Elands Bay Cave and the stone age of the Verlorenvlei, South Africa

John E. Parkington, Guillaume E Porraz

Southern African Humanities
VOLUME 29 • 2016

CONTENTS

Southern African Humanities 29, 2016

ISSN 1681-5564

Southern African Humanities

Volume 29, 2016

Elands Bay Cave and the Stone Age of the Verlorenvlei, South Africa

edited by

John Parkington and Guillaume Porraz

formerly *Natal Museum Journal of Humanities*

Southern African Humanities

VOLUME 29
DECEMBER 2016

KWAZULU-NATAL MUSEUM
PIETERMARITZBURG
SOUTH AFRICA

KwaZulu-Natal Museum
Private Bag 9070
Pietermaritzburg
3200 South Africa
www.nmsa.org.za
www.sahumanities.org.za

ISSN 1681–5564

CONTENTS

Southern African Humanities **29**: 1–15 December 2016 KwaZulu-Natal Museum

Three arcs: observations on the archaeology of the Elands Bay and northern Cederberg landscapes

Alex Mackay
Centre for Archaeological Science, School of Earth and Environmental Sciences,
University of Wollongong, Australia

ABSTRACT

The area around Elands Bay and the adjacent interior landscapes west of the Doring River have been subject to intense archaeological investigation over the last ~50 years. The result is a region with great depth and diversity of archaeological information. In this paper I discuss three general observations that arise from the integration of data across this region. The first is that redundancy in site occupation is limited: even where many sites are excavated in a small area, understanding of the regional sequence cannot be assumed to be complete. The second is that humans did not live in rock shelters: a focus on rock shelters alone, even where these are abundant, produces a skewed picture of occupational and demographic histories. The third is that the coast and its hinterland are intimately bound: interaction between the two zones is variable, and even where it is limited this observation is important to the understanding of both.

KEY WORDS: Elands Bay; Klipfonteinrand; occupational patterns; late Pleistocene; Holocene; megamiddens.

If you stand on the rocks at the point around which Elands Bay's famous left-hander peels, you can watch the wave start to break with the face of Baboon Point in the background, and behind it Elands Bay Cave and the massive middens over which it looks (Jerardino 1998). As the wave arcs slowly north and finally peters out you find yourself staring at Dunefield Midden (Parkington et al. 1992; Stewart 2008), some 12 km beyond which is Steenbokfontein (Jerardino & Yates 1996). Immediately behind you is Tortoise Cave (Robey 1984) and the mouth of the Verlorenvlei which extends to the northeast following a high sandstone ridge that some 14 km away breaks down into a series of koppies, in the most prominent of which is Diepkloof (Porraz et al. 2013). The view from Diepkloof takes in the west end of the vlei and a broad sweep of sandveld (Mazel 1981; Manhire 1984), ridges of which obscure Faraoskop (Manhire 1993) to the north but which on a clear day allow sight of the coastal mountain range and the high Cederberg the west flanks of which run into the Olifants River valley (Parkington & Poggenpoel 1971; Orton & Mackay 2008; Hallinan 2013) and the east flanks into its more tempestuous sister river the Doring. The Olifants-Doring system runs initially north before eventually curving back west to the sea around Ebenezer. Between them, those three watery arcs—the wave, the vlei and the river—circumscribe one of the most interesting and well-studied archaeological landscapes of southern Africa, with occupation documented over more than 100 000 years. The unusual density of archaeological data that has been generated here, coupled with the diversity of geological and environmental settings from which they derive and the extensive duration which they cover allows it to address questions of changing human behaviour and land use. In this paper I focus on what I view as three issues of general relevance that arise from the last 50 years of research—driven mainly by John Parkington and colleagues from UCT—in this area: inter-site occupational redundancy, occupational context and coastal/interior interactions.

ISSN 2305-2791 (online); 1681-5564 (print)

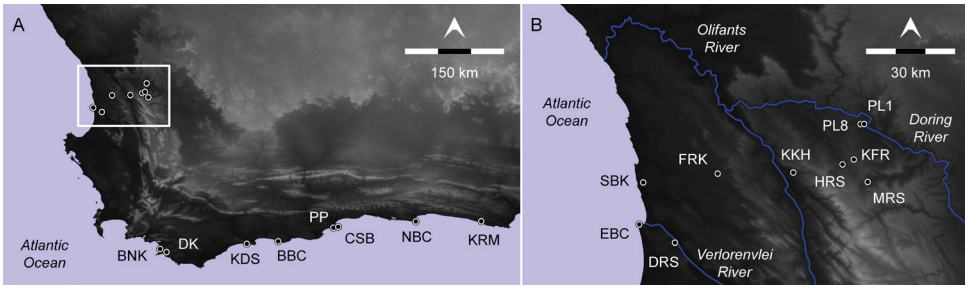

Fig. 1. Location of sites discussed in the text. (A) South western South Africa. BBC=Blombos Cave; BNK=Byneskranskop; CSB=Cape St. Blaize; DK=Die Kelders; KDS=Klipdrift Shelter; KRM=Klasies River; NBC=Nelson Bay Cave; PP=Pinnacle Point 13b & 5-6. White box highlights study areas shown in (B). (B) Sites in the main study area. DRS=Diepkloof Rock Shelter; EBC=Elands Bay Cave; FRK=Faraoskop; HRS=Hollow Rock Shelter; KFR=Klipfonteinrand; KKH=Klein Kliphuis; MRS=Mertenhof Rock Shelter; PL1=Putslaagte 1; PL8=Putslaagte 8; SBK=Steenbokfontein. Megamiddens occur from just south of Elands Bay Cave to north of Steenbokfontein.

INTER-SITE OCCUPATIONAL REDUNDANCY IS LIMITED

Prior to the advent of chronometry temporal schemes were built in relative terms using seriation. The characteristics of different items or assemblages of material were described, and placed in sequence with other items/assemblages. Sequencing could be approached in one of several ways. Prior to the availability of deep sequence excavation in southern Africa, researchers would form series either through comparison with already-developing European sequences (e.g. Peringuey 1911) or by assuming that technologies would become more sophisticated through time and thus arranging samples from less complex (older) to more complex (younger) (e.g. Gooch 1882). Some applied a mix of these approaches (e.g. Goodwin & Van Riet Lowe 1929; cf. Mackay 2016).

The excavation of multi-component sites allowed the development of local sequences independent of such assumptions. These also had the advantage of allowing assemblages from single component (usually open) sites to be fitted into the local sequence. Following this approach, particularly deep sequence sites with multiple components assumed considerable importance. The focus on key sequence sites, however, produced some curious results, most notably with the excavations of Klasies River, Nelson Bay Cave and Die Kelders on the south coast (Fig. 1). None of these major Pleistocene sites included a sample of bifacial points, contributing to the demise of the Still Bay as a cultural unit in the southern Cape (Sampson 1974; Volman 1981), even though its type marker was one of the earliest identified lithic artefact types in southern Africa (Minichillo 2005). It was not until the excavation of Blombos that the Still Bay lurched suddenly and vividly back to life on the south coast as a viable techno-cultural entity (Henshilwood et al. 2001).

Yet the absence of a given component from these otherwise impressive sites is not wholly surprising when the dataset from the south coast is considered in aggregate. Looking only at the known components of the Pleistocene sequence, we find fairly limited site-to-site redundancy (Table 1). So far, and in spite of at least nine deep sequence Pleistocene sites on the southern coast Blombos remains the only significant Still Bay sample (*pace* Minichillo 2005). Similarly, while the

TABLE 1

Occupational presence/absence by culture historic units for late Pleistocene sites on the southern Cape coast. Grey shading denotes periods of occupation. BKK = Bynensrkanskop; DK = Die Kelders; CSB = Cape St Blaize; BBC = Blombos Cave; KRM = Klasies River; KDS = Klipdrift; NBC = Nelson Bay Cave; PP13b = Pinnacle Point13b; PP5–6 = Pinnacle Point 5–6.

Unit	BBC	BKK	CSB	DK	KDS	KRM	NBC	PP13b	PP5–6
'Albany'									
Robberg									
Late MSA									
Post-Howiesons P.									
Howiesons Poort									
Pre-Howiesons P.									
Other MIS 4									
Still Bay									
Early MSA									

Howiesons Poort is present at four of nine sites, significant post-Howiesons Poort samples have only been reported from two. An early MSA occurs at most sites, but if proposed sub-divisions of this period (e.g. Wurz 2013) are stable and valid, and given that this unit potentially covers greater than 50 000 years at most sites, then the degree of consistency between sites is almost considerably less than implied by Table 1. Die Kelders has an MSA variant that may be absent from all other sites in the area, while Pinnacle Point 5–6 has a Howiesons Poort-like unit that possibly ante-dates the Howiesons Poort elsewhere in the area. Thus, even with nine sites, our understanding of the regional sequence would be sensitive to the removal of just one sample, and we cannot assume that our current knowledge of the southern Cape late Pleistocene sequence is complete. The problem can be described as one of limited inter-site occupational redundancy.

Elands Bay Cave (this issue) and Diepkloof (Porraz et al. 2013) (Fig. 1) replicate this pattern on the west coast very clearly (Parkington 2016 this issue; Porraz, Schmid et al. 2016 this issue). Both shelters have late Holocene components. But for the remainder of their sequences, the occupation of these two sites appears to have been entirely non-overlapping. If views of the occupation of the Verlorenvlei were based principally on the excavation of Elands Bay Cave, the perspective produced would have been one of weak occupation outside of the earliest MSA until the start of MIS 2. Thereafter, and with a few minor lacunae, populations would have been inferred to have been resident through until recent times. In contrast, if models were based on Diepkloof, the argument could have been developed for rich occupation during the MSA with abandonment during the coldest climates of MIS 2, and a return in the warm, stable conditions of the late Holocene.

A similar lack of inter-site occupational redundancy can be seen at interior sites in the Doring River catchment (Fig. 1).[1] For example, Hollow Rock Shelter and Klipfonteinrand are two rock shelters formed in Table Mountain Sandstones, and

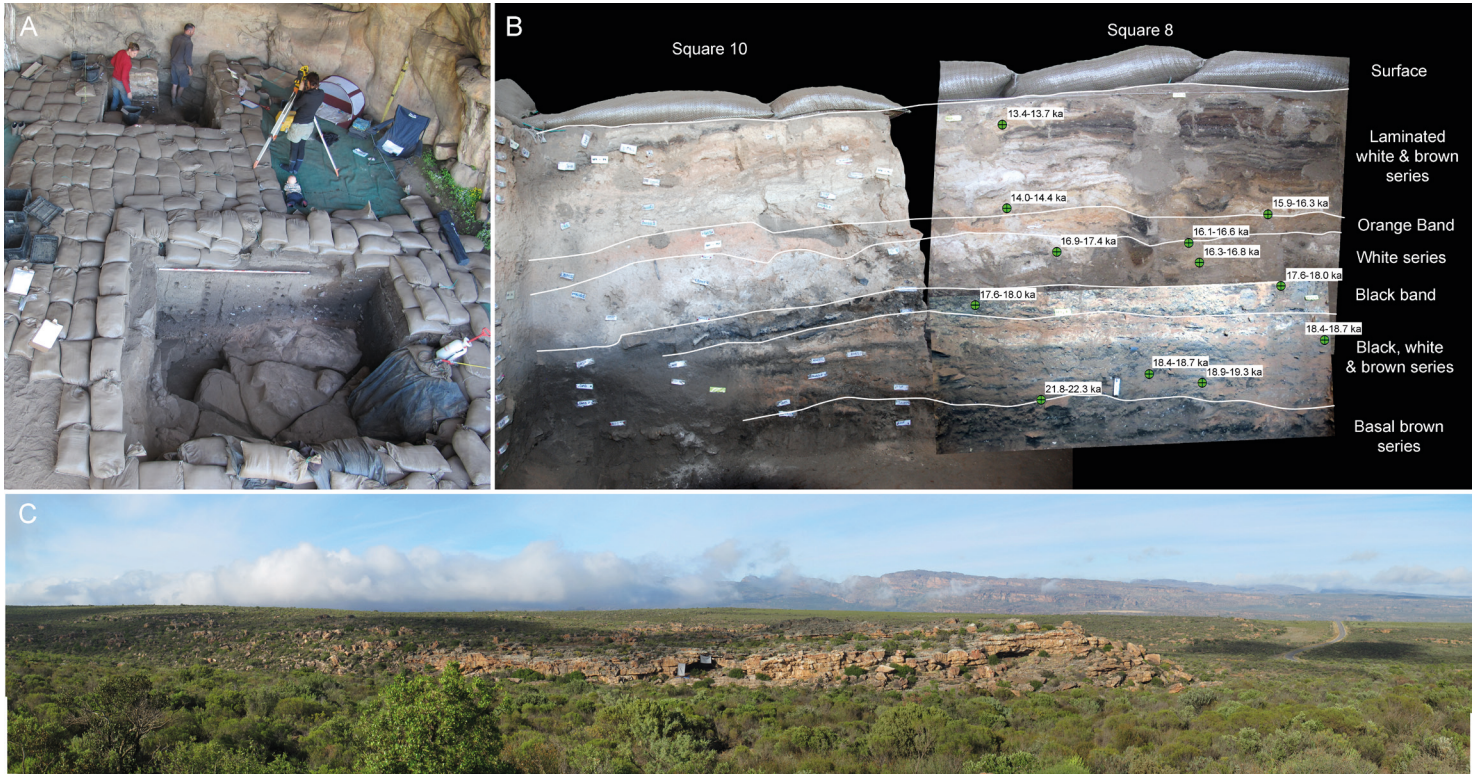

Fig. 2. Excavations at Klipfonteinrand. (A) Overview showing front and rear trenches. (B) South section of trench two composed from multiple images over multiple seasons. The western portion of this section is visible in panel (A). The upper stratigraphic group—Laminated White and Brown Series—is post-Robberg; the underlying Orange Band is unassigned pending further analysis; The White Series, Black Band, and Black, White and Brown Series are all Robberg; The Basal Brown series is Howiesons Poort. Ages are as per Table 2. (C) Setting of Klipfonteinrand with the Cederberg mountains in the background. Silver shade cloth was used to limit direct sunlight.

TABLE 2
Radiocarbon ages from Klipfonteinrand, rear trench. Calibration follows Hogg et al. (2013).

Stratum	square	Sample code	Uncalibrated age	Calibrated age
Laminated white and brown series	9	D-AMS 001836	11 723 ± 52	13 384–13 703
	8	D-AMS 002439	12 303 ± 41	14 003–14 425
Orange Band	8	D-AMS 003797	13 439 ± 56	15 897–16 314
	8	D-AMS 003798	13 584 ± 58	16 087–16 555
White series	8	D-AMS 002440	14 131 ± 61	16 885–17 407
	9	D-AMS 001837	13 722 ± 49	16 275–16 766
Black Band	9	D-AMS 003799	14 656 ± 55	17 606–17 979
	9	D-AMS 001838	14 706 ± 65	17 637–18 039
Black, white and brown series	8	D-AMS 002440	15 309 ± 65	18 355–18 710
	8	D-AMS 002441	15 342 ± 65	18 389–18 739
	9	D-AMS 003800	15 871 ± 59	18 902–19 276
	9	D-AMS 001839	18 232 ± 71	21 829–22 294

located 2 km apart. Both sites fall in the catchment of the Brandewyn River, albeit that the former is situated on the river and the latter on the adjacent ridge. Hollow Rock is an unusual site—a hollowed out boulder perched on the cliffs immediately above the Brandewyn River (Evans 1994).The depth of sediment is quite shallow, and the sequence is limited to two main components—a series of sedimentary units assigned to the 'Still Bay' layers and dating ~70 ka, from which >50 bifacial points have been recovered (Evans 1994; Högberg & Larsson 2011; Högberg 2014). These are underlain by a thin body of sediment lacking bifacial points and dating ~80 ka, which has been assigned to the early MSA (Mackay 2009).

Klipfonteinrand was excavated by Parkington in 1969, and again under my direction in 2011–12. The first excavations covered a large area of the site to a limited depth (~200 mm), with a single deep trench to bedrock at the front of the site. The more recent excavations widened the existing front trench and opened a second trench to bedrock at the back of the shelter (Fig. 2) (Table 2). The Klipfonteinrand sequence as we presently understand it features late Holocene, possible early Holocene, late MIS 2 ('Albany' or 'Oakhurst'), early MIS 2 (Robberg), Howiesons Poort and early MSA units. While Parkington's excavation diary reports that a single 'laurel leaf' point without stratigraphic reference, despite the now extensive spatial coverage of the site neither excavation there has produced any Still Bay finds in context. Furthermore there appears to be no significant sequence between the oldest MIS 2 layers dating ~22 ka, and the Howiesons Poort, likely antedating 60 ka (Jacobs et al. 2008; Tribolo et al. 2013).

Subsequent excavations of two square meters to bedrock at the site of Putslaagte 8, a further 20 km north, produced another long sequence, again with similar and different characteristics (Mackay et al. 2015). The site features late Holocene at the top, underlain by particularly rich layers dating to MIS 2. This includes the well-known Oakhurst and Robberg units, but also includes an early Later Stone Age component

dominated by hornfels blade production and dating ~22–25 ka. This component is otherwise unknown at other rock shelter sites in the region. Below this early MIS 2 component the archaeological record at Putslaagte 8 is persistent but material finds occur in low density. Thus while the site has very minor MIS 3 MSA, post-Howiesons Poort and Howiesons Poort assemblages, the total sample size for each is too low for technological or other behavioural characterisation. The existence of a Still Bay at the site is inferred from a couple of probable bifacial thinning flakes, but as with Klipfonteinrand we have no bifacial points recovered in context.

Finally, in 2013 we initiated excavations at the site of Mertenhof, located on the Bushmans Kloof property 10 km south of Klipfonteinrand (Will et al. 2015; Schmidt & Mackay 2016). The site has grass-bedding deposits towards the top that include glass beads and ceramic pipe fragments that probably date to the last few hundred years. None of the other sites mentioned above has produced archaeological materials likely to be so recent (though Nic Wiltshire noted a glass bead on the surface during a visit to Putslaagte 8). The remainder of the Mertenhof sequence can be described as follows. Underlying the grass-bedding deposits are sedimentary units (denoted R/GBS) the technological composition of which relates to the Robberg. Cut into R/BGS are a number of pits of unknown age, including two burials of human children, and several probable mongoose burials (Fig. 3). Underlying the Robberg at Mertenhof are three major sedimentary units (LGS, LRS, DGS) containing MSA materials, that almost certainly relate to the late or MIS 3 MSA—those absent or very scarce at the other sites in the area. Under these are rich post-Howiesons Poort and Howiesons Poort strata (BGG/WS), and under this Still Bay layers (RGS) that have so far produced half a dozen bifacial points in the limited excavation area—though this is notably far less than the sample from Hollow Rock Shelter. The Still Bay rests on the sedimentary unit DBS that can be characterised as early MSA pending more detailed study (bedrock has not yet been reached anywhere at Mertenhof).

The aggregate occupational data set from the excavated northern Cederberg rock shelter sites is presented in Table 3. The maximum distance across the four sites is 25 km—about a full day's walk for a hunter-gatherer (Kelly 1995). Most sites have produced at least one component that is lacking or weakly expressed in all of the others. Peak redundancy occurs in late Holocene and the MIS 2 Robberg unit. There may also be some redundancy in the early MSA, but again this cannot be assumed.

The implication of these observations is that no site on its own seems capable of resolving the occupational history of any given region, and that even large numbers of sites are often insufficient. The factors governing site selection in the past were clearly complex (Kandel et al. 2016), and given the present state of our data, effectively cryptic. In order to understand occupational histories, and to build something approximating a regional key-sequence, we need to amalgamate the results of as many sites as possible. And even then we are confronted by the fact that …

PEOPLE DID NOT LIVE IN ROCK SHELTERS

One of the great advantages of the Elands Bay and northern Cederberg regions is that the Table Mountain series geology produces a high frequency of rock shelters. In an otherwise erosional landscape, rock shelters are an attractive target for archaeological research because they can accumulate and protect sedimentary sequences. Away from

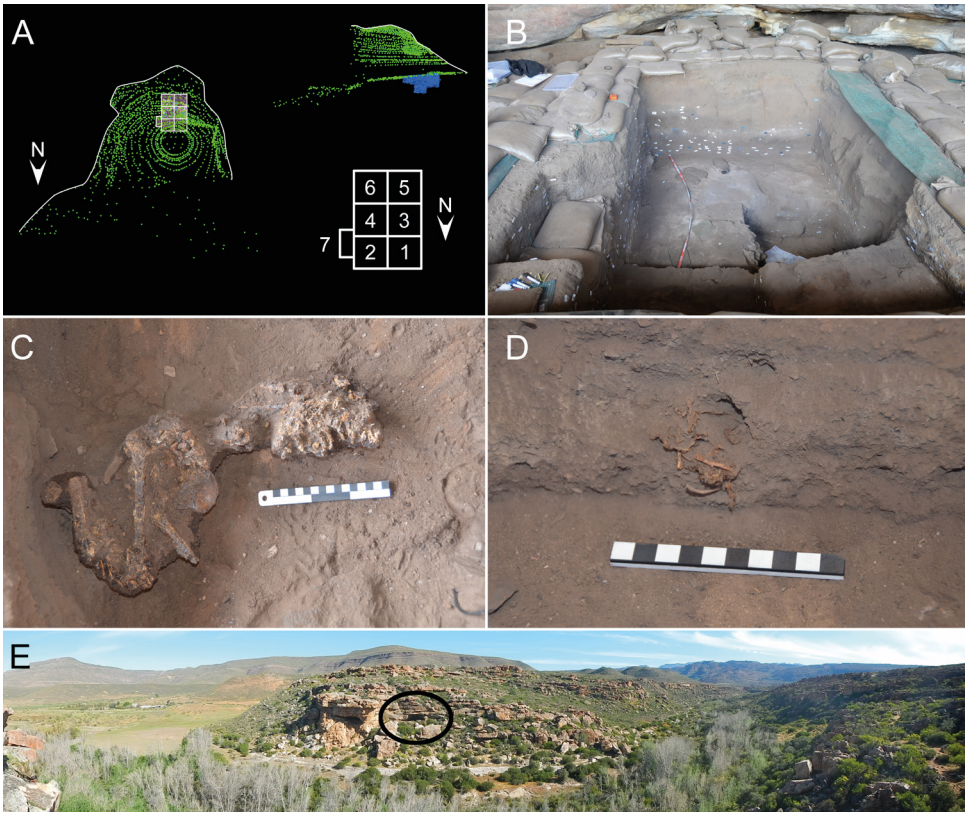

Fig. 3. Excavations at Mertenhof. (A) layout of shelter (green dots), plotted finds (blue dots) and excavation squares (numbered 1-7). North is arbitrarily oriented to shelter mouth. (B) Excavation area at end of season III. (C) Child post-crania, located at the junction of squares 2, 4 and 7. Skull had earlier been removed after it was first encountered in square 4 and became unstable by the time square 7 was opened to allow removal of remaining bones. The bones were extremely poorly preserved and were only recoverable with the aid of a consolidant (Paraloid B-72). The burial was covered by a low cairn of large rocks. (D) Partially articulated mongoose in small pit in north wall, square 7 – possibly a burial. (E) Location of Mertenhof shelter (black oval) with the Biedouw River in the foreground and the Cederberg visible on the right-hand side.

the coast it is often human occupation which drives sedimentation in rock shelter sites; despite recurrent and sometimes very long hiatuses, sterile sediment bands are effectively absent from the rock shelters of the interior in this region (Mackay 2010; Mackay et al. 2015) (Fig. 2). Thus excavation in rock shelters with any depth of sediment in these areas is likely to produce reasonably well-preserved sequences of behavioural information. Beyond the rock shelters, however, accumulation of sediment is spatially and temporally relatively rare, and in the case of the coastal sandsheet (or Sandveld), highly episodic (Chase & Thomas 2007). In most cases, material debris from human occupation is left on stable or actively eroding surfaces where preservation of organic material is poor, and where ages can only be assigned based on similarities with material from dated contexts—usually rock shelters. Where such open sites occur close to features that attract repeated occupation (e.g. water), they are susceptible to persistent

TABLE 3

Occupational sequences at major rock shelter sites in the Doring River catchment. HRS = Hollow Rock Shelter; KFR = Klipfonteinrand; PL8 = Putslaagte 8; MRS = Mertenhof Rock Shelter; PL1 = Putslaagte 1. PL1 is the only open site in the sample. Dark shading denotes the present of substantial volumes of deposit and/or large assemblages. Light shading denotes occupation but with little recovered material debris.

Unit	HRS	KFR	PL8	MRS	PL1
Historical					
Late Holocene (<3 ka)					
Mid Holocene (3–7 ka)					
Early Holocene (7–12 ka)					
Term. Pleistocene (~12–14 ka)					
MIS 2 Robberg (~16–22 ka)					
MIS 2 early LSA (~22–25 ka)					
MIS 3 MSA					
MIS 3/4 post-Howiesons Poort					
Howiesons Poort					
Still Bay					
Early MSA					

over-print, resulting in palimpsests from which time-sensitive information can be difficult to extract (Bailey 2007). The focus on rock shelters as a principal source of archaeological data in such areas is thus a rational use of finite research time.

There is, however, an important problem that arises from this research focus: people did not live in rock shelters. Extensive ethnographic studies (e.g. Kelly 1995; Binford 2001) reveal little evidence of rock shelters as occupational foci. Instead, people lived across landscapes, making use of a diverse array of variably-situated resources. Rock shelters account for a miniscule fraction of the landscape contexts used, the proportion of time spent in rock shelters was probably often very low, and ultimately there is no reason to assume that all behaviours in the habitual repertoires of human groups were expressed there. However, while the fact that rock shelters provide an imperfect record of the past is uncontroversial, more troubling is the possibility that the rock shelter record may be structurally biased.

This possibility is beautifully drawn out by Jerardino and Yates (1996), in their study of Holocene occupational patterns along the west coast. A persistent gap in the occupation of major rock shelter sites 2–4 ka may have been taken to imply a population absence from the region. However this is also the period in which the largest shell middens along the coast were formed—the so-called 'megamidden phase'. Thus, it seems that populations reorganised their movements in this period such that rock shelters saw comparatively little use.

Recent research in the interior reveals similar patterns in the Pleistocene. While MIS 3 MSA assemblages are persistently difficult to find in rock shelter sites in the northern Cederberg (Table 3) and indeed throughout the south west of southern Africa (Faith

2013; Mackay, Stewart & Chase 2014), it appears that rich sites dating to this period do occur in open contexts on the Doring River (Mackay, Sumner et al. 2014). Still Bay sites, which have historically not been abundant in rock shelters in the region are very commonly located in the open (Mackay et al. 2010; Hallinan 2013; Mackay, Sumner et al. 2014). Similarly, only Mertenhof has produced a sizeable post-Howiesons Poort sample in the northern Cederberg (Table 3), but extremely rich open-air post-Howiesons Poort sites have been reported on the Doring River and further inland (Hallinan & Shaw 2015, Will et al. 2015). Conversely, Howiesons Poort sites, which have extraordinarily high visibility in rock shelter sequences throughout southern Africa (Mackay 2010; Karkanas et al. 2015), have so far remained elusive despite extensive surveys across multiple catchments (Mackay & Hallinan in press).

A consequence of these observations is that inferences about changing occupation and demography through the last ~100 000 years, when drawn principally from rock shelters, has the potential to conflate rock shelter use with population presence/absence and potential even population size. Ultimately, intensive occupation of rock shelters—whether by larger groups of people, people visiting more often, people staying longer, or all of the above—can only really be understood to imply that rock shelters were being more heavily occupied. Extending that inference to the intensity of regional population more generally necessitates the assumption that rock shelters will be occupied proportional to regional population. And that assumption is risky, given that, for some periods it has proven to be false.

OCCUPATION OF THE COAST IS ENRICHED BY UNDERSTANDING OF THE INTERIOR

Parkington's (1977) seminal PhD research—*Follow the San*—was based on the principals of economic archaeology where different and potentially complementary resource zones were argued to have been occupied in sequence as part of a seasonal subsistence round. In the Elands Bay and northern Cederberg regions, the complementarity was suggested to have produced different signals of faunal exploitation in coastal and interior areas reflecting different seasons of occupation. Subsequent work by Sealy and Van der Merwe (1986, 1992) suggested that in fact the two populations in these different areas were largely discrete (though note Parkington 1991). Both studies, however, highlight some of the variable possibilities in coastal/interior interactions which have implications for our understanding of patterns in both.

The renewed excavations at Klipfonteinrand provide new comparative data that implies changing interior/coastal relations during MIS 2. Early in this stage (~22–16 ka), marine shell—necessarily a coastally acquired resource—is absent from the excavated sample. Meanwhile at coastal sites of this age, hornfels is uncommon (Manhire 1993; Orton 2006; Porraz, Igreja et al. 2016 this issue). While hornfels is available as pebbles in ancient terraces at the mouth of the Olifants (Mackay 2011), it is relatively abundant in the interior, being the dominant or sub-dominant rock at sites around the Doring River (Mackay, Sumner et al. 2014; Hallinan & Shaw 2015, Mackay et al. 2015; Will et al. 2015). The interior is thus the likely source for the examples found in coastal and near-coastal sites.

In later MIS 2, several interesting changes occur. From 14–13 ka at Klipfonteinrand, marine shell appears for the first time. The dominant species is white mussel (*Donax*

serra) with smaller contributions from black mussel (*Choromytilus meridionalis*), Argenville's limpet (*Scutellastra argenvillei*) and ribbed mussel (*Aulacomya ater*) (K. Bluff pers. comm. 2015). White mussel was used in the terminal Pleistocene and early Holocene coastal sites as a raw material for scrapers (Manhire 1993; Orton 2006). Conversely, by ~14 ka at Elands Bay Cave and ~12 ka at Faraoskop (Manhire 1993), the proportion of hornfels in assemblages begins to rise, reaching its peak at Elands Bay Cave ~13–10 ka (Orton 2006). Hornfels is particularly common in the retouched flake component, most notably in the form of large scrapers known as naturally backed knives (Orton 2006). This artefact type also makes its first appearance at Klipfonteinrand in this period. These data appear to suggest a complementarity of resource movement between coastal and interior zones in later MIS 2, and coincide suggestively with a period of unusually rapid sea-level rise (Stanford et al. 2006). Given the earlier absence of such evidence it seems plausible that the nature of interaction between these two areas was variable through the terminal Pleistocene, with increasing resource transfer potentially tracing the marine transgression at the end of MIS 2.

Further variance in this relationship is apparent in the mid to late Holocene (~2–4 ka). During this period, broadly coincident with the megamidden phase described earlier, proportions of hornfels in Sandveld sites is considerably lower than during the late Pleistocene (Manhire 1993; Jerardino 2010). Jerardino (1997, 1998, 2010, 2010, 2012, 2013), drawing on a wealth and diversity of data, has developed a demographic model to explain changes in coastal occupation in this period. This model contends that the megamidden period was driven principally by increased population density on the coast. The earliest signal of this population change is a reduction in the frequency of large game and intensification of small game procurement, followed by a subsequent shift in emphasis to sessile, resilient and highly productive marine resources. As part of the emphasis on sessile marine fauna, mobility decreased, duration of occupation increased, and indicators of circumscribed mobility—including interments of the dead—became common. The effect was one of resource intensification and increasingly exclusive use of coastal resource patches. While Jerardino's thesis has been influential, it has not been uncontested. Parkington (2012), for example, citing the dearth of artefacts, paucity of well-defined hearths, and equivocal nature of skeletal isotope data, has suggested that the megamiddens were not in fact residential occupational foci, but rather served as logistical processing locations. More specifically, they were locations where large quantities of black mussel were dried for transportation to and consumption in interior locations.

Two observations encourage development of a third explanation for the megamiddens, more similar to Jerardino's, but based on different underlying mechanisms. First, while the interior climate data are somewhat equivocal there appears to be a broad trend to aridity in the mid to late Holocene punctuated by briefer periods of humidity (Jerardino 1995; Chase et al. 2010, 2013; Valsecchi et al. 2013; Chase et al. 2015). Second, none of the major dated interior rock shelters in either the Olifants or Doring River valleys show occupation in the megamidden period (Parkington & Poggenpoel 1971; Manhire 1993; Orton & Mackay 2008; Mackay et al. 2015); the only clear evidence for occupation in the interior at this time takes the form of isolated child burials (Sealy et al. 2000).While the above-noted risk of conflating rock shelter use with population presence/absence needs to be borne in mind, the available evidence provides neither the environmental

context nor empirical support for population increase in the interior in the mid to late Holocene, nor for significant coastal/interior interaction.

One commonly used model to explain variance in hunter-gatherer land-use and territoriality is that proposed by Dyson-Hudson and Smith (1978). This model has seen considerable application in southern African archaeology (e.g. Ambrose & Lorenz 1990; McCall 2007; Marean 2014). The Dyson-Hudson and Smith model uses a simple 'high–low' dichotomy in two resource parameters—abundance and predictability—to generate a two-axis model of variance in mobility and territoriality. At one extreme, populations inhabiting areas with dense and predictable resources are suggested to form small 'geographically stable' territories, while at the other extreme, populations in unpredictable and resource depauperate environments are argued to be dispersed, highly mobile and to lack well-defined territorial areas.

While the model has been influential, it contains an important deviation from the 'economic defendability' model (Brown 1964) on which it was based. In that original model, resource density is considered relative to population size, and not an absolute property of environments. Where resources are rich relative to the number of foragers, there is little benefit to be accrued from defending the resource patch (Brown 1964: 162–3). The critical consideration is not the prevalence of resources, but the marginality of resources relative to the population base (Brown 1964: 160).

One of the ethnographic examples provided by Dyson-Hudson and Smith serves to highlight the difference. Prior to increasing disruptions brought about by the fur trade, the Ojibwa of the Canadian subarctic forests had access to large and small game, and generally focused on the exploitation of larger animals such as moose and caribou. This resource configuration effectively precluded the "formation of well-defined territories, since caribou migrations are not restricted by any artificially bounded regions"(Bishop 1974: 209). Later decreases in large game abundance brought about in part by fur traders led to an increased focus on small game. At this time, groups became increasingly territorial, and "[s]ocial sanctions against trespass apparently were an important aspect of defense of hunting territories" (Dyson-Hudson & Smith 1978: 33). Of course, the small game on which the Ojibwa were increasingly reliant had always been present. Thus, and precluding that significant population increase occurred as a response to *diminishing* subsistence resources, maintenance of a restricted, well-defined foraging territory was likely a means of increasing resource security under increasingly marginal conditions.

The megamidden phase in the Elands Bay area may have parallels with this case. Environmental data suggest aridification, and occupational evidence from the interior is weak. On the coast, the proportion of large game declines and subsistence comes to focus heavily on productive and resilient marine fauna, with some use of small terrestrial game. Interment of the dead—which may have served to circumscribe territorial associations—becomes more common, and the extent of interaction between coastal and remaining interior populations appears to be unusually limited. While absolute population increase has been suggested to account for this pattern, it is not necessary to explain it. Rather, facing diminishing resource abundance, coastal populations around Elands Bay, like the Canadian Ojibwa, may have attempted to sustain their number by relying increasingly heavily on the more resilient of the food items that had always been available in their zone, and improved the security of that resource by the exclusion of other coastal and non-coastal groups.

Combined, these observations suggest great variability in the nature and extent of interior and coastal interaction through the last ~22 ka. To that extent, our ability to understand occupational patterns in either is contingent on the incorporation of information from both.

DISCUSSION AND CONCLUSION

Southern Africa has been the subject of much recent research focus, due in large part to the discovery of relatively early evidence for behaviours inferred to reflect complex cognition. This has resulted, among other things, in the development of many new research projects, the excavation of new sites, and the re-excavation of old sites. Much of this work has been strongly site-specific, reflecting factors including the enduring value of deep sequence sites, increasingly refined but concomitantly slow modern excavation methods, and the increasing amount of post-excavation information that can be generated by specialist analyses. As discussed here, however, the significance of the occupation, abandonment and archaeological composition of any site—or even multiple sites—is hard to resolve without knowledge of the contemporaneous use of surrounding landscapes.

The site of Elands Bay Cave continues to play a central role in our understanding of the archaeology of the Elands Bay and northern Cederberg areas. Its long sequence and excellent Holocene organic preservation, coupled with the site's locational sensitivity to sea-level change, has made it an unmatched source of information about changing lifeways in the region. As much as the site itself is a key archive, however, the meaning of the information it contains has been enhanced by the degree to which it has been integrated into the archaeology of the surrounding landscapes and the broader region. This integration largely reflects the sustained effort of researchers from the UCT—more recently augmented by contributions from international scholars—and their continued sampling of the many different facets of the region's archaeology. Indeed, the three points made in this paper are largely Pleistocene extensions of the past work of Parkington and colleagues, with Elands Bay Cave central to all of them. Comparisons between Klipfonteinrand and Elands Bay Cave, for example, were components of the seasonal transhumance model, in which coastal and interior locations were presented as a two components of a single integrated subsistence system. Understanding of the imperfect perspective on regional occupational systems provided by rock shelters is evident from the occupational gaps at Elands Bay Cave and complementary occupation of megamiddens. Limited site redundancy could be inferred as early as the 1970s in contrasts between Elands Bay Cave and Diepkloof.

Ultimately, what work at Elands Bay Cave and the surrounding landscapes seems most strongly to suggest is that the archaeological information-richness of a region is a factor not only of the sequential depth and preservation quality of our available data, but also of its spatial density. Without the constraints provided by multiple sites of different types distributed across different landscape contexts, occupational hiatuses in a one or more deep-sequence shelters might be assumed to imply regional abandonment, while intense shelter use or resource intensification might be assumed to reflect increased population. And these patterns may well carry these implications. However, our ability to disentangle the significance of any given observation is contingent on our ability to situate it within the broader landscapes that people in the past unquestionably used.

NOTE

[1] I focus here on the Doring River rather than adjacent stretches of the Olifants where relatively few deep-sequence and/or multi-component sites have so far been excavated and published. Interesting detail on open site distribution and composition in the Olifants is available in Hallinan (2013).

ACKNOWLEDGEMENTS

I am very grateful to Guillaume Porraz for his invitation to contribute to this volume, and to John Parkington, Brian Stewart and a third anonymous reviewer for their advice in strengthening the paper. I am also extremely grateful to the staff and students at UCT for on-going support. Some of the research detailed here was funded by Australian Research Council grants DP#1092445 and DE#130100068.

REFERENCES

Ambrose, S.H. & Lorenz, K.G. 1990. Social and ecological models for the Middle Stone Age in southern Africa. In: P. Mellars, ed., *The emergence of modern humans*. Edinburgh: Edinburgh University Press, pp. 3–33.

Bailey, G. 2007. Time perspectives, palimpsests and the archaeology of time. *Journal of Anthropological Archaeology* **26** (2): 198–223.

Binford, L.R. 2001. *Constructing frames of reference: an analytical method for archaeological theory building using ethnographic and environmental data sets*. Berkeley and Los Angeles: University of California Press.

Bishop, C.A. 1974. *The Northern Ojibwa and the fur trade: an historical and ecological study*. Toronto: Holt, Rinehart and Winston of Canada.

Brown, J.L. 1964. The evolution of diversity in avian territorial systems. *Wilson Bulletin* **76**: 160–9.

Chase, B.M., Boom, A., Carr, A.S., Meadows, M.E. & Reimer, P.J. 2013. Holocene climate change in southernmost South Africa: rock hyrax middens record shifts in the southern westerlies. *Quaternary Science Reviews* **82**: 199–205.

Chase, B.M., Lim, S., Chevalier, M., Boom, A., Carr, A.S., Meadows, M.E. & Reimer, P.J. 2015. Influence of tropical easterlies in southern Africa's winter rainfall zone during the Holocene. *Quaternary Science Reviews* **107**: 138–48.

Chase, B.M., Meadows, M.E., Carr, A.S. & Reimer, P.J. 2010. Evidence for progressive Holocene aridification in southern Africa recorded in Namibian hyrax middens: implications for African Monsoon dynamics and the 'African Humid Period'. *Quaternary Research* **74** (1): 36–45.

Chase, B.M. & Thomas, D.S.G. 2007. Multiphase late Quaternary aeolian sediment accumulation in western South Africa: timing and relationship to palaeoclimatic changes inferred from the marine record. *Quaternary International* **166** (1): 29–41.

Dyson-Hudson, R. & Smith, E. 1978. Human territoriality: an ecological reassessment. *American Anthropologist* **80** (1): 21–41.

Evans, U. 1994. Hollow Rock Shelter, a Middle Stone Age site in the Cederberg. *Southern African Field Archaeology* **3**: 63–73.

Faith, J.T. 2013. Taphonomic and paleoecological change in the large mammal sequence from Boomplaas Cave, Western Cape, South Africa. *Journal of Human Evolution* **65** (6): 715–30.

Gooch, W.D. 1882. The Stone Age of South Africa. *Journal of the Royal Anthropological Institute* **11**: 124–83.

Goodwin, A.J.H. & Van Riet Lowe, C. 1929. *The Stone Age cultures of South Africa*. Edinburgh: Neill and Co.

Hallinan, E. 2013. *Stone Age landscape use in the Olifants River Valley, Western Cape*. MPhil, University of Cape Town.

Hallinan, E. & Shaw, M. 2015. A new Middle Stone Age industry in the Tanwka Karoo, Northern Cape Province, South Africa. *Antiquity Project Gallery* **89**: 344.

Henshilwood, C.S., Sealy, J.C., Yates, R., Cruz-Uribe, K., Goldberg, P., Grine, F.E., Klein, R.G., Poggenpoel, C., Van Niekerk, K. & Watts, I. 2001. Blombos Cave, southern Cape, South Africa: preliminary report on the 1992–1999 excavations of the Middle Stone Age levels. *Journal of Archaeological Science* **28** (4): 421–48.

Högberg, A. 2014. Chronology, stratigraphy and spatial distribution of artefacts at Hollow Rock Shelter, Cape Province, South Africa. *South African Archaeological Bulletin* **69**: 142–51.

Högberg, A. & Larsson, L. 2011. Lithic technology and behavioural modernity: new results from the Still Bay site, Hollow Rock Shelter, Western Cape Province, South Africa. *Journal of Human Evolution* **61** (2): 133–55.

Hogg, A.G., Hua, Q., Blackwell, P.G., Niu, M., Buck, C.E., Guilderson, T.P., Heaton, T.J., Palmer, J.G., Reimer, P.J., Reimer, R.W., Turney, C.S.M. & Zimmerman, S.R.H. 2013. SHCal13 Southern hemisphere calibration, 0–50,000 years cal BP. *Radiocarbon* **55** (4): 1889–903.

Jacobs, Z., Roberts, R.G., Galbraith, R.F., Deacon, H.J., Grun, R., Mackay, A., Mitchell, P., Vogelsang, R. & Wadley, L. 2008. Ages for the Middle Stone Age of southern Africa: implications for human behavior and dispersal. *Science* **322** (5902): 733–5.

Jerardino, A. 1995. Late Holocene neoglacial episodes in southern South America and southern Africa: a comparison. *The Holocene* **5**: 361–8.

Jerardino, A. 1997. Changes in shellfish species composition and mean shell size from a Late-Holocene record of the West Coast of Southern Africa. *Journal of Archaeological Science* **24** (11): 1031–44.

Jerardino, A. 1998. Excavations at Pancho's Kitchen Midden, Western Cape coast, South Africa: further observations into the megamidden period. *South African Archaeological Bulletin* **53**: 16–25.

Jerardino, A. 2010. Large shell middens in Lamberts Bay, South Africa: a case of hunter-gatherer resource intensification. *Journal of Archaeological Science* **37** (9): 2291–2302.

Jerardino, A. 2010. Prehistoric exploitation of marine resources in southern Africa with particular raference to sellfish gathering: opportunities and continuities. *Pyrenae* **41** (1): 7–52.

Jerardino, A. 2012. Large shell middens and hunter-gatherer resource intensification along the west coast of South Africa: The Elands Bay Case Study. *The Journal of Island and Coastal Archaeology* **7** (1): 76–101.

Jerardino, A. 2013. Two complementary Holocene lithic assemblages from Elands Bay and Lamberts Bay: implications for local changes in toolkit and group mobility. *South African Archaeological Bulletin* **68**: 188–99.

Jerardino, A. & Yates, R. 1996. Preliminary results from excavations at Steenbokfontein Cave: implications for past and future research. *South African Archaeological Bulletin* **51**: 7–16.

Kandel, A.W., Bolus, M., Bretzke, K., Bruch, A.A., Haidle, M.N., Hertler, C. & Märker, M. 2016. Increasing behavioral flexibility? An integrative macro-scale approach to understanding the Middle Stone Age of southern Africa. *Journal of Archaeological Method and Theory* **23** (2): 623–68.

Karkanas, P., Brown, K.S., Fisher, E.C., Jacobs, Z. & Marean, C.W. 2015. Interpreting human behavior from depositional rates and combustion features through the study of sedimentary microfacies at site Pinnacle Point 5–6, South Africa. *Journal of Human Evolution* **85**: 1–21.

Kelly, R.L. 1995. *The foraging spectrum: diversity in hunter-gatherer lifeways*. Washington, D.C.: Smithsonian Institution Press.

Mackay, A. 2009. *History and selection in the late Pleistocene archaeology of the Western Cape, South Africa*. PhD thesis, Australian National University.

Mackay, A. 2010. The Late Pleistocene archaeology of Klein Kliphuis rockshelter, Western Cape, South Africa: 2006 excavations. *South African Archaeological Bulletin* **65**: 132–47.

Mackay, A. 2011. Potentially stylistic differences between backed artefacts from two nearby sites occupied ~60,000 years before present in South Africa. *Journal of Anthropological Archaeology* **30** (2): 235–45.

Mackay, A. 2016. Technological change and the importance of variability: the Western Cape of South Africa from MIS 5 to MIS 2. In: S. Jones & B. A. Stewart, eds, *Africa from MIS 6–2: Population Dynamics and Paleoenvironments*. Dordrecht: Springer, pp. 49–63.

Mackay, A. & Hallinan, E. In press. Provisioning responses to environmental variation in the late Pleistocene of southern Africa. In: E. Robinson & F. Sellet, eds, *Lithic technological organization and paleoenvironmental change*. Springer.

Mackay, A., Jacobs, Z. & Steele, T.E. 2015. Pleistocene archaeology and chronology of Putslaagte 8 (PL8) rockshelter, Western Cape, South Africa. *Journal of African Archaeology* **13** (1): 71–98.

Mackay, A., Orton, J., Schwortz, S. & Steele, T.E. 2010. Soutfontein (SFT)-001: Preliminary report on an open-air bifacial point-rich site in southern Namaqualand, South Africa. *South African Archaeological Bulletin* **65**: 84–95.

Mackay, A., Stewart, B.A. & Chase, B.M. 2014. Coalescence and fragmentation in the late Pleistocene archaeology of southernmost Africa. *Journal of Human Evolution* **72**: 26–51.

Mackay, A., Sumner, A., Jacobs, Z., Marwick, B., Bluff, K. & Shaw, M. 2014. Putslaagte 1 (PL1), the Doring River, and the later Middle Stone Age in southern Africa's Winter Rainfall Zone. *Quaternary International* **350**: 43–58.

Manhire, A. 1993. A report on the excavations at Faraoskop Rock Shelter in the Graafwater District of the south-western Cape. *Southern African Field Archaeology* **2**: 3–23.

Manhire, A.H. 1984. *Stone tools and Sandveld settlement*. MSc thesis, University of Cape Town.

Marean, C.W. 2014. The origins and significance of coastal resource use in Africa and Western Eurasia. *Journal of Human Evolution* **77**: 17–40.

Mazel, A.D. & Parkington, J.E. 1981. Stone tools and resources: a case study from southern Africa. *World Archaeology* **13** (1): 16–30.

McCall, G.S. 2007. Behavioral ecological models of lithic technological change during the later Middle Stone Age of South Africa. *Journal of Archaeological Science* **34** (10): 1738–51.

Minichillo, T. 2005. *Middle Stone Age lithic study, South Africa: an examination of modern human origins*. PhD thesis, University of Washington.

Orton, J. 2006. The Later Stone Age lithic sequence at Elands Bay, Western Cape, South Africa: raw materials, artefacts and sporadic change. *Southern African Humanities* **18** (2): 1–28.

Orton, J. & Mackay, A. 2008. New excavations at Klein Kliphuis Rockshelter, Cederberg Mountains, Western Cape: the late Holocene deposits. *South African Archaeological Bulletin* **63**: 69–76.

Parkington, J.E. 1977. *Follow the San*. PhD thesis, Cambridge University.

Parkington, J.E. 1991. Approaches to dietary reconstruction in the Western Cape: are you what you have eaten? *Journal of Archaeological Science* **18** (3): 331–42.

Parkington, J.E. 2012. Mussels and mongongo nuts: logistical visits to the Cape west coast, South Africa. *Journal of Archaeological Science* **39** (5): 1521–30.

Parkington, J.E. 2016. Elands Bay Cave: keeping an eye on the past. *Southern African Humanities* **29**: 17–32.

Parkington, J.E., Nilssen, P., Reeler, C. & Henshilwood, C.S. 1992. Making sense of space at Dunefield Midden Campsite, Western Cape, South Africa. *Southern African Field Archaeology* **1**: 63–70.

Parkington, J.E. & Poggenpoel, C. 1971. Excavations at De Hangen, 1968. *South African Archaeological Bulletin* **26**: 3–36.

Peringuey, L. 1911. The Stone Ages of South Africa. *Annals of the South African Museum* **8**: 1–218.

Porraz, G., Igreja, M., Schmidt, P. & Parkington, J.E. 2016. A shape to the microlithic Robberg from Elands Bay Cave (South Africa). *Southern African Humanities* **29**: 203–47.

Porraz, G., Parkington, J.E., Rigaud, J.-P., Miller, C.E., Poggenpoel, C., Tribolo, C., Archer, W., Cartwright, C.R., Charrié-Duhaut, A., Dayet, L., Igreja, M., Mercier, N., Schmidt, P., Verna, C. & Texier, P.J. 2013. The MSA sequence of Diepkloof and the history of southern African Late Pleistocene populations. *Journal of Archaeological Science* **40** (9): 3542–52.

Porraz, G., Schmid, V.C., Miller, C.E., Tribolo, C., Cartwright, C.R., Charrié-Duhaut, A., Igreja, M., Mentzer, S., Mercier, N., Schmidt, P., Conard, N.J., Texier, P.-J. & Parkington J.E.2016. Update on the 2011 excavation at Elands Bay Cave (South Africa) and the Verlorenvlei Stone Age. *Southern African Humanities* **29**: 33–68.

Robey, T. 1984. *Burrows and bedding: site taphonomy and spatial archaeology at Tortoise Cave*. MA thesis, University of Cape Town.

Sampson, C.G. 1974. *The Stone Age archaeology of southern Africa*. New York: Academic Press.

Schmidt, P. & Mackay, A. 2016. Why was silcrete heat-treated in the Middle Stone Age? An early transformative technology in the context of raw material use at Mertenhof Rock Shelter, South Africa. *Plos One* **11** (2): e0149243.

Sealy, J., Pfeiffer, S., Yates, R., Willmore, K., Manhire, A., Maggs, T. & Lanham, J. 2000. Hunter-Gatherer child burials from the Pakhuis Mountains, Western Cape: growth, diet and burial practices in the late Holocene. *South African Archaeological Bulletin* **55**: 32–43.

Sealy, J. & Van der Merwe, N.J. 1986. Isotope assessment and the seasonal mobility hypothesis in the southwestern Cape of South Africa. *Current Anthropology* **27** (2): 135–50.

Sealy, J. & Van der Merwe, N.J. 1992. On 'Approaches to dietary reconstruction in the Western Cape: Are you what you have eaten?' A reply to Parkington. *Journal of Archaeological Science* **19** (4): 459–66.

Stanford, J.D., Rohling, E.J., Hunter, S.E., Roberts, A.P., Rasmussen, S.O., Bard, E., McManus, J. & Fairbanks, R.G. 2006. Timing of meltwater pulse 1a and climate responses to meltwater injections. *Paleoceanography* **21** (4): PA4103.

Stewart, B.A. 2008. *Refitting repasts: a spatial exploration of food processing, sharing and disposal at the Dunefied Midden Campsite, South Africa*. PhD thesis: University of Oxford.

Tribolo, C., Mercier, N., Douville, E., Joron, J.L., Reyss, J.L., Rufer, D., Cantin, N., Lefrais, Y., Miller, C.E., Porraz, G., Parkington, J.E., Rigaud, J.-P. & Texier, P.-J. 2013. OSL and TL dating of the Middle Stone Age sequence at Diepkloof Rock Shelter (South Africa): a clarification. *Journal of Archaeological Science* **40** (9): 3401–11.

Valsecchi, V., Chase, B.M., Slingsby, J.A., Carr, A.S., Quick, L.J., Meadows, M.E., Cheddadi, R. & Reimer, P.J. 2013. A high resolution 15,600-year pollen and microcharcoal record from the Cederberg Mountains, South Africa. *Palaeogeography, Palaeoclimatology, Palaeoecology* **387**: 6–16.

Volman, T. P. 1981. *The Middle Stone Age in the southern Cape*. PhD thesis, University of Chicago.

Will, M., Mackay, A. & Phillips, N. 2015. Implications of Nubian-like core reduction systems in southern Africa for the identification of early modern human dispersals. *Plos One* 10 (6): e0131824.

Wurz, S. 2013. Technological Trends in the Middle Stone Age of South Africa between MIS 7 and MIS 3. *Current Anthropology* **54** (S8): S305–19.

Southern African Humanities **29**: 17–32 December 2016 KwaZulu-Natal Museum

Elands Bay Cave: keeping an eye on the past

John Parkington
Department of Archaeology, University of Cape Town, Rondebosch, 7700 South Africa;
John.Parkington@uct.ac.za

ABSTRACT

Elands Bay Cave has been episodically occupied for many tens of thousands of years, but apparently always in fairly brief visits. It therefore contains an intermittent but sequentially organized record of environmental and behavioural events over a time period of perhaps 150 000 years. Here I look at the later Holocene record and assess what it reveals about marine food exploitation by hunter gatherers and later pastoralist groups. Because we have similar records from several other small caves, rock shelters and open sites around the Verloren Vlei and the associated shoreline, we can recognise periods of common use and disuse and understand the intermittent and changing use of the local shoreline resources over the past 5000 years.

KEY WORDS: Elands Bay Cave, Holocene, episodicity, shellfish gathering, strandloping.

THE VIEW FROM THE CAVE

Elands Bay Cave (EBC, Fig. 1) offers a permanently anchored location from which to view a changing landscape, generating a record in some sense, of what people did at this place when they were there. If space is defined by geographic co-ordinates, it becomes place when it is given meaning by people by living in it; the place is a synthesis of decisions and behaviours deemed appropriate for a particular location on the social and resource landscape. EBC has been such a place intermittently for over 100 000 or more years. I have chosen here to regard the cave as an eye on the past, seeing what it can see, recording what happens and open to interpretation by archaeologists. Like eyes, caves can blink and sleep: like eyes, caves can only see what is in front of them.

Our excavations at EBC in the 1970s were fairly extensive (Fig. 2) and resulted in the removal of some 100 m^3 of deposit, almost all screened through 12 mm and 3 mm mesh sieves. Occasionally the contents of sieved or unsieved samples were retained for more detailed analyses. A conventional metre square grid was used and features, but not all individual artefacts, were mapped *in situ*. The result is a fairly coarse spatial understanding of the distributions of objects that rarely penetrates a one-metre square provenience. This does, however, contribute usefully, sometimes quite significantly, to our understanding of the record.

Our decisions about stratigraphic distinctions were informed largely by macro-patterning in the shellfish, bedding, ash, fine-grain and roof-fall composition of the sediments excavated. Analytical units were kept at the minimal scale, with labelled layers, however similar, never amalgamated but kept separate, no doubt leading to some duplication of depositional envelopes (Fig. 3). We aimed for a fine-grained analysis of changes in artefactual and foodwaste content. These units, some 350 in all, provide a stratigraphic framework for understanding the temporal patterning of behaviours. I refer to each individual depositional event as a package and to the sets of near-contemporary packages as pulses of occupation: the chronology of these is of great interest in the understanding of local settlement history. A set of 35 radiocarbon dates (Fig. 4),

ISSN 2305-2791 (online); 1681-5564 (print)

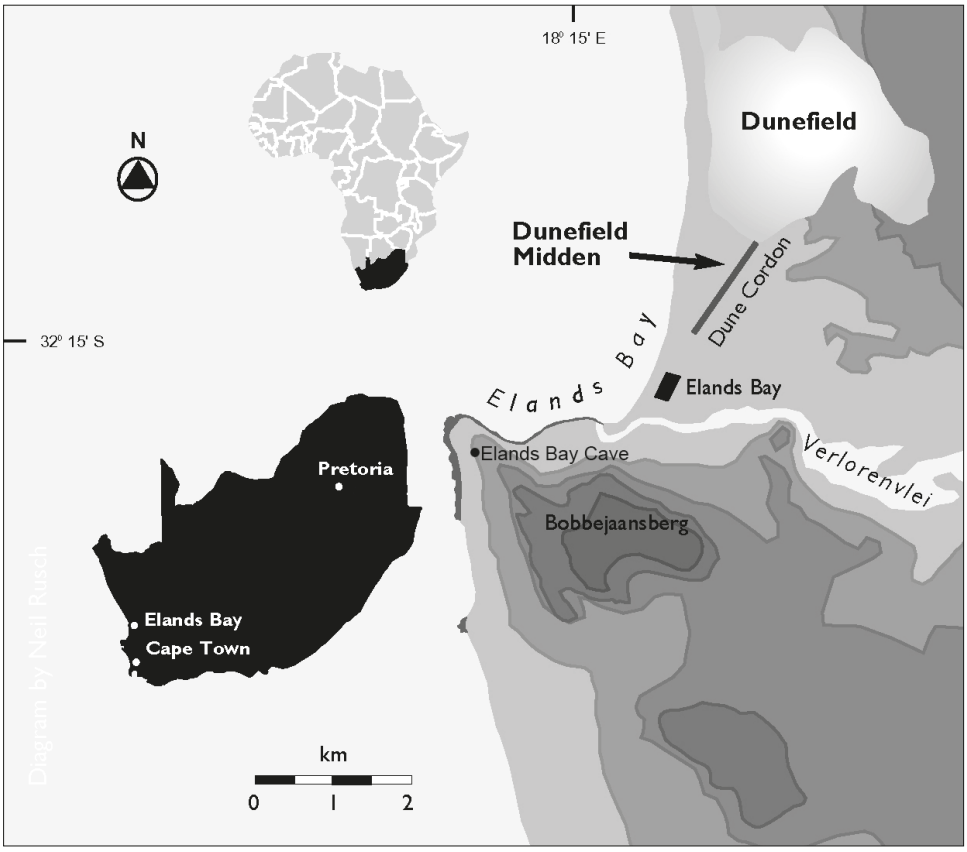

Fig. 1. The location of Elands Bay Cave.

extending beyond the effective discriminatory range of this method, calibrates the temporal order and allows us to think in terms of continuities and discontinuities. The time and space opportunity provided by grid and matrix are the platform for narratives of Holocene and Pleistocene behaviours. Here only the Holocene is of interest.

SEDIMENTS, DATES AND CAVE USE

Perhaps the most elementary pattern to emerge from this spatial and chronological framework is the episodicity of cave use. Because our excavations are so spatially extensive across the cave floor, we can confidently recognize periods of cave use and disuse. Interestingly, periods of avoidance are never marked by the accumulation of sterile sediment, simply by the close stratigraphic juxtaposition of quite distinct radiocarbon dates. This is a widespread pattern in southern African Stone Age sites, in fact, suggesting that most cave deposition is substantially anthropogenic. The most prominent exceptions are the southern Cape sites of Die Kelders, Blombos and Klasies River Main site, where during late Pleistocene lowered sea level, extensive sand deposits, blown off the exposed sandy coastal shelf, accumulated in these receptacles, generating deep sterile stratigraphic units.

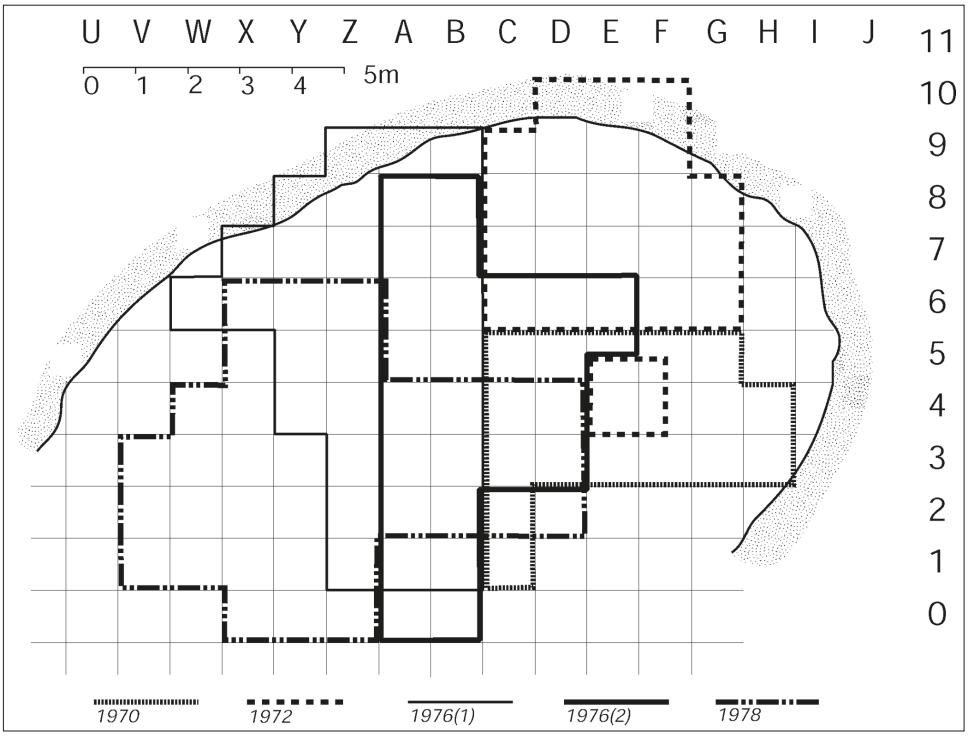

Fig. 2. The extent of excavation at Elands Bay Cave in the archaeological seasons between 1970 and 1978.

At EBC, several periods of relative, but not complete, abandonment are documented, notably those between about 7800 and 4300 years ago and between 3100 and 1800 years ago. I return to these episodes later when I discuss behavioural strategies. 'Abandonment' or 'avoidance', however, are relative terms as it is likely, but hard to demonstrate with the lack of precision of radiocarbon dating, that all time periods when the cave was in use are represented by sets of very brief occupations separated by time intervals varying between months and decades. The mean volume removed in the stratigraphic units of Figure 3 is far less than one cubic metre, suggesting that the visits responsible for these minimal depositional events were extremely brief. Usages are likely to have measured days or weeks, absences years, centuries or millennia. Effectively, Elands Bay Cave has been vacant for the vast majority of its 40 000 year-and-more occupation history, an eye more closed than open.

What is of local and regional interest, of course, is the question of shared episodicity. Here (partly shown in Fig. 5) I illustrate the shared patterns of cave, rock shelter and open site use among sites around the mouth of the Verlorenvlei, predominantly in the second half of the Holocene. Quite obviously, the more prominent absences are duplicated from site to site, with pronounced agreement between sites on the paucity of occupations across excavations at both open and rock shelter sites. As others have recently confirmed (Jerardino et al. 2014), the earlier and longer hiatus between about 7500 and 4500 years ago probably reflects drier, warmer conditions of the early mid-

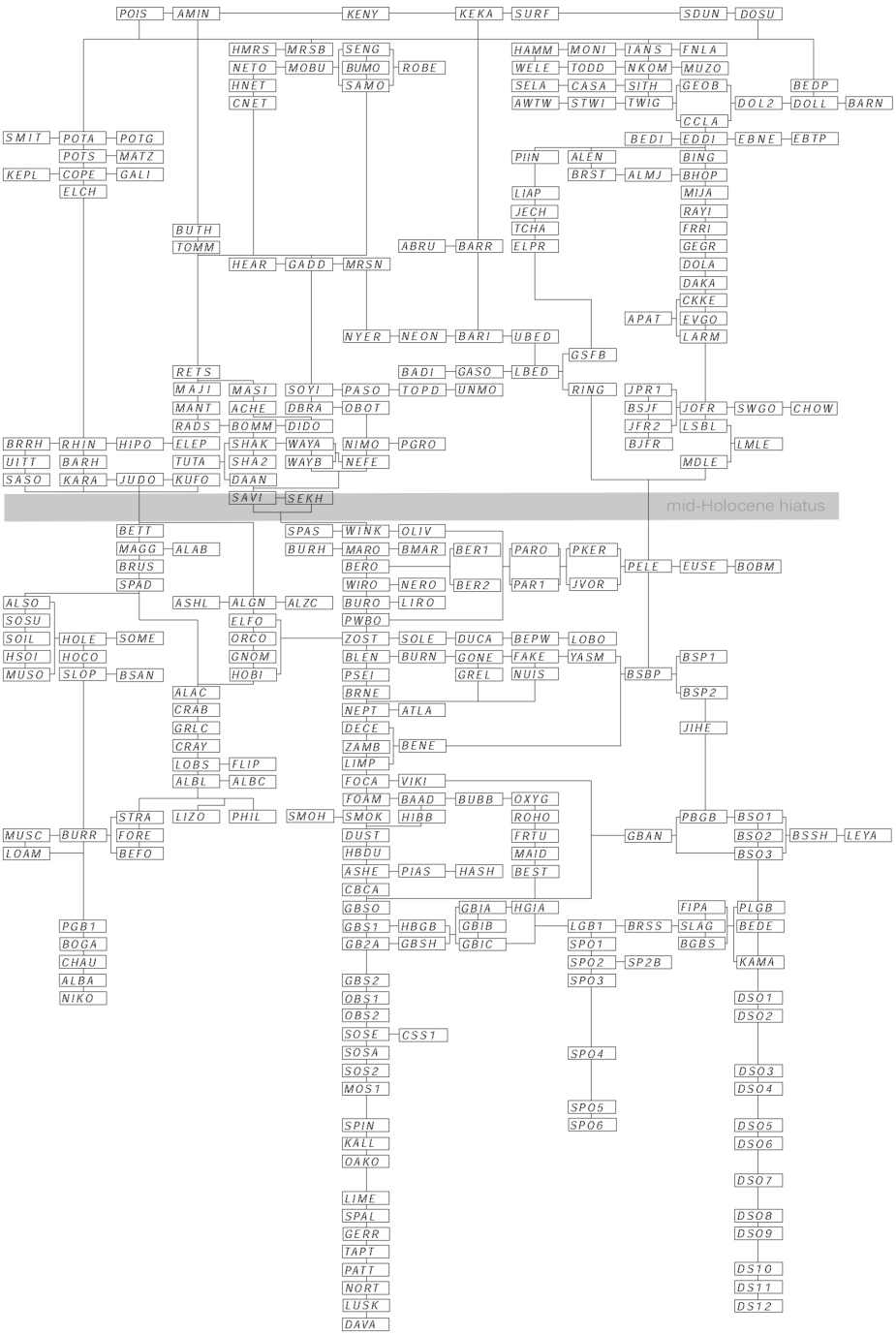

Fig. 3. A stratigraphic matrix showing the relationships between excavated depositional units or envelopes, which we refer to as packages. More than 340 individual packages were removed and materials and artefacts are counted and recorded by package.

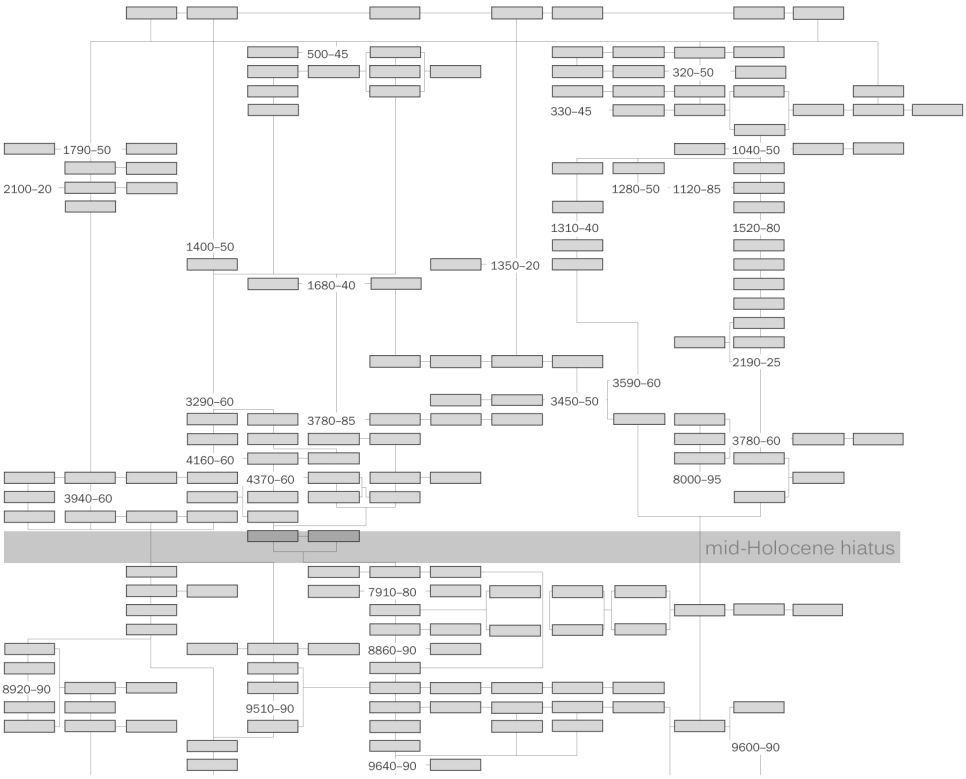

Fig. 4. Radiocarbon dates (uncalibrated) mapped onto the stratigraphic matrix. The link between envelope and age can be gauged by comparison of Figures 3 and 4.

Holocene. It is now well documented over some tens of kilometres of the Cape west coast, although, of course, it does not imply total abandonment of the shore and its resources. Rather, it is a period of reduced use-frequency, possibly also reduced duration of visits. Certainly, radiocarbon dates showing that some sites have only been occupied after this period marks a distinct shift in site preference from about the middle of the fifth millennium before the present. The fact that most of these occupational resumptions are in caves surely rules out the possibility that the pattern is simply the result of dune sand movements and site burial along the shore.

The later of the two hiatuses reflected at EBC is also widespread along this part of the coast, though we doubt it has anything primarily to do with climate change. In this case absences at the cave sites are compensated by very substantial presences at specific open locations. The very clear sandwiching of open 'megamidden' dates between clear periods of rock shelter use means this is a distinct preference shift (and back) by hunter gatherer groups. Visits to the local coastline between about 3100 and 1800 years ago were primarily scheduled next to highly productive mussel colonies that were exploited from adjacent sandy dune camps (Parkington 2012; Parkington et al. 2013; Parkington et al. 2015). We have argued that these can be seen as logistical visits from which large collections of dried mussel meat were gathered for

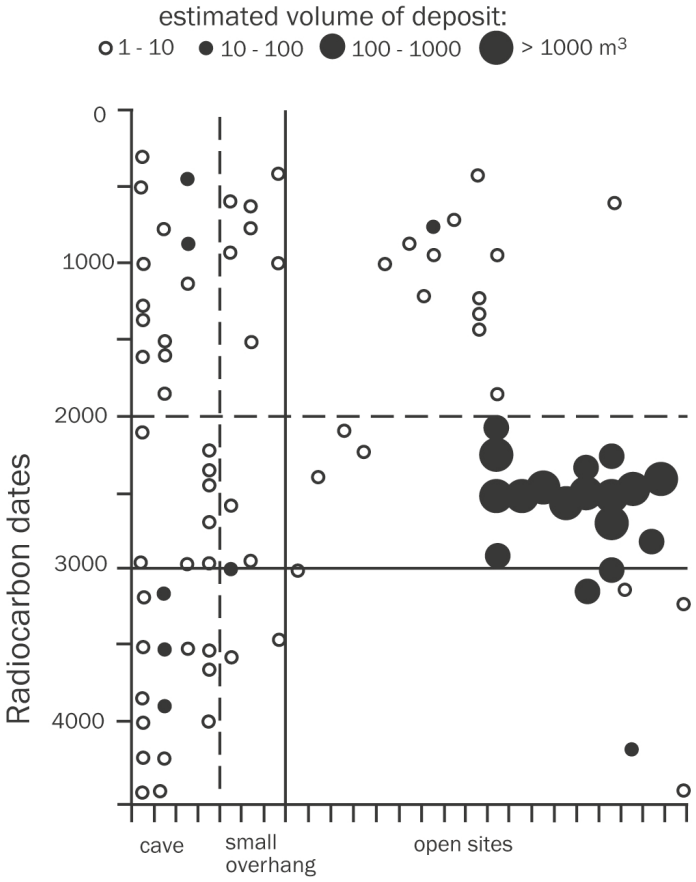

Fig. 5. Site choices over the last 4500 years around the mouth and lower reaches of the Verloren vlei, and the associated shoreline. Note that the diameters of the circles are not to scale, otherwise the sizes of 'megamidden' would overwhelm the diagram. The differences in location, size and frequency reflect major changes in settlement patterns before, during and after the 'megamidden' period.

transport inland. It is possible, however, that the choice of this strategy was ultimately influenced by shifting resource factors.

HOLOCENE BEHAVIOURAL CHANGES

I am interested in the extent to which changes are manifest within as well as between pulses and in the extent to which changes in particular manifestations may or may not coincide temporally. I begin from the perspective of the changes in the dominant depositional element in Holocene sedimentation, shell, and then look to see what other changes are associated.

Clearly the pre-megamidden (4500–3100) pulse at EBC is a period of stability in which little change is reflected until occupation is fairly abruptly replaced by abandonment, perhaps just before 3000 years ago. All excavated packages are characterized by high

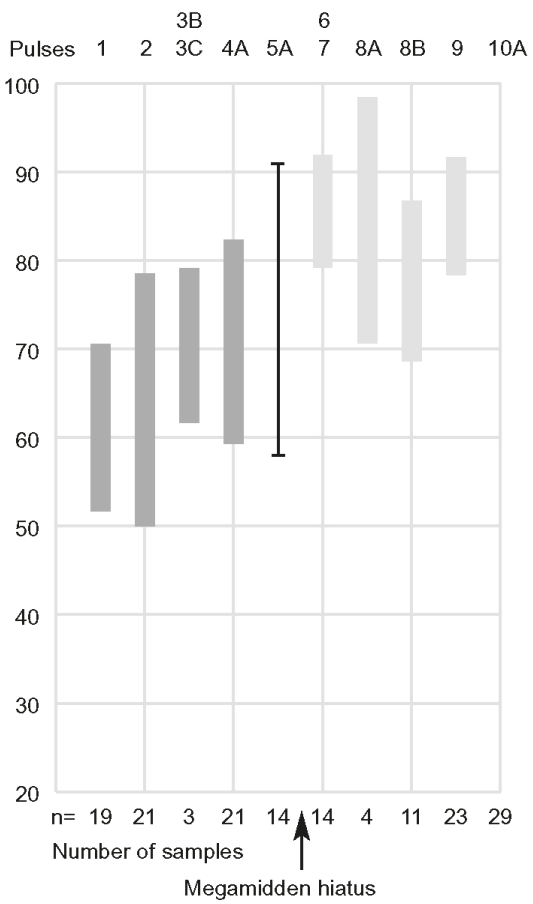

Fig. 6. Mussel (*Choromytilus meridionalis*) frequencies in packages through the Elands Bay depositional sequence. Each bar reflects several observations. The contrast between the frequencies before and after the 'megamidden' period is quite revealing.

mussel and low limpet frequencies (Fig. 6), large, but not exceptionally large, mussel mean sizes (Fig. 7), lots of tiny water-worn shell and pebble (Fig. 8), and very low frequencies of barnacles (Fig. 9). The densities of seal and sea bird bones are very low but fish bone, relative to later packages, is fairly common. The list of fish species represented is as long as anywhere else in the EBC sequence (Poggenpoel 1996: 44). There are, of course, no potsherds at this time. Before interpreting this pattern, it is as well to list the contrasting characteristics of the post-megamidden pulse.

When regular occupation at EBC resumes about 1800 years ago, we can presume from dated assemblages elsewhere in the region that ceramic-using pastoralists (or hunters with sheep) were a feature of the local social landscape (Orton et al. 2013), although perhaps not yet a dominant one. Because of this development and its sequential consequences, this pulse exhibits directional change, despite an overall contrast with the earlier pulse. Mussels, for example, dominate the earliest packages of the pulse but limpets become far more common after about 1500 years ago (Fig. 6). Markedly after

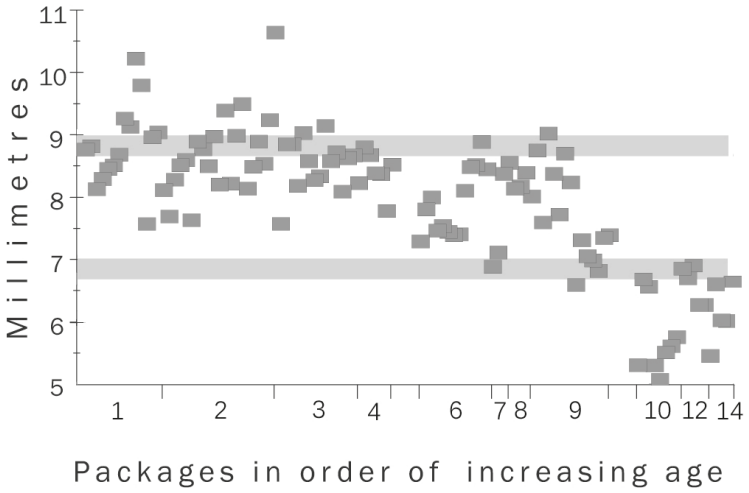

Fig. 7. The mean sizes of mussels (*Choromytilus meridionalis*) from packages through the Elands Bay Cave sequence. Only after 1500 years ago do means exceed 9.0 mm. The measurements are of the prismatic band that is proportional to the length of the shell and is far more frequently preserved than whole valves.

this latter point in time, mussel sizes are often very large (Fig. 7), water-worn shell and pebble much less common (Fig. 8) and barnacles (*Austromegabalanus cylindricus*, a subtidal species) more common (Fig. 9). Along with this, the density of seal bone is much higher, seabird bone likely higher too, and fish bone much less common. Only three species of fish are found after 1500 years ago (Poggenpoel 1996: 44).

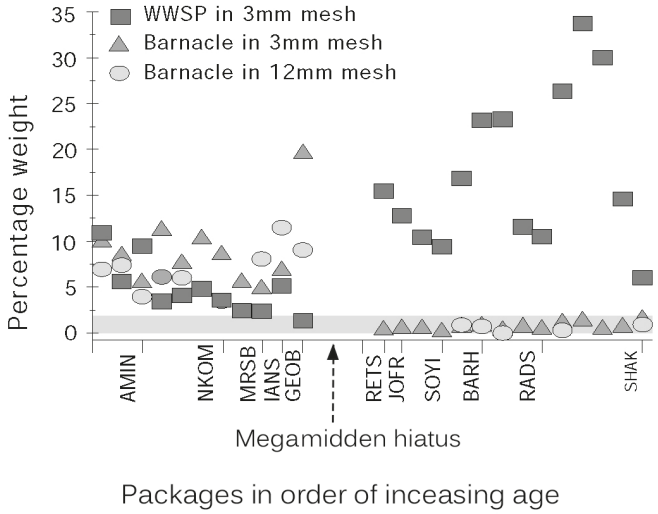

Fig. 8. Weights of water worn shell and pebble (WWSP) as a percentage of the total weight of shell in unsieved samples of packages from the Elands Bay Cave sequence. WWSP is defined and explained by Jerardino (1995).

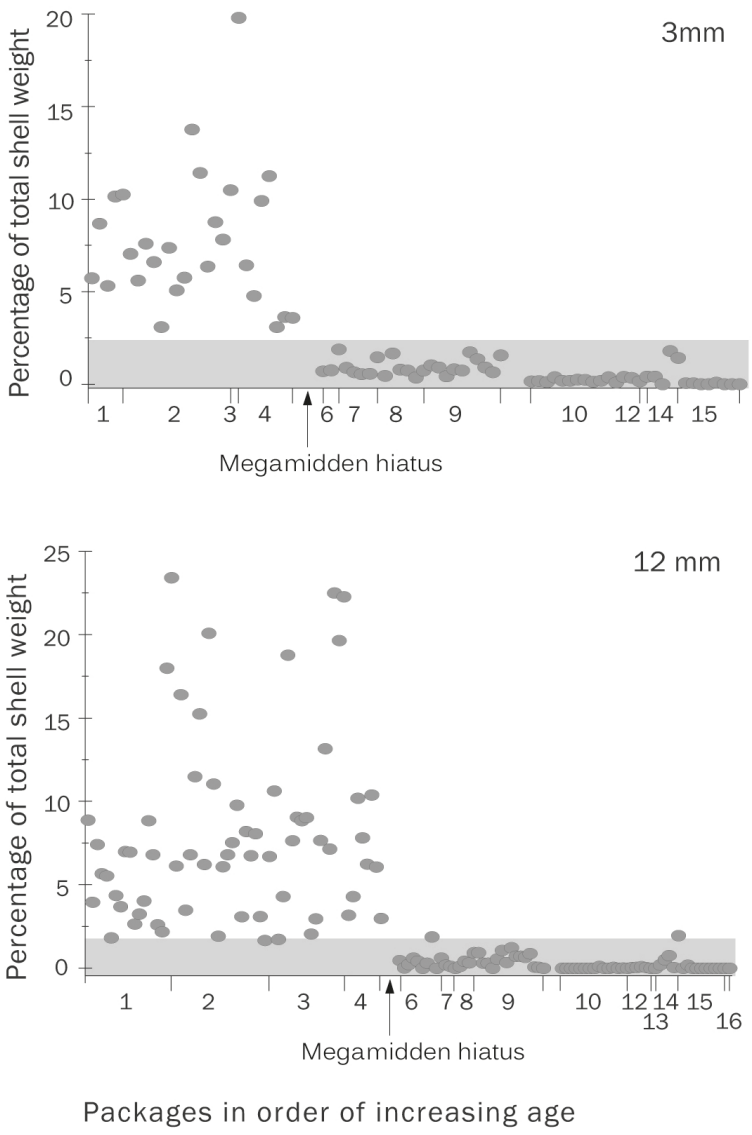

Fig. 9. The weight of barnacle (*Austromegabalanus cylindricus*) fragments as a percentage of the total weight of shell from sediments through the Elands Bay Cave sequence. Samples were sieved through 3 mm and 12 mm sieve meshes. Note that the contrasting pattern of values from before and after the 'megamidden' hiatus at Elands Bay Cave is dramatic.

Some of these details are likely to reflect changes in the lower reaches of the Verlorenvlei, a system that has clearly been massively affected by the sea level changes experienced since the terminal Pleistocene. Prior to 11 000 years ago, before shellfish were being routinely brought back to EBC, the proto-Verlorenvlei passed north of the rocky point where the cave is located, across a narrow rocky plain into a lowered sea level. As sea level rose rapidly through the Pleistocene-Holocene boundary, the

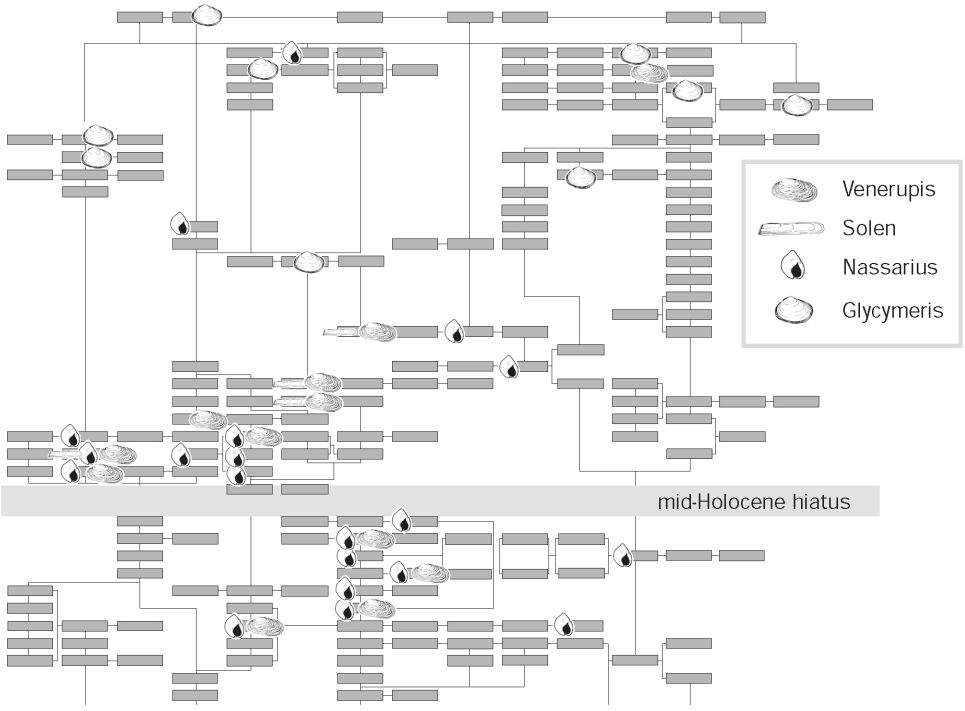

Fig. 10. The distribution of selected molluscs, ones not thought to be part of the human diet, considered by Jerardino (1995) as 'incidentals', mapped onto the stratigraphic matrix. The distribution of *Nassarius kraussiana* appears to reflect the open conditions of the Verlorenvlei in the mid-Holocene. This species is very much less common after about 1400 years ago. These observations derive *post hoc* from shells sampled from the sieves during sieving and sorting of shelly matrices.

coastline approached, the mouth of the river flooded back and became lagoonal, subsequently retreated until the lower reaches were estuarine and finally became the coastal lake it currently is (Grindley & Grindley 1987). The most persuasive evidence for these changes comes from molluscs and plant remains (Figs 10 & 11) plotted onto the stratigraphic matrix. In the pre-megamidden pulse the regular occurrence of eel grass (*Zostera capensis*), the tick shell (*Nassarius kraussianus*), the razor shell (*Solen capensis*) and the corrugated clam (*Venerupis corrugata*) imply that the Verlorenvlei mouth was open to the sea, as does the relatively high variety of fish species that include species that today require lagoonal or estuarine conditions (Poggenpoel 1996: 44). None of these fish species are found after 1500 years ago, when only those that can survive in a vlei with only intermittent access to the sea, are found. The EBC pattern is strongly supported by parallel observations from Tortoise Cave (Jerardino 1995), a vlei bank rather than coastal site.

Other changes, however, undoubtedly reflect shifts in the nature of the occupations before and after the megamidden phase, including changing coastal resource exploitation strategies. Perhaps a point of some significance is that the EBC packages that most closely resemble the megamidden signature are those immediately

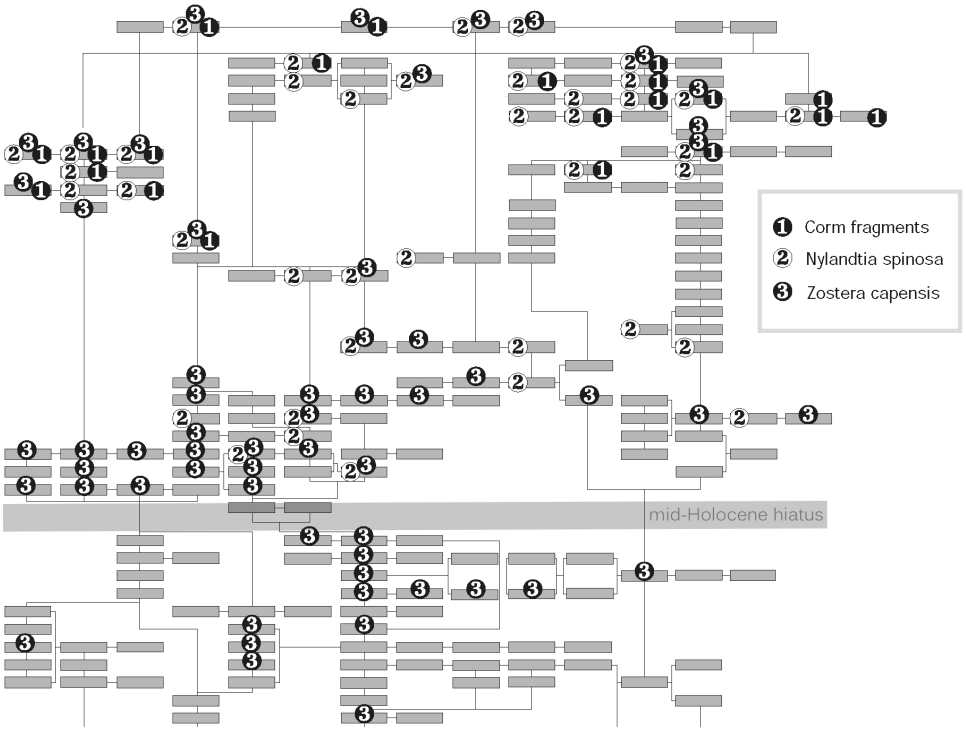

Fig. 11. The distribution of selected plant remains mapped onto the stratigraphic matrix. The strong presence of *Zostera capensis* from the mid-Holocene appears to reflect the open conditions of the Verlorenvlei at this time. Terrestrial grasses and corm parts appear only after 1400 years ago.

preceding and following that phase. Almost all of the 4300–3100 year old packages from EBC are mussel dominated, have very low artifact and animal bone densities and clearly reflect a food base dependant on the intertidal exploitation of mussel colonies. This is what megamiddens reflect too, except on a massive and exaggerated scale. Interestingly, the early post-megamidden (between about 1800 and 1500 years ago) deposits at EBC are also like this (Fig. 6). The situation only changes, quite dramatically, after about 1500 years ago, as described above.

What gives added significance to these observations is the repeated occurrence of them at other nearby sites, notably at Tortoise Cave, Spring Cave, Elands Bay Open and Pancho's Kitchen Midden. Sites with dated single occupations such as Dunefield Midden, Borrow Pit Midden, Connie's Limpet Bar and Hailstorm Midden, also conform to this pattern (Fig. 5, see also Parkington 2012: table 1, 1523–4).

What I have described is a multi-site pattern that involves not only co-occurrences of depositional pulsing, but also similarities of pulse contents. Using the vantage point of an extensively excavated space at Dunefield Midden (DFM) as a guide (Parkington et al. 2013; Parkington et al. 2014), we have argued that the complementary inverse patterning in frequencies of barnacles and water worn shell and pebble reflect a significant shift, although not a complete replacement, in the methods of exploitation of mussels. Prior to the mega-midden phase, collectors targeted the lower intertidal

where their gathered mussels included large quantities of tiny fragments of shell and pebble caught up in the byssus mat (Jerardino 1993: 483). After the mega-midden phase, whilst this practice continued, collectors paid more attention to, or were faced with increased opportunities from, the swathes of mussels wrenched from their sub-tidal holdfasts and thrown up onto the beaches. Note that this suggestion results not from the perceived optimal returns from washed up mussels (contra Jerardino 2014), but from the fact that the large barnacles, *Austromegabalanus cylindricus*, are otherwise unobtainable in the intertidal and have to have come from subtidal zones. Larger mussels are also more prevalent sub-tidally. The patterning in mussel size, water-worn shell and pebble frequency and barnacle numbers seems to make this interpretation the most plausible.

We have referred to the collection of beached mussels as an increase in 'strandloping', the systematic monitoring and exploitation of washed up marine foods along the shoreline. The fact that other likely stranded marine food sources such as birds and seals co-vary with the metrical and stratigraphic observations listed above (higher after the megamiddens than before), is further demonstration of a strategic shift in resource gathering along this part of the shore. It is not impossible that this shift was brought on by a recognition that the fishing opportunities in the lower Verlorenvlei were less attractive as sea level approached today's height after 1500 years ago (Parkington et al. 2014).

PATTERNS OF ARTEFACTUAL DISTRIBUTIONS IN REGIONAL CONTEXT

It is obviously important to tie the Elands Bay Cave occupation pulses into a larger landscape framework. The artefactual record at EBC, associated with some depositional shifts in content and location, for example, points to the period after 1400 years ago as registering a rather different exploitation system compared to the early post-megamidden occupations at the cave. Radiocarbon dates do not offer precision in these matters, but the critical centuries are those between 2100 and 1500 or 1400 years ago. These changes reflect an early phase of pastoralist impact, followed by a residual hunter gatherer phase that is likely the 'Soaqua' signature recognizable from the times of early colonial penetration (Parkington 1977, 1984). I suggest here that both environmental change, impacting resource availabilities, as well as social change, restricting settlement options, are involved. This latter begins with pastoralist intrusion and ends in the colonial devastation.

The relevant observations are as follows. Glass beads and metal objects have been found only in the uppermost packages, persuasively reflecting the overlap between terminal hunter-gatherer occupation and the penetration of colonial groups away from the Cape (Fig. 12). The small sample of seed beads also comes from these packages. Ceramics are documented at EBC frequently after 1400 years ago, somewhat less so back to 2100 years ago but very infrequently before that. The records at 2100 could be credible given the examples elsewhere back to 2050 years ago (Sealy & Yates 1994, 1996), but otherwise the small numbers below this reflect percolation by gravity. Sheep bones are mostly found after 1600 years ago at Elands Bay Cave and then in very small numbers, although they appear earlier at other regional sites such as Spoegrivier Cave (Webley 1992; Orton et al. 2013) and Blombos (Sealy & Yates 1994, 1996; Henshilwood 1996).

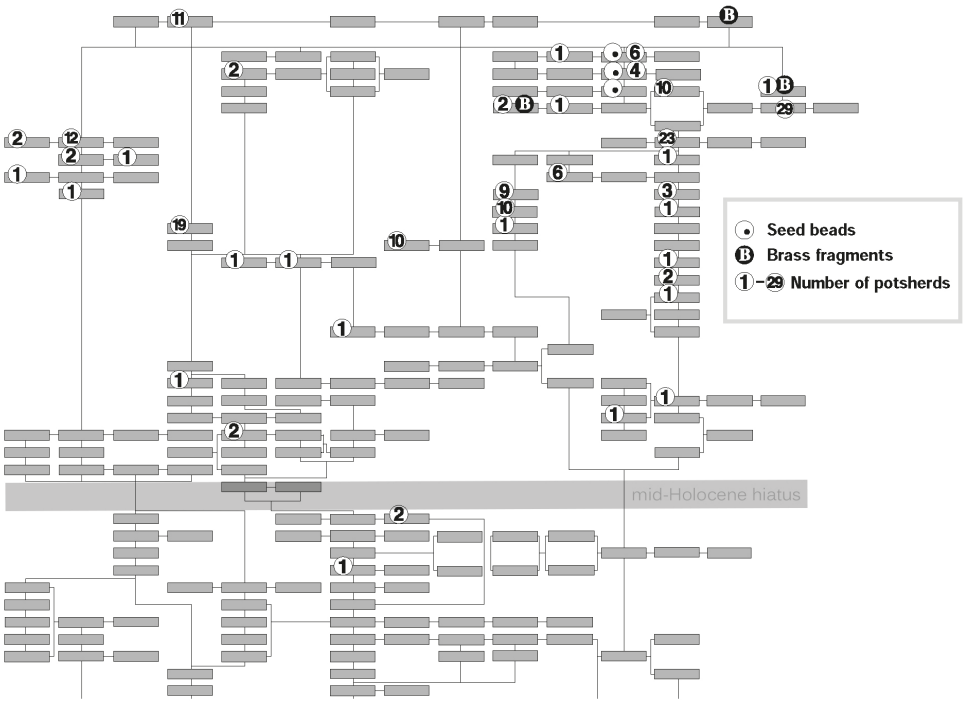

Fig. 12. The distribution of some artefactual remains mapped onto the Elands Bay Cave stratigraphic matrix.

What adds meaning to these stratigraphic distributions are the associated depositional envelopes in which they are found. Quite clearly the eelgrass *Zostera capensis*, collected from the lower reaches of the Verlorenvlei, is the bedding of choice from prior to the mid-Holocene hiatus until after the mega-midden interval, continuing into the period from 2100 to 1400 years ago (Fig. 11). Grass bedding, despite the material preservation of organic remains throughout the Holocene, is completely absent until after 1400 years ago at Elands Bay Cave. Perhaps not coincidentally, the seed beads, fragments of grass string and the inedible corm casings peeled off edible corms and discarded, are also restricted to packages with terrestrial grass wads. A similar and arguably contemporary shift is documented at Tortoise Cave, some 4 km up the Verlorenvlei from its mouth (Robey 1984, 1987; Jerardino 1995) and likely at other nearby sites.

This shift from estuarine to terrestrial grasses as bedding is given additional significance because the latter is the material of choice throughout the coastal plains and associated mountain chains to the east, from at least as early as 1700 years ago. We have coined the term bedding-and-ash sites for these rock shelter localities that include De Hangen (Parkington & Poggenpoel 1971), Diepkloof (Parkington & Poggenpoel 1987), Andriesgrond (Anderson 1991), Renbaan (Kaplan 1987), Klipfonteinrand 2 (Nackerdien 1989) and others (Liengme 1987). It may also be relevant that the bedding-and-ash deposits at all of these sites observe a strict spatial arrangement of bedding around the walls of caves or rock shelters and ashy deposits toward the

centre of them, however large or small (Liengme 1987). This is more or less the case at EBC, where terrestrial bedding hugs the rear wall.

Artefacts of stone and ostrich eggshell add to the feeling that although pastoralism is detectable at 2100 years ago, its final accommodation comes a few hundred years later. Royden Yates' measurements of ostrich eggshell beads throughout the Holocene Western Cape (Smith et al. 1991) have shown that mean sizes are an interesting reflection of, almost a metaphor for, the disruption of pastoralism. As others have also argued (Jacobson 1987), pre-pastoralist bead diameters are small, around 4 mm to 4.5 mm, whereas when pastoralism is detectable through sheep bones or ceramics, they rise quickly to mean sizes of 6 mm or 7 mm. Not only that, but bead mean sizes change first in areas where pastoralists dominate early, such as the nutritionally attractive coastal plains in the Western Cape, only later in mountainous areas where hunters could survive longer. When occupation of EBC resumes in earnest after 1800 years ago, bead sizes are unchanged since the mid-Holocene, only after 1400 years ago do they increase, never after that to diminish.

This complex of bone, stone, spatial and depositional patterning serves to link the final thousand years of the EBC record, from about 1400 to about 300 years ago, more intimately to the interior record captured by other eyes on the landscape than in earlier times. It also corresponds to the most terrestrial of isotope dietary signals in the region from throughout the Holocene (Parkington 2012). The only local Verlorenvlei individual from the last 1000 years reflects a strong terrestrial protein consumption (Parkington 2012). Put another way, skeletons reflecting more than 50 % intake of terrestrial (as opposed to marine) protein are six times as common after 1500 years ago as they are between 3000 and 1500 years ago. (This, it must be admitted, derives from a sample of coastally buried individuals from along the whole west coast not only that part near Elands Bay).

The number of small-volume archaeological, single phase occupations is by far larger in the years between 1400 and 300 years ago than in any previous comparable time periods (Parkington 2012). These sites are, in addition, far more variable in location than at any earlier time (Fig. 5). Strandloping, in the sense defined earlier, is more strongly recorded in the depositional record then than at any earlier period (Parkington et al. 2014). Similarities between the assemblages and depositional arrangements at inland and coastal locations are stronger then than previously. Strandloping, it seems, is associated with a stronger terrestrial protein intake, greater residential mobility, the ability to make use of smaller residential spaces and a more visible artefactual response to the presence of pastoralists on the landscape.

I suggest that after an introductory few centuries of modest pastoralist impact between about 1800, or perhaps a little earlier, and 1400 years ago, an agreed or at least tolerated arrangement of pastoralist and hunter-gatherer co-usage of the Western Cape space, still visible to, but not well understood by, colonial settlers, was established. From the features listed above, we might characterize this settlement pattern as residual, implying impoverished, restricted, diminished. I suggest it may reflect decreased overall numbers, smaller group sizes and a more cautious choice of site. This enters the written record as a 'soaqua' presence (Parkington 1984), but may also incorporate the rather poorly understood 'huriqua' identity.

CONCLUSION

The Elands Bay Cave 'eye' has recorded a variety of images, some of them reflections of environmental change, others the responses of the hunters, gatherers, fishers and herders who lived there. It has 'seen' some things that other local eyes have also seen, and other things that more distant 'eyes' could not. As a relatively deep stack of sediment with good preservation of organic materials, it stands as a reference framework for the evaluation of ideas and the construction of regional narratives about changing settlement. In order to progress, we need to document many more local stratigraphies and pursue these strands of connectivity, both between landscape locations and between material aspects of the recorded past.

REFERENCES

Anderson, G. 1991. Andriesgrond revisited: material culture, ideologies and social change. BA Hons dissertation, University of Cape Town.

Cowling, R.M., Cartwright C., Parkington, J.E. & Allsopp, J.C. 2001. Fossil wood assemblages from Elands Bay Cave, South Africa: implications for Late Quaternary vegetation and climates in the winter-rainfall fynbos biome. *Journal of Biogeography* **26** (2): 367–78.

Grindley, J.R. & Grindley, S.A. 1987. The ecology and biological history of Verlorenvlei. In: J.E. Parkington & M. Hall, eds, *Papers in the prehistory of the Western Cape, South Africa*. Oxford: B.A.R., pp 97–119.

Henshilwood, C. 1996. A revised chronology for pastoralism in southernmost Africa: new evidence of sheep at ca. 2000 bp from Blombos Cave, South Africa. *Antiquity* **70**: 945–9.

Jacobson, L. 1987. The size variability of ostrich eggshell beads from central Namibia and its relevance as a stylistic and temporal marker. *South African Archaeological Bulletin* **42**: 55–8.

Jerardino, A. 1993. Mid to Late Holocene sea level fluctuations: the archaeological evidence at Tortoise Cave, south Western Cape, South Africa. *South African Journal of Science* **89**: 481–8.

Jerardino, A. 1995. The problem with density values in archaeological analysis: a case study from Tortoise Cave, Western Cape, South Africa. *South African Archaeological Bulletin* **50**: 21–7.

Jerardino, A. 2014. Stranded rocky shore mussels and their possible procurement during prehistory on the West Coast of South Africa. *Journal of Archaeological Science* **49**: 536–45.

Jerardino, A., Wiltshire, N., Webley, L., Tusenius, M., Halkett, D., Hoffman, M.T. & Maggs, T. 2014. Site distribution and chronology at Soutpansklipheuwel, a rocky outcrop on the West Coast of South Africa. *The Journal of Island and Coastal Archaeology* **9** (1): 88–110.

Kaplan, J. 1987. Settlement and subsistence at Renbaan Cave. In: J.E. Parkington & M. Hall, eds, *Papers in the prehistory of the Western Cape, South Africa*. Oxford: B.A.R., pp 350–76.

Klein, R.G. & Cruz-Uribe, K. 1987. Large mammal and tortoise bones from Elands Bay cave and nearby sites, Western Cape Province, South Africa. In: J.E. Parkington & M. Hall, eds, *Papers in the prehistory of the Western Cape, South Africa*. Oxford: B.A.R., pp 132–63.

Liengme, C. 1987. Botanical remains from archaeological sites in the Western Cape. In: J.E. Parkington & M. Hall, eds, *Papers in the Prehistory of the Western Cape, South Africa*. Oxford: B.A.R., pp 237–61.

Matthews, T. 1999. Taphonomy and micromammals from Elands Bay Cave. *South African Archaeological Bulletin* **54**: 133–40.

Orton, J. 2006. The Later Stone Age lithic sequence at Elands Bay, Western Cape, South Africa: raw material, artefacts and sporadic change. *Southern African Humanities* **18** (2): 1–28.

Orton, J., Mitchell, P., Klein, R.G., Steele, T. & Horsburgh, K.A. 2013. An early date for cattle from Namaqualand, South Africa: implications for the origins of herding in southern Africa. *Antiquity* **87**: 108–20.

Nackerdien, R. 1989. Klipfonteinrand 2: a sign of the times. BA Hons thesis, University of Cape Town.

Parkington, J.E. 1977. Soaqua: hunter-fisher-gatherers of the Olifants River, Western Cape. *South African Archaeological Bulletin* **32**: 150–7.

Parkington, J.E. 1984. Soaqua and Bushman: hunters and robbers. In: C. Schrire, ed., *Past and present in hunter gatherer studies*. Orlando: Academic Press, pp 151–74.

Parkington, J.E. 2012. Mussels and mongongo nuts: logistical visits to the Cape west coast, South Africa. *Journal of Archaeological Science* **39**: 1521–30.

Parkington, J.E., Fisher Jr, J.W. & Kyriacou, K. 2013. Limpet gathering strategies in the Later Stone Age along the Cape west coast, South Africa. *Journal of Island and Coastal Archaeology* **8** (1): 91–107.

Parkington, J.E., Fisher Jr, J.W., Poggenpoel, C.A. & Kyriacou, K. 2014. Strandloping as a resource-gathering strategy in the Cape, South African Holocene Later Stone Age: the Verloren Vlei record. *Journal of Island and Coastal Archaeology* **9** (2): 219–37.

Parkington, J.E., & Poggenpoel, C.A. 1971. Excavations at De Hangen, 1968. *South African Archaeological Bulletin* **26**: 3–36.

Parkington, J.E. & Poggenpoel, C.A. 1987. Diepkloof Rock Shelter. In: J.E. Parkington & M. Hall, eds, *Papers in the prehistory of the Western Cape, South Africa.* Oxford: B.A.R., pp 269–93.

Poggenpoel, C.A. 1996. *The exploitation of fish during the Holocene in the South-Western Cape, South Africa.* MSc thesis, University of Cape Town.

Robey, T.S. 1984. *Burrows and bedding: site taphonomy and spatial archaeology at Tortoise Cave.* MA thesis, University of Cape Town.

Robey, T.S. 1987. The stratigraphic and cultural sequence at Tortoise Cave, Verlorenvlei. In: J.E. Parkington & M. Hall, eds, *Papers in the prehistory of the Western Cape, South Africa.* Oxford: B.A.R., pp 294–325.

Schweitzer, F.R. 1974 Archaeological evidence for sheep at the Cape. *South African Archaeological Bulletin* **29**: 75–82.

Sealy, J.C. & Yates, R. 1994. The chronology of the introduction of pastoralism to the Cape, South Africa. *Antiquity* **68**: 58–67.

Sealy, J.C. & Yates, R. 1996. Direct radiocarbon dating of early sheep bones: two further results. *South African Archaeological Bulletin* **51**: 109–110.

Smith, A.B., Sadr, K., Gribble, J. & Yates, R. 1991. Excavations in the south-western Cape, South Africa and the archaeological identity of prehistoric hunter-gatherers within the last 2000 years. *South African Archaeological Bulletin* **46**: 71–91.

Webley, L. 1992. Early evidence for sheep from Spoeg River Cave, Namaqualand. *Southern African Field Archaeology* **1**: 3–13.

Southern African Humanities **29**: 33–68 December 2016 KwaZulu-Natal Museum

Update on the 2011 excavation at Elands Bay Cave (South Africa) and the Verlorenvlei Stone Age

[1,2]**Guillaume Porraz**, [3,4]**Viola C. Schmid**, [5]**Christopher E. Miller**, [6]**Chantal Tribolo**, [7]**Caroline C. Cartwright**, [8]**Armelle Charrié-Duhaut**, [9]**Marina Igreja**, [10,11]**Suzan Mentzer**, [6]**Norbert Mercier**, [3]**Patrick Schmidt**, [3]**Nicholas J. Conard**, [12]**Pierre-Jean Texier** and [13]**John E. Parkington**

[1]CNRS, USR 3336, Institut Français d'Afrique du Sud, Johannesburg, South Africa; guillaume.porraz@mae.u-paris10.fr
[2]Evolutionary Studies Institute, University of the Witwatersrand, Johannesburg, South Africa
[3]Department of Early Prehistory and Quaternary Ecology, Eberhard Karls University of Tübingen, Tübingen, Germany; viola.schmid@uni-tuebingen.de
[4]UMR 7041, Equipe AnTET, Université Paris Ouest Nanterre La Défense, Nanterre Cedex, France
[5]Institute for Archaeological Sciences, and Senckenberg Centre for Human Evolution and Paleoenvironment, University of Tübingen, Rümelinstraße 23, 72070, Tübingen, Germany; christopher.miller@uni-tuebingen.de
[6]CNRS – Université de Bordeaux, UMR 5060, IRAMAT-CRP2A, Maison de l'archéologie, Esplanade des Antilles, 33607 Pessac cedex, France; ctribolo@u-bordeaux-montaigne.fr
[7]Department of Scientific Research, British Museum, London WC1B 3DG, United Kingdom
[8]CNRS, UMR 7140, Université de Strasbourg, Laboratoire de Spectrométrie de Masse des Interactions et des Systèmes (LSMIS), Strasbourg, France; acharrie@unistra.fr
[9]ENVARCH, CIBIO-INBIO, University of Porto, Portugal; maraujo_mar@yahoo.com
[10]Institute for Archaeological Sciences, University of Tübingen, Rümelinstraße 23, 72070 Tübingen, Germany; susan.mentzer@ifu.uni-tuebingen.de
[11]School of Anthropology, University of Arizona, 1009 E. South Campus Room 210, Tucson, Arizona 85721; USA
[12]CNRS, UMR 5199-PACEA, Université de Bordeaux 1, Talence, France ; pierre.texier@u-bordeaux.fr
[13]Department of Archaeology, University of Cape Town, South Africa; john.parkington@uct.ac.za

ABSTRACT

Elands Bay Cave (EBC) is one of the key sites for the analysis of the Late Pleistocene/Holocene record in southern Africa. It typifies an area of study, the West Coast of South Africa, which benefits from a long history of research, from the 1960s until today. The 2011 project of EBC was initiated within the framework of the Middle Stone Age (MSA) research at Diepkloof Rock Shelter (DRS). The objective was to build a local synthesis and a complementary picture on the basis of these two sites located 14 km apart from one another, on the left bank of the Verlorenvlei.

The excavation at EBC took place during May 2011 with the aim of clarifying the site formation processes, the chronology of the Late Pleistocene occupations as well as the nature of the technological sequence. Our excavation focused on a 1.2 m deep profile that records two main occupational phases separated by a significant hiatus: (1) the initial phase represents an early MSA technology (previously called 'MSA 1' by T. Volman 1981) within deposits that started accumulating ca. 250 ka years ago; (2) the second phase documents (late) MSA, Early Later Stone Age (ELSA) and Robberg occupations.

The present synthesis is part of a series of several papers that take a multidisciplinary perspective. In this paper, we introduce our 2011 excavation, present our main results and discuss the succession from the late MSA to the LSA at EBC. In an epilogue, we provide a comparison between the archaeological records of EBC and DRS and further explore the reasons why these two sites do not represent similar occupational sequences.

KEY WORDS: Early MSA, late MSA, Early LSA, Robberg, coastal site, Elands Bay Cave, Diepkloof, Verlorenvlei.

Elands Bay Cave (EBC) is located on the present shoreline of the West Coast of South Africa. Its (re)discovery followed the excavation in the Cederberg mountains in the late 1960s at De Hangen, where marine shells were found some 80 km away from

ISSN 2305-2791 (online); 1681-5564 (print)

the sea (Parkington & Poggenpoel 1971). The excavation conducted in the 1970s by Parkington and colleagues revealed a rich cultural and environmental record that rapidly positioned EBC as a prominent place for the study of the southern African Holocene (Parkington 1972, 1976, 1981, 1984, 1988; Parkington et al. 1988, 2014). But, EBC also documents older occupations. In the present paper we aim to give an update on the Pleistocene record of EBC and to provide a first narrative of the Verlorenvlei Stone Age on the southwestern tip of Africa.

Since the excavations at EBC in the 1970s, the area of the West Coast has benefited from intensive field activities as well as a wide scientific exposure, notably influenced by researchers from the University of Cape Town. As a consequence, the West Coast firmly represents one of the best known areas concerning the study of the Southern African Stone Age today. This assertion is certainly true for the Late Pleistocene and Holocene but much less for earlier periods. MSA and LSA sites have been discovered on the coast, in particular around the Saldanha peninsula, but also more inland such as in the Cederberg range, in shelters and in open air sites. The Stone Age of the West Coast also benefits from a fairly good mapping of the stone raw material availability (predominantly composed of quartz, quartzite and silcrete), as well as a good understanding of the palaeoenvironments (Cartwright & Parkington 1997; Cowling et al. 1999; Parkington et al. 2000; Chase & Thomas 2006; Cartwright 2013; Cartwright et al. 2014). Several publications from the 1970s onwards illustrate the progress and importance of the research conducted in this area (e.g. Parkington 1972, 1976, 1984, 1988, 2001; Klein 1974, 2001; Jerardino 1993, 2013; Orton 2006; Avery et al. 2008; Mackay 2009, 2010; Texier et al. 2010; Högberg & Larson 2011; Wurz 2012; Kandel & Conard 2012; Hallinan 2013; Jerardino et al. 2013; Porraz, Parkington et al. 2013, Will et al. 2013; Mackay et al. 2015; Parkington & Porraz 2016 this issue).

EBC relates to a wide and diversified landscape, but the position of the shelter itself, within the Verlorenvlei catchment, at the mouth of the vlei and on the present coast, defines a unique environment. The Verlorenvlei catchment can be framed as an 'enculturated landscape' (see Lovis & Whallon 2016), composed of several rock art places, burials but also living and eating places, paths and routes. This unique landscape, composed of various ecological and vegetational niches (Cartwright 2013; Cartwright et al. 2016 this issue), has favoured intense human occupation, notably during the Holocene. EBC is mostly known for its Holocene record, but the site provides older insights about the settlements of this area. EBC is one of the three sites (including Peers Cave and to a lesser extent, Bushman Rock Shelter) that led Volman (1981) to define what he considered to be the oldest stage of the MSA in South Africa, namely the 'MSA1'. In addition, EBC provides deposits associated with MIS 3 and MIS 2, generally associated with the succession from the MSA to the LSA.

EBC is a pivotal place for the Verlorenvlei Stone Age, but cannot define on its own the temporal range and behavioural diversity that characterized the occupation of this area. As Parkington (2016 this issue) points out with his metaphor of the blinking eye, the sequence of EBC is made of severe discontinuities in sedimentation and human occupations. Certainly, these discontinuities relate to an environment that was highly variable. However, these discontinuities more widely reflect the fragmentary nature of all archaeological records. From that perspective, the reconstruction of the Verlorenvlei Stone Age requires us to refer to other places as well, such as Diepkloof Rock Shelter

(DRS), actually discovered in 1973 within the framework of the 1970s EBC project (Parkington et al. 2013). Excavated from 1998 to 2013 by Rigaud, Texier, Poggenpoel and Parkington, DRS has revealed a 3 m deep sequence with (lithic) traditions being largely represented by Still Bay (SB) and Howiesons Poort (HP) occupations (Porraz, Texier et al. 2013), both of which are seemingly absent at EBC.

Within the project of DRS, questions related to the Pleistocene deposits and occupations of EBC came back into view. How could these two sites, located a few kilometers away from each other, present such differences in terms of their chrono-cultural record? How was the Verlorenvlei catchment occupied, under which circumstances and under which motivations? In 2011 and with these questions in mind, we decided to reopen EBC largely in order to clarify the nature of its Pleistocene occupations. The specific goals of our field work were threefold: 1) to understand the site formation processes, 2) to give a chronological framework for the human occupations, 3) to characterize the technical phases and successions.

This paper aims to provide a general background of our field research and to introduce results of our multidisciplinary approach. We clarify what our strategy of excavation has been, present our 2011 field data and establish correlations with the 1970s excavations. We summarize the main sedimentary phases at the site as well as their chronology and discuss the human occupations. Furthermore, we discuss the technological changes recorded from MIS 3 to MIS 2. We then compare the record of EBC with the record of DRS and explore the possible reasons why these two neighbouring sites record distinct occupational phases.

RESEARCH HISTORY AT ELANDS BAY CAVE

The shelter and its context (Fig. 1)

The West Coast region of South Africa, as we define it, extends from Cape Town to the Olifants River mouth, from the Atlantic coast to the Cederberg Mountains. It falls within the Winter Rainfall Zone and experiences precipitation that accumulates mostly from April to September, with an average of ca. 270 mm/year (Robertson 1980; Sinclair et al. 1986). The landscape of the West Coast is part of the larger Cape Floristic Region, with dominant fynbos vegetation and a sandveld landscape along the coastal plains. It includes a range of geological formations that are drained by several rivers flowing westward, including the Verlorenvlei.

The Verlorenvlei River catchment begins 40 km to the east of the Atlantic coast, nearby the town of Piketberg on the east of the Piketberg moutains. The river, fed by tributaries from the Piketberg, Olifantsrivier, Swartberg and Mannberg mountain ranges, turns progressively into a semi-estuarine and marshy coastal lake or vlei. It defines a wetland ecosystem of ca. 10 km^2 that provides rich resources within the semi-arid West Coast (Baxter 1997). This unusual ecological configuration finds its origin in the presence of a quartzitic sill that obstructs the river's mouth near the village of Elandsbaai.

The late Precambrian Malmesbury Formation and the Siluro-Devonian Table Mountain Group (TMG) dominate the bedrock of the area (Baxter 1997). The TMG bedrock forms buttes and ridges that run northwest-southeast and rise above the extensive surficial sands of the Sandveld. The left bank of the Verlorenvlei is marked

Fig. 1. Location of Elands Bay Cave on the West Coast of South Africa and below view of the Verlorenvlei mouth.

by a 120 m high ridge (Tankard 1976; Rogers 1987) that continues to the coast at Elands Bay and terminates at Baboon Point at the Atlantic Ocean, where the shelter of Elands Bay Cave is situated.

Elands Bay Cave is located at Cape Deseada, ca. 180 km north of Cape Town. The cave (or rock shelter) is ca. 18 m wide and 10 m long. It presents a rectilinear morphology that is defined by the bedding and jointing of the TMG bedrock. The site faces the ocean to the southwest at an altitude of ca. 42 m above sea level. This area has of course undergone significant change throughout the Quaternary as a result of fluctuating sea levels. During phases of maximum marine regression, sea levels at Elands Bay dropped more than 100 m below modern levels exposing 20–30 km of coastal plains and leading to significant down-cutting by the Verlorenvlei river.

A short introduction to the 1970s excavation

The first excavations carried out at EBC began in November 1970 by a team headed by John E. Parkington, Cedric Poggenpoel and Peter Robertshaw from the University of Cape Town. The excavation continued until December 1978 for a total of 20 weeks of fieldwork (Parkington 2016 this issue). In parallel, a large survey was conducted around the Verlorenvlei area and many new sites were discovered, including Tortoise Cave, Dunefield Midden as well as Diepkloof Rock Shelter (see Parkington 2016 this issue).

The team started to excavate the eroding, disturbed sediments in the southwestern area of the chamber and expanded the excavation area to 96 m^2. The excavators extensively unearthed the Holocene and terminal Pleistocene deposits but only explored the lower part in the form of two successive test-pits over an area of ca. 5 m^2. They reached the smooth undulating bedrock circa 3 m below the original surface of the deposits.

Parkington et al. excavated pursuant to depositional units that were distinguished on the grounds of composition, such as relative amounts of shell, bedding grasses, twigs, ash, roof spall, loamy matrix and gypsum. According to the local archaeological tradition, the excavated units were given arbitrary names, which have been reduced to a set of four letter acronyms afterwards. All features such as pits, post holes, disturbances as well as hearths and the boundaries of depositional units were mapped. Identifiable artefacts and bones were also recorded by square and depth. The excavated sediments were dry sieved with 12 mm and 3 mm mesh sieves. All of the recovered archaeological material is currently stored in the Iziko South African Museum.

Except for the lowermost part that lies beyond the range of radiocarbon dating, the large number of radiocarbon dates (> 60) showed that the sequence was clearly characterized by episodes of non-deposition and non-occupation. Thus, Parkington developed a classification of the sequence into so-called pulses (Parkington 2016 this issue), listed here from oldest to youngest:

> **Pulse H** lies directly on bedrock. It corresponds to a 300 to 400 mm thick deposit that represents homogenous quartzite rubble composed of quartzite artefacts and geofacts. It contains relatively little fine interstitial material and lacks plant and faunal remains (Miller 1987). This lithic assemblage was assigned to the MSA 1 by Thomas P. Volman (Volman 1981, 1984; Schmid et al. 2016 this issue).
>
> **Pulses G, F and E** consist of 1.3 m of sandy loams rich in charcoal, ash and occasional roof spall. The sands are coarse and exhibit a poor sorting with a high contribution of localised cave wall weathering. The pulses contain no shells, but do contain faunal remains, mostly terrestrial animals. Pulses G and F have been separated by the presence of the depositional unit PATT (a horizon associated with the presence of disintegrated quartzite blocks) while pulses F and E have been separated by the depositional unit SPAL characterized by an increase in roof spalls. Pulses G and F have C14 dates that fall beyond the range of radiocarbon dating (> 40 ka BP); pulse E has been dated between 21 ka to 17 ka uncal BP. These lithic assemblages have been classified as MSA and ELSA (Parkington 1992).

Pulse D reflects occupations across the terminal Pleistocene to the early Holocene boundary. Three sedimentary phases have been recognized within this pulse: (1) the lowermost part is composed of sandy loams from the terminal Pleistocene with ash and charcoal, high densities of artefacts as well as terrestrial faunal remains; (2) the middle part contains loams with shell from the terminal Pleistocene with a very high density of terrestrial and marine animal bones; (3) the uppermost part represents shell middens with a high loam content to finally shell middens without any substantial fine-grained components other than ash from the early Holocene. One striking element of pulse D is the presence of a burial from depositional unit ALBA dated to 10.86 ± 0.18 ka uncal BP (OxA478).

Pulse C dates between 4.3 and 3.2 ka uncal BP. The deposits are deep, loose and homogeneous shell middens with a substantial windblown component. Some of the thick depositional units contain dispersed remains of estuarine grass bedding or ash that have encouraged the excavators to conclude that these materials were originally deposited in basins in the rear of the site and later covered or repositioned by the cave occupants. Other depositional units of this period are *in situ* filling of a basin in the rear centre of the cave with shelly material and presumed estuarine bedding grass.

Pulses B and A are separated by only a short time interval. Pulse B has an age of 1.8 to 1.5 ka uncal BP and is associated with the appearance of ceramics; pulse A dates between 1.4 ka and 0.3 ka uncal BP. The densities of marine materials such as crayfish, seals and birds exceed those of the terminal Pleistocene in some depositional units. This assemblage of plant remains, such as twigs, grasses, corms and seeds, terrestrial bedding grasses and inorganic as well as organic artefacts, such as string, seed beads, brass and ceramics, resembles those of other coastal and, interestingly, inland sites.

THE 2011 EXCAVATION

Excavation strategy

In May 2011, we started a new excavation at EBC with the objective to clarify the nature of the pulses H to E: the Pleistocene occupations at the site. We achieved our research goals in a campaign of four weeks that focused on the 1970s test-pit area. Our 1 x 1 m excavation grid, which we established by using a total station, conformed to the one set up in the 1970s; however, we employed a different nomenclature to avoid confusion (Fig. 2). The squares were numbered serially and each square was subdivided into four quadrants (a–d).

The opening of the 1970s test pit revealed the strong impact of post-depositional processes on the stratigraphy. These post-depositional processes mostly take the form of secondary minerals, including large nodules of gypsum. Water actively percolates through the bedrock of the site and its effects are visible on the wall of the shelter and within the remaining deposits, causing some lateral variation within the stratigraphy (Miller et al. 2016 this issue). Based on these direct observations, we oriented our excavation towards the eastern profile that was the least affected by post-depositional agents. The east section had also the advantage of being well

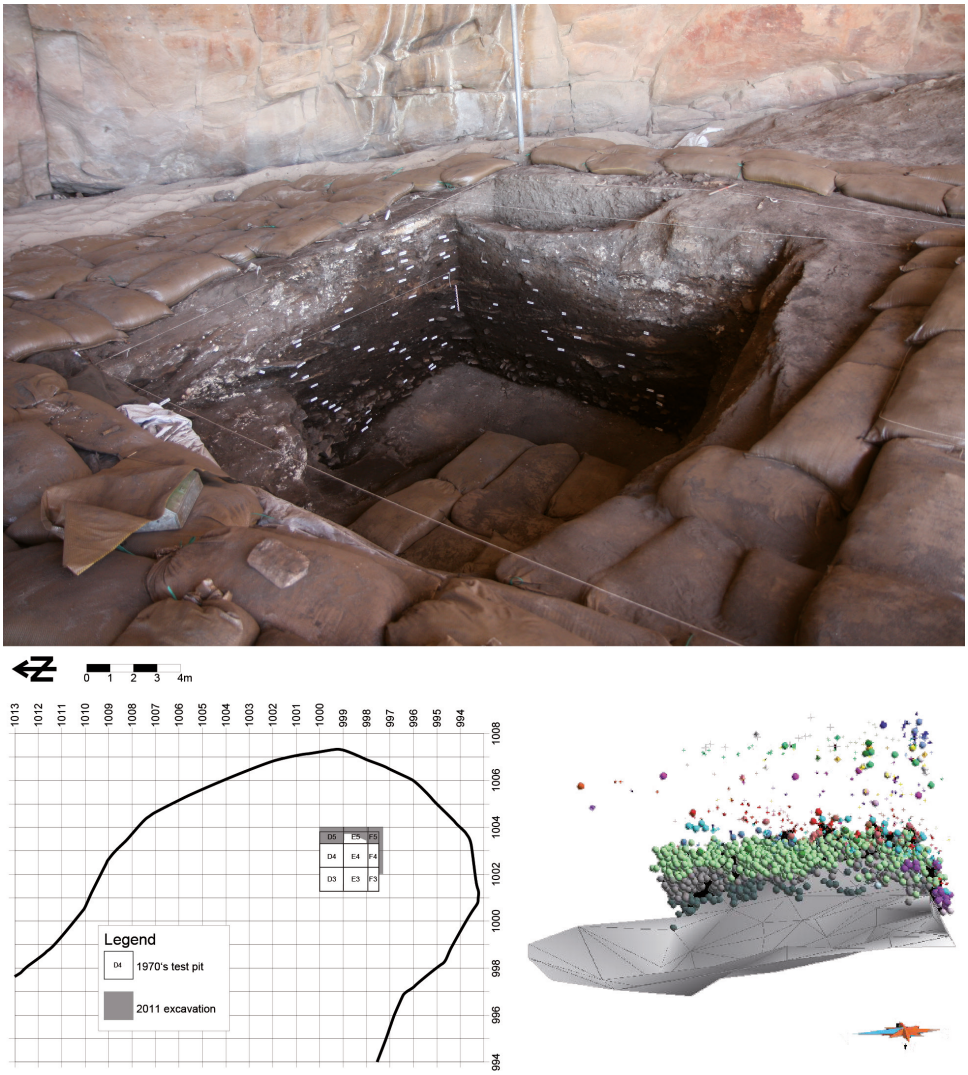

Fig. 2. View of the 2011 excavation area and projection of the plotted lithic artefacts per SUs.

exposed to the natural sunlight and in connection with the north section, for which we had field notes from the 1970s.

Before starting the excavation, we cleaned the eastern profile and individualized the main stratigraphic phases in order to provide an initial organisation of the deposits. We labelled each of these stratigraphic phases with a capital letter from L to C. Within each stratigraphic phase, we distinguished stratigraphic units (SUs) by giving informal names, but maintaining an internal alphabetical order. The SUs relate to the smallest identifiable sedimentary events that spread over an area larger than a quarter square meter. If a SU reached a depth over 25 mm, it was subsequently subdivided into successively numbered *décapages* ('spits') following concentrations of artefacts.

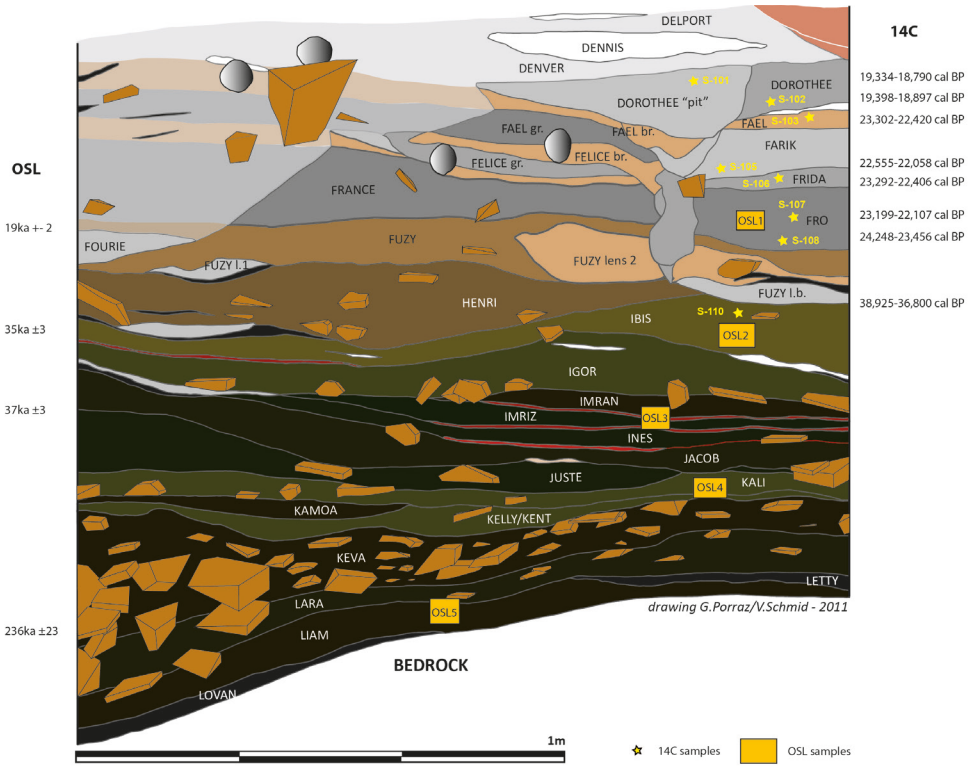

Fig. 3. 2011 eastern stratigraphic profile of Elands Bay Cave with the location of 14C and OSL samples.

The 2011 excavation focused on a narrow band of 2.5 m length and 0.5 m width. However, the eastern section also demonstrated lateral variations owing to post-depositional factors, most particularly towards its northern part, where gypsum formation was active. We therefore focused on the southern part of the east profile, which represents our main section. In addition, we straightened the south profile to get a better overview of the geometry of the deposits.

In the following, we describe the main stratigraphic phases as observed within our main section (Fig. 3) and as individualized during the excavation (see Miller et al. 2016 this issue):

Phase L (Letty to Lovan) has a maximum thickness of ca. 100 mm and consists of black and moist lenses within dark brown sediment. While a few archaeological finds occur, their origin is questioned and presently interpreted as a likely intrusion from the overlying unit.

Phase Keva/Lara exhibits a maximum thickness of ca. 350 mm. Keva and Lara contain a large accumulation of quartzite artefacts and roof spall with almost no interstitial matrix.

Phase K (Kent to Kali) is up to 150 mm thick. This comprises fine laminations visible in the southern section. Phosphatic lenses and nodules are present.

Phase J (Juste to Jacob) presents a maximum thickness of ca. 200 mm. The phase J is lighter than the phase K and laminations are not visible. Phosphatic lenses and nodules are also present.

Phase I (Ines to Igor) has a maximum thickness of approximately 250 mm. The phase I is darker than phase J and finely laminated with a succession of reddish laminations. Igor corresponds to yellowish sediment and its base is marked by a concentration of roof spall and small quartzite blocs between 50 to 150 mm of maximum dimension. The base of Ines corresponds to an accumulation of roof spalls, which are disintegrated. Phosphatic lenses, possibly related to ash, are present.

Phase H (Ibis to Harry) conforms to a phase of ca. 200 mm maximum in thickness. The phase H resembles phase I, but is lighter in colour. It is composed of homogeneous greyish to brownish sediment with occasional lenses. Quartz grains partly related to the alteration of roof spall occur abundantly within the sediments. All SUs show an inclination towards the south.

Phase F and D (Fuzy to Delport) has a maximum thickness of ca. 550 mm. It corresponds to a succession of units related to combustion activities indicated by the presence of ashes, charcoals and rubefied sediments, although post-depositional agents have modified their structures. Unlike phase D, phase F contains multiple interstratified depressions.

Phase C corresponds to a large pit composed of yellow brown sand that extends and slopes towards the southern wall of the shelter. The archaeological material is not abundant and mostly comprises shells. We observed no horizontal or vertical organization. This phase is a remnant of the Holocene deposits.

During the excavation of 2011, we used classic excavation methods and standards. All objects larger than 2 cm were recorded three-dimensionally with the total station using EDM software and field videos were taken on a daily basis. Cores, core fragments, tools and tools fragments regardless of their size were always recorded. Afterwards, the finds were put into bags with their individual find labels including their unique find number, square, sub-square and SU provenience. All of these single finds were washed and labelled with ink. Additionally, the sediments belonging to determined SUs of a sub-square were collected in buckets and recorded. These buckets were given unique find numbers starting with the letter T, referring to the French word for screen '*tamis*'. They were dry sieved with a superimposed screen of a 3 mm and a 1 mm mesh sieve to retrieve all the smaller pieces as well as the larger objects that were not detected in the field. The residues of the 3 mm screen were sorted and all the lithic finds were bagged by sub-square and SU. All lithic artefacts larger than 2 cm were analysed.

The material unearthed during the 2011 excavation is largely dominated by lithic artefacts made from rocks such as quartz, quartzite and silcrete, including a few iron-rich pieces ('ochre'). The fauna preservation in our excavated area has been strongly impacted by post-depositional processes; bones were identified during excavation but largely in the form of yellowish imprints. However, charcoal of a size generally smaller than 10 mm were numerous (Cartwright et al. 2016 this issue). To these categories

of finds, we should add the discovery of two hearths that were structured by the presence of quartzite stones. These two combustion features were found in the SUs Jacob and Furb respectively. Stones from the SU Furb were sampled and used for thermoluminescence dating (Tribolo et al. 2016 this issue).

We implemented the dating strategy by sampling a set of charcoal fragments that were directly collected from the profile at the end of the excavation. The radiocarbon dating has been complemented by five OSL samples that were collected by night in 2011, while dosimeters were removed a year later in 2012. During this second campaign of one week in 2012 we collected micromorphological samples and performed ground penetrating radar (GPR) at the site to evaluate the morphology of the bedrock.

The deposits and their chronology

In the excavated area, the bedrock presents an irregular topography with a strong inclination down towards the north. The GPR data (Miller et al. 2016 this issue) allows us to elaborate on the topography of the bedrock and to have a better understanding of the geometry of the deposits at the site. The GPR shows the presence of a topographic depression (*cuvette*) at the centre of the shelter and confirms that the excavations focused on the deepest part of the deposits.

The site formation processes are characterized by important post-depositional processes taking the form of rodent burrows as well as the formation of secondary minerals. These minerals benefited from the moist environment provided by the nearby Atlantic Ocean and from the presence of water percolating from the joints in the bedrock of the shelter.

The site formation processes and the chronology enable the recognition of four main phases:

Phase (1) (L–Keva): the filling of the depression of the bedrock consists of a rich accumulation of archaeological material and spall which corresponds to the phase L until Keva. The results of the micromorphological study question the preliminary interpretation of K. Butzer (1979) that this lower sedimentary phase represents a lag deposit (Miller et al. 2016 this issue). The luminescence chronology indicates that the deposits started forming at ca. 230 ka BP. However, due to the almost total absence of sand within this phase and the difficulty of sampling within the rocks, we could not collect samples directly within the archaeological units. We only have one TL age on a burnt quartzite rock coming from the SU *Keva* and dated to 83 ± 14 ka BP (but see Tribolo et al. 2016 this issue for a discussion of the ages). The archaeological occupations are therefore bracketed between 230 and 83 ka BP but comparative technological studies allow us to conclude that human occupations likely date back to MIS 6 (Schmid et al. 2016 this issue).

Phase (2) (main hiatus): the micromorphological analysis shows the presence of a hiatus on the top of SU Keva, as indicated by the presence of a thin lag deposit.

Phase (3) (K–H): this includes the SUs Kent to Fuzy and reflects both geogenic and anthropogenic sedimentation processes. Within this phase, we also notice the presence of two horizons rich in spall fragments that relate to the progressive deterioration of the shelter. The technological study

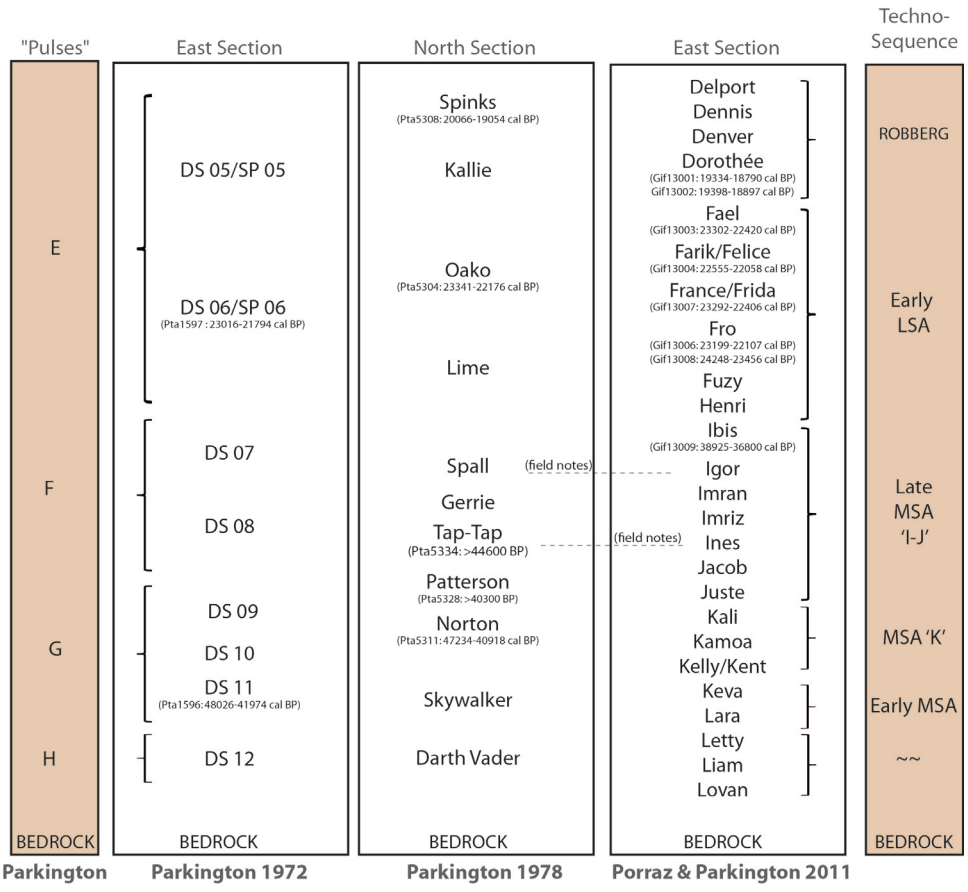

Fig. 4. Stratigraphic correlations between the 1972, the 1978 and the 2011 excavations at Elands Bay Cave.

suggests the lower lithic assemblages are reminiscent of post-HP occupations. The luminescence chronology together with the C14 dates indicates this phase (3) ends at ca. 35 ka BP.

Phase (4) (F–D): this phase of anthropogenic sedimentation comprises several combustion features and few spall fragments. This upper phase starts from SU Fro and lasts until the stratigraphic phase D which yielded a C14 date of ca. 19 ka cal. BP.

The 1970s and 2011 stratigraphic correlations (Fig. 4)

The stratigraphic correlations between the 1970s and the 2011 excavation concern the lower part of the deposits as exposed in the so-called deep sounding. This deep sounding was first excavated in squares E4 and F4 in 1972 and then enlarged towards north in 1978. In each of these two field seasons, Parkington used different names for the uncovered depositional units, as direct correlations were uncertain due to the lateral variation of the stratigraphy. In 1972, the units were called 'spits' with continuous numbers from DS 12 to DS 05, whereas in 1978, informal names were given. The 1972

and 1978 collections were subsequently grouped into pulses. For the present discussion, we establish correlations between the 1970s pulses and the 2011 excavation.

During our 2011 excavation, we focused on the east section of the deep sounding. We intended to establish direct stratigraphic correlations with the northern profile. However, direct observations of the profiles were limited and insecure due to the strong impact of secondary minerals in that part of the excavation. Our stratigraphic correlations (Fig. 4) combine and hierarchize different kinds of evidence that are based on sedimentary and field observations, C14 dating and techno-typological comparisons.

Correlations between the lower parts of the deposit have been facilitated by the presence of both sedimentary and lithic descriptions from the 1970s. The 2011 L phase (Keva included) clearly matches with the 'lag deposits' as described by Butzer (1979) and can be correlated with the pulse H and the base of the pulse G of Parkington. The main features in common are the rich accumulation of quartzite artefacts and roof spall with very little fine interstitial material, the absence of organic remains and a thickness of 400 to 500 mm. This is also supported by the technological comparison between the 1972 and 2011 lithic collections (Schmid et al. 2016 this issue).

Stratigraphic correlations regarding the intermediate part of the sequence, from phases K to H, has been more problematic due to 1) differences in sedimentation (the main section being more dilated), 2) differences in post-depositional preservation (the other sections being more degraded) and 3) a relatively low density of lithic artefacts. We focused primarily on some sedimentary markers that were independently observed during excavations. Firstly we correlate the depositional units Patterson and Norton—described as a 'Disintegrated Rock Horizon' in Parkington's field diary—with our SU Ines which represents the same processes of rock alteration occurring at a similar elevation. Secondly, we propose a stratigraphic correlation between the unit Spall and our SU Igor on the basis of a large concentration of quartzite slabs, also initially noticed by Parkington. Some specific typological markers were recovered from the 1970s such as a bifacial piece found in the unit Gerrie; one new specimen found in 2011 in SU Jacob. Based on our set of data, we correlate the 2011 phases K to H with the upper part of pulse G and with pulse F.

The upper part of our 2011 main section, phases F and D, correlates with pulse E. Finer correlations are possible due to the presence of C14 dates: our phase F is correlated with the unit Oako dated by radiocarbon from 20.5 ka uncal BP (J. Vogel 1980, unpublished); our phase D correlates with the unit Spinks dated by radiocarbon to 17.8 ka uncal BP. The technological comparisons support the present correlations.

THE PLEISTOCENE ARCHAEOSEQUENCE OF ELANDS BAY CAVE

Presentation of the 2011 lithic collection

The total collection of lithics is composed of 2592 artefacts > 20 mm. Apart from the lower units where artefacts are numerous, the Pleistocene sequence of EBC is characterized by a relatively low density of lithic artefacts (Table 1, all tables after references). Together with the limited area of our excavation and the variable extension of each SU, this has as a result some quantitative variations between SUs. To avoid important variations in counts and percentages, we therefore decided to group SUs that were adjacent and that

belong to a similar stratigraphic phase. These groupings have been undertaken in order to reach an arbitrary limit of a minimum number that we fixed at 30 pieces.

The different raw materials that compose the collection are represented by the local quartzite that comes from the TMG (classified here as 'Coarse-grained quartzite'), the quartz and the fine-grained quartzite that are available within the local conglomerates, the silcrete that is of exotic origin as well as a few other petrographic occurrences (classified as 'others') such as chert and hornfels (see Porraz et al. 2016 this issue for a better description of the regional lithologic resources). With the exception of phase D, where silcrete forms almost 50 % of the lithic assemblage, the raw material spectrum of the Pleistocene inhabitants of EBC is dominated by local rocks.

For the present study, the techno-typological classification has been limited to a few attributes in order to adapt to the low number of pieces as well as to simplify diachronic observations. Our distinction between flakes, blades and bladelets follow classic definitions, blades being twice as long as wide with parallel edges and bladelets being no wider than 11 mm. Within the present collection and with regard to the data known from the current literature, we paid special attention to evidence related to bipolar-on-anvil strategies. Typologically, the list has been simplified as well with regard to the low number of formal tools and their low range of internal variability.

The archaeo-stratigraphic sequence we propose rests on the study of the 2011 artefacts, but also includes some observations based on the 1970s collection. Schematically, we suggest introducing the sequence by individualizing three main phases: 1) the Early MSA; 2) the MSA to Early LSA; 3) the Robberg. As Schmid et al. (2016 this issue) describe specifically the Early MSA of EBC and Porraz et al. (2016 this issue) deal specifically with the Robberg of EBC, the present paper will focus more on the (late) MSA and ELSA lithic technologies than the other phases.

The Early MSA(Fig. 5)

The first phase of occupation of the shelter is characterized by a rich accumulation of quartzite artefacts and geofacts. The higher density of geofacts at the base of the accumulation, as observed during excavation, supports the hypothesis that the accumulation predates human occupations. In that case, the first EBC inhabitants would have partly taken benefit of the available raw materials. The main archaeological horizon is the SU Keva, with which we associate the SU Lara. We consider that the material of these two SUs belongs to one single archaeological assemblage, the field subdivision being related to different densities of sediments in the fine fraction.

The knappers have preferentially exploited the local quartzite, which accounts for 98–99 % of the lithic collection (Table 2). In association, we find a few artefacts made from quartz as well as a few others made from fine-grained rocks that originate from the local conglomerates. The spectrum of rocks, except for a few silcrete artefacts, documents an exploitation of rocks that was strictly local.

The reduction strategies we observe document the production of flakes of different morphologies. From a techno-typological perspective, the reduction sequences are reminiscent of the Levallois and the Discoid systems. However, we recognize a specific system that was adapted to the cubic morphology of the quartzite slabs that were exploited. We termed this system 'POL-reduction strategy' (Planar-Orthogonal-Linear) and defined it as a system based on various combinations of reduction of the three

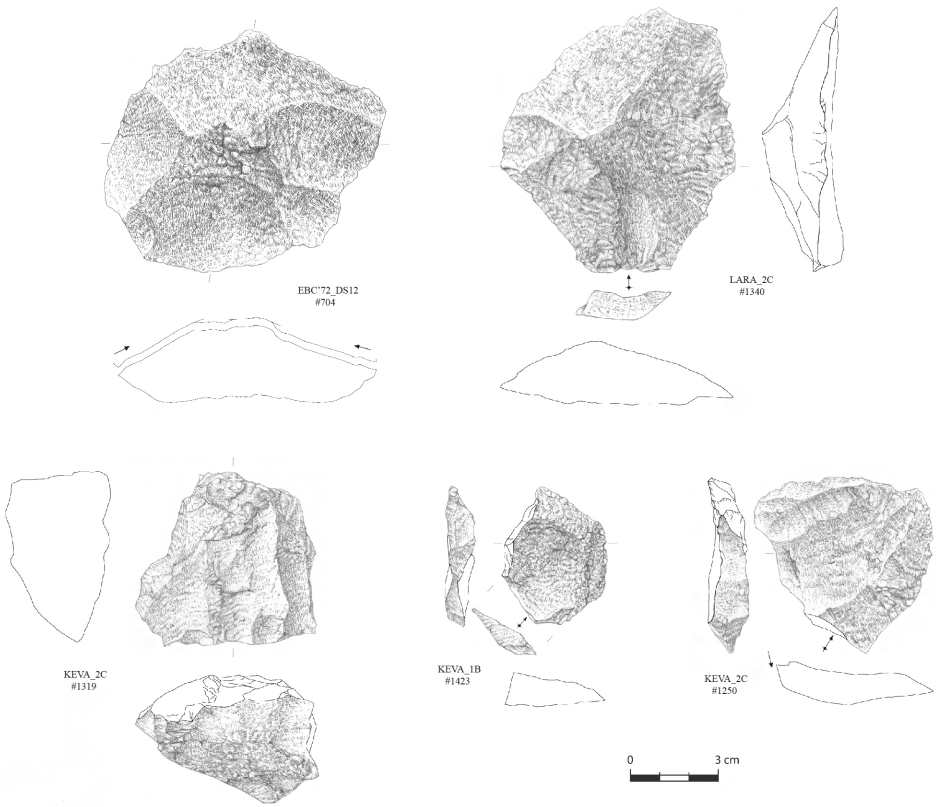

Fig. 5. Lithic artefacts from the EMSA of Elands Bay Cave (drawings by M. Grenet).

axes of the quartzite slabs that were selected (Schmid et al. 2016 this issue). In addition, we also recognized a laminar semi-prismatic reduction strategy, although it remains a small component of this lithic industry. The flakes have been rarely retouched (less than 1 % of the total collection) and are mostly transformed by notches.

Our study contests the hypothesis the site was occupied for short-term activities that were aimed at the exploitation of the local rocks and the export of end-products. We rather emphasize the fact that the reduction strategies were short and diversified and that the poor number of retouched tools is actually a consequence of a production system that was oriented toward the production of various morphologies and sizes. Apart from Peers Cave in the Western Cape, no other South African lithic collections for the moment share similarities with this assemblage from EBC. We encourage avoiding the classification as 'MSA1', but hypothesize that the lower occupations of EBC belongs to the suite of EMSA industries.

The MSA to the Early LSA

The second phase of occupations groups together the sedimentary phases K to F, from the SU Kent to the SU Fael. In the following description, we aim first at introducing the overall characteristics and then, to elaborate on some of the differences we recognize throughout the sequence.

These lithic assemblages are relatively homogeneous regarding the raw material procurement, which is dominated by quartz (Table 2). There is one exception documented in phase 'K', where the local quartzite seems to play a more substantial role than in the overlying deposits. Non-local occurrences are firstly represented by silcrete artefacts, present in small numbers but throughout all deposits, and secondly by hornfels and chert. Our excavation area has been restricted and thus limits our interpretation with regard to the raw material provisioning strategies. However, together with our observations based on the 1970s collections, we see a significant difference between the local rocks knapped *in situ* and the non-local rocks that were predominantly introduced in the form of finished pieces.

Since its first recognition, the identification of silcrete heat treatment has attracted increasing attention in southern African archaeological assemblages (mostly from the Western Cape where silcrete plays an important part as raw material). Its identification and the quantitative evaluation of its prevalence has also been improved by a set of new laboratory techniques, analysis protocols and experimental approaches that help define the characteristic attributes on artifacts (Brown et al. 2009; Schmidt et al. 2015; Delagnes et al 2016; Schmidt & Mackay 2016). In the context of EBC, evidence of silcrete heat treatment is identified from SU Juste onwards and is present throughout the subsequent sequence. As silcrete is represented only by a handful of pieces, it is difficult to further elaborate on its technological context. However, it is worth noting that in this context silcrete was heat-treated even though the rock only accounts for a small part of the raw material spectrum. This finding illustrates the necessity to extend the current research on lithic heat treatment from the MSA to the LSA.

There are several technological attributes that contribute to the conformity of the phases K to F. The first one relates to the overall domination of flakes over blades and bladelets (Table 3). One common element is the use of bipolar-on-anvil knapping (Fig. 6), as deduced from the cores as well as from the flakes themselves that can compose up to 50 % of the total of the flakes. This bipolar reduction is associated with different raw materials, although there is stronger association with quartz. This reduction strategy takes different forms: cores and products can document a polyhedral exploitation but the dominant form is the one favoring one main surface of removals. In this last case, some of the pieces overlap with the so-called category of the *pièces esquillées*.

Apart from the bipolar reduction strategies, we recognized a discoidal reduction strategy *sensu* Boëda (1993). This takes the form of typical thick *dos limité* flakes as well as a few cores with unifacial exploitation (Fig. 7). While this reduction strategy is identified throughout the sequence, the proportion of discoidal flakes is more important in the lower SUs of this archaeological phase (Table 3) and typical discoidal cores have only been identified within the K phase.

Blades and bladelets represent two minor technological components within the studied assemblages. Interestingly, they document two separate reduction sequences: the bladelets are mostly produced by bipolar flaking, while the blades are strictly associated with free-hand percussion (no clear evidence support the hypotheses that the bipolar bladelets come from later in the reduction chain than the freehand blades). We notice some diachronic changes within the blades. The ones of the lower SUs, especially phases K and I, are more regular and more numerous (Fig. 8). The blade

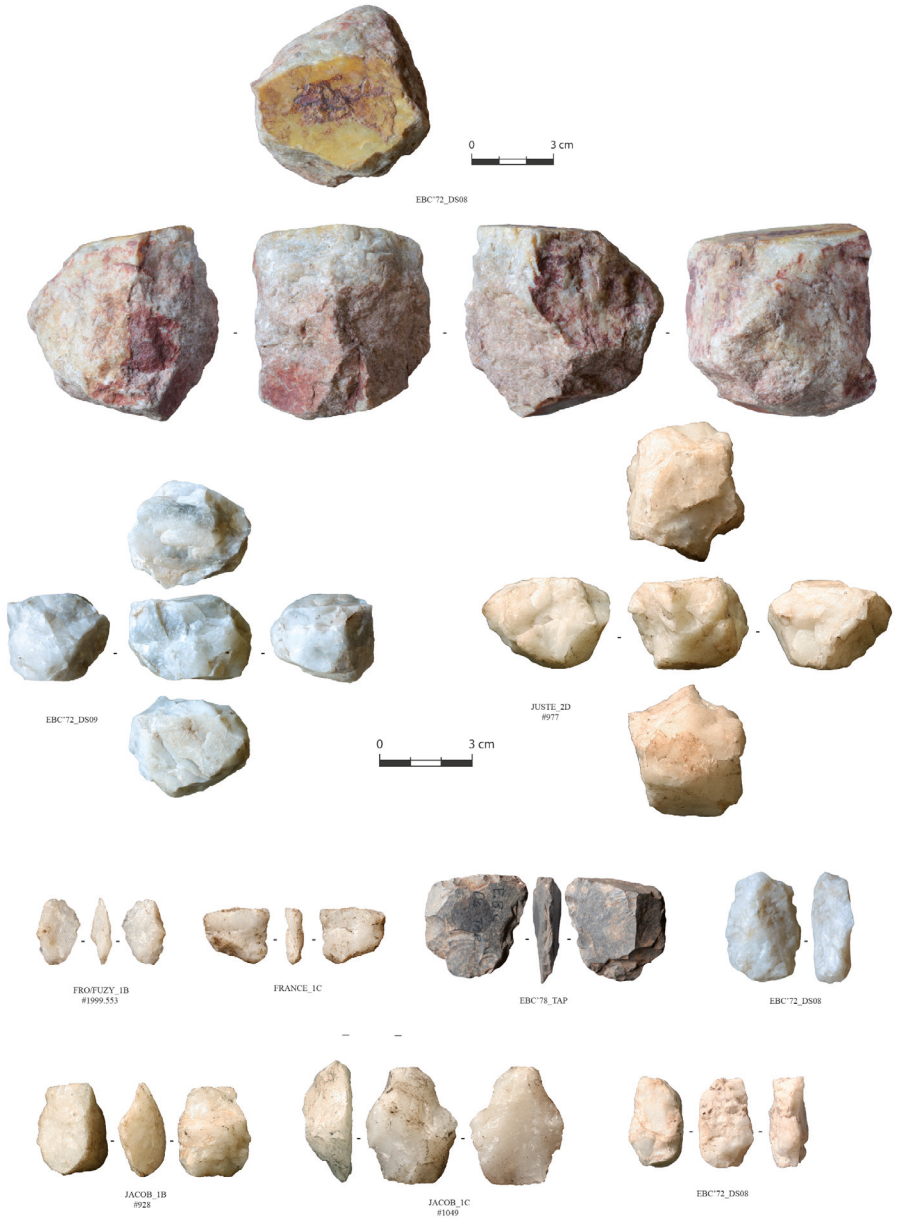

Fig. 6. Bipolar cores from the late MSA and ELSA of Elands Bay Cave.

technology of K and I can only partially be described as there are neither laminar cores nor technical products (or identified as such) present in the collections. The blades are represented by isolated products, some of them being very regular and suggesting a well-controlled execution and production. Based on our current set of information, we hypothesize a disjointed production of blades and flakes and are tempted to recognize two blade reduction sequences, one on the surface with an internal percussion and the

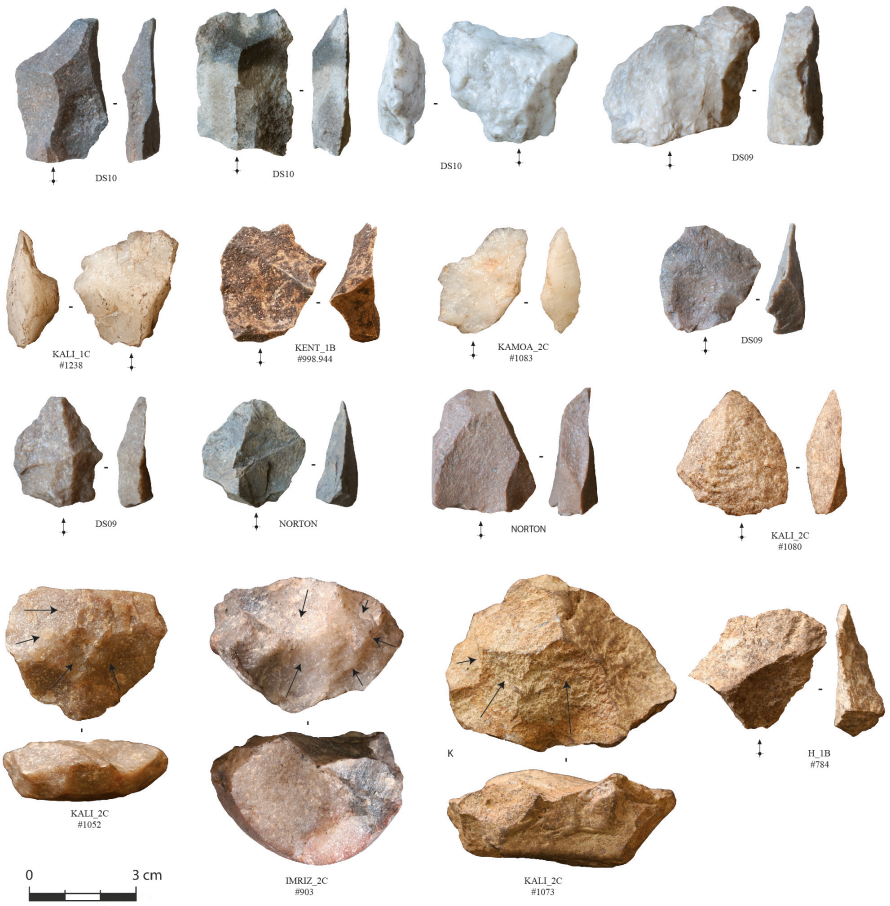

Fig. 7. Discoid blanks and cores from the MSA of Elands Bay Cave.

other being prismatic with a more tangential percussion. Strikingly, one regular blade exhibits a polish that shows use in a longitudinal motion together with other evidence that suggests that the blank was hafted (Fig. 9).

Regarding the typological corpus, the denticulates largely dominate the formal tools with more than 70 % of the total population (Table 4). These denticulates display a great degree of variability in terms of raw materials, blanks, morphologies, dimensions as well as manufacture (Fig. 10). With respect to this last attribute, the denticulates vary in the number of notches, their location (on the ventral or dorsal face) as well as their regularity, extension and depth; some denticulates having very marginal notches while others are much more invasive. As a general statement, the denticulates seem to represent a relatively expedient tool, as illustrated by their low degree of standardization. One good example is typified by a denticulate made on a silcrete heat shatter.

Apart from the denticulates, we also point out the discovery of one quartz bifacial piece in SU Jacob. A previous specimen in silcrete was found during the 1978 excavation. These two pieces show that bifacial technology was part of the technological repertoire of these populations and confirm that such technology was actually widely distributed

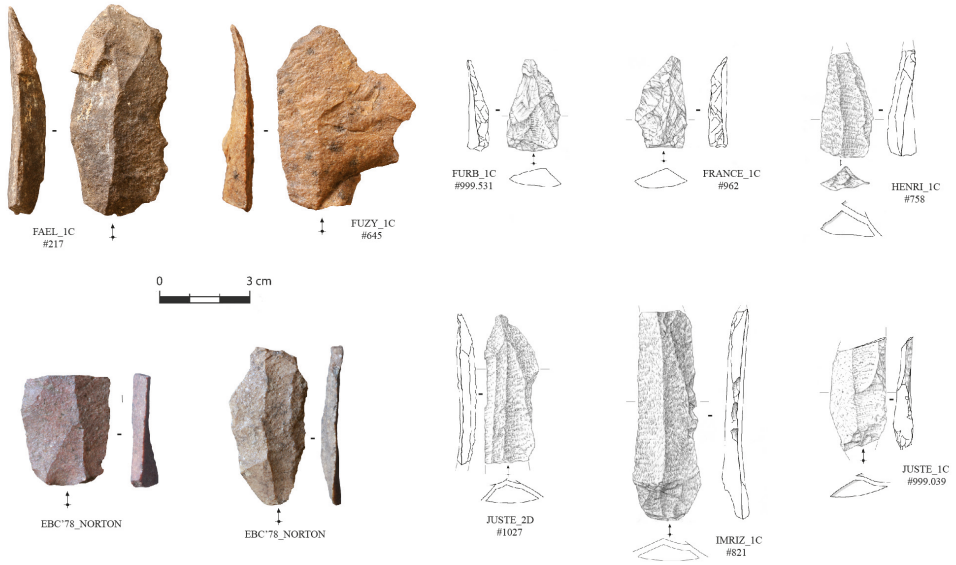

Fig. 8. Blades and elongated blanks from the MSA and ELSA of Elands Bay Cave (drawings by M. Grenet).

throughout the Late Pleistocene in southern Africa (de la Pena et al. 2013; Porraz, Texier et al. 2013; Soriano et al. 2015; Archer 2016; Will & Conard 2016).

In addition to our 2011 assemblage of formal tools, we should refer to the presence of a few typological pieces from the 1970s excavations that contribute to providing nuance to the present overview (Fig. 10). Additional to the two bifacial pieces, we may add the discovery of a single unifacial point (with a broken tip) that has been found in depositional unit DS10, which correlates with our phase K. Moreover, three 'truncated knives', falling into the category of the Asymmetric Convergent Tools (ACTs), have been found in depositional unit DS09, which correlates with our phase I. These tools, all on non-local rocks, have been made on regular blades and represent a distal retouch that backs the opposite edge into the straight and regular cutting edge. The functional analysis of one of these blades show a polish related to a longitudinal use (Fig. 9). Finally based on the 1970s collection, it appears that the *pièces esquillées* are more numerous in the upper SUs than in the lower. Note that a preliminary functional study performed on one of these artefacts (Fig. 9) shows the presence of a polish originating from long and repeated contact with an organic raw material, probably bone, and suggesting this lithic piece was either exclusively or alternatively used as a tool compared to the exploitation as core (see above).

This overview of the lithic industries from the phases K to F allows us to individualize the following common characteristics: 1) a low rate of lithic artefacts per SU; 2) raw material provisioning strategies based on the exploitation of local rocks and the episodic introduction of finished forms; 3) production primarily oriented towards flakes; 4) the important role of bipolar-on-anvil flaking; 5) a typological corpus dominated by denticulates. But within the phases K to F, we are inclined to sub-categorize the following trends:

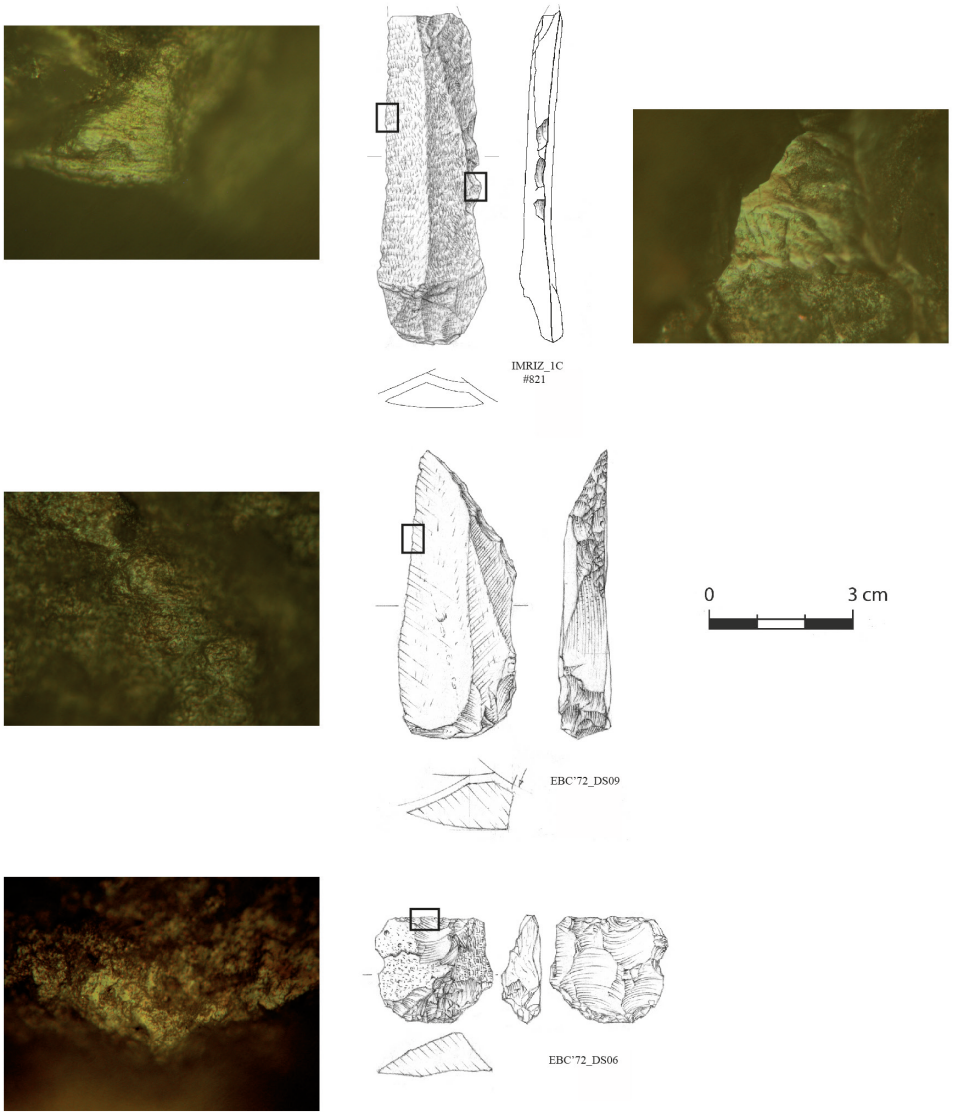

Fig. 9. MSA artefacts of Elands Bay Cave with microscopic use-wear traces. #821 (quartzite) left: rounded edge with parallel striation probably related to insertion of the blade in a handle (hafting), right: wood scraping polish. #DS09 (CCS) polish characteristic of use for soft material (animal) cutting. #DS06 (CCS) *pièce esquillée* with a polish showing contact with hard materials (magnification 200×, drawings by M. Grenet).

The phase K can be distinguished on the presence of a stronger emphasis on discoidal reduction, as well as on the presence of regular blades and a greater selection of the local quartzite. Typologically, the phase K includes the sole unifacial point that has been found so far at EBC. This phase finds echo in other post-HP assemblages, such as Klein Kliphuis (Mackay 2010) and Border Cave (Beaumont et al. 1978; Villa et al. 2012) from South Africa as well as Ha Soloja,

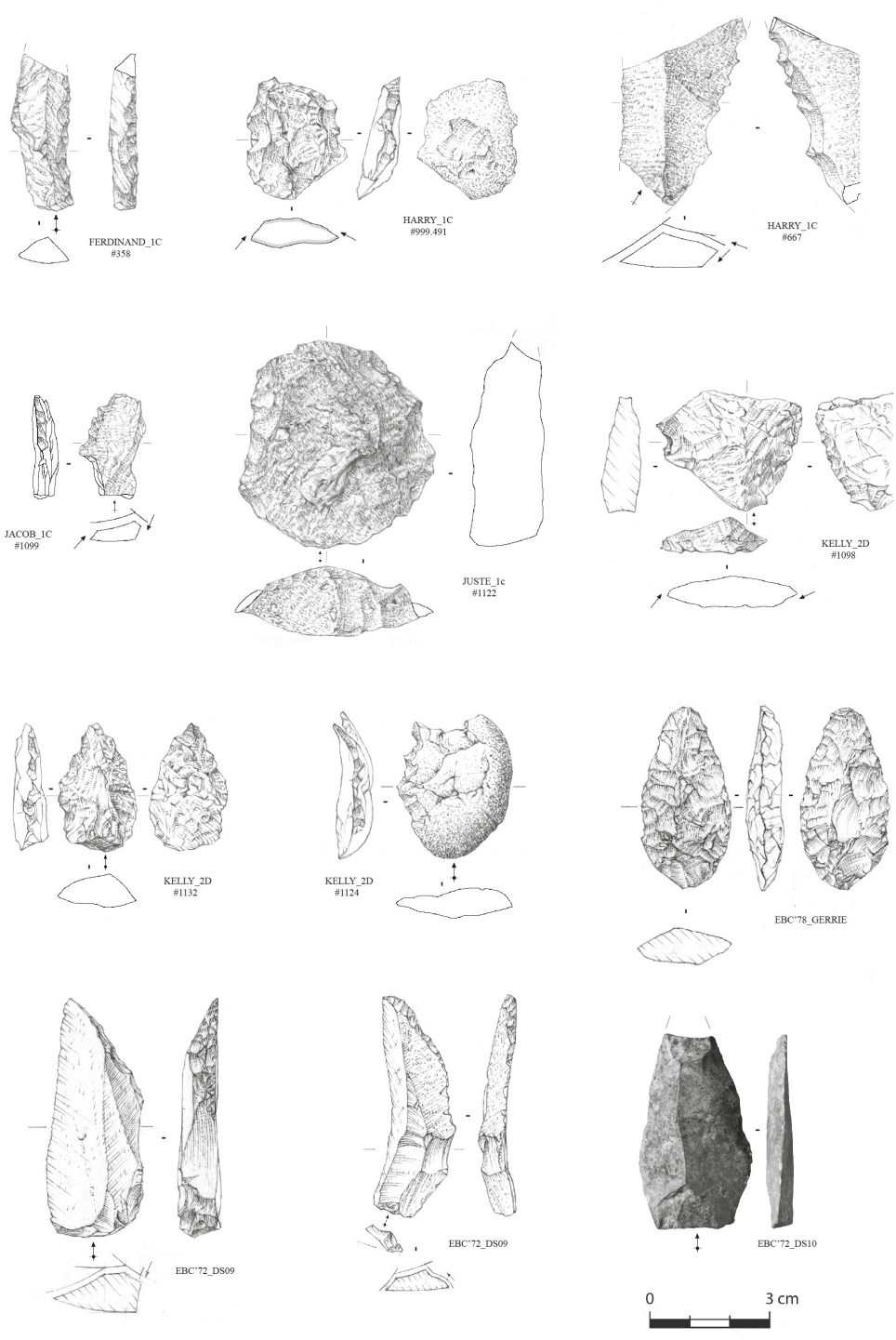

Fig. 10. Formal tools from the MSA and ELSA of Elands Bay Cave (drawings by M. Grenet).

Lesotho (Carter & Vogel 1974; Mitchell & Steinberg 1992), though the presence of a discoidal reduction sequence has so far not been reported in the literature. The only exception are some post-HP layers from Sibudu (Porraz pers. observation; Conard & Will 2015), which suggests to us that this actually might be a more widespread technology than presently assumed. The discoidal reduction sequence contributes to clarify the technological identity of the industries informally called 'post-HP' (Conard et al. 2012).

The phase J–I is characterized typologically by a certain diversity, as expressed by the presence of bifacial pieces and 'truncated knives'. Another element that characterizes the phase I—J is the drop observed in discoidal reduction while regular blades are still present. Its mean OSL ages is 36 ± 3 (SUs Imriz/Ibis), its mean TL age is 30 ± 4 (SU Furb), while a C14 date from the upper part gives an age of ca. 39–37 ka cal BP.

This phase resembles other MIS 3 lithic assemblages such as Klein Kliphuis (Mackay 2010) and Pugtslaagte 8 (Mackay et al. 2015; Law & Mackay 2016) from the West Coast, though bifacial pieces and truncated blades have so far not been noticed. But the occurrence of a bifacial technology in the MIS 3 of EBC is not an isolated case in southern Africa; we may for example refer to Sibudu where bifacial pieces are documented together with hollow-based points at ca. 39–35 ka BP (Wadley 2005).

The phase H–F is largely dominated by bipolar-on-anvil flaking, oriented towards the production of small flakes and bladelets, and documents a low degree of preparation of the production. The typological corpus only represents denticulates. The C14 dating brackets a time period between ca. 24 and 22 ka cal BP. This phase can be considered as part of the suite of ELSA technologies.

The Robberg

The third phase represents Robberg occupations (Porraz et al. 2016 this issue). This phase, strictly associated with D, dates back to 19 398–18 790 ka cal. BP. It corresponds to depositional units Kallie and Spinks from the 1978 excavation and to the depositional unit DS05 of 1972. However, our comparisons between these collections show differences (notably in terms of the flake component) that we interpret as a consequence of mixing with the underlying units due to the poor stratigraphic integrity of the area excavated in the 1970s. We therefore do not integrate the 1970s collections in the present summary.

Our 2011 lithic assemblage groups together 175 artefacts > 20mm (Table 3). It is predominantly made from quartz and silcrete (Table 2). For silcrete, evidence of heat treatment, post-heating removal scars or heat-induced-non-conchoidal fractures, are common. The lithic assemblage suggests that non-local rocks were introduced in various forms (end-products and cores) and that only short sequences of production took place in the shelter.

The lithic assemblage is dominated by microlithic products (Fig. 11), i.e. bladelets and bladelet cores with a length smaller than 25 mm. The Robberg is characterized by bladelets of various morphologies, coming from different reduction sequences that have the use of single platform cores and the association of direct marginal soft stone

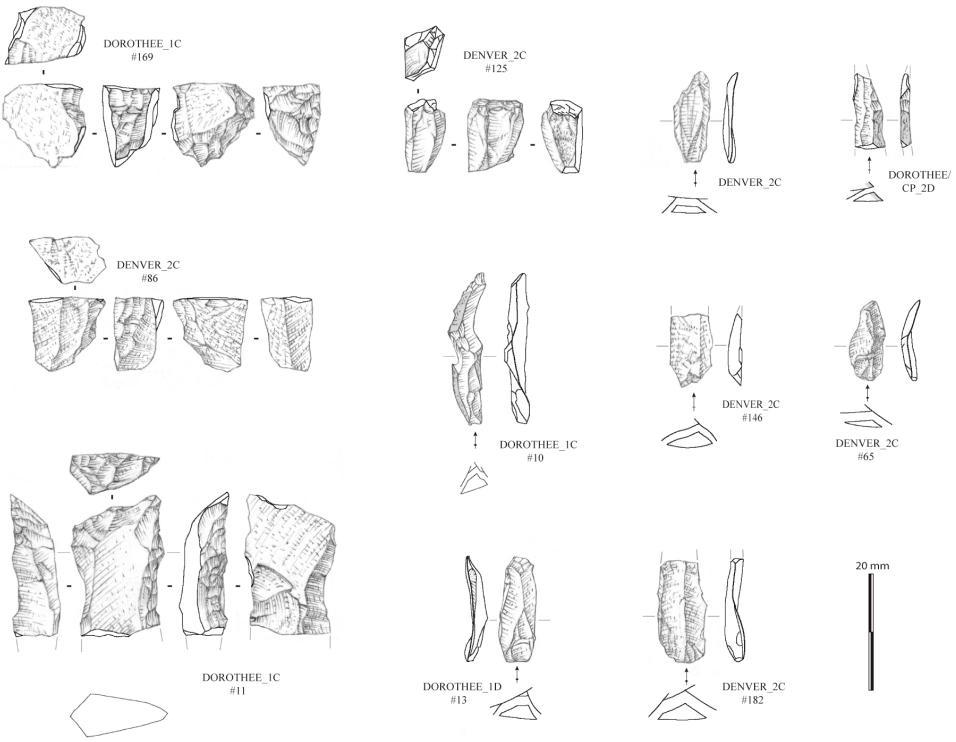

Fig. 11. Lithic artefacts from the earliest Robberg at Elands Bay Cave (drawings by M. Grenet).

hammer percussion with anvil/bipolar percussion in common. A few blades have been found but they remain rare and flakes are mostly associated with the local quartzite. The typological corpus of this Robberg D phase is represented by three pieces, composed of two modified bladelets with a shallow retouch and one retouched silcrete flake, as well as two denticulates.

EBC AND THE MSA TO LSA SUCCESSION IN SOUTHERN AFRICA

Our 2011 excavation allowed a refining of the stratigraphy of the MIS 3 and MIS 2 deposits at EBC as well as the nature of their occupations, in terms of technology, succession and chronology. Of importance and worth discussion is the appearance and definition of the so-called ELSA in southern Africa. The ELSA was first introduced by Beaumont and Vogel (1972) based on their discoveries at the site of Border Cave (BC), with the oldest ELSA layer dated to a time period between 44 and 43 ka cal BP. More recently, two papers (d'Errico et al. 2012; Villa et al. 2012) have confirmed the antiquity of these discoveries as well as clarified their nature. From about 40 000 years ago at BC, ELSA inhabitants were working and engraving bones, using OES, marine pendants and bored stones as well as mixing compound adhesives—all proxies that the authors (d'Errico et al. 2012) associate with earliest San practices (see Mitchell 2012; Pargeter 2014 for discussion). One important result of their study is the discrepancy between the linear changes observed in lithic technology and the abrupt (re)appearance

of bone technologies and symbolic proxies that suggest to them the beginning of the LSA in southern Africa.

The ELSA lithic assemblages of BC features a microlithic technology that is based on quartz and bipolar-on-anvil percussion oriented towards the production of small blanks (flakes and bladelets) that were used unretouched. Additionally, the authors note the presence of free-hand hard hammer percussion associated with the production of unstandardized flakes and blades. However, the observations that have so far been published in the literature (see Kaplan 1989; Deacon 1995; Mitchell 2002; Lombard et al. 2012; Ossendorf 2013; Mackay et al. 2015) display an ELSA characterized by a greater technological diversity with lithic assemblages said to be microlithic or not, based on prepared or unprepared cores and with various formal tools (e.g. scrapers, backed pieces etc.), or none. It is worth remembering that these reflect different analytical approaches and have been extracted from different archaeological contexts (stratigraphy and dating), both of which may contribute to an explanation of the poorly resolved picture presently associated with the nature of lithic technologies at the end of the MIS3 in southern Africa.

At EBC, the phase F is dated to 24–22 ka cal BP, a time period conventionally associated with the ELSA (see Lombard et al. 2012). The ELSA at EBC typifies an expedient microlithic technology characterized by (1) the use of local raw materials, predominantly quartz; (2) the application of bipolar-on-anvil and free-hand percussions; (3) the reduction of unprepared cores oriented towards the production of small flakes and bladelets; (4) the virtual absence of formal tools (low diversity and low frequency). This set of observations suggests some similarities between the ELSA technology of EBC and the one of BC, although these two assemblages are separated in time by more than 15 000 years.

The sequence of EBC includes several discontinuities. However, we are inclined to notice some technological continuity from the MSA to the ELSA, reflected notably by the nature of the raw material provisioning strategies as well as a common use of bipolar-on-anvil percussion. The main change from the MSA to the ELSA relates to the impoverishment in formal tools and the increasing importance of bipolar-on-anvil technologies concomitant with the disappearance of prepared core technologies.

Within the sequence of EBC, the main technological change we recognize occurs between the F phase and the D phase, in other words between the ELSA and the first Robberg occupations. This technological discontinuity is illustrated by a change in the raw material provisioning strategies (Table 2) together with a change in the main techno-typological attributes (Table 3). While non-local rocks are a minor component in the ELSA, silcrete reaches up to ca. 50 % of the raw materials spectrum within the first Robberg SU. In addition, we observe new reduction sequences that are based on single platforms cores oriented towards the production of regular bladelets (Porraz et al. 2016 this issue).

Bladelets occur during the ELSA at EBC and can actually be subdivided into two main populations. The first and larger population represents quartz bladelets with a low degree of regularity, mainly produced by bipolar-on-anvil percussion. The second population of bladelets is represented by three silcrete pieces (2 bladelets, one core). But we question the association of these three elements with the ELSA due to 1) their very low number, 2) their similarities with the overlying Robberg and 3) their difference

with regard to other ELSA lithic artefacts. One bladelet comes from the SU Fael, which is immediately below the Robberg SU Dorothee; the other one originates from the SU Furb; the bladelet core comes from the top of the SU France (*décapage* France 1), in the square 2D, which is an area where the stratigraphy starts to be destroyed by secondary gypsum formation. Based on our present set of data and observations, we reject the existence of a silcrete bladelet component in association with the ELSA at EBC and favor the hypothesis of contamination from the overlying deposits.

The ELSA and the Robberg of EBC have in common the microlithic technology, the use of bipolar-on-anvil percussion technique and the manufacture of denticulates. However, the ELSA and the Robberg differ radically with regard to their raw material provisioning strategies and the nature of their reduction sequences. While the succession between the ELSA and the Robberg is abrupt at EBC, the existence of a hiatus estimated to ca. 2 000 years between these two phases does not allow further elaboration on the nature of this succession. However, the observations from EBC suggest to us that this change might have been 'rapid' at a regional scale.

In the present discussion, our aim was to provide a well-controlled case study of the technological changes experienced by southern African societies from MIS 3 to MIS 2. We have avoided some epistemological questions and tried to stay distant from a clear-cut compartmentalization between the MSA and the LSA (Parkington 1990; Mitchell 2008), focusing more on the observations and the processes of change they document.

The present set of information available for South Africa indicates some technological fragmentation at the end of MIS 3 and the beginning of MIS 2. This is suggested, first, by the chronology of the ELSA occupations at BC. While an ELSA technology developed on the edge of the Highveld area ca. 40 000 years ago, MSA technologies persisted much longer in time until ca. 25 ka BP in the Western Cape, some 2000 km westward. Interestingly, MSA technologies vanished and transformed in a similar way as the one described at BC, i.e. towards more miniaturization and less predetermination (but see Mackay et al. 2015). This technological fragmentation during MIS 3 might reflect a process of regionalization, maybe in relation with the arrival of new populations as suggested by d'Errico et al. (2012). The miniaturization that concurs with the definition of the ELSA finds its full expression within the Robberg, a pan-southern African tradition that appears more or less around 23–22 ka cal BP in a scenario that still needs to be understood (slow and gradual, rapid and gradual or abrupt?). The reinvestigation of further key sites such as Heuningneskrans, Rose Cottage, Sehonhong and Boomplaas will likely contribute to a clarification of the MSA to LSA succession in southern Africa (e.g. Beaumont 1981; Deacon 1995; Mitchell 1994; Clark 1997).

DIEPKLOOF AND ELANDS BAY CAVE IN THE VERLORENVLEI CATCHMENT

The Verlorenvlei currently represents 10 km² of a coastal and marshy lake, obstructed by a quartzitic sill. Unlike the left side of the bank where the hill of the TMG formation dominates, the right side of the river is characterized by a more sandy landscape with small isolated kopjes. It defines an area rich in resources due to the multiplicity of geological formations and ecological influences. The catchment represents a natural

west-east axis of circulation allowing one to bypass the Piketberg Mountains located to the south and it is located at about 50 km from the Olifants River that follows the Cederberg Mountains.

While many open air and sheltered Holocene sites have been recorded in the Verlorenvlei catchment, only DRS and EBC presently document occupations from the Late Pleistocene and earlier. We began the present project at EBC within the framework of the excavation carried out at DRS. It was part of a research perspective aiming to characterize the Pleistocene Stone Age of the Verlorenvlei area.

These two sites, at a distance of 14 km from each other, are two rock shelters located on the left side of the coastal lake. DRS is a large rock shelter, about 25 m wide and 20 m long, providing about 200 m² of protected space. It is located ca. 120 m above the Verlorenvlei and opens towards the east, with good views on the lake and the rocky hills that emerge from the sandy landscape. It is located at the end of the natural lake, about 14 km from the present shoreline. Excavations exposed a ca. 3 m deep sequence recording MSA occupations overlain by shallow Holocene deposits. The MSA sequence, which has not been completely explored yet, starts with occupations dated to MIS 5 and lasts until MIS 4 (Tribolo et al. 2013). There is an ongoing controversy on the luminescence age of the deposits (Jacobs et al. 2008; Tribolo et al. 2013; Jacobs & Roberts 2015), but both teams agree that the MSA occupations of the shelter are not recorded after ca. 45 ka BP.

EBC is a shelter that provides about 150 m² of protected space. It is located on the modern shoreline ca. 42 m a.s.l. a kilometer or so from the current mouth of the Verlorenvlei. It opens west and faces the Atlantic Ocean and its coast. The excavations exposed a ca. 3 m deep sequence recording MSA and LSA occupations, with shallow deposits at the base that started forming at ca. 230 ka BP and the main sequence accumulating from MIS 3 onwards (Tribolo et al. 2016 this issue).

While these two sites are located near to each other and in a similar environment, excavations document different occupational sequences. The sequence of DRS is concentrated on MIS 5 and MIS 4, while the sequence of EBC, with some shallow pre-MIS 5 deposits at its base, mostly accumulated from MIS 3 onward. This first comparison between the two well-controlled stratigraphic sequences may suggest that these two sites were not inhabited at the same time and eventually that the occupation of one shelter implied the exclusion of the other one. But inhabitants of DRS and EBC were both likely aware of the existence of the other shelter. We have evidence that DRS inhabitants frequented the shoreline (and most likely the EBC area), as depicted by the marine resources that were brought back to the site (Steele & Klein 2013). Concomitantly, we have evidence that EBC inhabitants frequented the inland area, as silcrete artefacts macroscopically similar to the raw materials from Redelinghuys have been found in the lithic assemblages. The exploitation of the Redelinghuys silcrete outcrop, located on the left side of the Verlorenvlei about 20 km eastward of the present shoreline, indicates that EBC people had to pass by DRS.

Various reasons, not exclusive of one another, may explain why the records from DRS and EBC differ so radically. These reasons might relate to changes in the settlement systems of the populations and/or in their subsistence strategies, to climatic factors as well as to differences in the way inhabitants of the Verlorenvlei culturally perceived this living area. Consequently, there might be different scenarios explaining why DRS

and EBC do not record similar occupational events. But the null hypothesis is to interrogate the site formation processes. Are there any observations that support the hypothesis that these two sites might have recorded similar occupations that would have been later erased by post-depositional agents?

At DRS, the micromorphological study done by Miller et al. (2013) indicates a fairly continuous depositional sequence. There is no evidence in the studied sequence for major phases of erosion or significant hiatuses in deposition, although trampled surfaces have been identified which are suggestive of minor discontinuities. However, the overall archaeological record (Porraz, Texier et al. 2013, Parkington et al. 2013) is consistent with the study of Miller et al. (2013) and supports a fairly continuous record. Thus, the main question unresolved—besides the lower deposits that remain unexcavated—concerns the post-MIS 4 deposits. At DRS, the deposits on top of the MSA take the form of shallow LSA bedding and a few pits that date to about 2 ka BP (Parkington & Poggenpoel 1987). This suggests a major hiatus (in sedimentation and possibly occupation) of more than 50 000 years, which, if reflecting an absence of occupation, would be enigmatic considering the prominent place of Diepkloof in the landscape as well as the set of evidence that testifies to a local presence during that time period.

Although the sequence at DRS suggests more or less continuous sedimentation until ca. 45 ka, at EBC, the situation is clearly different (Miller et al. 2016 this issue). In contrast to DRS, the site is largely exposed to atmospheric elements that have favoured the formation of secondary minerals and contributed to the disturbance of the stratigraphy in some areas. The shelter itself is formed by tabular joints favoring the circulation of water that is still active today. With regard to the question of continuities and discontinuities, the micromorphological study indicates a sharp and clear contact between SU Keva, associated with EMSA occupations, and the SUs Kelly/Kent which reflect post-HP occupations. In this context, deposits contemporaneous to those from DRS might have existed at EBC, but subsequent post-depositional agents including erosion likely would have removed them. Maybe DRS inhabitants occupied the shelter of EBC too, but the deposits recording their visits have been subsequently eroded, making it difficult to construct a narrative on how these two sites complemented one another during MIS 5 and MIS 4. Regardless of whether we have the full picture of human occupation in the Verlorenvlei or not, we are still left with the question of why was EBC favoured by hunter-gatherers in MIS 3 and onwards?

This comparison between DRS and EBC first aims at emphasizing the richness and importance of the archaeological heritage of the Verlorenvlei area. We recognize that our narrative requires integrating more sources of information: firstly the archaeological data from the landscape (Mackay 2016 this issue), secondly the palaeoenvironmental data from the riverine and sea coring. However, we regard this discussion as a first attempt to build and explain a local scenario before trying to integrate a large set of archaeological data from a regional to a macro-regional and sub-continental scale. DRS and EBC are two important landmarks in the Verlorenvlei area. Why these two sites present such different occupational records surely relates to the geological factors that have contributed to erase the past, as well as to the environmental settings that have changed through time and that have impacted the subsistence strategies of population. But, we finally have to acknowledge that a territory is also a cultural representation that belongs to a memory and the set of symbols defining the living world of the populations.

The temporary depopulation of an area and/or the replacement of a population might introduce major breaks in cultural transmission and territorial representation. Such mechanisms could be one alternative factor explaining changes in living places within the Verlorenvlei catchment.

By introducing and discussing the Verlorenvlei Stone Age, our intention was to provide an additional piece in the chrono-cultural puzzle of the Late Pleistocene Stone Age of South Africa. We also take a strong stand for continuing efforts to revisit and revise sites that have been previously excavated. As we believe the work presented in this special volume shows, this approach allows us to not only study and secure these important stratigraphic sections, but it also provides new insights into the sites' formation histories, their chronologies, and the lifeways and technological know-how of their Pleistocene inhabitants.

ACKNOWLEDGMENTS

We thank the French Ministry of Foreign Affairs and the Deutsche Forschung Gemeinschaft(Grant number: 17091015) for funding the excavation at EBC and the National Research Agency for the dating study (ANR-09-JCJC-0123-01). We thank the University of Cape Town and the Iziko Museum for their support as well as the South African Heritage Resources Agency for providing the research permit (2011/04/001). Many thanks to Sébastien Bernard-Guelle and Will Archer for their presence and inputs during our fieldwork, to David Brown for the loan of the total station as well as to Louisa Hutten and Dolores Jacobs for their constant help. We finally express our gratitude to the French Institute of South Africa and to PAST for funding the publication, to Richard Klein and Alex Mackay for their comments and inputs as well as to Gavin Whitelaw, who helped and assisted all along the compilation of the EBC papers.

REFERENCES

Archer, W., Gunz, P., van Niekerk, K.L., Henshilwood, C.S., & McPherron, S.P. 2015. Diachronic change within the Still Bay at Blombos cave, South Africa. *PloS ONE* **10** (7): e0132428.

Avery, G., Halkett, D.J., Orton, J., Steele, T., Tusenius, M. & Klein, R.G. 2008. The Ysterfontein 1 Middle Stone Age Rock Shelter and the evolution of coastal foraging. *South African Archaeological Society Goodwin Series* **10**: 66–89.

Baxter, A.J. 1997. *Late Quaternary palaeoenvironments of the Sandveld, Western Cape Province, South Africa*. PhD dissertation, University of Cape Town.

Beaumont, P.B. 1981. The Heuningneskrans Shelter. In: E.A. Voigt, ed., *Guide to archaeological sites in the northern and eastern Transvaal*. Prepared for the Southern African Association of Archaeologists Excursion, 6–11 June, pp. 132–45.

Beaumont, P.B. & Vogel, J.C. 1972. On a new radiocarbon chronology for Africa south of the Equator: Part 2. *African Studies* **31** (3): 155–182.

Beaumont, P.B., De Villiers, H. & Vogel, J.C. 1978. Modern man in sub-Saharan Africa prior to 49 000 years B.P.: a review and evaluation with particular reference to Border Cave. *South African Journal of Science* **74**: 409–19.

Boëda, É. 1993. Le débitage Discoïde et le débitage Levallois récurrent centripète. *Bulletin de la SociétéPréhistorique Française* **90**: 392–404.

Brown, K.S., Marean, C.W., Herries, A.I., Jacobs, Z., Tribolo, C., Braun, D., Roberts D.L., Meyer M.C. & Bernatchez, J. 2009. Fire as an engineering tool of early modern humans. *Science* **325** (5942): 859–62.

Butzer, K.W. 1979. Geomorphology & Geo-archaeology at Elandsbaai, Western Cape, South Africa. *Catena* **6**: 157–66.

Carter, P.L. & Vogel, J.C. 1974. The dating of industrial assemblages from stratified sites in eastern Lesotho. *Man* **9**: 557–70.

Cartwright, C.R. 2013. Identifying the woody resources of Diepkloof Rock Shelter (South Africa) using scanning electron microscopy of the MSA wood charcoal assemblages. *Journal of Archaeological Science* **40**: 3463–74.

Cartwright, C.R. & Parkington, J.E. 1997. The wood charcoal assemblages from Elands Bay Cave, southwestern Cape: principles, procedures and preliminary interpretation. *South African Archaeological Bulletin* **52**: 59–72.

Cartwright, C.R., Parkington, J.E. & Cowling, R.M. 2014. Understanding late and terminal Pleistocene vegetation change in the Western Cape, South Africa: the wood charcoal evidence from Elands Bay Cave, In: C.J. Stevens, S. Nixon, M.A. Murray & D.Q. Fuller, eds., *Archaeology of African Plant Use*. Left Coast Press, Walnut Creek, California, pp. 59–72.

Cartwright, C., Parkington, J.E. & Porraz, G. 2016. The wood charcoal evidence from renewed excavations at Elands Bay Cave. *Southern African Humanities* **29**: 249–58.

Chase, B.M. & Thomas, D.S.G. 2006. Late Quaternary dune accumulation along the western margin of South Africa: distinguishing forcing mechanisms through the analysis of migratory dune forms. *Earth and Planetary Science Letters* **251**: 318–33.

Clark, A.M.B. 1997. The MSA/LSA transition in southern Africa: new technological evidence from Rose Cottage Cave. *South African Archaeological Bulletin* **52**: 113–21.

Conard, N.J., Porraz, G. & Wadley, L. 2012. What is in a name? Characterising the post-Howieson's Poort at Sibudu. *South African Archaeological Bulletin* **67**: 180–99.

Conard, N.J. & Will, M. 2015.Examining the causes and consequences of short-term behavioral change during the Middle Stone Age at Sibudu, South Africa. *PloS ONE* **10** (6): e0130001.

Cowling, R.M., Cartwright C., Parkington, J.E. & Allsopp, J.C. 1999. Fossil wood assemblages from Elands Bay Cave, South Africa: implications for Late Quaternary vegetation and climates in the winter-rainfall fynbos biome. *Journal of Biogeography* **26** (2): 367–78.

Deacon, H.J. 1995.Two late Pleistocene-Holocene archaeological depositories from the southern Cape, South Africa. *South African Archaeological Bulletin* **50**: 121–31.

Delagnes, A., Schmidt, P., Douze, K., Wurz, S., Bellot-Gurlet, L., Conard, N.J., Nickel, K.G., Van Niekerk, L. & Henshilwood, C.S. 2016. Early evidence for the extensive heat treatment of silcrete in the Howiesons Poort at Klipdrift Shelter (Layer PBD, 65 ka), South Africa. *PLoS ONE* **11** (10): e0163874.

d'Errico, F., Backwell, L., Villa, P., Degano, I., Lucejko, J.J., Bamford, M.K., Higham T.F.G., Colombini M.P. & Beaumont, P.B. 2012. Early evidence of San material culture represented by organic artifacts from Border Cave, South Africa. *Proceedings of the National Academy of Sciences* **109** (33): 13214–19.

Hallinan, E. 2013. *Stone Age landscape use in the Olifants River Valley, Western Cape*. MPhil, University of Cape Town.

Högberg, A. & Larsson, L. 2011. Lithic technology and behavioural modernity: new results from the Still Bay site, Hollow Rock Shelter, Western Cape Province, South Africa. *Journal of Human Evolution* **61**: 133–55.

Jacobs, Z., Roberts, R.G., Galbraith, R.F., Deacon, H.J., Grün, R., Mackay, A., Mitchell, P.J., Vogelsang, R. & Wadley, L. 2008. Ages for the Middle Stone Age of southern Africa: implications for human behavior and dispersal. *Science* **322**: 733–5.

Jacobs, Z. & Roberts, R.G. 2015. An improved single grain OSL chronology for the sedimentary deposits from Diepkloof Rockshelter, Western Cape, South Africa. *Journal of Archaeological Science* **63**: 175–92.

Jerardino, A. 1993. Mid to Late Holocene sea level fluctuations: the archaeological evidence at Tortoise Cave, south Western Cape, South Africa. *South African Journal of Science* **89**: 481–8.

Jerardino, A. 2013.Two complementary Holocene lithic assemblages from Elands Bay and Lamberts Bay: implications for local changes in toolkit and group mobility. *South African Archaeological Bulletin* **68**: 188–99.

Jerardino, A., Klein, R.G., Navarro, R.A., Orton, J. & Horwitz, L.K. 2013.Settlement and subsistence patterns since the terminal Pleistocene in the Elands Bay and Lamberts Bay areas. In: A. Jerardino, A. Malan & D. Braun, eds., *The archaeology of the West Coast of South Africa*. Cambridge Monographs in African Archaeology 84. BAR International Series 2526. Oxford: BAR, pp. 85–108.

Kandel, A.W. & Conard, N.J. 2012. Settlement patterns during the Earlier and Middle Stone Age around Langebaan Lagoon, western Cape (South Africa). *Quaternary International* **270**: 15–29.

Kaplan, J.M. 1989. 45 000 years of hunter-gatherer history in Natal as seen from Umhlatuzana Rock Shelter. *South African Archaeological Society Goodwin Series* **6**: 7–16.

Klein, R.G. 1974. Environment and subsistence of prehistoric man in the southern Cape Province, South Africa. *World Archaeology* **5** (3): 249–84.

Klein, R.G. 2001. Southern Africa and modern humans origins. *Journal of Anthropological Research* **57**: 1–16.

Lombard, M., Wadley, L., Deacon, J., Wurz, S., Parsons, I., Mohapi, M., Swart, J. & Mitchell, P. 2012. South African and Lesotho Stone Age sequence updated I. *South African Archaeological Bulletin* **67**:120–44.

Lovis, W.A. & Whallon, R. 2016. *Marking the land: hunter-gatherer creation of meaning in their environment*. Routledge.

Mackay, A. 2009. *History and selection in the late Pleistocene archaeology of the Western Cape, South Africa*. PhD, Australian National University.

Mackay, A. 2010. The late Pleistocene archaeology of Klein Kliphuis rock shelter, Western Cape, South Africa: 2006 excavations. *South African Archaeological Bulletin* **65**: 132–47.

Mackay, A., Jacobs, Z. & Steele, T.E. 2015.Pleistocene archaeology and chronology of Putslaagte 8 (PL8) rockshelter, Western Cape, South Africa. *Journal of African Archaeology* **13** (1): 71–98.

Mackay, A. 2016. Three arcs: observations on the archaeology of the Elands Bay and northern Cederberg landscapes. *Southern African Humanities* **29**: 1–15.
Miller, C.E., Goldberg, P. & Berna, F., 2013. Geoarchaeological investigations at Diepkloof Rock Shelter, Western Cape, South Africa. *Journal of Archaeological Science* **40** (9): 3432–52.
Miller, C.E., Mentzer, S., Berthold, C., Leach, P., Schulz H., Tribolo, C., Parkington, J. & Porraz, G. 2016. Site formation processes of the Middle Stone Age deposits from Elands Bay Cave, South Africa. *Southern African Humanities* **29**: 69–128.
Miller, D. 1987. Geoarchaeology at Elands Bay. In: J.E. Parkington & M. Hall, eds, *Papers in the prehistory of the western Cape, South Africa*. Oxford: BAR, pp. 46–77.
Mitchell, P.J. 1994. Understanding the MSA/LSA transition: the pre-20,000 BP assemblages from new excavations at Sehonghong rock-shelter, Lesotho. *Southern African Field Archaeology* **3**: 15–25.
Mitchell, P.J. 2002. *The archaeology of southern Africa*. Oxford, Cambridge University Press.
Mitchell, P.J. 2008. Developing the archaeology of Marine Isotope Stage 3. *South African Archaeological Society Goodwin Series* **10**: 52–65.
Mitchell, P.J. 2012. San origins and transition to the Later Stone Age: new research from Border Cave, South Africa. *South African Journal of Science* **108** (11–12): 5–7.
Mitchell, P.J. & Steinberg, J.M. 1992. A Middle Stone Age Sequence from western Lesotho. *South African Archaeological Bulletin* **47**: 26–33.
Orton, J. 2006. The Later Stone Age lithic sequence at Elands Bay, Western Cape, South Africa: raw material, artefacts and sporadic change. *Southern African Humanities* **18** (2): 1–28.
Ossendorf, G. 2013. *Spätpleistozäne Jäger-Sammler des südwestlichen Namibias*. PhD thesis, University of Cologne.
Pargeter, J. 2014. The Later Stone Age is not San prehistory. *The Digging Stick* **31**: 1–4.
Parkington, J.E. 1972. Seasonal mobility in the late Stone Age. *African Studies* **31**: 223–44.
Parkington, J.E. 1976. Coastal settlement between the mouths of the Berg and the Olifants rivers, Cape Province. *South African Archaeological Bulletin* **31**: 127–40.
Parkington, J.E. 1981. The effects of environmental change on the scheduling of visits to the Elands Bay Cave, Cape Province, South Africa. In: I. Hodder, G. Isaac & N. Hammond, eds, *Pattern of the past: studies in honour of David Clarke*. Cambridge: Cambridge University Press, pp. 341–59.
Parkington, J.E. 1984. Changing views of the Later Stone Age of South Africa. *Advances in World Archaeology* **3**: 89–142.
Parkington, J.E. 1988. The Pleistocene/Holocene transition in the Western Cape, South Africa: observations from Verlorenvlei. In: J. Bower & D. Lubell, eds., *Prehistoric cultures and environments in the Late Quaternary of Africa*. Cambridge Monographs in African Archaeology 26. BAR International Series 405. Oxford: BAR, pp. 197–206.
Parkington, J.E. 1990. A view from the south: southern Africa before, during and after the Last Glacial Maximum. In: C. Gamble & O. Soffer, eds., *The World at 18 000 BP: the low latitudes*. London: Unwin Hyman, pp. 214–28.
Parkington, J.E. 1992. Making sense of sequence at the Elands Bay cave, western Cape, South Africa. In: A. Smith & B. Mütti, eds, *Guide to archaeological sites in the south-western Cape*. Prepared for the Southern African Association of Archaeologists Excursion, 5–9 July, pp. 6–12.
Parkington, J.E. 2001. Milestones: the impact of systematic exploitation of marine foods on human evolution. In: P.V. Tobias, M.A. Raath, J. Moggi-Cechi & G.A. Doyle, eds, *Humanity from African naissance to coming millenia*. Florence: Florence University Press, pp.327–36.
Parkington, J.E. 2016. Elands Bay Cave: keeping an eye on the past. *Southern African Humanities* **29**: 17–32.
Parkington, J.E. & Poggenpoel, C.A. 1971. Excavations at De Hangen, 1968.*South African Archaeological Bulletin* **26**: 3–36.
Parkington, J.E. & Poggenpoel, C.A. 1987.Diepkloof Rock Shelter. In: J.E. Parkington & M. Hall, eds, *Papers in the prehistory of the Western Cape, South Africa*. Oxford: B.A.R., pp 269–93.
Parkington, J.E., Poggenpoel, C.A., Buchanan, W., Robey, T., Manhire, A. & Sealy, J. 1988. Holocene coastal settlement patterns in the Western Cape. In: G. Bailey & J.E. Parkington, eds., *The archaeology of prehistoric coastlines*. Cambridge, Cambridge University Press, pp. 22–41.
Parkington, J.E., Baxter, A., Cartwright, C., Cowling, R.M. & Meadows, M. 2000.Palaeovegetation at the last glacial maximum in the Western Cape, South Africa: wood charcoal and pollen evidence from Elands Bay Cave. *South African Journal of Science* **96** (11–12): 543–6.
Parkington, J.E., Rigaud, J.-P., Poggenpoel, C., Porraz, G. & Texier, P.-J. 2013. Introduction to the project and excavation of Diepkloof Rock Shelter (Western Cape, South Africa): a view on the Middle Stone Age. *Journal of Archaeological Science* **40**: 3369–75.
Parkington, J.E., Fisher Jr, J.W., Poggenpoel, C.A. & Kyriacou, K. 2014.Strandloping as a resource gathering strategy in the Cape, South African Holocene Later Stone Age: the Verlorenvlei record. *Journal of Island and Coastal Archaeology* **9** (2): 219–37.

Parkington, J.E. & Porraz, G. 2016. Elands Bay Cave and the Stone Age of the Verlorenvlei, South Africa. *Southern African Humanities* **29**: 1–306.
Porraz, G., Parkington, J.E., Rigaud, J.-P., Miller, C.E., Poggenpoel, C., Tribolo, C., Archer, W., Cartwright, C.R., Charrié-Duhaut, A., Dayet, L., Igreja, M., Mercier, N., Schmidt, P., Verna, C. & Texier, P.-J. 2013. The MSA sequence of Diepkloof and the history of southern African Late Pleistocene populations. *Journal of Archaeological Science* **40**: 3542–52.
Porraz, G., Texier, P.-J., Archer, W., Piboule, M., Rigaud J.-P. & Tribolo, C. 2013. Technological successions in the Middle Stone Age sequence of Diepkloof Rock Shelter, Western Cape, South Africa. *Journal of Archaeological Science* **40**: 3376–400.
Porraz, G., Igreja, M., Schmidt, P. & Parkington, J.E. 2016. A shape to the microlithic Robberg of Elands Bay Cave (South Africa). *Southern African Humanities* **29**: 203–47.
Robertson, H.N. 1980. *An assessment of the utility of Verlorenvlei water*. MSc thesis, University of Cape Town.
Rogers, J. 1987. The evolution of the continental terrace between St Helena Bay and Lambert's Bay. In: J. E. Parkington & M. Hall, eds., *Papers in the Prehistory of the Western Cape, South Africa*. Oxford: B.A.R., pp. 35–45.
Schmid, V.C., Conard, N.J., Parkington, J.E., Texier P.-J. & Porraz, G. 2016. The 'MSA 1' of Elands Bay Cave (Western Cape Province, South Africa) in the context of the southern African Early Middle Stone Age technologies. *Southern African Humanities* **29**: 153–201.
Schmidt, P., Porraz, G., Bellot-Gurlet, L., February, E., Ligouis, B., Paris, C., Texier, P.-J., Parkington, J.E., Miller, C.E., Nickel, K.G. & Conard, N.J. 2015. A previously undescribed organic residue sheds light on heat treatment in the Middle Stone Age. *Journal of human evolution* **85**: 22–34.
Schmidt, P. & Mackay, A. 2016. Why was silcrete heat-treated in the Middle Stone Age? An early transformative technology in the context of raw material use at Mertenhof Rock Shelter, South Africa. *PLoS ONE* **11**: e0149243.
Sinclair, S.A., Lane, S.B. & Grindley, J.R. 1986. In: A.E.F. Heydorn & P.D. Morant, eds, *Estuaries of the Cape, Part 2: synopses of available information on individual system*. Report 32, Verlorenvlei. Report 431. Stellenbosch: Council for Scientific and Industrial Research.
Soriano, S., Villa, P., Delagnes, A., Degano, I., Pollarolo, L., Lucejko, J.J., Henshilwood, C.S. & Wadley, L. 2015. The Still Bay and Howiesons Poort at Sibudu and Blombos: understanding Middle Stone Age technologies. *PLoS ONE* **10**: 1–46.
Steele, T.E. & Klein, R.G. 2013. The Middle and Later Stone Age faunal remains from Diepkloof Rock Shelter, Western Cape, South Africa. *Journal of Archaeological Science* **40** (9): 3453–62.
Tankard, A.J. 1976.Pleistocene history and coastal morphology of the Ysterfontein-ElandsBay area, Cape Province. *Annals of the South African Museum* **69**: 73–119.
Texier, P.-J., Porraz, G. Parkington, J.E., Rigaud, J.-P., Poggenpoel, C.A., Miller, C.E., Tribolo, C., Cartwright, C.R., Coudenneau, A., Klein, R.G., Steele, T. &Verna, C. 2010. A Howiesons Poort tradition of engraving ostrich eggshell containers dated to 60,000 years ago at Diepkloof Rock Shelter, South Africa. *Proceedings of the National Academy of Sciences of the United States of America* **107**: 6180–5.
Tribolo, C., Mercier, N., Douville, E., Joron, J.-L., Reyss, J.-L., Rufer, D., Cantin, N., Lefrais, Y., Miller, C.E., Parkington, J.E., Porraz, G., Rigaud, J.-P. & Texier, P.-J. 2013. OSL and TL dating of the Middle Stone Age sequence of Diepkloof Rock Shelter (Western Cape, South Africa): a clarification. *Journal of Archaeological Science* **40**: 3401–11.
Tribolo, C., Mercier, N., Valladas, H., Miller, C.E., Parkington, J.E. & Porraz, G. 2016. Chronology of the Pleistocene deposits at Elands Bay Cave (South Africa) based on charcoals, burnt lithics, and sedimentary quartz and feldspar grains. *Southern African Humanities* **29**: 129–52.
Villa, P., Soriano, S., Tsanova, T., Degano, I., Higham, T., d'Errico, F., Backwell, L., Lucejko, J., Colombini, M.P. & Beaumont, P.B. 2012. Border Cave and the beginning of the Later Stone Age in South Africa. *Proceedings of the National Academy of Sciences* **109** (33): 13208–13.
Volman, T.P. 1981. *The Middle Stone Age in the southern Cape*. PhD thesis, University of Chicago.
Volman, T.P. 1984. Early prehistory of southern Africa. In: R.G. Klein, ed., *Southern African Prehistory and Palaeoenvironments*. Rotterdam: Balkema, pp. 169–220.
Wadley, L. 2005. A typological study of the final Middle Stone Age stone tools from Sibudu Cave, KwaZulu-Natal. *South African Archaeological Bulletin* **60**: 51–63.
Will, M., Parkington, J.E., Kandel, A.W. & Conard, N.J. 2013. Coastal adaptations & the Middle Stone Age lithic assemblages from Hoedjiespunt 1 in the Western Cape, South Africa. *Journal of Human Evolution* **64**: 518–37.
Will, M. & Conard, N.J. 2016. What drives cultural change in the Middle Stone Age of Sibudu, KwaZulu-Natal? *Quaternary International* **404**: 206.
Wurz, S. 2012. The significance of MIS 5 shell middens on the Cape coast: a lithic perspective from Klasies River and Ysterfontein 1. *Quaternary International* **270**: 61–9.

TABLE 1
Density of lithic artefacts at Elands Bay Cave based on the 2011 excavation.

	Total Lithics > 20mm (N)	Excavated volume (L)	Density Lithics/L
Delport	34	unknown	unknown
Dennis	13	unknown	unknown
Denver	71	20	3,5
Dorothee	57	12	4,5
Fael	24	8	3
Fannie	15	29	0,5
Farik	13	3	4,5
Fatim	18	21	1
Felice	22	7	3
Ferdinand	10	4	2,5
Flavie	6	6	1
France	133	40	3,5
Frida	25	6	4
Fro	30	6	5
Furb	58	22	2,5
Fuzy	71	27	2,5
Harry/Ha	20	10	2
Hazel	24	16	1,5
Henri	70	54	1,5
Ian/I	8	6	1
Ibis	31	39	1
Igor	34	55	0,5
Imran/Ilian	30	49	0,5
Imriz	14	27	0,5
Ines	22	25	1
Jacob	125	43	3
Juste	112	41	2,5
Kali/Kamoa	60	32	2
Kelly	23	16	1,5
Kent	30	16	2
Keva	615	54	11,5
Lara	274	62	4,5
Liam/Letty	500	50	10
TOTAL	2592	-	-

TABLE 2
Classification (%) per raw material of the 2011 lithic collection from Elands Bay Cave.

		Coarse-grained quartzite	Quartz	Silcrete (N heated)	Fine-grained quartzite	Hornfels	CCS	Others	Total % (N)
Robberg	**Delport/Dennis**	23	49	28 (7)	0	0	0	0	**100 % (47)**
	Denver	8	46	41 (18)	3	0	2	0	**100 % (71)**
	Dorothee	5	43	49 (15)	0	0	3	0	**100 % (57)**
ELSA	**Fael/Fannie**	10	72	10	5	0	3	0	**100 % (39)**
	Farik/Fatim	22	72	3 (1)	3	0	0	0	**100 % (31)**
	Felice/Ferdinand	7	87	3 (1)	3	0	0	0	**100 % (32)**
	Flavie/France	13	80	4 (1)	1	0	1	1	**100 % (139)**
	Frida/Fro	13	73	2 (1)	4	5	3	0	**100 % (55)**
	Furb	15	78	5	2	0	0	0	**100 % (58)**
	Fuzy	12	72	11 (3)	1	4	0	0	**100 % (67)**
	Harry/Hazel	8	70	11 (1)	9	0	2	0	**100 % (44)**
	Henri	20	67	6 (2)	6	1	0	0	**100 % (70)**

TABLE 2 (*continued*)
Classification (%) per raw material of the 2011 lithic collection from Elands Bay Cave.

		Coarse-grained quartzite	Quartz	Silcrete (N heated)	Fine-grained quartzite	Hornfels	CCS	Others	Total % (N)
Late MSA J–I	**Ian/Ibis**	13	79	5 (1)	3	0	0	0	**100 % (39)**
	Igor	0	97	3	0	0	0	0	**100 % (34)**
	Imran/Ilian	7	83	0	7	3	0	0	**100 % (30)**
	Imriz/Ines	14	83	0	3	0	0	0	**100 % (36)**
	Jacob	7	84	6 (3)	2	0	1	0	**100 % (125)**
	Juste	7	82	8 (7)	3	0	0	0	**100 % (112)**
MSA K	**Kali/Kamoa**	23	55	12	10	0	0	0	**100 % (60)**
	Kelly/Kent	41	45	6	4	0	2	2	**100 % (53)**
EMSA	**Keva**	98	0,5	0,5	0,5	0	0,5	0	**100 % (615)**
	Lara	99	1	0	0	0	0	0	**100 % (274)**
	Liam/Letty	98	1	0,5	0,5	0	0	0	**100 % (500)**

TABLE 3
Technological classification of the 2011 lithic collection from Elands Bay Cave.

		Flakes	Bipolar flakes	Discoid flakes	Blades	Bladelets	Cores	Anvil/ Bipolarcores	Fragments > 20mm	Total % (N)
Robberg	Delport/Dennis	36	6	0	6	23	8	16	5	**100 % (47)**
	Denver	24	7	0	3	42	10	8	6	**100 % (71)**
	Dorothee	12	0	0	7	51	7	12	11	**100 % (57)**
ELSA	Fael/Fannie	39	20	0	2	8	0	10	21	**100 % (39)**
	Farik/Fatim	39	19	3	0	6	0	3	30	**100 % (31)**
	Felice/Ferdinand	40	16	0	3	9	0	6	26	**100 % (32)**
	Flavie/France	42	24	1	0	1	1	7	24	**100 % (139)**
	Frida/Fro	27	22	2	0	5	0	14	30	**100 % (55)**
	Furb	41	19	5	2	3	0	5	25	**100 % (58)**
	Fuzy	44	20	1	6	7	1	3	18	**100 % (71)**
	Harry/Hazel	41	7	2	0	4	0	7	39	**100 % (44)**
	Henri	48	11	4	1	6	1	0	29	**100 % (70)**

TABLE 3 (*continued*)
Technological classification of the 2011 lithic collection from Elands Bay Cave.

		Flakes	Bipolar flakes	Discoid flakes	Blades	Bladelets	Cores	Anvil/ Bipolarcores	Fragments > 20mm	Total % (N)
Late MSA J–I	**Ian/Ibis**	36	26	5	0	3	0	5	25	**100 % (39)**
	Igor	29	18	3	9	0	0	12	29	**100 % (34)**
	Imran/Ilian	27	23	7	7	3	3	13	17	**100 % (30)**
	Imriz/Ines	44	17	3	5	3	3	11	14	**100 % (36)**
	Jacob	41	21	5	5	0	1	3	24	**100 % (125)**
	Juste	41	26	5	5	2	0	4	17	**100 % (112)**
MSA K	**Kali/Kamoa**	50	22	10	8	0	5	0	5	**100 % (60)**
	Kelly/Kent	53	15	15	6	0	4	0	7	**100 % (53)**
EMSA	**Keva**	76	2	8	3	0	5	0	6	**100 % (615)**
	Lara	78	3	9	2	0	6	0	2	**100 % (274)**
	Liam/Letty	36	1	4	1	0	2	0	56	**100 % (500)**

TABLE 4

Typological classification of the 2011 lithic collection from Elands Bay Cave.

		Denticulates/ notches	Scrapers	Convergent scrapers	Bifacial pieces	Retouched bladelets	Fragments / others	Total (N)
Robberg	Delport/Dennis	1	0	0	0	0	0	1
	Denver	1	0	0	0	3	0	4
	Dorothee	0	1	1	0	2	0	4
ELSA	Fael/Fannie	1	0	0	0	0	0	1
	Farik/Fatim	0	0	0	0	0	0	0
	Felice/Ferdinand	1	0	0	0	0	0	1
	Flavie/France	2	2	0	0	0	0	4
	Frida/Fro	1	1	0	0	0	0	2
	Furb	1	0	0	0	0	0	1
	Fuzy	2	0	1	0	0	0	3
	Harry/Hazel	2	1	0	0	0	0	3
	Henri	1	1	0	0	0	0	2
Late MSA J–I	Ian/Ibis	0	0	0	0	0	0	0
	Igor	0	0	0	0	0	0	0
	Imran/Ilian	1	0	0	0	0	0	1
	Imriz/Ines	0	0	0	0	0	0	0
	Jacob	2	1	0	1	0	0	4
	Juste	3	2	0	0	0	0	5
MSA K	Kali/Kamoa	2	0	0	0	0	0	2
	Kelly/Kent	6	0	0	0	0	0	6
EMSA	Keva	4	1	0	0	0	0	5
	Lara	2	3	0	0	0	1	6
	Liam/Letty	0	1	0	0	0	0	1

Southern African Humanities **29**: 69–128 December 2016 KwaZulu-Natal Museum

Site-formation processes at Elands Bay Cave, South Africa

[1]**Christopher E. Miller,** [2,3]**Susan M. Mentzer**, [4]**Christoph Berthold**, [5]**Peter Leach**, [6]**Bertrand Ligouis**, [7]**Chantal Tribolo**, [8]**John Parkington** and [9,10]**Guillaume Porraz**

[1]Institute for Archaeological Sciences, and Senckenberg Centre for Human Evolution and Paleoenvironment, University of Tübingen, Rümelinstraße 23, 72070, Tübingen, Germany; christopher.miller@uni-tuebingen.de

[2]Institute for Archaeological Sciences, University of Tübingen, Rümelinstraße 23, 72070 Tübingen, Germany; susan.mentzer@ifu.uni-tuebingen.de

[3]School of Anthropology, University of Arizona, 1009 E. South Campus Room 210, Tucson, Arizona 85721; USA

[4]Competence Center Archaeometry – Baden Wuerttemberg (CCA-BW) Applied Mineralogy, University of Tübingen, Wilhelmstraße 56, 72076 Tübingen, Germany; christoph.berthold@uni-tuebingen.de

[5]Department of Anthropology, University of Connecticut, 354 Mansfield Road, Storrs, Connecticut 06269, USA; peter.leach@uconn.edu

[6]Laboratories for Applied Organic Petrology AND Institute for Archaeological Sciences, University of Tübingen, Rümelinstraße 23, 72070, Tübingen, Germany; Bertrand.ligouis@uni-tuebingen.de

[7]CNRS – Université de Bordeaux, UMR 5060, IRAMAT-CRP2A, Maison de l'archéologie, Esplanade des Antilles, 33607 Pessac cedex, France; ctribolo@u-bordeaux3.fr

[8]Department of Archaeology, University of Cape Town, South Africa; John.Parkington@uct.ac.za

[9]CNRS, USR 3336, Institut Français d'Afrique du Sud, Johannesburg, South Africa; guillaume.porraz@mae.u-paris10.fr

[10]Evolutionary Studies Institute - Honorary Research Fellow, University of the Witwatersrand, South Africa

ABSTRACT

Elands Bay Cave is a small coastal rock shelter formed in quartzite that contained up to ca. 3 m of anthropogenic and geogenic deposits with archaeological materials dating to the Middle Stone Age through Later Stone Age. Today, only the lower portion of the sedimentary sequence, comprising ca. 1.2 m of sediment remains. A geoarchaeological study of the remaining deposits was undertaken in conjunction with renewed excavations of the site (2010–2012). A ground penetrating radar survey revealed that the excavation area targeted the deepest portion of the sedimentary infill within the rock shelter. Furthermore, micromorphological analyses of the remaining Middle and Later Stone Age deposits indicate that combustion features are present. Fourier transform infrared spectroscopy and x-ray diffraction measurements were used to identify secondary minerals, including taranakite, hydroxylapatite, gypsum, variscite, ardealite, opal, and whitlockite. The distributions of these secondary minerals—present mainly as microcrystalline nodules—track zones of moisture within the sediment, as well as areas where calcium carbonate (e.g. ashes, shell) and bones are not preserved. In addition to the chemical dissolution of several components of the archaeological assemblage, secondary processes impacting the Elands Bay Cave deposits include bioturbation and mechanical fragmentation of rocks and charcoal. Despite the effects of post-depositional alteration, our study indicates a good degree of localized preservation of the stratigraphic units.

KEY WORDS: micromorphology, site formation processes, diagenesis, FTIR, XRD, SEM-EDS, ground penetrating radar, organic petrology, rock shelter, cave, combustion features, environmental archaeology, Middle Stone Age.

Elands Bay Cave is a widely cited case study used to introduce students to the fundamental concepts of environmental archaeology. Highlighted in first-year texts such as Renfrew and Bahn (2008), the site provides a compelling story that links Later Stone Age human habitation of the cave and exploitation of local marine resources with paleoenvironmental proxy data. Less well-known, but still significant to the

ISSN 2305-2791 (online); 1681-5564 (print)

southern African archaeological community are the Middle and earlier Later Stone Age deposits within the site, which in combination with the Later Stone Age midden, provided Parkington and colleagues a medium for the development of a unique method of stratigraphic nomenclature that facilitates lithostratigraphic analysis and today is employed throughout the Western Cape (e.g. Porraz et al. 2013). For geoarchaeologists, the site is additionally significant due to the presence of deposits that range from merely rich in anthropogenic sediment to the midden that is composed almost entirely of material of human origin. The site thus provides a laboratory for the study of anthropogenic deposits, as well as the post-depositional processes unique to siliceous bedrock settings that impact their preservation.

The geoarchaeological study described here expands upon previous stratigraphic and sedimentological studies conducted at the site (e.g. Butzer 1979), and aims to reconstruct the formation processes that operated at a site scale, including human and non-human depositional mechanisms. We employ a combination of high-resolution analytical methods including micromorphology, microspectroscopy, organic petrology and elemental compositional analyses of present-day moisture inputs to the site in order to: 1) make micro-scale observations of mm- to cm-scale stratigraphic units and features defined on the basis of sediment composition, fabric and structure; and 2) to document the mineralogical traces of post-depositional chemical diagenesis. The results of these analyses are integrated with site-scale observations of cm- to dm-scale stratigraphic units and lateral variation therein with the aim of reconstructing a probable sequence of deposition and stasis—intimately related to human occupation of the site—and the post-depositional chemical and physical processes that contribute to the distribution of archaeological materials and features observed today.

SITE LOCATION, GEOGRAPHY AND GEOLOGY

Elands Bay Cave (alt. Elandsbaai) is located at the northern extent of St Helena's Bay at Cape Deseada on the west coast of South Africa, approximately 180 km north of Cape Town (Fig. 1). The site, along with other important localities such as Diepkloof Rock shelter and Kraal (Parkington & Poggenpoel 1987; Porraz et al. 2013), Tortoise Cave (Robey 1987) and Dunefield Midden (Parkington et al. 1992), forms part of a Middle and Later Stone Age archaeological landscape centred around the Verlorenvlei (Parkington 1981)-a rich, wetland ecosystem that provides a wealth of resources in a mostly semi-arid coastal landscape (Baxter 1997). The Verlorenvlei consists of a river, a marsh and a large, semi-estuarine coastal lake or vlei that is 13.5 km long, 1.4 km wide at its widest point, and covers an area of 10 km^2 (Baxter 1997). The Verlorenvlei River catchment, covering ca. 1890 km^2 (Noble & Hemens 1978), begins 40 km to the west, fed by tributaries that drain the Piketberg, Olifants River, Swartberg and Mannberg mountain ranges. The river follows a northwest/southwest structural trend across the sandy coastal plain until the town of Redelinghuys, where the marshy, meandering landscape becomes constricted by a narrow valley that extends westward to Grootdrift. Here the river transitions into a marsh which opens up at Diepkloof, marking the beginning of the open-water vlei. The coastal lake continues until Verlorenvlei Farm, where the lake becomes marshy again. Here the Verlorenvlei narrows to a single channel, which trends south until crossing a narrow rock ridge and terminating at a sand bar at the beach of Elands Bay (Baxter 1997).

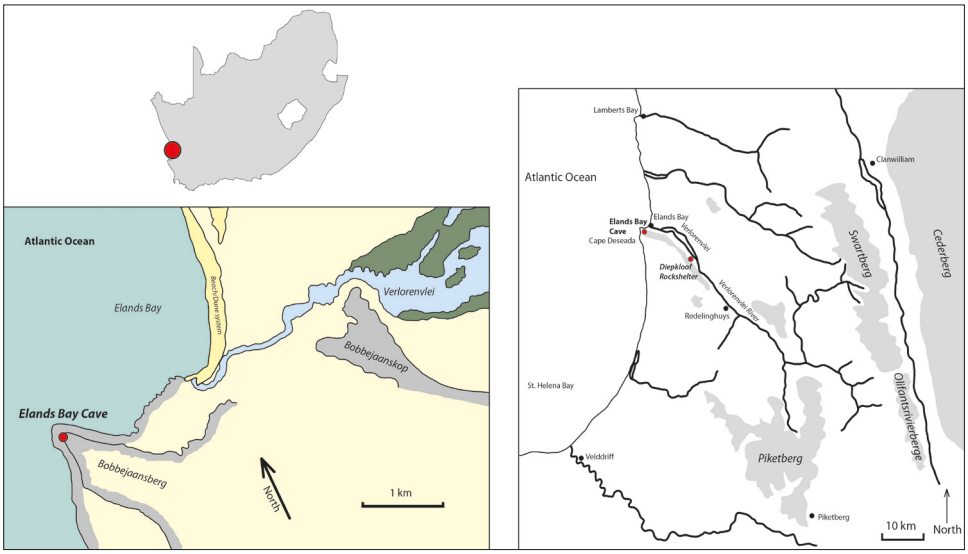

Fig. 1. Maps showing location of Elands Bay Cave and other localities mentioned in text. Adapted from Baxter (1997) and Sinclair et al. (1986).

South of Elands Bay the coast follows a steep sandstone cliff that rises locally to 160 m above modern sea level and trends south-southeast for ca. 6 km until merging with the coastal plain (Miller 1987). In front of this cliff line is a sandy beach with an extensive dune system reaching up to 16 m in height. North of Elands Bay, the coast is less rocky and consists of an undulating, hilly coastal plain that rises about 20–30 m above modern sea level and is dominated by an active dune field that locally exceeds elevations of 90 m.

The landscape surrounding the Verlorenvlei is commonly called the Sandveld and is part of the larger Cape Floristic Region. The juxtaposition of cold, upwelling Atlantic waters, the arid coast, and a source of fresh water provides a unique combination of vegetation types, including West Coast Strandveld, Lowland Sand Plain Fynbos, Karroid Shrubland, Dry Mountain Fynbos, and Marsh Vegetation (Sinclair et al. 1986; Baxter 1997). Despite the obvious source of fresh water, the area surrounding Elands Bay Cave is semi-arid and meets the criteria for classification as a Mediterranean-type climate (Baxter 1997). The Verlorenvlei area falls within the winter rainfall zone so that precipitation, which averages ca. 270 mm/year (Robertson 1980), is highly seasonal, with nearly 80 % of rain accumulating from April to September (Sinclair et al. 1986). Temperature data from Cape Columbine, the nearest weather station, record average July minimums at 10°C and the February maximum as 21.1°C, with an annual temperature amplitude of 4.3°C and daily temperature amplitude of 6.9°C (Butzer 1979). Maximum temperature inland from Elands Bay can reach over 40°C in the summer, and Baxter (1997) reports personal anecdotes of night-time frost in interior valleys during the winter; however, the temperature fluctuations at Elands Bay are modulated by the sea. Advective fog is common along the coast, particularly in the spring and autumn, providing a much needed source of moisture for coastal vegetation. Despite these coastal effects, the hot, dry summers lead to high evaporation, recorded

at Lambert's Bay to the north of Elands Bay as 1400 mm, or seven times the annual rainfall (Robertson 1980).

The late Precambrian Malmesbury Formation and the Siluro-Devonian Table Mountain Group make up the bedrock of the area, with the latter comprising ca. 30 % of the surficial geology in the area (Baxter 1997). The Table Mountain Group within the Verlorenvlei drainage is composed of weakly-metamorphosed, red-coloured, medium- to coarse-grained sandstones, cross-bedded, fine-grained, shaley sandstones, and conglomerates. The fluvial conglomerates comprise the Piekenierskloof Formation, which is overlain by the estuarine shaley sandstones, which comprise the Graafwater Formation (Visser & Toerien 1971; Theron 1983). The Table Mountain Group bedrock forms minor escarpments, kopjes (buttes), and ridges that follow the regional northwest-southeast structural trend and stand above the extensive surficial sands of the Sandveld. The southern bank of the Verlorenvlei River is marked by such a ridge, which follows a northwest-southeast trending strike-fault (Tankard 1976; Rogers 1987) beginning at Redelinghuys. This 120 m high ridge continues to the coast at Elands Bay, where it is known as either Elandsberg or Bobbejaansberg, and terminates at Baboon Point at the modern coastline, where Elands Bay Cave is located.

The bedrock around Verlorenvlei and across the area known as the Sandveld is draped in aeolian and fluvial sandy deposits, locally up to 67 m thick that likely formed as a result of fluctuating sea-levels during the Tertiary and Quaternary (Baxter 1997). Rogers (1982) places these sands into three distinct formations. The lowermost is the Elandsfontyn formation, which consists of peaty clay and sand. This is overlain by the Varswater formation, which is a conglomeratic phosphorite; and the uppermost, which Rogers (1982) places within the Bredasdorp formation and subdivides into three units, the youngest of which is unconsolidated sands. Butzer (1979) suggests that these unconsolidated sands were emplaced around 12 500 BP. The modern soils that form within the sandy deposits are well-drained arenosols that are mostly fine-grained, loose, and poor in nutrients and weatherable minerals (Talbot 1947; Schloms et al. 1983). Interior soils are generally acidic, whereas littoral soils are generally alkaline and show an enrichment in phosphorous and nitrogen relative to other soils along the west coast (Talbot 1947; Baxter 1997). Calcretes, ferricretes and other hard pans are common (Baxter 1997).

QUATERNARY LANDSCAPE CHANGE AND LOCAL PALEOENVIRONMENTAL RECORDS

Although the Verlorenvlei is an important component of the modern ecology of Elands Bay, the vlei and coastline were not always in their current configuration since the area has undergone significant change throughout the Quaternary as a result of fluctuating sea levels. Visser and Toerien (1971) report a series of marine terraces along the coast near Elands Bay ranging from 120 m to 3 m above modern sea level. The highest erosional marine terrace is found north of Elands Bay and is covered in fossiliferous phosphatic sands, likely dating to the late Tertiary; a later terrace at 60 m above modern sea level is also recorded nearby (Visser & Toerien 1971). Miller (1987) argues that Elands Bay Cave itself, and other nearby shelters located at around 40 m above modern sea level, may have been scoured during previous marine high stands. Tankard (1976) also reports a relict boulder beach near Elands Bay Cave at 13 m above

modern sea level—possibly correlating with early Pleistocene high-stand markers from Saldana Bay—and argues that the ca. 5 m above modern sea level wave-cut platform at Baboon Point found directly below Elands Bay Cave may have formed initially during the middle or early Pleistocene, but was probably re-scoured during the late Pleistocene marine transgression.

During phases of marine regression, sea levels at Elands Bay dropped more than 100 m below modern levels exposing 30–40 km of coastal plains and leading to significant down cutting by the Verlorenvlei River (Baxter 1997). Additionally, the bedrock ridge of Elandsberg Mountain and Baboon Point, which forms a rocky, submerged groyne at the entrance to Elands Bay today, would have been subaerially exposed. Faunal evidence from Elands Bay Cave (Klein & Cruz-Uribe 1987) suggests that during the last glacial, the exposed continental shelf likely supported a grassland ecosystem inhabited by large grazers; however, this does not necessarily imply that conditions were significantly drier during the terminal Pleistocene and Last Glacial Maximum. To the contrary, charcoal and pollen recovered during excavations at Elands Bay Cave contained species assemblages including Afromontane taxa, indicating higher available soil moisture than today (Baxter 1997; Cartwright & Parkington 1997; Cartwright 2013). Cowling et al. (1999) hypothesized that this higher moisture was caused by sustained precipitation resulting from westerly cyclonic fronts along the western portion of the Cape Fold Belt. In contrast, more arid conditions in the eastern part of the fynbos biome resulted from cooler and more restricted moisture driven by the Agulhas current. The argument for wetter conditions during the Last Glacial Maximum along the western coast, and particularly at Elands Bay, is supported, according to Parkington et al. (2000), by the presence of hedgehog (*Erinaceus frontalis*) remains from Pleistocene layers at the cave. Furthermore, measurements made by Klein (1991) on dune molerat (*Bathyergus suillus*) humeri from Elands Bay Cave imply more humid conditions in the region between 9500 and 13 600 BP (Parkington et al. 2000; Klein & Cruz-Uribe 2016 this issue).

During the marine transgression following the Last Glacial Maximum low stand, the shoreline migrated landwards, submerging the exposed coastal plain and, together with temperature amelioration and intensified aridity, led to significant alteration of the regional ecology. Sea levels, which rose at a rate of 50 cm per 100 years, also transgressed during the Holocene, particularly at 8000 BP, 5500 BP and 4000 BP, with the later event appearing to exceed modern sea-levels (Baxter 1997). Afromontaine elements became significantly reduced by the terminal Pleistocene and by 6500 BP, and floral communities generally resembling those found today in the Sandveld appear to have become established at this time. The trend towards aridification, particularly pronounced in the mid-Holocene, is implied, according to Parkington (1987) by the secondary formation of gypsum within Elands Bay Cave.

The changing landscape around Elands Bay Cave is also reflected in changing subsistence practices of its inhabitants. During the terminal Pleistocene, when the exposed coastal plain was only partially submerged, the occupants at the site exploited the large grazers found in the grasslands; however, by ca. 11 000 BP, when the shoreline was about 5 km from the cave, the inhabitants began exploiting marine resources, evidenced by the presence of shellfish remains at the site. By 9000 BP fully developed shell-midden deposits are found at Elands Bay Cave. At the same time, many of the

larger grazer species disappear from the archaeological record and are replaced by smaller browsers (Klein & Cruz-Uribe 1987).

Paleoenvironmental data for time periods prior to the terminal Pleistocene and Last Glacial maximum are more sparse. Butzer (1979) constructed a composite stratigraphic sequence for the region, relying largely on colluvial deposits and paleosols exposed about 1 km east of Elands Bay Cave near a train tunnel excavated through the Elandsberg. He argues that the base of the sequence, a wave cut platform at 13 m above modern sea level, likely corresponds to MIS 9 and is overlain by colluvial deposits and aeolian sands that he attributes to a cold-period and phase of marine transgression corresponding to MIS 8 and 7. A polyphased soil, consisting of a subsurface horizon with prismatic structure overprinted by calcrete, formed on top of these units and likely corresponds to several different climatic phases of MIS 7. This soil is overlain at the Elandsberg tunnel section by colluvial deposits, what Butzer called *grèzes litées*, and which he argued were representative of cold-climatic conditions during MIS 6b. Furthermore, he correlated the colluvial materials with the lowermost stratigraphic units at Elands Bay Cave, which contain large angular debris and coincide with the earliest evidence for Middle Stone Age occupation at the site. Butzer argued that the transition between MIS 6a and 5e is represented by an accumulation of aeolian transgressive sands at the Elandsberg tunnel section, and that 5e proper is represented by the 6 m above modern sea level beach deposit and associated lagoonal deposits at Verlorenvlei. The correlation of this beach deposit with MIS 5e contradicts Hendey and Volman (1986) who argue that the 3 m above modern sea level shorelines found across the Western Cape Province correspond to 5e, and those at higher elevation likely pre-date the last interglacial. At the Elandsberg tunnel section, Butzer described strongly prismatic soils which formed on the aeolian sand deposited during the transition between MIS 6a and 5e. He correlated this soil with deeply oxidized cambic soils found at Verlorenvlei and also other 'aeolian soils' found in the uplands, and argues that this paleo-catena represents the last major phase of pedogenesis in the Elands Bay area. He noted that this period of soil formation is followed by a phase of slope denudation, corresponding with MIS 5b, with the well-developed red soils being subjected to slope wash at both the Elandsberg tunnel section and also in the Verlorenvlei. These reddish-coloured slope deposits are cemented by a calcrete, which Butzer correlated to MIS stage 5a and which is overlain by a rockier, colluvial deposit which he suggested corresponds to colder conditions during MIS 4.

In addition to the contribution in this issue (Cartwright 2016) the most detailed study to date of botanical remains from the Verlorenvlei area pre-dating the terminal Pleistocene comes from the Middle Stone Age site of Diepkloof Rock shelter, which is located about 17 km inland from Elands Bay along the Verlorenvlei River (Cartwright 2013; see also Fig. 1). Cartwright identifies several key changes in vegetation throughout the Diepkloof sequence, beginning in deposits containing pre-Still Bay artefacts and continuing through the post-Howiesons Poort deposits. She notes that the pre-Still Bay charcoal remains are dominated by Afromontane species and that with the beginning of the Still Bay, the assemblages shift towards favouring more thicket-like vegetation. At the same time, the Still Bay is when we see the earliest evidence for wetland vegetation associated with the Verlorenvlei. More taxa associated with these wetland environments are present in the Howiesons Poort, at the same time that plant communities appear

to become more diverse and representative of thicket and shrubland environments. Cartwright (2013) notes that the presence of Afromontane taxa in the Diepkloof sequence parallels a similar pattern in the Middle Stone Age charcoal record from Elands Bay Cave (Cartwright & Parkington 1997). The higher diversity of fynbos taxa within the Diepkloof sequence relative to that from Elands Bay Cave may reflect the influence of sea levels on the vegetation communities around the coastal site (Cartwright 2013). Cartwright (2013) urges caution, however, in using the data from these sites to directly infer environmental change. Rather, she points out that the charcoal assemblages at sites like Elands Bay Cave and Diepkloof reflect not only the available floral resources surrounding the site, but also human selection of these resources, potentially biasing a purely environmental interpretation.

Previous geoarchaeological studies at Elands Bay Cave

Elands Bay Cave and the landscape surrounding the Verlorenvlei have been the focus of relatively intensive geoarchaeological research for the past several decades (Butzer 1979; Miller 1981, 1987; Baxter 1997; Miller et al. 2013). Butzer (1979) published the first geoarchaeological study of the sediments from Elands Bay Cave as part of a larger geomorphic and geoarchaeological study of the region around the Verlorenvlei. He noted the presence of three distinct lithostratigraphic units at the site: 1) a basal, 30 cm thick unit composed of 'frost-shattered rubble' that corresponds with phase L of the recent excavations (see Porraz, Schmid et al. 2016 this issue); another unit above, around 1.3 m thick, that was composed of "lenticular hearth and refuse deposits rich in charcoal powder", corresponding roughly to phases K through D of the current excavations; and 3) the LSA shell-midden deposits which were dug by Parkington (1976) in the original excavations of the 1960s and 70s (Butzer 1979: 162–3). For Butzer, the presence of 'frost-shattered', angular rubble at the base of the sequence, and the presence of similar deposits at Diepkloof and across the landscape of Elands Bay suggested to him that the western coast of South Africa experienced harsh climatic conditions during the Middle Pleistocene, particularly during MIS 6 (Butzer 1979, 2004). Butzer collected a total of 6 sediment samples from Elands Bay Cave for more detailed granulometric and compositional analysis. His results showed that the inorganic component of the sediment prior to 12 500 BP had mean grain sizes between 200 and 500 μm. Younger sediments at the site were better sorted and contained grains ranging between 100 and 200 μm. He interpreted this pattern as reflecting a shift in the source of sediment to the cave, such that the younger, finer sediments represented a greater influence of aeolian 'backshore sands', probably related to the terminal Pleistocene marine transgression. He also argued that the contribution of autochthonous sediment from the cave bedrock decreased by 50 % between 20 000 and 11 000 BP, and that the increase in aeolian sands at the terminal Pleistocene caused an increase in overall sedimentation rates.

Miller (1981, 1987) conducted a more detailed study of the sediments from Elands Bay Cave, collecting a total of 90 loose sediment samples on which he conducted granulometric analyses focusing on the 32 μm to 2 mm size fraction. Miller agreed with Butzer's assertion that the deposit of coarse angular blocks found in the lowermost unit (phase L) formed as a result of freezing of the cave ceiling and walls. He termed this layer a 'basal lag' and argued that finer material was leached from the lower part of this

layer, based on an increase in coarseness with depth. He thought that the removal of a portion of the fine fraction may have occurred during a period of prolonged exposure of the surface of this layer and that an increase in the fine fraction at the top of the layer may indicate the downward translocation of finer sediment from overlying deposits. Miller's analyses also reproduced the trend in grain size distributions found by Butzer; the older deposits (layers 24–12, or following the current stratigraphic designations phases K through D) were more poorly sorted and coarser, and younger deposits, dating between 12 500 to 8000 BP were finer and better sorted. However, Miller interpreted the trends differently. He argued that "more vigorous winds … during the last glacial and immediately post glacial" accounted for the presence of coarser grains and the poor sorting of the older sediments at the site (Miller 1987: 64). These winds may have also contributed to an increase in the addition of autochthonous material derived from the cave walls and ceiling, according to Miller (1987).

Geochemical analyses and diagenesis of bone

Butzer (1979), as part of his geoarchaeological study of Elands Bay Cave, conducted several geochemical analyses of the sediment, in addition to presenting field descriptions and particle-size data. He reported a general trend of decreasing calcium carbonate and increasing phosphorous with depth within the second lithostratigraphic unit (phases I through D), a pattern that Butzer interpreted as changing patterns in the presence of 'fired shell' and 'bone phosphate' (Butzer 1979: 163).

Sillen and Parkington (1996) conducted a more detailed study of bone chemistry and chemical diagenesis at Elands Bay Cave. They measured the carbon and nitrogen content of bone, and also measured the crystallinity of the mineral fraction of the bone, using infrared spectroscopy to determine the splitting factor (Weiner & Bar-Yosef 1990; Bar-Yosef et al. 1993). The goals of this study were to assess the use of crystallinity measurements as a tool in determining relative chronology and to examine the link between organic and mineral processes in bone diagenesis. Sillen and Parkington (1996) reported a relatively strong correlation between age and crystallinity index measurements for bones younger than 20 000 BP at the site, but weak correlation between age and crystallinity index for older bones. They noted a strong correlation between nitrogen content and crystallinity index, which they interpreted as implying a link between diagenetic processes influencing the organic and mineral components of the bone. Sillen and Parkington (1996) also argued that since the nitrogen, carbon, and crystallinity measurements correlate better between themselves than with the dates of their corresponding stratigraphic layers, either 'microenvironmental' factors influenced the rate of diagenesis, or there was mixing between stratigraphic layers at the site. They favoured the latter explanation, ruling out spatial variation in the degree or type of diagenesis at the site, and instead argued that measurements similar to those made in their study can be used to assess the stratigraphic integrity of archaeological sites.

RESEARCH GOALS OF THE CURRENT GEOARCHAEOLOGICAL STUDY

Elands Bay Cave has been the focus of intensive archaeological research for several decades and, as described above, numerous geoarchaeological studies have been carried out on the site's deposits. In the current study our aim is twofold: 1) to provide detailed stratigraphic and geoarchaeological observations that can help us

interpret the cultural, environmental and geochronological data collected during the recent excavations and 2) to provide a formation history of the site and specifically the Middle and earlier Later Stone Age deposits. The previous geoarchaeological studies conducted by Butzer (1979) and Miller (1987) were largely aimed at placing the site's sequence within a climato-stratigraphic framework that the researchers could then correlate with environmental change that occurred across the broader landscape. These research questions fit well with the goals of the previous Elands Bay Cave excavations, which pioneered an environmental approach to archaeological investigations. We share these goals; however, our approach is different. Rather than viewing the deposits as largely an archive of environmental change, we view the deposits as having accumulated as a result of geologic, biologic and anthropogenic agents. Additionally, we recognize that following accumulation, these deposits were variably influenced by sometimes intensive post-depositional alteration. Therefore, our goal is to identify the sources for sedimentary components at the site, to determine the agents of accumulation, and to identify the processes that caused the sediments to become altered following deposition. By unravelling these various processes that influenced the site over time, we can construct a site-formation model that allows us to contextualize the results of other researchers and also identify natural and cultural influences on the site's deposits.

METHODS

For this study we employed a combination of field and laboratory techniques. Field-based methods included site and profile description combined with ground-penetrating radar (GPR) survey. We also collected environmental water samples for chemical analysis and sediment block samples for microcontextual analysis.

GPR

We carried out a GPR survey of the cave's deposits with the goal of estimating the depth to bedrock across the site and to investigate any larger scale patterns in the geometry of the deposits. For this survey we employed a Geophysical Survey Systems, Inc. (GSSI) SIR-3000 control unit with a 400 MHz central-frequency antenna and an externally-mounted survey wheel with 2 cm triggering interval. We collected the GPR data within a single geophysical survey grid measuring 11 x 12 m, which covered the majority of the cave's floor and which was referenced to the established site datum. The data were collected unidirectionally along the Y and X axes at lines spaced at 20 cm intervals. In order to maximize data collection in irregular survey areas, particularly along the back wall of the cave, we extended the survey beyond the area of the grid. Despite in-field gain corrections raw GPR profiles exhibited weakly contrasting amplitudes below modern sand, and required experimentation with band pass filtering to enhance weak stratigraphic boundaries.

Post-processing routines for the GPR data were conducted in GSSI's RADAN software and included position correction (time zero), background removal (for removal of banding related to digital noise), hyperbolic-based migration (for depth calibration), high and low pass filtering (for suppression of unwanted noise), and time-varied gain enhancement (for enhancing signal degradation with increased depth). For all spatially coincident survey data, profile lines were combined into one

file using the Super3D function of RADAN and processed simultaneously. The data were interpreted in cross-section view (2D) and as time slices. Ground-truthing data for refining depths to significant strata, including bedrock basement, were provided by the recent archaeological excavations.

Water chemistry

In order to determine the source for various elemental inputs to the deposits, we collected samples of rain water and water seeping through a joint in the bedrock at the front of the cave. The samples were collected during a late summer rain storm that began in the evening and continued into the following morning. We gathered water in plastic flasks at the start of the precipitation event and on the morning of the following day. At the end of the rain storm, we collected a sample of water that had begun to flow and drip from the joint. We sealed the water sample flasks with Parafilm® and electrical tape and kept the samples refrigerated prior to analysis.

We filtered the water samples and split them in order to preserve some of the water for later analysis. We also ran a blank for control of possible contamination from the filters. Determination of the elements Al, B, Ba, Ca, Cr, Cu, Fe, K, Li, Mg, Mn, Na, Ni, P, Sr, and Zn was performed using an inductively coupled plasma-optical emission spectrometer (ICP-OES) Perkin Elmer Optima 5300 DV with a Meinhard nebulizer and a baffled cyclonic spray chamber housed in the Laboratory of Soil Science and Geoecology at the University of Tübingen. The optimal instrumental conditions for axial view were: RF generator power 1.4 kW, plasma gas flow rate: 15 L min^{-1}, nebulizer gas flow rate, auxiliary gas flow rate: 0.3 L min^{-1}, pump rate: 1.0 mL min^{-1}. The following analytical lines were used for determination of the analytes: Al 396.153 nm; B 249.677 nm; Ba 233.527 nm; Ca 317.933 nm; Cr 267.716 nm; Cu 327.393 nm; Fe 238.204 nm; K 766.490 nm; Li 670.784 nm; Mg 285.213 nm; Mn 285.213 nm; Na 589.592 nm; Ni 231.604 nm; P 213.617 nm; Sr 407.771 nm; Zn 206.200 nm.

Microcontextual analysis

Micromorphology

We collected a total of eight block samples of intact, oriented archaeological sediment for micromorphological and microcontextual analyses. We removed the blocks from profiles exposed during the recent excavations and stabilized them for transport using plaster-of-Paris bandages or toilet paper and packaging tape. In the laboratory we dried the samples at 40°C for at least 24 hours and then indurated them under vacuum with a mixture of polyester resin and styrene in a ratio of 7:3. We used methylethylketone peroxide as a catalyst with 3–5 ml per litre of resin and styrene. Once the mixture had gelled, we heated the indurated samples again at 60°C for at least 24 hours in order to completely harden the resin. We then sliced the blocks with a tile saw, producing chips measuring 6 x 9 cm. When this size of chip did not offer complete coverage of the block sample, we sub-sampled so that some block samples have two corresponding thin sections, with sub-sample A located stratigraphically higher than sub-sample B. Panagiotis Kritikakis (Geoarchaeology Laboratory, University of Tübingen) thin-sectioned the resulting chips to 30 μm thickness. We scanned the thin sections using a flat-bed scanner (Arpin et al. 2002) and analysed them under the naked eye and at magnification up to 200 x using plane-polarized light (PPL), cross-polarized light (XPL), oblique incident

light (OIL) and blue-light fluorescence. We described the thin sections using protocols and terminology developed by Stoops (2003) and Courty et al. (1989).

Fourier Transform infrared (FTIR) spectroscopy and Fourier Transform infrared microspectroscopy (μFTIR)

In addition to block samples, we also collected loose samples of sediment and samples of visible nodules from the exposed profiles for mineralogical analysis. We analysed the loose samples with a Cary 630 (Agilent Technologies) portable FTIR with a diamond-crystal attenuated total reflectance (ATR) attachment. Spectra were initially collected using the MicroLab PC software, and later exported to the Essential FTIR software package for further mineral identification and analysis. The spectra were generated from 32 co-added scans at 4 cm-1 resolution over a spectral range of 400–4000 cm-1. Initial mineral identifications were made using a spectral library search with databases composed of KBr and ATR spectra generated by S. Weiner (http://www. weizmann. ac. il/kimmel-arch/infrared-spectra-library), the RRUFF project (www. RRUFF. info; Lafuente et al. 2015), and using a personal mineral collection (S. Mentzer).

Analysis of loose samples of sediment and nodules can provide valuable information about mineral assemblages present within a site and their spatial and stratigraphic distribution (e.g. Weiner & Goldberg 1990; Weiner et al. 2002). However, this approach is not always useful for determining the sequence of formation of secondary minerals or their relationship to other sedimentary or diagenetic components or processes. Therefore, we decided to conduct FTIR analysis directly on the thin sections using a Cary 610 FTIR microscope connected to a Cary 660 FTIR bench (Agilent Technologies). We collected spectra on secondary minerals, bone fragments and other components in thin section using a germanium-ATR (Ge-ATR) objective with 32 co-added scans at 4 cm-1 resolution between 4000 and 570 cm-1. We collected the data as individual point measurements (sampling area ~50–70 μm diameter), as well as automated measurements on a grid using the Resolutions Pro software package. As with the loose samples, mineral identifications were conducted using spectra exported to the Essential FTIR software package and searched against reference spectral libraries, including a library generated from heated bone reference samples in thin section. All spectra generated from this study are available to view online (www. geoarchaeology. info/FTIR).

μ-XRD

In order to confirm and clarify several of the mineral identifications made using FTIR, we conducted analyses directly on thin sections and loose mineral nodules using a μ-XRD^2 diffractometer (BRUKER D8-Discover GADDS) located in the microanalytical laboratory of the CCA-BW in the Applied Mineralogy at the University of Tübingen. The microdiffractometer was equipped with a Co-sealed tube running at 30 kV/30 mA. Measurements were performed using either a 50 μm polycapillary X-ray optic or a larger 500 μm monocapillary X-ray optic with 300 μm pinhole, and a 14 cm two-dimensional detector (BRUKER VANTEC-500) covering 40°2θ in one diffraction image. Diffraction patterns were produced by integrating two diffraction images measured on different detector positions. Measurement times of each pattern were typically four minutes. In some cases, samples were rotated about a fixed vertical

axis in order to suppress single crystal intensities generated from oriented crystallites or single grains. Mineral identifications were conducted using the PDF-database of the International Centre for Diffraction Data (ICDD).

Scanning electron microscopy (SEM)
Mineral identifications using FTIR and μ-XRD[2] were aided in part by elemental data collected directly on minerals visible in thin section using a LEO 1450 VP SEM housed in the Department of Geosciences at the University of Tübingen. The thin sections were sputter coated in gold to minimize charging. Compositional analyses were conducted over points and areas using an EDS detector.

Autoradiography
Because at least one of the identified secondary minerals contained K, and could therefore influence how we calculate dose-rate for the luminescence age estimates, we conducted autoradiography on chips corresponding to the analysed thin sections. The autoradiography was performed using an imaging plate (IP-Fuji 25 cm x 25 cm), which contains beta sensitive crystals (BaFBr:Eu+2). The chip was placed on the imaging plate, in a shielding lead box, for 43 days. We then scanned the imaging plate (Dürr Medical HD-CR 35 Bio). Under lighting, each pixel emits a light whose intensity is related to the beta dose received during the exposure of the imaging plate to the sample. The resulting image represents the spatial distribution of beta dose in the sample (Rufer & Preusser 2009).

Organic petrology
Organic petrology is a field that studies the organic components of rocks and deposits using qualitative and quantitative microscopy. The approach is widely used in geology, particularly for the assessment and analysis of coal and other organic rich rocks of economic interest (Taylor et al. 1998); however, it has recently been applied successfully in archaeology, and specifically geoarchaeology as part of a microcontextual research strategy (e.g. Ligouis 2006; Goldberg et al. 2009; Stahlschmidt, Miller, Ligouis, Goldberg et al. 2015; Stahlschmidt, Miller, Ligouis, Hambach et al. 2015).

The organic petrologic analyses in this study were carried out at the Laboratory for Applied Organic Petrology at the University of Tübingen on well-polished indurated blocks that corresponded to thin sections analysed using micromorphology and other microanalytical techniques (EBC-12-01 and EBC-12-04). The samples were analysed using reflected white light and fluorescence and focused on describing the form and properties (e. g., anisotropy) of organic particles, referred to as 'macerals'. Further analysis, including measurement of the reflectance values of the macerals, was conducted on a Leitz DMRX-MPVSP microscope photometer in reflected white and blue-light, using oil immersion objectives between 20x and 50x. Analysis of the form, property and reflectance of the macerals can help identify the origin of the organic material, and assess its degree of humification and/or charring.

RESULTS

Field observations
Elands Bay Cave is situated at 42 m above modern sea level within a cliff of Table Mountain Group bedrock at Baboon Point (Fig. 2). The cave, which is ca. 18 m across

Fig. 2A. View of Baboon Point, composed of Table Mountain Group quartzites and conglomerates, in which Elands Bay Cave is located. 2B) View of Elands Bay Cave.

and 10 m deep, faces the ocean to the southwest. Because the site is wider than it is deep, and since daylight reaches most corners of the site, Elands Bay Cave is best described as a rock shelter; however, because of the long history of research referring to the site as a cave, we will continue this convention. The morphology of the site is generally rectilinear and follows the sub-horizontal bedding planes and vertical joints of the Table Mountain Group bedrock.

The present excavations focused on a small portion of the site initially exposed by Parkington as a test pit (squares F5, E5, and D5) during his original excavations. We established a new grid system for the site in order to facilitate the collection of spatial data using a total station (see Porraz, Schmid et al. 2016 this issue for details). Although all exposed profiles in the test pit were described and studied, excavations focused on the eastern profile of the pit, particularly sub-squares 1c, 2c, 2d, 11c, and 11d.

During excavation and field description we identified 8 major phases of deposition, which we assigned letter designations (see Porraz, Schmid et al. 2016 this issue for details) (Fig. 3). Each phase is composed of more than one layer or Stratigraphic Unit (SU), which was the smallest unit of excavation and archaeological analysis. Following standard practice on the western coast of South Africa, the SUs were generally given names that begin with the letter of the phase in which the SU is grouped. For example, SUs grouped into phase K have names including Kelly and Kent.

The lowermost phase, L, rests directly on the bedrock and has a maximum thickness of 10 cm. It appears mostly as black lenses within dark brown sandy sediment. Bones were absent from the basal SUs, which include Letty to Lovan. This phase is overlain by another phase up to 35 cm thick called 'Keva/Lara', referring to the two layers present within the main stratigraphic sequence. It is composed of large, angular blocks of quartzite roof spall and artefacts which exhibit a horizontal to sub-horizontal orientation. In some portions of this sedimentary phase, the deposits appear clast-supported. This phase corresponds with the basal deposits of the sequence described by Butzer (1979) and Miller (1987) as a 'frost-shattered' deposit. As in the deposits from phase L, Keva/Laura contained no faunal remains. The deposits are particularly rich in lithic artefacts and likely correspond to an early phase of the Middle Stone Age (Porraz, Schmid et al. 2016 this issue; Schmid et al. 2016 this issue). Tribolo et al. (2016 this issue) report an uncertain age of 83 ± 14 ka on a burnt fragment of quartzite from Keva/Laura.

Phase K which includes SUs from Kali to Kent is easily distinguished from the underlying deposits by its general lack of large, angular roof spall. It is ca. 15 cm thick and appears dark brown in colour, and is composed of sandy silt. Clear bedding, laminations and lenses are present within this phase, and are particularly noticeable within the southern portion of the eastern profile. Phase J, which is ca. 20 cm thick and corresponds to SUs Jacob to Kelly in the main stratigraphic sequence, appears generally lighter in colour compared to phase K and displays similar bedding structures and laminations. These phases remain undated.

Phase I corresponds to SUs Igor to Ines and has a maximum thickness of 25 cm. The sediments of this phase appear generally dark brown in colour and exhibit light-coloured lenses and fine laminations, some of which appear reddish in colour. Igor appears yellowish in the field, and the base of the layer is marked by a laterally discontinuous concentration of angular roof spall, mostly 5–15 cm in size. Ines, at the base of phase I consists largely of degraded fragments of roof spall. Radiocarbon measurements

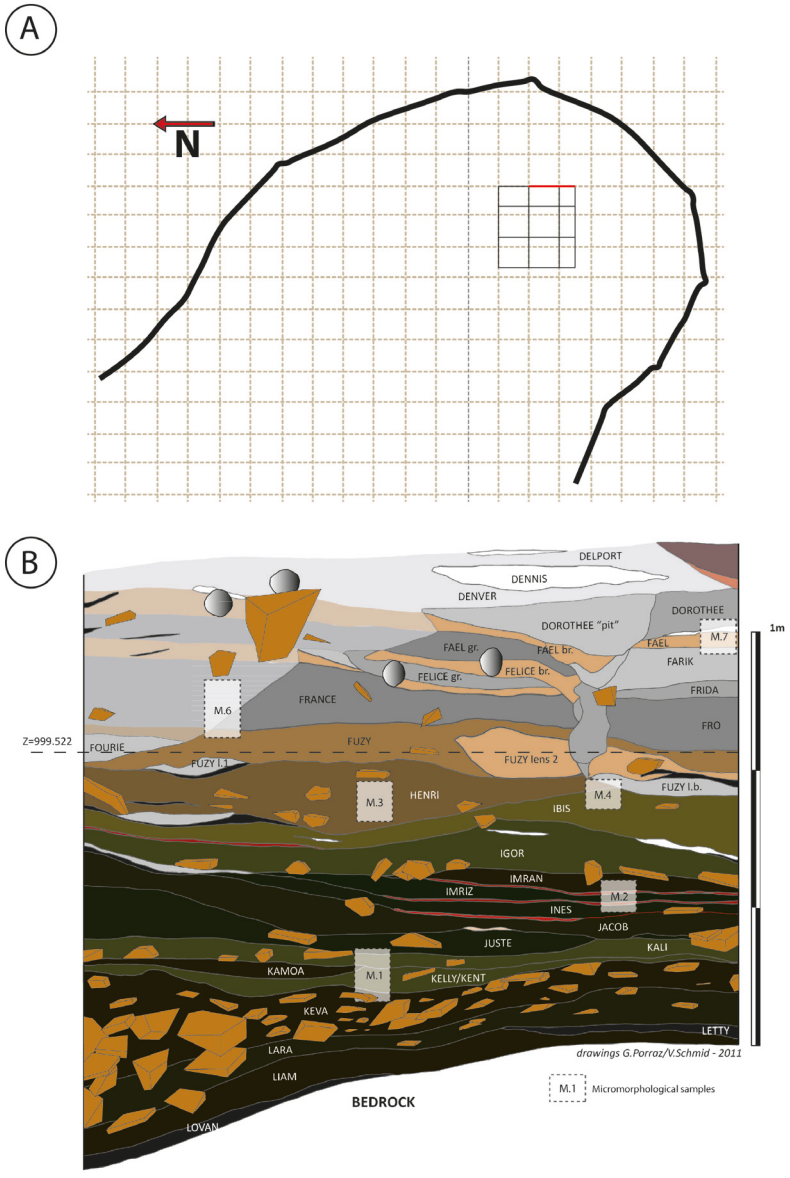

Fig. 3A. Excavation grid indicating the areas excavated by Parkington and Porraz during the current campaign. The main profile of study for this work is the eastern profile, a drawing of which is presented in 3B. Here, the location of micromorphological samples is indicated by the squares, with sample numbers included (e.g. M.1 is EBC-12-01).

obtained on charcoal from this phase returned ages between 36.8 and 38.9 ka cal BP and optically stimulated luminescence (OSL) ages were consistent with these dates (Tribolo et al. 2016 this issue). The lithic industry in phase I is consistent with a late phase of the Middle Stone Age (Porraz, Schmid et al. 2016 this issue). Phase I is overlain by phase H which is up to 20 cm thick and shows a slight inclination to the south. It includes SUs

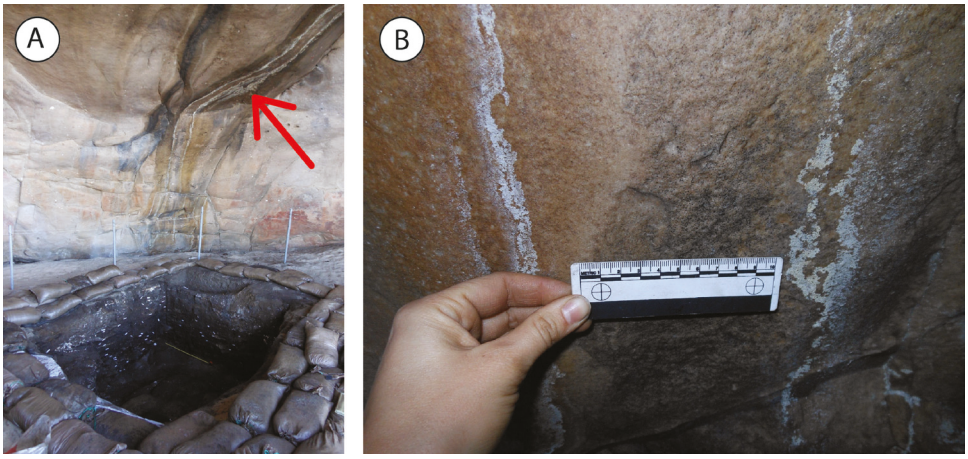

Fig. 4A. Photograph of the interior of Elands Bay Cave with the excavation area exposed. Note the joint in the back wall along which water seeps during rain events (red arrow). The white streaks are secondary minerals that form as the water evaporates. Also note that within the excavation area, the deposits appear darker to the south and east, indicating a wetting front associated with the joint. 4B) A close-up view of the secondary minerals forming along the back wall.

Harry to Ibis. Phase H appears generally homogenous and is sandier than underlying deposits. Bones were not found in phases I, H, J or K during excavation.

Phases D and F include SUs Delport to Fuzy and they together comprise a total thickness of around 55 cm. This phase is composed of interstratified lenses and pits that are light in colour and resemble *en cuvette* hearths. Radiocarbon dating of charcoal from phase F places deposition between 22.1 and 24.2 ka cal BP, although luminescence ages on quartzite blocks from the base of the phase suggest a slightly earlier start to accumulation (Tribolo et al. 2016 this issue). Radiocarbon dates on charcoal obtained from phase D returned ages between 19.4 and 18.8 ka cal BP (Tribolo et al. 2016 this issue). Porraz, Igreja et al. (2016 this issue) identify the lithic industry from phase F as corresponding to the early LSA, and phase D as corresponding to the Robberg. Faunal remains were found during excavation in these phases, but were poorly preserved.

The stratigraphically highest unit excavated during the most recent excavations was phase C which consisted of a large pit that sloped towards the southern wall of the cave and that contained yellowish-brown sand and some marine shell. Artefacts in this unit were not abundant.

A vertical joint in the bedrock of the cave runs along the top and back of the cave ceiling and wall, oriented perpendicular to the entrance of the site (Fig. 4). When it rains, water seeps and runs along this joint and when the water evaporates, it deposits a rim of secondary minerals parallel to the orientation of the joint. The effects of this water seep appear to continue from the joint into the archaeological deposits as a wetting front: the southeastern corner of the excavations in squares F5, E5 and F4 exhibits an inverted cone-shaped zone where few, if any, large secondary mineral nodules appear. The rest of the profiles in the current excavation area, particularly to the north and west, are thoroughly permeated by large, white powdery nodules,

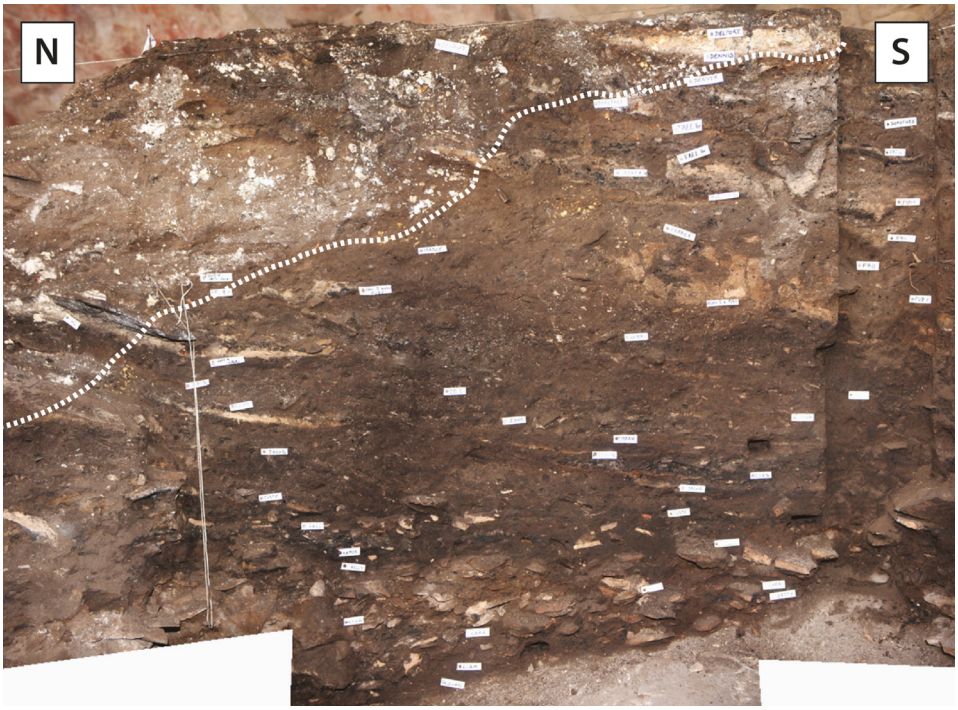

Fig. 5. Photograph of the eastern profile, showing the wetting front. To the north of the dotted white line, large secondary nodules, mostly of gypsum, form and physically disturb the deposits. To the south of the line, secondary nodules are smaller and do not significantly alter the physical structure of the deposits.

some larger than 10 cm in diameter (Figs 5, 6). Parkington identified the secondary mineral as gypsum ($CaSO_4 \cdot 2H_2O$), and suggested that its formation was linked to increasing influence of marine aerosols during and following the late Pleistocene marine transgression (Parkington 1987). Our FTIR measurements on loose samples of these nodules confirmed their identification as gypsum (Table 1). Within the wetting front, nodules are present, but are much smaller-generally less than 1 cm in diameter-

TABLE 1

A list of secondary minerals identified in this study, along with their chemical formulae.

Gypsum	$CaSO_4 \cdot 2H_2O$
Hydroxylapatite	$Ca_{10}(PO_4)_6(OH)_2$
Taranakite	$(K,Na)_3(Al,Fe^{3+})_5(PO_4)_2(HPO_4)6 \cdot 18H_2O$
Ardealite	$Ca_2(HPO_4)(SO_4) \cdot 4H_2O$
Whitlockite	$Ca_{18}Mg_2H_2(PO_4)_{14}$
Variscite	$AlPO_4 \cdot 2H_2O$
Opal	SiO_2 (amorphous, hydrated)
Dawsonite	$NaAlCO_3(OH)_2$

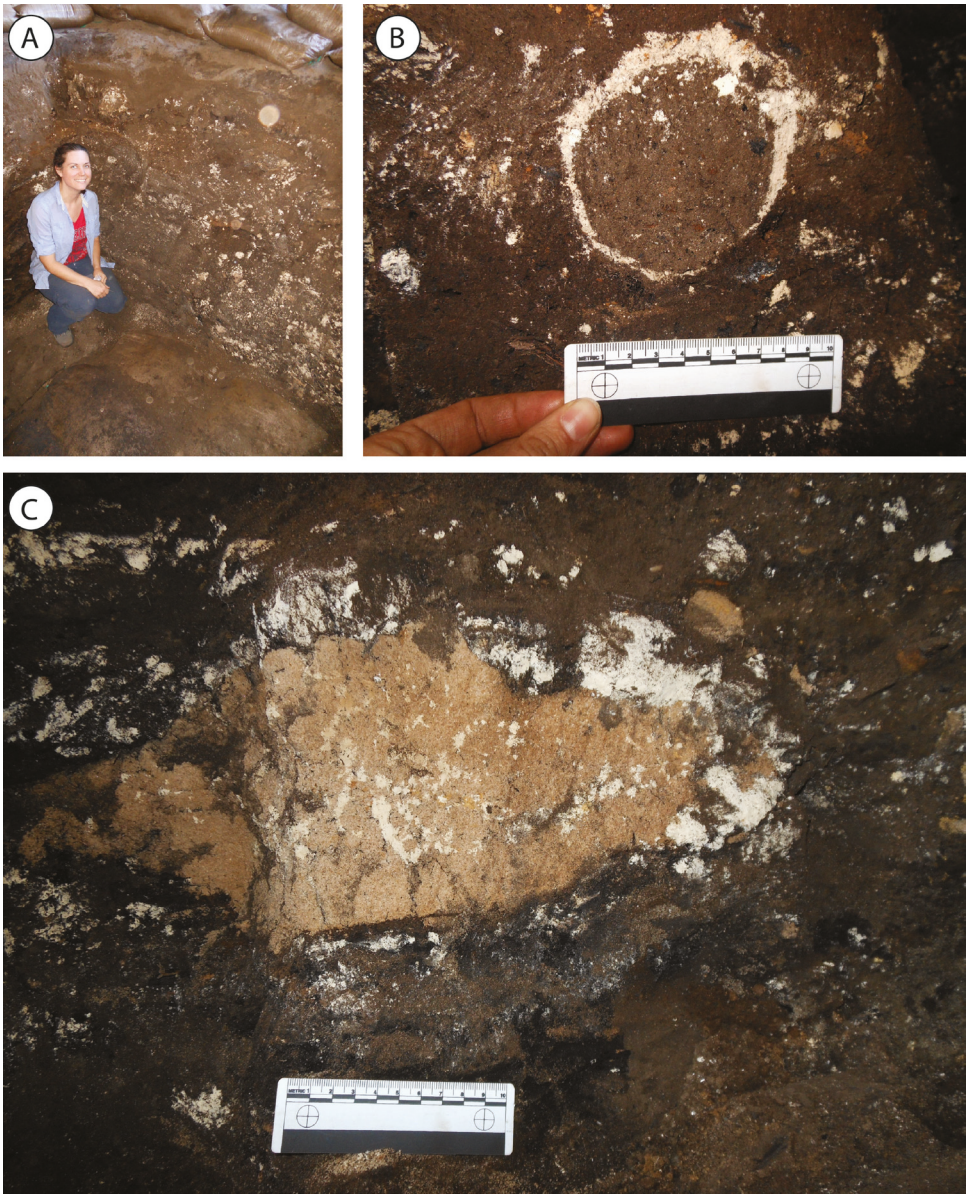

Fig. 6A. Photograph of the western profile, showing extensive impregnation of the deposits by secondary nodules. 6B) A krotovina along which secondary gypsum has formed. 6C) A block of quartzite that has been partially destroyed by the formation of secondary gypsum.

and appear as small flecks or thin veins with a beige colour. FTIR measurements on loose samples of these nodules revealed that they are composed of taranakite ($(K, Na)_3(Al,Fe^{3+})_5(PO_4)_2(HPO_4)6{\cdot}18H_2O$). SEM-EDS measurements indicate that the mineral is rich in potassium. Towards the outer edge of the wetting front, round, cm-sized, yellowish nodules appear. FTIR measurements on loose samples of these

nodules identified them as hydroxylapatite ($Ca_{10}(PO_4)_6(OH)_2$). Additional minerals identified from loose samples include quartz (SiO_2), which is present in the bedrock and sand grains, white masses of opal (amorphous hydrated SiO_2), cream-colored nodules of ardealite ($Ca_2(HPO_4)(SO_4)\cdot 4H_2O$) mixed with gypsum, aragonite ($CaCO_3$) in fragments of marine shell, and dawsonite ($NaAlCO_3(OH)_2$), which is present as small green crystals which formed on the aluminium casing of the dosimeters used for luminescence dating.

The extensive formation of large, secondary nodules of hydroxylapatite, taranakite, and in particular, gypsum, has had a significant impact on the physical preservation of the deposits. Some large blocks of *éboulis* have been physically broken down by the formation of the nodules. In addition, the growth of the nodules has led to disturbance of the stratigraphic layers. Within the wetting front, laminations and lenses are clearly distinguishable. Outside of this zone, the large gypsum nodules appear to have homogenized the deposits, making it difficult, if not impossible, to follow distinct layers across the entire excavation pit. Bioturbation has also played a role in disturbing the deposits, but to a much lesser degree. Several krotovinas are visible in the profiles, including one where secondary gypsum has grown along the edge of the burrow. The excavators also noted that bones were found through much of the deposits outside the wetting front, but were almost completely absent from within it. Shells were only present within burrows.

GPR

Surface conditions at Elands Bay Cave comprised a layer of sand fill. Obstructions were minimal, though a barrier fence limiting access to the rock art was slightly restrictive. Initial field data showed relatively low dielectric contrasts due to aridity of the area, and there was attenuation from salt spray and long-term salt accumulation in the deposits. Field data therefore displayed weak signal amplitudes with few strong reflectors below the interface of modern sand and archaeological strata. Post-fieldwork digital processing served to enhance the data and increased interpretability, significantly enhancing GPR profiles and enabling time slicing of the dataset. Time slicing delineated a large excavation block from previous excavations (Fig. 7), and facilitated spatial correlation between this and more recent excavations to the south. Of note are the distinct reflections from sand bags in the more recent unit, and clear boundaries of previous excavation blocks.

Stratigraphic profiles at the site were briefly exposed when sand bags were removed from the recent excavation units. GPR profiles were consistent with excavation profiles and showed at least four discernible units overlying a pronounced and undulating bedrock reflector (Fig. 7). These units identified in the GPR survey likely correspond with phases L and Keva/Laura (unit I), phases J-I (unit II), phases D-F (unit III) and the modern sand fill (unit IV). Phase L (unit I) is apparent in the GPR data and appears to fill a bedrock depression. This unit pinches-out to the north, where bedrock or roof fall is exposed at the ground surface. In some locations unit I appears to thicken to the south and then thins toward the southern cave wall. Parallel to the rear wall the other units follow this general pattern, while perpendicularly, units thicken toward the entrance following the bedrock trend.

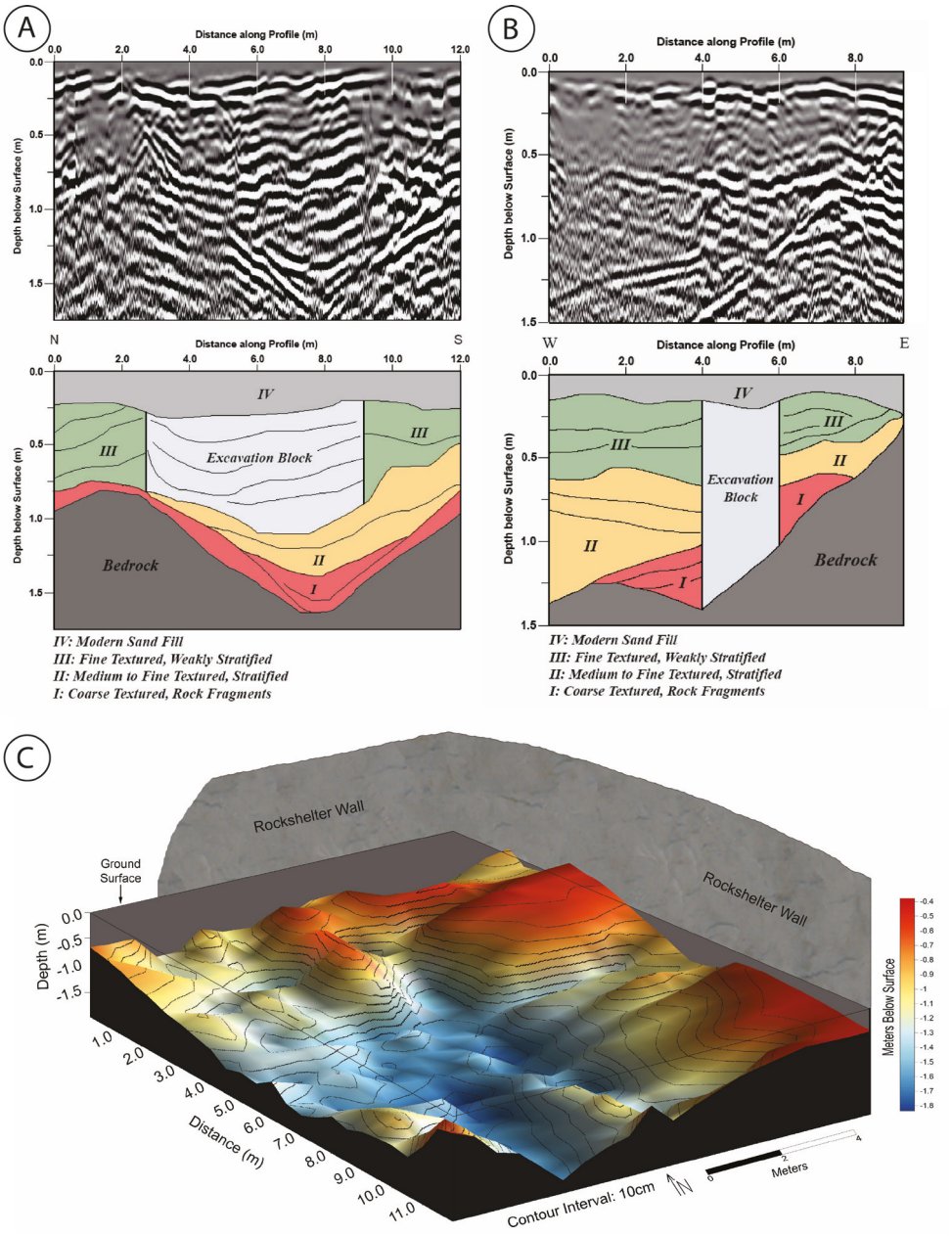

Fig. 7A. Post-processed and interpreted example of north-south trending GPR profile. This profile crossed the area of the current excavations. 7B) Post-processed and interpreted example of west-east trending GPR profile. This profile also crossed the area of the current excavations. 7C) Three-dimensional reconstruction of bedrock topography from GPR data. Note variable bedrock surface and relatively deep depression in south-central section of the site. This basin is infilled with the coarse deposits of phases L and K.

Water and sediment chemistry results

The results of the elemental analysis of drip water collected from along the joint is presented in Table 2. Most measured elements showed a general trend towards enrichment following percolation through the bedrock and overlying deposits. Of particular note, Ca, K, Mg, Na, and P were particularly enriched relative to the rainwater collected outside of the cave. Because the rainstorm occurred during the late summer, this water composition likely represents a seasonal end-member of dripwater composition that ranges from concentrated in contaminants to more dilute, as rains flush through bird guano, dassie middens, and other organic materials accumulated above the site during the dry season (spring, summer and fall). We expect late winter dripwater to have a different composition.

Micromorphology and microcontextual analysis

We collected a total of eight block samples for micromorphological analysis (Table 3) and 33 loose samples for other mineralogical analyses. Sampling for micromorphology

TABLE 2

Elemental analysis of rain and seep water from Elands Bay Cave, along with measurements made on the blank. Values are reported as mg/L. Sample 1 was collected on 30 March 2012 from rain water, a day after it had started to storm. Sample 2 was collected on the 29 March 2012, from rain water when it had just begun to storm. Sample 3 was collected on the 30 March 2012, from seep water within the cave.

Element	Water sample 1	Water sample 2	Water sample 3	Blank
Al	0.014	0.102	0.593	Below detection limit of 0.004
B	0.038	0.101	0.463	0.011
Ba	0.008	0.021	0.027	0.001
Ca	2.635	13.220	79.403	0.381
Cr	Below detection limit of 0.002	Below detection limit of 0.002	0.003	Below detection limit of 0.002
Cu	Below detection limit of 0.003	0.022	0.010	Below detection limit of 0.003
Fe	0.015	0.101	0.788	0.002
K	2.067	11.327	101.457	Below detection limit of 0.073
Li	Below detection limit of 0.005	Below detection limit of 0.005	0.017	Below detection limit of 0.005
Mg	1.330	9.522	97.464	0.168
Mn	Below detection limit of 0.002	0.003	0.003	Below detection limit of 0.002
Na	7.409	65.621	811.178	0.388
Ni	Below detection limit of 0.002	0.002	0.004	Below detection limit of 0.002
P	0.501	1.357	2.169	Below detection limit of 0.007
Sr	0.008	0.109	0.778	0.001
Zn	0.003	0.036	0.018	0.005

TABLE 3
A list of block samples collected for microcontextual analysis, along with sample location, and stratigraphic, chronologic and cultural information.

Sample	Profile location	Stratigraphic designation	Chronocultural designation
EBC-12-08	Southern profile	Contact of phases D/F	Early LSA (phase F), dates between 24.2 and 22.1 ka cal BP; Robberg (phase D), dates between 19.4 and 18.8 ka cal BP.
EBC-12-07	Eastern profile	Farik, Fael, Dorothee	Early LSA (phase F), dates between 24.2 and 22.1 ka cal BP; Robberg (phase D), dates between 19.4 and 18.8 ka cal BP.
EBC-12-06 (a and b)	Eastern profile	Fuzy, France	Early LSA, dates between 24.2 and 22.1 ka cal BP.
EBC-12-03	Eastern profile	Henri	Late phase of MSA, not directly dated
EBC-12-05	Southern profile	Phase I (above Imriz)	Late phase of MSA, dates between 36.8 and 38.9 ka cal BP.
EBC-12-04	Eastern profile	Ibis	Late phase of MSA, dates between 36.8 and 38.9 ka cal BP.
EBC-12-02	Eastern profile	Ines, Imriz, Imran	Late phase of MSA, dates between 36.8 and 38.9 ka cal BP.
EBC-12-01	Eastern profile	Keva, Kelly/Kent	Contact between early phase of MSA and a later, undated phase of the MSA.

focused on the eastern profile, known as the Main Section (squares 1c, 2d and 2c), since 1) this was the primary profile of investigation for the current excavations, 2) it provided us with complete diachronic coverage of the sequence excavated by the current excavations, and 3) this profile exhibited the least amount of physical disturbance by secondary nodule formation. However, we aimed to examine not only diachronic variations in the deposits, but lateral variations as well. Therefore, we also collected block samples from the southern profile. Below we provide the results of micromorphological and microcontextual analyses, beginning with the stratigraphically lowest sample.

EBC-12-01

We collected this sample from the contact between SU Keva and SU Kelly/Kent, which is the top of the coarse, 'frost-shattered' deposits of the MSA I overlain by later Middle Stone Age occupations. The contact is clearly visible in the block so that it was possible to divide the thin section into two distinct depositional units (Fig. 8).

In both Keva and Kelly/Kent the groundmass exhibits a close to single-spaced enaulic c/f-related distribution, with the coarse fraction composed mostly of a poorly sorted mixture of fine-to-medium sand-sized, subangular grains of quartz and rare feldspar. The fine-fraction is mostly composed of microaggregated silt-sized fragments of finely-comminuted organic material, some of which appears humified and some carbonized. The characteristics of the groundmass identified here are similar throughout most of the Elands Bay sequence, and also resemble the groundmass identified at other Middle Stone Age quartzite rock shelters, such as Sibudu (Goldberg et al. 2009) and

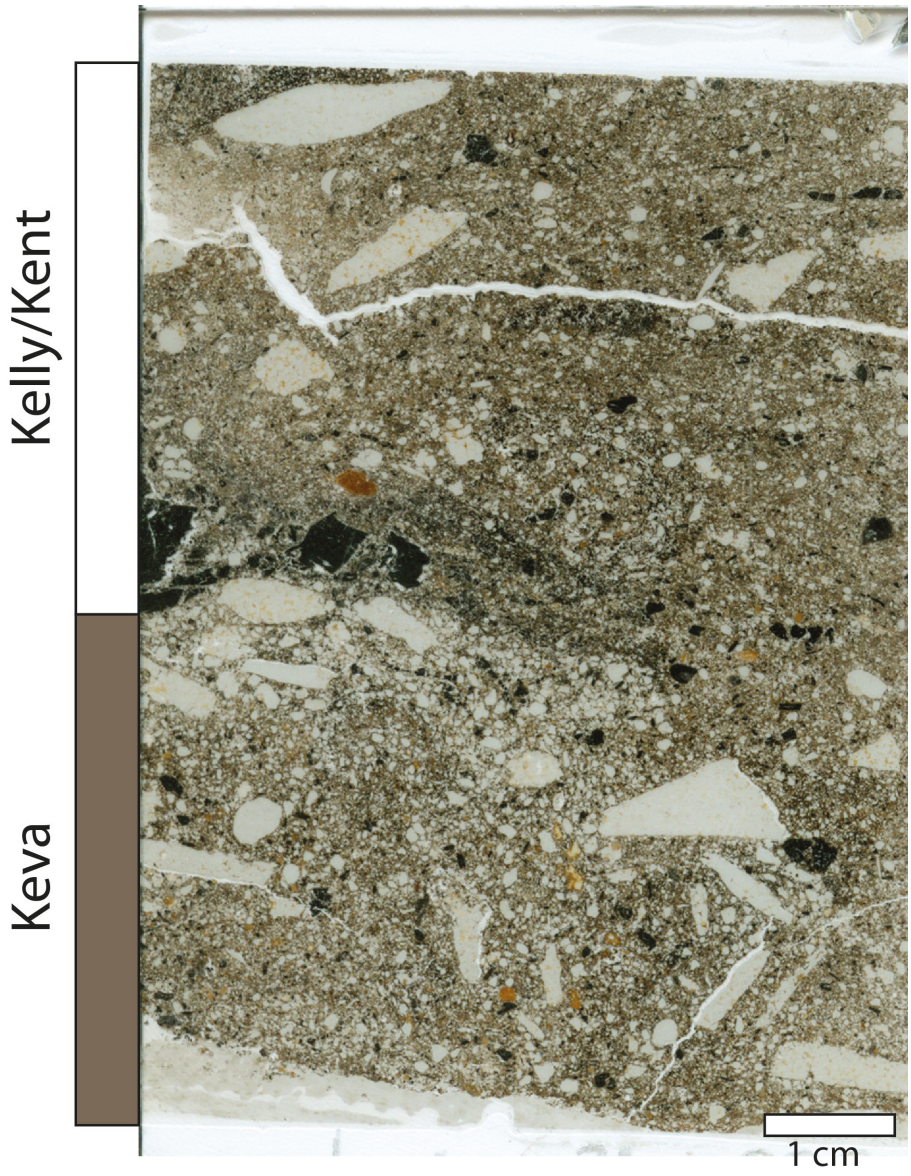

Fig. 8. Flatbed scan of EBC-12-01. This sample was collected from the contact between Keva and Kelly/Kent, which represents a significant unconformity in the Elands Bay sequence.

Diepkloof (Miller et al. 2013). Material coarser than medium sand is also present at about 20–30 % abundance. The coarser components include: 1) well-rounded, coarse sand-sized grains of single crystal and polycrystalline quartz, 2) centimetre-sized, angular, elongated fragments of weakly metamorphosed quartzite, likely derived from spalling of the cave ceiling and walls, and 3) sub-angular fragments of woody charcoal, generally less than 0. 5 cm in size. Some of the fragments of quartzite roof spall appear

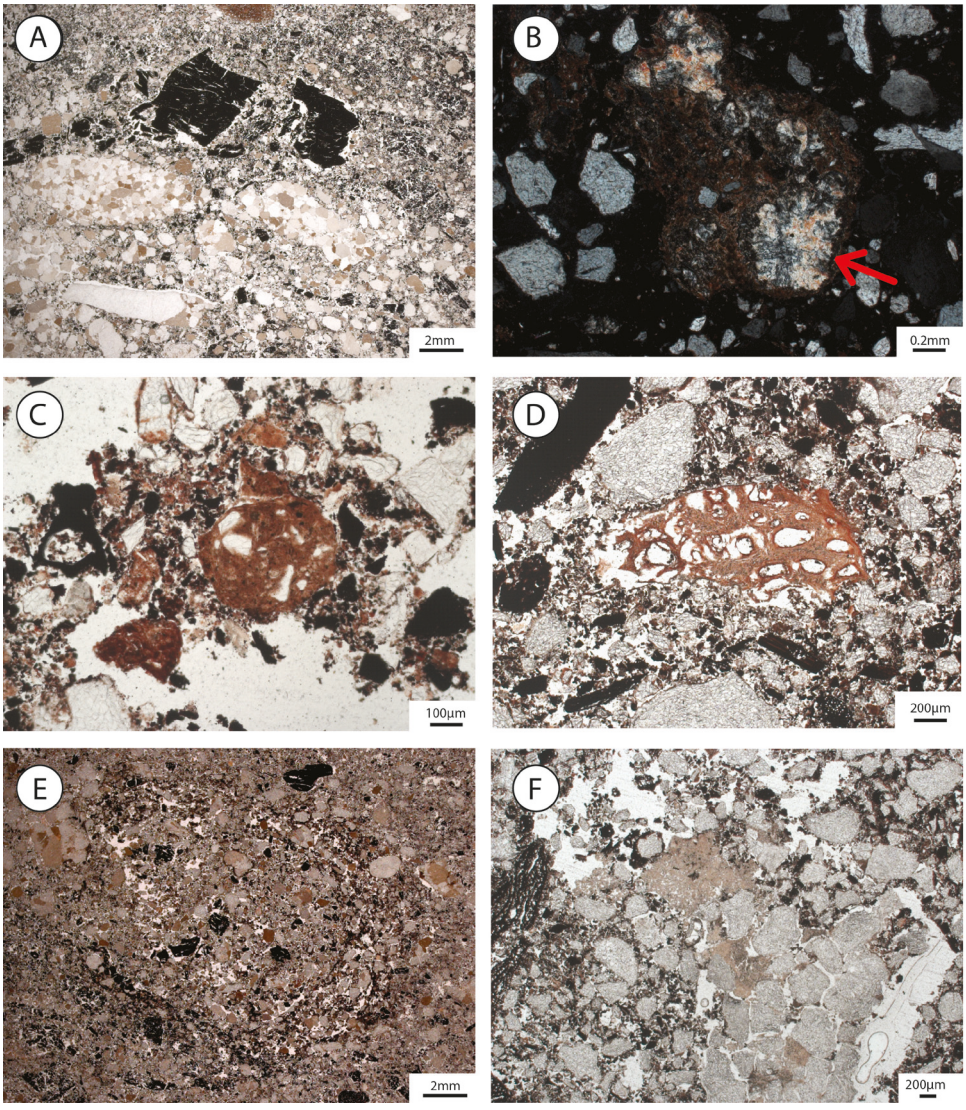

Fig. 9. Microphotographs from EBC-12-01. 9A) The contact between Keva and Kelly/Kent. Note the horizontally oriented clasts of quartzite, indicating the erosional surface on Keva. On top of this surface is a lenticular concentration of charcoal, possibly representing a combustion feature. PPL. 9B) A clay rich aggregate in which secondary nodules of variscite have formed, SU Keva. XPL. 9C) Another clay rich aggregate, SU Kelly/Kent, note the absence of variscite, which is only found in aggregates in SU Keva. PPL. 9D) Fragment of bone, partially dissolved. Bone was not found in these SUs during excavation, but a few sand-sized fragments, often altered, have been identified in thin section. PPL. 9E) Burrow, indicating bioturbation. Evidence for bioturbation at Elands Bay Cave is mostly limited to discrete passage features, as those seen here. PPL. 9F) Fragment of quartzite derived from the bedrock, undergoing in situ granular disaggregation as the result of secondary formation of taranakite. PPL.

to have disaggregated *in situ*, contributing to the sand-sized fraction of the ground mass (Fig. 9). Additionally, the elongated quartzite fragments in most of Keva show no preferred fabric; rather they display a random orientation. There are a few, rounded, medium-to-coarse sand-sized aggregates of silt and clay present in Keva. The clay fraction in these aggregates display a stipple-speckled to striated b-fabric. Some of these aggregates show evidence for chemical alteration in the form of radial, crystalline intergrowths that exhibit low-order grey and yellow interference colours. We analysed the composition of these intergrowths directly in thin section using μFTIR, SEM-EDS and μXRD. FTIR spectra obtained from these crystals had a broad peak around 1620,a shoulder at 1140, and peaks at 1025, 1005, 905, 585 wave numbers. The EDS measurements indicated that the mineral contained Al and P. μXRD measurements made directly on the thin section identified the mineral as variscite ($AlPO_4 \cdot 2H_2O$). Other nodules of secondary minerals were visible in Keva in addition to the variscite found forming in the silty clay aggregates. These nodules are typically 1–2 mm in size and appear pale yellow in PPL, exhibit low-order greys in XPL, and strongly fluorescing under blue-light fluorescence. At higher magnifications (200x) individual crystals, up to 30 μm in size, are visible and display a platy habit in parallel aggregates. We collected μFTIR measurements of these nodules directly on the thin section and obtained spectra with diagnostic peaks at 1097, 1056, 1013, 949, 696, 642, and 601 wave numbers, confirming an identification of taranakite, $(K,Na)_3(Al, Fe^{3+})_5(PO_4)_2(HPO_4)_6 \cdot 18H_2O$, with SEM-EDS analyses suggesting that the phase is rich in K.

The contact between Keva and Kelly/Kent is locally sharp and clear. The upper portion of the lower depositional unit shows an increase in the coarser fraction (medium to coarse sand). Furthermore, elongated fragments of quartzite roof spall exhibit a horizontal, preferred orientation at the contact. The sharp, upper portion of the contact is directly overlain by a cm-thick lens containing angular, 0.5 cm fragments of charcoal. This lens also appears to have a lower proportion of coarse sand compared to sediment above or below, and is dominated by fine sand. The sharp contact and charcoal-rich lens do not appear to be laterally continuous across the thin section, but both appear to be locally disturbed by mesofauna biogalleries.

The upper depositional unit (Kelly/Kent) contains similar sedimentary components and exhibits generally similar micromorphological characteristics as those described for the lower unit (Keva). The c/f-related distribution is close- to single-spaced fine enaulic; however, the coarse fraction here appears slightly finer than that described for Keva. Additionally, there are fewer cm-sized fragments of quartzite roof spall (ca. 10 % abundance). These appear to exhibit a horizontal to sub-horizontal preferred orientation which parallels the weakly expressed, sub-cm thick sedimentary bedding visible in the thin section. Silt and clay aggregates exhibiting stipple-speckled and striated b-fabric are also present in Kelly/Kent, albeit finer grained (0. 5 mm) and in lower abundance (< 5 %) compared to those found in Keva. Additionally, the aggregates in Kelly/Kent do not exhibit any secondary crystal intergrowths. Other secondary nodules are present and appear similar in appearance and abundance to those described in Keva. μFTIR measurements of these nodules made in thin section confirmed that they are also composed of taranakite.

Organic petrographic analyses confirm the observation that finely comminuted organic material constitutes a significant portion of the sediment in these samples

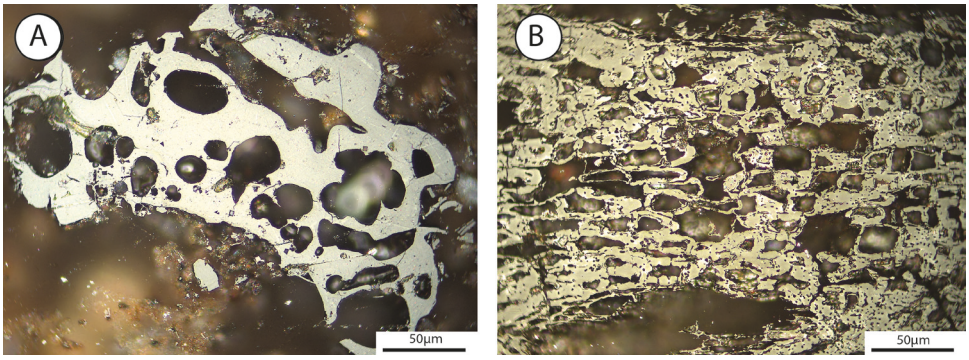

Fig. 10. Photomicrographs collected in reflected light used in the organic petrographic analysis 10A) a fragment of fat-derived char from Kelly/Kent in sample EBC-12-01. Fat-derived char is relatively common at Elands Bay Cave and suggests that the occupants were either burning bone or cooking at the site. 10B) Kelly/Kent, EBC-12-01.A fragment of permineralized charcoal showing evidence of fungal attack. The large voids are the cell walls, and the smaller voids were caused by fungal attack. Many of the plant tissues at Elands Bay Cave show evidence for humification and fungal attack prior to burning.

(Fig. 10). The fine fraction of organics is composed of both woody and herbaceous tissues, with one well-preserved leaf fragment visible. Many of the tissue fragments show evidence of having been humified: their cell walls are swollen or incompletely dissolved by cellulose hydrolysis, giving them a corroded appearance. Gelified humus colloid droplets as well as fillings occur in the cell lumens. Additionally, the cell walls of most of the tissues are perforated as the result of fungal degradation. The observation of fungal degradation is supported by the presence of sclerotia within this sample.

Interestingly, the humification of these tissues appear to have occurred prior to combustion. In Keva, reflectance values range from 0.82 % to 1.87 % Ro, although most occur between 0.82 and 1.49 % Ro, allowing us to classify those with the lower values as low-reflecting fusinite (charcoal) whereas those with the highest values correspond with typical fusinite. These values are different from those measured in Kelly/Kent, where the tissue fragments exhibit values ranging between 0.62 and 1.22 % Ro.

Bone is almost completely absent from both Keva and Kelly/Kent. Only a single, sand-sized fragment of bone was found at the base of Kelly/Kent, and it appeared etched and did not fluoresce under blue light.

EBC-12-02

This sample was collected from SUs Ines, Imriz and Imran. In the field, these layers appeared laminated and contained thin, light-coloured lenses. In thin section, we were able to identify six discrete depositional units (Fig. 11). The mineral component in the lowermost unit, unit 1, is poorly sorted and composed of coarse silt/fine sand to coarse sand. The fine fraction is largely composed of finely comminuted organic material that exhibits a granular microstructure. Rare fragments of quartzite bedrock are present, all under 0.5 cm in size, and display no preferred orientation. Unit 1 is capped by a thin (0.75 cm) lens of subangular fragments of charcoal (unit 2), ranging from silt-sized fragments up to 0.5 cm in size. The upper and lower units of this lens are sharp and clear. Mineral grains are almost completely absent from unit 2, a characteristic observed

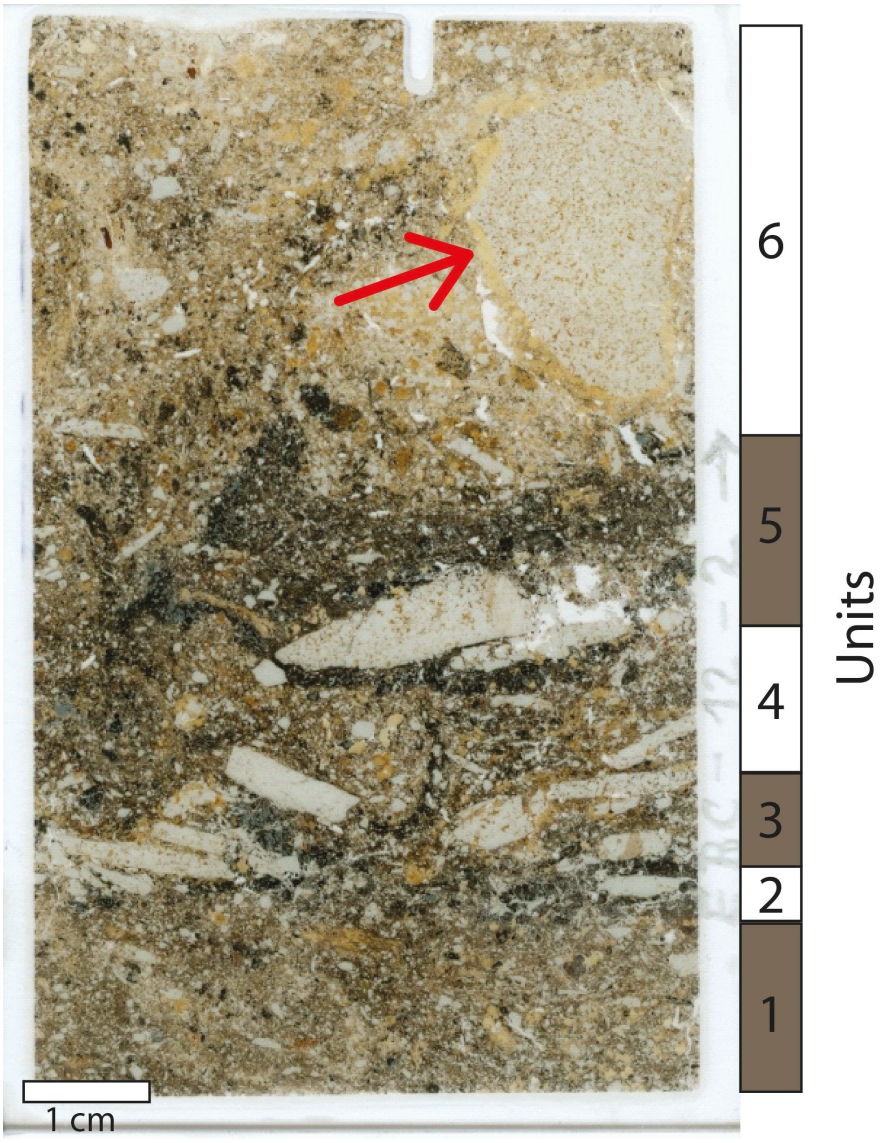

Fig. 11. flatbed scan of EBC-12-02 indicating the depositional units identified in thin section. Note the large block of quartzite around which a crust of taranakite has formed. Here one can see that units 2 and 5 are rich in charcoal, and unit 5 has a sharp lower contact.

from other charcoal lenses at similar Middle Stone Age sites, such as Diepkloof (Miller et al. 2013). The third depositional unit is dominated by cm-sized, elongated, angular fragments of bedrock that display a clear horizontal orientation. The interstitial material between the fragments of bedrock is composed of sand-sized mineral grains and microgranular organic material, resembling the groundmass described for unit 1 in this sample. The charcoal lens and overlying angular bedrock fragments likely

marks the contact between layers Ines and Imriz. The contact between unit 3 (the bedrock fragment unit) and the overlying unit (unit 4) is gradational. Here, the fine organic component appears coarser than that described for unit 1; rounded fragments of charcoal, about 0.5 mm in diameter, are common. Additionally, the fine granular organic component appears partially aggregated, reducing the overall porosity of the unit. The upper contact of unit 4 is sharp and clear, apart from a small portion that is disturbed by passage features. Unit 5 is largely composed of sub-angular fragments of charcoal; the fine fraction is also composed of charcoal, but exhibits a granular microstructure. Mineral grains are absent from the base of unit 5 although a large, horizontally-oriented, cm-sized fragment of bedrock is present. Above this fragment, mineral grains ranging in size from coarse silt to sand are present but not at the frequency encountered in units 1 or 4. The upper contact of unit 5 is clear but diffuse and appears disturbed, likely as a result of bioturbation. Unit 6 appears much lighter in colour than the other depositional units encountered in this sample. It contains mineral grains that are poorly sorted and range in size from coarse silt to coarse sand. Fragments of charcoal or organic material are rare and when present, appear rounded. A few rounded aggregates of clay and silt are present. Bedrock fragments are also rare, apart from a large, 2 cm sized rounded fragment.

The fine fraction of unit 6 is composed almost exclusively of secondarily-formed materials, accounting for the light colour of the unit. Throughout the rest of this sample, secondary nodules are also common and appear generally similar to the material found in unit 6. In PPL the nodules range in colour from pale yellow to dark orange and present as either discrete nodules, often no larger than 1–2 mm in size to 1.5 mm sized crusts and weakly-developed veins. In XPL the nodules range from anisotropic to weakly isotropic, exhibiting low order grey to yellow interference colours. In units 1–5, the secondary components appear more nodular, whereas in unit 6 they are diffuse, comprising a dominant part of the fine fraction. We collected FTIR spectra on the nodules and crusts directly on the thin section confirming that many are composed of taranakite, as identified in sample EBC-12-01. Other nodules are composed of amorphous silica, or opal (Fig. 12). In addition, the large, rounded fragment of quartzite bedrock in unit 6 is coated in a 1.5 mm thick crust of taranakite.

We collected an autoradiograph image of the corresponding chip from this sample (Fig. 13). The taranakite crust forming on the quartzite block clearly showed higher radioactivity relative to the surrounding sediment, suggesting that the taranakite was rich in potassium. Within this crust we noted several distinct voids that appear bladey and have a radial distribution. The morphology of the voids, and their orientation, suggests that they are pseudomorphic after a crystal intergrowth of gypsum which has subsequently dissolved. Very few, sand-sized fragments of bone are present and appear sub-rounded, stained and altered. These fragments do not fluoresce under blue light and FTIR measurements collected directly from the thin section suggest that the bones are composed of the original hydroxylapatite.

EBC-12-04

This sample was collected from layer Ibis, and is stratigraphically lower than EBC-12-03, but higher in terms of depth below datum. In the field, and in thin section, the sample appeared laminated, and in thin section we were able to identify seven distinct

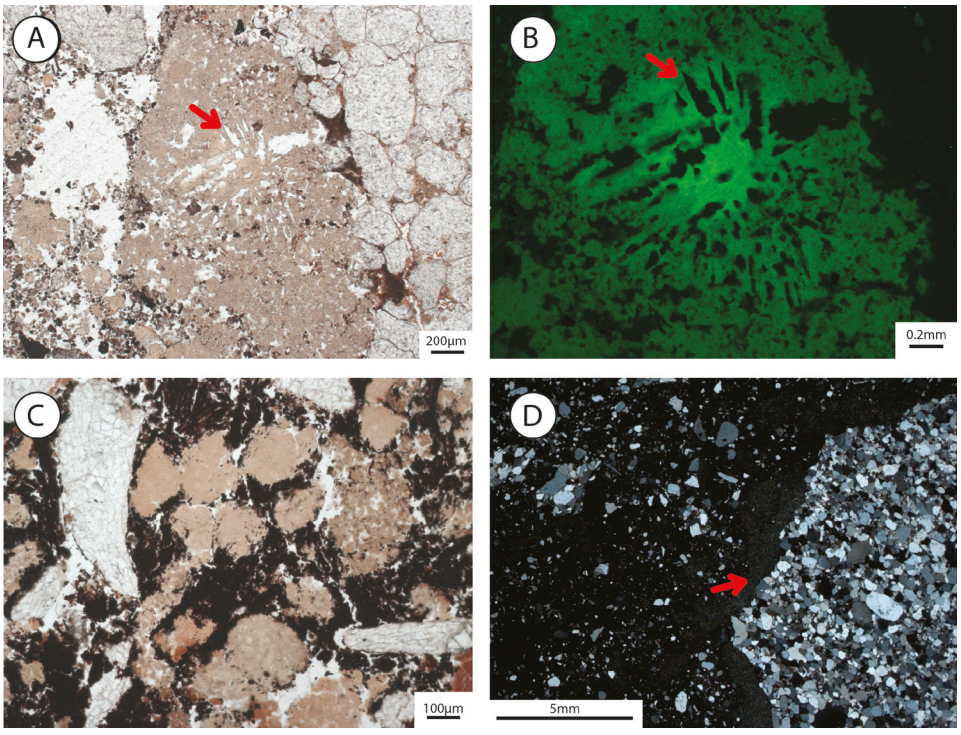

Fig. 12. Microphotographs of EBC-12-02. 12A) The taranakite crust growing on the large quartzite fragment, with pseudomorphic voids after gypsum. PPL. 12B) Same view as 12A, but at higher magnification and under blue light fluorescence. 12C) Nodules of taranakite growing within a fragment of charcoal, and physically destroying it. 12D) The quartzite bock with the taranakite crust, XPL.

depositional units (Fig. 14). The lowermost unit, unit 1, appears lighter coloured than most other units described in this sample. The mineral grains range in size from coarse silt to coarse sand and are poorly sorted. They also appear slightly more rounded than mineral grains described in samples collected stratigraphically below EBC-12-04. The fine fraction is composed largely of finely-comminuted, organic material and individual phytoliths are also present. Organic petrographic analysis and associated reflectance measurements on the tissues indicate that they are derived from herbaceous and woody plants and have been burnt. Apart from a large, cm-sized block of quartzite at the top of the unit, there are only a few, sub-rounded granule-sized fragments of quartzite bedrock. Aggregates of clay and silt are present and are more abundant than in either EBC-12-01 or EBC-12-02. These aggregates appear throughout sample EBC-12-04. In addition, many of the aggregates composed of clay and silt appear to be chemically altered and even partially dissolved. We collected one FTIR spectrum on a soil aggregate that confirmed that it was composed of quartz and clay. However, another spectrum collected from a different aggregate showed that it was composed of amorphous silica. Sand-sized and even larger fragments of bone are present in unit 1 at ca. 5–10 % abundance and appear more frequent towards the top of unit 1. The bones appear partially dissolved and stained and altered. They do not fluoresce in blue light.

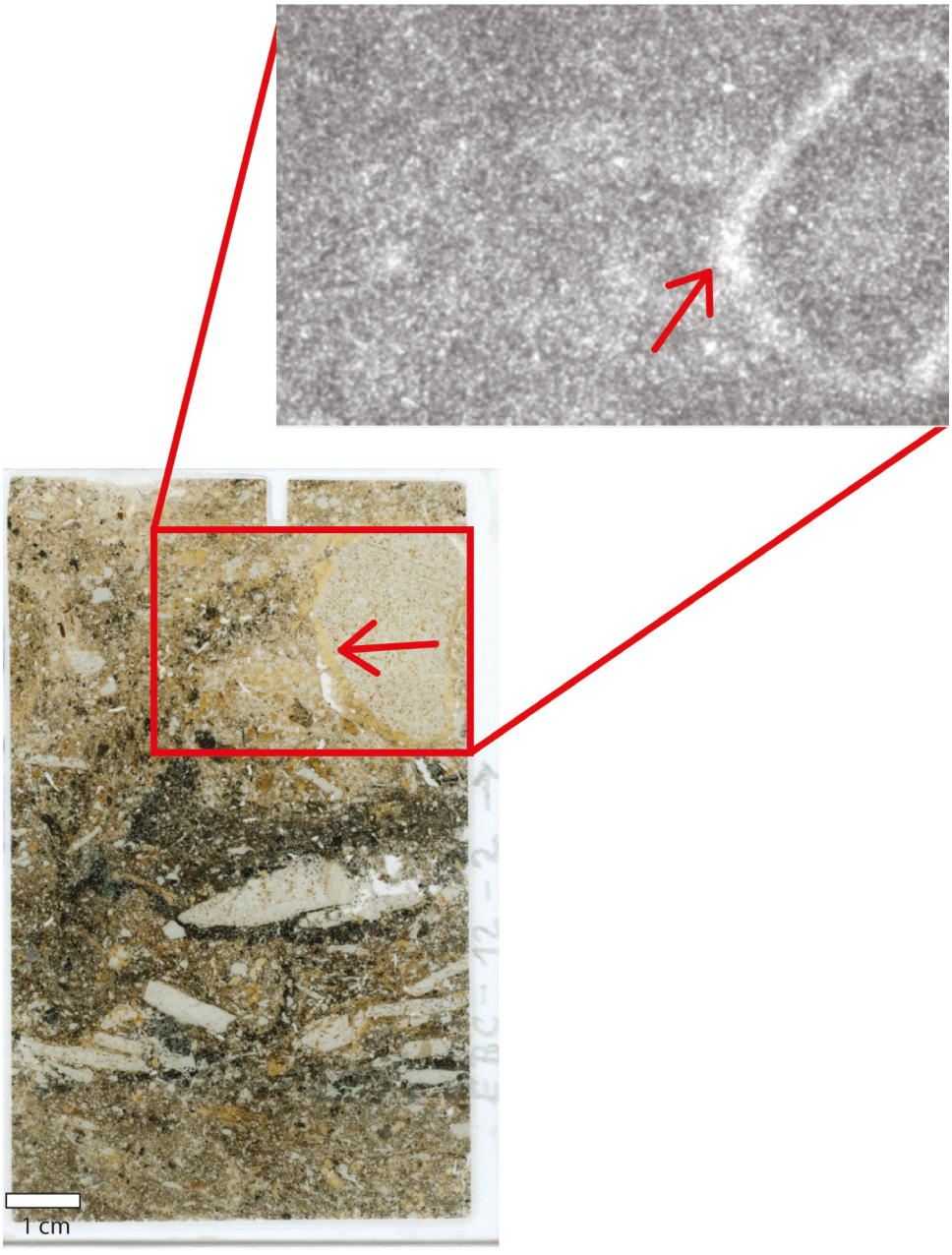

Fig. 13. Autoradiography image of a portion of sample EBC-12-02.The white ring (indicated by the arrow) is the taranakite crust forming on the quartzite block. The slight variation in morphology compared to the thin section is because the image was produced from the chip. These results indicated that the taranakite is the potassium-rich end member, an observation confirmed by the SEM-EDS results.

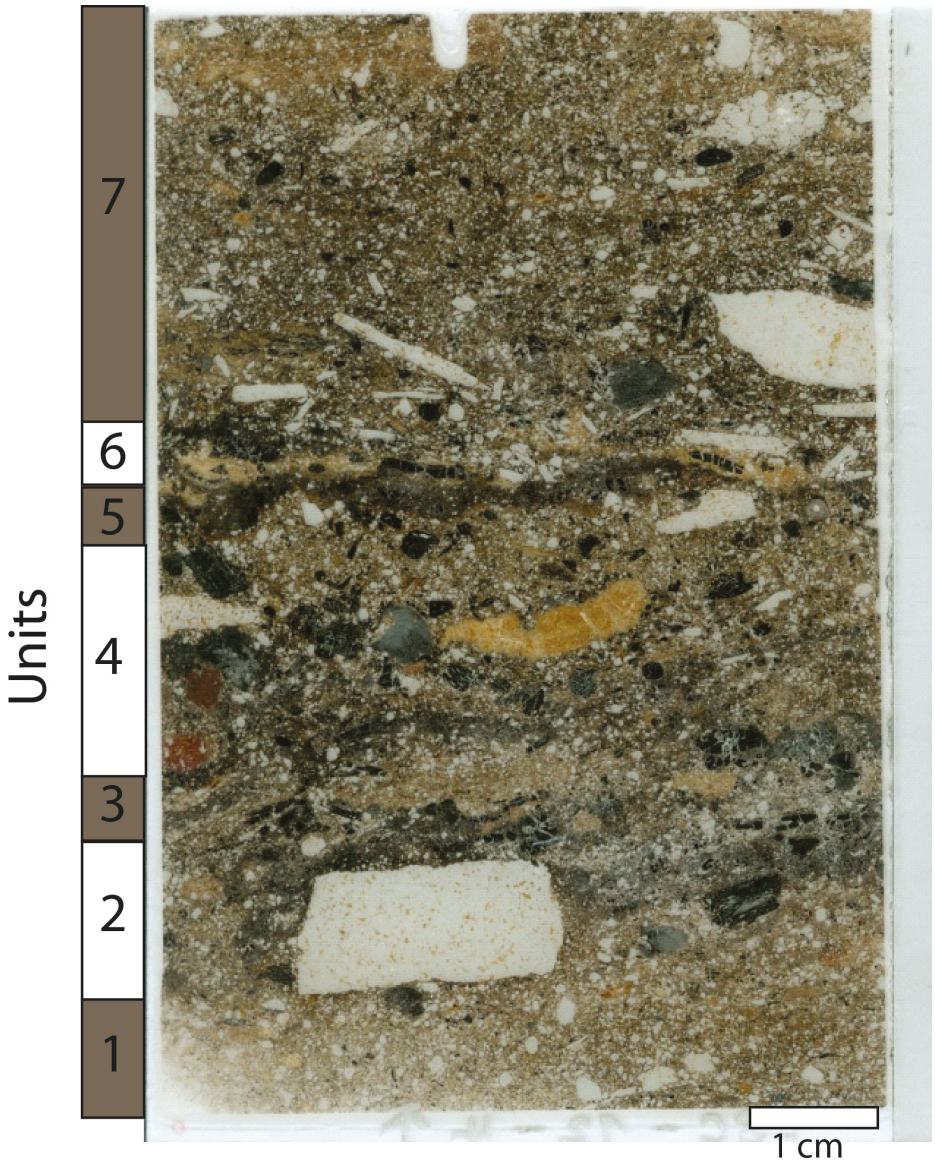

Fig. 14. Flatbed scan of EBC-12-04 indicating the depositional units identified in thin section.

The contact between units 1 and 2 is clear yet diffuse. The fine and coarse fraction of unit 2 is largely composed of charcoal, including 0.5 cm sized sub-angular fragments of woody charcoal, and smaller fragments of herbaceous charcoal. Mineral grains are present, and appear similar to those in unit 1, albeit in lower proportions. The contact between unit 2 and the overlying unit 3 is sharp but irregular. Unit 3 appears to be a lens that is relatively light-coloured in PPL and generally resembles unit 1; however, the fine fraction appears to be more granular here and contains more mineral

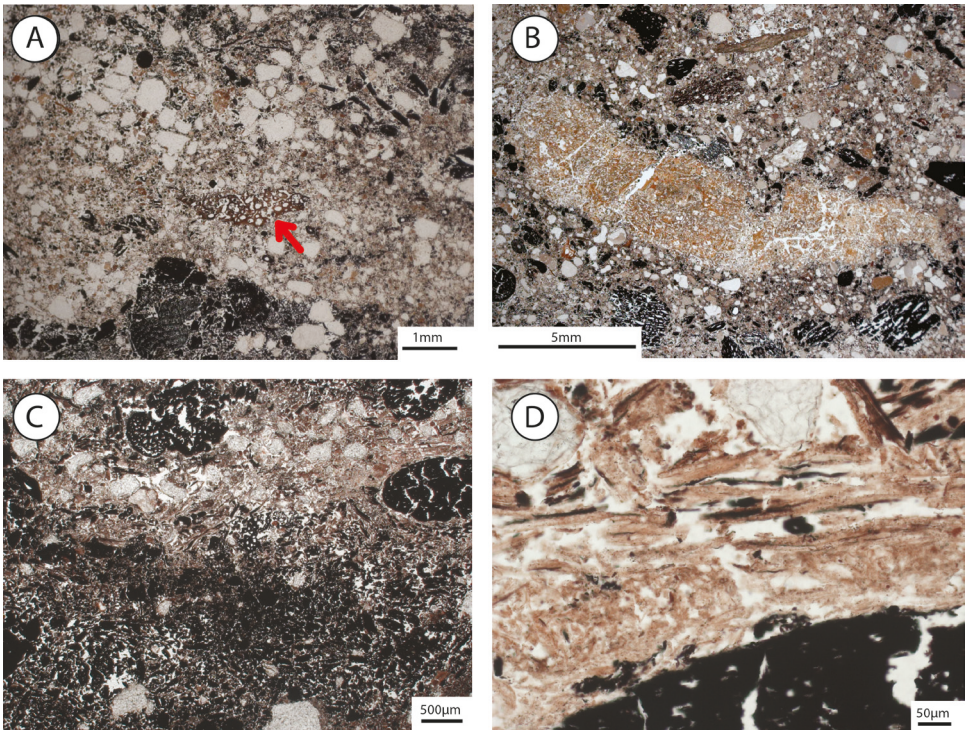

Fig. 15. Microphotographs of sample EBC-12-04. 15A) A sand-sized fragment of spongey bone that appears altered. 15B) A weathered, fissured rock fragment, likely derived from the local conglomeritic bedrock. It is surrounded by fragments of charcoal. PPL. 15C) A thin lens of charcoal. PPL. 15D) Laminated, articulated phytoliths. PPL.

constituents, including clay minerals. Fine-sand-sized, rounded fragments of charcoal are present, as are fine-sand-sized, rounded aggregates of clay and silt. A single, sub-angular fragment of partially dissolved spongy bone, 1.5 mm long, is present in the centre of the lens.

The contact between unit 3 and 4 is clear and locally diffuse. The layer is lighter coloured, and in this respect resembles both units 1 and 3; however, it can be distinguished from the underlying unit 3 by a very thin and discontinuous lens of herbaceous charcoal. Unlike units 1 and 3, the abundance of sub-rounded fragments of granule-sized charcoal is about 20 %. In addition, unit 4 contains three fragments of rock that are distinct from the more typical quartzite (Fig. 15). These include a centimetre-sized fragment of what appears to be an extensively weathered metamorphic rock, a fragment of iron-rich siltstone, and a smaller fragment of a weathered, possibly sedimentary rock. These may derive from the local conglomeritic bedrock, the Piekenierskloof Formation. The contact between unit 4 and 5 is sharp, clear and continuous across the thin section. The fine fraction at the top of unit 4 appears compacted, such that the c/f-related distribution appears porphyric. Additionally, the top of this unit contains numerous granule-sized, subangular fragments of spongey bone that appear stained and also partially altered and dissolved. They do not fluoresce under blue light.

Unit 5 is composed almost exclusively of charcoal that is mostly sub-angular and medium-sand sized. Much of it appears herbaceous. A few fragments of clearly non-carbonized (i.e. humified) plant material is also present. Organic petrographic analysis identified several elongated, permineralized organic clasts that are rich in silt-sized grains of quartz and that exhibit a network-porous texture reminiscent of peat. These fragments do not appear to have been heated, but appear humified. Mineral components are almost completely absent from this unit. The contact with the overlying unit 6 is clear, and sharp to diffuse. This unit is locally discontinuous across the thin section and is light coloured in PPL, and isotropic in XPL. The sediment generally lacks mineral components at its base, but contains quartz, ranging in size from coarse silt to coarse sand at its top. The lower part of the unit is composed almost exclusively of articulated phytoliths. The contact with the overlying unit, where present, is sharp and clear, and is marked by a thin lens of charcoal and elongated, mm-sized fragments of quartzite bedrock located at the base of unit 7. This unit displays the typical single-spaced to close fine enaulic c/f-related distribution found elsewhere at the site; however, the structure fine fraction appears more compact than that described for units 1 and 3 in this sample. Additionally, there are several thin lenses and horizontal concentrations of charcoal that give the unit a weakly laminated to bedded appearance. Of particular note is a 2–3 mm thick, laterally discontinuous lens of horizontally oriented herbaceous charcoal and laminated, articulated phytoliths. Charcoal is finely comminuted and generally dispersed evenly through the unit. Larger, subangular fragments, ranging in size between 3 mm to 8 mm are present as well, at 5–10 % abundance.

There are very few secondary mineral nodules present in this sample, especially when compared to sample EBC-12-02. Several mm-sized nodules of what appears to be taranakite are present at both the base and top of this sample. Direct μFTIR measurements made on these nodules in thin section, shows however, that they are composed of amorphous silica.

EBC-12-05

This sample was collected from the south profile, directly above layer Imriz within depositional phase I, making it roughly stratigraphically equivalent to samples EBC-12-02 and EBC-12-04. As noted in the field, and described from other thin sections from phase I, the deposits in this sample appear bedded and laminated, and 6 distinct depositional units could be identified in thin section (Fig. 16). Only a very small area of the lowermost unit, unit 1, is present in the thin section. The unit appears light brown in PPL it is more compact than other deposits, such that at lower magnification it appears partially porphyric. There is a single, sand-sized, sub-angular fragment of bone present. The upper portion of this unit appears partially reddened and it has a sharp, irregular contact with the overlying unit 2. Portions of this contact have been disturbed by bioturbation. Unit 2 is locally up to 1cm thick and is composed of sand-sized, subrounded fragments of woody and fibrous charcoal, with more elongate fragments displaying a preferred, horizontal orientation. Sand and silt-sized grains of quartz are less abundant here than in unit 1, at about 10 %.

Unit 2 has a gradual to locally sharp contact with the overlying unit 3, which appears lighter in colour and is generally similar to unit 1 in composition and microstructure; however, this unit contains more and larger sub-angular sand-sized fragments of

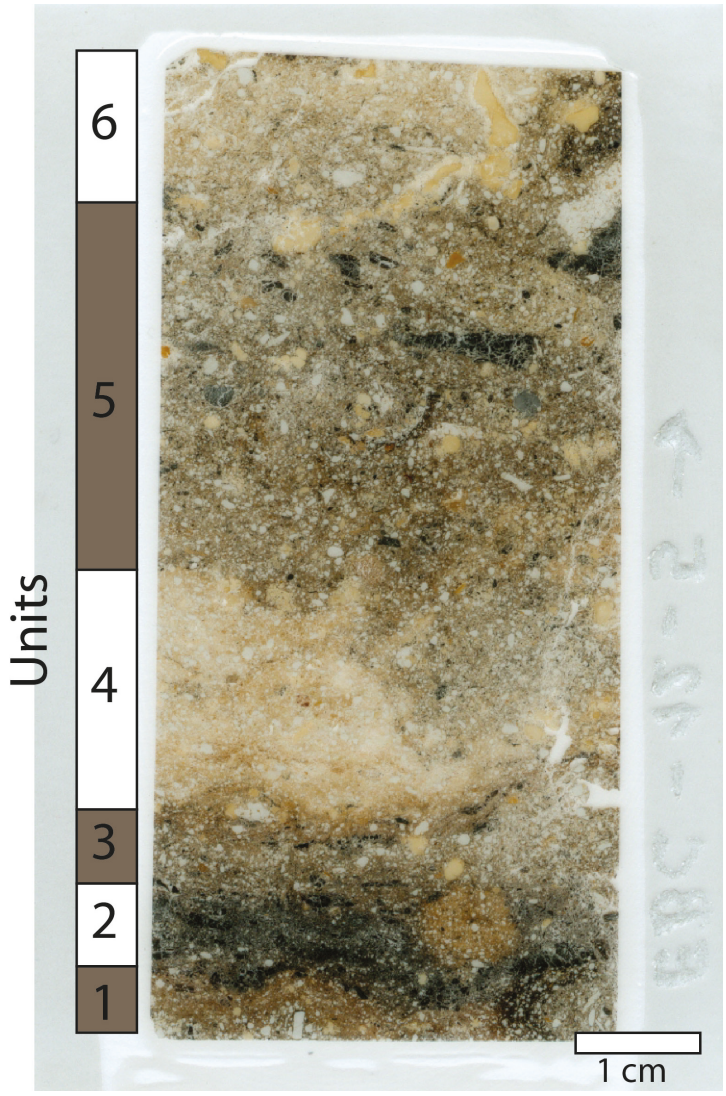

Fig. 16. Flatbed scan of EBC-12-05 indicating the depositional units identified in thin section. Note the sharp contact between the charcoal-rich unit 2 and the underlying reddened unit. Additionally, note the yellowish crust at the top of unit 5.

fibrous and woody charcoal, at about 20 % abundance (Fig. 17). Stringers of articulated phytoliths are present, as are angular fragments of what appears to be fat-derived char (Goldberg et al. 2009). A large passage feature in this unit indicates some degree of disturbance by bioturbation.

The contact with unit 4 is gradual and marked by a lighter colour in PPL and a significant decrease in the amount of charcoal present. This unit has a similar frequency and occurrence of quartz grains as described for unit 3 and 1; however, the fine fraction is composed largely of phytoliths, many articulated but showing no preferred orientation

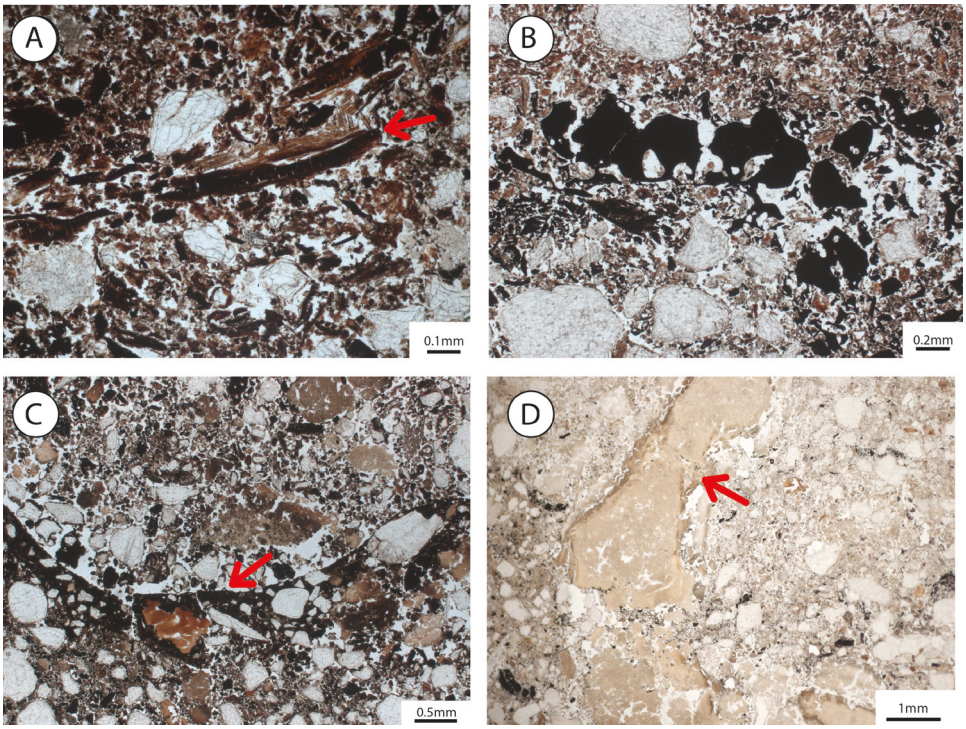

Fig. 17. Microphotographs of sample EBC-12-05. 17A) A stringer of articulated phytoliths. PPL. 17B) Fragments of fat-derived char. PPL. 17C) The outer rim of a biogallery. PPL. 17D) a crust that formed at the contact between units 5 and 6. MicroFTIR analysis of this crust shows that it is composed of opal and taranakite. PPL.

and appearing chemically altered. Finely comminuted organic material is also present as are silt-sized, ovular crystal aggregates with weak, low-order interference colours. μFTIR measurements made on these aggregates in thin section identified them as opal. Some bone fragments are present in this unit; all are sand-sized and sub-rounded. Direct measurements on these bone fragments in thin section with the FTIR suggests that they have been burnt, based on comparison with experimental reference samples in thin section and molecular changes to bone apatite with heating reported by Thompson et al. (2013). One in particular appears greyish in colour in PPL and has been heated to high temperature, as indicated by the presence of a peak at 625 cm-1. As with other units in this sample, unit 4 appears partially disturbed by bioturbation.

The contact with overlying unit 5 is relatively sharp and irregular. This unit generally resembles unit 3 in appearance. It contains several sub-angular, sand-sized fragments of bone that appear partially dissolved, as well as sand-sized aggregates of clay and silt. Unit 5 is relatively thick, ca. 2 cm, and exhibits no clear structural features or fabric. The top of this unit is capped by a mm-thick crust that appears yellow to brown in PPL. In XPL the lighter-yellow coloured areas appear strongly birefringent and exhibit first-order grey and white interference colours. The darker brown areas are isotropic. μFTIR measurements made on this crust in thin section show that it is variably composed of opal and taranakite. In places it appears partially disturbed and fragmented, likely as a

result of bioturbation. Where the crust is still in place, the contact with overlying unit 6 is sharp but where disturbed by bioturbation, the contact is more diffuse. Unit 6 has a similar composition to units 1, 3, 4, and 5 as described in this sample. The base of the unit contains sand-sized fragments of sub-angular charcoal; however, the proportion of charcoal in the unit dramatically decreases, so that the upper portion of the unit generally resembles unit 4. It contains articulated phytoliths, but at a lower frequency than unit 4, as well as opal, and finely comminuted, humified organic material.

In addition to the diagenetic crust, secondary nodules, ranging in size from ca. 100 μm to 2 mm, are also present throughout this sample. They are generally pale yellow to dark brown or orange in PPL. The nodules that appear darker in PPL also generally appear more isotropic in XPL, whereas the pale yellow nodules exhibit weak interference colours under XPL, with lower order greys to yellows. The optical characteristics of these nodules are generally similar to those described from sample EBC-12-02. *In situ* measurements made with the μFTIR confirm that they are composed of amorphous silica and taranakite.

EBC-12-03

This sample was collected from layer Henri and appeared relatively homogenous both in the field and in thin section. Coarse-sand-sized and larger, sub-angular to sub-rounded fragments of woody and herbaceous charcoal are present at 10–20 % abundance and are evenly distributed throughout the sample. Additionally, sand-sized, sub-angular fragments of what appears to be cortical bone are more numerous in this sample than in any of the stratigraphically lower samples. The fragments of bone appear stained, and altered or partially dissolved. Elongated, angular fragments of quartzite bedrock, most under 1cm in size, are present throughout the sample and do not exhibit any preferred orientation. Rounded aggregates of clay and silt, most mm-sized, are present as well.

Secondary nodules, most between 0.5 and 2 mm in size, are present throughout the sample (Fig. 18). Some of the nodules appear dense, light yellow in PPL, isotropic, and fluoresce under blue light. Others are less dense and appear greyish yellow in PPL. These nodules display low-order grey to yellow interference colours under XPL and fluoresce more strongly than the other nodules. In many instances, both types of material are found in the same nodule. In general, these nodules resemble those found in samples EBC-12-01 and EBC-12-02 and FTIR measurements made on them directly in thin section confirm that they are composed of either taranakite, opal, or a combination of both. In some places, the secondary nodules have grown within fragments of charcoal, thereby causing physical breakup of the charcoal.

Passage features are common in this sample, suggesting that bioturbation accounts for the general homogenous appearance of the deposit and the lack of orientation of elongated fragments of bedrock. There are two cm-sized, sub-rounded fragments of laminated organic material that may hint at a former fabric of the deposit that has since been destroyed.

EBC-12-06

We collected this sample at the contact between layers Fuzy, France, and the stratigraphically undifferentiated portion of the eastern profile that has been significantly affected by nodule growth. Because of the size of this sample we subsampled for thin

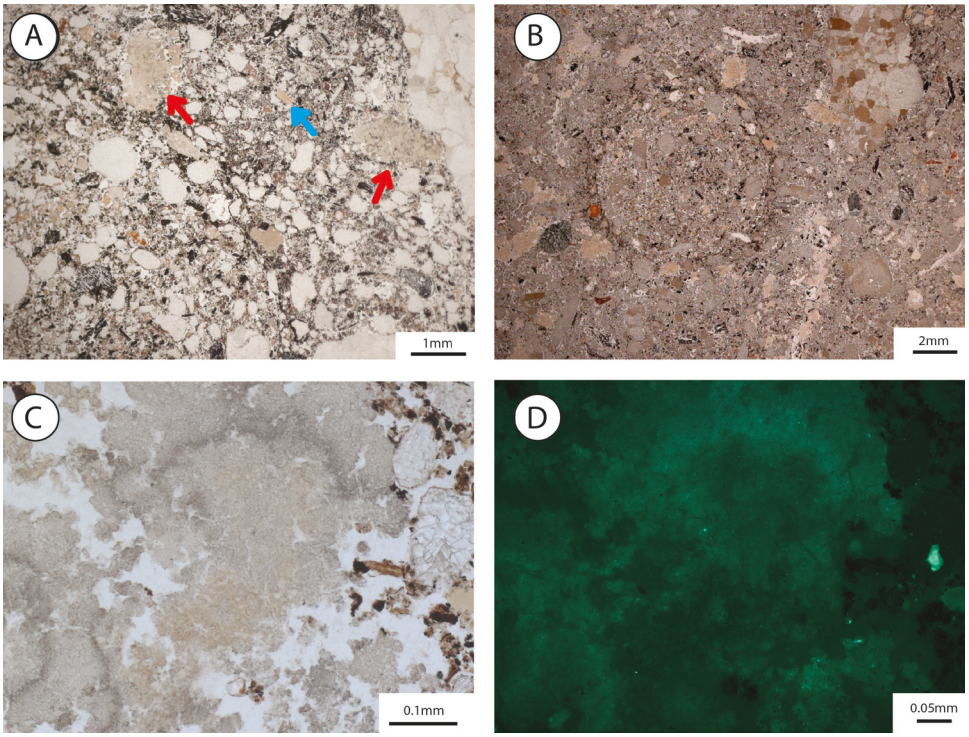

Fig. 18. Microphotographs of sample EBC-12-03. 18A) A general view of the deposits, showing secondary nodules of taranakite and opal, as well as a few fragments of bone. Bone was not found during excavation, but sand-sized fragments were visible in thin section. PPL. 18B) A biogallery, indicating the effects of bioturbation on the deposits. 18C) A secondary nodule composed of taranakite and opal, based on microFTIR analysis conducted directly on the thin section. PPL. 18D) Same view, but under blue light fluorescence.

sectioning, so that thin section EBC-12-06B is stratigraphically below EBC-12-06A (Fig. 19). Distinct units are visible in thin section that likely correspond to the units described in the field. The lower 2 cm of EBC-12-06B likely corresponds to Fuzy and contains a poorly sorted mixture of mineral grains ranging in size from coarse silt to coarse sand which is embedded within a fine matrix of finely comminuted organic material. There is little to no pore space between the silt-sized grains of organic material, such that this portion of the sample exhibits a porphyric c/f-related distribution. The upper portion of this sample has a similar composition to the lower portion; however, it is more porous, so that it displays a close to single-space fine enaulic c/f-related distribution. Passage features are present in this sample, suggesting some influence of bioturbation on fabric and composition of the deposit.

Unlike the other samples collected from Elands Bay Cave, EBC-12-06 contains a significant amount of fragmented bone, present at about 10 % abundance. The fragments of bone range from angular to sub-rounded, range in size from fine-sand to gravel, and appear stained, altered and partially dissolved; however, the proportion of bone that appears altered is lower than that described from stratigraphically lower samples. Measurements made directly on the bones in thin section using the μFTIR

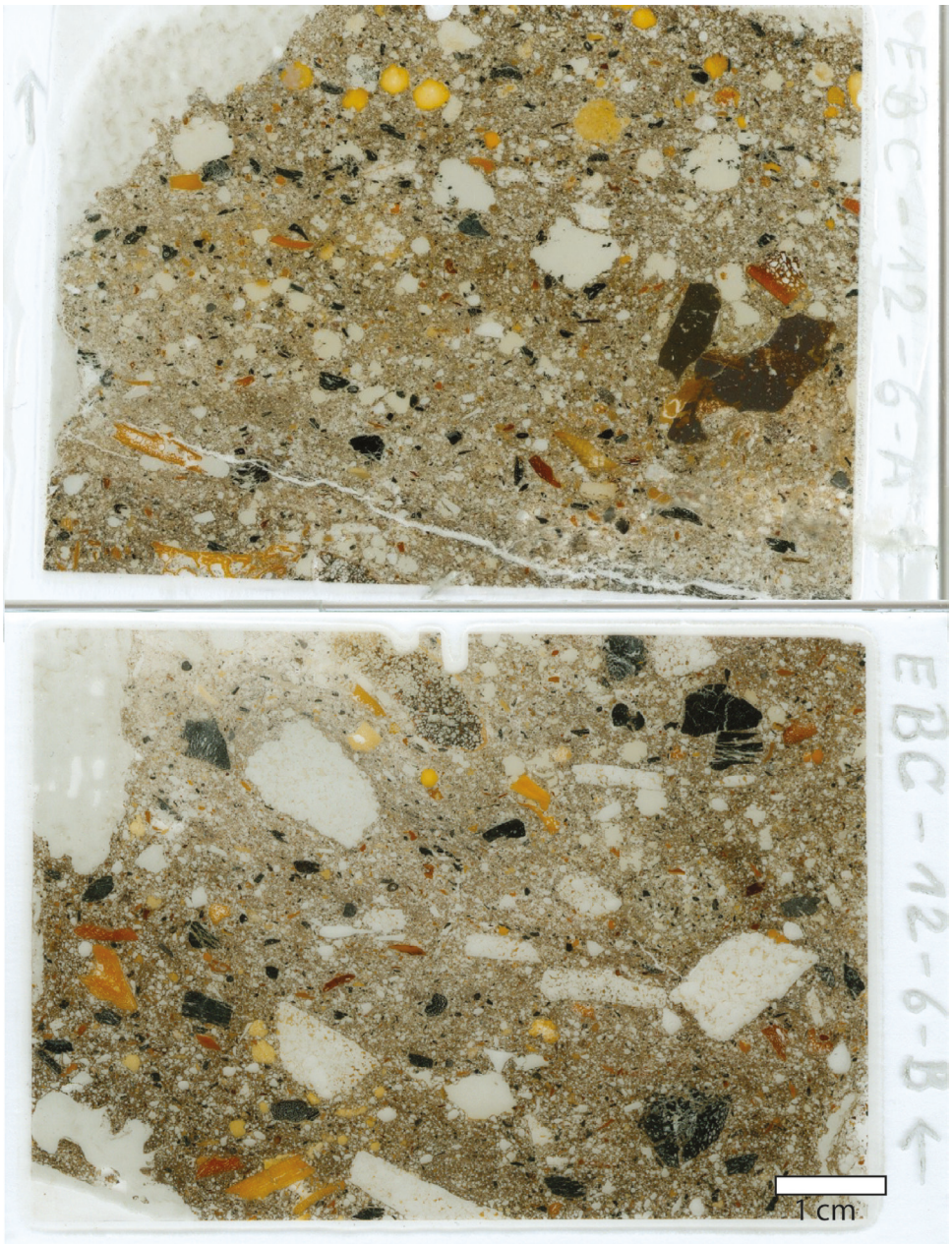

Fig. 19. Flatbed scan of sample EBC-12-06 (top and bottom). Note the presence of fragments of bone and secondary nodules.

show that some are burnt. Elongated fragments of bone display no preferred orientation and they appear to be more frequent in the lower portion of the sample (layer Fuzy) compared to the rest of the sample, which likely corresponds to layer France.

Gravel-sized fragments of quartzite bedrock are also present in this sample, and are distributed evenly throughout, at an abundance of ca. 20 %. Unlike bedrock fragments found in other samples, here the fragments do not appear elongated but rather are more equant. One rounded fragment of sandstone, ca. 2 cm in size, exhibits a textural coating of silt and sand. Since textural pedofeatures are otherwise almost completely absent from the deposits at Elands Bay Cave, it is likely that this coating was inherited from the original source of the grain, possibly a soil from outside of the cave. As in other samples collected from Elands Bay Cave, this sample contains aggregates of clay and silt. Larger, gravel-sized, sub-angular to sub-rounded fragments of woody charcoal are also present at a slightly lower abundance compared to the fragments of bedrock, and are evenly distributed throughout the thin section.

The upper thin section from this sample, EBC-12-06A, covers the stratigraphically undifferentiated deposit. The micromorphological characteristics of this sample are very similar to those described for EBC-12-06B, apart from some weakly expressed lamination towards the bottom of the thin section. Additionally, a cm-sized angular fragment of iron oxide is present in this sample. This fragment also displays well-developed, laminated limpid clay coatings, suggesting that it, like the rounded grain of sandstone found in EBC-12-06B, likely originated from a soil outside of the cave. However, it is possible that it was collected and transported to the site by humans.

Secondary nodules, generally ranging in size from 200 μm to ca. 1 cm are present in both thin sections (Fig. 20). FTIR measurements on loose samples of these nodules collected in the field identified the minerals as gypsum and apatite, which was confirmed by measurements made with the μFTIR directly on the thin sections. Further measurements made with the μFTIR confirmed that some of the nodules are also composed of whitlockite ($Ca_{18}Mg_2H_2(PO_4)_{14}$), based on the presence of a multi-component peak centred at 984 cm-1, a sharp peak at 601 cm-1 and a doublet at 555 and 542 cm-1. A single nodule containing ardealite was also identified in EBC-12-06. Additionally, μFTIR measurements confirmed the presence of taranakite nodules within the sample. The nodules of gypsum and whitlockite are difficult to distinguish from one another in thin section when relying solely on optical characteristics. Both exhibit bladey crystals, ca. 20 μm in size, with low-order white and grey interference colours, with random crystal orientation. They do not fluoresce under blue light. Some nodules of gypsum appear slightly yellowish in PPL at low magnification, whereas others are transparent and exhibit no obvious colour. Hydroxyapatite nodules are yellowish in PPL and appear cryptocrystalline to amorphous. Others appear to be composed of parallel bundles of individual crystals that have a booklet-like appearance. The hydroxylapatite nodules are either isotropic in XPL or exhibit weak, low-order white and grey interference colours. They fluoresce under blue light. The nodules of taranakite are generally sand-sized and appear grey in PPL. They fluoresce strongly under blue light and are either isotropic or exhibit milky, low order interference colours under XPL. Taranakite, gypsum and hydroxylapatite nodules occur throughout all of EBC-12-06; however, their spatial distribution is variable. Taranakite is more common towards the

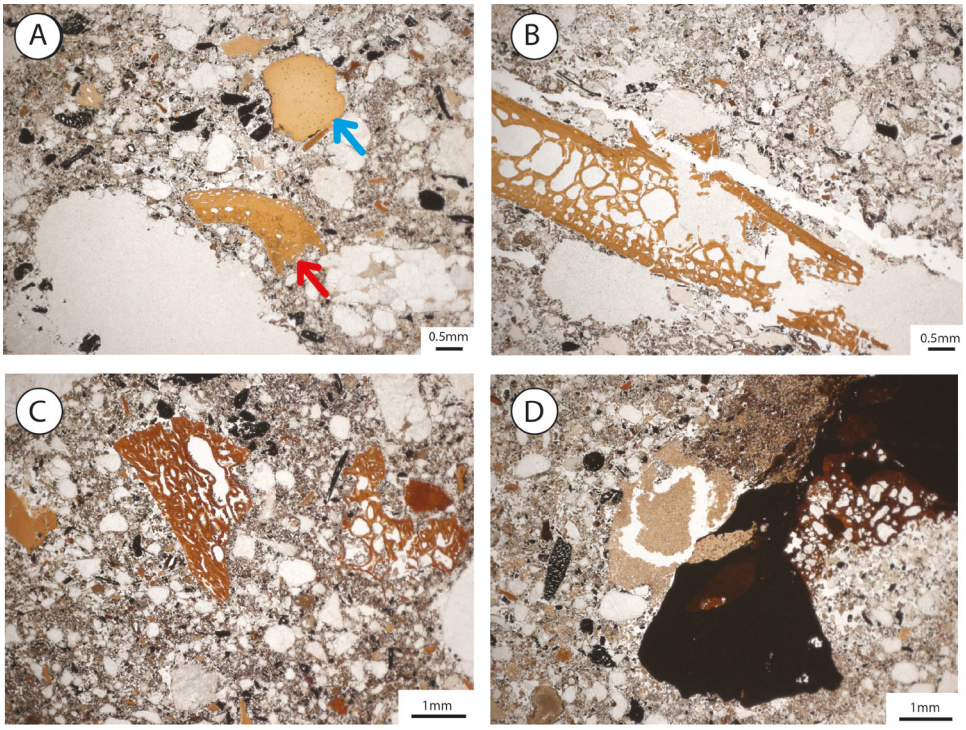

Fig. 20. Microphotographs of EBC-12-06. 20A) Larger, better preserved fragments of bone are more common in this portion of the site. Here, secondary nodules of hydroxylapatite and gypsum are visible. PPL. 20B) Some of the fragments of bone have been physically broken apart by the growth of secondary minerals, here, gypsum. PPL. 20C) Although bones are better preserved here than elsewhere in the site, some still exhibit evidence of partial dissolution, as exhibited by their irregular form. PPL. 20D) a fragment of iron oxide. PPL.

base of EBC-12-06b whereas gypsum and hydroxylapatite are more common towards the top of EBC-12-06a.

EBC-12-07

We collected this sample from the eastern profile from layers Farik, Fael and Dorothee, although no obvious stratigraphic units were identifiable in the thin section. The mineral grains in this sample seem to be present at a higher abundance than in other samples, up to 50 %. Sand-sized, sub-rounded to sub-angular fragments of charcoal are present in relatively low abundance (5–10 %). Bone is relatively abundant, at about 10 %, and appears most frequently as sand-sized, subangular fragments that display a range of colours, from yellow to orangish-brown in PPL. Some appear greyish-white and appear milky in XPL, suggesting that they are calcined. Other fragments of bone appear partially dissolved. Elongated components, such as fragments of bedrock, bone and charcoal, do not display any preferred orientation. This, and the presence of passage features, suggests that these deposits were influenced by bioturbation.

Nodules are present in this sample, although they are generally smaller than elsewhere, such as in sample EBC-12-06. Here they are generally mm or smaller in size and range

in colour from grey to pale yellow in PPL. Under XPL they appear isotropic to weakly birefringent with lower order interference colours. Measurements made on these nodules in thin section using the μFTIR confirmed that they are variably composed of hydroxylapatite and opal.

EBC-12-08

We collected this sample from the south profile near the contact between stratigraphic phases F and D, making it stratigraphically equivalent to sample EBC-12-7. There is only one depositional unit within this sample. This sample is distinct from most other samples from Elands Bay Cave in that it contains a relatively higher proportion (ca. 15 %) of angular, equant fragments of quartzite, likely derived from the cave ceiling and walls. Additionally, this sample has a relatively higher proportion of gravel-sized, sub-rounded fragments of charcoal, present at about 30 % abundance. Sand-sized, subangular fragments of bone are also present, at ca. 10 % abundance, and display a range of colours and states of preservation, similar to those described in sample EBC-12-07. Elongated components do not appear to display any preferred orientation.

Nodules are present in this sample and are similar in size and frequency to those described in sample EBC-12-07. They appear grey in colour in PPL and exhibit milky white interference colours in XPL, and sometimes occur as coatings on grains of quartz. *In situ* measurements made on these nodules in thin section using the μFTIR showed that these are variably composed of hydroxylapatite and opal. A single round nodule displayed similar characteristics to the other nodules found in this sample, but contained several spherulitic crystals within it and appeared yellow in PPL and displayed lower order grey and yellow interference colours in XPL (Fig. 21). Measurements on this nodule made with the μFTIR suggest that this nodule is heat-altered phosphate, based on the presence of the 625 cm-1 peak (Thompson et al. 2013).

DISCUSSION

The results from our study show that the deposits of Elands Bay Cave formed through various depositional and post-depositional processes influenced by geologic, biologic and anthropogenic agents. Here we discuss the roles that these various agents played in the accumulation of sediments at the site and integrate these results to present a synthetic formation model.

Geologic processes and sources

Both Butzer (1979) and Miller (1987) argued that Elands Bay Cave itself is a former sea cave scoured out during a previous marine high stand. We see no evidence supporting or rejecting this claim. However, we believe that a more significant feature governing the formation of the cave is a vertical joint in the bedrock that runs the entire length of the ceiling and along the back wall. GPR data collected during this study suggests that this joint continues under the sediments and is the cause for the basin-like structure in the buried bedrock of the cave. Erosional processes-whether initially induced by wave action or not-likely exploited the joint as a zone of weakness, so that enhanced erosion along the joint eventually led to the formation of the cavity. The main processes of bedrock erosion within the cave today seem to be spalling, granular disaggregation, and possible aeolian abrasion, which is implied by the smooth surfaces on the walls of the

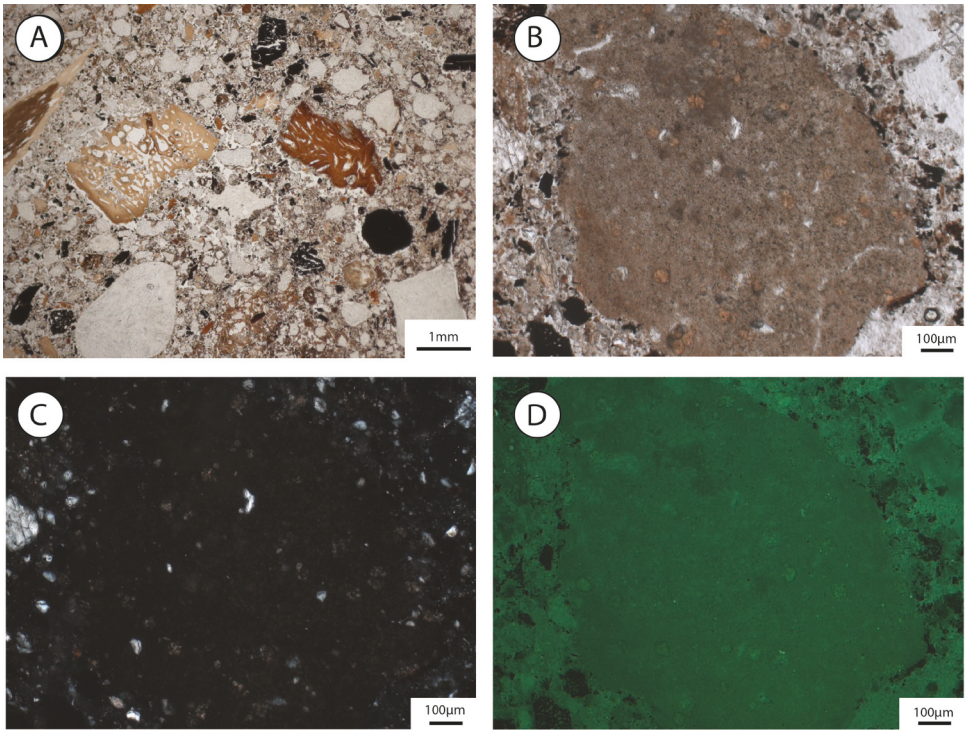

Fig. 21. Microphotographs of EBC-12-08. 21A) Bone fragments are relatively common here, but still exhibit evidence of dissolution. PPL. 21B) A nodule of hydroxylapatite that has been heated, based on measurements collected with the microFTIR directly on the thin section. PPL. 21C) Same view, but XPL. 21D) Same view, but under blue light fluorescence.

cave. The presence of ancient rock art on the cave walls suggests that modern erosion of the cave walls occurs at a very slow rate. These erosive processes, particularly spalling and granular disaggregation, contributed to the accumulation of geogenic deposits within the cave. Both Butzer (1979) and Miller (1987) suggested that the formation and accumulation of roof spall within the site, particularly in phase L, was induced by frost action. Given that modern-day temperatures in the area around Verlorenvlei do not regularly fall below freezing, this claim would imply that the climate on the west coast during the Pleistocene was at times significantly cooler than today. Butzer (1979) correlated the spall-rich deposit at Elands Bay Cave with other colluvial deposits found outside the cave. He used these observations to argue for a wide spread period of cold conditions during MIS 6 (Butzer 1979).

We find the arguments for frost-induced spalling at Elands Bay Cave equivocal. The link between coarse-grained, spall-rich layers in caves and cold climatic conditions was argued by researchers such as Laville (1973) working in the Paleolithic caves of southwestern France. These formation models generally interpreted red-coloured layers within the caves as representing *in situ* pedogenesis initiated during warm, wet interglacial periods. Layers rich in spall, or *éboulis*, formed as a result of frost-induced spalling and could therefore be correlated with cold, glacial periods. Subsequent geoarchaeological

studies showed that the red-coloured layers were not *in situ* soils, but were composed of colluvially reworked soil material (Goldberg 1979). Additionally, studies on the effects of frost action on rock suggests that formation of *éboulis* is a more stochastic process than was previously assumed, making it difficult to directly correlate a spall-rich layer with a specific climatic period (Lautridou & Ozouf 1982; Bertran 1994; Goldberg & Macphail 2008). Furthermore, the occurrence of a layer rich in coarse material does not necessarily imply a higher rate of accumulation of coarse material. A similar pattern can appear when the rate of *éboulis* accumulation remains constant, but the accumulation of finer sediment is variable. Therefore, we see no reason to apply outdated formation models developed for karstic caves in temperate Europe to sandstone shelters in semi-arid Africa. Rather, the more parsimonious explanation for the formation and accumulation of spall at Elands Bay Cave is salt-crystal growth. Salt-induced spalling is an active process occurring in Elands Bay today. The salts that form in the cave likely have their ultimate source from the ocean; however, the occurrence of salt-induced spalling is not necessarily a proxy for shoreline proximity: salt-induced spalling has been observed as a modern-day process at more interior sites as well, such as Diepkloof and Sibudu (Goldberg et al. 2009; Miller et al. 2013; Miller & Mentzer pers. observation).

Individual silt- and sand-sized grains of quartz and occasionally feldspar are a significant geogenic component of the sediments at Elands Bay Cave. Based on our qualitative observations of the thin sections, we estimate that they occur at between 10 % and 50 % abundance. Both Butzer (1979) and Miller (1987) addressed the issue of source and deposition for the sandy component of sediments at Elands Bay Cave. They both noted that the sand-sized fraction from phases L through D was poorly sorted, but Miller concluded that this was a result of high energy winds, whereas Butzer thought that this was a result of a strong influence of sand grains derived from the cave ceiling and walls. In thin section we also observed that the mineral fraction is poorly sorted, and displays a wide range of degree of rounding, with some grains appearing sub-angular and others appearing well-rounded. Given the heterogeneity of the mineral grains, we would tend to agree with Butzer's interpretation. It is likely that most of these grains derived from granular disaggregation of the cave ceiling and walls. However, as Butzer (1979) pointed out, some of the grains also likely derived from the *in situ* break down of blocks of bedrock contained within the deposits. We observed this process in the field, as large nodules of gypsum appeared to have broken apart sandstone blocks that were soft and saprolitic. Additionally, in thin section, we observed smaller blocks of bedrock that appeared partially disaggregated as a result of secondary mineral formation. These observations show that post-depositional processes can contribute sand-sized grains of quartz to deposits, suggesting that we should be cautious when attempting to interpret granulometric data from sandstone rock shelters or caves as purely a function of depositional energy. Furthermore, the process of in situ disaggregation of sandy bedrock could contribute a portion of quartz grains to the sediment that have not been completely bleached, complicating luminescence age estimates (Tribolo 2016 this issue).

Another significant geogenic component of the deposits at Elands Bay Cave are sand-sized aggregates of sand, silt and clay. Based on the stipple-speckled and striated b-fabric exhibited by the clay fraction of these aggregates, and the lack of any obvious

autochthonous source of clay within Elands Bay Cave, we believe that these aggregates derived from soils located outside of the cave. Similar aggregates have been reported from a variety of cave and rock shelter sites around the world, often associated with ashy deposits (Goldberg 2001, 2003; Pinhasi et al. 2014; Villagran et al. 2016). Although the abundance of the aggregates varies from layer to layer at Elands Bay Cave, they are ubiquitous throughout the studied sequence. Modern-day soils in the vicinity of Elands Bay Cave are almost exclusively weakly-developed arenesols that lack well-developed argillic horizons. However, Butzer (1979) reported the presence of more strongly developed paleosols in the region. He did not provide detailed descriptions of the horizons within the paleosols but did note that some of them display deep cambic horizons and some display blocky structures. Unfortunately, we do not have any reference samples from these paleosols to compare to the soil aggregates found in the cave. However, given the sandy nature of modern soils in the region, we believe that these aggregates derived from soils that formed under much different environmental conditions than those prevailing today.

In other South African rock shelters, the presence of soil aggregates may be due to human activity. For example, Miller et al. (2013) and Goldberg et al. (2009) reported the presence of soil aggregates at the Middle Stone Age sites of Diepkloof and Sibudu. In Sibudu Goldberg et al. (2009) documented gleyed soil aggregates containing diatoms, which they argued were most likely transported to the shelter on the roots of sedges collected by humans from the nearby Tongati River for the construction of bedding.

The soil aggregates at Elands Bay Cave do not appear more frequently in layers that we interpret as anthropogenic features, making it unlikely that the aggregates indicate a human mode of accumulation. Butzer (1979), in his description of a section exposed near the Elandsberg tunnel, noted the presence of reddish-coloured colluvial deposits that he interpreted as pedosediments formed during a phase of landscape denudation in MIS 5b. The ubiquity of soil aggregates throughout the sequence at Elands Bay Cave suggests that they cannot be linked directly to any specific climatic event; however, it is possible that processes contributing to landscape denudation posited by Butzer were also responsible for the deposition of soil aggregates within Elands Bay Cave.

Anthropogenic deposits and processes

Sedimentary components that are likely anthropogenic in origin are ubiquitous throughout the sequence at Elands Bay Cave. These components include fragments of charcoal, chipped stone, bones (both burnt and unburnt) and phytoliths. Many of these components are found as individual, isolated occurrences within the ground mass; however, these components also occur as distinct lenses and laminations that likely represent discrete anthropogenic depositional events. We encountered most of the anthropogenic lenses within depositional phase 'I' which appeared laminated in the field. The most common type of anthropogenic deposit found in the Elands Bay Cave samples were charcoal lenses. The charcoal in these lenses appeared both woody and herbaceous; however, some of the charcoal in these lenses was present as silt-sized aggregates, implying some degree of post-depositional alteration, possibly as a result of soil microfauna preferentially ingesting the charcoal, a process observed at other sites (Mentzer et al. 2014; Baykara et al. 2015). Silt- and sand-sized grains of quartz are generally absent from these lenses, or present in relatively low abundance (ca. 5 %),

particularly when compared to other microstratigraphic units where grains of quartz are generally present at much higher abundances (up to 50 %). Goldberg et al. (2009) and Miller et al. (2013) also noted that in other Middle Stone Age sandstone shelters in South Africa, grains of quartz are often absent or present in low abundances from charcoal-rich lenses. They argued that this implies a rapid accumulation of the charcoal, suggesting that these lenses represent anthropogenic combustion features. At Sibudu and Diepkloof, charcoal lenses are sometimes overlain by lenses of calcareous ashes or phosphatic or siliceous material which may have been derived from the diagenetic alteration of ashes. In the deposits examined in this study at Elands Bay Cave, calcareous materials, including ashes, are completely absent, which is likely a result of dissolution induced by acidic conditions within the sediments (see below). Unlike Sibudu and Diepkloof, however, we see little evidence for phosphatised or otherwise altered lenses of ashes above the charcoal lenses. An exception to this is found within Phase I where some of the charcoal lenses appear capped by lenses of laminated, articulated phytoliths. The charcoal in these lenses is generally herbaceous and also appears laminated. Goldberg et al. (2009), Wadley et al. (2010) and Miller et al. (2013) interpreted the association of laminated herbaceous charcoal with a capping lens of laminated phytoliths as representing burnt plant bedding. Given reports of laminated phytolith layers from several Middle Stone Age sites, including Sibudu (Goldberg et al. 2009; Wadley et al. 2011; Miller 2015) and Diepkloof (Miller et al. 2013; Miller 2015), it is possible that the phytolith layers at Elands Bay Cave also represent burnt bedding. However, unlike Sibudu, where numerous examples of phytolith layers have allowed researchers to carefully study their occurrence, we only have a few examples of this type of deposit at Elands Bay. Therefore, we make the identification of burnt bedding at Elands Bay Cave cautiously.

The occurrence and structure of combustion features within the Middle and earlier Later Stone Age deposits at Elands Bay Cave appear diachronically variable, at least within the studied section. Anthropogenic deposits from phase I appear thin and laminated, whereas combustion features within stratigraphically later phases, such as phase D and F exhibit a basin-like morphology, resembling *en cuvette* hearths, and appear superimposed. Samples collected from phases D and F, particularly samples EBC-12-07 and EBC-12-08, were rich in burnt anthropogenic components, such as charcoal and burnt bone; however, the components in these samples were not organized into any clear microstructure but rather appeared dispersed throughout the ground mass. This pattern is in contrast to the thin, sometimes laminated anthropogenic lenses identified in samples from phase I, particularly in EBC-12-02 and EBC-12-04. As in many Middle Stone Age sites in South Africa, the deposits at Elands Bay Cave preserve evidence for discrete depositional episodes where humans were the main agents of accumulation. In phase I, the anthropogenic lenses are not directly stacked on top of one another, but are often separated by thin layers that appear more geogenic in nature. These separating layers do not exhibit any clear bedding structures, but consist of homogenous mixtures of quartz sand, finely comminuted organic material, and anthropogenic components, such as charcoal and occasionally bone. In other instances, such as in sample EBC-12-02, combustion features are capped by, or rest directly on, thin layers composed largely of angular blocks of roof spall. Other micromorphological studies of anthropogenic deposits from Middle Stone Age sites in South Africa report

a similar pattern of anthropogenic materials or deposits separated from one another by deposits with a more natural origin. For example, at Die Kelders, Goldberg et al. (2000) reported thin layers and lenses of burnt organic material and bone that appeared to rest on distinct microsurfaces and which were separated from other similar layers by deposits composed largely of aeolian sand. Karkanas et al. (2015), working at Pinnacle Point 5–6, reported similar anthropogenic layers, rich in carbonized plant material, ashes and burnt bone, that were separated by layers of geogenic sands. They noted that the density of the anthropogenic layers relative to the geogenic layers increased during MIS4, a pattern they interpreted as indicating an intensification of use of the site. At Diepkloof, Miller et al. (2013) reported that the deposits associated with the Intermediate Howiesons Poort and earlier occupations consisted of discrete lenses of charcoal and ash that were separated by reddish-coloured layers composed of sand- and silt-sized grains of quartz, humified organic material, and sand-sized fragments of bone and charcoal. Although these reddish layers contained components that have a clear anthropogenic source, they also contained a high proportion of geogenic and biogenic components. However, unlike at Die Kelders or Pinnacle Point, Miller et al. (2013) suggested that these deposits were significantly influenced by anthropogenic trampling, an interpretation also offered by Goldberg et al. (2009) to explain similar deposits associated with Howiesons Poort and earlier occupations at Sibudu. The deposits from phase I at Elands Bay Cave are most similar to those described at Die Kelders and the Intermediate HP at Diepkloof. These deposits are in contrast to those described from post-Howiesons Poort occupations at Sibudu (Goldberg et al. 2009) and those associated with Intermediate to post-Howiesons Poort occupations at Diepkloof (Miller et al. 2013): here, anthropogenic lenses and layers of charcoal, ash and phytoliths rest directly on top of each other and are not separated by layers with a more geogenic nature.

Given the limited spatial extent of the current excavations and the micromorphological sampling at Elands Bay Cave, it is difficult to interpret the frequency and occurrence of anthropogenic deposits throughout the sequence in terms of intensity of site use or organization of domestic space, as was attempted at Diepkloof (Miller et al. 2013) and Sibudu (Goldberg et al. 2009; Wadley et al. 2011). However, the occurrence of combustion features separated by geogenic layers seems to imply that at least during the accumulation of phase I, repeated periods of occupation were followed by longer periods of limited or no occupation.

Biogenic processes of accumulation and alteration

Biological sources of sediment and processes of deposition can be difficult to identify and distinguish from anthropogenic sources and processes. Sand-sized fragments of bone which, despite adverse preservation conditions, are found throughout the deposits at Elands Bay Cave, could have been deposited by humans or animals. While burnt bones are usually assumed to be indicative of human activity, it is not always clear if the burning of the bone was intentional or accidental. Even more ambiguous in terms of anthropogenic versus biologic source is the finely comminuted organic material that makes up a significant portion of the fine fraction of deposits from Elands Bay Cave. Much of this material is silt-sized and displays a reddish- or chestnut-brown colour in PPL, implying that it is humified and not carbonized. However, many of

the silt-sized fragments of organic material appear black and opaque, suggesting that at least some proportion may have been carbonized. Distinguishing between humified and carbonized organic material can be difficult in thin sections (Stahlschmidt, Miller, Ligouis, Hambach et al. 2015); however, organic petrographic analysis of two of the Elands Bay Cave samples has clarified the nature of the fine organic fraction. Most exhibit reflectance values classifying them as fusinite, implying that they have been altered to some degree by heating and are therefore charcoal. However, our analysis also shows that prior to burning, the organic material underwent varying degrees of humification. This observation has two possible interpretations. One, the occupants of Elands Bay Cave collected plant material for their fires that was old and partially humified, a behaviour proposed for the site of Lapa do Santo in Brazil, based on similar observations (Villagran et al. 2016). Or two, the occupants of Elands Bay Cave built their fires directly on humic-rich surfaces, leading to unintentional combustion of organic material already contained within the sediment (Mallol et al. 2013). Scenario one would imply a largely anthropogenic source for the organic material at the site, whereas scenario two could imply either a biological or anthropogenic source. Based on the current samples and observations at Elands Bay, it is not possible for us to state which scenario is more likely.

Biologic influences on the deposits at Elands Bay Cave are more readily apparent as post-depositional processes. Evidence for bioturbation is prevalent at the site. In thin section, passage features, usually 1 cm or smaller in diameter, are relatively common and in the field, krotovinas, often ca. 5 cm in diameter, are easily identified. One krotovina from the northern profile of the current excavations is particularly noteworthy. It exhibits a white crust of secondary minerals, most likely gypsum, which formed along its outer boundary resulting in a ring-like appearance in profile. This krotovina was first encountered during Parkington's initial test excavations into the Middle Stone Age deposits (per. comm.) and served as a key reference point for correlation between his and the current excavations. Although evidence for bioturbation is common at Elands Bay Cave, the burrowing animals did not completely homogenize the deposits. Even in areas of the excavation where we find passage features and krotovinas, preservation of distinct layers and laminations imply relatively minimal stratigraphic disturbance, at least within the wetting front.

Chemical diagenesis at Elands Bay Cave

Significant observations that may be linked to biologic processes at Elands Bay Cave are the effects of post-depositional chemical diagenesis. All of the deposits analysed in this study have undergone some degree of chemical and physical alteration as the result of dissolution or secondary precipitation of diagenetic minerals.

Chemical diagenesis of archaeological cave deposits has only been intensively studied from limited contexts: most studies have targeted limestone caves with ashy sediments from the eastern Mediterranean (Goldberg & Nathan 1975; Weiner & Goldberg 1990; Weiner et al. 1993; Karkanas et al. 1999; Karkanas et al. 2000; Weiner et al. 2002). There, the main agent of diagenetic alteration is phosphoric acid, along with other types of acids, which in these caves is often assumed to derive from the decomposition of bird and bat guano (Shahack-Gross et al. 2004). Researchers working at sites such as Kebara, Hayonim, Tabun and Theopetra showed that phosphate-rich

solutions reacted with the calcite from limestone blocks and ashes to form secondary minerals composed of apatite. Under conditions of low pH, apatite itself is not stable and other phosphate minerals—some containing K, Al, and/or Fe—preferentially form, such as montgomeryite, crandallite, or taranakite. For example at Kebara, Weiner et al. (1993) identified a block of dolomite that fell to the floor of the cave and was subsequently buried. The carbonate-rich rock reacted with the phosphate-solution in the deposits, forming a reaction rim of secondary minerals on the rock's surface. The first mineral to form was apatite (or dahllite, as they reported it), which was replaced by a non-stoichiometric calcium-phosphate phase which was in turn coated by crandallite, montgomeryite and leucophosphite. The succession of mineral formation found on this block suggested to the authors that these minerals represented a reaction cascade, with minerals replacing one another over time. Karkanas et al. (1999), working at Theopetra Cave, reported a similar reaction cascade, but one found across several meters within the sediments of a single geological layer, that progressed from calcite to apatite to montgomeryite or crandallite, and finally taranakite. Both the reaction rim on the dolomitic block from Kebara and the alteration zone in the sediments from Theopetra show a pattern of initially high Ca proportions in the original material progressing towards secondary minerals with higher proportions of Al, Fe, and K. Karakanas et al. (2000) point out that these elements can be found in ashes derived from the burning of wood, but that they can also be found in clays, which would begin to breakdown under low pH conditions (Shahack-Gross et al. 2004). These studies suggested that the presence of more 'advanced' phosphate minerals, such as taranakite or leucophosphite, implies the occurrence of a reaction cascade through the preceding minerals. However, Karakanas (2010) points out, based on the calculation of mineral phase diagrams, that although apatite is the stable phosphate mineral under alkaline pH conditions, the phosphate mineral phase that forms under acidic conditions is not solely dependent on pH but also on the available ions in solution. For instance, in situations where Ca ions are not available, such as in an already decalcified deposit, low pH phosphate minerals containing Ca, such as crandallite, will not form, but rather taranakite and other minerals lacking Ca will preferentially form. Similarly, the availability of Al in solution can govern whether the formation of crandallite or montgomeryite is preferred.

The formation of secondary phosphate minerals is governed by the specific chemistry of the solutions present in the deposits, which can vary spatially within a site, can change over time and can be different from site to site. Therefore, the identification of secondary minerals can be informative about variation in past sedimentary conditions, such as pH, moisture availability, and oxidation conditions. Furthermore, by understanding how these types of conditions have changed over time, we can better assess the preservation of certain classes of artefacts and deposits at archaeological sites (Karkanas 2010). For example, under high concentrations of phosphorous in solution, materials commonly found at archaeological sites that are composed of carbonates-such as limestone blocks, shells and ashes-will alter to form secondary calcium phosphate minerals, such as hydroxylapatite. Under low pH conditions, other secondary phosphate minerals, such as crandallite or montgomeryite, can preferentially form since apatite is not stable under these conditions. Under low pH conditions, other common archaeological materials composed of apatite, such as

bone, will also not be stable. Berna et al. (2004) experimentally demonstrated that bone contained within sediment with a pH above 8.1 is stable and that bone in sediment with a pH of 7.4 to 8.1 will recrystallize and be replaced by more stable forms of apatite. When pH of the sediment drops below 7, bone readily dissolves releasing P ions into solution which can then form secondary phosphate minerals. Therefore, the presence of secondary, low-pH phosphate minerals in an archaeological deposit can tell us about past conditions that may have been adverse for the preservation of shell, ashes and even bones. At Kebara, Weiner and others (Weiner et al. 1993, 2007) used the spatial distribution of taranakite and other minerals that can form under low pH conditions in the cave's deposits to explain the presence or absence of bone. They noted that taranakite, crandallite and montgomeryite were present in deposits where bone was absent. Apatite and calcite were present where bones were found. Therefore, they argued that the spatial variation in occurrence of bone was not linked to human behaviour, but rather to chemical diagenetic processes influencing the deposits after burial.

The study of chemical diagenesis in archaeological cave and rock shelter sites in South Africa has been limited when compared to those of the Levant. At Die Kelders, Goldberg et al. (2000) reported that calcareous sands and ashes underwent phosphatisation thereby leading to slumping and physical deformation of the deposits. They did not conduct mineralogical analyses such as FTIR on the deposits, but identified the main secondary phosphate mineral forming at Die Kelders as apatite, based on micromorphological thin section analysis. Schiegl and Conard (2006) also reported secondary minerals found forming in the deposits from Sibudu. Using FTIR analysis of loose samples, they identified apatite and gypsum as the main diagenetic minerals found at the site; however, using SEM-EDS analysis of polished and carbon-coated blocks of indurated sediment, they identified traces of leucophosphite, taranakite and crandallite. Karkanas and Goldberg (2010) similarly noted the presence of secondary apatite and sulfate minerals at Pinnacle Point 13-B. Here they identified lozenge-shaped crystals of gypsum that had been replaced by anhydrite. Miller et al. (2013), working at Diepkloof Rock Shelter, also reported the presence of several diagenetic minerals found at the site. They noted the presence of secondary apatite and gypsum, but also noted that niter (KNO_3) forms extensive surficial crusts at the site, and sveite ($KAl_7(NO_3)_4(OH)16Cl_2{\bullet}8H_20$) forms along cracks in the wall of the shelter.

The secondary minerals found at Elands Bay Cave generally fit with those identified at the Levantine and South African cave sites and include gypsum, hydroxylapatite, taranakite and variscite. We also identified three more uncommon minerals: ardealite, whitlockite and dawsonite. Ardealite has been identified in non-archaeological contexts within Eastern Mediterranean caves (Shahack-Gross et al. 2004), as well as in numerous studies of guano deposits (Marincea et al. 2004; Onac et al. 2006; Frost et al. 2011). Whitlockite has been identified in limited archaeological contexts, including within bones and dental calculus (Preus et al. 2011; Monge et al. 2014), as well as in secondary crusts attributed to decomposition of bird guano (Watchman et al. 2001). Both whitlockite and ardealite have been identified in South Africa at Sibudu (Mentzer et al. 2014), but their formation histories at this site are presently unknown. To the best of our knowledge, dawsonite has never been identified in an archaeological context, although it was documented as a weathering product in soils located in Olduvai Gorge (Hay 1963; Hay & Reeder 1978).

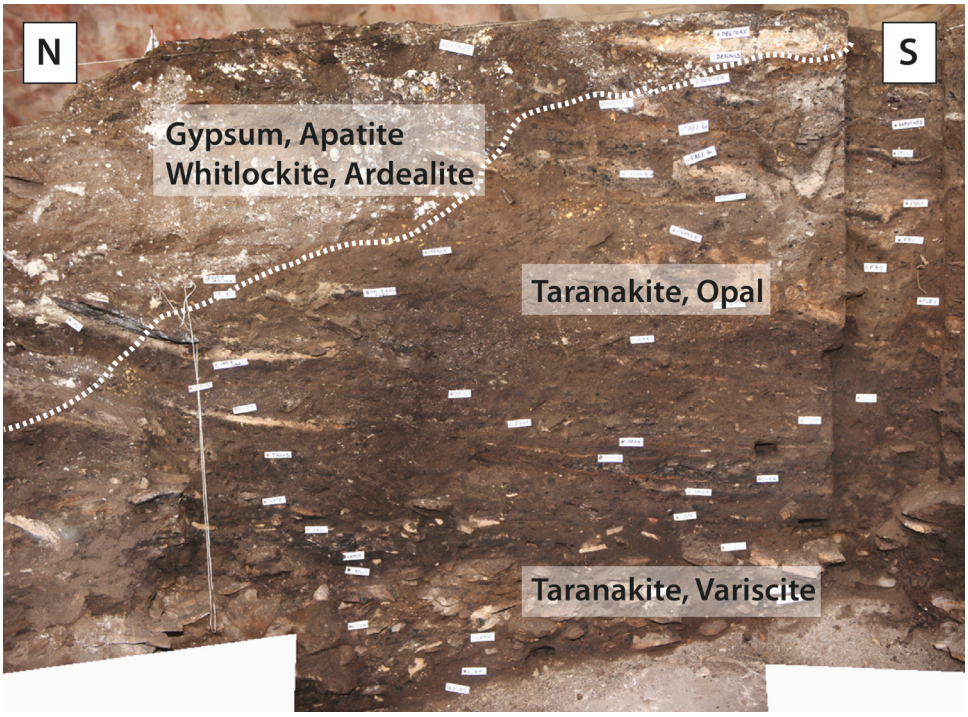

Fig. 22. Photograph of the eastern profile, showing the general distribution of secondary minerals.

Like at Kebara (Weiner et al. 1993), Hayonim (Weiner et al. 2002) and Theopetra (Karkanas et al. 1999), the distribution of secondary diagenetic minerals exhibits spatial variability at Elands Bay Cave (Fig. 22). Variscite was only identified in sample EBC-12-01 within layer Keva, which was the stratigraphically lowest sample collected for this study. Here, variscite is exclusively found as alteration nodules formed within soil aggregates. Variscite is known to form as a result of reaction between phosphate-enriched groundwater and aluminium-rich rocks (Larsen 1942; Frost et al. 2004) or clays (Odriozola et al. 2010) and crystallizes under generally acidic conditions (Kittrick & Jackson 1955; Hsu 1982). Karkanas et al. (1999) report the presence of variscite as a cementing mineral within the lowermost unit of Theopetra cave and Weiner et al. (2002) noted its presence in sediments from Hayonim in association with leucophosphite and montgomeryite. Karkanas et al. (2000) also note that at Kebara, bone found at the transition between sediments containing apatite and those containing montgomeryite had transformed to variscite. Interestingly, the soil aggregates which have partially altered to variscite only appear in layer Keva. Based on the lithic assemblages found within Keva and underlying layers, the top of Keva likely represents a significant unconformity within the stratigraphic sequence. Soil aggregates found directly above this contact-within the same thin section-do not display evidence for variscite alteration. Therefore, the stratigraphic association of variscite with the oldest deposits at the site may imply an early phase of chemical diagenesis that predates the deposition of layers Kelly/Kent.

Taranakite has been widely reported as a secondary diagenetic mineral found in archaeological cave and rock shelter sites (e. g. Karkanas et al. 2000; Weiner et al. 2002; Schiegl & Conard 2006; Mentzer et al. 2014) and generally forms under low pH conditions. At Elands Bay Cave, taranakite has been found in almost every sample, but is particularly abundant in samples collected from within the wetting front, towards the southern end of the main section. In the field, we observed the taranakite as small, mm-sized flecks and similarly small rootlet-like veins. In thin section, the taranakite appears as small mm-sized nodules, often associated with secondary opal, and as crusts. Towards the edge of the wetting front taranakite is still present, but significantly less abundant than to the south; additionally, other minerals are present at this transition.

In the field, the edge of the wetting front is marked by the occurrence of large, white nodules of gypsum which are found extensively across the site. Millimetre to cm-sized nodules of gypsum are present in sample EBC-12-06, which was collected at the edge of the wetting front. Parkington et al. (1987) noted the presence of gypsum nodules and suggested that these likely formed as a result of marine aerosols entering the cave, which had an increasing significance as sea-levels transgressed the coast during the terminal Pleistocene and early Holocene. Given the proximity of the site to the modern shoreline, and the presence of dissolved ions within the drip water collected from the site, it is likely that at least some of the sulfate responsible for the formation of gypsum has a marine origin. However, gypsum has been noted in archaeological sites in South Africa that are not close to the modern shoreline, such as Diepkloof (Miller et al. 2013), Sibudu (Schiegl & Conard 2006; Goldberg et al. 2009), Bushman Rock Shelter (Badenhorst & Plug 2012), and Wonderwerk Cave (Goldberg et al. 2015). Furthermore, gypsum can form as a secondary mineral during the decay of organic material, in particular guano (Shahack-Gross et al. 2004). Karkanas and Goldberg (2010) suggest that the decay of guano is the likely source for gypsum found in deposits at Pinnacle Point 13B, another coastal, Middle Stone Age site in South Africa. In general, the source and formation of gypsum at Elands Bay Cave and other cave and rock shelter sites in South Africa seems to be complex and not linked to a single cause. Further adding to the complexity of gypsum formation at archaeological sites is the mineral's high solubility, which allows it to readily and quickly dissolve and reprecipitate. At Elands Bay Cave the gypsum found in profile appeared to have become more extensive during the decades separating the original excavations of Parkington and those of the current team (Parkington & Porraz, personal observation). In addition, there is evidence in the thin sections that the spatial extent of gypsum at the site was variable in the past. In sample EBC-12-02-located towards the south of the main section within the wetting front-we identified voids formed within a crust of taranakite that appear pseudomorphic after gypsum. Today, gypsum is absent from this part of the site. The pseudomorphic voids suggest that gypsum was initially present here and that it predated the formation of taranakite within the deposits. The subsequent dissolution of the gypsum implies that this area of the site became wetter at some point in the past.

Most secondary nodules of hydroxylapatite are found in sample EBC-12-06; however, they also occur in samples EBC-12-07 and EBC-12-08. Of particular interest is the occurrence of secondary nodules of hydroxylapatite in sample EBC-12-08 (from depositional phase D and F) that appear to have been heated. The heating of these nodules was likely incidentally caused by fires built by the occupants of the site. This

would imply that some chemical alteration of the deposits had taken place prior to human occupation of the site during phase D and F, which Tribolo et al. (2016 this issue) date to ca. 19 000 BP.

We identified other secondary phosphate minerals in sample EBC-12-06, including whitlockite and ardealite. In total, these minerals were only identified in three nodules (two in thin section and one loose sample), and therefore it is difficult to propose specific formation pathways. However, both of these minerals have also been identified at Sibudu (Mentzer et al. 2014). As at Elands Bay Cave, ardealite at Sibudu occurs at a transition between a zone that contains sulfate minerals and a zone that lacks sulfate minerals. Whitlockite, on the other hand, needs magnesium to be present in order to form; currently we are not able to identify a possible source for the Mg at Elands Bay, but note that Mg is present within the dripwater at 97.464 mg/L. Further study of the occurrence of whitlockite and ardealite at South African rock shelter sites will hopefully clarify their formation in these types of contexts.

Although some taranakite is found at the edge of the wetting front, secondary nodules of hydroxylapatite are also present and are more numerous than any other type of secondary phosphate minerals in sample EBC-12-06. The nodules of hydroxylapatite appear in the field as yellowish, mm- to cm-sized round nodules, which are also clearly identifiable in thin section. The presence of secondary hydroxylapatite at the transition zone suggests that moisture contained within the sediments was more alkaline towards the north, compared to the zone where taranakite formed. The co-occurrence of gypsum-which is highly soluble-and hydroxylapatite-which is stable under alkaline conditions-suggests that the zone of alteration represents a spatial trend in moisture availability and pH conditions across the site: with wetter, more acidic conditions dominating to the south of the main section, and drier, more basic conditions dominating to the north of the main sector. The most likely source for this moisture is the bedrock joint along which today moisture collects during periods of rainfall. This moisture likely seeps from the joint into the adjacent deposits, creating a wetting front with spatially variable moisture and chemical properties.

The effects of this wetting front are not only visible in the secondary minerals which formed, but also in the preservation of the archaeological remains and deposits themselves. No calcareous materials, such as plant-derived ashes, were found in the deposits despite frequent evidence for burning in the form of charcoal. Furthermore, within the area of the site where taranakite is dominant, no bones were recovered during excavation. In thin section we observed small, sand-sized fragments of bones within this zone, but many of them appeared partially dissolved or altered. Outside of this zone, where hydroxylapatite and gypsum are more dominant, bone was found during excavation and also more frequently in thin section. The absence of calcareous ashes and shell, and the spatial variation in distribution of bones at the site is likely a result of the acidic water which seeped through the joint in the bedrock and permeated the archaeological deposits. However, it is unlikely that the phosphorous found in the secondary phosphate minerals such as variscite and taranakite comes solely from the dissolution of bone. While the chemical break down of bone certainly released phosphorous into the deposits, it is interesting to note that the elemental composition of the drip water collected along the bedrock joint is enriched in elements necessary for the formation of the secondary minerals

found at the site. Phosphorous, which is required to form secondary hydroxylapatite, taranakite, variscite, ardealite and whitlockite, is found in relatively high abundance within the drip water along the bedrock joint as is calcium, which is necessary for the formation of hydroxylapatite, ardealite and whitlockite. Additionally, potassium and magnesium, which are enriched within the drip water, are necessary for forming taranakite and whitlockite, respectively. Other elements, such as aluminium, required to form secondary minerals such as variscite and taranakite likely derive from the dissolution and alteration of components contained within the deposits. We see evidence for this in the form of partially dissolved and altered clay-rich soil aggregates. In general, although the suite of minerals found at Elands Bay Cave is roughly similar to those reported from the Levantine and eastern Mediterranean Middle Paleolithic cave sites (Goldberg & Nathan, 1975; Weiner & Goldberg 1990; Weiner et al. 1993; Karkanas et al. 1999; Karkanas et al. 2000; Weiner et al. 2002), we do not see a need to invoke a reaction cascade (e. g. Weiner et al. 1993) to explain the occurrence of taranakite or other more extreme phosphate minerals.

The effects of the percolating water and secondary mineral formation on the site were not only chemical but also physical. The secondary formation of taranakite has led to the physical destruction of pieces of charcoal and fragments of bedrock. In addition, the growth of large nodules of gypsum has caused significant disturbance to the stratigraphic units and has led to the physical breakdown of large blocks of *éboulis*. The spatial variation in the formation of these minerals means that areas within the zone of taranakite formation preserve the original, finely laminated and bedded aspect of the deposits, but lack bone preservation; areas within the hydroxylapatite and gypsum zone have bones preserved, but have been physically reworked by extensive growth of secondary nodules.

Site formation model

Initial occupation of the site began during deposition of phase L. At this time salt-induced spalling produced a high proportion of quartzite flakes from the ceiling and roof of the shelter that filled in the basin-like bedrock base of the site. These quartzite roof spall flakes were likely exploited by the inhabitants for stone tool production; however, it is also likely that the inhabitants transported some higher-quality quartzite from further away (Schmid et al. 2016 this issue). In addition to the accumulation of roof spall, humans built fires, contributing charcoal and burnt bones, and either humans or other biologic agents transported plant material to the site that resulted in the accumulation of humified organic silt. Granular disaggregation of the bedrock and colluvial movement of soil aggregates also contributed to the accumulation of sediment within the site. At some point, accumulation ceased and the deposits were partially eroded leaving an unconformity on top of layer Keva. In thin section, the unconformity is indicated by a thin lag deposit composed of coarse grains of sand and horizontally oriented fragments of roof spall. It is difficult to estimate how much time is missing in the sequence between Keva and Kelly/Kent, especially since it was not possible to obtain reliable ages for these lower deposits (Tribolo et al. 2016 this issue). Furthermore, it is impossible for us to identify what process is responsible for the erosion. However, techno-typological analysis of the lithics suggests that the hiatus may represent a significant period of time, given that there are few similarities

between the assemblages from phase Land Keva/Lara and those from the nearby Middle Stone Age site of Diepkloof (Schmid et al. 2016 this issue; Porraz, Schmid et al. 2016 this issue). The hiatus found in the Elands Bay Cave sequence may represent a period of time covering almost the entirety of the Diepkloof sequence; however, more reliable geochronological data will be necessary to confirm this hypothesis. Prior to, or synchronous with the phase of erosion, acidic water seeping into the deposits through the bedrock joint likely caused decalcification of the deposits and led to the secondary formation of variscite within soil aggregates.

Prior to ca. 40 000 BP, sedimentation recommenced within Elands Bay Cave. Natural modes of accumulation-including roof spalling, granular disaggregation, and soil aggregate deposition-which were active in the earlier deposits, continued to be active in the later phases as well. Humans were also present at Elands Bay Cave with the initiation of sedimentation following the period of erosion. We can see clear evidence for this in the form of a thin charcoal lens, possibly representing a hearth, which was built directly on the erosional surface at the top of layer Keva. Overlying sediments associated with this phase contain multiple thin laminations and lenses of charcoal and laminated phytoliths. Interestingly, these anthropogenic deposits are often separated from one another by thin layers containing higher proportions of geogenic material, suggesting that occupation at Elands Bay during the latter part of the Middle Stone Age was sporadic and likely separated by periods of low-intensity site use or non-occupation. At some point during or after the accumulation of phases K-D, the deposits suffered chemical alteration. Initially, small nodules of gypsum were present as secondary minerals in the deposits, implying some degree of aridity. However, at some point the acidic water from the bedrock joint, which caused decalcification and variscite formation in phase K, also caused the gypsum closest to the joint to dissolve. Additionally, the acidic water seeping through the deposits led to decalcification, alteration of clays within the soil aggregates, and dissolution of bone. The dissolved bone released phosphorous into the deposits and this, combined with additional phosphorous and other ions from the seep water, led to the formation of secondary minerals such as taranakite. Further away from the joint the deposits were drier and pH conditions more alkaline, thereby enhancing the preservation of bone but also promoting the formation of secondary gypsum and hydroxylapatite which caused significant physical disturbance to the previously finely laminated deposits. It is difficult to determine when this phase of chemical alteration occurred at Elands Bay Cave. Parkington et al. (1987) suggested that the gypsum largely formed during the mid-Holocene as a result of climatic aridification. We find no evidence to support or refute this hypothesis. However, we would note that we have identified the presence of heat-altered nodules of hydroxylapatite within phases D-F, implying that at least some chemical alteration of phases K-D had occurred prior to ca. 19 000 BP.

Our study focused solely on the Middle and earlier Later Stone Age deposits at Elands Bay Cave. Most of the later period deposits were largely removed during previous excavations. Therefore, we can only offer a detailed site formation model for these time periods. However, the studies conducted by Butzer (1979) and Miller (1987) allow us to extend our model into the Later Stone Age. With the end of the Pleistocene and beginning of the Holocene, rising sea levels brought the coast line ever closer to Elands Bay Cave. With the transgressing sea, aeolian sands began to contribute significantly

to the geogenic accumulation of sediment within the site, outcompeting the effects of granular disaggregation and roof spalling of the bedrock. Human occupation continued, but the dramatically changing landscape forced the inhabitants to change their subsistence strategies to exploit the ever closer coastline. The change in subsistence strategies also had a significant effect on the nature of anthropogenic deposition within the site. Beginning at 11 000 BP, marine shell is found within the deposits. Given the extensive decalcification of the lower deposits, any marine shell brought to the site by Middle Stone Age humans would have likely been dissolved. However, it seems likely given the spatial limits of the wetting front and zones of chemical alteration that the Later Stone Age deposits were largely outside of the effects of the acidic water seep. By 9 000 BP humans became the most significant depositional agent at Elands Bay Cave, forming a large shell midden which extensively filled up the site.

CONCLUSIONS

The aims of our study were to provide a detailed geoarchaeological and stratigraphic data set that could be used to interpret the results from the recent excavation and also to develop a site formation model. Additionally, our study also allowed us to clarify some aspects of previous geoarchaeological studies (Butzer 1979; Miller 1987).

Field observations and the GPR survey provided valuable information regarding the formation and morphology of the shelter. In particular the GPR survey showed that the bedrock joint running along the wall and ceiling of the cave also continues into the floor, forming a basin that was filled in with the coarse angular debris of phase L. Furthermore, these results show that the test pit excavated by Parkington reached the bedrock of the site, and that there are no stratigraphically lower deposits present.

We also agree with Butzer's (1979) argument that the sandy component of the earlier deposits likely derives from the cave's bedrock, in contrast to Miller's (1987) argument that these grains are aeolian in origin. We agree with both Butzer (1979) and Miller (1987) that aeolian sands likely became a much more significant component of the site's sediments during the late Pleistocene and Holocene, when the transgressing shoreline contributed a more significant amount of dune sand. However, we disagree with Butzer's (1979, 2004) and Miller's (1987) assertion that the coarse angular debris found at the base of the sequence (phase L) formed as a result of frost action. We believe that salt-induced spalling is a more likely process at Elands Bay Cave, given the ubiquity of this process at other sandstone shelters across southern Africa.

Micromorphological analysis of the contact between SU Keva and the overlying deposits confirmed the presence of a significant unconformity, an observation made by previous excavators and geoarchaeologists (e. g. Miller 1987) and suggested also by the current excavations (Schmid et al. 2016 this issue; Porraz, Schmid et al. 2016 this issue). We were able to identify the presence of a thin lag deposit which had formed on the surface of SU Keva, implying a phase of erosion within the site. Our results showed that phase L at the base of the sequence is not a 'basal lag' (Butzer 1979; Miller 1987) but rather a deposit on which a thin lag eventually developed. Our results also showed that initial occupation following the phase of erosion occurred directly on this surface, as seen by the presence of a thin charcoal lens found directly on the surface of the lag deposit.

Elands Bay Cave is known for its late Pleistocene and Holocene material, in particular the Later Stone Age shell midden: a large, anthropogenic deposit. Our study focused on the underlying Middle and earlier Later Stone Age deposits and showed that during this time, humans also contributed significantly to the accumulation of sediment at the site. The Middle Stone Age deposits at Elands Bay Cave, particularly those from phase I are laminated like many other similarly aged sites in southern Africa and contain evidence for anthropogenic deposition in the form of charcoal and phytolith lenses. Our study showed that anthropogenic depositional events were often separated by periods of more natural accumulation, possibly implying a more sporadic use of the site.

Although portions of the sequence at Elands Bay Cave contain well-preserved laminations, much of the sequence has been disturbed by post-depositional chemical alteration. This study presents one of the first, detailed analyses of chemical diagenesis occurring within a non-calcareous cave or rock shelter. Although many of the secondary minerals identified are similar to those found in similar studies of karstic sites in the eastern Mediterranean and Levant, our study also identified other minerals, such as whitlockite. Furthermore, our study suggested that the reaction chain, argued for at sites like Kebara and Hayonim (Weiner et al. 1993, 2002) may not be necessary to explain the formation of taranakite or the dissolution of bone. Furthermore, our study of chemical diagenesis at Elands Bay Cave provided an explanation for the spatial variation in occurrence of bone and the preservation of stratigraphic units across the site.

Despite the strong effects of post-depositional alteration occurring within the deposits at Elands Bay Cave which limited to some extent our ability to date (Tribolo et al. 2016 this issue) and excavate the site, our results show that a geoarchaeological study that integrates field and microcontextual analyses can help unravel the often complex processes influencing a site's formation.

ACKNOWLEDGEMENTS

The authors would like to acknowledge the Deutsche Forschungsgemeinschaft (DFG) for providing funding for this project (MI 1748/1–1). Additionally, we would like to thank Hartmut Schultz for providing assistance with the SEM, and Peter Kühn and Sabine Flaiz for the elemental analysis.

REFERENCES

Arpin, T. L., Mallol, C. & Goldberg, P. 2002. A new method of analyzing and documenting micromorphological thin sections using flatbed scanners: applications in geoarchaeological studies. *Geoarchaeology* **17**: 305–13.

Badenhorst, S. & Plug, I. 2012. The faunal remains from the Middle Stone Age levels of Bushman Rock Shelter in South Africa. *South African Archaeological Bulletin* **67:** 16–31.

Baxter, A.J. 1997. *Late Quaternary palaeoenvironments of the Sandveld, Western Cape Province, South Africa.* PhD dissertation, University of Cape Town.

Baykara, İ., Mentzer, S.M., Stiner, M.C., Asmerom, Y., Güleç, E.S. & Kuhn, S.L. 2015. The Middle Paleolithic occupations of Üçağızlı II Cave (Hatay, Turkey): Geoarcheological and archeological perspectives. *Journal of Archaeological Science: Reports* **4**: 409–26.

Berna, F., Matthews, A. & Weiner, S. 2004. Solubilities of bone mineral from archaeological sites: the recrystallization window, *Journal of Archaeological Science* **31**: 867–82.

Bertran, P. 1994. Degradation des niveaux d'occupation paléolithiques en contexte périglaciare: exemples et implications archéologiques. *Paléo* **6**: 285–302.

Butzer, K.W. 1979. Geomorphology and geo-archaeology at Elandsbaai, western Cape, South Africa. *Catena* **6**: 157–66.

Butzer, K.W. 2004. Coastal eolian sands, paleosols, and Pleistocene geoarchaeology of the Southwestern Cape, South Africa. *Journal of Archaeological Science* **31**: 1743–81.

Cartwright, C.R. 2013. Identifying the woody resources of Diepkloof Rock Shelter (South Africa) using scanning electron microscopy of the MSA wood charcoal assemblages. *Journal of Archaeological Science* **40**: 3463–74.

Cartwright, C.R., Porraz, G. & Parkington, J.E. 2016. The wood charcoal evidence from renewed excavations at Elands Bay Cave. *Southern African Humanities* **29**: 249–58.

Carthwright. C.R. & Parkington, J. 1997. The wood charcoal assemblages from Elands Bay Cave, southwestern Cape: principles, procedures and preliminary interpretations. *South African Archaeological Bulletin* **52**: 59–72.

Courty, M.-A., Goldberg, P. & Macphail, R.I. 1989. *Soils and micromorphology in archaeology*. Cambridge University Press.

Cowling, R.M., Cartwright, C.R., Parkington, J.E. & llsopp, J. 1999. Fossil wood assemblages from Elands Bay Cave, South Africa: a wetter glacial in the winter rainfall fynbos biome. *Journal of Biogeography* **26**: 367–78.

Frost, R.L., Palmer, S.J., Henry, D.A & Pogson, R. 2011. A Raman spectroscopic study of the 'cave' mineral ardealite Ca2(HPO4)(SO4). 4H2O. *Journal of Raman Spectroscopy* **42**: 1447–54.

Frost, R.L., Weier, M.L., Erickson, K.L., Carmody, O. & Mills, S. 2004. Raman spectroscopy of phosphates of the variscite mineral group. *Journal of Raman Spectroscopy* **35**: 1047–55.

Goldberg, P. 1979. Micromorphology of Pech-de-l'Azé II sediments. *Journal of Archaeological Science* **6**: 17–47.

Goldberg, P. 2000. Micromorphology and site formation at Die Kelders Cave I, South Africa. *Journal of Human Evolution* **38**: 43–90.

Goldberg, P. 2001. Some micromorphological aspects of prehistoric cave deposits. *Cahiers d'Archéologie du CELAT* **10**: 161–75.

Goldberg, P. 2003. Some observations on Middle and Upper Palaeolithic ashy cave and rock shelter deposits in the Near East. In: A.N. Goring-Morris & A. Belfer-Cohen, eds., *More than meets the eye: studies on Upper Palaeolithic diversity in the Near East*. Oxford: Oxbow, pp. 19–32.

Goldberg, P., Berna, F. & Chazan, M. 2015. Deposition and diagenesis in the Earlier Stone Age of Wonderwerk Cave, Excavation 1, South Africa. *African Archaeological Review* **32**: 613–43.

Goldberg, P. & Macphail, R.I. 2008. *Practical and theoretical geoarchaeology*. Blackwell Publishing.

Goldberg, P., Miller, C.E., Schiegl, S., Ligouis, B., Berna, F., Conard, N.J. &Wadley, L. 2009. Bedding, hearths and site maintenance in the Middle Stone Age of Sibudu Cave, KwaZulu-Natal, South Africa. *Archaeological and Anthropological Sciences* **1**: 95–122.

Goldberg, P.S. & Nathan, Y. 1975. The phosphate mineralogy of et-Tabun cave, Mount Carmel, Israel. *Mineralogical Magazine* **40**: 253–8.

Hay, R.L. 1963. Zeolitic weathering in Olduvai Gorge, Tanganyika. *Geological Society of America Bulletin* **74**: 1281–6.

Hay, R.L. & Reeder, R.J. 1978. Calcretes of Olduvai Gorge and the Ndolanya beds of northern Tanzania. *Sedimentology* **25**: 649–73.

Hendey, Q.B. & Volman, T.P. 1986. Last interglacial sea levels and coastal caves in the Cape Province, South Africa, *Quaternary Research* **25**: 189–98.

Hsu, P.H. 1982. Crystallization of variscite at room temperature. *Soil Science* **133**: 305–13.

Karkanas, P. 2010. Preservation of anthropogenic materials under different geochemical processes: a mineralogical approach. *Quaternary International* **214**: 63–9.

Karkanas, P., Bar-Yosef, O., Goldberg, P. & Weiner, S. 2000. Diagenesis in prehistoric caves: the use of minerals that form in situ to assess the completeness of the archaeological record. *Journal of Archaeological Science* **27**: 915–29.

Karkanas, P., Brown, K.S., Fisher, E.C., Jacobs, Z. & Marean, C.W. 2015. Interpreting human behavior from depositional rates and combustion features through the study of sedimentary microfacies at site Pinnacle Point 5–6, South Africa. *Journal of Human Evolution* **85**: 1–21.

Karkanas, P. & Goldberg, P. 2010. Site formation processes at Pinnacle Point Cave 13B (Mossel Bay, Western Cape Province, South Africa): resolving stratigraphic and depositional complexities with micromorphology. *Journal of Human Evolution* **59**: 256–73.

Karkanas, P., Kyparissi-Apostolika, N., Bar-Yosef, O. & Weiner, S. 1999. Mineral assemblages in Theopetra, Greece: a framework for understanding diagenesis in a prehistoric cave. *Journal of Archaeological Science* **26**: 1171–80.

Kittrick, J.A. & Jackson, M.L. 1955. Application of solubility product principles to the variscite-kaolinite system. *Soil Science Society of America Journal* **19**: 455–7.

Klein, R.G. 1991. Size variation in the Cape dune molerat (*Bathyergus suillus*) and Late Quaternary climatic change in the southwestern Cape Province, South Africa. *Quaternary Research* **36**: 243–56.

Klein, R.G. & Cruz-Uribe, K. 1987. Large mammals and tortoise bones from Elands Bay Cave and nearby sites, western Cape Province, South Africa. In: J.E. Parkington & M. Hall, eds., *Papers in the prehistory of the Western Cape, South Africa*. International Series 332. Oxford: B.A.R., pp. 132–63.

Klein, R.G. & Cruz-Uribe, K. 2016. Large mammals and tortoise bones from Elands Bay Cave (South Africa): implications for Later Stone Age environment and ecology. *Southern African Humanities* **29**: 259–82.

Lafuente, B., Bowns, R.T., Yang, H. & Stone, N. 2015. The power of databases: the RRUFF project. In: T. Armbruster, T. & R.M. Danisi, eds., *Highlights in mineralogical crystallography*. Berlin: W. De Gruyter, pp. 1–30.

Larsen, E.S. 1942. The mineralogy and paragenesis of the variscite nodules from Near Fairfield, Utah part 1. *American Mineralogist* **27**: 281–300.

Latridou, J.P. & Ozouf, J.C. 1982. Experimental frost shattering: 15 years of research at the Centre de Géomorphologie du CNRS. *Progress in Physical Geography* **6**: 215–32.

Laville, H. 1973. *Climatologie et chronologie du Paléolithique en Périgord: étude sédimentologique de dépots en grottes et sous abris*. Thèse de Doctorat d'Etat ès Sciences Naturelles, Université de Bordeaux I.

Ligouis, B. 2006. Jais, lignite, charbon et autres matières organiques fossils: application de la pétrologie organique à l'étude des éléments de parure et des fragments bruts. In: J. Bullinger, D. Leesch & N. Plumettaz, eds., *Le site magdalénian de Monruz, 1. Premiers éléments pour l'analyse d'un habitat de plein air*. Neuchâtel: Service et Musée Cantonal d'Archéologie, pp. 197–216.

Mallol, C., Hernández, C.M., Cabanes, D., Sistiaga, A., Machado, J., Rodríguez, Á., Pérez, L. & Galván, B. 2013. The black layer of Middle Palaeolithic combustion structures: interpretation and archaeostratigraphic implications. *Journal of Archaeological Science* **40**: 2515–37.

Marincea, Ş., Dumitraş, D. G., Diaconu, G. & Bilal, E. 2004. Hydroxylapatite, brushite and ardealite in the bat guano deposit from Peştera Mare de la Mereşti, Perşani Mountains, Romania. *Neues Jahrbuch für Mineralogie-Monatshefte* **10**: 464–88.

Mentzer, S.M., Miller, C.E., Kloos, P., Wadley, L. & Conard, N.J. 2014. The distribution of authigenic minerals in the Middle Stone Age deposits of Sibudu (South Africa), and implications for the preservation of archaeological features. Poster presented at the 4th Annual Meeting of the European Society for the Study of Human Evolution, Florence, Italy.

Miller, D. 1981. Geoarchaeological research at Elands Bay. BSc (Hons) thesis, University of Cape Town.

Miller, D. 1987. Geoarchaeology at Elands Bay. In: J.E. Parkington & M. Hall, eds., *Papers in the prehistory of the Western Cape, South Africa*. International Series 332. Oxford: B.A.R., pp. 46–77.

Miller, C.E. 2015. High-resolution geoarchaeology and settlement dynamics at the Middle Stone Age sites of Diepkloof and Sibudu, South Africa. In: N.J. Conard & A. Delagnes, eds., *Settlement dynamics of the Middle Paleolithic and Middle Stone Age, vol. IV*. Tübingen: Kerns Verlag, pp. 27–46.

Miller, C.E., Goldberg, P. & Berna, F. 2013. Geoarchaeological investigations at Diepkloof Rock Shelter, Western Cape, South Africa. *Journal of Archaeological Science* **40**: 3432–52.

Monge, G., Carretero, M.I., Pozo, M. & Barroso, C. 2014. Mineralogical changes in fossil bone from Cueva del Angel, Spain: archaeological implications and occurrence of whitlockite. *Journal of Archaeological Science* **46**: 6–15.

Noble, R.G. & Hemens, J. 1978. *Inland water ecosystems in South Africa: a review of research needs*. South African National Scientific Programmes Report 34. Pretoria: Council for Scientific and Industrial Research.

Odriozola, C.P., Linares-Catela, J.A. & Hurtado-Pérez, V. 2010. Variscite source and source analysis: testing assumptions at Pico Centeno (Encinasola, Spain). *Journal of Archaeological Science* **37**: 3146–57.

Onac, B.P., Zaharia, L., Kearns, J. & Vereş, D. 2006. Vashegyite from Gaura cu Muscă Cave. *International Journal of Speleology* **35**: 67–73.

Parkington, J. 1976. Coastal settlement between the mouths of the Berg and Olifants rivers, Cape Province. *South African Archaeological Bulletin* **31**: 127–40.

Parkington, J. 1981. The Elands Bay Cave sequence: cultural stratigraphy and subsistence strategies. In: R.E. Leakey & B.L. Ogot, eds., *Proceedings of the 8th Pan-African Congress of Prehistory and Quaternary Studies*. Tillmiap: Nairobi.

Parkington, J. 1987. Changing views of prehistoric settlement in the Western Cape. In: J. E. Parkington & M. Hall, eds., *Papers in the Prehistory of the Western Cape, South Africa*. International Series 332. Oxford: B.A.R., pp. 4–32.

Parkington, J., Cartwright, C., Cowling, R.M., Baxter, A. & Meadows, M. 2000. Palaeovegetation at the Last Glacial Maximum in the Western Cape, South Africa: wood charcoal and pollen evidence from Elands Bay Cave. *South African Journal of Science* **96**: 543–6.

Parkington, J.E., Nilssen, P., Reeler, C. & Henshilwood, C. 1992. Making sense of space at Dunefield Midden campsite, Western Cape, South Africa. *Southern African Field Archaeology* **1**: 63–70.

Parkington, J. & Poggenpoel, C. 1987. Diepkloof rock shelter. In: J.E. Parkington & M. Hall, eds., *Papers in the Prehistory of the Western Cape, South Africa*. International Series 332. Oxford: B.A.R., pp. 269–93.

Pinhasi, R., Meshveliani, T., Matskevich, Z., Bar-Oz, G., Weissbrod, L., Miller, C.E., Wilkinson, K., Lordkipanidze, D., Jakeli, N., Kvavadze, E. & Higham, T.F. 2014. Satsurblia: new insights of human response and survival across the Last Glacial Maximum in the southern Caucasus. *Plos One* **9**: e111271.

Porraz, G., Igreja, M., Schmidt, P. & Parkington, J.E. 2016. A shape to the microlithic Robberg from Elands Bay Cave (South Africa). *Southern African Humanities* **29**: 203–47.

Porraz, G., Parkington, J.E., Rigaud, J.P., Miller, C.E., Poggenpoel, C., Tribolo, C., Archer, W., Cartwright, C.R., Charrié-Duhaut, A., Dayet, L. & Igreja, M., 2013. The MSA sequence of Diepkloof and the history of southern African Late Pleistocene populations. *Journal of Archaeological Science* **40**: 3542–52.

Porraz, G., Schmid, V.C., Miller, C.E., Tribolo, C., Cartwright, C.C., Charrié-Duhaut, A., Igreja, M., Mentzer, S., Mercier, N., Schmidt, P., Conard, N.J., Texier, P.-J. & Parkington J.E.2016. Update on the 2011 excavation at Elands Bay Cave (South Africa) and the Verlorenvlei Stone Age. *Southern African Humanities* **29**: 33–68.

Preus, H.R., Marvik, O.J., Selvig, K.A. & Bennike, P. 2011. Ancient bacterial DNA (aDNA) in dental calculus from archaeological human remains. *Journal of Archaeological Science* **38**: 1827–31.

Renfrew, C. & Bahn, P.G. 2008. *Archaeology: theories, methods and practice*. Thames & Hudson.

Robertson, H.N. 1980. *An assessment of the utility of Verlorenvlei water*. MSc thesis, University of Cape Town.

Robey, T. 1987. The stratigraphic and cultural sequence at Tortoise Cave, Verlorenvlei. In: J. E. Parkington & M. Hall, eds., *Papers in the Prehistory of the Western Cape, South Africa*. International Series 332. Oxford: B.A.R., pp. 46–77.

Rogers, J. 1982. Lithostratigraphy of the Cenozoic sediments between Cape Town and Elands Bay. *Palaeoecology of Africa* **115**: 121–37.

Rogers, J. 1987. The evolution of the continental terrace between St Helena Bay and Lambert's Bay. In: J. E. Parkington & M. Hall, eds., *Papers in the Prehistory of the Western Cape, South Africa*. International Series 332. Oxford: B.A.R., pp. 35–45.

Rufer, D. & Preusser, F. 2008. Potential of Autoradiography to Detect Spatially Resolved Radiation Patterns in the Context of Trapped Charge Dating. *Geochronometria* **34**: 1–13.

Schiegl, S. & Conard, N.J. 2006. The Middle Stone Age sediments at Sibudu: results from FTIR spectroscopy and microscopic analyses. *Southern African Humanities* **18** (1): 149–72.

Schloms, B.H.A., Ellis, F. & Lambrechts, J.J.N. 1983. Soils of the Cape coastal platform. In: H.J. Deacon, Q.B. Hendey, & J.J.N. Lambrechts, eds., *Fynbos palaeoecology:a preliminary synthesis*. South African National Scientific Programmes Report 75. Pretoria: Council for Scientific and Industrial Research, pp. 70–86.

Schmid, V., Conard, N.J., Parkington, J.E., Texier P.-J, & Porraz, G. 2016. The 'MSA 1' of Elands Bay Cave (Western Cape Province, South Africa) in the context of the southern African Early Middle Stone Age technologies. *Southern African Humanities* **29**: 153–202.

Shahack-Gross, R., Berna, F., Karkanas, P. & Weiner, S. 2004. Bat guano and preservation of archaeological remains in cave sites. *Journal of Archaeological Science* **31**: 1259–72.

Sillen, A. & Parkington, J. 1996. Diagenesis of bones from Eland's Bay Cave. *Journal of Archaeological Science* **23**: 535–42.

Sinclair, S.A., Lane, S.B. & Grindley, J.R. 1986. *Estuaries of the Cape, Part 2: synopses of available information on individual systems,* Report 32, Verlorenvlei (CW 13): 1–95.

Stahlschmidt, M.C., Miller, C.E., Ligouis, B., Goldberg, P., Berna, F., Urban, B. & Conard, N.J. 2015. The depositional environments of Schöningen 13 II-4 and their archaeological implications. *Journal of Human Evolution* **89**: 71–91.

Stahlschmidt, M.C., Miller, C.E., Ligouis, B., Hambach, U., Goldberg, P., Berna, F., Richter, D., Urban, B., Serangeli, J. & Conard, N.J. 2015. On the evidence for human use and control of fire at Schöningen. *Journal of Human Evolution* **89**: 181–201.

Stoops, G. 2003. *Guidelines for analysis and description of soil and regolith thin sections*. Soil Science Society of America.

Talbot, W.J. 1947. *Swartland and Sandveld*. Oxford University Press, Cape Town.

Tankard, A.J. 1976. Pleistocene history and coastal morphology of the Ysterfontein-ElandsBay area, Cape Province. *Annals of the South African Museum* **69**: 73–119.

Taylor, G.H., Teichmüller, M., Davis, A., Diessel, C.F.K., Littke, R. & Robert, P. 1998. *Organic Petrology*. Berlin: Gebrüder Borntraeger.

Theron, J.N. 1983. Geological setting of the fynbos. In: H.J. Deacon, Q.B. Hendey, & J.J.N. Lambrechts, eds., *Fynbos palaeoecology: a preliminary synthesis*. South African National Scientific Programmes Report 75. Pretoria: Council for Scientific and Industrial Research, pp. 21–34.

Thompson, T.J.U., Islam, M. & Bonniere, M. 2013. A new statistical approach for determining the crystallinity of heat-altered bone mineral from FTIR spectra. *Journal of Archaeological Science* **40**: 416–22.

Tribolo, C., Mercier, N., Valladas, H., Miller, C.E., Parkington, J.E. & Porraz, G. 2016. Chronology of the Pleistocene deposits at Elands Bay Cave (South Africa) based on charcoals, burnt lithics, and sedimentary quartz and feldspar grains. *Southern African Humanities* **29**: 129–52.

Villagran, X.S., Straus, A., Miller, C., Ligouis, B. & Oliveria, R. 2016. Buried in ashes: site formation processes at Lapa do Santo rock shelter, east-central Brazil. *Journal of Archaeological Science*. http://dx.doi.org/10.1016/j.jas. 2016.07.008

Visser, H.M. & Toerien, D.K. 1971. *Die geologie van die gebied tussen Vredendal en Elandsbaai, toeligting van blaaie 321 BC Doringbaai en 321 BA Lambertsbaai*. Geological Survey Publication No. 62813–1. Pretoria: Department of Mines.

Wadley, L., Sievers, C., Bamford, M., Goldberg, P., Berna, F. & Miller, C. 2011. Middle Stone Age bedding construction and settlement patterns at Sibudu, South Africa. *Science* **334**: 1388–91.

Watchman, A., Ward, I., Jones, R. & O'Connor, S. 2001. Spatial and compositional variations within finely laminated mineral crusts at Carpenter's Gap, an archaeological site in tropical Australia. *Geoarchaeology* **16**: 803–24.

Weiner, S. & Goldberg, P. 1990. On-site Fourier Transform-Infrared spectrometry at an archaeological excavation. *Spectroscopy* **5**: 46–50.

Weiner, S., Goldberg, P. & Bar-Yosef, O. 2002. Three-dimensional distribution of minerals in the sediments of Hayonim Cave, Israel: diagenetic processes and archaeological implications. *Journal of Archaeological Science* **29**: 1289–1308.

Weiner, S., Goldberg, P. & Bar-Yosef, O. 1993. Bone preservation in Kebara Cave, Israel using on-site Fourier transform infrared spectrometry. *Journal of Archaeological Science* **20**: 613–27.

Weiner, S., Berna, F., Cohen, I., Shahack-Gross, R., Albert, R. M., Karkanas, P., Meignen, L. & Bar-Yosef, O. 2007. Mineral distributions in Kebara Cave: diagenesis and its effect on the archaeological record. In: O. Bar-Yosef & L. Meignen, eds., *Kebara Cave, Mt. Carmel, Israel: The Middle and Upper Paleolithic Archaeology, Part I*. American School of Prehistoric Research Bulletin 49. Harvard University, Peabody Museum of Archaeology and Ethnology, Cambridge MA, pp. 131–46.

Southern African Humanities **29**: 129–52 December 2016 KwaZulu-Natal Museum

Chronology of the Pleistocene deposits at Elands Bay Cave (South Africa) based on charcoals, burnt lithics, and sedimentary quartz and feldspar grains

[1]**Chantal Tribolo**, [1]**Norbert Mercier**, [2]**Hélène Valladas**, [1]**Yannick Lefrais**, [3]**Christopher E. Miller**, [4]**John Parkington** and [5,6]**Guillaume Porraz**

[1]IRAMAT-CRP2A, CNRS, Université de Bordeaux, UMR 5060, Maison de l'archéologie, Esplanade des Antilles, 33607 Pessac cedex, France; ctribolo@u-bordeaux-montaigne.fr; norbert.mercier@u-bordeaux-montaigne.fr; yannick.lefrais@u-bordeaux-montaigne.fr

[2]Laboratoire des Sciences du Climat et de l'Environnement, LSCE/IPSL, CEA-CNRS-UVSQ, Université Paris-Saclay, Avenue de la terrasse, bât 12, 91198 Gif-sur-Yvette, France; Helene.Valladas@lsce.ipsl.fr

[3]Institute for Archaeological Sciences, University of Tübingen, Rümelinstrasse 23, 72070 Tübingen, Germany; christopher.miller@uni-tuebingen.de

[4]Department of Archaeology, University of Cape Town, Rondebosch, 7700 South Africa; John.Parkington@uct.ac.za

[5]CNRS, USR 3336, French Institute of South Africa, 62 Juta Street, Braamfontein, 2113 South Africa; guillaume.porraz@mae.u-paris10.fr

[6]Evolutionary Studies Institute, University of the Witwatersrand, Johannesburg, South Africa.

ABSTRACT

In 2011 we conducted a field campaign at the site of Elands Bay Cave (EBC), on the West coast of South Africa, with the aim of clarifying the nature and chronology of its human Pleistocene occupations. In the present paper, we present the results of a chronology based on various materials and methods: radiocarbon (C14) dating was applied to 8 fragments of charcoal whereas luminescence dating methods (OSL, IRSL and TL) were applied to quartz and feldspar grains extracted from 5 sediment samples and to 4 burnt fragments of quartzite rock.

For the upper part of the sequence, the luminescence ages are either in agreement with or slightly younger than the C14 ages. The results suggest that the upper part of the EBC sequence extends from MIS3 to MIS2, including successively late Middle Stone Age (starting from 38 ± 3 ka), Early Later Stone Age (ending 22 ka ago) and Robberg occupations (starting 19.1 ± 0.3 ka ago). The lower part of the EBC sequence, associated with Early Middle Stone Age assemblages, remains poorly constrained: the sediment sample taken above could be a mixture of different layers and could not be dated, whereas OSL ages for sediments below are 236 ± 23 ka and only one stone sample could be dated within this layer (83 ± 14 ka). Considering both the chronological and techno-cultural points of view, the EBC sequence is complementary to the Diepkloof sequence, located less than 20 km eastward.

KEY WORDS: Middle Stone Age, Later Stone Age, luminescence dating, radiocarbon, TL, OSL, IRSL

The Middle Stone Age (MSA) of Southern Africa has received significant attention during the last decades. In particular, this research has mainly focused on the Still Bay (SB) and Howiesons Poort (HP) techno-complexes, largely within the framework of researching the origins of 'modern behavior' (e.g. Henshilwood et al. 2002; Jacobs et al. 2008; Henshilwood & Dubreuil 2011; Porraz, Parkington et al. 2013a; Tribolo et al. 2013; Conard et al. 2014; Soriano et al. 2015; Wadley 2015). By comparison, other techno-complexes, whether defined in long sequences such as those at Border Cave, Klasies River or Bushman Rock Shelter or in other shorter sequences (Beaumont et al. 1978; Singer & Wymer 1982; Volman 1984; Wurz 2002; Porraz et al. 2015), have received little attention and their chronology is poorly defined.

ISSN 2305-2791 (online); 1681-5564 (print)

Elands Bay Cave (EBC), located on the South Western coast of South Africa, is particularly interesting in this context since it retains Early MSA lithic assemblages that were used by Volman (1984) for defining the MSA 1 techno-complex (see Schmid et al. 2016 this issue) and it also presents a well-developed Late Pleistocene to Holocene sequence. EBC should therefore be complementary to the nearby site (< 20 km) of Diepkloof Rock Shelter (Parkington et al. 2013; Porraz, Parkington et al. 2013; Texier et al. 2010, 2013), which mainly preserved SB and HP occupations.

EBC was first studied in the seventies by Parkington et al. (see Parkington 2016 this issue). Their study focused mainly on the upper Later Stone Age (LSA) remains. The lower LSA and MSA layers were excavated over a limited area only (2 x 2.5 m on ~1.5 m deep) and only a > 40 ka C14 age was available for the MSA levels. In order to enlarge the archaeological collection and contextualize it from both a geological and chronological perspective, an excavation was undertaken in April 2011 (Porraz, Schmid et al. 2016 this issue). Eight charcoal samples were taken for radiocarbon dating along with five sediment samples and ten potentially burnt fragments of quartzite were selected for luminescence dating. In this paper, we present the main analytical steps of the dating process and discuss the chronology.

SITE AND CONTEXT

Short introduction to Elands Bay Cave

Details about the geological setting, history of excavation and stratigraphy can be found in other papers in this issue (Miller et al.; Parkington; Porraz, Schmid et al.). Only the main aspects are reported here.

EBC is located near the small town of Elandsbaai and is currently ca. 50 m from the Atlantic coast line, 42 m above sea level (see fig.1 in Porraz, Schmid et al. 2016 this issue). The cavity (about 10 m deep, 18 m wide) is formed in the sandstone of the Table Mountain Group and opens toward the northwest. The shelter contains Pleistocene and Holocene deposits that form a sequence of about 3 m thick.

So far, much of the fieldwork and studies focused on the Holocene deposits and less attention was paid to earlier occupations. In 2011, we reopened the two test-pits made by J.E. Parkington in 1972 and 1978. We excavated a narrow band along the Eastern section (Fig. 1) where the succession of deposits was clearly visible. Eight stratigraphic blocks subdivided into ca. 30 stratigraphic units (SUs), named in alphabetical order from top to bottom, were individualized and three main 'cultural' entities were recognized during excavation.

Main sedimentological and technological phases

The main sedimentary phases from our 2011 excavation can be summarized as follows: Phases D and F (SUs Delport to Fuzy), on the top 50 cm, display the remains of numerous combustion features: ashes, charcoals and rubefied sediments. In particular, a hearth structured with quartzite stones was discovered in the SU Furb. Fauna is poorly preserved.

Phases H to K (SUs Harry to Kent) are darkish, laminated sediments, including yellowish lenses. Phase H appears generally homogeneous and sandier than phase K. In these units no organic remains are preserved, with the exception of a few small charcoals in the SU Jacob.

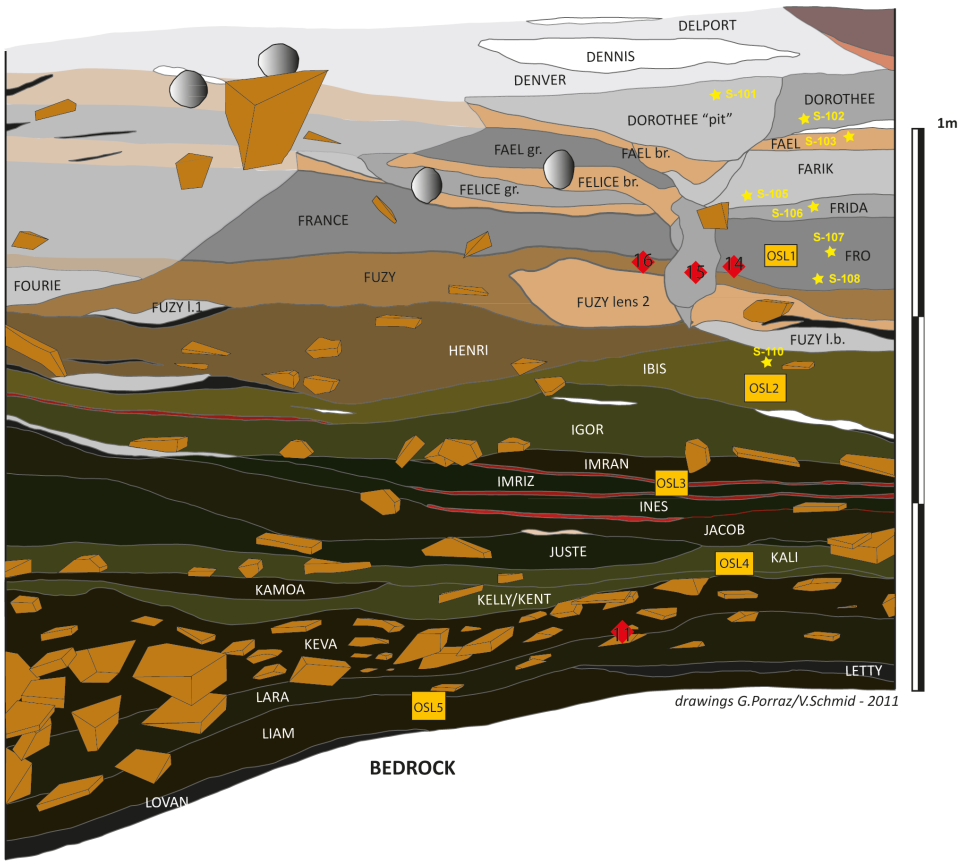

Fig. 1. Eastern section displaying the main units and the location of the OSL (sediment; orange rectangle), TL (burnt quartzites; red diamonds) and C14 (charcoals; yellow stars) samples. Note that the SU Furb where the TL samples EBC14, 15 and 16 come from is not drawn on the section: it was a combustion feature of limited extension located between the SUs Fro and Fuzy.

Phase Keva/Lara, with a maximum thickness of 35 cm, is characterized by a large accumulation of quartzite artifacts and roof spalls with almost no fine sediment in between. No organic material is preserved.

Phase L at the bottom (max. 10 cm thick) lies directly on the substratum. It is composed of dark brown sediments with black moist lenses. There are very few archaeological finds that likely represent intrusive artefacts from the overlying SU. Again, organic materials are not preserved.

The main technological phases can be summarized as follow:

Phase D. The lithic assemblages are composed of small cores and bladelets in quartz and silcrete that are characteristics of the Robberg techno-complex (Porraz, Igreja et al. 2016 this issue).

Phase F to K. The lithic assemblages, of relatively low densities, are characteristically MSA, with laminar and discoid reductions sequences, together with denticulates. But some diachronic change is evident from the base to the top (Porraz, Schmid et al. 2016

this issue). The phase F in particular, with the highest proportion of quartz, the use of bipolar percussion, and a low degree of normalization, typifies what is generally referred to as Early LSA.

Phase Keva/Lara. This is the richest lithic assemblage of the sequence. It is characterized by the production of various blanks in local quartzite (Schmid et al. 2016 this issue). This assemblage was initially used by Volman to define what he named the MSA 1 (Volman 1984).

Geoarchaeological background to the study

The sediments are strongly influenced by chemical diagenesis (Miller et al. 2016 this issue). Nodules of secondary gypsum in particular have completely transformed the appearance of the different units in the west, north and south sections. In the southern part of the eastern section, the aspect of the layers was preserved due to a still-active cone of water percolation that has prevented gypsum crystallization. However the percolation has induced chemical transformations, including the formation of secondary apatite, variscite and taranakite. The percolating water is also likely responsible for the dissolution of bone within this area of the site. Micromorphological examination of these deposits suggests that there were likely multiple phases of chemical diagenesis throughout the history of EBC, and the moisture which led to secondary mineral growth and bone dissolution was likely variable in the past (Miller et al. 2016 this issue).

The complex history of chemical diagenesis at the site raises the question of stability over time of the dose rate, which must be assessed for calculating the luminescence ages, and of the representativeness of the present one, measured both in the field and in the laboratory. Comparisons with radiocarbon ages and uses of different materials, for which the ratio of internal and external dose rates are different, are expected to give insight into the general reliability of the results.

Some biological activity was also noted during excavation, mostly in the upper portion of the deposits in the form of burrows and insect hollows. We collected OSL samples as far away from these disturbances as possible.

SAMPLING AND METHODS

Sediments

Samplings

Five sediment samples were taken at night under subdued red light in the eastern profile for dating with the OSL method (Aitken 1998). EBC1 comes from the SU Fro associated to the Early LSA phase, EBC2 and EBC3 come respectively from the SUs Ibis and Imran/Imriz, associated to the Late MSA. It was not possible to sample sediments directly from the SUs embedding the MSA 1 techno-complex as there were too many stones and not enough pockets of fine sediments. EBC4 was then taken above the 'MSA 1' layers, in the SU Kali, and EBC5 below, in the SU Liam (Fig.1).

De estimate

Each sediment sample was put into light-tight black plastic bags and brought back to the IRAMAT-CRP2A laboratory (Pessac, France) where they were processed. The 200–250 μm quartz and feldspar grains were extracted by mechanical and chemical

treatments: wet sieving, HCl (10 %) and H_2O_2 (30 %) for removal of carbonates and organic material respectively, followed by density separation with hetero-polytungstate of sodium (LST) at 2.58 and 2.72 g/cm^3. The feldspar grains were rinsed with distilled water and dried, while the quartz grains were further etched for 60 min with HF (48 %) and rinsed with HCl (10 %) and water. The absence of feldspars in the quartz sample was checked with IRSL tests (Duller 2003). The grains were dispersed on three different supports: silicon oil coated standard stainless steel discs (quartz, 5 mm mask) or cups (feldspar, 1 mm mask) along with a single grain disc (quartz, 100 cylindrical holes, 300 μm diameter x 300 μm deep).

The measurements were performed on a TL/OSL-DA20 Risø reader (Duller et al. 1999; Bøtter-Jensen et al. 2000, 2003) equipped with clusters of blue LED (470 ± 20 nm) or infra-red LED (870 ± 30 nm) for excitation of multi quartz and feldspar grains respectively (estimated reproducibility: 1.5 %). Excitation of single quartz grains was done by a 10 mW Nd:YVO_4 diode-pump-laser (532 nm) (2.7 % reproducibility). The luminescence signals were detected with a Q9235 photomultiplier tube preceded by either 7.5 mm of Hoya U340 filter for detection in the UV range (280–380 nm) (quartz), or Schott BG39+Corning 7-59 filters for detection in the blue range (320–460 nm) (feldspar). A $^{90}Sr/^{90}Y$ beta source delivering 0.15 Gy/s attached to the reader was used for artificial irradiation. Analyses of the measurements were performed with the Analyst software (Duller 2015) and the baSAR function was used for Bayesian statistics (Mercier et al. in press).

Linearly modulated OSL measurements and comparison with the Risø calibration quartz suggest that in all samples the signal is dominated by the fast-component (data not shown). The estimate of the equivalent dose (De) for the quartz grains was thus based on a Single Aliquot and Regenerative dose protocol applied to single grains (SAR, Murray & Wintle 2000, 2003; Fig. 2A). The protocol tests and results are given in section "analyses of the luminescence dating data sets" below. For the feldspar grains, only those extracted from sample EBC 5 were measured. The estimate of the equivalent dose was done on multi-grain single aliquots following two different protocols (Figs 2B, 2C): InfraRed Stimulated Luminescence (IRSL) at 50°C (IR50) after Auclair et al. (2003) and Post IR-IRSL at 290°C (PIR-IR290) after Buylaert et al. (2009).

Dose rate estimate

The cosmic dose rate (Dr) was estimated with the equation of Prescott and Hutton (1994), taking into account the geometry of the cave. The gamma Dr was determined with Al_2O_3: C chips dosimeters (e.g. Richter et al. 2010): these ones were inserted into the outcrops for about one year at the location where each sediment sample had been taken.

The beta Dr was based on the determination of the U, Th and K contents of each sediment sample, with separate examination of the coarse and fine fractions, following Tribolo et al. (accepted) and Martin (2015). A fraction of the sediment sample was dried in the oven (45°C) for one week and sieved at 2 mm. The > 2 mm and < 2 mm fractions were then finely crushed separately for the analyses: estimates of U, Th and K contents were then deduced from high resolution gamma spectrometry for the < 2 mm fraction and with ICP-MS or ICP-AES instruments for the > 2 mm fraction. Attenuation factors of Guérin et al. (2012) and conversion factors of Guérin et al. (2011) were applied.

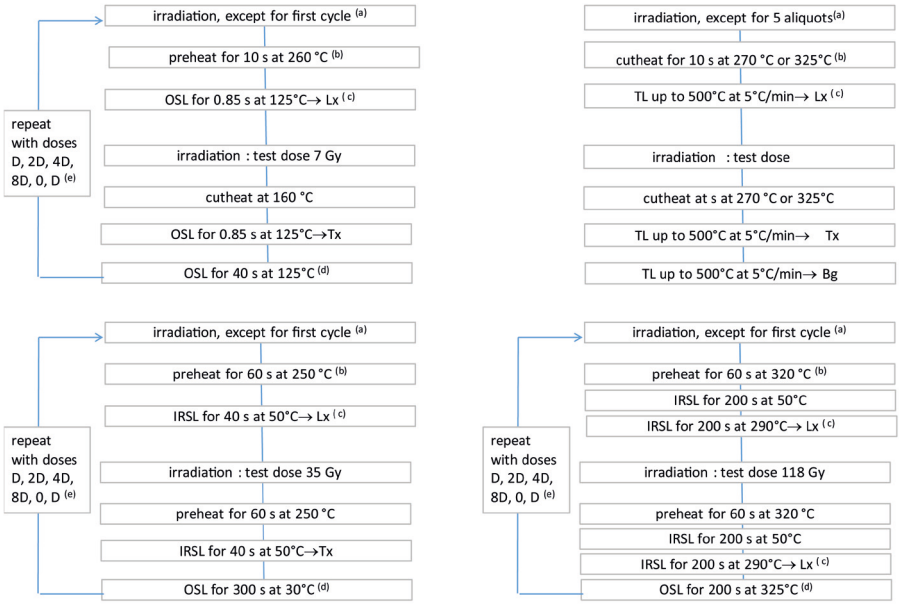

Fig. 2. Protocols. A) SAR protocol applied for the OSL-single quartz grain study. a) For the dose recovery tests, a dose (3D, close to the estimated De) was given during the first cycle. b) For the preheat plateau tests, the preheat temperature was set at 220, 240, 260 or 280°C; they were performed with multi-grain aliquots, and the OSL signals were measured with the blue LED at 125°C for 40s. c) For the single grain signal analyses, the first 0.05 s and last 0.10 s were used as signal and background respectively; the background of the natural or regenerative dose signal was taken for the following test dose signal. d) The optical wash was performed with the blue LED. e) The regenerative dose were chosen so that 3D was close to the central De.
B) SAR – IR50 protocol applied to the multi-aliquot feldspar grains.
C) PIR-IR290 protocol applied to the multi-aliquot feldspar grains; f) the first 6 and last 16.4 seconds were used as signal and background. D) Protocol applied to each aliquot for the multiple aliquot additive and regenerative dose protocol; g) integration was done on the plateau area. h) the regenerative doses were given after annealing at 450°C for 1h45 min; i) the preheat was 300°C for EBC14, 15 and 16 and 325°C for EBC11. The normalized luminescence signal was calculated as (Lx-Bg)/(Tx-Bg), first on 5°C wide steps (plateau tests) then on a temperature range where the De estimate is stable.

The alpha Dr was assumed negligible for the quartz grains since the HF etching had theoretically removed most of the outer layer of the grains irradiated by the alpha particles. The external alpha dose for the feldspar grains was based on the U, Th contents of the sediment and assumed an a-value of 0.08 ± 0.02 (Rees-Jones 1995). The internal Dr of the K-feldspar grains was derived from the internal K content, estimated 10.0 ± 0.5 % after measurements on single grains with MEB-EDX, and from an assumed Rb content of 400 ± 100 ppm (Huntley & Baril 1997; Huntley & Hancock 2001).

Rock samples

Sampling and initial tests

Ten quartzite samples were initially selected and brought to the IRAMAT-CRP2A laboratory for dating with luminescence technics. Preliminary tests using blue TL signal showed however that only four were not saturated; the others were too close to

saturation for being dated with standard blue TL protocols. Further tests were done with other protocols (ITL, after Tribolo & Mercier 2012; Red TL, e.g. Fattahi & Stokes 2003) for which working at doses close to the saturation level is feasible, or for which the saturation of the signal comes at higher doses than for the blue TL. Unfortunately none of these were useful in this project.

The four stones passing the tests come from the hearth of SU Furb (EBC14, 15, 16) and from SU Keva (EBC11), associated with the Early LSA and Early MSA techno-complexes respectively.

Equivalent dose estimate

These four selected samples were sawed and their core crushed, sieved at 100–160 μm and briefly treated with HCl 10 %. The luminescence measurements were performed with the same device as for the luminescence analyses of the sediments, except that the detection window was a combination of HEBO B03, B39 and V01 filters for a detection in the blue at 380 ± 20 nm, and the doses were given in an external irradiator equipped with a $^{90}Sr/^{90}Y$ beta source delivering 0.06 Gy/s. The De was estimated using an additive and regenerative multiple aliquot protocol (Valladas 1992) (Fig. 2D). A total of 40 aliquots of 5.28 ± 0.13 mg of 100–160 μm grain size powder was used per sample. The regenerative doses were given after annealing at 450°C for 105 min.

Dose rate estimate

The cosmic Dr was the same as for the sediment samples. The closest dosimeters were used for the determination of the gamma Dr, taking into account the shape and weight of each stone for the attenuation of the gamma rays (Valladas 1985). The contribution from external beta and alpha Drs were negligible since the irradiated outer layer of each stone sample (at least 2 mm thick) had been removed by sawing.

The internal alpha and beta Drs were based on the determination of the U, Th, K contents (by ICP-MS and ICP-AES). The same model as the one used for Diepkloof rock samples was applied (Tribolo et al. 2013): the U, Th and K emitters were assumed to be mainly in the grains boundaries, implying an attenuation for the alpha Dr and none for the beta Dr. For the alpha Dr the attenuation factors of Brennan et al. (1991) were applied, the mean size of the quartz grains within the stone being estimated with the aid of thin section observations.

Charcoal samples

Eight charcoal samples were selected directly on the eastern profile at the end of the excavation (Fig. 1). They are labelled S101 to S110 and come from phases D (S101 and S102), F (S103 to S108) and I (S110). They were processed at the LSCE (CEA-CNRS-UVSQ at Gif-sur-Yvette, France) and measured on the Artemis AMS facility (LMC-14, CEA, Saclay). Before the C14 analysis the samples were submitted to a chemical treatment to eliminate contamination by extraneous carbon. It involved a succession of 'acid (HCl, 0.5 N)—base (NaOH, 0.1 N)—acid treatments (HCl, 0.5 N)' which first dissolve the carbonates that may have come from the sediment or ground water, then the humic acids arising from the transformation of organic matter, and bacteria or other living microorganisms. Whatever remained were oxidized to CO_2

then reduced to graphite and compressed into pellets for the accelerator measurement (Cottereau et al. 2007).

ANALYSES OF THE LUMINESCENCE DATING DATA SETS

Quartz grains

Quartz grains dose rate

The current gamma Drs recorded by the dosimeters range between 702 and 500 μGy/a and decrease from top to bottom. This might be partly related to the increasing content with depth of quarzitic rock fragments, whose mean radioisotope content is usually lower than for fine sediments.

As mentioned earlier, for the determination of the beta Dr, care was taken to measure the U, Th and K contents on the coarse (> 2 mm) and fine (< 2 mm) fractions separately. The U, Th, activities and K contents for the < 2 mm fraction of the five sediment samples are shown on Table 1a (all tables after the references). It can be noticed that the U family decay chain is at equilibrium for EBC1 and 2 but displays a disequilibrium between the pre-^{226}Ra and post-^{226}Ra parts for EBC3, 4 and 5: the activity of the pre-^{226}Ra part is about 40 % higher than the activity of the post-^{226}Ra part. However the overall contribution from the U chain to the total Dr is sufficiently low (currently 26–30 %) for not having a significant effect on the age estimate: taking extreme scenarios where equilibrium would have prevailed up to recently, the actual dose rate would be down to 3 % lower (e.g. recent arrival of ^{234}U) or up to 10 % higher (e.g. recent loss of ^{226}Rn) than the dose rate calculated with the current activities. As mentioned earlier, the variation of K over time suggested by the analysis of the diagenetic process is a more important concern (currently, the K contribution is 36–48 %). This will be further discuss when comparing the age estimates, calculated from the current K, U and Th contents.

For the > 2 mm fractions, the U, Th and K contents or activities are, as expected, significantly (37 % to 84 %) lower than the U, Th, K contents of the fine fraction (Table 1b) (except for Th in EBC3). It has been suggested that the true beta Dr stands between the Dr estimated from the fine and the Dr estimated from the coarse + fine (i.e. total) radioisotope contents (Table 1c) (Martin 2015; Tribolo et al. accepted). These two extreme beta Dr estimates are given in Table 2. The differences between them are quite low (3–9 %), however, since the effect of the relative lower radioisotope contents for the coarse fraction is counterbalanced by its low relative weight (< 14 % of the total mass). The average of these two extreme beta Dr estimates has been used for calculating the age, as suggested by Martin (2015).

The current water contents, ranging from 8 to 18 %, are also given in Table 2. The presence of pseudomorphic voids, likely the result of gypsum dissolution, formed within a taranakite crust in the lower SUs (Ines to Imran) suggests that the sediment has been drier sometime in the past (Miller et al. 2016 this issue). However, the ages have been calculated with the current water content. If overestimated, the ages should be overestimated as well (about 1 % of the initial age estimate per percentage of water content overestimation).

The total Drs, assuming the persistence of the observed current conditions, for water and radioisotope contents, are presented on Table 2. They are rather low, ranging from 1.28 ± 0.08 to 1.62 ± 0.11 Gy/ka.

Quartz equivalent doses

The SAR protocol is presented on Figure 2a. During the analysis of the luminescence data, single quartz grains were systematically rejected if (1) the natural test dose signal was less than 3 times background, (2) the recycling ratio was not consistent at one sigma with the [0.9 , 1.1] interval, 3) recuperation ratio was more than 5 % of natural signal, 4) natural test dose uncertainty was more than 10 %.

In the following, we proceed with successive steps: first, we test the reliability of the measurement protocol; then we present the De distributions and discuss whether or not they might be consistent with a single mean/central De; finally, we discuss and compare the way the calculation of this single De is performed. In particular, we compare results obtained with the Central Age Model (Galbraith et al. 1999), which is basically a frequentist statistical approach, to the results obtained with the recently developed Bayesian statistical approach (Combès et al. 2015). In both cases, a saturating exponential fit (i.e. $Lx/Tx = a[1-\exp(-(D + c)/D_0]$, where Lx/Tx is the sensitivity corrected luminescence signal, D the regenerative dose and a, c and D_0 characterize the growth curve) was used.

A basic requirement of the protocol is the ability to recover a laboratory given known dose. Dose recovery tests were performed on each sample. The samples were mounted on single grain discs, left under a solar simulator (Hölne SOL500) for one minute and a dose close to the equivalent dose was given in the reader. Results are shown on Figures 3a, b, c, where the ratios of observed to given dose for a set of aliquots are displayed against their minimum characteristic D_0 dose, following the suggestion of Thomsen et al. (2016). EBC1, 2 and 3 display the same pattern and only EBC1 is shown on Figure 3a. For theses samples (given dose between 32 and 50 Gy), the dose recovery ratios are independent of the minimum D_0 and consistent with unity at two sigma. Conversely for EBC4 and 5 (given doses of 91 and 228 Gy respectively), the dose recovery ratios increase with the minimal D_0 value, then a plateau, consistent with unity at two sigma, is reached when D_0 is over about 100 Gy: grains with low D_0 value are unable to recover high doses and must be discarded (Thomsen et al. 2016). The final ratios are summarized in Table 3. Additional selection of grains based on the D_0 values has thus also been applied to the final De analyses.

In addition, we verified the temperature stability of the De over different preheat conditions by performing a preheat plateau test. It was done on multi-grain aliquots for EBC1, 2 and 3. Preheat temperatures between 220 and 280°C were applied. No significant effect was observed (data not shown). We assumed that it was also the case for EBC4 and 5.

Figure 4 shows the dependence of the central De on the minimal D_0 value. Similar patterns as those observed for the dose recovery tests are observed: for EBC1, the central De are independent on D_0. EBC2 and EBC 3 show similar patterns and are not plotted. For EBC4 and 5, for which the central De values are significantly higher, these ones increase with the minimal D_0 and reach a plateau when D_0 is close to 100 Gy. The distributions plotted on Figure 5 are cleared of the data corresponding to low D_0 values for EBC4 and 5.

The overdispersions (OD, Galbraith et al. 1999) stand between 23 ± 1 and 31 ± 2 % for EBC1, 2, 3 and 5 (Fig. 6, Table 4). They are, as expected (Thomsen et al. 2005, 2012), higher than the OD for the bleached and beta dosed samples (dose recovery

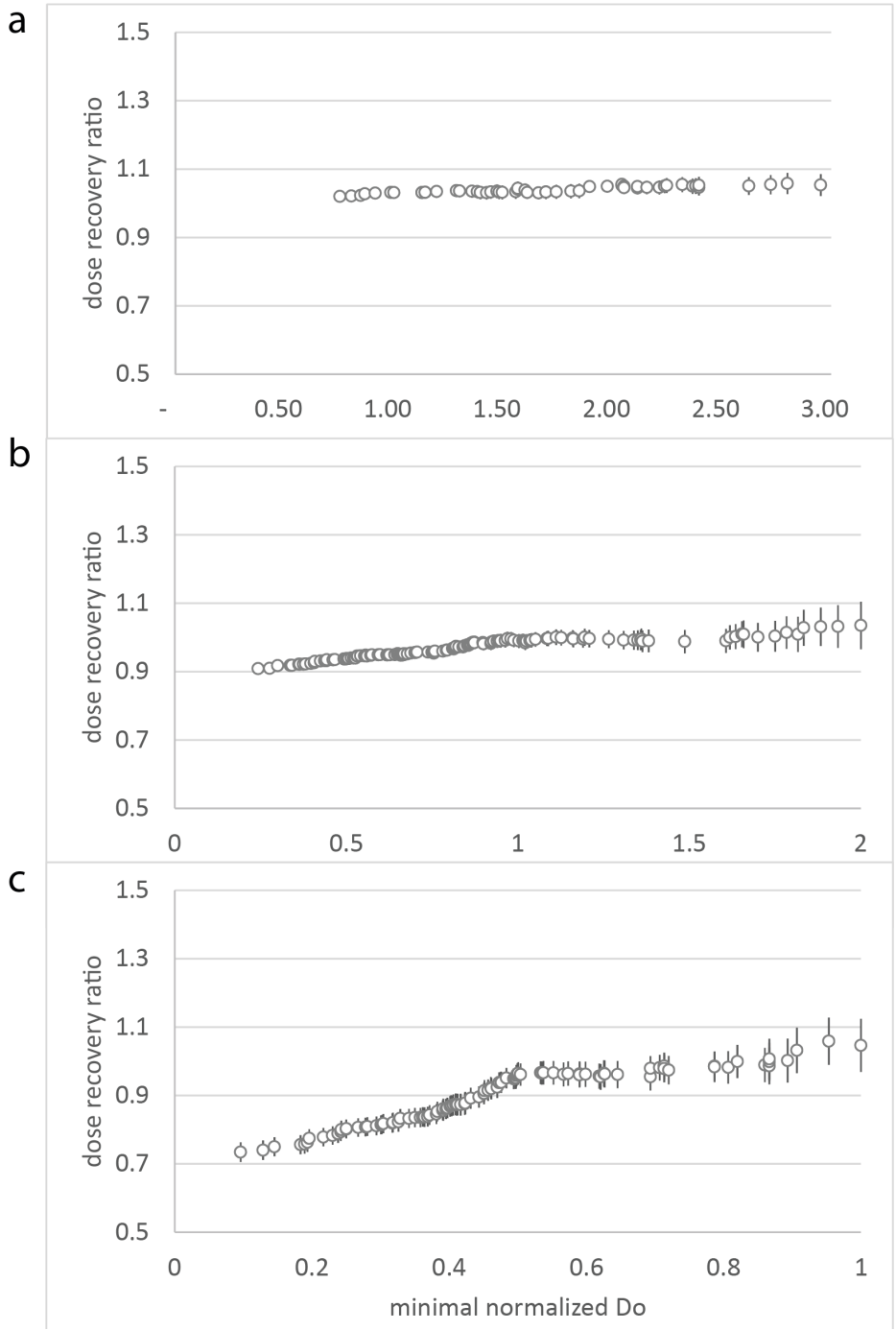

Fig. 3. Dose recovery ratio in function of the minimum D_0. The central doses used in the calculation of the ratio are estimated from exponential fit of individual growth curves and from the central age model of Galbraith et al. (1999). a) EBC1, b) EBC4, c) EBC5.

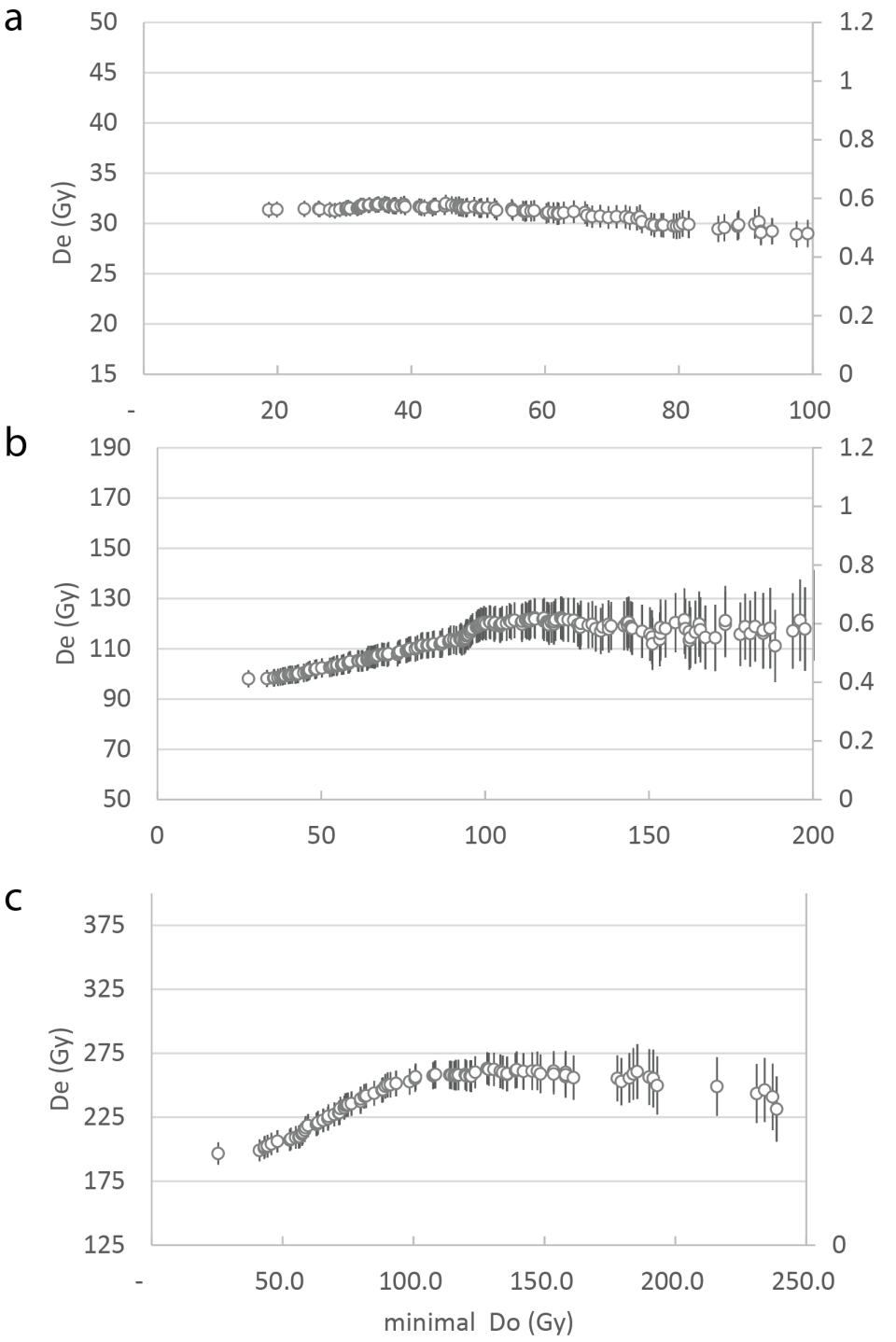

Fig. 4. Central (CAM) De in function of the minimal D_0 value. a) EBC1, b) EBC4, c) EBC5.

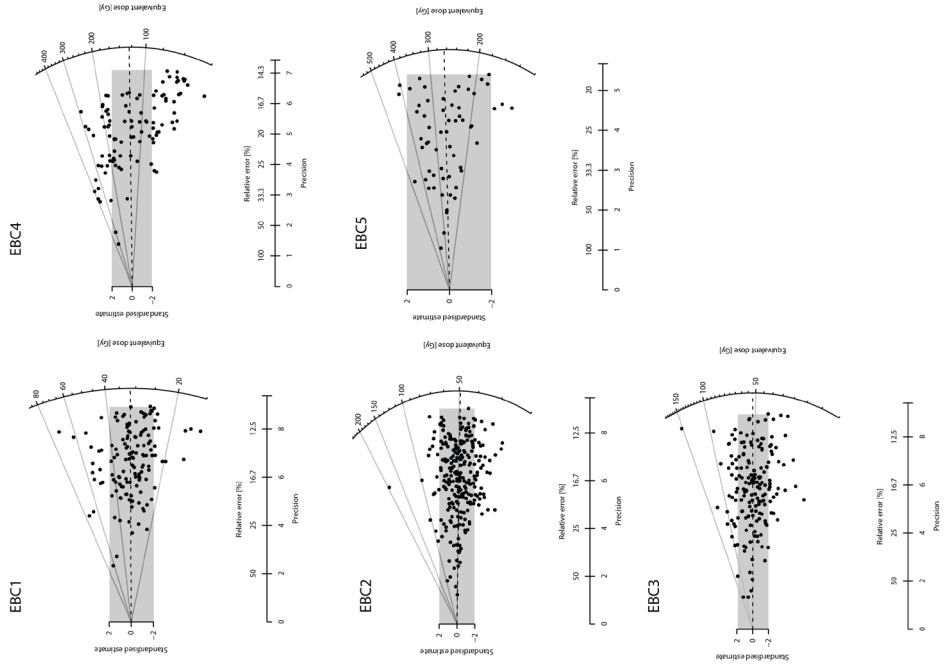

Fig. 5. Radial plots of the single grain De distribution. Note the distributions took into account the low D_0 values criterion for EBC4 and EBC5, and the intrinsic overdispersions estimated from the dose recovery test have been taken into account for the plot of the relative error so that the dispersion due only to extrinsic factors is highlighted.

tests: 7 ± 2 to 17 ± 3 %). It has been suggested (Thomsen et al. 2012) that the OD for bleached and not in situ (gamma or beta) dosed samples is higher than the OD for bleached and *in situ* beta dosed samples and therefore is a more accurate estimate of the intrinsic OD of each sample. We tested this for EBC4 and EBC5 but no significant difference was observed (Fig. 6). This is consistent with what Thomsen et al. (2016) observed once the D_0 criteria has been used.

The quadratic difference between the OD for distributions of natural De and artificial De values can have several sources such has a heterogeneous beta Dr, bad bleaching or bioturbation. Here, we have assumed that microdosimetry was the main contributor for EBC1, 2, 3 and 5, i.e., the distributions are consistent with a single population. However, in the absence of any estimate of the beta Dr heterogeneity, the main support for this assumption comes a posteriori from the comparisons with C14 ages for EBC1, 2 and 3 data and, to a lesser extent, with feldspars ages for EBC5. EBC4 could be more complex: while the OD for the bleached and beta or gamma dosed samples are as low as for the other samples (10 ± 2 % and 13 ± 5 % respectively), its natural OD is significantly higher (53 ± 4 %) (Fig. 6, Tables 3, 5). Based on the micromorphological analysis, there is a clear erosional contact with a thin 'lag' deposit on top of Keva, overlain by charcoal lenses and small scale burrows that slightly disturb it in localized places. As Keva was quite thin and difficult to sample, we cannot rule out the possibility that we sampled the contact and the overlying lenses at the same time, leading to some mixing

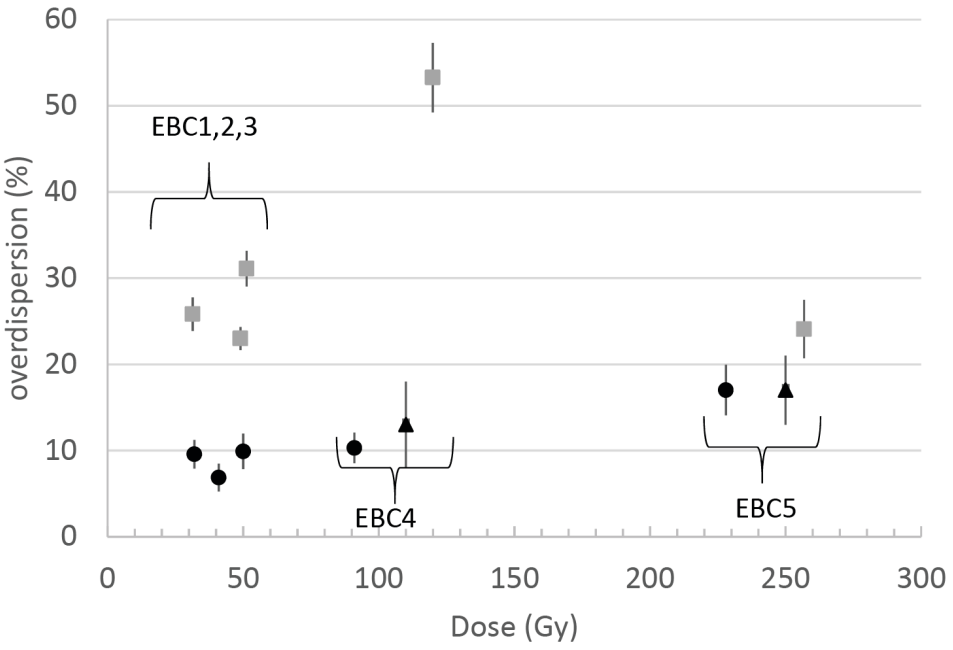

Fig. 6. OD values for natural (grey squares), bleached and beta dosed (black circles) and bleached and gamma dosed (black triangles) samples (after eventual additional selection based on the D_0 values).

of grains. Assuming two populations of grains and applying the finite mixture model (Roberts et al. 2000), the components are found to cover about 45 and 55 % of the grains. If these proportions of grains in each component are correct, the question of the representativeness of the mean Dr for calculating an age is raised. It seems more reasonable at this stage to conclude that the central De model is likely not correct for EBC4, but that no age can be given with confidence using any mixture model.

For the results discussed above (both the dose recovery test and De), the (frequentist) Central Age Model has been applied. The dose recovery ratio and the De values obtained with the Bayesian statistical treatment (on the same set of selected grains as for the Central Age Model approach) are displayed on Tables 3 and 4 respectively (note we have applied it to the De data of EBC4 as well for comparison with the bayesian model, even though it may have no meaning for calculating an age). It can be observed that the dose recovery ratio are in all cases either consistent with unity at two sigma or within 5 % of unity. For EBC1 to EBC4, the Bayesian De are consistent with the frequentist De, as expected from the dose recovery tests. For EBC5 however, the Bayesian central De is significantly higher than the frequentist one. The reason why it is so and what value is relevant for the final age estimate are open questions. Combès et al. (2015) however have suggested that the Bayesian approach is more rigorous: in contrast to the frequentist approach, it avoids the decomposition of "the global inference into a set of consecutive assessments, [that] is likely to lead to a significant loss of information at each step of the process, and can result in an inference of limited coherency with respect to the original data" (Combès et al. 2015: 63). Guérin et al. (2015), by comparing

results of both statistical approaches with known age samples, have also suggested that the bayesian approach was more accurate. Therefore, for the final age estimates, the bayesian De have been used.

Feldspar grains

The Dr for the feldspar grains of EBC5 are shown on Table 2. The internal Dr contributes for 35 % to the total Dr (0.74 ± 0.04 and 2.07 ± 0.10 Gy/ka respectively).

The De obtained with the PIR-IR290 protocol on 7 multi-grain aliquots of EBC5 is 470.3 ± 34.1 Gy. Following Thomsen et al. 2011, neither correction for fading, nor residual dose at the beginning of burial, were taken into account. The De obtained with the IR50 protocol on 20 multi-grain aliquots is, as expected, much lower because of the anomalous fading (308 ± 21.1 Gy). The g_{2days} value is rather variable, from 0.03 ± 0.06 to 6.17 ± 0.08 %/decade (mean 4.20 ± 0.36). With the dose rate correction (DRC) method for fading correction (Lamothe et al. 2003), the final De is 516.2 ± 39.2 Gy, consistent with the PIR-IR290 De value. With the fading correction method of Huntley and Lamothe (2001), the final De is 478.0 ± 32.1 Gy, also consistent with the PIR-IR290 and IR50 DRC corrected estimates, though the growth curves are not in the linear region where the Huntley and Lamothe correction theoretically applies. The DRC-corrected IR50 De and PIR-IR290 De values are kept for further age calculation and comparisons.

Quartzites

Figures 7a and b display the TL glow and growth curves for sample EBC11. They show that the De is independent of the temperature at least on the peak area and that the additive and regenerative growth curves have similar shapes. Similar observations were done for the other samples. Different fits (quadratic or saturating exponential) and different methods of calculation of the De (either extrapolation or slide technics—e.g. Mercier et al. 1992) were applied. The estimated De show no significant dependency on these methods of fit/calculation, although the slide methods give more precise estimates (data not shown). For the final age calculation, the exponential fit with slide method was used. The De for EBC14, 15 and 16 are close to each other and stand between 25.5 ± 0.9 and 26.6 ± 0.5 Gy (statistic uncertainty). For sample EBC 11, the De is significantly higher, 60.8 ± 1.9 Gy.

The U, Th and K contents of the quartzite samples are displayed on Table 5. Macroscopic observations of the four selected stone samples suggest that they are composed of coarse quartz grains. This is confirmed with the observation of thin sections: most grains sizes stand between 300 and 1000 μm and some can be over 2 mm. It can be assumed that the emitters stand mainly between the quartz grains (see Tribolo et al. 2013 and references therein for discussion about the model). The alpha particles are therefore strongly attenuated and the internal Dr is consequently dominated by the beta Dr. The internal Dr represents 34–37 % of the total Dr, which stand between 0.73 ± 0.11 Gy/ka and 0.89 ± 0.10 Gy/ka (Table 5).

AGES AND DISCUSSION

The final age estimates are displayed on Table 6a for the luminescence results and 6b for the radiocarbon results. They are gathered on Figure 8.

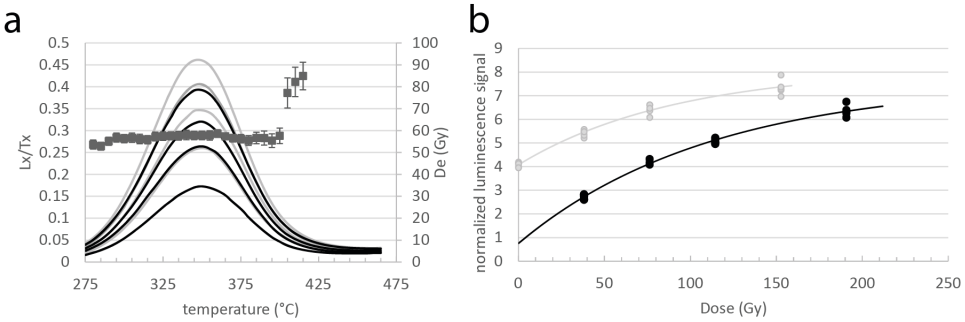

Fig. 7. Example of TL curves. a) Additive (grey) and regenerative (black) glow curves for sample EBC11 and De (black squares) in function of the integration zone (5°C wide intervals). Each curve is the mean of 5 TL glow curves for five aliquots, normalized with a TL measurements after a test dose. b) TL growth curves for sample EBC11 fitted with a saturating exponential. Signals were integrated on the plateau region between 315 and 380°C.

The D phase, associated to Robberg industry is dated by two radiocarbon analyses which yield the calibrated time interval 19400–18900 cal BP (Hogg et al. 2013; Reimer et al. 2013).[1] This is consistent with previous ages get for Robberg industries in South Africa (see Mitchell 2002), which are said to initiate from 23 ka cal BP and last until the terminal Pleistocene. At EBC, the D phase represents the oldest Robberg occurrences at the site, which indicates that the earliest Robberg occupations are not documented, unlike at other regional sites such as Klein Kliphuis (Mackay 2010).

The F phase, associated to Early LSA assemblages, is dated by 5 radiocarbon results yielding a calibrated time interval ranging from 24.3 to 22.4 ka cal BP. The OSL age of quartz grains at 19 ± 2 ka (EBC 1) seems thus slightly underestimated, though consistent at two sigma. The 3 TL ages (burnt quartzites EBC 14, 15 and 16) at the base of the F phase are slightly older though consistent at two sigma with the C14 estimates (29 ± 4 to 31 ± 4 ka). The I phase, associated to final MSA, is dated by one radiocarbon analysis on charcoal giving the calibrated age interval of 38.5–36.4ka cal BP and two OSL (quartz grains: EBC 2 and 3) estimates (35 ± 3 and 37 ± 3 ka). They are all consistent.

The sedimentological analyses suggest that some potassium might have been introduced through the water dripping during burial (Miller et al. 2016 this issue). This might explain why the age for EBC1 is slightly underestimated. The agreement between the radiocarbon and the OSL and TL ages for the other samples in these upper phases suggests, however, that this eventual change of K-content over time in the sediment has been moderate and had no significant impact on the dose rate determination.

For the K phase, associated with MSA assemblages, only one sediment sample (EBC4) was studied. As discussed earlier, the large OD for the De distribution together with micromorphological observations suggest that the distribution is not representative of a single age population. Applying a finite mixture model does not help, as the model suggests that if any, the mixing is important (about 45/55 %) and the mean dose rate is meaningless for calculating ages.

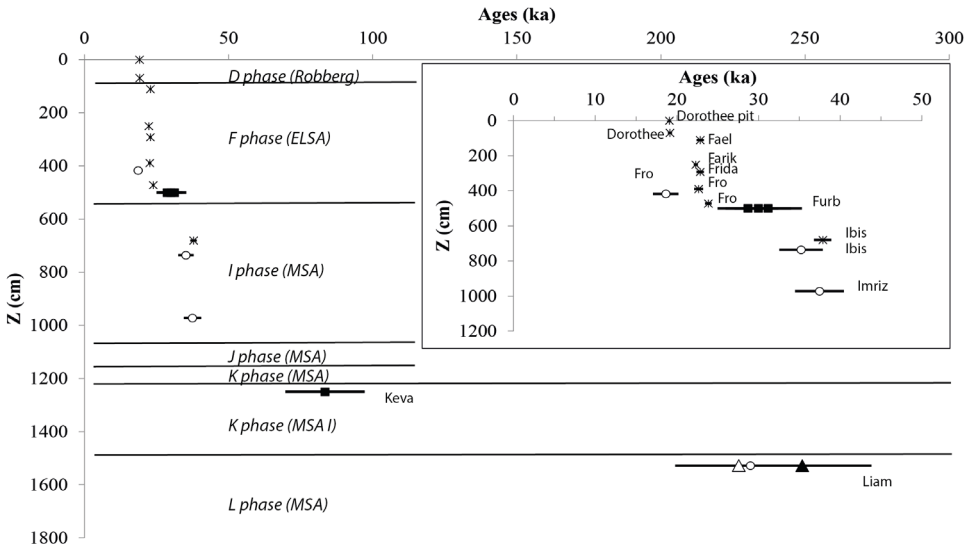

Fig. 8. Synthesis of the dating results for Elands Bay Cave. Ages are displayed against the relative depth of the samples. The name of the units where the samples come from are indicated, as well as the main phases (see section 2). Cross symbol: charcoal-radiocarbon; open circle: quartz grains-OSL; black triangle: feldspar grains-IR50; white triangle: feldspar PIR-IR290; black squares: burnt quartzites-TL.

The Keva-Lara phase, associated with Early MSA assemblages, is dated by one TL-burnt quartzite estimate at 83 ± 14 ka (EBC11). This age is unexpectedly low given the technological differences of the 'MSA 1' with other MIS 4 and MIS 5 sequences from the Western Cape and particularly from Diepkloof Rock Shelter (Porraz, Texier et al. 2013, Tribolo et al. 2013, Schmid et al. 2016 this issue). However, it must be taken with caution as we have one estimate only. Problems with the De and internal Dr of this sample seem unlikely, since it looks similar to EBC14, 15, 16, whose ages are consistent with their stratigraphic position and other age estimates. Is the external Dr of EBC11 overestimated? This possibility cannot be excluded, though we lack strong arguments: would that be due to an increase of K-content over time in that particular location? Or to a poor matching between the gamma Dr recorded by the dosimeter and the gamma Dr to which the sample was submitted (i.e. spatial variation)? Unfortunately, the dating of the Liam unit, below the Keva unit, gives poor age constraint for this one. The estimates for sample EBC5 are indeed much higher than those for EBC4 and EBC11: 231 ± 20 ka (quartz), 249 ± 24 ka (feldspar, IR50) or 227 ± 22 ka (feldspar, PIR-IR290). As quartz and feldspar measured at 50°C or 290°C have different bleaching rates, the consistency between the different estimates argue against any poor bleaching problem. And since the feldspar Dr includes a 35 % internal contribution, while the quartz does not, the consistency also suggests, as for the top units, that the problem of K instability could be minimized. Present studies and technological comparisons between the Early MSA from EBC and other South African sites (see Schmid et al. 2016 this issue) suggest the Keva-Lara phase likely forms during the MIS6, which is consistent with our present results.

CONCLUSION

Luminescence and radiocarbon dating have been performed at EBC on quartz and feldspars grains, burnt quartzite and charcoal samples. Concerning the luminescence method, questions were raised about the stability of the Dr over time, due to the observation of strong diagenesis implying the formation of minerals containing potassium. However, but for one sample in the Early LSA layers, the consistency between the radiocarbon and OSL estimates and between quartz and feldspar estimates suggests that the current Dr may not be significantly different from the past mean one. Both radiocarbon and luminescence dating allow us to obtain good chronological control for the upper units and assemblages, including the Robberg at 19.1 ± 0.3 ka, Early LSA from 29 ± 4 to ca. 22 ka ago, and late MSA at 38 ± 3 to 35 ± 3 ka. The Early MSA (or 'MSA1') is constrained by a *terminus post quem* age of 236 ± 23 ka (mean of quartz and feldspar estimates).

NOTE

[1] The interval presented simply uses the lowest and highest dates for the samples concerned and is not based on any bayesian analysis.

ACKNOWLEGMENTS

This work was funded by the French Ministry of Foreign Affairs (Projet Diepkloof) and the French National Research Agency (ANR-09-JCJC-0123-01). We would like to thank James Feathers and Sébastien Huot for the helpful comments they provided in their reviews.

REFERENCES

Aitken, M.J. 1998. *An introduction to optical dating: the dating of Quaternary sediments by the use of photon-stimulated luminescence.* Oxford University Press.

Auclair, M., Lamothe M. & Huot S. 2003. Measurement of anomalous fading for feldspar IRSL using SAR. *Radiation Measurements* **37**: 487–92.

Beaumont, P.B., de Villier, H. & Vogel, J.C. 1978. Modern man in sub-saharan Africa prior to 49 000 BP: a review and evaluation with particular reference to Border Cave. *South African Journal of Science* **74**: 409–19.

Bøtter-Jensen, L., Bulur, E., Duller, G.A.T. & Murray, A.S. 2000. Advances in luminescence instrument systems. *Radiation Measurements* **32**: 523–8.

Bøtter-Jensen, L., Andersen, C.E., Duller, G.A.T. & Murray, A.S. 2003. Developments in radiation, stimulation and observation facilities in luminescence measurements. *Radiation Measurements* **37**: 535–41.

Brennan, B.J., Lyons, R.G., & Phillips, S.W. 1991. Attenuation of alpha particle track dose for spherical grains. *Nuclear Tracks and Radiation Measurements* **18**: 249–53.

Bronk Ramsey C., Scott, M. & van der Plicht, J. 2013. Calibration for archaeological and environmental terrestrial samples in the time range 26–50 ka cal BP. *Radiocarbon* **55** (4): 2021–7.

Buylaert, J.P., Murray, A.S., Thomsen, K.J. & Jain M. 2009. Testing the potential of an elevated temperature IRSL signal from K-feldspar. *Radiation Measurements* **44**: 560–65.

Combès, B., Philippe, A., Lanos, P., Mercier, N., Tribolo, C., Guérin, G., Guibert, P. & Lahaye, C. 2015. A Bayesian central equivalent dose model for optically stimulated luminescence dating. *Quaternary Geochronology* **28**: 62–70.

Conard, N.J., Bader, G.D., Schmid, V.C. & Will, M. 2014. Bringing the Middle Stone Age into clearer focus. *Mitteilungen der Gesellschaftfür Urgeschichte* **23**: 121–8.

Cottereau, E., Arnold, M., Moreau, C., Baqué, D., Bavay, D., Caffy, I., Comby, C., Dumoulin, J-P., Hain, S., Perron, M., Salomon, J. & Setti, V. 2007. Artemis, the new ^{14}C AMS at LMC14 in Saclay, France. *Radiocarbon* **49** (2): 291–9.

Duller, G.A.T. 2003. Distinguishing quartz and feldspar in single grain luminescence measurements. *Radiation Measurements* **37**: 161–5.

Duller, G.A.T. 2015. The Analyst software package for luminescence data: overview and recent improvements. *Ancient TL* **33**: 35–42.

Duller, G.A.T., Bøtter-Jensen, L., Kohsiek, P. & Murray, A.S. 1999. A high sensitivity optically stimulated luminescence scanning system for measurement of single sand-sized grains. *Radiation Protection Dosimetry* **84**: 325–30.

Fattahi, M. & Stokes, S. 2003. Red emission luminescence from quartz and feldspar for dating applications: an overview. *Radiation Measurements* **37**: 383–95.

Guérin, G., Mercier, N. & Adamiec, G. 2011. Dose rate conversion factors: update. *Ancient TL* **29**: 5–8.

Guérin, G., Mercier, N., Nathan, R., Adamiec, G. & Lefrais, Y. 2012. On the use of the infinite matrix assumption and associated concepts: A critical review. *Radiation Measurements* **47**: 778–85.

Guérin, G., Combès, B., Tribolo, C., Lahaye, C., Mercier, N., Guibert, P. & Thomsen, K.J. 2015. Testing the accuracy of a single grain OSL Bayesian central dose model with known-age samples. *Radiation Measurements* **81**: 62–70.

Henshilwood, C.S., D'Errico, F., Yates, R., Jacobs, Z., Tribolo, C., Duller, G.A.T., Mercier, N., Sealy, J.C., Valladas, H., Watts, I. & Wintle, A.G. 2002. Emergence of modern human behaviour: Middle Stone Age engravings from South Africa. *Science* **295**: 1278.

Henshilwood, C.S. & Dubreuil, B. 2011. The Still Bay and Howiesons Poort, 77–59 ka: symbolic material culture and the evolution of the mind during the African Middle Stone Age. *Current Anthropology* **52**: 361–80.

Hogg, A.G., Hua, Q., Blackwell., P.G., Niu, M., Buck, C.E. & Zimmerman, S.R.H. 2013. SHCAL13 Southern Hemisphere calibration, 0–50,000 years cal BP. *Radiocarbon* **55**: 1889–903.

Huntley, D.J. & Baril, M.R. 1997. The K content of the K-feldspars being measured in optical dating or in thermoluminescence dating. *Ancient TL* **15**: 11–13.

Huntley, D.J. & Hancock, R.G.V. 2001. The Rb contents of the K-feldspar grains being measured in optical dating. *Ancient TL* **19**: 43–6.

Huntley, D.J. & Lamothe, M. 2001. Ubiquity of anomalous fading in K-feldspars and the measurement and correction for it in optical dating. *Canadian Journal of Earth Sciences* **38**: 1093–106.

Jacobs, Z., Roberts, R.G., Galbraith, R.F., Deacon, H.J., Grün, R., Mackay, A., Mitchell, P., Vogelsang, R. & Wadley, L. 2008. Ages for the Middle Stone Age of southern Africa: implications for human behavior and dispersal. *Science* **322**: 733–5.

Lamothe, M., Auclair, M., Hamzaoui, C. & Huot, S. 2003. Towards a prediction of long-term anomalous fading of feldspar IRSL. *Radiation Measurements* **37**: 493–8.

Mackay, A. 2010. The late Pleistocene archaeology of Klein Kliphuis rock shelter, Western Cape, South Africa: 2006 excavations. *South African Archaeological Bulletin* **65**: 132–47.

Martin, L. 2015. *Caractérisation et modélisation d'objets archéologiques en vue de leur datation par des méthodes paléo-dosimétriques. Simulation des paramètres dosimétriques sous Geant4*. PhD thesis, University of Bordeaux Montaigne.

Mercier, N., Valladas, H. & Valladas, G. 1992. Observations on palaeodose determination with burnt flints. *Ancient TL* **10**: 28–32.

Mercier, N., Kreutzer, S., Christophe, C., Guérin, G., Guibert, P., Lahaye, C., Lanos, P., Philippe, A. & Tribolo, C. in press. Bayesian statistics in luminescence dating: the 'baSAR'-model and its implementation in the R package 'Luminescence'. *Ancient TL*.

Miller, C.E., Mentzer, S., Berthold, C., Leach, P., Schulz H., Tribolo, C., Parkington, J. & Porraz, G. 2016. Site formation processes of the Middle Stone Age deposits from Elands Bay Cave, South Africa. *Southern African Humanities* **29**: 69–128.

Mitchell, P. 2002. *The archaeology of southern Africa*. Cambridge University Press.

Murray, A.S. & Wintle, A.G. 2000. Luminescence dating of quartz using an improved single-aliquot regenerative-dose protocol. *Radiation Measurements* **32**: 57–73.

Murray, A.S. & Wintle, A.G. 2003. The single aliquot regenerative dose protocol: potential for improvements in reliability. *Radiation Measurements* **37**: 377–81.

Parkington, J.E. 2016. Elands Bay Cave: keeping an eye on the past. *Southern African Humanities* **29**: 17–32.

Parkington, J.E., Rigaud, J.-P., Poggenpoel, C., Porraz, G. & Texier, P.-J. 2013. Introduction to the project and excavation of Diepkloof Rock Shelter (Western Cape, South Africa): a view on the Middle Stone Age. *Journal of Archaeological Science* **40**: 3369–75.

Porraz, G., Igreja, M., Schmidt, P., Valladas, H. & Parkington, J.E. 2016. A shape to the microlithic Robberg of Elands Bay Cave (South Africa). *Southern African Humanities* **29**: 203–47.

Porraz, G., Parkington, J.E., Rigaud, J.-P., Miller, C.E., Poggenpoel, C., Tribolo, C., Archer, W., Cartwright, C.R., Charrié-Duhaut, A., Dayet, L., Igreja, M., Mercier, N., Schmidt, P., Verna, C. & Texier, P.-J. 2013. The MSA sequence of Diepkloof and the history of southern African Late Pleistocene populations. *Journal of Archaeological Science* **40**: 3542–52.

Porraz, G., Schmid, V., Miller, C.E., Tribolo, C., Cartwright, C., Charrié-Duhaut, A., Igreja, M., Mentzer, S., Mercier, N., Schmidt, P., Conard, N., Texier, P.-J. & Parkington, J.E. 2016. Update on the 2011 excavation at Elands Bay Cave (South Africa) and the Verlorenvlei Stone Age. *Southern African Humanities* **29**: 33–68.

Porraz, G., Texier, P.-J., Archer, W., Piboule, M., Rigaud J.-P., & Tribolo, C. 2013. Technological successions in the Middle Stone Age sequence of Diepkloof Rock Shelter, Western Cape, South Africa. *Journal of Archaeological Science* **40**: 3376–400.

Porraz, G., Val, A., Dayet, L., de la Peña, P., Douze, K., Miller, C.E., Murungi, M., Tribolo, C., Schmid, V.C. & Sievers, C. 2015. Bushman Rock Shelter (Limpopo, South Africa): a perspective from the edge of the Highveld. *South African Archaeological Bulletin* **70**: 166–79.

Prescott, J.R. & Hutton, J.T. 1994. Cosmic ray contributions to dose rates for luminescence and ESR dating: large depths and long-term time variations. *Radiation Measurements* **23**: 497–500.

Rees-Jones, J. 1995. Optical dating of young sediments using fine-grain quartz. *Ancient TL* **13**: 9–14.

Reimer, P. J., Bard, E., Bayliss, A., Beck, J. W., Blackwell, P. G., Bronk Ramsey, C., Buck, C. E., Cheng, H., Edwards, L., Friedrich, M., Grootes, P. M., Guilderson, T.P., Haflidason, H., Hajdas, I., Hatté, C., Heaton, T., Hoffmann, D. L., Hogg, A. G., Hughen, K. A., Kaiser, K. F., Kromer, B., Manning, S. W., Niu, M., Reimer, R. W., Richards, D. A., Scott, E. M., Southon, J. R., Staff, R. A., Turney, C. S. M. & van der Plicht, J. 2013. IntCal13 and Marine 13 Radiocarbon age calibration curves 0–50 000 years cal BP. *Radiocarbon* **55**: 1869–87.

Richter, D., Dombrowski, H., Neumaier, S., Guibert, P. &Zink, A. 2010. Environmental gamma dosimetry with OSL of α-Al2O3: C for in situ sediment measurements. *Radiation Protection Dosimetry* **141**: 27–35.

Roberts, R.G., Galbraith, R.F., Yoshida, H., Laslett, G. &Olley, J.M. 2000. Distinguishing dose populations in sediment mixtures: a test of single-grain optical dating procedures using mixtures of laboratory-dosed quartz. *Radiation Measurements* **32**: 459–65.

Schmid, V., Conard, N.J., Parkington, J.E., Texier P.-J, & Porraz, G. this issue. The 'MSA 1' of Elands Bay Cave (Western Cape Province, South Africa) in the context of the southern African Early Middle Stone Age technologies. *Southern African Humanities* **29**: 153–201.

Singer, R. & Wymer, J. 1982. *The Middle Stone Age at Klasies River Mouth in South Africa.* University of Chicago Press, Chicago.

Soriano, S., Villa, P., Delagnes, A., Degano, I., Pollarolo, L., Lucejko, J.J., Henshilwood, C. & Wadley, L. 2015. The Still Bay and Howiesons Poort at Sibudu and Blombos: understanding Middle Stone Age technologies. *PLoS ONE* **10**: 1–46.

Texier, P.-J., Porraz, G., Parkington, J., Rigaud, J.-P., Poggenpoel, C., Miller, C., Tribolo, C., Cartwright, C., Coudenneau, A., Klein, R., Steele T. & Verna, C. 2010. A Howiesons Poort tradition of engraving ostrich eggshell containers dated to 60,000 years ago at Diepkloof Rock Shelter, South Africa. *Proceedings of the National Academy of Sciences* **107**: 6180–5.

Texier, P.J., Porraz, G., Parkington, J., Rigaud, J.P., Poggenpoel, C. & Tribolo, C. 2013. The context, form and significance of the MSA engraved ostrich eggshell collection from Diepkloof Rock Shelter, Western Cape, South Africa. *Journal of Archaeological Science* **40**: 3412–31.

Thomsen, K, Murray, A.S. & Bøtter-Jensen, L. 2005. Sources of variability in OSL dose measurements using single grains of quartz. *Radiation Measurements* **39**: 47–61.

Thomsen, K., Murray, A. & Jain, M. 2011. Stability of IRSL signals from sedimentary K-feldspar samples. *Geochronometria: Journal on Methods & Applications of Absolute Chronology* **38**: 1–13.

Thomsen, K.J., Murray, A.S. & Jain, M. 2012. The dose dependency of the over-dispersion of quartz OSL single grain dose distributions. *Radiation Measurements* **47**: 732–9.

Thomsen, K, Murray, A.S., Buylaert, J.P., Jain, M., Hansen, J.H. & Aubry, T. 2016. Testing single-grain quartz OSL methods using sediment samples with independent age control from the Bordes-Fitterockshelter (Roches d'Abilly site, Central France). *Quaternary Geochronology* **31**: 77–96.

Tribolo, C. & Mercier, N. 2012. Towards a SAR-ITL protocol for the equivalent dose estimate of burnt quartzites. *Ancient TL* **30**: 17–26.

Tribolo, C., Mercier, N., Douville, E., Joron, J.-L., Reyss, J.-L., Rufer, D., Cantin, N., Lefrais, Y., Miller, C.E., Parkington, J., Porraz, G., Rigaud, J.-P. & Texier, P.-J. 2013. OSL and TL dating of the Middle Stone Age sequence of Diepkloof Rock Shelter (Western Cape, South Africa): a clarification. *Journal of Archaeological Science* **40**: 3401–11.

Tribolo, C., Asrat, A., Bahain, J.-J., Chapon, C., Douville, E., Fragnol, C., Hernandez, M., Hovers, E., Leplongeon, A., Martin, L., Pleurdeau, D., Pearson, O., Puaud, S. & Assefa, Z. Accepted. Across the gap: geochronological and sedimentological evidence for the Middle and Later Stone Age sequence of GodaButicha, southeastern Ethiopia. *Plos One.*

Valladas, H. 1985. *Datation par la thermoluminescence de gisements moustériens du sud de la France*. PhD thesis, Muséum National d'Histoire Naturelle et Université Paris VI.
Valladas, H. 1992. Thermoluminescence dating of flint. *Quaternary Science Reviews* **11**: 1–5.
Volman, T.P. 1984. Early prehistory of Southern Africa. In: R.G. Klein, ed., *Southern African prehistory and paleoenvironments*. Rotterdam: Balkema, pp. 169–220.
Wadley, L. 2015. Those marvellous millennia: the Middle Stone Age of southern Africa. *Azania: Archaeological Research in Africa* **50**: 155–226.
Wurz, S. 2002. Variability in the Middle Stone Age lithic sequence, 115 000–60 000 years ago at Klasies River, South Africa. *Journal of Archaeological Science* **29**: 1001–15.

TABLE 1

U, Th activities and K contents determined: A) by high resolution gamma spectrometry for the < 2mm fraction; B) by ICP-MS and ICPAES for the > 2 mm fraction; C) mean U, Th activities and K contents for the whole samples, i.e. calculated using data from Table 1A and 1B, weighted by the relative weight of the < 2 mm and > 2 mm fractions.

	sample	K (%)		^{232}Th (Bq/kg)		U (after ^{234}Th) (Bq/kg)		U (after ^{214}Bi and ^{214}Pb) (Bq/kg)		U (after ^{210}Pb) (Bq/kg)	
			±		±		±		±		±
A	EBC1	0.91	0.02	22.1	0.3	26.1	1.3	24.6	0.4	24.0	2.0
	EBC2	0.72	0.02	20.9	0.3	22.4	1.2	20.9	0.4	21.7	1.9
	EBC3	0.60	0.01	22.6	0.2	31.2	0.7	21.0	0.2	22.5	1.0
	EBC4	0.64	0.02	26.4	0.3	34.4	1.2	23.8	0.3	27.4	1.7
	EBC5	0.68	0.01	30.0	0.3	36.7	1.1	24.0	0.3	24.6	1.6

	sample	K (%)		^{232}Th (Bq/Kg)		^{238}U(Bq/kg)		massic ratio of coarse fraction
			±		±		±	
B	EBC1	0.39	0.02	8.05	0.29	11.0	0.2	4 %
	EBC2	0.10	0.01	13.05	0.35	6.8	0.1	7 %
	EBC3	0.10	0.01	25.31	0.44	10.4	0.1	14 %
	EBC4	0.12	0.01	16.25	0.44	9.8	0.1	11 %
	EBC5	0.31	0.02	16.12	0.26	12.1	0.2	11 %

	sample	K (%)		^{232}Th (Bq/kg)		U (after ^{234}Th) (Bq/kg)		U (after ^{214}Bi and ^{214}Pb) (Bq/kg)	
			±		±		±		±
C	EBC1	0.89	0.02	21.55	0.31	25.5	1.2	24.1	1.7
	EBC2	0.68	0.02	20.31	0.32	21.5	1.2	20.1	1.6
	EBC3	0.53	0.01	22.97	0.25	28.2	0.7	19.1	0.7
	EBC4	0.58	0.01	25.32	0.32	31.7	1.2	21.9	1.2
	EBC5	0.64	0.01	28.44	0.31	34.0	1.1	22.2	1.0

TABLE 2

Summary of data for Dr estimates for the sediment samples at Elands Bay Cave. Gamma Drs are deduced from the Al2O3:C dosimeters inserted for one year into the sections. Beta Drs are deduced from the U, Th and K contents measured with high resolution gamma spectrometry and ICP-MS or ICP-OES; the calculation for the U contribution is done with both the head and middle of chain estimates, assuming the disequilibrium has always prevailed. The current water content has been used. Beta-1 and Total-1 refer to the U, Th, K contents in the fine (<2 mm) fraction only, while beta-2 and Total-2 are deduced from the U, Th and K content for the whole samples. Cosmic Drs were calculated from Prescott and Hutton (1994), taking into account the geometry of the cave. The internal Dr of the K-feldspar grains was derived from the internal K content (10.5 ± 0.5%), and an assumed Rb content of 400 ± 100 ppm. The alpha dose is based on the U, Th and K contents of the sediment and assumes an a value of 0.08±0.02. The Drs uncertainties include systematic uncertainties.

sample	layer	cultural attribution	material	current water content	dose rate Gy/ka									
					alpha	gamma	cosmics	internal	beta-1	total-1	beta-2	total-2	total mean	
EBC1	Fro	ELSA	quartz	13%		0.70 0.07	0.04 0.01		0.90 0.09	1.63 0.12	0.87 0.08	1.61 0.11	1.62	0.11
EBC2	Ibis	MSA	quartz	8%		0.63 0.07	0.04 0.01		0.78 0.07	1.44 0.10	0.74 0.07	1.40 0.08	1.42	0.09
EBC3	Imran/ Imriz	MSA	quartz	8%		0.63 0.07	0.04 0.01		0.74 0.06	1.40 0.09	0.67 0.05	1.34 0.07	1.37	0.08
EBC4	Kali	above MSA1	quartz	11%		0.59 0.07	0.04 0.01		0.78 0.07	1.41 0.10	0.72 0.06	1.35 0.07	1.38	0.09
EBC5	Liam	below MSA1	quartz	18%		0.50 0.06	0.04 0.01		0.77 0.08	1.31 0.10	0.72 0.07	1.26 0.08	1.28	0.09
			felds-paths		0.05 0.01			0.74 0.04		2.09 0.11		2.04 0.09	2.07	0.10

TABLE 3

Results of the Dose recovery tests following different statistical approaches (frequentist-CAM versus Bayesian), and without or with selection based on the D_0 values. n/N: number of accepted grains/number of measured grains.

		all grains passing standard rejection criteria							additionnal selection D_0 >x							
sample	dose to recover (Gy)	frequentist					Bayesian		x (Gy)	frequentist					Bayesian	
		ratio	±	OD	±	n/N	ratio	±		ratio	±	OD	±	n/N	ratio	±
EBC1	32	1.02	0.02	10	2	69/400	1.03	0.02								
EBC2	41	1.03	0.01	7	2	81/400	1.04	0.01								
EBC3	50	0.99	0.02	10	2	53/400	1.00	0.02								
EBC4	91	0.91	0.02	16	2	149/1100	0.94	0.01	78	0.98	0.02	10	2	69/1100	0.97	0.02
EBC5	228	0.73	0.03	36	3	113/1000	0.86	0.03	114	0.96	0.03	17	3	44/1000	0.98	0.03

TABLE 4

Results for the equivalent doses following different statistical approaches (frequentist-CAM/Bayesian) after additional selection based on the D_0 value. n/N: number of accepted grains over number of measured grains.

		frequentist- CAM					Bayesian	
Sample	D_0 threshold (Gy)	De (Gy)	±	OD (%)	±	n/N	De (Gy)	±
EBC1	none	31.4	0.8	26	2	142/700	30.0	0.6
EBC2	none	49.0	0.8	23	1	258/1400	49.2	0.7
EBC3	none	51.3	1.4	31	2	170/1200	52.8	1.8
EBC4	100	119.9	6.6	53	4	104/3300	114.7	8.8
EBC5	100	256.8	10.2	24	3	61/1700	297.1	10.5

TABLE 5

Dr estimates for the 4 stone samples. U, Th and K contents within the rock samples were estimated with ICP-MS and ICP-OES. The Drs indicated here take into account the attenuation factors, the difference of sensitivity for the alpha Dr and current water content for the external Dr. Statistic uncertainties are shown for the internal and external dose rates. For the total Dr, a 10% systematic uncertainty of the beta, gamma and alpha Drs is also taken into account (e.g. calibration with standards of the ICP-MS and OES).

sample	internal contents			gamma attenuation	dose rates (Gy/ka)												
					internal						external				ratio internal/ total	total	
					alpha		beta		gamma		gamma		cosmic				
	U (ppm)	Th (ppm)	K (%)														
EBC14	0.577	3.541	0.105	0.74	0.005	0.001	0.266	0.001	0.062	0.000	0.52	0.10	0.036	0.006	37%	0.89	0.10
EBC15	0.327	2.425	0.167	0.75	0.003	0.001	0.248	0.000	0.039	0.000	0.53	0.11	0.036	0.006	34%	0.85	0.11
EBC16	0.536	3.516	0.067	0.75	0.005	0.001	0.229	0.005	0.057	0.000	0.53	0.11	0.036	0.006	34%	0.85	0.11
EBC11	0.482	3.291	0.055	0.81	0.005	0.001	0.205	0.001	0.040	0.000	0.44	0.11	0.036	0.006	34%	0.73	0.11

TABLE 6

Summary of the ages estimates: A) luminescence dating results for quartz grains, feldspar grains and burnt quartzites; B) C14 results obtained on the charcoal specimens and calibrated time intervals deduced using OxCal v4.2.4 software (Bronk Ramsey et al. 2013; Hogg et al. 2013) (age intervals at 95.4 % of confidence level).

	sample	SU	cultural attribution	material	Dr (GY/ka)	De (Gy)	Age (ka)
A	EBC1	Fro	ELSA	quartz	1.62 ± 0.11	30.0 ± 0.6	19 ± 2
	EBC14	Furb	ELSA	burnt quartzite	0.89 ± 0.10	25.5 ± 0.9	29 ± 4
	EBC15	Furb	ELSA	burnt quartzite	0.85 ± 0.11	26.6 ± 0.5	31 ± 4
	EBC16	Furb	ELSA	burnt quartzite	0.85 ± 0.11	25.6 ± 0.7	30 ± 4
	EBC2	Ibis	MSA	quartz	1.42 ± 0.09	49.2 ± 0.7	35 ± 3
	EBC3	Imran/ Imriz	MSA	quartz	1.37 ± 0.08	51.4 ± 1.4	37 ± 3
	EBC4	Kali	above MSA1	quartz	1.38 ± 0.09		
	EBC11	Keva	MSA 1	burnt quartzite	0.73 ± 0.11	60.8 ± 1.9	83 ± 14
	EBC5	Liam	below MSA1	quartz	1.28 ± 0.09	297.1 ± 10.5	231 ± 20
				feldspaths	2.07 ± 0.10	516.2 ± 39.2	249 ± 24
					2.07 ± 0.10	470.3 ± 34.1	227 ± 22

	sample	Lab reference	SU	cultural attribution	material	masse (mg)	Age (a) uncal BP	Age interval (a) cal BP (95 %)
B	EBC 2011 S101	GifA 13001/ SacA 31983	Dorothee pit	Robberg	charcoal	0.82	15830 ± 60	19223–18875
	EBC 2011 S102	GifA 13002/ SacA 31984	Dorothee	Robberg	charcoal	0.87	15970 ± 60	19445–18993
	EBC 2011 S103	GifA 13003/ SacA 31985	Fael	ELSA	charcoal	0.51	19120 ± 90	23338–22665
	EBC 2011 S105	GifA 13004/ SacA 31986	Farik	ELSA	charcoal	0.38	18720 ± 90	22802–22357
	EBC S106	GifA 13006/ SacA 31988	Frida	ELSA	charcoal	0.43	18780 ± 90	23300–22629
	EBC 2011 S107	GifA 13007/ SacA 31989	Fro	ELSA	charcoal	1.52	19100 ± 90	22863–22400
	EBCS108	GifA 13008/ SacA 31990	Fro	ELSA	charcoal	1.24	19960 ± 100	24257–23670
	EBCS110	GifA 13009/ SacA 31991	Ibis	MSA	charcoal	1.13	33270 ± 430	38534–36356

Southern African Humanities **29**: 153–201 December 2016 KwaZulu-Natal Museum

The 'MSA 1' of Elands Bay Cave (South Africa) in the context of the southern African Early MSA technologies

[1,2]**Viola C. Schmid**, [1,3]**Nicholas J. Conard**, [4]**John E. Parkington**, [5]**Pierre-Jean Texier** and [6,7]**Guillaume Porraz**

[1]Department of Early Prehistory and Quaternary Ecology, Universität Tübingen, Tübingen, Germany; viola.schmid@uni-tuebingen.de
[2]UMR 7041, Equipe AnTET, Université Paris Ouest Nanterre La Défense, Nanterre Cedex, France
[3] Senckenberg Center for Human Evolution and Paleoenvironment, Universität Tübingen, Tübingen, Germany; nicholas.conard@uni-tuebingen.de
[4]Department of Archaeology, University of Cape Town, Cape Town, South Africa; john.parkington@uct.ac.za
[5]CNRS, UMR 5199-PACEA, Université de Bordeaux 1, Talence, France ; pierre.texier@u-bordeaux.fr
[6]CNRS, USR 3336, IMIFRE 25, Institut Français d'Afrique du Sud, Johannesburg, South Africa; guillaume.porraz@mae.u-paris10.fr
[7]Evolutionary Studies Institute, University of the Witwatersrand, Johannesburg, South Africa

ABSTRACT

The Early Middle Stone Age (EMSA) of southern Africa represents a poorly defined period in terms of chronology, palaeoenvironments, subsistence strategies and technological traditions. This lack of understanding is directly related to the low number of EMSA deposits that have been excavated, but concomitantly, it also reflects the poor interest accorded by most of the recent archaeological projects. In this context, the excavation that we undertook at Elands Bay Cave (EBC) in the West Coast of South Africa in 2011 provides a good opportunity to discuss the oldest occupations at the site, which have been assigned to the 'MSA 1' by T. Volman (1981) and which purportedly belong to the earliest MSA traditions of southern Africa.

In the present paper, we provide a technological study of the 'MSA 1' lithic assemblage. Our results demonstrate the near-exclusive use of local quartzite by the inhabitants of EBC. This raw material was preferentially selected in the form of slabs and large flakes to produce blanks that were used without further retouching. We identified various reduction sequences that we unify under a concept referred to as 'POL-reduction strategy'. Furthermore, we perform intersite technological comparisons and conclude that on technological grounds the 'MSA 1' of Elands Bay Cave dates back to MIS 6, in agreement with the luminescence dating. We acknowledge current difficulties in building a chrono-cultural framework at a subcontinental scale. Thus, we discuss the relevance of the term 'MSA 1' and instead advocate a more neutral and generic label of 'EMSA' (understood here as late Middle Pleistocene MSA technologies). The analysis of the EMSA of EBC sheds new light on the patterns and changes that characterise behaviours and organisations of Anatomically Modern Humans over the last 200 ka.

KEY WORDS: Early Middle Stone Age, chrono-cultural sequence, innovations, lithic technology and economy.

Recent findings on the Middle Stone Age (MSA) have highlighted the early occurrence of distinct innovations within the material culture repertoire in southern Africa (e.g. Henshilwood et al. 2002; Mourre et al. 2010; Texier et al. 2010; d'Errico et al. 2012). However, the timing, nature and interpretation of these changes remain disputed (McBrearty & Brooks 2000; Parkington 2001; Klein 2001; Wadley 2001; Henshilwood & Marean 2003; Conard 2008; Porraz, Texier et al. 2013; Wurz 2013). Some of the difficulties might be related to the overemphasis, particularly over the past two decades, placed on two late Pleistocene sub-stages of the MSA, the Howiesons Poort (HP) and the Still Bay (SB). Both of these techno-complexes seem to express early proxies of innovative behaviours but comparatively little research has addressed the preceding

ISSN 2305-2791 (online); 1681-5564 (print)

sub-stages of the MSA (but see: Wurz 2002; Thompson et al. 2010). This lack of understanding challenges our perception of how the history of Anatomically Modern Humans (AMHs) in southern Africa developed and what could have been the driving forces that accompanied their cultural evolution.

In East Africa, several long archaeological sequences (e.g. Wendorf & Schild 1974) indicate that the transition from the Earlier Stone Age to the Middle Stone Age occurred between 300 ka and 250 ka (McBrearty & Brooks 2000; McBrearty & Tryon 2005; Tryon et al. 2005; Herries 2011). In southern Africa, little is known about the beginning of the MSA, but it is generally assumed that it also started around 300 ka (Herries 2011; Lombard et al. 2012; Wurz 2014; Wadley 2015). The MSA is considered to be a time period linked to the disappearance of large cutting tools and the development of prepared core technologies to produce flakes, blades and triangular flakes with faceted platforms (Goodwin & Van Riet Lowe 1929; Wurz 2014; Wadley 2015). As such, the appearance of the MSA would represent a major shift in the way that people were manufacturing as well as using their tools, and consequently in the way that they were organizing their subsistence. Several authors associate the onset of the MSA with a diversification in lithic technology that would be related to the cultural regionalization of past populations (Goodwin & Van Riet Lowe 1929; Clark 1988; McBrearty & Brooks 2000; Tryon et al. 2005; Wurz 2012). Such changes in the organization of societies would mark a turning point in the history of Stone Age populations.

The limited knowledge associated with the Early MSA (EMSA) in southern Africa, understood here as embracing all late Middle Pleistocene MSA technologies (300–130 ka) (see also Lombard et al. 2012), contrasts with the numerous publications dealing with the palaeoenvironmental and cultural record from MIS 5 to MIS 3. The EMSA currently represents a vague concept in terms of chronology, palaeoenvironments, subsistence and technologies. This reinforces the idea that societies experienced dramatic behavioural changes ca. 100 ka, before which people were relatively 'informal' in their adaptations and did not show an explicit trend of advancing complexity (for a synthesis, see Wurz 2013). However, the low number of new excavations (although see Thompson et al. 2010; Porraz et al. 2015) and few new analyses represent a major bias behind this premise.

In 2011, we reinvestigated the site of Elands Bay Cave (EBC) located ca. 14 km westward of Diepkloof Rock Shelter along the Verlorenvlei. One of the main motivations was to explore the MSA occupations at the site, which were assigned to the 'MSA 1' by Thomas P. Volman. Volman (1981, 1984) defined this sub-stage on the basis of the two sites EBC and Peers Cave, both in the Western Cape Province, to which he added Bushman Rock Shelter located in Limpopo Province. In his synthesis, Volman considered it to be the earliest stage of the MSA in southern Africa. He also described the 'MSA 1' as the most problematic phase of the MSA, characterised by "very little formal retouch, small broad flakes with few facetted butts, and a high proportions of cores for the production of flakes with intersecting dorsal scars. Retouched points are absent in the assemblages and scraper retouch is very rare" (Volman 1984: 201).

By reinvestigating the site of EBC, our aim was to verify the stratigraphy and to take samples for geoarchaeological studies as well as luminescence dating. Moreover, our goal was to revise the characterization of the lithic assemblage assigned to the 'MSA 1' through technological analysis (Boëda et al. 1990; Geneste 1991; Inizan et al. 1999;

Soressi & Geneste 2011). Traditionally, a typological approach has been favoured to analyse and classify MSA lithic assemblages (e.g. Sampson 1974; Volman 1981; Singer & Wymer 1982; Thackeray & Kelly 1988). However, this methodology which focuses only on formal tools holds a high potential for biases, in particular regarding the fact that lithic assemblages of the EMSA are said to contain a very limited quantity of formal tools.

Our main research goal is to explore the spatial and temporal variability of the EMSA in southern Africa and to test the hypothesis that considers these lithic assemblages to be 'informal' and 'homogeneous'. Given the current state of the art, our research addresses the following questions: What is the 'MSA 1'? What technological trends do we observe for this period in southern Africa? What are the implications regarding the history of AMHs?

BACKGROUND TO THE STUDY

EBC on the West Coast of South Africa

The site of EBC (Western Cape Province) is located on the West Coast of South Africa (Fig. 1). The whole area falls within the winter rainfall zone and currently is a semi-desertic environment characterised by seasonal variations in precipitation. The West Coast area is delimited by the Atlantic coast to the west, the Great Escarpment to the east, the Olifants River mouth to the north and the Cape of Good Hope to the south. The present-day vegetation of the fynbos biome varies in plant community composition with distance from the coast and mountains (Cartwright 2013). Three main geological formations compose the West Coast, determining its topography: the quartzitic formations of the Table Mountain Group, the coastal formation of the Cape Granite Suite and the argillaceous formations of the Malmesbury group (Coertze 1984). The geological substrate is overlain by Quaternary coastline landscapes that consist of dune formations and blow-outs forming an extensive layer of calcareous sand (Chase & Thomas 2006; Roberts et al. 2009). Several permanent rivers traverse the West Coast plains, including the estuarine coastal freshwater lake Verlorenvlei. The mouth of the Verlorenvlei lies a few hundred meters away from the site.

EBC is situated on the Atlantic coast on the headland of Baboon Point ca. 180 km north of Cape Town. The cave is one of numerous cavities and shelters cut into the northwest-facing quartzitic Table Mountain Sandstone cliff, located at an altitude of 42–45 m above present sea level and in close proximity to the rocky and sandy shores. The change in sea levels through time would have transformed the environment from an inland riverine to a coastal estuarine setting (Parkington 1981). However, the variations of the Pleistocene shoreline were relatively minimal due to the relatively abrupt topography of the submerged coastal plain (see Porraz, Texier et al. 2013).

Only 14 km eastward of EBC, along the Verlorenvlei, is another well-known MSA site, Diepkloof Rock Shelter, containing a long MSA sequence. Unlike EBC, Diepkloof is not a coastal site, but rather was exploited as a strategic place positioned at the interface of distinct ecological niches (Porraz, Parkington et al. 2013). Other notable MSA sites in the region include Hoedjiespunt, Sea Harvest, Ysterfontein and Peers Cave on the present coast as well as Hollow Rock Shelter, Klein Kliphuis, Putslaagte 1, Varsche Rivier and Klipfonteinrand inland to the north and east (Fig. 1).

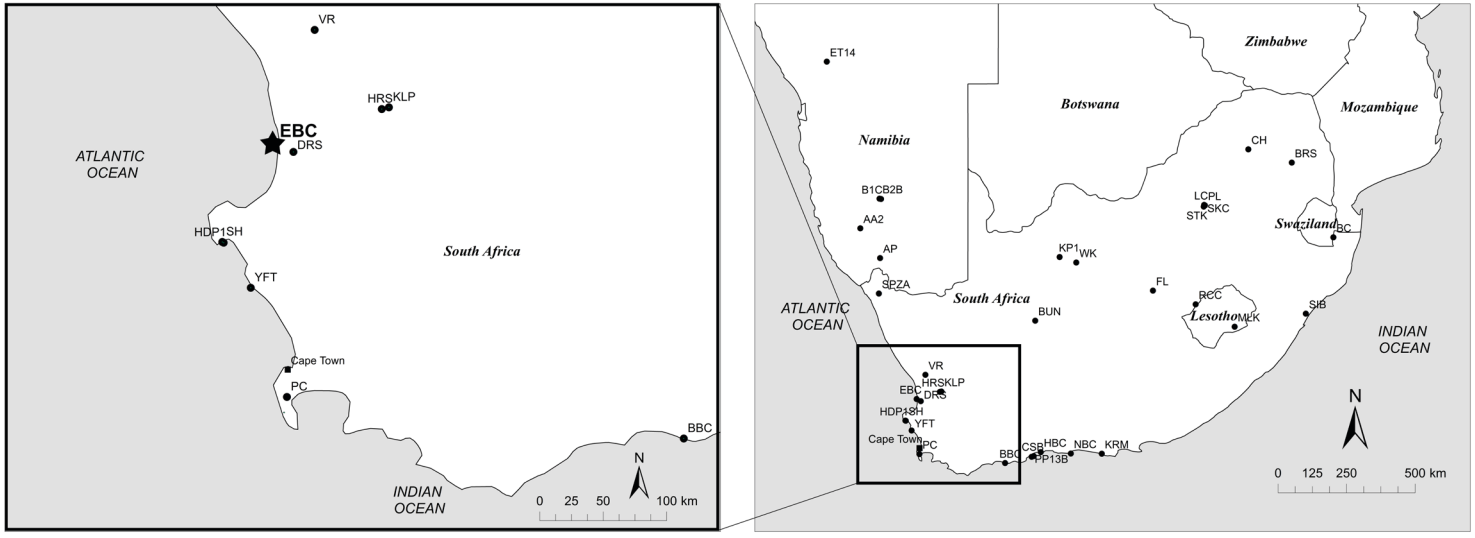

Fig. 1. Location maps depicting Elands Bay Cave (EBC) and MIS 6 to MIS 5 sites (AA2-Aar 2; AP-Apollo 11 Rock Shelter; BBC-Blombos Cave; BC-Border Cave; B1C-Bremen 1C; B2B-Bremen 2B; BUN-Bundu Farm; BRS-Bushman Rock Shelter; CSB-Cape St. Blaize; CH-Cave of Hearths; DRS-Diepkloof Rock Shelter; ET14-Etemba 14; FL-Florsibad; HBC-Herolds Bay Cave; HDP1-Hoedjiespunt 1; HRS-Hollow Rock Shelter; KP1-Kathu Pan 1; KRM-Klasies River main site; KLP-Klipfonteinrand; LC-Lincoln Cave; MLK-Melikane Rock Shelter; NBC-Nelson Bay Cave; PC-Peers Cave; PP13B-Pinnacle Point 13B; PL-Plovers Lake; RCC-Rose Cottage Cave; SH-Sea Harvest; SIB-Sibudu Cave; SPZA-Spitzkloof A Rock Shelter; STK-Sterkfontein; SKC-Swartkrans Cave; VR-Varsche Rivier 003; WK-Wonderwerk Cave; YFT-Ysterfontein 1).

First research at EBC

The investigation of EBC began in November 1970, when John Parkington, Cedric Poggenpoel and Peter Robertshaw from the University of Cape Town conducted the first excavations there and found a great potential for intact deposits. The fieldwork continued from November 1970 until December 1978. The team started to excavate the sediments in the southwestern area of the chamber with a size of ca. 18 x 13 m and expanded the excavation area to 96 m^2. Despite the total area covered, the smooth undulating bedrock was only reached in the deep sounding covering 5 m^2, ca. 3 m below the original summit of the mound of the shell midden.

Depositional units were treated as the smallest stratigraphic events and were distinguished by composition in terms of relative amounts of shell, bedding grasses, twigs, ash, roof spall, loamy matrix and gypsum. Uniform layers with a depth of more than 50 mm were subdivided into arbitrary spits. The large number of radiocarbon dates (over 60) collected throughout the whole sequence indicated significant time differences between some of the depositional units directly above or below each other (Parkington 2016 this issue). This is most probably connected due to explicit episodes of non-deposition; thus, Parkington classified the depositional units with radiocarbon dates of a close range into so-called pulses (Porraz et al. 2016 this issue).

Pulse H represents the lowest phase at EBC. It is described as quartzite rubble almost exclusively consisting of artefacts and relatively little fine interstitial material, lying directly on bedrock (Miller 1987). This lithic assemblage was studied by Volman (1981, 1984).

During the excavation most of the quartzite pieces of Pulse H were considered as artefacts and the rest was interpreted as frost-shattered, angular rubble related to harsh climatic conditions (Butzer 1979; Butzer 2004). At that time, Karl Butzer established a provisional reconstruction of geomorphic events near Elandsbaai, a small town close to EBC. According to his model, the formation of this basal rubble unit must have been contemporary with the formation of sorted block rubbles on nearby slopes, including the one directly below the cave, and was associated with cold-climate slope denudation probably dating to MIS 6b (Butzer 1979; Butzer 2004). Furthermore, the fact that no organic remains are preserved led Butzer (1979) to the assumption that Pulse H could represent a residual lag deposit, from which all organic and fine materials have been removed by percolating water.

As an alternative to this interpretation as a residual lag, Parkington (pers. comm.) suggests that the character of the Pulse H assemblage is affected by the function of the site and could represent a quarry site, based on the high homogeneity of the raw material and the paucity of formal tools.

Volman's analysis

Volman studied the lithic artefacts of the depositional unit Spit 12, which forms a part of Pulse H, in the course of his doctoral thesis (Volman 1981). He classified this assemblage as 'MSA 1' according to his system of classification. In total, he analysed 1537 lithics, comprising 1007 flakes, 25 cores and 505 angular debris. He described the use of primarily local quartzite (n = 1504) to manufacture blanks, amounting to 97.9 % of the total assemblage. Only 32 pieces of quartz were present, and Volman identified one silcrete flake.

In general, the quartzite flakes (n = 995) had a square shape. This observation was also statistically determined with an average width-length ratio of 0.89. The length of the quartzite blanks averaged 48 mm. Only 20 flakes had a length over 70 mm and not a single piece was longer than 110 mm. Twenty-four of the cores were made on quartzite and one on quartz. Volman classified most cores as intersecting ridge cores (definitions of the cores according to Volman 1981). Most of the quartzite flakes exhibited intersecting dorsal scars. Triangular blanks with convergent dorsal scars and flakes with parallel or sub-parallel scars are very rare.

Formally retouched pieces did not appear in the assemblage. Evidence of utilisation in the form of edge damage was found on five quartzite artefacts as well as on one quartz piece and the only silcrete artefact. Additionally, Volman mentioned one specimen, a large flake fragment, which showed minimal heavy-duty alternating retouch. He identified a high proportion of artefacts with this kind of heavy-duty retouch in the Peers Cave sample that he also designated 'MSA 1'. Further similarities between EBC and Peers Cave are the short length and the square shape of the blanks.

STRATIGRAPHIC CONTEXT

The 2011 excavation

One of the main objectives of the excavation in 2011 was to get a better understanding of the lower part of stratigraphy of EBC. Thus, the deep sounding of the former excavation led by Parkington from 1970 to 1978 was re-opened.

The new excavation focused primarily on the southern part of the eastern section of the deep sounding (Fig. 2), because the stratigraphy was best preserved in this area (Miller et al. 2016 this issue; Porraz et al. 2016 this issue). A narrow band 2.5 m in length and 0.5 m in width was excavated. Before the actual excavation began, the exposed sections were used to identify specific sedimentation cycles, so-called stratigraphic phases. Eight main phases could be identified and have been labelled with the letters C to L. Each phase could be subdivided into different stratigraphic units (SUs). These units were recorded and given informal names (e.g. Lovan, Liam, Letty etc.) due to the local archaeological tradition, but maintaining an internal alphabetical order. The SUs relate to the smallest stratigraphic events that spread over an area larger than a quarter square metre. If a SU reached a depth over 25 mm, it was subdivided into *décapages* (Porraz et al. 2016 this issue).

The base of the sequence is formed by phase L, comprising SUs Letty to Lovan. This phase has a maximum thickness of 100 mm and consists of black and moist lenses within dark brown sediment. Archaeological finds occur, but an intrusion from the overlying SUs, especially concerning the lowermost layer Lovan, is very likely, as the artefacts show a strong incline downward toward the north. The SUs of this phase in particular show a strong inclination towards the north due to the topography of the substrate (see Miller et al. 2016 this issue). The following phase spanning SUs Keva and Lara is ca. 350 mm thick and contains an accumulation of quartzite artefacts as well as roof spalls with virtually no sedimentary matrix. The two units Karl and Kirsten have only been excavated in the southern section. These two SUs belong to the same phase as Keva to Lara excavated in the eastern profile and are also characterised by a rich accumulation of quartzite artefacts and a similar lack of sedimentation. However, a distinction was made since tracking the deposits laterally was not possible due to the geometry of the deposits.

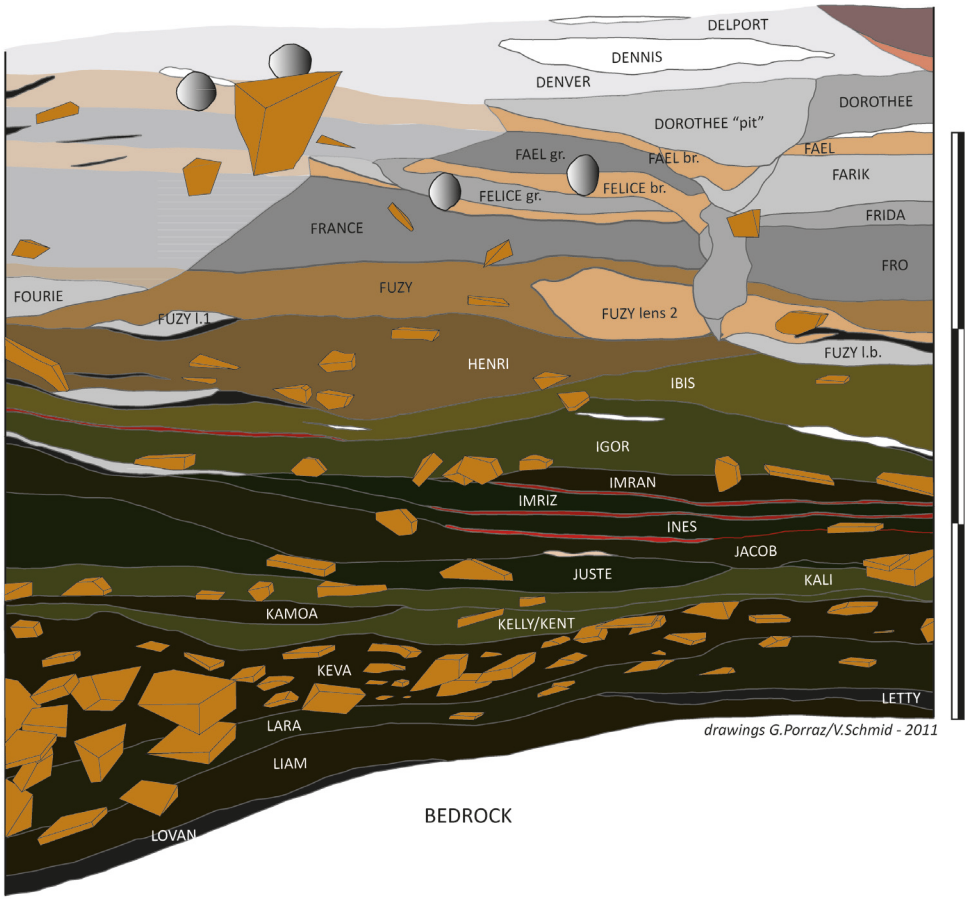

Fig. 2. East section showing stratigraphic sequence of the 2011 excavation.

The SUs Keva to phase L are characterised by an accumulation of quartzite artefacts with some roof spalls. We refer to this archaeological phase as lower MSA.

Site formation processes and chronology of the lower deposits of EBC

The main characteristic of the deposits of the lower MSA is an accumulation of quartzite artefacts and natural quartzite slabs with almost no sedimentary matrix. We found no preferential orientation of the objects. Furthermore, the morphology of the lower layers is affected by the underlying substrate that inclines towards north and forms a depression in the centre of the excavated zone. The sediments of the lower MSA as well as the sediments of EBC in general are strongly influenced by chemical diagenesis. A cone of water percolating in the southern part of the eastern section has on the one hand prevented gypsum crystallization that caused transformation of the appearance of the SUs in other parts of the site. But on the other hand, the water percolation most likely led to the complete dissolution of bone in this area (Miller et al. 2016 this issue).

Concerning the age of the lower MSA, SU Keva was dated directly by TL to 83 ± 14 ka. However, this date represents only one age estimate and thus must be regarded with caution (see Tribolo et al. 2016 this issue). The lower lying SU Liam immediately under the main archaeological SUs Keva and Lara attests an age of 236 ± 23 ka using the OSL-dating (Tribolo et al. 2016 this issue). For the moment, we can securely claim that the lower MSA post-dates 236 ka and is older than MIS 4.

Stratigraphic correlations between the 1970s and the 2011 excavations

Parkington excavated the deep sounding first in squares E4 and F4 in 1972 and later enlarged it to the north in 1978. In each of these two field seasons, he applied a different naming system to the stratigraphic sequence as a direct correlation was extremely difficult due to great lateral variations. The assemblage from the 1978 enlargement layer Darth Vader comprises only a few undiagnostic pieces. However, most of the blanks are made from local quartzite and also share similar morphological characteristics to the flakes of the assemblage from Spit 12 from 1972.

The sedimentary observations during the fieldwork in 2011, together with altitude indications and technological comparisons, made stratigraphic correlations between the different excavations in the deep sounding possible (see Porraz et al. 2016 this issue). Based on diagnostic stratigraphic and archaeological features, sedimentary phases L and Keva/Lara correspond to Pulse H, including Spit 12 and Darth Vader, and probably the base of the subsequent Pulse G, including Spit 11 (1972 excavation) and Skywalker (1978 excavation). First, we observed an accumulation of quartzite artefacts and roof spalls with very little fine interstitial material (Miller 1987; Miller et al. 2016 this issue). Secondly, no organic remains are preserved (Butzer 1979; Parkington pers. comm.). Thirdly, the maximum thickness of the pulse is between 400 and 500 mm (Parkington pers. comm.). Finally, the lithics assigned to the 'MSA 1' by Volman (Volman 1981, 1984) and those of the lower MSA from the new excavation share the same technological and techno-economic features and can be regarded as one assemblage.

ARCHAEOLOGICAL SAMPLE AND METHOD OF STUDY

The excavation of 2011 used modern excavation standards. All objects larger than 20 mm were recorded three-dimensionally with a total station, but cores, core fragments, tools and tool fragments were recorded regardless of their size. The screen residues were sorted and all the lithic finds were bagged by sub-square and sedimentary unit. All the lithic artefacts larger than 20 mm coming from the sieves were washed and labelled. The sum of all these lithic artefacts larger than 20 mm was analysed.

The main data set of this study derives from the lower MSA, comprising SUs Liam, Letty, Lara, Keva, Karl and Kirsten, and is based on a total of 1518 lithic artefacts larger than 20 mm (Table 1), including retouched objects smaller than 20 mm. The lithic material of the main section comes from a volume of ca. 166 l, representing an artefact density of 8.4 n/l (see Porraz et al. 2016 this issue). We grouped the assemblages of these SUs together based on common technological components. A total of 1543 lithic artefacts from Spit 12 of the excavation conducted by Parkington was also analysed and used for comparative purposes. However, our calculations and tables only relate to the 2011 assemblage.

The study of the lithic material is based on a technological approach. Lithic technology concerns all actions of past humans related to the manufacture and use of lithic artefacts (Inizan et al. 1999). Thus, the technological analysis attempts to understand the processes concerning the whole assemblage, from the initial stage of raw material procurement to the final stage of the discard of used artefacts. We therefore applied the technological approach, *chaîne opératoire*, as advocated elsewhere (e.g. Boëda et al. 1990; Geneste 1991; Inizan et al. 1999; Soressi & Geneste 2011). The typological classification is based on terminology commonly used in MSA lithic analysis (Sampson 1974; Singer & Wymer 1982; Wurz 2000; Porraz, Texier et al. 2013).

Additionally, systematic refitting analysis was carried out, as it provides insights into the technological processes involved in the reduction sequence (Cahen 1976; Cziesla et al. 1990; Nigst 2012).

Finally, we recorded edge damage and thermal alterations to evaluate the condition of the lithic material.

RAW MATERIALS

Raw material availabilities

The study of the provenance and composition of the raw materials of an assemblage yields information about human mobility, land-use/foraging patterns and site occupational histories. Moreover, raw material availability and quality affect the size of the blanks as well as the assemblage composition (Nigst 2012). Systematic geological fieldwork is required to gain knowledge of the available raw materials in a region and to make further statements about the techno-economic system. Our results are based on several field surveys that we conducted during the EBC excavation and within the Diepkloof project. We refer to 'local', in accordance with ethnographic and archaeological observations, as an economic zone less than 5 km around the site, while 'semi-local' means more than 5 km but less than 20 km, and 'exotic' is more than 20 km from the site (Geneste 1985, 1988; Porraz et al. 2008).

The main rock type available in the area surrounding EBC is the quartzite of the Table Mountain Group geology, in which the rock shelter itself was also formed. However, different qualities of quartzite occur, depending on the size of the quartz grains as well as their homogeneity within the rock. During our survey, we did not observe lateral variations in terms of quartzite distribution but rather recognised vertical variations, related to the beddings of the geological formation. In general, the local quartzite can be regarded as a rock of poor quality due to the heterogeneity of its inclusions and the presence of large quartz grains, although some varieties of a better quality have been found.

Another local rock source is the conglomeratic formations inter-bedded within the Table Mountain Group. The formation occurs in the form of pebbles and an important variation in terms of pebble size was observed, with a maximum size of ca. 20 cm. Furthermore, the rock types have been deeply affected by the presence of faults in the Table Mountain, which constrain their suitability for knapping. However, the selection of rocks implies procurement on the beach or on the slopes of the hills directly. The main rock available within the conglomerates by far is milky quartz, found everywhere around the shelter and along the Verlorenvlei. In general, this quartz is of

poor-to-medium knapping quality, but some larger pebbles exist and can be flaked. The second rock that appears in the conglomerates is a fine-grained quartzite. Some of its varieties exhibit a good knapping quality. The third rock type is chert, corresponding to fine-grained siliceous rocks. Very few occurrences of conglomerate chert have been reported and only in the form of small pebbles.

The geological contextualization of the silcrete artefacts in the EBC lower MSA assemblage is based on a survey conducted during the Diepkloof project (Porraz, Texier et al. 2013). More than 60 outcrops of silcrete were sampled and recorded. Of greatest interest for the present study are the two silcrete outcrops identified along the Verlorenvlei. The first outcrop, at Elandsbaai, is located near to the site of EBC and consists of large siliceous crusts and blocs of grey colour. The second outcrop, at Redelinghuys, is located about 20 km east of EBC, consisting of boulders of yellowish-brown colour. Both silcrete sources present a quartzitic structure, and do not present the best knapping qualities in comparison to other types available in the wider region.

Raw material provenances and composition

The archaeological assemblage has been divided into six main rock categories, identified as coarse-grained Table Mountain quartzite, quartz, fine-grained quartzite, chert, medium- to coarse-grained yellowish-brown silcrete and fine- to medium-grained silcrete. We distinguished three cortex types: 1) weathered cortex, well-polished and shiny, 2) natural surface, often flat, stepped, and occasionally oxidized, and 3) pebble cortex with a regular surface, generally convex, with numerous shocks.

The assemblage is characterised by the dominant exploitation of local quartzite (Fig. 3.1), accounting for 98.7 % of the raw material total (Table 2). The quartzite has natural surfaces as the main cortex type, indicating its collection in the shelter or on the slope in front. This kind of cortex, as it does not induce problems during the utilization of the working edge, may have influenced the MSA people of EBC to not necessarily remove it. Indeed, cortex occurs on 84.6 % of the artefacts made from local quartzite (Table 3) which is relatively high compared to experimental lithic assemblage replications (Geneste 1985, 1988, 1992). Two alternative hypotheses could explain this high ratio: either this indicates that the reduction sequences were short or that the 'MSA 1' people exported the end-products from the site.

The second rock type that is known to be of strictly local origin is quartz (Fig. 3.2). Interestingly, while quartz pebbles are also abundantly available in the surroundings of the site and largely used during other periods (Porraz et al. 2016 this issue), 'MSA 1' inhabitants rarely used this rock for blank production, with only 0.8 % of the artefacts made from this rock type. This pattern reflects that the knappers preferred local Table Mountain quartzite over quartz particularly due to its characteristics rather than simply due to the availability. The stratigraphic unit Karl in the south section contains a higher proportion of quartz than all the other layers, but the sample remains too small (n = 35) to draw any meaningful conclusion.

Three pieces (0.2 %) of fine-grained quartzite (Fig. 3.3) and two pieces (0.1 %) of chert were documented in the assemblage (Fig. 3.5). Although they are randomly available in the form of pebbles eroded out of the Table Mountain Formation conglomerates, past people hardly ever used them for tool-making. Finally, three pieces of silcrete are present in the assemblage. None of these silcretes are macroscopically

TABLE 1

EBC, lower MSA: Count of artefacts larger than 20 mm by SUs.

SU	(N > 20 mm)	%
East Section		
KEVA	615	40.5 %
LARA	274	18.1 %
LETTY	146	9.6 %
LIAM	354	23.3 %
South Section		
KARL	35	2.3 %
KIRSTEN	94	6.2 %
Total	**1518**	**100 %**

TABLE 2

EBC, lower MSA: Raw material frequency of artefacts larger than 20 mm by SUs.

Raw Mat.	KEVA		LARA		LETTY		LIAM		KARL		KIRSTEN		Total	
	(N)	%	(N)	%	(N)	%	(N)	%	(N)	%	(N)	%	(N)	%
Quartzite local	606	98.5 %	272	99.3 %	145	99.3 %	348	98.3 %	33	94.3 %	94	100 %	**1498**	**98.7 %**
Quartz	4	0.7 %	2	0.7 %	1	0.7 %	3	0.8 %	2	5.7 %	0	0 %	**12**	**0.8 %**
Chert	2	0.3 %	0	0 %	0	0 %	0	0 %	0	0 %	0	0 %	**2**	**0.1 %**
Quartzite fine-grained	1	0.2 %	0	0 %	0	0 %	2	0.6 %	0	0 %	0	0 %	**3**	**0.2 %**
Silcrete	2	0.3 %	0	0 %	0	0 %	1	0.3 %	0	0 %	0	0 %	**3**	**0.2 %**
Total	**615**	**100 %**	**274**	**100 %**	**146**	**100 %**	**354**	**100 %**	**35**	**100 %**	**94**	**100 %**	**1518**	**100 %**

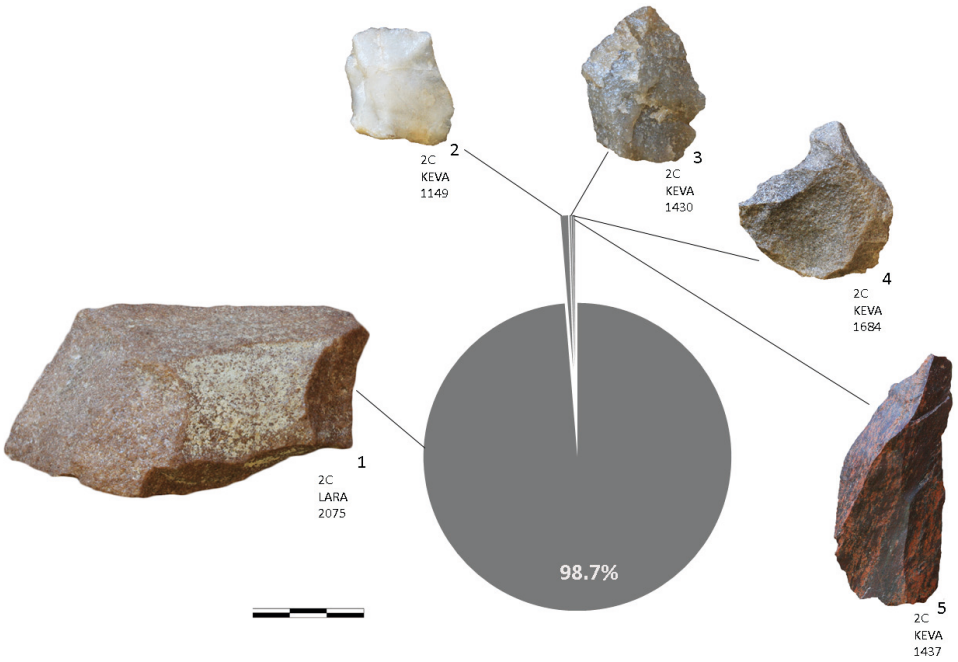

Fig. 3. Pie chart showing the occurring rock types at Elands Bay Cave, lower MSA. 1: Local quartzite; 2: Quartz; 3: Fine-grained quartzite; 4: Silcrete; 5: Chert.

similar to the Elandsbaai silcrete outcrop, but two artefacts of a yellowish-brown colour (Fig. 3.4) most probably come from the semi-local Redelinghuys outcrop. The origin of the third piece is unknown.

The study of the raw material frequencies shows that sources around the site, particularly the local quartzite, were primarily exploited. The other rock types, in particular the silcretes, are exclusively present as blanks, attesting that isolated finished blanks were brought to the site (Table 4). This dominance of local quartzite suggests that the MSA tool-makers of EBC put minimal investment in the procurement of rock types, although they selected it over the evenly available quartz.

LITHIC TECHNOLOGY

The reduction system of only the quartzite artefacts is discussed here, as only a few pieces of the other raw materials are present. Later we discuss and compare how these individual pieces correspond to what we observe for the local quartzite.

The quartzite assemblage contains various coexisting reduction sequences. The main reduction is directed towards the production of flakes, which compose 66.9 % of the whole assemblage, including cores and angular debris (Table 4). Fifty-two of the cores, representing 89.7 % of the total cores, were clearly oriented towards the manufacture of flakes (Table 5).

The products are in general rather short than elongated and have a rectangular to trapezoidal shape and occasionally a triangular one (Table 6). The majority of the blanks exhibit cortical or plain platforms; only a few pieces exhibit a faceted platform.

TABLE 3

EBC, lower MSA: Cortex type frequency of artefacts larger than 20 mm made from local quartzite (without angular debris).

Cortex Type	(N)	%
no cortex	144	13.2 %
weathered	21	1.9 %
natural surface	925	84.6 %
pebble cortex	4	0.4 %
Total	**1094**	**100 %**

TABLE 4

EBC, lower MSA: Technological classification of artefacts larger than 20 mm by rock types.

Techn. Class.	Quartzite		Quartz		Quartzite fine-grained		Chert		Silcrete		Total	
	(N)	%	(N)	%	(N)	%	(N)	%	(N)	%	(N)	%
Flake	1002	66.9 %	10	83.3 %	3	100 %	2	100 %	3	100 %	**1020**	**67.2 %**
Blade	34	2.3 %	0	0 %	0	0 %	0	0 %	0	0 %	**34**	**2.2 %**
Core	58	3.9 %	0	0 %	0	0 %	0	0 %	0	0 %	**58**	**3.8 %**
Angular debris	404	27.0 %	2	16.7 %	0	0 %	0	0 %	0	0 %	**406**	**26.7 %**
Total	**1498**	**100 %**	**12**	**100 %**	**3**	**100 %**	**2**	**100 %**	**3**	**100 %**	**1518**	**100 %**

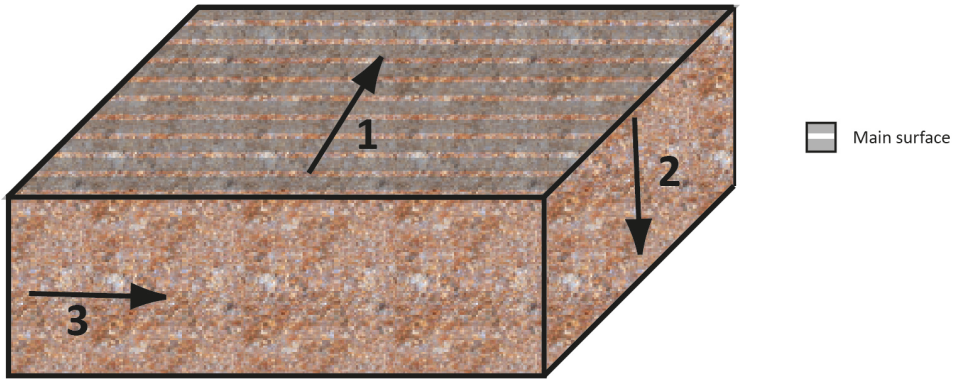

Fig. 4. Three planes of symmetry of a cuboid/parallelogram. 1: Planar plane; 2: Orthogonal plane; 3: Linear plane.

Flake Reduction Strategy

One notable feature is that quartzite slabs and large flakes were almost exclusively selected by EBC knappers (Table 7). Our analysis was therefore adapted to take account of the morphological characteristics of slabs in order to investigate how the knappers of the MSA manipulated their specific geometry. These three-dimensional objects resemble cuboids/parallelograms and have three axes of symmetry (see Carmignani 2010). These axes represent three planes that define the orientation of the geometry and reduction sequence of the cores:

(a) The exploitation of the planar plane describes the detachment of the blanks from the widest main surface (Fig. 4.1).
(b) The exploitation of the orthogonal plane refers to blanks that are detached orthogonally to the main surface. The detachment is carried out on the narrow surface transversally (Fig. 4.2).
(c) The exploitation of the linear plane concerns the longitudinal detachment of the blanks from the narrow surface (Fig. 4.3).

The planar plane

The knappers exploited the slabs and large flakes on their planar plane (Fig. 5.1–3), as documented by 13 (22.4 %) of the cores. The typical products show primarily unidirectional dorsal removals, but also bidirectional or orthogonal removals occur. Products are at least as wide as long and have a transverse edge opposed to the platform (Fig. 5.4–6). The use of internal percussion with a hard hammerstone has been exclusively employed. Some flakes—morphologically similar to pseudo-Levallois points (or *dos limités*)—with a short cortical back also resulted from this reduction sequence (Table 6). We observed no phase of preparation and the reduction sequence is generally short. Two of these cores are made on large flakes and show no cortex coverage. The other eleven cores exhibit cortex remnants often on the exploitation surface, attesting a short reduction sequence. The flakes resulting from an early stage in the reduction have either remaining cortex or a part of an old ventral face on their dorsal face. Some flakes can be identified as Kombewa flakes (Table 6), verifying that some of the cores are made on flakes (Table 7).

TABLE 5
EBC, lower MSA: Core type frequency (all in local quartzite).

Core Type	(N)	%
Flake Production		
Planar exploitation Core	13	22.4 %
Orthogonal exploitation Core	28	48.3 %
Linear exploitation Core	4	6.9 %
Orthogonal & Planar exploitation Core	7	12.1 %
Blade Production		
Unidirectional Levallois Core	1	1.7 %
Blade Core	3	5.2 %
Initialized or Indetermined broken Cores		
Initialized Core	1	1.7 %
Indeterminate broken Core	1	1.7 %
Total	**58**	**100 %**

TABLE 6
EBC, lower MSA: Frequency of flakes according to their morphological and technological features (all in local quartzite).

Flake Type	(N)	%
'pseudo-Levallois point'	82	8.2 %
elongated flake	107	10.7 %
plunging flake	78	7.8 %
core edge flake	11	1.1 %
bipolar flake	14	1.4 %
Kombewa flake	11	1.1 %
prepared flake	7	0.7 %
rectangular to trapezoidal flake	254	25.3 %
triangular flakes	87	8.7 %
not diagnostic flake	351	35.0 %
Total	**1002**	**100 %**

TABLE 7
EBC, lower MSA: Original blank frequency of all cores (all in local quartzite).

Core blank	(N)	%
Flake	8	13.8 %
Slab	39	67.2 %
Indetermined	11	19.0 %
Total	**58**	**100 %**

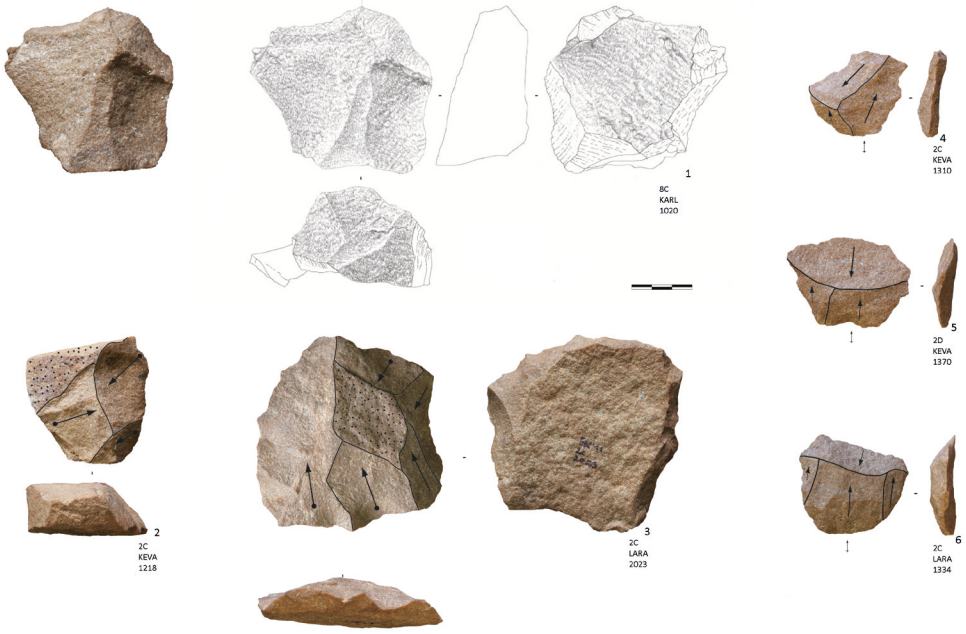

Fig. 5. Elands Bay Cave, lower MSA. 1–3: Planar exploited core (drawing: M. Grenet); 4–6: Rectangular to trapezoidal flakes with bidirectional dorsal scars.

The orthogonal plane

Secondly, the dominant reduction sequence observed on 28 of the cores (48.3 %) corresponds to the exploitation of slabs and flakes on their orthogonal plane (Fig. 6.1–6). The length of these cores' exploitation surfaces shows that the thickness of the selected slabs was generally bracketed between 20 to 40 mm (Fig. 7.1). Some of these cores exhibit only a few flake removals, while others attest a longer exploitation sequence and some were even completely exhausted based on their small dimensions. The average length of the last complete removals (n = 22), excluding knapping accidents, is 22.4 mm (Fig. 7.2), indicating that this is the minimum range of blank size. The products are either as wide as long or even wider as long and always show unidirectional dorsal scars. Their platforms types are cortical or plain.

Two main types of products could be distinguished. The first type corresponds to plunging flakes, which exhibit a rectangular shape and are generally thick (Fig. 6.7–10). These blanks indicate a longer sequence of reduction and (in)directly served to manage the distal convexity of the exploitation surface of the core. These products enable the maintenance of the distal convexity for a further exploitation by free hand. Otherwise, the knappers employed the bipolar-on-anvil percussion as another solution to ensure the continuation of the exploitation (see below). The second type is represented by rectangular to trapezoidal flakes that are thinner than the plunging flakes. Instead of showing an overshot, these products have a transversal edge opposed to their butt and have strictly unidirectional scars (Fig. 6.11–14). These blanks share the same features concerning morphology and direction of dorsal removals as those described for the rectangular to trapezoidal flakes coming from the planar plane reduction. We observed

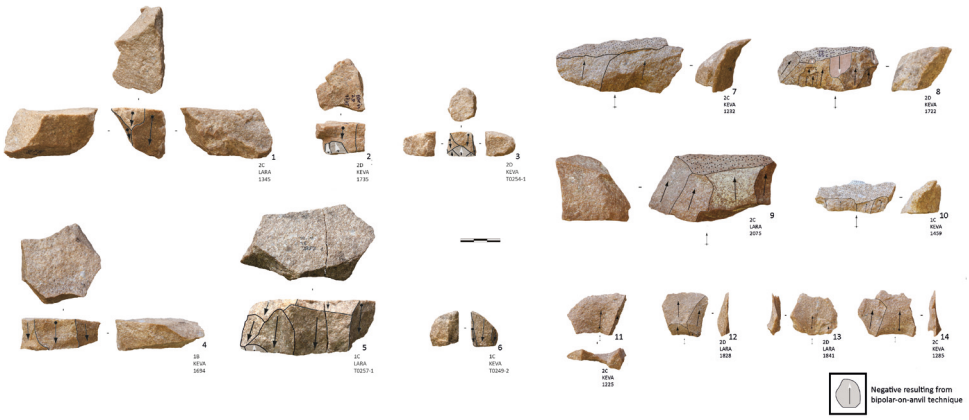

Fig. 6. Elands Bay Cave, lower MSA. 1,4,6: Orthogonal exploited cores; 2,3,5: Orthogonal exploited cores exhibiting traces of bipolar-on-anvil technique; 7,9,10: Plunging flakes of rectangular shape with unidirectional dorsal scars; 8: Plunging flakes of rectangular shape exhibiting traces of bipolar-on-anvil technique; 11–14: rectangular to trapezoidal flakes.

a certain degree of overlap between the flakes resulting from the reduction of these two planes and a clear distinction is only possible if the orientation of the dorsal scars is not unidirectional.

The cores and the products reflect the use of internal percussion with a hard hammerstone, yet alternatively or at the final stage of exploitation, the knappers also used bipolar-on-anvil percussion to exploit the slabs. Some of the flakes exhibit typical features of bipolar-on-anvil percussion, such as traces of 'repercussion' (*contre-coup*) on the distal part initiated by the contact point between the core and the anvil (Fig. 8.4), opposed impact scars on both ends of the ventral face (Fig. 8.3), radial fractures (Fig. 8.1–2) and V-shaped ends (Fig. 8.5). Some of the cores also show explicit characteristics of bipolar-on-anvil percussion, such as 'repercussion' marks observed on the base of these cores (Fig. 6.2–3, 5). A box plot of core length demonstrates that the cores connected to bipolar-on-anvil percussion are located within the lower range of the orthogonal cores that were reduced by direct hard-hammer percussion (Fig. 7.3). The same is true for the length of the last complete removals (Fig. 7.4). This fact supports the hypothesis that bipolar-on-anvil percussion was used at a later stage or at the last stage of reduction. The reduction sequence involves no preparation of the cores. However, in order to ensure continuous exploitation, the convexities of the cores were controlled by employing the different types of percussion and the removal of plunging flakes.

The linear plane

A further reduction sequence recognised on four cores (6.9 %) shows exploitation on the linear plane of the slabs and flakes (Fig. 9.1). The scars on these cores indicate the detachment of elongated flakes with a unidirectional reduction strategy. The MSA tool-makers managed the convexities of the cores with removals from the exploitation surface. The distal convexities were controlled with elongated plunging products (Figs 9.2–3), with 22.2 % of the elongated flakes having plunging terminations. The lateral convexities were established with elongated flakes that removed a part of the

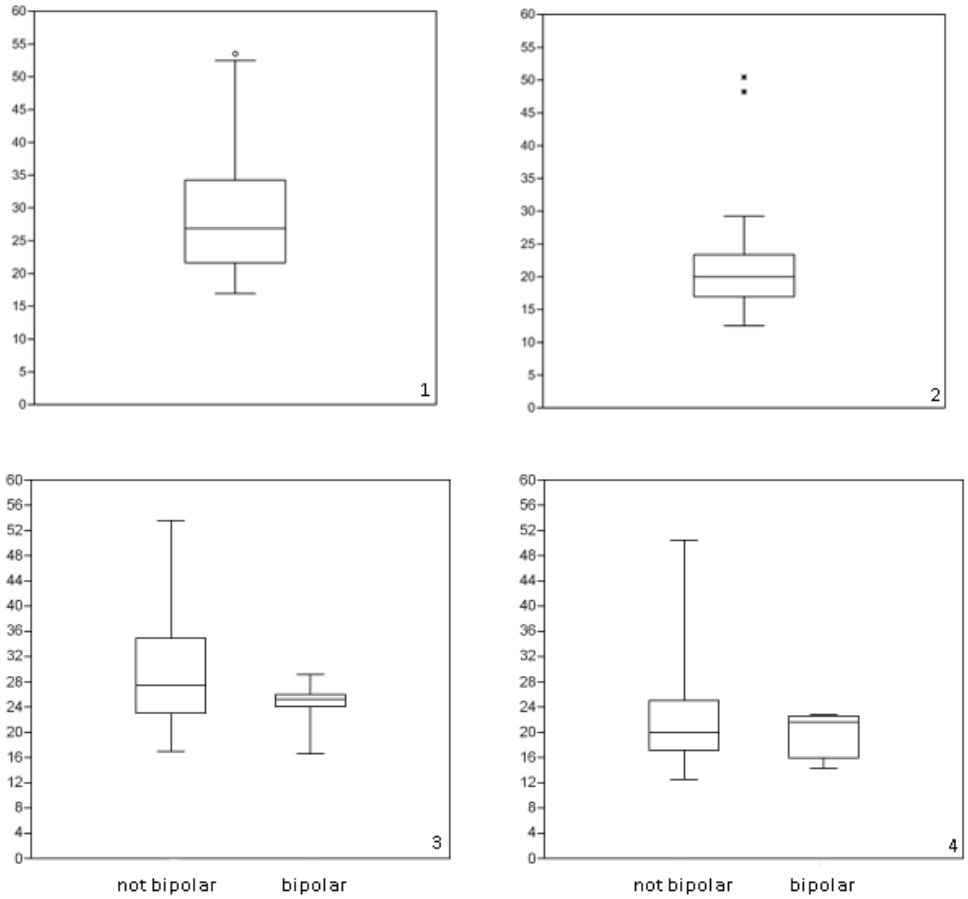

Fig. 7. Elands Bay Cave, lower MSA. 1: Box plot of the length of all the exploitation surfaces of all orthogonal exploited cores (n = 28); 2: Box plot of the length of the last complete removals of the orthogonal exploited cores (n = 22), excluding the accidents; 3: Box plot of the length of exploitation surfaces of orthogonal exploited cores (n = 22) and orthogonal exploited cores connected to the bipolar-on-anvil technique (n = 6); 4: Box plot of the length of last complete removals of orthogonal exploited cores (n = 17) and orthogonal exploited cores connected to the bipolar-on-anvil technique (n = 5).

core edge (*éclats débordants*) (Fig. 9.5). No phase of preparation was observed. Internal percussion with hard hammerstone is the dominant percussion technique, but some of the cores and products clearly demonstrate features of bipolar-on-anvil percussion (Fig. 9.4), indicating that this technique was used either alternatively or at the last stage of exploitation. There is a certain degree of overlap with the flakes resulting from the use of bipolar-on-anvil percussion during the orthogonal core reduction and the main distinctive characteristic is greater flake length.

The multi-plane

Finally, some of the cores were exploited on multiple planes of the slab. To begin with, a combination of exploitation of both the orthogonal and planar planes was observed

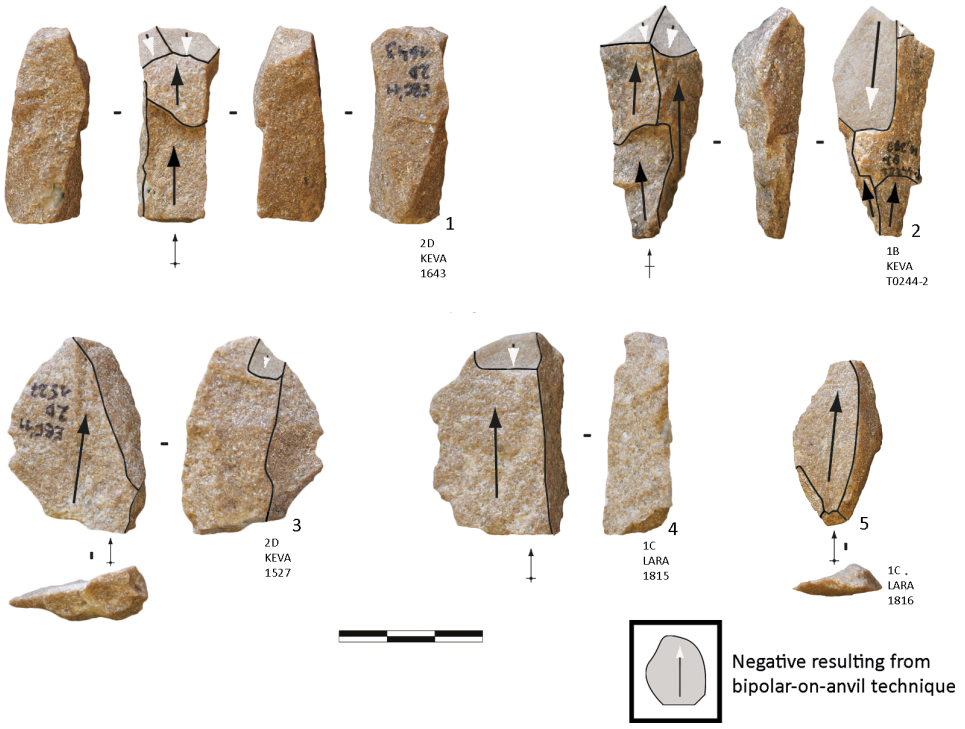

Fig. 8. Elands Bay Cave, lower MSA. 1–2: Bipolar flakes with radial fractures; 3: Bipolar flake with opposed impact scars on both ends of the ventral face; 4: Bipolar flake with exhibit 'repercussions (*contre-coups*) on the distal part; 5: Bipolar flake with V-shaped end.

Fig. 9. Elands Bay Cave, lower MSA. 1: Linear exploited core; 2–3: Plunging elongated flakes; 4: Elongated flake exhibiting traces of bipolar-on-anvil technique; 5: Elongated flake that removed a part of the core edge (*éclats débordant*); 6–7: Elongated flakes.

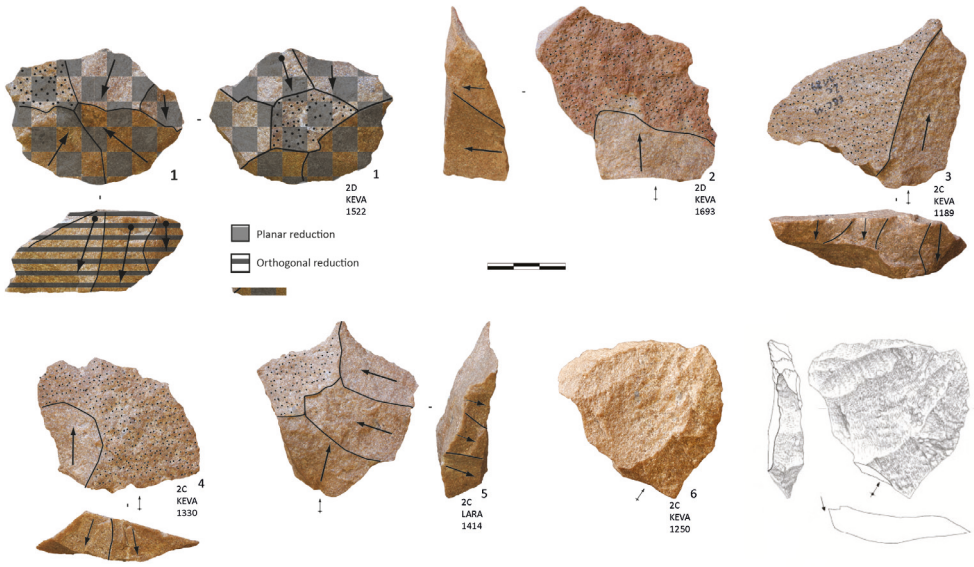

Fig. 10. Elands Bay Cave, lower MSA. 1: Orthogonal and planar combined exploited core; 2, 3, 5: Thick flake with a back formed by invasive removals; 4: Thick flake exhibiting invasive removals on the butt; 6: Thick flake with a back formed by invasive removals (drawing: M. Grenet).

on seven of the cores (12.1 %) (Fig. 10.1). The chronology of removals on these cores indicates that the last operations of the knappers were carried out on the planar plane; they generally started with the exploitation of the orthogonal plane and continued with the planar plane. Some of the plunging flakes typical of the orthogonal plane exploitation exhibit a plain rather than a cortical butt and thus attest that after the initial reduction of the orthogonal plane, the two planes were exploited alternately. The diagnostic flakes resulting from this reduction strategy are thick as well as wide and have a back. These flakes were detached from the planar plane of the core and their backs are formed by invasive removals that came from the exploitation of the orthogonal plane and making the back appear like a denticulation (Fig. 10.2–3, 5–6). A few flakes do not have a back but instead exhibit these invasive removals on their butt (Fig. 10.4).

Additionally, some of the flakes indicate the rotation of the core from the orthogonal to the linear plane. These typical blanks show a series of dorsal scars that are orthogonal to the new axis of percussion (Fig. 11). However, no cores of this type were identified in the assemblage.

The POL-reduction strategy'

We observe that the EBC knappers combined different options to orientate and exploit the slabs. While the blanks do not all share the same features, we identify similarities based on: 1) the selection of the slabs and flakes, 2) the use of direct hard-hammer percussion, and 3) a limited number of options concerning the reduction. To characterise these reduction strategies and unify what we consider to be one 'concept', we call it the Planar-Orthogonal-Linear-reduction system or POL-reduction system.

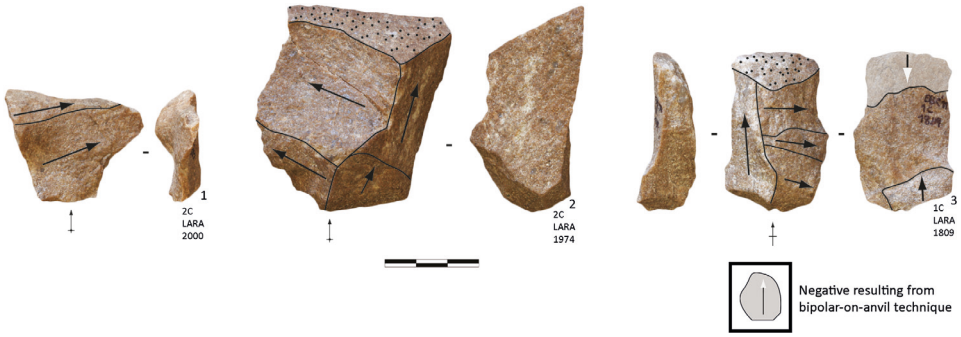

Fig. 11. Elands Bay Cave, lower MSA. 1–2: Flakes showing a series of dorsal scars that are orthogonal to the new axis of percussion; 3: Bipolar flake showing a series of dorsal scars that are orthogonal to the new axis of percussion.

Blade Reduction Strategy

In addition, we identify 4 cores with a morphology that does not overlap with our definition of the POL-reduction strategy. These cores document the production of blades and we are inclined to distinguish two reduction sequences.

The first reduction strategy is seen on three blade cores, representing 5.2 % of all cores in the assemblage (Table 5), which were prepared in order to exploit large flakes or slabs (Fig. 12). The ridge formed by the natural geometry of the slab was used to detach the initial blade. The following detachment led to the removal of elongated convergent blanks with one cortical side (Fig. 13.6, 10). The continuing reduction

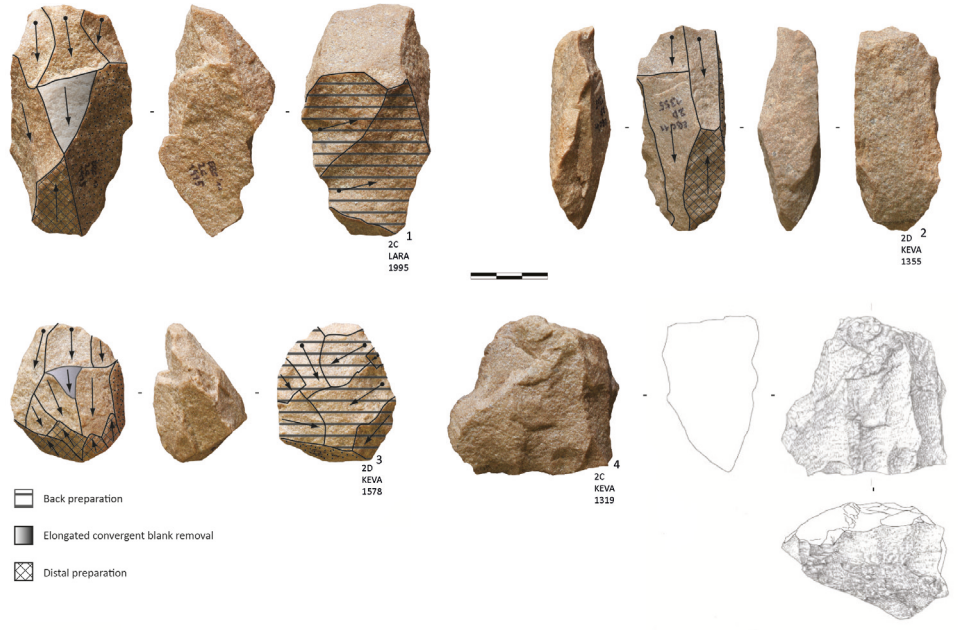

Fig. 12. Elands Bay Cave, lower MSA. 1–3: Blade cores; 4: Unidirectional parallel recurrent Levallois core (drawing: M. Grenet).

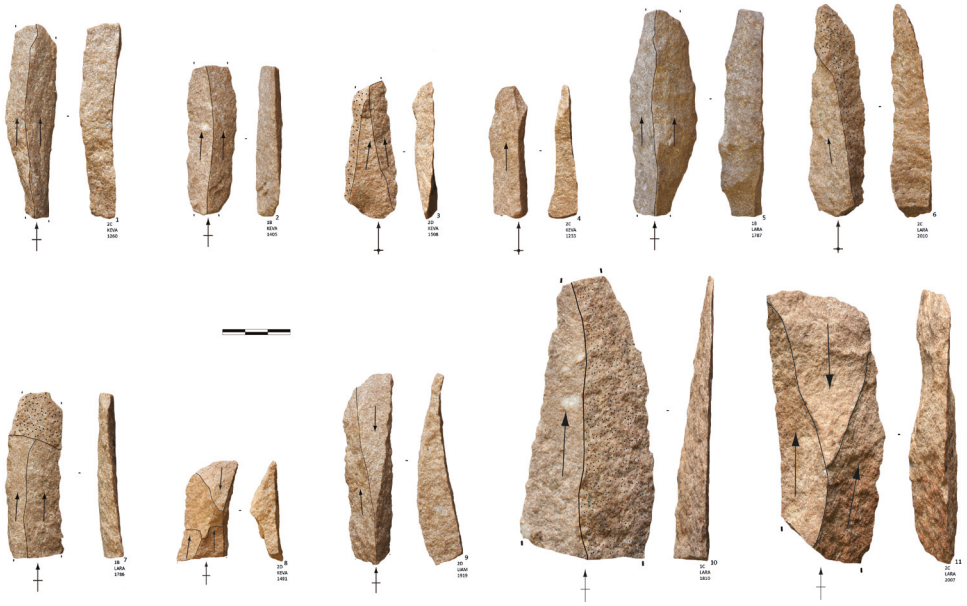

Fig. 13. Elands Bay Cave, lower MSA. 1–7, 10: Blades with unidirectional dorsal scars. 8–9, 11: Blades with bidirectional dorsal scars due to distal preparation.

sequence on the narrow frontal surface is unidirectional and usually parallel. This reduction sequence seems to be short. However, one core shows greater exhaustion and its progressive reduction demonstrates an increased investment in preparation of the back and distal part of the exploitation surface (Fig. 12.3). These cores correspond to single platform cores.

The platforms are generally not faceted as documented by the cores, but also by the blades, as 90 % of them have a plain or cortical butt (Table 8). The cores show that the distal convexity of the exploitation surface was managed by removals originating from the base of the core, opposed to the platform, and 14.7 % of all blades exhibit bidirectional dorsal scars (Fig. 13.8–9, 11; Table 9). The opposed removals on the blades with a bidirectional dorsal scar pattern rather originate from a preparation of distal convexity than from a bidirectional exploitation, as the quantity of blades with bidirectional removals is low and the cores confirm to a unidirectional reduction sequence.

The second blade reduction strategy is shown by only one core, which has two distinct surfaces that are hierarchized (Fig. 12.4). The striking platform is faceted and the angle between the platform and the exploitation surface is approximately 90°. The reduction strategy attests a unidirectional exploitation and is reminiscent of a unidirectional parallel recurrent Levallois system (Boëda 1994).

The knapping characteristics observed on the cores and on the products attest the strict application of internal percussion with a hard hammerstone in both blade reduction strategies.

Blades are not numerous in our lithic assemblage (2.3 %) and present a great range of dimensions (Fig. 13), with some specimens being very large (max. 119 mm)

(Fig. 13.10–11). The small blade sample does not allow a further determining of the diagnostic morphometric characteristics and the potential differences that would be related to the two reduction strategies we recognize.

A point requiring clarification is the nature of the differences between the linear plane reduction strategy and the blade reduction strategies. If the geometries of the cores differ, there might be some morphometric overlap between the blanks. Some products thus do not exhibit definite characteristics to allow the assignment to one or the other reduction strategy. Based on our observation of the cores, we acknowledge the existence of differences regarding the regularities of the blanks. This is why we distinguished the elongated flakes (from the Linear plane reduction strategy) versus blades, based, first, on the parallelisation of the edges, and second, the length to width ratio. Some other technical criteria were taken into account. For example, blanks with bidirectional dorsal scar patterns or evidence of core preparation were considered as originating from the blade reduction strategy (see below). Additionally, elongated blanks with traces of bipolar-on-anvil percussion were assigned to the linear plane reduction.

Formal Tools

The lower MSA of EBC contains a low percentage of formal tools. Only 11 of all quartzite artefacts larger than 20 mm (0.7 %) are retouched (Table 10). Notched pieces dominate the typological corpus, followed by scrapers. Marginal retouch and burins are represented by one piece each in the assemblage. Furthermore, one quartz object shows marginal retouch.

Only the local raw material categories include retouched artefacts. The blank types used for tool production are exclusively flakes. As a general trend, the retouch that we observe is not invasive and often limited to a small part of the blank to correct an angle or a delineation. Present data converge to argue that the transformation of the blanks by retouch was not part of the daily technological repertoire of these populations.

EBC LITHIC CHARACTERISTICS AND OCCUPATIONS

Technical system of the lower MSA of EBC

The lithic technology of the lower MSA is characterised by a clear selection of the local quartzite for the manufacturing of blanks. Two main reduction sequences were recognized. One is oriented towards the production of flakes, while the other concerns the production of blades.

Regarding blade production, which plays a discrete role in this assemblage, two distinct reduction strategies were identified. On the one hand, blade cores feature the exploitation of a narrow surface, and on the other hand, one core is a unidirectional parallel recurrent Levallois core. Both reduction sequences include phases of preparation of the volume before the detachment of the predetermined end-products. The products and the cores attest the strict use of direct hard-hammer percussion. Some of the blanks exhibit bidirectional dorsal removals demonstrating the preparation of the cores to manage the distal convexity.

Flake production is the more common objective of reduction. The original blanks of the cores are slabs and large flakes of local quartzite. The reduction of quartzite

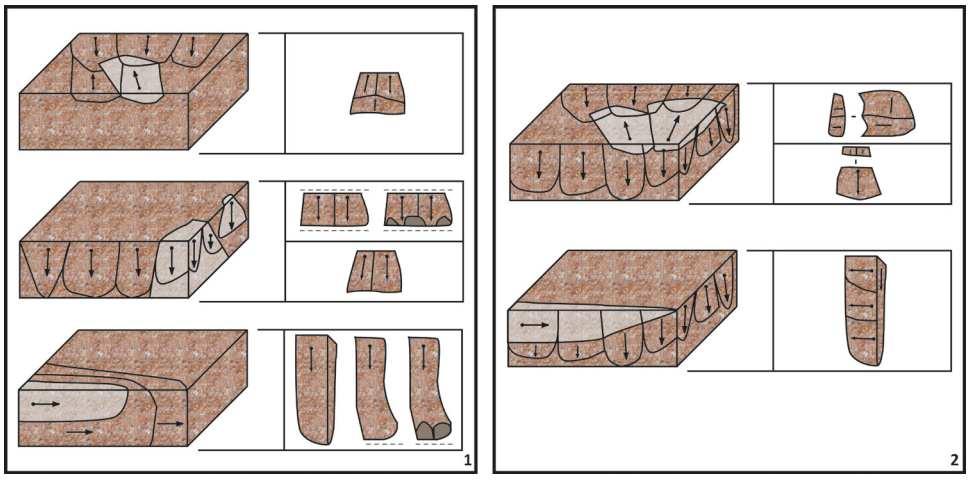

Fig. 14. Elands Bay Cave, lower MSA. 1: Scheme of independent planar, orthogonal and linear slab reduction strategies; 2: Scheme of orthogonal and planar as well as orthogonal and linear combined slab reduction strategies.

is not related to any kind of raw material constraints because surveys showed that other morphologies and other raw materials are available around the site. Therefore, the slab reduction strategy at EBC that we refer to as the 'POL'-reduction strategy can be considered as an original and deliberate character for this assemblage. Three different modalities of the POL-reduction system occur independently (Fig. 14.1) or in a combination (Fig. 14.2). The principle of this reduction strategy is based on the exploitation of the natural geometry of slabs. The reduction sequences include mostly short episodes of production, although the diminutive size of some cores document higher degrees of exhaustion. The exploitation on three axes entailed the production of different flake types that do not attest a high degree of morphological control as no preparation of the volumes occurred. However, the production of flakes with similar characteristics was possible due to adhering to the POL-reduction system. Therefore, it is confirmed that the use of slabs and large flakes as cores has broad implications for the morphological features of the blanks. The majority of the desired end-products are either elongated flakes or trapezoidal to rectangular short flakes with a working edge opposed to a thick proximal part. The flakes morphologically similar to pseudo-Levallois points are the exception.

To additionally control the reduction system, two different percussion techniques were used within the POL-system: direct hard-hammer percussion and bipolar-on-anvil percussion. Bipolar-on-anvil percussion permitted the knappers to obtain a significant recurrent series of flakes with a certain degree of morphological control on raw material morphologies where the maintenance of the reduction with a classic direct percussion would be difficult (Mourre et al. 2011). Thus, this percussion technique was either employed during the reduction or at the end of reduction to extend the production rather than to reshape the exploitation surface. The heavily exhausted cores, as well as some of the products, exhibit stigmata originating from the use of bipolar-on-anvil percussion.

TABLE 8

EBC, lower MSA: Platform type frequency (all in local quartzite).

Techn. Class.	cortical		plain		dihedral		faceted		crushed		indet.		Total	
	(N)	%	(N)	%	(N)	%	(N)	%	(N)	%	(N)	%	(N)	%
Flake	245	48.9 %	204	40.7 %	12	2.4 %	12	2.4 %	5	1.0 %	23	4.6 %	**501**	**100 %**
Blade	4	40.0 %	5	50.0 %	1	10.0 %	0	0 %	0	0 %	0	0 %	**10**	**100 %**
Total	**249**	**48.7 %**	**209**	**40.9 %**	**13**	**2.5 %**	**12**	**2.3 %**	**5**	**1.0 %**	**23**	**4.5 %**	**511**	**100 %**

TABLE 9

EBC, lower MSA: Dorsal scar orientation frequency of all blanks (all in local quartzite).

Techn. Class.	unidir.		bidir.		orthogonal		centripetal		cortex		Kom-bewa		indet.		Total	
	(N)	%	(N)	%	(N)	%	(N)	%	(N)	%	(N)	%	(N)	%	(N)	%
Flake	470	46.9 %	16	1.6 %	258	25.7 %	62	6.2 %	185	18.5 %	10	1.0 %	1	0.1 %	**1002**	**100 %**
Blade	29	85.3 %	5	14.7 %	0	0 %	0	0 %	0	0 %	0	0 %	0	0 %	**34**	**100 %**
Total	**499**	**48.2 %**	**21**	**2.0 %**	**258**	**24.9 %**	**62**	**6.0 %**	**185**	**17.9 %**	**10**	**1.0 %**	**1**	**0.1 %**	**1036**	**100 %**

TABLE 10

EBC, lower MSA: Frequency of formal tools (all in local quartzite).

Formal Tool	(N)	%
Denticulate/Notch	6	54.5 %
Scraper	3	27.3 %
Burin	1	9.1 %
Marginal retouch	1	9.1 %
Total	**11**	**100 %**

Retouching of the blanks is rare in the assemblage. Only minimal modification was applied to correct the angle of the working edges. Thus, the tool-makers of EBC established a reduction system that enabled the production of end-products that could be used immediately as implements for different tasks without great investment in any kind of further modification to shape tools.

Having defined the POL-reduction system, it is important to justify how this differs from or resembles other systems described in the literature, such as the exploitation of unprepared and orthogonal knapping surfaces (cf. S.S.D.A.: Forestier 1993), the Discoid system and the Levallois system. First, the S.S.D.A. (Système par Surface de Débitage Alterné) is similar to the POL-reduction system as the cores exhibit no preparation and still the end-products share predetermined morphological features. In contrast to the reduction system of EBC, the selection of the original core morphologies does not represent a key phase in the S.S.D.A. as knappers managed the organisation of the reduction sequence by establishing orthogonal exploitation surfaces. Secondly, the cores of the POL-reduction system cannot be considered as Discoid because the percussion direction is not sideward (*cordal*) to maintain the peripheral convexity as it is the case for the Discoid method (Boëda 1993, 1995). Some of the cores and products could be confused with Discoid cores and products due to their morphological features. However, these cores reflect the last stage of reduction which is not necessarily representative for the whole reduction sequence. The cores within the context of this assemblage clearly represent a combination of the exploitation of two different planes of slabs. Finally, the cores cannot be considered as Levallois (Boëda 1994) because the two surfaces are not hierarchical; the exploitation alternates from one surface to the other. The exploitation surfaces are not prepared by removals to establish an optimal convexity for the detachment of predetermined products, and the platforms of the cores do not exhibit any faceting.

From our perspective, the POL-reduction strategy represents the main technological characteristic of the lower MSA of EBC. This reduction system is not specific to EBC and shares similarities within other contexts, such as the late Mousterian from the Grotta del Cavallo in Italy (Carmignani 2010). In both examples, the reduction strategy is not opportunistic and the selection of slabs to be exploited as cores is a crucial phase in the reduction sequence.

Techno-economic system of the lower MSA of EBC

One of the questions that challenges the study is how far the assemblage is representative of the lithic tradition of the EBC inhabitants. Therefore we have to further investigate what technological activities were performed at the site and what this reveals in terms of territorial organisation.

The local quartzite component supports the notion that knapping activities took place on site since all phases of the different core reduction sequences are present. Additionally, the high frequency of cortical pieces, including first flakes (*entame*) (Table 11), together with cores, angular debris and chips (pieces smaller than 20 mm) attest that the local quartzite was exploited on site without or with only minimal previous preparation of the cores (Table 12). However, the large proportion of cortical blanks could either be related to short reduction sequences or to the export of end-products. We argue that in general, the reduction sequences that characterise the lower MSA of

EBC were short. First, the blank to core ratio, which represents a proxy for the intensity of raw material utilization (Dibble & McPherron 2006), is relatively low (Table 13), and second, a lot of the cores exhibit remnants of cortex on their exploitation surface.

Although quartz pebbles are also present locally in large quantities, this rock type was rarely used. Ten flakes are made from quartz, yet no cores are present. Three of these quartz flakes show clear traces of bipolar-on-anvil percussion. Very little use was made of the better-quality rocks found in the Table Mountain Formation conglomerates. Three flakes made from fine-grained quartzite and two elongated flakes from chert are present in the assemblage. One of the chert blanks exhibits a faceted platform, suggesting that the knappers invested more in the preparation and realisation of these end-products. Silcrete is represented by three flakes, transported to the cave from sources potentially over 20 km away. The isolated blanks of exotic raw material indicate that they were introduced exclusively as end-products.

The raw material identification and the above summarized technological analysis aim to determine the provisioning strategy adopted by hunter-gatherers (Kuhn 1995). As the local quartzite presents the predominant raw material and the entire reduction sequence of this rock type took place at the rock shelter, the population coped with their anticipated requirements by a so-called 'provisioning of place' strategy (Kuhn 1995).

Different hypotheses about the quartzite-dominated composition of the assemblage exist. One of these hypotheses is that the rich accumulation of quartzite geofacts (natural roof spalls), which occur in a considerable number together with the artefacts, and artefacts would be related to quarry activities (Parkington pers. comm.). EBC inhabitants would have visited the cave in order to take advantage of the natural accumulation of raw material. We acknowledge that the presence of raw material within the cave could have been one criterion that motivated the occupation of the cave. But our data converge to indicate that no major sample was exported outside of the cave and that the reduction sequence was entirely conducted *in situ*. While we acknowledge the lack of faunal preservation and potential for use-wear analysis (necessary to elucidate the various activities carried out at the site), our data suggest to us that the assemblage should firstly be viewed and interpreted as the result of activities that were diversified implying the renewal of blanks/tools. As a consequence, we do not regard EBC as a quarry site.

The dominance of the local quartzite as well as the scarcity of retouched blanks is an integrant of the technical system of the lower MSA of EBC.

THE LOWER MSA OF EBC AND THE 'MSA1' IN THE CURRENT CHRONO-CULTURAL FRAMEWORK OF SOUTHERN AFRICA

Towards a clarification of the 'MSA1"

In his attempt to summarize human cultural developments in southern Africa, Volman published a subdivision of the MSA based on the archaeological record (Volman 1981, 1984). On a cultural basis, he defined four sub-stages of the MSA, which from oldest to youngest are 'MSA 1', 'MSA 2a', 'MSA 2b', Howiesons Poort and 'MSA 3', but these were hampered by the lack of confirmation by absolute dating. Arabic numerals were used to distinguish this classification from the terminology for Klasies River established by Singer and Wymer (1982). Volman's 'MSA 1' represented the earliest phase of the MSA recognizable in southern Africa, but this was also the most problematic. It was

TABLE 11

EBC, lower MSA: Cortex position of artefacts larger than 20 mm by rock types (without angular debris).

Raw Mat.	no cortex		100 % cortex		first flake		backed		lateral		distal		proximal		centre		indet.		Total	
	(N)	%	(N)	%	(N)	%	(N)	%	(N)	%	(N)	%	(N)	%	(N)	%	(N)	%	(N)	%
Quartzite local	145	13.3 %	99	9.0 %	85	7.8 %	31	2.8 %	317	29.0 %	292	26.7 %	44	4.0 %	75	6.9 %	6	0.5 %	**1094**	**100 %**
Quartz	7	70.0 %	0	0 %	0	0 %	0	0 %	2	20.0 %	0	0 %	0	0 %	1	10.0 %	0	0 %	**10**	**100 %**
Quartzite fine-grained	1	33.3 %	0	0 %	0	0 %	0	0 %	0	0 %	2	66.7 %	0	0 %	0	0 %	0	0 %	**3**	**100 %**
Silcrete	1	33.3 %	0	0 %	0	0 %	1	33.3 %	1	33.3 %	0	0 %	0	0 %	0	0 %	0	0 %	**3**	**100 %**
Chert	2	100 %	0	0 %	0	0 %	0	0 %	0	0 %	0	0 %	0	0 %	0	0 %	0	0 %	**2**	**100 %**
Total	**156**	**14.0 %**	**99**	**8.9 %**	**85**	**7.6 %**	**32**	**2.9 %**	**320**	**28.8 %**	**294**	**26.4 %**	**44**	**4.0 %**	**76**	**6.8 %**	**6**	**0.5 %**	**1112**	**100 %**

TABLE 12

EBC, lower MSA: Technological classification of artefacts by rock types.

Techn. Class.	Quartzite local		Quartz		Quartzite fine-grained		Chert		Silcrete		Total	
	(N)	%	(N)	%	(N)	%	(N)	%	(N)	%	(N)	%
Flake	1002	60.1 %	10	26.3 %	3	100 %	2	100 %	3	100 %	**1020**	**59.5 %**
Blade	34	2 %	0	0 %	0	0 %	0	0 %	0	0 %	**34**	**2 %**
Core	58	3.5 %	0	0 %	0	0 %	0	0 %	0	0 %	**58**	**3.4 %**
Angular debris	404	24.2 %	2	5.3 %	0	0 %	0	0 %	0	0 %	**406**	**23.7 %**
Chips	170	10.2 %	26	68.4 %	0	0 %	0	0 %	0	0 %	**196**	**11.4 %**
Total	**1668**	**100 %**	**38**	**100 %**	**3**	**100 %**	**2**	**100 %**	**3**	**100 %**	**1714**	**100 %**

TABLE 13

EBC, lower MSA: Ratio of all complete and proximal preserved blanks larger than 20 mm to cores (all in local quartzite.

SU	(N of Blanks)	(N of Cores)	Blank/Core Ratio
East Section			
KEVA	377	31	12,16129032
LARA	182	17	10,70588235
LETTY	20	3	6,666666667
LIAM	120	6	20
South Section			
KARL	19	1	19
KIRSTEN	9	0	-
Total	**727**	**58**	**12,53448276**

suggested that this stage of the MSA dates to MIS 6. The assigned assemblages are characterised by a low frequency of formal tools, small broad flakes with few faceted platforms and a high proportion of intersecting ridge cores (definition according to Volman 1981, 1984). Denticulates are the most frequent tool types.

Besides EBC, Volman identified the 'MSA 1' at the sites of Peers Cave and Bushman Rock Shelter (Fig. 1; Table 14, after the references). We provide here a short description of the main typo-technological features that characterise these two assemblages.

Peers Cave (PC), Western Cape Province (also known as Skildergat, Fish Hoek, Peers' Shelter or B/102), was excavated several times by different teams beginning in the 1920s. Volman (1981) studied the material of the latest excavation conducted by Barbara W. Anthony in 1963. Three archaeological horizons were identified in the excavation area called Trench II. During Volman's analysis, it became clear that the two upper layers were homogenous so he combined the two and referred to them as Upper sample and Lower sample. Furthermore, his study revealed that although the two samples differ in some aspects, overall they exhibit the same tendencies and can be considered as closely related assemblages within a technological tradition, most probably dating to MIS 6 (Volman 1981). Volman (1981, 1984) designated these undated assemblages from PC to the 'MSA 1'. Fittingly, he recognized explicit similarities between PC and EBC. Both Upper and Lower samples of PC feature a high frequency of local quartzite. Both show a low proportion of retouched elements, the most common tool types being denticulates and notched pieces. Flakes are the preferred end-products. Most of the platforms of the blanks are not faceted, but rather plain or cortical. Cores are absent in the Lower sample, while the Upper sample contains minimal, radial and change of orientation cores (Volman 1981). Besides these other features, the most striking phenomenon of the assemblages is the appearance of "a high proportion of cobbles, slabs and even some large flakes with rather crude, alternating and/or bifacial retouch" (Volman 1984: 201) (Fig. 15). Following our analysis of the EBC assemblage, we hypothesize these artefacts to be similar to the orthogonal cores of the POL-reduction strategy rather than tools, due to the size as well as the angle of the removals and the implied percussion technique. The removals are relatively large and their angles are steep. Moreover, they were detached by applying direct hard-hammer percussion. However, a new analysis of the PC lithic material is necessary to confirm this hypothesis.

Bushman Rock Shelter (BRS), Limpopo, contains a long cultural sequence that is currently undated (Eloff 1969; Plug 1981; Badenhorst & Plug 2012; Underhill 2012; Porraz et al. 2015). Volman (1984) proposed that the lowermost levels 31–105 most probably belong to the 'MSA 1'. In these layers, formally retouched artefacts are rare or absent. Quartzite is used more frequently for blank production in these deposits than in the overlying strata, though it is not the dominant material. The blanks are in general short and thick (Volman 1981). Underhill (2012) published a comparative study of the lithics from layers 95–105, observing that knappers most frequently used quartz, followed by hornfels and quartzite. Retouched artefacts consist of notched pieces, denticulates and side scrapers. The reduction sequences include unidirectional and 'alternating platform cores' as well as one Discoid core, aiming towards the production of flakes, though a few blades occur (Underhill 2012). The production of flakes primarily of a short and thick morphology and the toolkit encompassing notched pieces and denticulates are features similar to EBC, but a more detailed

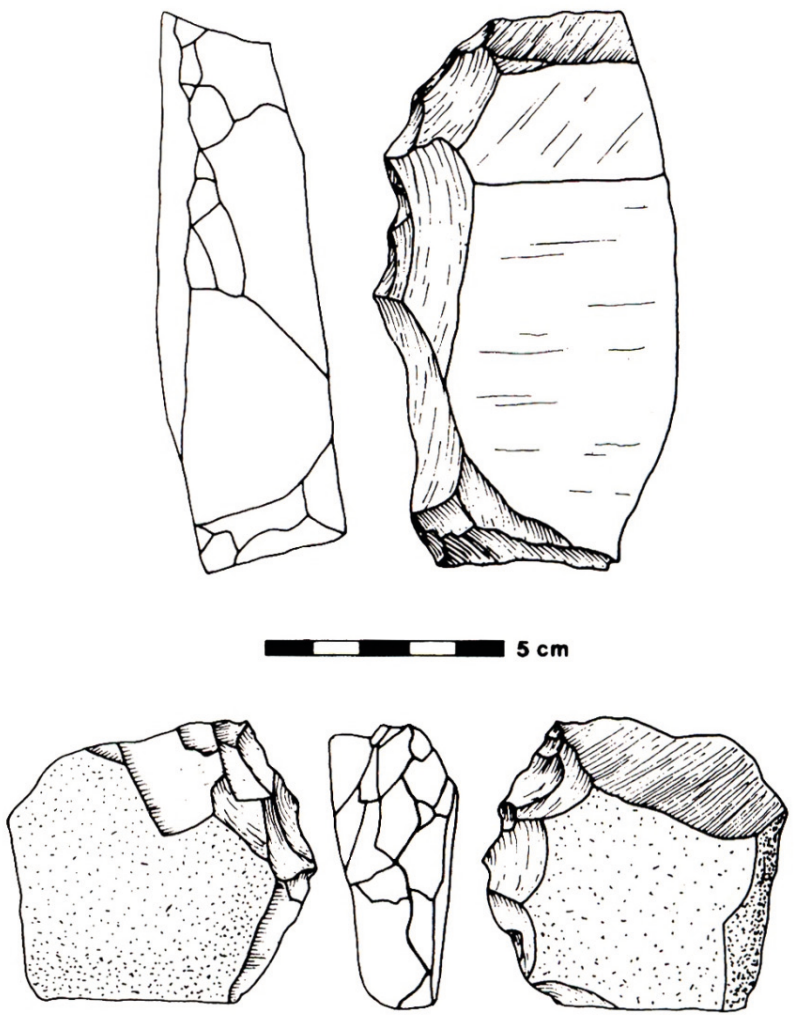

Fig. 15. Peers Cave: quartzite slabs reminiscent of the POL-reduction system as recognized at EBC. Top: orthogonal exploited core described as "slab with heavy-duty unifacial retouch"; bottom: orthogonal exploited core described as "weathered slab with heavy-duty bifacial retouch" (modified after Volman 1984: fig. 7).

technological study is required to confirm or reject the resemblances between these two industries.

The open-air site Duinefontein 2, Western Cape Province, was also originally assigned to the 'MSA 1' (Volman 1981, 1984), but has been reclassified as Earlier Stone Age (ESA) given the presence of Acheulean elements (Klein et al. 1999). Since Volman (1981, 1984) published his subdivision of the MSA, Thompson et al. (2010) have compared the Pinnacle Point 13B assemblages dating to MIS 6 (see below) with the 'MSA 1'. The low number of formal tools, relative frequencies of plain platforms and predominance of local quartzite are listed as similarities with the

'MSA 1' and consequently with EBC. However, some differences are pointed out, namely the presence of bladelet production and the relatively low quantity of "cores with convergent flake scar patterning" (Thompson et al. 2010: 372).

In our attempt to revise the definition of the 'MSA 1', several limitations that Volman (1981, 1984) himself identified still remain. First, the small sample size impedes a clear determination of significant features defining the techno-complex. Second, the large investigation area spanning South Africa hinders the comparability of assemblages. Third, a possible long time frame due to the lack of absolute dating compromises the integrity of the 'MSA 1' as a definite sub-stage of the MSA. Finally, Volman's analysis primarily relied on typological criteria, although he himself acknowledged that most MSA assemblages usually contain less than 1 % of formal tools and thus his approach has a high potential of for bias (Volman 1981, 1984). We assert that only a comprehensive study of variability in a regional context can enable a subsequent understanding of large-scale cultural phenomena and trajectories.

New radiometric ages, including TL and OSL, are essential to build a new chrono-cultural framework. In addition, more systematic studies of the lithic assemblages are required. Technological studies are superior to typological studies alone, since these involve whole assemblages and provide more detailed information about the way people adapted to their resources and transmitted their traditions (Inizan et al. 1999; Pelegrin 1991; Pigeot 1991; Soressi & Geneste 2011). Therefore, we agree with Volman, who insisted that his classificatory system was informal (Volman 1981, 1984) and argue that the 'MSA 1' lacks the preconditions of spatio-temporal relevancy to represent a homogeneous entity. We assert that the term 'MSA 1' should not be used anymore and rather substituted by the generic expression EMSA, understood here as all MSA industries dating back to the late Middle Pleistocene.

The lower MSA of EBC in a regional context

The lower MSA of EBC is bracketed by luminescence dates of 236 ka and 83 ka (see Tribolo et al. 2016 this issue). Due to the lack of good chronological control, we argue that its implicit assignment to the set of EMSA industries should be tested by chronologically more extensive technological comparisons. We first examine variability on a regional scale between MIS 5 assemblages.

Diepkloof Rock Shelter (DRS), Western Cape Province, is a particularly important site in this context, containing a long regional reference sequence of the MSA. DRS includes pre-SB occupations with notably a lithic assemblage that refers to the so-called MSA type 'Mike' (Porraz, Texier et al. 2013; Porraz, Texier et al. 2014). This MSA-Mike dates back to 118–90 ka according to Tribolo et al. (2013) and to 97.7–83.8 ka according to Jacobs and Roberts (2015). The MSA-Mike assemblage is dominated by local raw materials, predominantly quartzite. Formal tools are rare, mainly being notched pieces and denticulates. Different reduction sequences are present, oriented towards the production of triangular flakes, blades and flakes. Two distinct reduction strategies for the manufacture of triangular flakes occur. One falls within the range of Levallois points, while the other results in the production of triangular flakes with a triangular section that exhibit a unidirectional or orthogonal preparation ('accourcies' points). Additionally, there are semi-prismatic prepared cores aimed at the production of blades. Finally, a Levallois centripetal core reduction sequence yielded flakes, including the detachment of pseudo-Levallois points.

Interestingly, although DRS, with its long well-dated sequence of the MSA (Porraz, Texier et al. 2013; Tribolo et al. 2013), and EBC are located in close proximity to each other, none of the technological phases share any great similarities with the lower MSA of EBC. The MSA-Mike and EBC assemblages have a number of features in common: the exploitation of local quartzite and the low frequency of formal tools, mainly notched pieces and denticulates. However, they clearly differ in terms of reduction strategies and the aims of the reduction sequences.

Klasies River main site (KRM), Eastern Cape Province, represents another crucial site with a long, well-dated sequence of pre-SB deposits (Volman 1981, 1984; Singer & Wymer 1982; Wurz 2000, 2002; Wurz 2014). Two sub-stages of the MSA, originally named 'MSA I' and 'MSA II', are differentiated at KRM (Singer & Wymer 1982; Wurz 2002, 2013). With their pioneer definitions of the 'MSA I' and 'MSA II', Singer and Wymer (1982) intended only to describe the MSA sequence of KRM; they did not mean to establish a new classification scheme for southern Africa because of the uncertainty of its applicability to other sites (Singer & Wymer 1982). Sarah Wurz later performed a reanalysis of the lithic assemblages from the MSA sequence of KRM to clarify the validity of the sub-stages (Wurz 2000, 2002). The study confirmed the subdivision established by Singer and Wymer (1982); however, Wurz proposed formal designations and suggested in contrast to Singer and Wymer (1982) that the sub-stages are of relevance on a sub-continental scale (Wurz 2002). More recently, Lombard et al. (2012) published a revision of the South African and Lesotho Stone Age sequence and reaffirmed the 'Klasies River' ('MSA I') and the 'Mossel Bay' ('MSA II') as distinct techno-complexes within the MSA.

The 'MSA II' or 'Mossel Bay' dates between approximately 85–70 ka (Feathers 2002) and the reference assemblage from KRM occurs in the SAS and RF Members. The blades are shorter, thicker and more irregular than those from the 'MSA I' or 'Klasies River' sub-stage. Levallois points constitute end-products with carefully prepared platforms, regular dorsal scar patterns and a central ridge. Platform characteristics, such as often splintered bulbs, well-developed ripples and no dorsal thinning, imply the exclusive use of hard-hammer percussion. The reduction systems reflect unidirectional convergent and parallel Levallois methods. The small proportion of formal tools is dominated by denticulates and notched pieces (Wurz 2002, 2013; Lombard et al. 2012). Diepkloof MSA-Mike (see above) (Porraz, Texier et al. 2013), Blombos Cave (BBC) M3 phase (Douze et al. 2015) and Pinnacle Point 13B dating to MIS 5 (Thompson et al. 2010)—all sites from the Western Cape Province—are reminiscent of the 'MSA II' or 'Mossel Bay' of KRM, suggesting the existence of an unified techno-complex on at least a regional scale during MIS 5.

The 'MSA I' or 'Klasies River' ranges from ca. 115 to 110 ka (Feathers 2002) and the type assemblage is associated with the LBS and RBS Members at KRM (Wurz 2002; Lombard et al. 2012). This sub-stage is characterised by the exploitation of local raw materials and the production of blades and triangular flakes, of which around 30 % exhibit features associated with soft-hammer percussion. The blanks are relatively thin and symmetrical. Both a laminar and a unidirectional recurrent Levallois reduction system are present. The knappers exploited cobbles as pyramidal or flat cores and clearly invested in their preparation, indicated by the high frequency of end-products with faceted platforms. The small number of formal tools are dominated by denticulates and notched pieces (Wurz 2000, 2002, 2012).

The regional context of the MSA from MIS 5 is quite well-documented when compared to the preceding time periods. However, the lower MSA of EBC corresponds neither to 'MSA I' nor 'MSA II'. Indeed, the use of local raw materials and the low frequency of formal tools represent similarities. Yet the aim towards the production of blades and triangular flakes, involving a high investment in the preparation of the end-products, and the appearance of the Levallois method clearly differ from the lower MSA of EBC. Moreover, retouched points occur, whereas this tool type is completely absent at EBC.

In this context, Ysterfontein 1 (YFT), Western Cape Province, has to be mentioned (Halkett et al. 2003; Avery et al. 2008; Wurz 2012). Four OSL ages between 132.1 ± 8 and 120.6 ± 6.6 ka exist, but are considered to be too old since the MIS 5e sea level high stand must have flushed out all previous contents of the site. An age within MIS 5c–a is suspected (Avery et al. 2008). The artefacts from Groups 1–13 exhibit the same characteristics and therefore are considered as one assemblage (Wurz 2012). The majority of artefacts are made from silcrete, followed by calcrete, with both material types being locally available. The assemblage is characterised by a relatively high tool component dominated by denticulates, notched pieces and scrapers. Some tools exhibit a remarkably refined converging denticulation towards a point. The reduction sequence is oriented towards the manufacture of short flakes. The cores are minimally prepared and thick-sectioned blanks removing a part of the core edge are frequent. Most of the blanks show plain platforms (Halkett et al. 2003; Klein et al. 2004; Avery et al. 2008; Wurz 2012). YFT shares great similarities with two further coastal sites from the West Coast, Hoedjiespunt 1 (HDP1) and Sea Harvest (SH), suggesting either chronologically distinct or regional variants (Wurz 2012, 2013).

These three sites, YFT, HDP1 and SH, probably all dating to the Last Interglacial, strongly conform in technology as well as economy (Wurz 2013; Mackay et al. 2014; Douze et al. 2015). In comparison with EBC, obvious differences stand out with regard to the raw material economy. The main raw material at HDP1 is quartz, followed by calcrete and quartz porphyry. In addition to the local rock types, knappers also used semi-local or exotic silcrete, especially for tool production. The assemblages of YFT and SH are dominated by semi-local silcrete. These three sites clearly demonstrate a higher diversity of raw materials and the usage of rocks with better knapping qualities than at EBC. The high frequency of formal tools also strikes a clear contrast to EBC. However, all assemblages are flake based. Blades occur to a minor degree and triangular forms are almost absent. The cores and blanks demonstrate no or minimal preparation. The reduction sequences differ further, as the technical system of EBC does not include inclined core reduction.

Hollow Rock Shelter (HRS) and Klipfonteinrand (KLP) are inland sites in the Cederberg Mountains, thus differ substantially in context from EBC and the other coastal and near-coastal sites. Although the use of local quartzite is most frequent in HRS and KLP, as in the lower MSA of EBC, other rock types often of better knapping suitability make up a higher proportion of the assemblage. HRS and KLP also exhibit a low percentage of retouched pieces. However, unifacial points dominate the toolkit of KLP, whereas these are completely absent from EBC. The reduction sequence at HRS is oriented towards the production of flakes and blades mainly from radial cores, while the reduction strategy at KLP clearly aims to manufacture blades and triangular

flakes. Thus, both the HRS and KLP assemblages show distinctive features, but do not correspond to the technological tradition of EBC.

To summarize, we argue that EBC does not resemble any other MIS 5 industry identified in the Western and Eastern Cape Provinces. In particular, EBC differs from the 'MSA I' and 'MSA II' defined at KRM and recognized in other sites (see Lombard et al. 2012). At a closer regional scale, we also observe clear differences between the lithic assemblages of EBC and those of DRS, YFT, HDP1 and SH. The differences concern the raw material provisioning strategies, the reduction strategies and/or the types of formal tools, suggesting that EBC is an idiosyncratic technological expression at a regional scale in comparison with other MIS 5 industries.

As an exception, it is worth mentioning the site of PC, which exhibits some similar trends to EBC as previously noticed by Volman (1981). The assemblages consist mostly of products from local raw materials, systematically selected by knappers as part of their provisioning strategy. Past people invested in blank predetermination rather than modification of blanks into tools. The reduction sequence is oriented towards the production of flakes involving different methods. Core preparation is minimal to absent. According to Volman's publications, drawings and descriptions, we tentatively suggest that the POL-reduction strategy was an integral part of the technical system of PC. Certainly, a detailed technological analysis is needed to further verify our hypothesis. However, if it can be demonstrated that this reduction strategy represents a main characteristic of PC, the assemblages of EBC and PC could be interpreted as belonging to the same technological tradition in the region.

The comparison of EBC to the MSA sites of the wider region highlights that EBC belongs to a different technological tradition and shows only resemblance to the hitherto undated site PC. The implications of the comparison suggest, in terms of relative chronology, that EBC likely predates MIS 5, which is in accordance with the luminescence dates (Tribolo et al. 2016 this issue).

Comparisons with dated EMSA lithic assemblages from southern Africa

There are relatively few MIS 6 deposits in southern Africa that have been recently excavated, dated and studied. Thus, the comparison of the lower MSA of EBC with other MIS 6 lithic assemblages should be regarded as preliminary and does not pretend to encompass the whole range of variability. Our aim is to highlight the main technological trends that these MIS 6 assemblages exhibit and to better position the lower MSA of EBC within the bigger picture. For the following comparison, we excluded the sites with undated or disturbed deposits and/or with lithic assemblages that were questionable, such as Bundu Farm (Kiberd 2006), Lincoln Cave (Reynolds et al. 2007) and Sterkfontein (Post-Member 6 Infill: Ogola 2009). Table 14 provides however a large overview and presentation of sites preceding the SB from southern Africa.

Pinnacle Point 13B (PP13B), Mossel Bay, Western Cape Province, has three excavation areas that have yielded seven layers of the MSA (Marean et al. 2010; Thompson et al. 2010). The north-eastern area contains two layers, LC MSA Lower, with a weighted mean age of 162 ± 5 ka, and LC-MSA Upper/Middle, dated to 125 ± 5 ka. The western area comprises one MIS 6 assemblage from DB Sands 4 a–c with an age ranging from 166 to 134 ka (Marean et al. 2010). The MIS 6 assemblages of PP13B

share overall major similarities. All assemblages are dominated by local quartzite and also include quartz, both available as cobbles in the immediate surroundings of the site. After the local rock types, fine-grained silcrete is the next most common raw material and originates from semi-local gravels and conglomerates. In general, the transformation of the blanks by retouch is relatively low and takes various forms: bulbar thinning, notching, backing, denticulation, burin-like retouch and also bifacial retouch, though this is said to be rare. Blank production is dominated by flakes, a small number of which are Levallois. Blades and triangular flakes are present. Triangular flakes are more common in the layers from the western area, while in the other areas blades are most common (Thompson et al. 2010). Bladelet technology is also claimed to be present (Marean et al. 2007; Thompson et al. 2010). LC-MSA Lower is the only layer where the proportion of bladelets clearly exceeds 1 %. Plain platforms are slightly more common than faceted platforms. Many of the cores in the PP13B assemblage are highly reduced and evidence for significant core rejuvenation is also shown by technical core rejuvenation flakes. Irregular cores and prepared cores, which include Levallois cores, are the most common types.

The lower MSA of EBC and the assemblages of PP13B share similarities such as the use of local raw materials, the low proportion of tools and the dominance of flakes. However, major differences can be observed in the reduction strategies, the morphology of the blanks—triangular flakes appear to be more important at PP13B—and the set of formal tools that demonstrate a greater variability at PP13B.

Kathu Pan 1 (KP1), Northern Cape Province, contains a reworked MSA artefact-bearing stratigraphic unit, Stratum 3 (Porat et al. 2010; Wilkins 2013). This deposit provides an OSL age estimate of 291 ± 45 ka (Porat et al. 2010). The assemblage is dominated by flake production, including Levallois flakes. Blades comprise less than 4 % of all lithic artefacts, and unifacial as well as bifacial points are present (Wilkins 2013). These retouched points and the use of the Levallois method are significant differences between the KP1 and EBC assemblages.

Florisbad (FL), Free State, comprises three different assemblages of the MSA that are of interest in the context of our paper (Kuman 1989; Kuman et al. 1999). The basal deposits N, O, P, associated with a hominid cranium (Dreyer 1935; Rightmire 1978; Clarke 1985), yielded the oldest but only a small assemblage dated between 327 and 208 ka, based on a combination of ESR and OSL (Grün 2006; Herries 2011). The raw materials used are more varied than in the subsequent layers: igneous rocks, hornfels and to a minor degree quartzite. Very few formal tools are present. Blank production is flake-oriented with a high proportion of broad, side-struck flakes. Multi-platform cores are most frequent (Kuman et al. 1999). The following Unit M was dated by OSL to 157 ± 21 ka (Grün et al. 1996). Hornfels is the main raw material. The assemblage contains a significant amount of tools, including mainly medium-sized side scrapers. Flakes were produced by exploiting different core types, such as single and multi-platform cores, Discoid and Levallois cores. Sampson (1974) termed these lithic artefacts of Unit M the 'Florisbad Industry', emphasizing that it presented the first sealed, unselected assemblage of highly retouched MSA in the region. The archaeologically rich Unit F was dated to 121 ± 6 ka using ESR, and 133 ± 31 ka and 128 ± 22 ka using OSL (Grün et al. 1996). Hornfels is the most common rock type. Formal tools, including minimally retouched cutting tools, side scrapers and burins,

occur in very low frequencies. Laminar flakes and triangular flakes together make up a large proportion of all complete blanks over 2 cm. Most of the blanks have plain platforms, followed by faceted or dihedral platforms. The majority of cores are multi-platform but prepared cores for producing triangular flakes are present (Kuman 1989).

The assemblages of FL are relatively small. However, the basal layers N, O, P include only a few formal tools and the manufacturing of flakes is dominant, conforming to the lower MSA of EBC. By contrast, the multi-platform cores are indicative of another reduction sequence. Unit M clearly differs from EBC due to the high proportion of tools and the presence of Discoid and Levallois methods. The assemblage of Unit F comprises triangular flakes coming from prepared cores and includes different tool types, albeit in low proportions, as seen in the lower MSA of EBC.

Border Cave (BC), KwaZulu-Natal, yielded several MSA deposits, with associated human remains (Beaumont et al. 1978; Grün et al. 1990; Grün & Beaumont 2001; Grün 2006). The layers 4BS, 4WA, 5BS and 5WA contain assemblages classified as pre-HP Pietersburg (Beaumont et al. 1978; Grün & Beaumont 2001; Wadley 2007). Beaumont et al. (1978), as well as Volman (1981), highlight similarities between these assemblages from Border Cave and those at KRM (see below). In broad agreement with U-series, amino acid epimerization (AAR) and TL dating, the results from ESR show that these strata date between 238 and 80 ka (Grün & Beaumont 2001; Grün 2006). Felsite is the dominant raw material. Retouched pieces are rare, and the most frequent tool types are bifacial, unifacial and laterally retouched points. Flakes and blades were produced as well as an abundance of triangular flakes. Some of the blades are of large dimensions. Evidence for the use of the Levallois method is observed (Eggers 1970; Sampson 1974; Beaumont et al. 1978). The assemblages share similarities with the undated Beds 5–9 at the Cave of Hearths (CH) which are identified as Middle to Upper Pietersburg (Sampson 1974; Beaumont et al. 1978).

Wonderwerk Cave (WK), Northern Cape Province, is a large solution cavity in the Kuruman Hills-Asbestos Mountains (Beaumont & Vogel 2006; Chazan & Horwitz 2009). Peter B. Beaumont (McGregor Museum) and colleagues excavated seven areas, Excavation 1–7, inside the cave yielding a great quantity of lithic and organic remains from the ESA, MSA and Later Stone Age (LSA) (Chazan & Horwitz 2009). The lithic assemblages of Major Unit (MU) 2 belong to the MSA (Beaumont & Vogel 2006). With regard to the age of MU 2, Beaumont and Vogel (2006: Tab. 2) published 12 U-series dates ranging from 234 to 74 ka. However, the relationship between the dated stalagmite from the top part of the MSA layers in Excavation 2 with an age of 234–206 ka and the deposits themselves is not clear. On the one hand, water activity definitely occurred at the site and could have moved it from elsewhere into the deposits; on the other hand, a stalagmite from a lower part of the section is dated to between 182 and 154 ka (Herries 2011). The best age estimation of the MSA layers of Wonderwerk Cave ranges from 182 to 118 ka, excluding the date from Excavation 6 and the Excavation 2 age of 234–206 ka; however, it remains unclear why the three dates younger than 100 ka are also excluded (see Herries 2011; Lombard et al. 2012). The lithic assemblage is dominated by prepared core technology, including large Levallois cores. Moreover, the manufacture of blades is present and Levallois, unifacial and bifacial points occur. These features are again typical for the Middle to Upper Pietersburg known from Beds 5–9 at CH (Beaumont & Vogel 2006).

Both BC and WK resemble Beds 5–9 of CH (Table 14D) and are assigned to the Pietersburg techno-complex (Sampson 1974), whose assignation to the MIS 6 and/or MIS 5 still requires clarification. They share features, such as the production of large elongated elements with the Levallois method, and the production of unifacial and bifacial points. In that regard, the lithic assemblages from BC and WK differ from the lower MSA of EBC.

The lower MSA from EBC within the context of the southern African MSA

Our short review of the archaeological record from the MSA of MIS 6 and 5 shows that the data are very diverse in many respects (Table 14). In the following section, we extend our scope and compare EBC with other MSA sites in southern Africa. We focus on comparisons between raw material use, retouch, and reduction sequences.

In general, all of the assemblages from MSA sites, either pre-dating or dating to MIS 5 before the Still Bay, show a dominance of local raw materials (Table 14) (see also Mackay et al. 2014). However, the knapping suitability of these rock types is variable and offers different preconditions for the manufacturing of blanks. Other sites, including BC and FL (Table 14C), had access to fine-grained raw materials in their proximity. The choice of raw materials represents the first stage in the technological system and affects the subsequent stages of blank production.

Moreover, another important distinguishing feature is the frequency of modification by retouch and the types of tools produced. The overall percentage differs between the assemblages, though a general trend can be observed that formal tools rarely exceed a proportion of 10 % (Table 14). The most common tool types are denticulates and notched pieces. Different types of side scrapers as well as various laterally retouched pieces also occur at some sites. Retouched triangular flakes (points), which are completely absent in the MSA of EBC, represent a part of the toolkits from the KRM, BBC as well as possibly PP13B and Nelson Bay Cave (see also Douze et al. 2015). In contrast to EBC, CH (mainly the assemblages assigned to the Later Pietersburg) (Table 14D), as well as BC and WK (which are considered to resemble the Later Pietersburg of CH) (Table 14C) comprise unifacial and bifacial points. Bifacial technology occurs also in KP1.

In explaining the low frequency of retouched tools, in general it seems that during MIS 6 and 5, MSA people invested in controlling blank morphology rather than subsequent modification of blanks into tools. Insofar as we could glean the information from the literature, the significance of slabs and large flakes as original core morphologies is not described for any other MSA assemblages, apart from possibly PC (see above). KRM, BBC, PP13B, Nelson Bay Cave, Cape St. Blaize and layer F of FL clearly differ from EBC, as these assemblages contain reduction sequences oriented towards the production of triangular flakes documented by prepared cores attested by core preparation and end-products (see also Douze et al. 2015) (Table 14). The Namibian sites of earlier MSA phases, including Aar 2, Apollo 11, Bremen 1C, Bremen 2B and Etemba 14 (Table 14D), demonstrate different reduction strategies and in contrast to EBC, the Discoid method is of great importance. The Levallois method played a role at Varsche Rivier 003, CH, BC, WK and Swartkrans Cave, however inhabitants of EBC did not use this method to produce predetermined blanks.

The whole corpus of dated EMSA industries consists of only a few sites, as stated above, and even some of these are highly problematic due to probable mixing, unclear stratigraphic correlations and unsecure chronology. They still show some general trends concerning the predominant use of local raw materials and the low frequency of formal tools. Nevertheless, we notice that various distinctive reduction systems have been described in the literature, which could either reflect different regional adaptations or traditions, or different phases within the EMSA. EBC stands out with its slab reduction strategy and the predetermination given by the original core blanks and not by the preparation of the cores. Based on the current set of published data, we argue that the lower MSA of EBC share some similarities with other MIS 6 industries and that the lower MSA of EBC should be viewed as one technological expression within the southern African EMSA.

CONCLUSION

The technological analysis of the lower MSA of EBC shows that this assemblage is clearly technologically distinctive despite the absence of typological markers. The so-called POL-reduction strategy was identified as the main defining characteristic. This reduction strategy is based on the exploitation of local quartzite slabs. Although past inhabitants of the rock shelter neither depended on this rock type, nor on this specific original core morphology, they specifically selected slabs and large flakes of quartzite. Therefore, the process of raw material selection represented a key phase in their technological system and had clear intended impact on blank production. The reduction of the three planes of these slab cores led to the manufacture of rectangular to trapezoidal short or elongated blanks, without investment in core preparation. The knappers gained further control of the reduction by integrating two percussion techniques: direct hard-hammer and bipolar-on-anvil percussion.

Our comparison with other MSA assemblages shows that the technical system at EBC differs from Late Pleistocene assemblages with regard to the reduction sequences and the aims of the blank production. This appears most clearly when comparing EBC with the neighbouring site of DRS, as well as with the well-studied MIS 5 sequence of KRM. Based on the current state of data, we argue that the lower MSA of EBC belongs to the corpus of EMSA industries.

Volman (1981, 1984) suggested previously that the EBC assemblage is part of an independent techno-complex which he referred to as 'MSA 1'. Although we advocate that the term 'MSA 1' should no longer be used, we tentatively confirm the similarities between EBC and PC and propose the POL-reduction system as the defining element shared by both.

Since Volman's (1981, 1984) publication of the subdivision of the MSA of southern Africa, multiple new attempts have been made to revise the sequence, defining the characteristics of the sub-stages of the MSA preceding the SB (Herries 2011; Lombard et al. 2012; Mackay et al. 2014; Wurz 2014). In spite of this, we argue that at present, a number of difficulties—such as the paucity of excavation projects, technological analyses and absolute dates—impede our ability to build a secure chrono-cultural framework of the EMSA on a sub-continental scale. Rather, we claim to follow a heuristic approach, like others have done before (e.g. Herries 2011; Wurz 2013; Mackay

et al. 2014; Wurz 2014), and identify the main trends of adaptations and changes of AMHs on a regional scale. The EMSA of EBC is thus seen as a specific adaptation. Only a few sites from this time period are interrelated and it remains unclear whether this phenomenon is due to preservation, study bias or lower population densities.

ACKNOWLEDGEMENTS

We thank the Iziko Museum for granting the permission to study the lithic material. We thank the University of Cape Town and especially Judith Sealy for offering space to analyse the lithic artefacts. We also thank Emily Hallinan for the English editing. This research was part of the project "The lithic technology of the Early Middle Stone Age in southern Africa" (Grant number: 17091015) funded by the DFG (German Research Foundation). It also benefited from the support of the French ministry of foreign affairs. We finally thank Sarah Wurz, Katja Douze and a third anonymous reviewer, who contributed to enhance the manuscript.

REFERENCES

Avery, G., Halkett, D.J., Orton, J., Steele, T., Tusenius, M. & Klein, R.G. 2008. The Ysterfontein 1 Middle Stone Age Rock Shelter and the evolution of coastal foraging. *South African Archaeological Society Goodwin Series* **10**: 66–89.

Badenhorst, S. & Plug, I. 2012. The faunal remains from the Middle Stone Age levels of Bushman Rock Shelter in South Africa. *South African Archaeological Bulletin* **67**: 16–31.

Beaumont, P.B., de Villiers, H. & Vogel, J.C. 1978. Modern man in sub-Saharan Africa prior to 49 000 years B.P.: a review and evaluation with particular reference to Border Cave. *South African Journal of Science* **74**: 409–19.

Beaumont, P.B. & Vogel, J.C. 2006. On a timescale for the past million years of human history in central South Africa. *South African Journal of Science* **102**: 217–28.

Boëda, É. 1993. Le débitage Discoïde et le débitage Levallois récurrent centripète. *Bulletin de la Société Préhistorique Française* **90**: 392–404.

Boëda, É. 1994. *Le concept Levallois: variabilité des méthodes*. Paris: Édition du CNRS.

Boëda, É. 1995. Steinartefakt-Produktionssequenzen im Micoquien der Kulna-Höhle. *Quartär* **45–46**: 75–98.

Boëda, É., J.-M. Geneste & L. Meignen 1990. Identification de chaînes opératoires lithiques du Paléolithique ancien et moyen. *Paléo* **2**: 43–80.

Brink, J.S. & Deacon, H.J. 1982. A study of a last interglacial shell midden and bone accumulation at Herolds Bay, Cape Province, South Africa. *Palaeoecology of Africa* **15**: 31–9.

Butzer, K.W. 1979. Geomorphology & geo-archaeology at Elandsbaai, Western Cape, South Africa. *Catena* **6**: 157–66.

Butzer, K.W. 2004. Coastal eolian sands, paleosols, and Pleistocene geoarchaeology of the Southwestern Cape, South Africa. *Journal of Archaeological Science* **31**: 1743–81.

Cahen, D. 1976. Das Zusammensetzen geschlagener Steinartefakte. *Archäologisches Korrespondenzblatt* **6**: 81–93.

Carmignani, L. 2010. L'industria litica del livello FIIIe di Grotta Del Cavallo Nardò, Lecce. Osservazioni su una produzione lamino-lamellare in un contesto del Musteriano Finale. *Origini XXXII* **Nuova Serie IV**: 7–26.

Cartwright, C.R. 2013. Identifying the woody resources of Diepkloof Rock Shelter (South Africa) using scanning electron microscopy of the MSA wood charcoal assemblages. *Journal of Archaeological Science* **40**: 3463–74.

Chase, B.M. & Thomas, D.S.G. 2006. Late Quaternary dune accumulation along the western margin of South Africa: distinguishing forcing mechanisms through the analysis of migratory dune forms. *Earth and Planetary Science Letters* **251**: 318–33.

Chazan, M. & Horwitz, L.K. 2009. Milestones in the development of symbolic behaviour: a case study from Wonderwerk Cave, South Africa. *World Archaeology* **41**: 521–39.

Clark, J.D. 1988. The Middle Stone Age of East Africa and the beginnings of regional identity. *Journal of World Prehistory* **2**: 235–305.

Clarke, R.J. 1985. A new reconstruction of the Florisbad cranium with notes on the site. *Ancestors: the hard evidence* **301**: 305.

Coertze, F.J. 1984. *Cape Town and environs*. Explanation: Sheet Maps (1:50 000) 3318 CD and DC, 3418 AB, AD and BA. Geological Survey. Department of Mineral and Energy Affairs, p. 77.

Conard, N.J. 2008. A critical view of the evidence for a southern African origin of behavioral modernity. *South African Archaeological Society Goodwin Series* **10**: 175–9.
Cziesla, E., Eickhoff, S., Arts, N. & Winter, D. 1990. *The big puzzle*. Bonn: Holos Verlag.
d'Errico, F., Backwell, L.R. & Wadley, L. 2012. Identifying regional variability in Middle Stone Age bone technology: The case of Sibudu Cave. *Journal of Archaeological Science* **39**: 2479–95.
Dewar, G. & Stewart, B.A. 2012. Preliminary results of excavations at Spitzkloof Rockshelter, Richtersveld, South Africa. *Quaternary International* **270**: 30–9.
Dibble, H.L. & McPherron, S.P. 2006. The missing Mousterian. *Current Anthropology* **47**: 777–803.
Douze K., Wurz, S. & Henshilwood, C.S. 2015. Techno-cultural characterization of the MIS 5 (c. 105–90 Ka) lithic industries at Blombos Cave, Southern Cape, South Africa. *Plos One* **10** (11): e0142151. doi:10.1371/journal.pone.0142151
Dreyer, T.F. 1935. A human skull from Florisbad, Orange Free State, with a note on the endocranial cast, by C. U. Ariens Kappers. *Proceedings of the Academy of Science of Amsterdam* **38**: 119–28.
Eggers, V. 1970. *Border Cave*. PhD thesis, University of California, Berkeley.
Eloff, J.F. 1969. Bushman Rock Shelter, Eastern Transvaal: excavations, 1967–68. *South African Archaeological Bulletin* **24**: 60.
Evans, U. 1994. Hollow Rock Shelter, a Middle Stone Age site in the Cederberg. *Southern African Field Archaeology* **3**: 63–73.
Feathers, J.K. 2002. Luminescence dating in less than ideal conditions: case studies from Klasies River main site and Duinefontein, South Africa. *Journal of Archaeological Science* **29**: 177–94.
Forestier, H. 1993. Le Clactonien: mise en application d'une nouvelle méthode de débitage s'inscrivant dans la variabilité des systèmes de production lithique du Paléolithique ancien. *Paléo* **5**: 53–82.
Geneste, J.-M. 1985. *Analyse lithique d'industries moustériennes du Périgord: approche technologique du comportement des groupes humaine au Paléolithique moyen*. PhD thesis, Université de Bordeaux.
Geneste, J.-M. 1988. Systèmes d'approvisionnement en matières premières au Paléolithique moyen et supérieur en Aquitaine. In: M. Otte, ed., *L'Homme de Néandertal*. Liège: ERAUL, pp. 61–70.
Geneste, J.-M. 1991. Systèmes techniques de production lithique: variations techno-économiques dans les processus de réalisation des outillages paléolithiques. *Techniques et culture* **17**: 1–35.
Geneste, J.-M., 1992. L'approvisionnement en matières premières dans les systèmes de production lithique: la dimension spatiale de la technologie. In: R. Mora, X. Terradas, A. Parpal & C. Plana, eds, *Tecnologia y cadenas operativas liticas*. Barcelona: Treballs d'Arqueologia, Universitat Autonòma de Barcelona, pp. 1–36.
Goodwin, A.J.H. & Van Riet Lowe, C. 1929. The Stone Age cultures of South Africa. *Annals of the South African Museum* **27**: 1–289.
Grine, F.E. & Klein, R.G. 1993. Late Pleistocene human remains from the Sea Harvest site, Saldanha Bay, South Africa. *South African Journal of Science* **89**: 145–52.
Grün, R. 1996. Direct dating of Florisbad hominid. *Nature* **382**: 500–1.
Grün, R. 2006. Direct dating of human fossils. *Yearbook of Physical Anthropology* **49**: 2–48.
Grün, R. & Beaumont, P.B. 2001. Border Cave revisited: a revised ESR chronology. *Journal of Human Evolution* **40**: 467–82.
Grün, R., Beaumont, P.B. & Stringer, C.B. 1990. ESR dating evidence for early modern humans at Border Cave in South Africa. *Nature* **344**: 537–39.
Halkett, D.J., Hart, T., Yates, R.J., Volman, T.P., Parkington, J.E., Orton, J., Klein, R.G., Cruz-Uribe, K. & Avery, G. 2003. First excavation of intact Middle Stone Age layers at Ysterfontein, Western Cape Province, South Africa: implications for Middle Stone Age ecology. *Journal of Archaeological Science* **30**: 955–71.
Hendey, Q.B. & Volman, T.P. 1986. Last interglacial sea levels & coastal caves in the Cape Province, South Africa. *Quaternary Research* **25**: 189–98.
Henshilwood, C.S., d'Errico, F., Yates, R.J., Jacobs, Z., Tribolo, C., Duller, G.A.T., Mercier, N., Sealy, J.C., Valladas, H., Watts, I. & Wintle, A.G. 2002. Emergence of modern human behavior: Middle Stone Age engravings from South Africa. *Science* **295:** 1278–80.
Henshilwood, C.S. & Marean, C.W. 2003. The origin of modern human behavior: critique of the models and their test implications. *Current Anthropology* **44**: 627–51.
Herries, A.I.R. 2011. A chronological perspective on the acheulian and its transition to the Middle Stone Age in southern Africa: the question of the Fauresmith. *International Journal of Evolutionary Biology* **30** 1–25.
Högberg, A. & Larsson, L. 2011. Lithic technology and behavioural modernity: new results from the Still Bay site, Hollow Rock Shelter, Western Cape Province, South Africa. *Journal of Human Evolution* **61**: 133–55.

Inizan, M.-L., Reduron-Ballinger, M., Roche, H. & Tixier, J. 1999. *Technology of knapped stone*. Nanterre: CREP.

Jacobs, Z., Duller, G.A.T., Wintle, A.G. & Henshilwood, C.S. 2006. Extending the chronology of deposits at Blombos Cave, South Africa, back to 140 ka using optical dating of single & multiple grains of quartz. *Journal of Human Evolution* **51**: 255–73.

Jacobs, Z. & Roberts, R.G. 2015. An improved single grain OSL chronology for the sedimentary deposits from Diepkloof Rockshelter, Western Cape, South Africa. *Journal of Archaeological Science* **63**: 175–92.

Kiberd, P. 2006. Bundu Farm: a report on archaeological and palaeoenvironmental assemblages from a pan site in Bushmanland, Northern Cape, South Africa. *South African Archaeological Bulletin* **61**: 189–201.

Klein, R.G. 2001. Southern Africa and modern humans origins. *Journal of Anthropological Research* **57**: 1–16.

Klein, R.G., Avery, G., Cruz-Uribe, K., Halkett, D., Hart, T., Milo, R.G. & Volman, T.P. 1999. Duinefontein 2: an Acheulean site in the Western Cape Province of South Africa. *Journal of Human Evolution* **37**: 153–90.

Klein, R.G., Avery, G., Cruz-Uribe, K., Halkett, D.J., Parkington, J.E., Steele, T., Volman, T.P. & Yates, R.J. 2004. The Ysterfontein 1 Middle Stone Age site, South Africa, and early human exploitation of coastal resources. *Proceedings of the National Academy of Sciences of the United States of America* **101**: 5708–15.

Kuhn, S.L. 1995. *Mousterian lithic technology: an ecological perspective*. Princeton: Princeton University Press.

Kuman, K.A. 1989. *Florisbad and ≠Gi: the contribution of open-air sites to study of the Middle Stone Age in southern Africa*. PhD thesis, University of Pennsylvania.

Kuman, K.A., Inbar, M. & Clarke, R.J. 1999. Palaeoenvironments and cultural sequence of the Florisbad Middle Stone Age hominid site, South Africa. *Journal of Archaeological Science* **26**: 1409–25.

Lombard, M., Wadley, L., Deacon, J., Wurz, S., Parsons, I., Mohapi, M., Swart J. & Mitchell, P. 2012. South African and Lesotho Stone Age sequence updated I. *South African Archaeological Bulletin* **67**: 120–44.

Mackay, A., Stewart, B.A. & Chase, B.M. 2014. Coalescence and fragmentation in the late Pleistocene archaeology of southernmost Africa. *Journal of Human Evolution* **72**: 1–26.

Marean, C.W., Bar-Matthews, M., Bernatchez, J., Fisher, E., Goldberg, P., Herries, A.I.R., Jacobs, Z., Jerardino, A., Karkanas, P., Minichillo, T., Nilssen, P.J., Thompson, E., Watts, I. & Williams, H.M. 2007. Early human use of marine resources and pigment in South Africa during the Middle Pleistocene. *Nature* **449**: 905–8.

Marean, C.W., Matthews, M., Fisher, E., Goldberg, P., Herries, A.I.R., Karkanas, P., Nilssen, P.J. & Thompson, E. 2010. The stratigraphy of the Middle Stone Age sediments at Pinnacle Point Cave 13B (Mossel Bay, Western Cape Province, South Africa). *Journal of Human Evolution* **59**: 234–55.

Mason, R.J. 1962. *Prehistory of the Transvaal*. Johannesburg: Witwatersrand University Press.

McBrearty, S. & Brooks, A.S. 2000. The revolution that wasn't: a new interpretation of the origin of modern human behavior. *Journal of Human Evolution* **39**: 453–563.

McBrearty, S. & Tryon, C.A. 2005. From Acheulean to Middle Stone Age in the Kapthurin Formation, Kenya. In: E. Hovers & S.L. Kuhn, eds., *Transitions before the Transition*. New York: Springer, pp. 257–77.

McNabb, J. & Sinclair, A. 2009. *The Cave of Hearths: Makapan Middle Pleistocene research project: field research by Anthony Sinclair and Patrick Quinney, 1996–2001*. Oxford: Archaeopress.

Miller, C.E., Mentzer, S., Porraz, G. 2016. Site-formation processes of the Middle Stone Age deposits from Elands Bay Cave, South Africa. *Southern African Humanities* **29**: 69–128.

Miller, D. 1987. Geoarchaeology at Verlorenvlei. In: J.E. Parkington & M. Hall, eds, *Papers in the Prehistory of the Western Cape, South Africa*. Oxford: B.A.R., pp. 46–77.

Mitchell, P. 2002. *The archaeology of southern Africa*. Cambridge: Cambridge University Press.

Mourre, V., Jarry, M., Colonge, D. & Lelouvier, L.A. 2011. Le débitage sur enclume aux Bosses Lamagdelaine, Lot, France: La percussion directe au percuteur dur et la diversité de ses modalités d'application. *Paléo* **numéro spécial**: 49–62.

Mourre, V., Villa, P. & Henshilwood, C.S. 2010. Early use of pressure flaking on lithic artifacts at Blombos Cave, South Africa. *Science* **330**: 659–62.

Nigst, P.R. 2012. *The early Upper Palaeolithic of the Middle Danube Region*. Leiden: Leiden University Press.

Ogola, C.A. 2009. *The Sterkfontein western breccias: stratigraphy, fauna & artefacts*. PhD thesis, University of the Witwatersrand, Johannesburg.

Parkington, J.E. 1981. The effects of environmental change on the scheduling of visits to the Elands Bay Cave, Cape Province, South Africa. In: I. Hodder, G. Isaac & N. Hammond, eds, *Pattern of the past: studies in honour of David Clarke*. Cambridge: Cambridge University Press, pp. 341–59.

Parkington, J.E. 2001. Milestones: the impact of systematic exploitation of marine foods on human evolution. In: P.V. Tobias, M.A. Raath, J. Moggi-Cechi & G.A. Doyle, eds, *Humanity from African naissance to coming millenia*. Florence: Florence University Press, pp. 327–36.

Parkington, J.E. 2016. Elands Bay Cave: keeping an eye on the past. *Southern African Humanities* **29**: 17–32.

Pelegrin, J. 1991. Sur une recherche technique expérimentale des techniques de débitage laminaire et quelques résultats. In: *Archéologie expérimentale. Tome 2. La Terre*. Actes du Colloque International «Expérimentation en archéologie: bilan et perspectives», (Archéodrome de Beaune, 6–9 avril 1988). Paris: Editions Errance, pp. 118–28.

Pigeot, N. 1991. Réflexions sur l'histoire technique de l'homme: de l'évolution cognitive à l'évolution culturelle. *Paléo* **3**: 167–200.

Plug, I. 1981. Bushman Rock Shelter. In: E.A. Voigt, ed., *Guide to archaeological sites in the Northern and Eastern Transvaal*. Prepared for the Southern African Association of Archaeologists excursion, 6–11 June, pp. 111–31.

Porat, N., Chazan, M., Grün, R., Aubert, M., Eisenmann, V. & Horwitz, L.K. 2010. New radiometric ages for the Fauresmith industry from Kathu Pan, southern Africa: implications for the Earlier to Middle Stone Age transition. *Journal of Archaeological Science* **37**: 269–83.

Porraz, G., Parkington, J.E., Rigaud, J.-P., Miller, C.E., Poggenpoel, C., Tribolo, C., Archer, W., Cartwright, C.R., Charrié-Duhaut, A., Dayet, L., Igreja, M., Mercier, N., Schmidt, P.,Verna, C. & Texier, P.-J. 2013. The MSA sequence of Diepkloof and the history of southern African Late Pleistocene populations. *Journal of Archaeological Science* **40**: 3542–52.

Porraz, G., Schmid, V., Miller, C.E., Tribolo, C., Cartwright, C., Charrié-Duhaut, A., Igreja, M., Mentzer, S., Mercier, N., Schmidt, P., Conard, N., Texier, P.-J. & Parkington, J.E.. 2016. Update on the 2011 excavation at Elands Bay Cave (South Africa) and the Verlorenvlei Stone Age. *Southern African Humanities* **29**: 33–68.

Porraz, G., Texier, P.-J., Archer, W., Piboule, M., Rigaud, J.-P. & Tribolo, C. 2013. Technological successions in the Middle Stone Age sequence of Diepkloof Rock Shelter, Western Cape, South Africa. *Journal of Archaeological Science* **40**: 3376–400.

Porraz, G., Texier, P. J., & Miller, C. M. 2014. Le complexe bifacial Still Bay et ses modalités d'émergence à l'abri Diepkloof (Middle Stone Age, Afrique du Sud). In: *Transitions, ruptures et continuité en Préhistoire*. XXVII^{ème} congrès préhistorique de France, Bordeaux-les Eyzies, 31 mai-5 juin 2010. Mémoires de la Société Préhistorique Française, pp. 155–75.

Porraz, G., Texier, P.-J., Rigaud, J.-P., Parkington, J.E., Poggenpoel, C. & Roberts, D.L. 2008. Preliminary characterization of an MSA lithic assemblage preceding the classic Howiesons Poort complex at Diepkloof Rock Shelter, Western Cape Province, South Africa. *South African Archaeological Society Goodwin Series* **10**: 105–21.

Porraz, G., Val, A., Dayet, L., de La Peña, P., Douze, K., Miller, C.E., Murungi, M., Tribolo, C., Schmid, V.C. & Sievers, C. 2015. Bushman Rock Shelter Limpopo, South Africa: a perspective from the edge of the Highveld. *South African Archaeological Bulletin* **70**: 166–79.

Reynolds, S.C., Clarke, R.J. & Kuman, K.A. 2007. The view from the Lincoln Cave: mid- to late Pleistocene fossil deposits from Sterkfontein hominid site, South Africa. *Journal of Human Evolution* **53**: 260–71.

Rightmire, G.P. 1978. Florisbad & human population succession in southern Africa. *American Journal of Physical Anthropology* **48**: 475–86.

Roberts, D.L., Bateman, M.D., Murray-Wallace, C.V., Carr, A.S. & Holmes, P.J. 2009. West coast dune plumes: climate driven contrasts in dunefield morphogenesis along the western and southern South African coasts. *Palaeogeography, Palaeoclimatology, Palaeoecology* **271**: 24–38.

Sampson, C.G. 1974. *The Stone Age archaeology of southern Africa*. London: Academic Press.

Schmidt, I. 2011. A Middle Stone Age assemblage with discoid lithic technology from Etemba 14, Erongo mountains, northern Namibia. *Journal of African Archaeology* **9**: 85–100.

Singer, R. & Wymer, J.J. 1982. *The Middle Stone Age at Klasies River Mouth in South Africa*. Chicago: University of Chicago Press.

Soressi, M. & Geneste, J.-M. 2011. The history and efficacy of the *chaîne opératoire* approach to lithic analysis: studying techniques to reveal past societies in an evolutionary perspective. *Paleoanthropology* **Special Issue**: 334–50.

Steele, T., Mackay, A., Orton, J. & Schwortz, S. 2012. Varsche Rivier 003, a new Middle Stone Age site in southern Namaqualand, South Africa. *South African Archaeological Bulletin* **67**: 108–19.

Texier, P.-J., Porraz, G. Parkington, J.E., Rigaud, J.-P., Poggenpoel, C., Miller, C.E., Tribolo, C., Cartwright, C.R., Coudenneau, A., Klein, R.G., Steele, T. & Verna, C. 2010. A Howiesons Poort tradition of engraving ostrich eggshell containers dated to 60 000 years ago at Diepkloof Rock Shelter, South Africa. *Proceedings of the National Academy of Sciences of the United States of America* **107**: 6180–85.

Thackeray, A.I. & Kelly, A.J. 1988. A technological & typological analysis of Middle Stone Age assemblages antecedent to the Howiesons Poort at Klasies River main site. *South African Archaeological Bulletin* **43**: 15–26.

Thompson, E. & Marean, C.W. 2008. The Mossel Bay lithic variant: 120 years of Middle Stone Age research from Cape St Blaize Cave to Pinnacle Point. *South African Archaeological Society Goodwin Series* **10**: 90–104.

Thompson, E., Williams, H.M. & Minichillo, T. 2010. Middle & late Pleistocene Middle Stone Age lithic technology from Pinnacle Point 13B (Mossel Bay, Western Cape Province, South Africa). *Journal of Human Evolution* **59**: 358–77.

Tribolo, C., Mercier, N., Douville, E., Joron, J.-L., Reyss, J.-L., Rufer, D., Cantin, N., Lefrais, Y., Miller, C.E:, Parkington, J.E., Porraz, G., Rigaud, J.-P. & Texier, P.-J. 2013. OSL and TL dating of the Middle Stone Age sequence of Diepkloof Rock Shelter Western Cape, South Africa: a clarification. *Journal of Archaeological Science* **40**: 3401–11.

Tribolo, C., Mercier, N., Selo, M., Valladas, H., Joron, J.-L., Reyss, J.-L., Henshilwood, C.S., Sealy, J.C. & Yates, R.J. 2006. TL dating of burnt lithics from Blombos cave South Africa: Further evidence for the antiquity of modern human behaviour. *Archaeometry* **48**: 341–57.

Tribolo, C., Mercier, N., Valladas, H., Miller, C.E., Parkington, J.E. & Porraz, G. 2016. Chronology of the Pleistocene deposits at Elands Bay Cave (South Africa) based on charcoals, burnt lithics, and sedimentary quartz and feldspar grains. *Southern African Humanities* **29**: 129–52.

Tryon, C.A., McBrearty, S. & Texier, P.-J. 2005. Levallois lithic technology from the Kapthurin Formation, Kenya: Acheulian origin & Middle Stone Age diversity. *African Archaeological Review* **22**: 199–229.

Underhill, D. 2012. *The Fauresmith: the transition from the Earlier to Middle Stone Ages in northern South Africa*. PhD thesis, University of Southampton, Southampton.

Vogelsang, R. 1998. *Middle Stone Age Fundstellen in Südwest-Namibia.* Köln: Heinrich Barth Institut.

Vogelsang, R., Richter, J., Jacobs, Z., Eichhorn, B., Linseele, V. & Roberts, R.G. 2010. New excavations of Middle Stone Age deposits at Apollo 11 Rock Shelter, Namibia: stratigraphy, archaeology, chronology and past environments. *Journal of African Archaeology* **8**: 185–218.

Volman, T.P. 1978. Early archaeological evidence for shellfish collecting. *Science* **201**: 911–3.

Volman, T.P. 1981. *The Middle Stone Age in the southern Cape*. PhD thesis, University of Chicago.

Volman, T.P. 1984. Early prehistory of southern Africa. In: R.G. Klein, ed., *Southern African Prehistory and Palaeoenvironments*. Rotterdam: Balkema, pp. 169–220.

Wadley, L. 2001. What is cultural modernity? A general view and a South African perspective from Rose Cottage Cave. *Cambridge Archaeological Journal* **11**: 201–21.

Wadley, L. 2007. Announcing a Still Bay industry at Sibudu Cave, South Africa. *Journal of Human Evolution* **52**: 681–9.

Wadley, L. 2015. Those marvellous millennia: The Middle Stone Age of southern Africa. *Azania: Archaeological Research in Africa* **50**: 155–226.

Wendorf, F. & Schild, R. 1974. *A Middle Stone Age sequence from the Central Rift Valley, Ethiopia*. Wroclaw: Polska Akademia Nauk Instytut Historii Kultury Materialnej.

Wilkins, J. 2013. *Technological change in the Early Middle Pleistocene: the onset of the Middle Stone Age at Kathu Pan 1, Northern Cape, South Africa*. PhD thesis, University of Toronto, Toronto.

Will, M., Parkington, J.E., Kandel, A.W. & Conard, N.J. 2013. Coastal adaptations and the Middle Stone Age lithic assemblages from Hoedjiespunt 1 in the Western Cape, South Africa. *Journal of Human Evolution* **64**: 518–37.

Wurz, S. 2000. *The Middle Stone Age at Klasies River, South Africa*. PhD thesis, University of Stellenbosch.

Wurz, S. 2002. Variability in the Middle Stone Age lithic sequence, 115 000–60 000 years ago at Klasies River, South Africa. *Journal Archaeological Science* **29**: 1001–15.

Wurz, S. 2012. The significance of MIS 5 shell middens on the Cape coast: lithic perspective from Klasies River & Ysterfontein 1. *Quaternary International* **270**: 61–9.

Wurz, S. 2013. Technological trends in the Middle Stone Age of South Africa between MIS 7 & MIS 3. *Current Anthropology* **54** Supplement 8: S305–S319.

Wurz, S. 2014. Southern and East African Middle Stone Age: geography & culture. In: *Encyclopedia of global archaeology.* New York: Springer, pp. 6890–912.

TABLE 14

Summary of relevant MSA sites for the present study with the assemblage description available (the approximate quantity is indicated as follows: +++ for > 50 %, ++ for < 50 %, + for < 10 % and (+) for unknown approximate quantity). The age ranges are specified with the maximum and minimum ages resulting from dating. N/A = not ascertainable.

Site	Layer	Dating	Age	Levallois	Flake	Blade	Triangular Flake	% of tools	Dominant Raw Mat.	Ref.
(A) Assemblages originally assigned to 'MSA 1'										
Elands Bay Cave	SUs Keva, Lara, Letty, Liam, Karl, Kirsten	OSL, TL	259–69 ka		+++	+	+	0.7	Quartzite	Volman 1981; Volman 1984; Schmid et al. 2016 this issue; Tribolo et al. 2016 this issue
Peers Cave	Upper sample			(+)	+++	+		6.3	Quartzite	Volman 1981; Volman 1984
	Lower sample				+++	+		1.2	Quartzite	
Bushman Rock Shelter	Layers 31–105				+++	+		N/A	Quartz, Hornfels, Quartzite	Eloff 1969; Plug 1981; Badenhorst & Plug 2012; Underhill 2012; Porraz et al. 2015
(B) Regional Assemblages dated to MIS 5										
Diepkloof Rock Shelter	MSA-Mike – SUs Mike & Lauren	OSL, TL	118–90 ka	++	+++	++	++	2.0	Quartzite	Porraz, Texier et al. 2013; Tribolo et al. 2013
Klasies River main site	Klasies River – LBS & RBS Members	AAR, U-series, OSL/IRSL	119–94 ka	+	+++	+	+	5.9	Quartzite	Singer & Wymer 1982; Wurz 2000; Wurz 2002; Wurz 2014
	Mossel Bay – SAS & RF Members	AAR, U-series, ESR, OSL/IRSL	108–63 ka	++	+++	+	+	14.7	Quartzite	

TABLE 14 (*continued*)

Summary of relevant MSA sites for the present study with the assemblage description available (the approximate quantity is indicated as follows: +++ for > 50 %, ++ for < 50 %, + for < 10 % and (+) for unknown approximate quantity). The age ranges are specified with the maximum and minimum ages resulting from dating. N/A = not ascertainable.

Site	Layer	Dating	Age	Levallois	Flake	Blade	Triangular Flake	% of tools	Dominant Raw Mat.	Ref.
Ysterfontein 1	Groups 1–13	OSL	140–114 ka		+++	++		19.0	Silcrete, Calcrete	Halkett et al. 2003; Avery et al. 2008; Wurz 2012
Hoedjiespunt 1	AH I–III	context	MIS 5e		+++	+		4.1	Quartz	Will et al. 2013
Sea Harvest			MIS 5e		+++	+		13.2	Silcrete, Quartz, Quartz porphyry	Volman 1978; Volman 1981; Grine & Klein 1993
Hollow Rock Shelter	Depth 20 cm	OSL	93–81 ka		+++	+		2.8	Quartzite	Evans 1994; Högberg & Larsson 2011
Klipfontein-rand	Spits 7–9				(+)	(+)	(+)	N/A	Quartzite	Volman 1981; Mackay et al. 2014
Pinnacle Point 13B	LC MSA Upper/Middle	OSL	130–120 ka	+	+++	++	+	1.7	Quartzite	Marean et al. 2010; Thompson et al. 2010
	Lower Roof Spall Facies	OSL	114–106 ka		+++	++	+	0.0	Quartzite	
	DB Sands 2–3/ LB Sands 1–2	OSL, U-series	102–91 ka	+	+++	+	++	4.0	Quartzite	
	Shelly Brown Sand Facies/ Upper Roof Spall	OSL	98–91 ka	+	+++	++	+	2.1	Quartzite	

TABLE 14 (*continued*)

Summary of relevant MSA sites for the present study with the assemblage description available (the approximate quantity is indicated as follows: +++ for > 50 %, ++ for < 50 %, + for < 10 % and (+) for unknown approximate quantity). The age ranges are specified with the maximum and minimum ages resulting from dating. N/A = not ascertainable.

Site	Layer	Dating	Age	Levallois	Flake	Blade	Triangular Flake	% of tools	Dominant Raw Mat.	Ref
Blombos Cave	M2 Lower – Layers CGAA to CGAC	OSL, TL	91–69 ka	not published yet						Jacobs et al. 2006; Tribolo et al. 2006; Douze et al. 2015
	M3 – Layers CH to CPA	OSL, U/Th	105–91 ka	+	+++	+	++	2.3	Silcrete, Quartzite, Quartz	
(C) Assemblages dated to MIS 6										
Pinnacle Point 13B	LC MSA Lower	OSL	167–157 ka	+	+++	++	+	0.8	Quartzite	Marean et al. 2010; Thompson et al. 2010
	DB Sands 4 a–c	OSL	166–134 ka	+	+++	+	++	3.3	Quartzite	
Kathu Pan 1	Stratum 3	OSL	336–246 ka	+	+++	+		N/A		Porat et al. 2010; Wilkins 2013
Florisbad	N/O/P	ESR, OSL	327–208 ka		+++			N/A	Igneous rock, Hornfels	Dreyer 1935; Sampson 1974; Rightmire 1978; Clarke 1985; Kuman 1989; Grün et al. 1996; Kuman et al. 1999; Grün 2006
	M	OSL	178–136 ka	(+)	+++	(+)		N/A	Hornfels	
Bundu Farm	Groups 2 & 3	ESR, fauna	162–130 ka	(+)	+++	+		N/A	Quartzite, Quartz	Kiberd 2006
Border Cave	4BS, 4WA, 5BS & 5WA	U-series, AAR, TL, ESR	238–80 ka	(+)	+++	(+)	(+)	N/A	Felsite	Beaumont et al. 1978; Grün et al. 1990; Grün & Beaumont 2001; Grün 2006

TABLE 14 (*continued*)

Summary of relevant MSA sites for the present study with the assemblage description available (the approximate quantity is indicated as follows: +++ for > 50 %, ++ for < 50 %, + for < 10 % and (+) for unknown approximate quantity). The age ranges are specified with the maximum and minimum ages resulting from dating. N/A = not ascertainable.

Site	Layer	Dating	Age	Levallois	Flake	Blade	Triangular Flake	% of tools	Dominant Raw Mat.	Ref.
Wonderwerk Cave	MU 2	U-series	182–74 ka	(+)	+++	(+)		N/A	N/A	Beaumont & Vogel 2006; Chazan & Horwitz 2009
Lincoln Cave	Lincoln Cave North	U-series	288–108 ka					N/A		Reynolds et al. 2007
	Lincoln Cave South	geological and archaeological correlation	288–211 ka		+++	+		N/A	Quartz	
Sterkfontein	Post-Member 6 Infill	ESR	426–211 ka		+++	(+)		6.0	Quartz	Reynolds et al. 2007; Ogola 2009
(D) Assemblages associated with MIS 6 or MIS 5 pre-SB										
Varsche Rivier 003	Layers I-04 & I-05			(+)	+++			N/A	Quartz	Steele et al. 2012
Herolds Bay Cave			MIS 5e		+++	(+)	(+)	N/A	Quartzite	Brink & Deacon 1982; Mitchell 2002; Hendey & Volman 1986; Wurz 2012
Cape St. Blaize	Layers CU, C1–C4				+++	++	+	1.9-12.6	Quartzite	Thompson & Marean 2008
Nelson Bay Cave	Level 8				+++	+	+	1.4	Quartzite	Volman 1981, 1984
	Levels 9–10				+++	++	(+)	0.5	Quartzite	

TABLE 14 (*continued*)

Summary of relevant MSA sites for the present study with the assemblage description available (the approximate quantity is indicated as follows: +++ for > 50 %, ++ for < 50 %, + for < 10 % and (+) for unknown approximate quantity). The age ranges are specified with the maximum and minimum ages resulting from dating. N/A = not ascertainable.

Site	Layer	Dating	Age	Levallois	Flake	Blade	Triangular Flake	% of tools	Dominant Raw Mat.	Ref.
Cave of Hearths	Bed 4			+	+++	++	++	2.2	Quartzite, Quartz, Andesite	Mason 1962; 1988; McNabb & Sinclair 2009
	Bed 5			+	+++	+	++	2.9	Quartzite, Quartz, Chert	
	Bed 6–9			+	+++	+	+	2.7-7.6	Quartz, Quartzite, Chert	
Swartkrans Cave	Member 4	U-Th	< 108 ka	(+)	+++	+		10.0	Quartz, Quartzite, Diabase	Sutton et al. 2009; Sutton 2013
Spitzkloof A Rock Shelter	Brian				+++	(+)		N/A	Quartz	Dewar & Stuart 2012
	Genevieve				+++	(+)		N/A	Quartz, Silcrete	
Apollo 11 Rock Shelter	MSA phase 2: Komplex 1 – Units V–X		> 73 ka		+++	++	+	5.5	Quartzite, Calcareous Mudstone	Vogelsang 1998; Vogelsang et al. 2010
	MSA phase 1: Komplex 1 – Units Y & Z		> 73 ka		+++	++	+	4.2	Quartzite, Calcareous Mudstone	
Bremen 1C	Basis-komplex				+++	++		N/A	Quartzite	Vogelsang 1998
Bremen 2B	Sediment-schicht I				++	+++		1.5	Quartzite	Vogelsang 1998
Aar 2	Sediment-schichten I–IV				++	++	(+)	1.0	Quartz, Quartzite	Vogelsang 1998
Etemba 14	Unit V				+++	+		1.0	Quartz, Dyke Rock	Schmidt 2011

Southern African Humanities **29**: 203–47 December 2016 KwaZulu-Natal Museum

A shape to the microlithic Robberg from Elands Bay Cave (South Africa)

[1,2]**Guillaume Porraz**, [3]**Marina Igreja**, [4]**Patrick Schmidt** and [5]**John E. Parkington**

[1]CNRS, USR 3336, Institut Français d'Afrique du Sud, Johannesburg, South Africa; guillaume.porraz@mae.u-paris10.fr
[2]Evolutionary Studies Institute, University of the Witwatersrand, Johannesburg, South Africa
[3]ENVARCH, CIBIO–INBIO, University of Porto, Portugal; maraujo_mar@yahoo.com
[4]Eberhard Karls University of Tübingen, Department of Prehistory and Quaternary Ecology, Schloss Hohentübingen, 72070 Tübingen, Germany; patrick.schmidt@uni-tuebingen.de
[5]Department of Archaeology, University of Cape Town, South Africa; john.parkington@uct.ac.za

ABSTRACT

Elands Bay Cave (EBC) is a key South African site allowing discussion of technological change and adaptations that occurred from the Upper Pleniglacial to the Holocene. In 2011, we set out a new field campaign aiming to clarify the nature and chronology of the earliest Robberg occupations at the site, a technocomplex whose appearance closely relates to the Last Glacial Maximum. Our results document the appearance of the Robberg technology at ca. 19 398–18 790 cal BP, succeeding a phase commonly referred to as the Early Later Stone Age. In this paper, we further develop the definition of the Robberg by providing a technological and functional study of the MOS1 lithic assemblage at EBC, dated to 14 605–14 278 cal BP. Our results show that EBC occupants dominantly selected local quartz in addition to heat-treated silcrete that was introduced from distances greater than 30 km. Robberg inhabitants applied different reduction strategies combining bipolar/anvil and soft stone hammer percussion. Reduction sequences were oriented toward the production of a set of small artefacts (< 25 mm long) that can be generically classified as bladelets. The low incidence of retouched forms and the absence of geometrics, together with our functional study, testify to a flexible composite microlithic technology. We also discuss the raw material provisioning strategies of EBC Robberg inhabitants and develop the question of the intra- and inter-assemblages variability. Finally, we attempt to discuss its temporal trends and conclude on the originality of the Robberg technology within the context of other Late Pleistocene microlithic traditions.

KEY WORDS: Later Stone Age, Robberg, Last Glacial Maximum, bladelets, microlithic technology, projectile, hafting, silcrete heat treatment, use-wear analysis.

The Robberg technocomplex, first recognized at Rose Cottage Cave (see Wadley 1996), was initially defined at Nelson Bay Cave on the Robberg Peninsula (Klein 1974; Deacon 1978). It represents a bladelet tradition whose appearance is conventionally associated with the regional beginning of the Later Stone Age (LSA) in southern Africa (Deacon & Deacon 1999; Mitchell 2002; but see Villa et al. 2012). Because the Robberg seems to coincide with the Last Glacial Maximum (LGM), this technology has been viewed as an innovation selected by groups in a context of unpredictable resources (e.g. Deacon 1983; Deacon 1988, 1990; Mitchell 1988a; Wadley 1993).

The LGM is referred to as the maximum global ice volume of the Late Pleistocene (Ehlers & Gibbard 2007). It corresponds to a cooling of about 5°C (20–33 % lower than present average temperatures; Mix et al. 2001) and marks an intensified aridity that substantially modified the paleoenvironmental conditions. But the timing and ecological impact of the LGM, centered around 21 ka cal. BP (Mix et al. 2001), varied significantly (Clark et al. 2009). Southern Africa, composed of multiple biomes, provides one good context in which to assess the nature of behavioral changes and adaptations that might have occurred at the onset of the Pleniglacial.

ISSN 2305-2791 (online); 1681-5564 (print)

The oldest Robberg occupations presently known in South Africa date back to ca. 23–22 ka cal. BP and extend throughout different biomes, from the Western Cape to Limpopo (Beaumont 1981; Deacon 1984; Mitchell 1988a, b, 1990, 1995; Wadley 1993, 1996; Deacon 1995; Lombard et al. 2012; Loftus et al. 2016). Current 14C dates suggest an occurrence of the Robberg in the LGM and Late Glacial (LG), with the most recent occupations that would have persisted until the Holocene at ca. 11–10 ka cal. BP (Wadley 1993, 1996; Mitchell 1995, 2002).

Although establishing the chronology of the Robberg has benefited from more recent studies and excavations, its regional variants and temporal developments remain uncertain. Regional adaptations related to, for example, geological contexts have been noticed (Mitchell 1988b). And there are diachronic changes that have been observed in raw material preferences at sites such as Boomplaas (Deacon 1984) and Putslaagte 8 (Mackay et al. 2015), in the way bladelets were used at Sehonghong (Mitchell 1995), as well as in the morphologies of the bladelets that were produced at Sehonghong (Pargeter & Redondo 2015). But the nature of these changes and their significance still require clarification.

Studies document Robberg populations exploiting a wide range of mineral, botanical and faunal resources (Deacon 1984; Wadley 1993; Mitchell 2005). Robberg populations used bone tools (Deacon 1984; Mitchell 1995; Wadley 1996) and also symbols for communication, as documented by the presence of engraved ostrich eggshells (Schweitzer & Wilson 1982) and beads made from ostrich egg and marine shell (Deacon 1976; Deacon 1984; Wadley 1996; Manhire 1993). The finding at Sehonghong, within the Drakensberg range, of a marine bead (Mitchell 1995, 2002) suggests long distance circulation or the existence of extended regional networks between groups during the Robberg. But the most distinctive feature typifying the Robberg is its lithic technology.

The Robberg yielded a microlithic technology based on unmodified bladelets that were produced from single platform cores (Deacon 1984; Wadley 1993; Mitchell 1995; Parkington 1990). We acknowledge the existence of a rich literature and discussion on the definition of a microlithic industry (e.g. Elston & Kuhn 2002). By microlithic, we here mean a technology that is based on diminutive blanks (bladelets or small flakes), with or without their transformation into geometrics. In that sense, we establish consecutively a distinction between microlithic tools and 'microliths', the latter corresponding to a formal tool category represented by geometric miniaturized forms (see Tixier 1965; Barrière et al. 1969).

Authors have recognized different reduction strategies during the Robberg, with emphasis being put on the standardization of the products and on the common use of bipolar percussion. Formal tools are very rare and generally composed of lightly modified bladelets, sometimes backed, together with a corpus of scrapers and denticulates. Though the spread of the Robberg technology might be associated with a decisive change in hunting techniques (e.g. Deacon 1983; Mitchell 1988c), pioneer functional studies document bladelets that were involved in both hunting and domestic activities (Binneman 1997; Binneman & Mitchell 1997). Additionally, and diagnostically, black organic adhesives found on Robberg products suggest that they were used as inserts as part of a composite technology (Binneman & Mitchell 1997).

The aim of this paper is to provide further insight into the Robberg technology by focusing on the lithic assemblages from Elands Bay Cave (EBC), located on the West

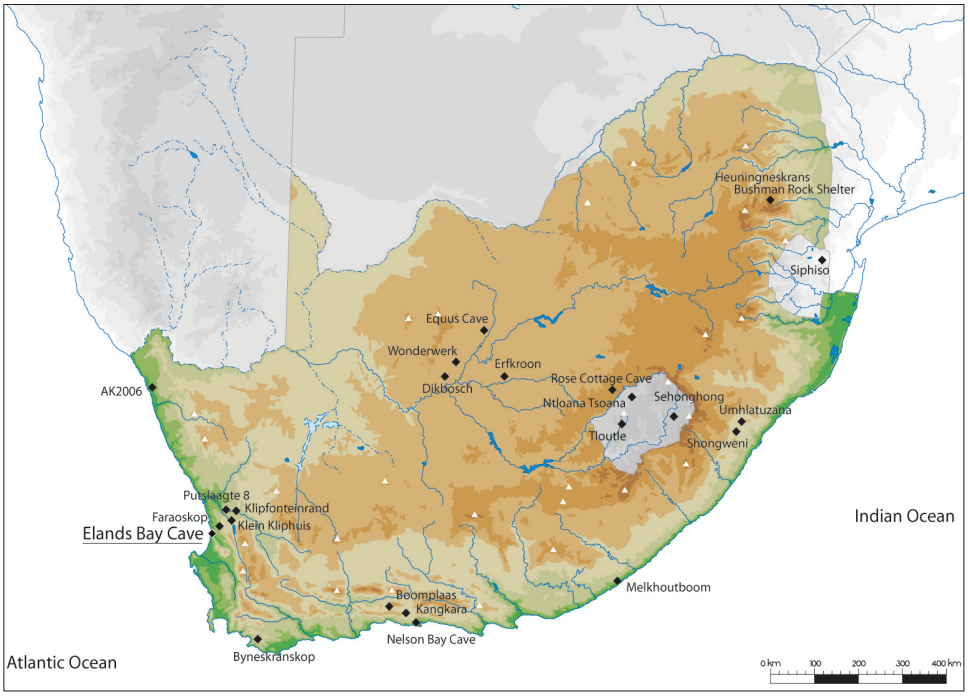

Fig. 1. Location of Elands Bay Cave (West Coast of South Africa) and of the main Robberg Sites.

Coast of South Africa. We first clarify the scenario and chronology of the appearance of the Robberg at EBC, and then conduct technological and functional analyses of one Robberg layer dating to ca. 14.5–14 ka cal BP. We fuel the question of the intra- and inter-assemblage variability of Robberg lithic assemblages and discuss the temporal evolution of this technocomplex. Our conclusions highlight the Robberg as an original and southern African trajectory within the context of Late Pleistocene microlithic technologies.

THE LATER STONE AGE RECORD AT ELANDS BAY CAVE

EBC is located on the current Atlantic coast about 200 km north of Cape Town (Western Cape, South Africa; Fig. 1). It is a large shelter opening to the west and located on a promontory of the Table Mountain Group, a few hundred meters southward of the natural lake (vlei) that formed at the Verlorenvlei River mouth. EBC is within an area rich in Holocene occupations as recorded at Tortoise Cave, Dunefield Midden and other sites including Diepkloof Rock Shelter that is located about 15 km eastward.

The main excavations at EBC were undertaken in the 1970s by John Parkington (Parkington 2016 this issue). He exposed a ca. 3 m deep sequence with the upper part being the remnant of a Holocene shell midden. The set of 14C dates indicates several pulses of human occupations from the end of the late Pleistocene to the late Holocene (Tribolo et al. 2016 this issue), with first occupations being Middle Stone Age (Schmid et al. 2016 this issue). Major climatic changes are documented throughout the sequence, indicating important modifications in the topographic setting of the area. At

the maximum glacial, local data suggest that the coast moved ca. 20–30 km away from its present location (Jerardino et al. 2013; Porraz et al. 2016 this issue).

The EBC LSA record has been well studied, with some of the main questions being related to Holocene coastal changes and adaptations (e.g. Parkington 1976, 1981, 1988; Parkington et al. 1988; Woodborne et al. 1995; Jerardino et al. 2013). The quality of organic preservation has allowed the recovery of a large set of botanical remains (Cowling et al. 1999; Parkington et al. 2000; Cartwright et al. 2016 this issue) but also a range of bone tools and food remains. Most spectacular is the presence of large adhesive artefact and adhesive imprints on tools recovered from Holocene layers (Charrié-Duhaut et al. 2016 this issue). Another important contribution is the analysis by Orton (2006) that has provided the first lithic overview of the LSA sequence at EBC, in which he observes changes in raw material procurements and lithic technology as well as some atypical features with regard to similarly dated assemblages.

While the terminal Pleistocene to Holocene record from EBC has received much attention, there are uncertainties regarding the nature and chronology of human occupations during the LGM, supposedly the period reflecting the technological succession from the Early LSA (ELSA) to the Robberg. It was with the intention to clarify the chronology and the contact between the ELSA and the first Robberg occupations at EBC that we decided to reopen the site in April 2011 (Porraz et al. 2016 this issue).

FIRST ROBBERG OCCUPATIONS AT ELANDS BAY CAVE

Parkington's 1970s excavation focused on the removal of the upper layers across a large surface of the shelter and on the preliminary exploration of the lower layers by opening a test pit of 5 m². In 2011, this test pit was reopened and worked on the east profile, where the deposits were most clearly stratified (Miller et al. 2016 this issue). We excavated a sequence of ca. 150 cm deep, uncovering LSA, ELSA and MSA occupations (Fig. 2), until bedrock was reached.

Schematically, the deposits of the test pit can be subdivided into 3 main sedimentary parts consisting, from the top to the bottom, of (1) a dominant anthropogenic matrix with combustion features, (2) a dominant geogenic matrix with isolated combustion features and (3) a thick accumulation of plaquettes overlying a blackish, moist sediment. The LSA from our 2011 excavation is strictly associated with the ca. 55 cm thick sedimentary part (1). During excavation, (1) was subdivided into two stratigraphic phases that received the letters D and F respectively.

Both stratigraphic phases are characterized by a relatively low density of lithic artefacts and the absence of organic material (see Miller et al. 2016 this issue). Phase D includes the stratigraphic units (SUs) Delport, Dennis, Denver and Dorothee. The excavation yielded 271 lithic artefacts > 20 mm, most of which are small quartz and silcrete bladelets (Fig. 3). Phase F, starting with the SU Faël, yielded 430 lithic artefacts > 20 mm. This latter phase mostly contains quartz flaking, bipolar technology and denticulates that are reminiscent of ELSA occupations (see Synthesis & Porraz et al. 2016 this issue for further descriptions).

To secure the chronology, charcoal samples were collected from the profile section at the end of the excavation: 2 samples from within phase D (S–101 and

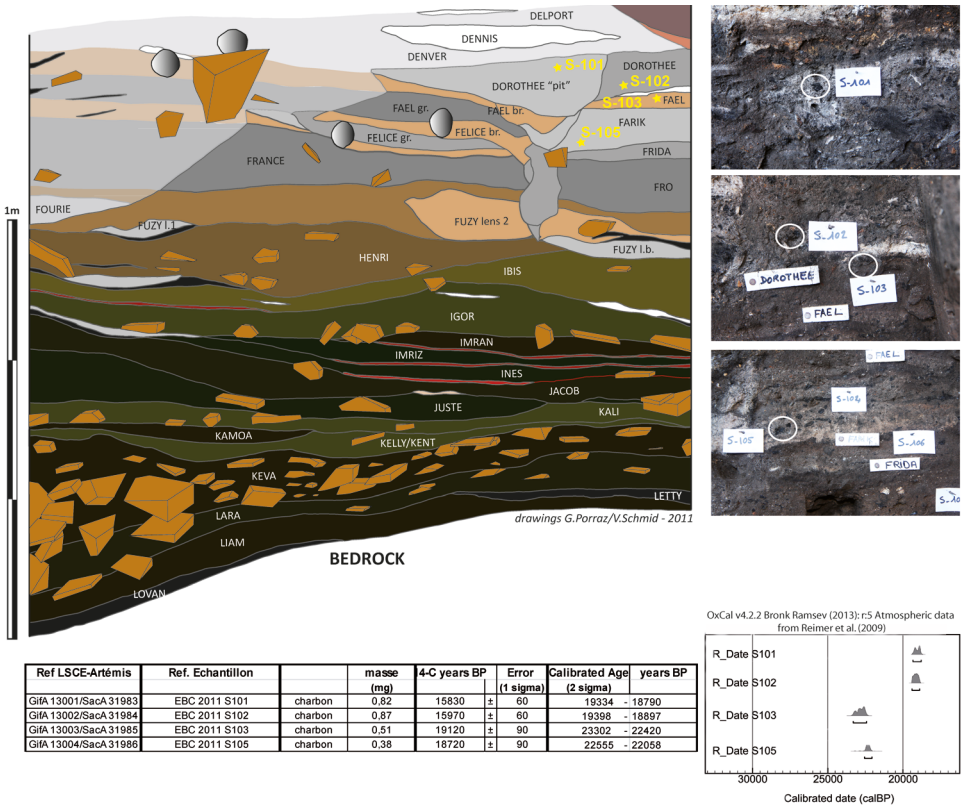

Ref LSCE-Artémis	Ref. Echantillon		masse (mg)	14C years BP		Error (1 sigma)	Calibrated Age (2 sigma)	years BP
GifA 13001/SacA 31983	EBC 2011 S101	charbon	0,82	15830	±	60	19334 - 18790	
GifA 13002/SacA 31984	EBC 2011 S102	charbon	0,87	15970	±	60	19398 - 18897	
GifA 13003/SacA 31985	EBC 2011 S103	charbon	0,51	19120	±	90	23302 - 22420	
GifA 13004/SacA 31986	EBC 2011 S105	charbon	0,38	18720	±	90	22555 - 22058	

Fig. 2. Western stratigraphic profile of Elands Bay Cave (2011 excavation), location of 14C samples (S-101 to S-104) and calibrated dates. The grey shade (top left) indicates post-depositional modification of the stratigraphy.

S–102) and 2 samples from the upper part of phase F (S–103 and S–105). The results are consistent and indicate an initial Robberg occupation at EBC dating to an interval between 19 398–18 790 cal. BP and a final ELSA occupation dating to an interval of 23 302–22 058 cal BP (Fig. 2). At EBC, the Robberg and the ELSA are separated by a hiatus in sedimentation and in human occupation that lasted for about 2500 years.

THE LITHIC TECHNOLOGY OF THE MOS1 ROBBERG AT ELANDS BAY CAVE: ANALYTICAL BACKGROUND

Because our 2011 excavation was limited and recovered only a small collection of lithic artefacts and because the correlation with the 1970s excavation could not be totally secured, we focus in the present study on the lithic assemblage from layer MOS1 that was excavated in the 1970s. MOS1 represents the oldest Robberg occupation extensively excavated by Parkington. It directly overlies our phase D. It was published as layer 20 by Parkington (1984; Fig.4) and as part of the phase A by Orton (2006). MOS1 is described as a loamy matrix with isolated hearths and is directly dated (Pta 4321: 13 600 ± 600 uncal BP) to 14 605–14 278 cal BP (calibration intcal13).

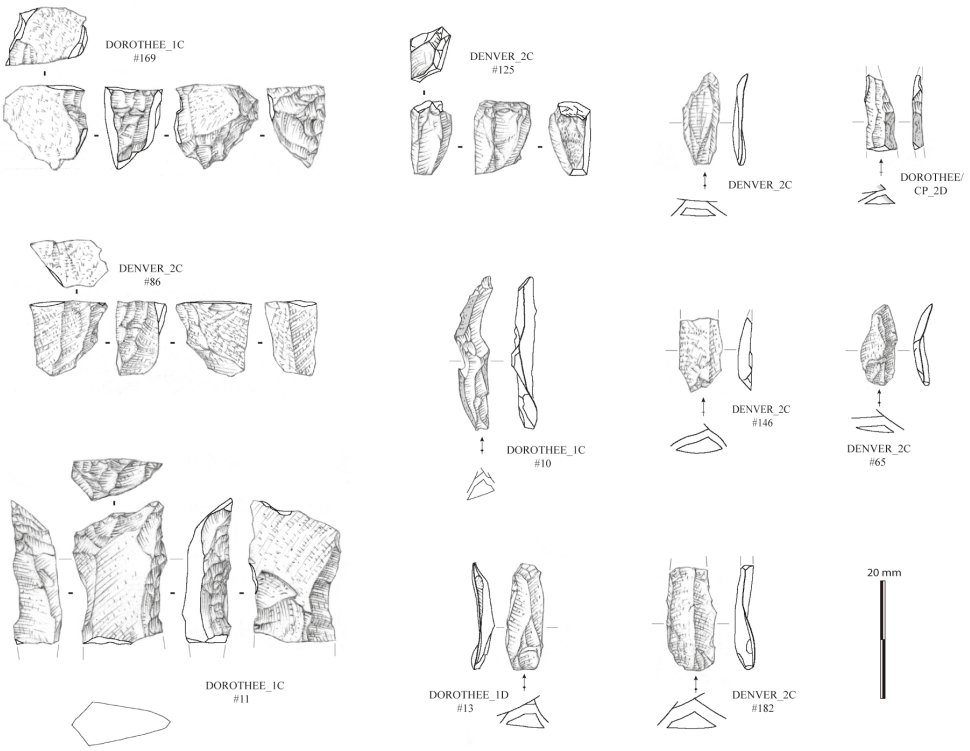

Fig. 3. 2011 lithic collection from the earliest Robberg occupations at Elands Bay Cave. #169, #86 (silcrete) and #125 (chert) are bladelet cores (to notice the dimensional homogeneity at their stage of discard), #11 is a reduced scraper with bladelet removals on its narrow side. The other products are all bladelets in silcrete except #146 (quartz). All silcrete products have been heat treated (drawings by M. Grenet).

Principles and methods

Our analytical procedure follows the general principles of the *chaîne opératoire* (Leroi-Gourhan 1964–65; Tixier 1980; Geneste 1992; Boëda et al. 1990), the aim being to inscribe each artefact within a succession of technological events from the acquisition of the rock to the use of the tool and its discard. The nature of the analysis itself is descriptive and purports to assert a craft knowledge. The interpretations behind this knowledge, in terms of variability and diversity, relate to a theoretical background that varies depending on the analysts and the research questions (Fig. 5).

The analytical background of lithic technological studies is based on one basic principle: the fracture of conchoidally fracturing rocks is subject to three constraints that dictate the way the fracture propagates. These three main physical constraints are: (1) the mechanical properties of the rocks (elasticity, hardness, homogeneity, fracture toughness, etc.), (2) the geometric shape of the volume (including longitudinal and transversal convexities, number of surfaces and angles of intersections) and (3) the application of the force (type and nature of the contact in terms of mode of application and of motion). Once these constraints are assimilated by the knapper, they become

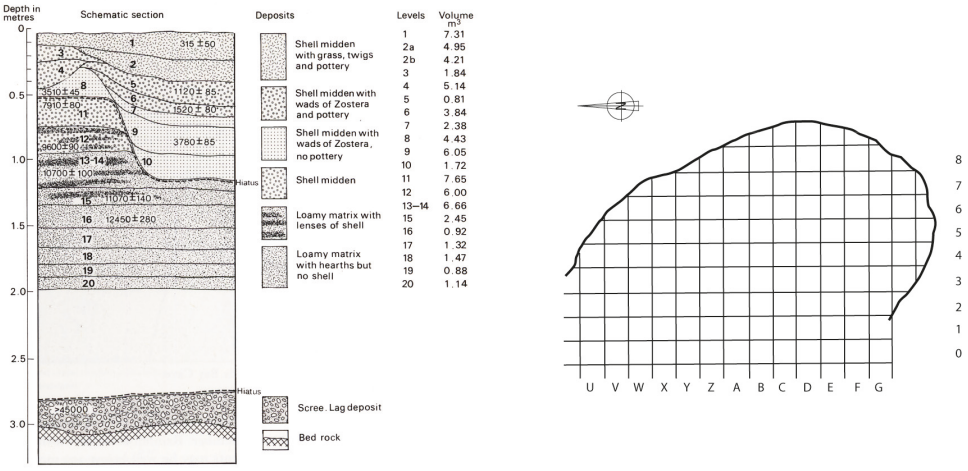

Fig. 4. Stratigraphy (after Parkington 1984) and grid of the 1970s excavation at Elands Bay Cave.

rules. With these rules in mind, it is thereafter possible to control and anticipate the fracture (i.e. notion of predictability and intentionality).

The intention is to manufacture a tool. A tool is an object defined by its efficiency, its kinetics as well as by its ergonomic and non-utilitarian aspects (Fig. 5). Schematically, a tool associates two main parts: a transformative part that is intended to be in contact with the worked material and a passive part that is intended to be handled/hafted (see Lepot 1993; Boëda 2001; 2013; Conard et al. 2012). Tools vary in shape and volume, depending on the actions intended with them (motion of the user and properties of the worked material), the technical sub-systems (e.g. the mode of propulsion, the hafting structure), the body techniques and the beliefs of the tool-making populations.

However, understanding a tool itself also requires us to consider all the technical steps behind its manufacture. The manufacturing stages vary with the skill of the knapper, the geological resources available in the environment as well as with the system of subsistence and with the traditions of the group. Applying such a global technological

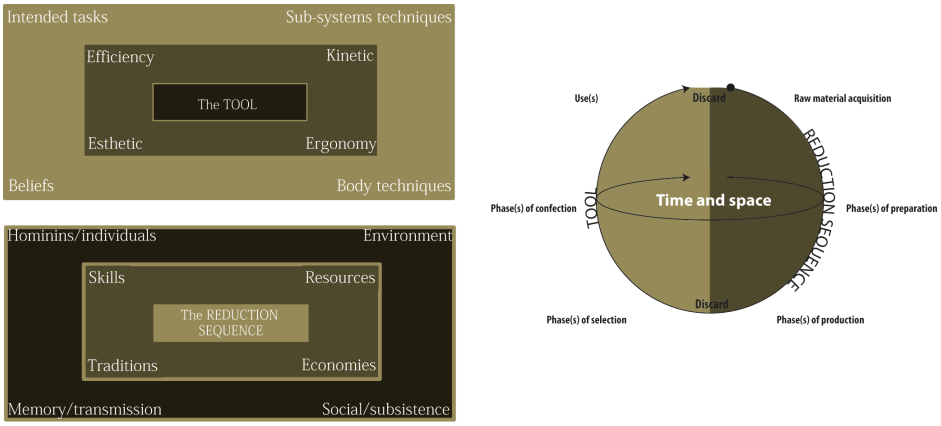

Fig. 5. Theoretical framework of the present technological study.

approach, the objective is to describe the different technical events that led to a lithic assemblage and to understand their associations and characteristics. Through a system of inferences (Gardin 2002), it is then possible to develop a narrative from a short- to a long-term perspective.

What raw materials were selected and for which raw material provisioning strategies?
Raw material characterization has a long history of research, targeting in particular to improve the sourcing of the rocks as well as their interpretative frameworks (e.g. Geneste 1992; Kelly 1995; Kuhn 1995; Féblot-Augustins 1997). The first analytical step is to characterize the geological environment to which populations had to adapt. In the context of EBC, the dominant geology is formed by the Table Mountain Group sandstone. EBC is formed in the lowest layer of the Table Mountain Series which is referred to as the Piekenierskloof Conglomerate. The pebble composition of this conglomerate is dominated by vein quartz, but it also includes a few fine-grained varieties of quartzite and chert.

Silcrete is locally available at the Verlorenvlei mouth. There it can be found as greyish hard silicified crust that, through experimental studies, has been found to be of rather low quality for knapping. The second nearest outcrop is the yellowish silcrete from Redelinghuys, located ca. 20 km eastward of EBC, along the Verlorenvlei. This silcrete is of medium knapping quality and presents a coarse grain-supported and heterogeneous texture. Silcrete of better knapping quality only occurs in more distant areas (Porraz et al. 2013). The first one is located north of Piketberg, ca. 40 km eastward of EBC: this silcrete presents a fine texture and is greyish with brownish features. The second silcrete can be found at the mouth of the Berg River, ca. 50 km southwards of EBC: this silcrete has a fine texture and is mostly shiny greyish to reddish. The third main area of silcrete distribution is located at the mouth of the Olifants river, ca. 70 km northward of EBC. Silcrete of this area is abundant in secondary position as pebbles that can be collected in alluvial terraces.

Hydrothermal vein quartz (henceforth only called 'quartz' for simplicity), quartzite, sandstone and silcrete represent the main regionally available raw materials. Hornfels occurs in minor amounts. So far, this rock has only been found within the terraces close to the Olifants river mouth, ca. 70 km northward of EBC.

Petrographic identifications were made at mesoscopic scale (10x–56x) using a regional geological database for comparison (see Porraz et al. 2013). Each lithic artefact was classified according to two criteria: the nature of the rock and, when present, the type of its surface or 'cortex' (weathered, rolled, fresh, indeterminate).

This technological study was completed by a detailed fracture surface analysis (Schmidt et al 2015) aiming to determine whether the silcrete component of the studied assemblage was heat-treated in the Robberg, as previously only documented in the regional MSA (Brown et al. 2009; Schmidt et al. 2015). During this analysis we identified three proxies: (1) Pre-heating removal scars: relatively rough fracture surfaces corresponding to the removal of flakes from unheated silcrete; (2) Post-heating removal scars: relatively smooth fracture surfaces that correspond to the removal of flakes from heat-treated silcrete; (3) Heat-induced-non-conchoidal (HINC) fractures: surfaces produced by thermal fracturing in a fire (sometimes termed overheating; Schmidt 2014). HINC fracture surfaces can be recognized due to their strong surface

roughness, the presence of scalar features on the surface and concave morphologies with frequent angular features. We only identify such a fracture surface as HINC when it is associated with a post-heating surface. Tempering-residue, a black organic tar (wood tar) produced by dry distillation of plant exudations during contact with glowing embers (Schmidt et al. 2015), might represent a fourth proxy but it has not been observed in the EBC collection.

To securely recognize pre- and post-heating scars on the EBC artefacts, we compared them with our reference collection of unheated and heat-treated silcrete from the region (Schmidt et al. 2013, 2015). The three heat treatment proxies were observed macroscopically and at a 10x magnification. Visual criteria were the surface roughness of removal scars and, in the case of HINC fractures, the presence of scalar features. No further equipment was used to measure flake scar roughness and no gloss-meter was used. The correct assignment of fracture surfaces to either pre- or post-heating fracture scars at EBC was verified with our experimental collection and aided by an 'internal calibration' (Schmidt & Mackay 2016). Such an internal calibration consists in first finding artefacts that show both smooth post- and rough pre-heating scars. The roughness of pre- and post-heating scars on other artefacts can then be compared with these 'diagnostic pieces' in order to verify their assignment to either heating proxy class. EBC artefacts that could not be clearly identified as belonging to one of the frequently occurring silcrete types and to which we could not find a clear match in the West Coast reference collection were left undetermined as to whether they were heat-treated or not.

What are the main core reduction sequences and for which technique(s)?

Our description of the lithics is based on an abundant literature combining both experimental and archaeological case studies (e.g. Tixier 1980; Pélegrin 1995; Inizan et al. 1999). The goal is to propose a scheme representing the different technical steps followed by the knapper. These steps are usually inferred from combining both 'mental' and 'physical' refitting.

A technological narrative implies a constant two way comparison between cores and products. We focused on all cores, cortical blanks, and all products that have, intentionally or accidently, been taken away from a large portion of the core. This last category includes over-plunged blanks, débordant/ridge blanks and core tablets. At this stage of the study, the aim is to decode the geometry of the cores and their transformation from initial shaping to discard.

Our description starts with the identification of the block that was selected to be knapped. A block is defined by its size and shape, which can be angular or rounded, regular or irregular, symmetric or asymmetric. In the context of EBC, we defined four main types of blocks: rounded pebbles, irregular fragments, slabs and flakes. Subsequent to this, the aim was to describe the initial shaping, starting with the way the block was oriented. This shaping aims to set up the surface of removals by establishing the appropriate convexities and angles. The description of the main surface(s) of removals allows us to reach an initial understanding of the types of blanks that were produced, as well as of the rhythms of the production.

The characterization of the technique of detachment of the blanks combines observations on the cores and on the products (e.g. Soriano et al. 2007). It is based on

the description of the platform (plain or prepared, thickness, amplitude), of the ventral surface (lip, contact point, interference waves) and of the dorsal surface (abrasion, removals, etc.). This description goes together with the calculation of the platform angle which, in the present study, was only taken on the cores. Additionally, special attention was paid to possible signs related to the presence of anvil repercussions. The Robberg lithic assemblages were long associated with the use of bipolar percussion and recent works (e.g. de la Peña 2015) have shown how this technique varies together with body techniques and objectives. In our paper, we follow the terminology advocated by Callahan (1987), who established a distinction between bipolar percussion involving an axial percussion, and anvil percussion involving a more slanted percussion.

What are the main categories of blanks and for which functional purposes were they struck?
In terms of classification, we distinguished the blades from the flakes on the base of their dimensions and regularity: the category 'blade' includes all products with sub-parallel to convergent edges that are twice or more as long as wide. For all categories, and assuming that size matters, we distinguished the following groups: blades (≥ 15 mm wide), microblades (≥ 12 mm), bladelets (≤ 11 mm) and microbladelets (≤ 5 mm). Similarly, we distinguished flakes from micro-flakes (≤ 20 mm long).

One of our research questions implied by the study of the Robberg industry addresses size and morphology and how these two variables relate. We measured the length (within the axis of percussion), the breadth (at the middle of the piece) and the thickness (at the intersection between length and breadth) of all products.

To identify any morphological patterns within the bladelet reduction sequence, we subdivided blanks into three main classes: (1) parallel bladelets, with their proximal and medial parts being 'equally' wide; (2) triangular bladelets: convergent and symmetric bladelets with a proximal part wider than their medial part; (3) comma-like bladelets: convergent asymmetric bladelets, often twisted, with one convex edge and one concave edge. In addition, we identified trapezoidal bladelets (flakes with divergent edges) and naturally backed bladelets (asymmetric in section).

Regarding the typological classification of the formal tools, we followed a simple subdivision into three categories that distinguish modified bladelets (regardless of the type of modification), products with notches/denticulations and scraper-like tools that are not of bladelet proportions.

For the functional study, we combined the observation of macroscopic edge damage features with the search for microscopic use-wear traces (see Semenov 1964; Keeley 1980). The contact between a tool and a given worked material chemically and mechanically modifies the edge and surface of the tool creating a specific set of use-wear traces. These modifications are visible under low magnifications as scars, fractures, edge rounding, and under the microscope where polishes, striation and micro edge rounding can be observed. Combined, they are reliable indicators of the nature of the material worked and of the actions performed.

Artefacts were first examined using a binocular microscope (Olympus, magnifications up to 100X) and then using a metallurgical incident light microscope equipped with Differential Interference Contrast (DIC) objective (Olympus, magnification up to 200x), following the standard procedures used in use-wear analysis (e.g. Plisson 1985; Gonzalez-Urquijo & Ibanez-Estevez 2004). Photomicrographs were taken with a

digital camera Canon EOS 600D. Interpretations of the functionality of stone tools are based on a large experimental reference collection of use-wear traces recorded on tools made from different raw materials and based on both African Stone Age and European Paleolithic replications (Igreja 2009; Igreja & Clemente-Conte 2009; Igreja & Porraz 2013; Porraz et al. 2015).

Given that much effort has already been expended to establish Diagnostic Impact Fractures (DIFs), shown through experiments (Fischer et al. 1984; Lombard 2005; Lombard & Pargeter 2008; Iovita et al. 2014), as well as possible effects of taphonomic disturbance on stone tools, we use the main DIF breakage types that have been commonly recognized as projectile impact damage based on the morphology of fracture initiation and termination (Fischer et al. 1984; Hayden 1979): step terminating bending fractures; spin-off fractures > 6 mm; bifacial spin-off fractures and impact burinations. Step terminating fractures and spin-off fractures have been referred to as the primary DIF types to identify the potential use of stone tipped weaponry (Lombard 2005; Lombard & Pargeter 2008; Villa et al. 2009). Snap, feather and hinge terminating fractures and tip crushing are recorded during macrofracture analyses to describe the complete range of damage seen on a tool. Such damage can result from a variety of other activities (such as trampling and knapping) and should not be used alone as potential indicators of projectile impact.

TECHNOLOGICAL AND FUNCTIONAL ANALYSIS OF THE MOS1 ROBBERG

Our sample (Table 1) represents 4263 lithic artefacts coming from the squares A2, A3, B2, D2, C2 and Z3 (Fig. 4) and includes 106 pieces originating from layer DS03 (square E4). MOS1 and DS03 were excavated at different times (in 1978 and 1970 respectively) and different areas, but field and technological observations support the hypothesis that they originate from the same archaeological horizon. All deposits were dry sieved with a 3 mm mesh.

Fragments (i.e. pieces that could not be assigned to any other technological category) ≤ 20 mm comprise the vast majority of our sample with a total of 3077 pieces: they represent 41 % of the silcrete and as much as 75 % of the quartz. The following observations and calculations exclude all fragments ≤ 20 mm and are based on a total collection of 1186 lithic artefacts.

What raw materials were selected and for which raw material provisioning strategies?

The collection is predominantly composed of quartz (82 %), which is available in the direct environment of the shelter. Most quartz pebbles are semi-spherical with mean sizes ranging from 5 to 15 cm long. The proportion of cortical flakes (ca. 10 %), the high number of cores, the number of small fragments and small flakes (Table 1) suggest that quartz was introduced as pebbles and exploited *in situ*. This raw material category includes a small proportion of well crystallized quartz or rock crystal (< 2 %).

The second main raw material in the lithic collection is silcrete (15 %). Our study allows us to distinguish two main categories.

(1) The first is represented by a yellowish coarse-grained silcrete, which represents 18 % of the silcrete collection. Seven cortical surfaces on a total of 11 pieces

TABLE 1
List of the MOS1 lithic assemblage from Elands Bay Cave (in bracket are the retouched pieces).

	Quartz	**Local Silcrete**	**Exotic silcrete**	**Coarse Quartzite**	**Fine Quartzite**	**Chert**	**Hornfels**	**Undeterm.**	**TOTAL**
Flakes	53 (3)	3	15 (2)	15	1	2	6 (1)	1	**96 (6)**
Blades (≥ 15 mm)	3	3	3	0	0	0	0	0	**9**
Micro-Blades (≥ 12 mm)	6	0	1	1	0	1	0	1	**10**
Bladelets (≤11 mm)	304 (12)	10	57 (8)	0	0	4	1	2	**378 (20)**
Micro-bladelets (≤5 mm)	238 (19)	8	36 (4)	0	3	4	0	0	**289 (23)**
Micro-flakes (≤20 mm)	105 (5)	5	30 (3)	1	1	3	0	0	**145 (8)**
Cores	63	1	3	0	0	1	1	0	**69**
Core-reduced pieces	136	1	0	0	0	1	1	0	**139**
Manuport	0	0	0	1	0	0	1	0	**2**
Fragments >20 mm	35	0	4	5	2	3	0	0	**49**
TOTAL	**943 (39)**	**31 (0)**	**149 (17)**	**23 (0)**	**7 (0)**	**19 (0)**	**10 (1)**	**4 (0)**	**1186 (57)**
Fragments ≤20 mm	2853	6	120 (2)	42	11	13	32	0	**3077 (2)**
TOTAL	**3796**	**37**	**269**	**65**	**18**	**32**	**42**	**4**	**4263 (59)**

were determinable and all show a weathered surface that documents their collection in a primary context. Macroscopically, this yellowish silcrete is similar to the one from Redelinghuys located ca. 20 km eastward of EBC.

(2) The second is classified as 'exotic'. Exotic silcrete varies macroscopically in colour and content of inclusions, suggesting that it originates from different sources. Cortical pieces that were determinable are represented by eight pieces (of a total of 11): five exhibit a weathered surface and three a rolled surface, indicating different places of collection (in primary and secondary contexts). Our present knowledge of the regional geology suggests these raw materials were collected and transported from distances greater than 30 km.

During our analysis, we identified all three heat treatment proxies described in section 4.2 (Fig. 6), but 16 artefacts (12 %) had removal scars that could not be clearly assigned to either pre- or post-heating removals. These groups, the total count and the relative percentages of artefacts in each group are summarized in Table 2. The percentages in these groups demonstrate that the majority of the silcrete artefacts were manufactured on heat-treated raw material. Depending on whether undetermined pieces are included in the calculation or not, 81–92 % of the artefacts were knapped from heat-treated silcrete, as indicated by the presence of post-heating removal scars. On 19 % of these heat-treated artefacts, rough pre-heating removal scars from before heat treatment are preserved alongside a second generation of smooth post-heating removal scars. The abundance of heat-treated artefacts that show HINC-fractures (9.4 %), i.e. that show traces of overheating after which knapping continued, reveals that heat induced failure occurred during the procedure of heat treatment. We notice some differences between the yellowish coarse-grained silcrete (assumed to be local) and the finer grained varieties. When separated from the total, it can be noted that 40 % of the local silcrete could not be determined as 'heated' or 'unheated'. Two hypotheses may explain this higher number of indeterminate pieces on this type of silcrete: the difference might be related 1) to an analytical bias due to the coarse nature of the first type or 2) to a different technological treatment applied to this silcrete type (local silcrete of poorer quality would have been less frequently heat-treated or not at all).

Our lithic collection allows us to develop two main observations about heat treatment. First, raw blocks and flakes were both heated by EBC inhabitants and selected as cores. The presence of HINC-fracture surfaces (n = 10) suggests that silcrete frequently broke during heat treatment and that this was not a criterion to discard the blocks. From this observation it may be inferred (cf. infra) that shaping of the volume before heat treatment was minimal, though some cores preserve pre-heating removals. The second observation is that the number of small thermal fragments and pot-lids is low in our collection, suggesting that heat treatment was not necessarily conducted on site.

Only three silcrete cores are present in our collection (one of local silcrete, two of exotic silcrete), which contrasts with the relative high number of bladelets, micro-flakes and small fragments (Table 1). This data suggest that silcrete was introduced in two main technological forms: 1) as end-products: this is suggested by the high number of bladelets and their petrographic diversity; 2) as cores: this is suggested by the number of fragments ≤ 20 mm that most likely originate from knapping. Following this assumption, the low number of silcrete cores in our collection may suggest that some cores were

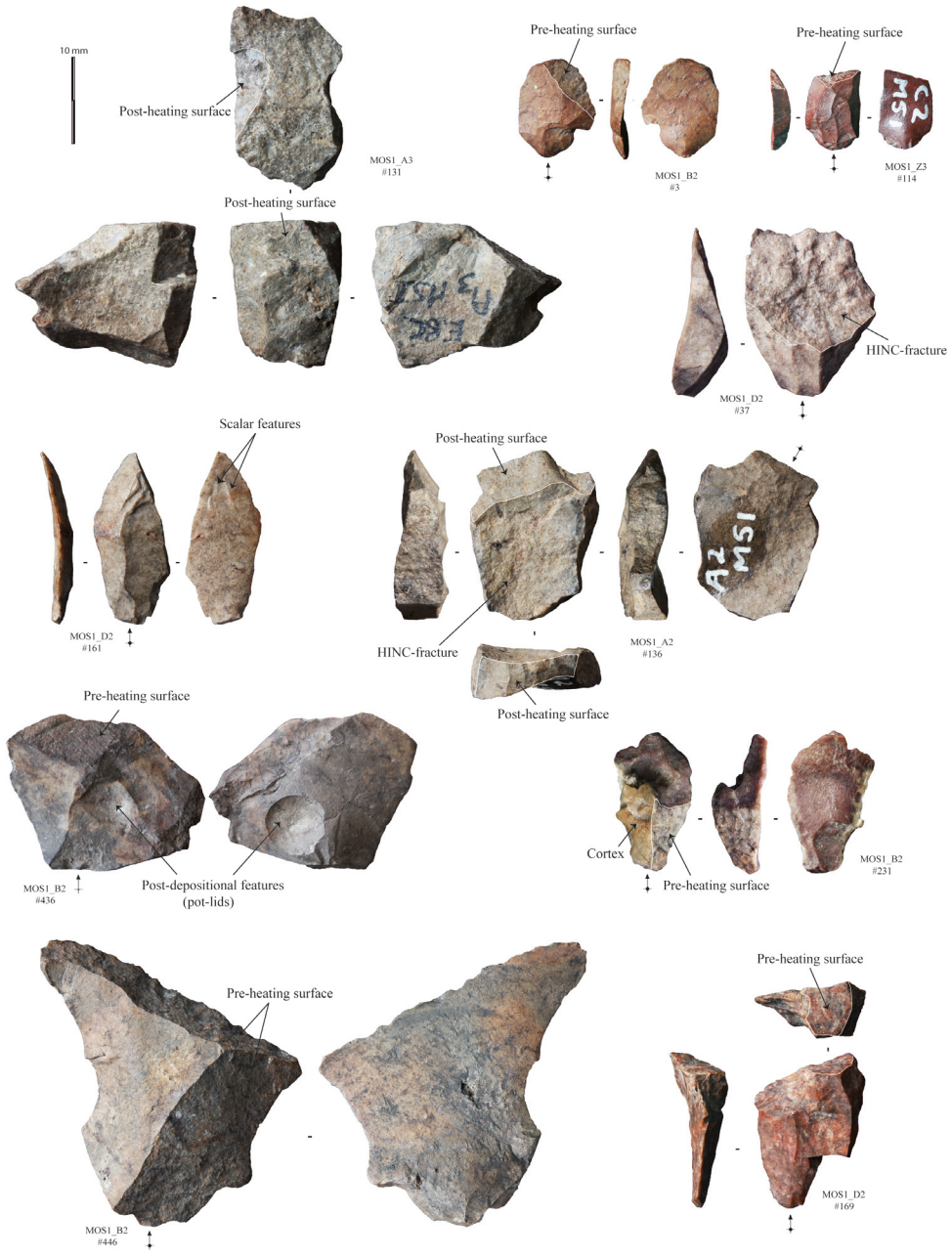

Fig. 6. Silcrete products bearing various indications of heat treatment. #131 is a frontal bladelet core with surfaces suggesting the volume was partly shaped before heat treatment. #3 is a microflake. #114 is a microflake with microbladelets removals. #37 is a technical flake intended to shape the transversal convexity of a bladelet core. #161 is a bladelet. #136 is a bladelet core-tablet. #436 is a flake. #231 is a technical flake intended to correct a removal that hinged (from an opposed platform). #446 is a flake. #169 is an irregular bladelet with opposed incidental removals indicating the use of anvil percussion.

TABLE 2

Results of the analysis of the silcrete artefacts MOS1 layer from Elands Bay Cave. Percentages under 'Percent total' refer to the total of analysed artefacts in the layers, percentages under 'Percent det.' refer to all determinable artefacts in the given layer but exclude non-diagnostic artefacts. Percentages under 'Percent HT' refer to the number of heat-treated artefacts in the layer.

	Count	% Total	% Determined	% Heat-treated
Non-diagnostic artefact	16	12 %		
Not-heated artefacts	9	7 %	8 %	
Artefacts with post-heating surfaces *Of which:*	106	81 %	92 %	
with both pre- and post-heating surfaces	20			19 %
with HINC-fracture surfaces	10			9 %
TOTAL	131	100 %	100 %	

introduced into the site, exploited *in situ* and taken away to another site ('ghost cores'; Porraz 2008). To these lines of evidence we may add the introduction as well of a few large silcrete flakes that were potentially exploited both as tools and as cores.

The other raw materials compose 3 % of the collection. This category includes coarse-grained locally available quartzite of poor quality for knapping. This coarse-grained quartzite is dominantly represented by flakes (n = 15/22). The other categories of rocks are represented by chert and by another type of finer grained quartzite, which are both locally available. However, the small number of artefacts, their high macroscopic diversity and the total absence of cortical products suggest that chert and fine-grained quartzite might be of non-local origin. The last petrographic group is hornfels. This rock was collected from secondary contexts, as indicated by the presence of pebble cortex (n = 4/5), and likely originate from terraces ca. 50 km northward of EBC. Hornfels was discarded at the site as flakes and small fragments.

What are the main core reduction sequences and for which technique(s)?

The collection is characterized primarily by the production of small artefacts, i.e. (micro-)bladelets and micro-flakes (Table 1). Blades, microblades and flakes represent only a minor component of the industry and together compose less than 10 % of the collection (Table 1). Blades seem to have mostly originated from an initial stage of the production (61 % of the blades have a cortical surface). Some of the flakes derive from an independent and expedient reduction strategy, as suggested by the quartzite category, but no core supports this assertion.

Aside from the expedient flake production, we are inclined to identify five main reduction strategies (Table 3, Figs 7, 8). Our sample represents 67 cores to which we associate 147 bipolar cores. It includes 12 undetermined cores that represent fragmented pieces or putative 'preforms'.

The 'high-backed' bladelet cores

This category, also called wedge-shaped bladelet cores in Mitchell (1995), was initially defined by Deacon (1978). The terminology reflects some ambiguity surrounding these

TABLE 3
List of the MOS1 cores from Elands Bay Cave.

	Quartz	Local Silcrete	Exotic silcrete	Quartzite	'Chert'	Hornfels	TOTAL
'High-backed' core	12	0	0	0	0	0	**12**
'Narrow-sided' cores	16	0	0	0	0	1	**17**
'Frontal' core	9	1	3	0	0	0	**13**
'Conic' core	4	0	0	0	1	0	**5**
Bipolar cores	8	0	0	0	0	0	**8**
Core-reduced pieces	136	1	0	0	1	1	**139**
Preforms & indetermined	12	0	0	0	0	0	**12**
TOTAL	**197**	**2**	**3**	**0**	**2**	**2**	**206**

pieces, initially called 'high-backed scrapers' due to the crushing along the platform that was similar to that along a scraper working edge (Deacon 1978).

The cores from our collection are all made from quartz (n = 12). EBC knappers preferentially selected quartz flakes that were produced by bipolar percussion. The knappers either oriented the flakes according to their long or short axis to position the removal surface. The shaping of the core consisted in the removals of two large flakes intended to flank the future removal surface, setting up the convexities of the core. The removal surface presents a conic shape and has a longitudinal convexity generally accentuated toward its base.

The reduction sequence can be considered as discontinuous, meaning that after the removals of a series of end-products, the knapper needed to reshape the surface in order to keep the same objective of production. The main products coming from this reduction sequence are bladelets. Direct observations on the (discarded) cores suggest final bladelets had a mean length between 8 and 11 mm and a mean breadth of 3 to 5 mm (Fig. 8). The conical shape of the surface did favour the production of bladelets that were pointed and slightly curved. From this reduction sequence, we expect to find three main categories of products: lateral flakes (for the transversal convexity), central bladelets (expected to be triangular) and lateral bladelets (expected to have a comma-like morphology). The platform is generally plain with mean angles ranging from 70 to 80°.

The 'narrow-sided' bladelet cores

This category corresponds to cores that have been exploited on their narrow surface (cores on edge). In our collection, they are all made of quartz (n = 16) except one made of hornfels. However, some technical products indicate that this reduction sequence also applied to silcrete.

The reduction sequence started with the selection of a quartz flake produced by bipolar percussion or, alternatively, by the selection of a slab with a triangular shape. The EBC knapper oriented the flake in order to locate the removal surface on its narrow side, generally in the longer axis. When necessary, a single (often partial) crest was realized to start or regularize the production. The shaping of the core could include

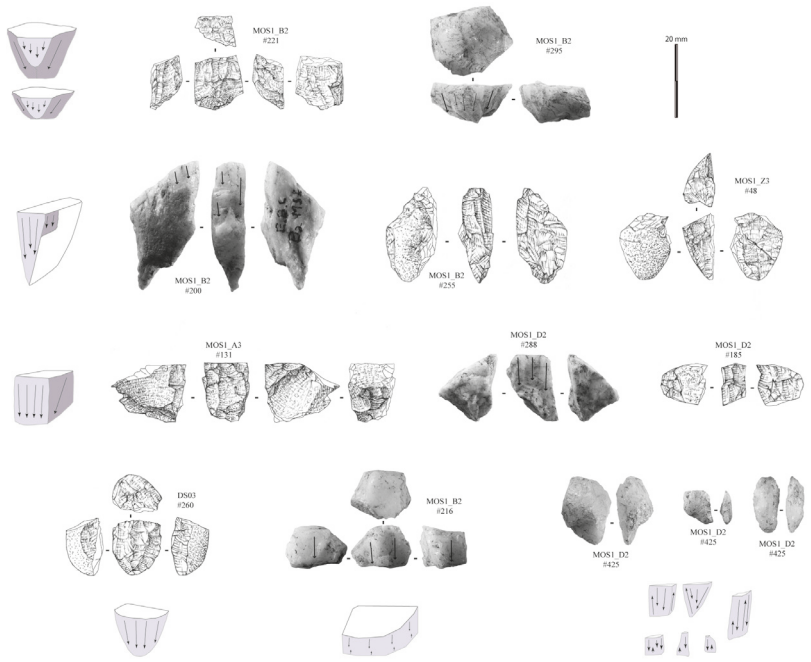

Fig. 7. Cores from the Robberg MOS1 lithic collection from Elands Bay Cave. #221 (silcrete) and #295 (quartz) represent 'high-backed' bladelets cores. #200, #255 and #48 (all in quartz) represent 'narrow-sided' bladelets cores. #131 (silcrete), #288 (quartz) and #185 (silcrete) represent 'frontal' bladelets cores. #260 (quartz) represents a 'conic' bladelet core. #216 (quartz) is a bipolar core. #425 (quartz) are bipolar-reduced pieces (drawings by Michel Grenet).

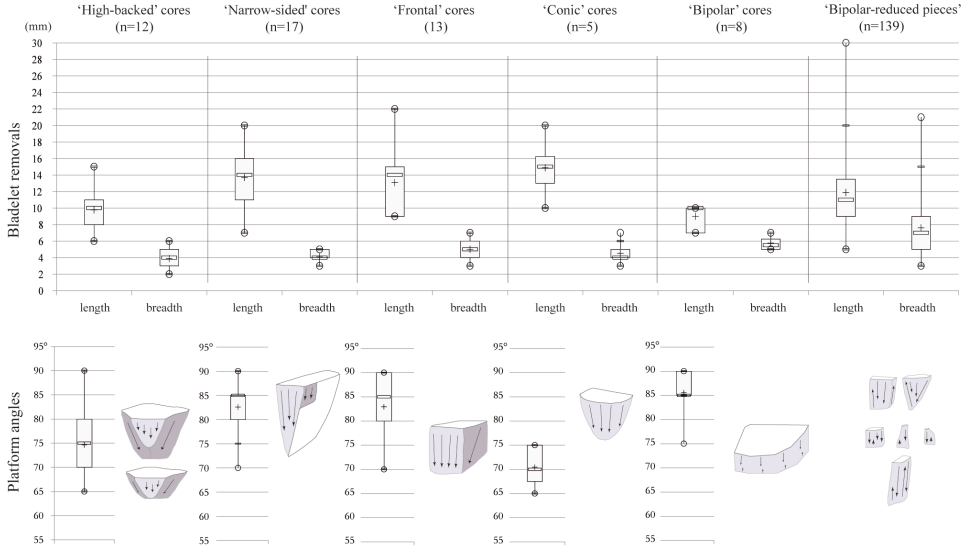

Fig. 8. Dimensional boxplots showing the variability within and between the individualized categories of cores.

some removals at its base, as illustrated by four cores. These removals at the base of the core, prior knapping, might have two purposes (not mutually exclusive): to facilitate the prehension of the core and/or to calibrate the length of the removal surface.

The general shape of the removal surface is 'conic'. The reduction progresses in the same axis all along the production, with one adjacent surface being partially invaded (1/3 prismatic). The reduction is continuous, meaning that the exploitation of the core doesn't require a new shaping after a series of removals. The control of the transversal convexity is managed by lateral bladelets (with often a cortical, a HINC-surface or a 'Kombewa' side) and the control of the longitudinal convexity by plunged products.

The bladelets are rectilinear and narrow; most of them present a triangular section and are pointed. The main morphology is expected to be parallel. The dimensions of the cores vary from 8 to 35 mm in length and 5 to 10 mm in breadth, but the removals do not always extend over the whole surface as indicated by the last removals: the dimensions of the bladelets range from 11 to 16 mm in length and 4 to 5 mm in breadth (Fig. 8). The platform is generally plain (one prepared and one cortical platform on a total of 16 cores) with mean angles between 80 and 85°. Some cores exhibit anvil scars at their base, suggesting they could have been held on a block while being knapped.

The 'frontal' bladelet cores

The 'frontal' bladelet cores share with the 'sided' cores the fact that for both the removal surface is located on the narrower surface of the core. But unlike the 'sided' cores, the frontal cores have a rectangular and 'flat' removal surface. Ten of these cores are made of quartz, four of silcrete.

The reduction sequence starts with the selection of a fragment or a large flake. The knapper oriented the fragment in order to exploit its narrower surface. When necessary, large flakes were detached to flank the main removal surface. The shaping of the core leads to create a removal surface that is relatively flat in its longitudinal and transversal sections. On four cores, we observe the presence of removals at the base of the core that we interpret as an option to calibrate the length of the removal surface (cf. supra).

The reduction sequence is continuous, meaning that the core doesn't need to be shaped after a first series of removals. The rhythm of the production keeps the surface more or less flat and doesn't invade largely the sides of the core. The convexities are controlled by the detachment of lateral bladelets and the use of bipolar technique. The bladelets coming from this reduction sequence are expected to be rectilinear with parallel edges and a triangular to trapezoidal section. Final bladelet removals are 9–15 mm long and 4–6 mm breadth. The platform is plain and has an angle bracketed between 80 and 90°. This reduction sequence implies the combination of bipolar and free hand percussion.

The 'conic' bladelet cores

The 'conic' bladelets cores might be considered as the most typical single platform cores with a semi-prismatic shape. This category includes five specimens, four made of quartz and one of chert.

The reduction sequence starts with the selection of a small block, a fragment or a flake. Little information about the initial shaping of the core can be inferred from our lithic assemblage. Some of these cores show orthogonal removals from their (raw) back

as well as from their base to set up the convexities, but the rhythm of the production seems to be firstly controlled by the removal of lateral and plunging bladelets. Most of these bladelets are slightly curved, with a triangular or a comma-like morphology. Final bladelet removals on the cores have a length between 13 to 16 mm and a mean width between 4 and 5 mm. The platform is kept plain and presents a mean angle of 70°.

The bipolar cores

The first group is composed of what we interpret as 'cores-to-cores' (n = 3, all in quartz). The reduction sequence starts with a selection of a pebble or a large fragment. These cores show different and independent removal surfaces that can give a polyhedral structure to the core at its stage of discard. Bipolar percussion is used to avoid problems of convexities. Regarding the general characteristics of our lithic assemblage, we interpret this reduction sequence as a way to fragment quartz pieces into smaller pieces intended afterwards to be exploited as cores.

The second group is represented by 'small-flake cores' (n = 5, all in quartz). The knapper starts by selecting a pebble, a slab or a large flake. There is no shaping of the core. The production starts directly by removing products on the thickness of the slab, progressively giving a semi-rotating structure to the core. The products are short, large and rectilinear, with a mean length between 7 and 10 mm and a mean breadth between 5 and 7 mm.

The third group is represented by the 'bipolar-reduced pieces'. The bipolar-reduced pieces form a large category that includes core reduced pieces and small and flat bladelet cores (Deacon 1984), *pièces esquillées* (Deacon 1978), 'rice-grain cores' and all other diminutive forms involving bipolar percussion. This category differs from the first two categories in their dimensions, their shapes as well as by the nature of the blanks that were produced, though they might represent one last stage in the reduction. This category represents the largest population of cores with 139 specimens, all except two being in quartz. These cores have either a plan-parallel or triangular shape and have a chisel-like platform. Removals on the cores show a 'radial' fracture, characteristic of bipolar production. Various blanks might have been selected to be exploited: flakes, small fragments as well as cores at their final stage of exploitation. The products show variability in shape, but are generally elongated. Though they are irregular, many of these products can be classified as (micro-)bladelets. The dimensional range of the last removals, as measured on the bipolar-reduced pieces, overlaps those from all other cores (Fig. 8).

The techniques of detachment

Authors have formulated different hypotheses regarding the nature of the techniques of detachment that were used by Robberg populations, but one agreement emerges from the literature, which is a common use of bipolar percussion. In the MOS1 assemblage, such evidence is indeed numerous. One interesting aspect regarding the use of this technique is that it was applied in different ways and for different purposes. Bipolar percussion appears for example to represent a common technique that was used to fragment quartz pebbles and to exhaust small cores. But anvil percussion was also regularly applied, as illustrated by the presence of anvil marks at the base of some bladelet cores. The common use of anvil percussion seems to have been a solution

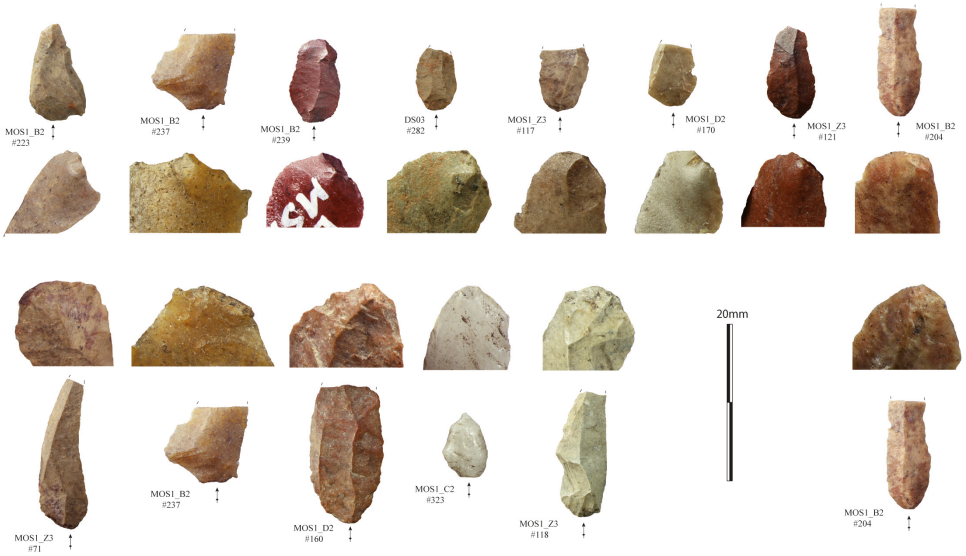

Fig. 9. Technical stigmata on the bladelets of the MOS1 Robberg from Elands Bay Cave (all in silcrete, except #323 in quartz). The presence of contact points (#223, #239, #282, #170, #121), of shattered bulbs (#282, #117) and shallow lips (#237, #204) together with the presence of intense abrasions (#71, #237, #160, #323, #118 and #204) suggest the application of a percussion slightly tangential with the use of (soft) stone hammer.

applied in response to different technical requirements: as a way to facilitate the support of small-sized bladelet cores, and as a way to correct accidents on the removal surfaces. Evidence of bipolar percussion is common among quartz pieces, but is also found on other raw materials including heat-treated silcrete. This technique cannot be interpreted as a direct adaptation to raw material properties; neither can it be related to a technical system that was predominantly oriented toward poorly standardized bladelets. This technique was part of the technical repertoire of the Robberg populations and contributes to define their technology.

Beside bipolar percussion, our observations on cores and bladelets lead us to reject the hypothesis of indirect percussion in favour of free hand percussion (Fig. 9). Abraded platforms indicate percussion that was intended to be marginal (a few millimetres inside); small contact points on the ventral faces indicate a localized contact (versus diffused); shattered bulbs indicate a hard contact and shallow lips indicate a percussion with a slightly tangential motion. All data converge to hypothesize the main use of soft stone hammer percussion to produce bladelets.

What are the main categories of blanks and for which functional purposes were they struck?

The reduction sequences were oriented toward the production of small blanks and notably of bladelets. The MOS1 bladelet corpus is composed of a majority of fragments that approaches 60 % of the population. Though the question related to the origin of these fractures requires further analyses, our preliminary observations allow us to propose that most breakages produced at the time of the knapping. The complete specimens

ANOVA Table for Length

	DDL	Sum of the squares	Medium Square	F value	p value	Lambda	Power
Rock 1	1	411,694	411,694	20,726	<,0001	20,726	,999
Residu	207	4111,775	19,864				

Table of means for Length
Effect: rock 1

	Number	Medium	Standard Dev.	Standard. Error
Quartz	134	11,287	3,296	,285
Silcrete	75	14,213	6,003	,693

Graphic of interactions for Length
Effect: Rock 1
Error Bar: interval of confidence 95%

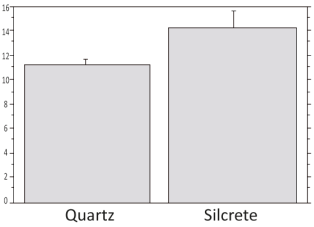

PLSD test of Fisher for Length
Effect: Rock 1
Significant: 5%

	Mean diff.	Crit. Diff.	p value	
Quartz, Silcrete	-2,926	1,267	<,0001	S

Table of means for Breadth
Effect: rock 1

	Number	Medium	Standard Dev.	Standard. Error
Quartz	134	5,910	2,194	,190
Silcrete	75	6,573	2,868	,331

Table of means for Thickness
Effect: rock 1

	Number	Medium	Standard Dev.	Standard. Error
Quartz	314	1,764	,907	,051
Silcrete	99	2,197	1,277	,128

Fig. 10. Data showing the dimensional means of quartz and silcrete bladelets from the MOS1 assemblage of EBC and statistical analysis discriminating the quartz and the silcrete bladelets (normality of the distribution verified).

document a mean length comprised between 8 and 16 mm (mean of 11.2 mm for the quartz and of 14.2 mm for the silcrete), a mean breadth comprised between 3 and 7 mm (mean of 5.9 mm for the quartz and of 6.5 mm for the silcrete) and a thickness centered around 2 mm (mean of 1.7 mm for the quartz and of 2.2 mm for the silcrete) (Fig. 10).

The dimensional analysis allows two main statements:

(1) We observe a significant difference ($p < 0{,}0001$) between the dimensions of the bladelets in quartz and those in silcrete (Fig. 10). This difference is clear when focusing, for example, on the length, with the bladelets in silcrete being significantly longer (by 3 mm) than those in quartz.

(2) Our study (Fig. 11) suggests that two silcrete populations can be statistically discriminated based on their length. The boundary between the two silcrete groups appears to be positioned between 13 and 15 mm, with one group of bladelets being ≤ 13 mm long and one group being ≥ 15 mm long.

The results of our dimensional analysis suggest a distinct raw material economy, between the quartz and the silcrete, and different reductions strategies within the silcrete. The implications are discussed further in the synthesis.

ANOVA Table
Breadth vs Length

	DDL	Sum of the squares	Medium Square	F value	p value
Regression	1	68,651	68,651	17,312	<,0001
Residu	70	277,217	3,96		
Total	71	345,778			

Regression coef.
Breadth vs Length

	Coefficient	standard error	standard. Coef.	t value	p value
cst. Term	2,928	,819	2,928	3,573	,0006
Length	,245	,059	,445	4,161	<,0001

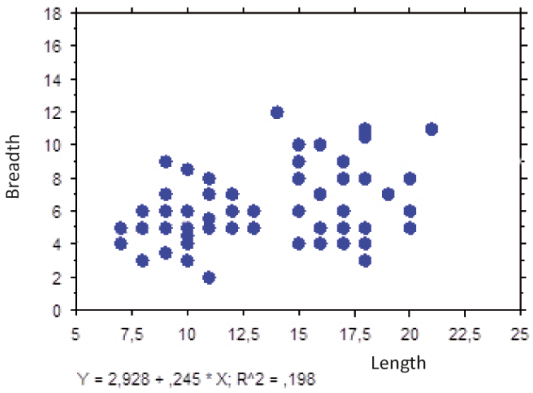

Fig. 11. Statistical analysis suggesting that two populations of silcrete bladelets can be discriminated based on their length (normality of the distribution verified).

The reduction sequences were oriented toward the production of small blanks with various morphologies (Fig. 12). Among the bladelets that could have been assigned to a morphological category (ca. 75 %), we observe a clear dominance of parallel bladelets (50 %) over the triangular (10 %) and the comma-like (5 %). Bladelets are dominantly rectilinear (62 %).

As well as the bladelets and the small flakes, there are a few blanks of bigger size represented by (micro-)blades and flakes. Blades and flakes do not show a high degree of preparation but all present regular edges. Interestingly, flakes often present a natural back opposed to a sharp edge.

The typological corpus of the MOS1 Robberg collection from EBC (Table 4) is characterized by three main characteristics:

(1) The proportion of modified pieces is more important than initially assumed (ca. 5 % of the whole assemblage): 7 % of the bladelets and 4.5 % of the flakes are modified, composing ca. 10.5 % of all silcrete products and ca. 4 % of all quartz products. Within the modified bladelets corpus, we observe an interesting pattern related to the morphotypes that were selected, with the parallel bladelets being under-represented (only ca. 9 % of the modified bladelets) by comparison with the triangular morphology (14 % of the modified bladelets) and the comma-like morphology (22.5 % of the modified bladelets).

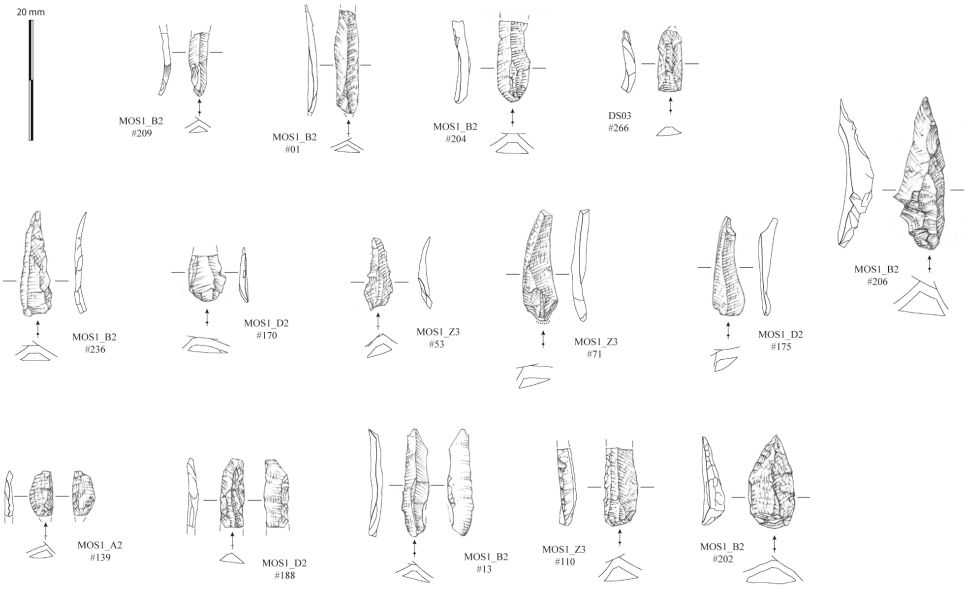

Fig. 12. Bladelets from the Robberg MOS1 lithic collection from Elands Bay Cave. #209, #01, #204, #13 #110 (all in silcrete) and #266, #139, #188 (quartz) are classified as 'parallel' bladelets. #236 (silcrete) and #170 (chert) are classified as triangular bladelets. #53 (quartz), #71 (silcrete) and #175 (chert) are classified as comma-like bladelets. #206 shows the preparation of a partial neo-crest. #139 (quartz), #188 and #13 (both silcrete) are ventrally blunted bladelets. #110 is a dorsally backed/blunted bladelet. #202 is a pointed retouched bladelet (drawings by Michel Grenet).

Out of a total of 47 bladelets, one originates from of a bipolar reduction sequence. We note also the high proportion of silcrete among formal tools (32 %) in comparison with the whole assemblage (15 %).

(2) The second element that typified the typological corpus is the low degree of transformation that characterizes the modified pieces. The retouch is always limited to a small portion of the products and/or is never invasive. Some actions were intended to sharpen the tool while others seem to have been intended to blunt the edge. If we focus on the modified bladelets, we have to acknowledge the occasional difficulty in discriminating what derives from use and what originates from retouch. In our study, we grouped together all bladelets bearing edge modification, regardless of their origins. In the MOS1 Robberg assemblage, it would appear that the very limited retouch was aimed more at correcting deficiencies of morphology rather than to shape, curate or re-sharpen the blanks.

(3) The third and last element that typified the typological corpus is the low diversity of the formal tools we identified. We separated 3 main categories which are 1) the modified bladelets, including blunted, backed and retouched specimens, 2) the notches and denticulates, and 3) the scrapers. The blunted bladelets represent bladelets that have been laterally transformed by a shallow and often irregular retouch, while backed bladelets have more

TABLE 4
List of the MOS1 modified pieces from Elands Bay Cave (in bracket: number of broken pieces).

	Quartz	Silcrete	hornfels	TOTAL
Modified bladelets - asymetric	8 (2)	4 (1)	0	12 (3)
Modified bladelets - symetric	18 (10)	6 (4)	0	24 (14)
Scrapers	3 (1)	4 (1)	1	8 (2)
Notches	6 (4)	2 (1)	0	8 (5)
denticulates	3 (3)	1 (1)	0	4 (4)
Fragment indetermined	1 (1)	2 (2)	0	3 (3)
TOTAL	**39 (21)**	**19 (10)**	**1**	**59 (31)**

regular and abrupt retouch. Modification of the bladelets occurs either laterally, or on the apex, but never on its base. Lateral modifications are always limited to one edge and are unifacial (ventral or dorsal) or bifacial. The notches (n = 8), the denticulates (n = 4) and the scrapers (n = 8) are dominantly of diminutive size but lack standardization; they were made on flakes and bladelets.

The present functional study rests on a total of 123 artefacts made of quartz and silcrete. The sample covered in particular the category of unmodified bladelets (n = 94) due to the high proportion of this class of artefacts, but it also includes modified bladelets (n = 19), flakes (n = 6), blades (n = 2) and *pièces esquillées* (n = 2). Overall, the edges and surfaces of artefacts are well preserved and allow for the use-wear analysis within reliable analytical conditions (Table 5). From the 123 artefacts analyzed, 62 show no signs of natural weathering but 18 exhibit edges and surfaces moderately damaged by post-depositional phenomena, presumably linked with a mechanical origin since the surfaces are marked by striae and flat bright polishes.

The analysis rests on a set of observations ranging from macro- to micro-traces. In our collection, three pieces show the presence of a black deposit that likely corresponds to remnant adhesive. Two of them show a black imprint with a diagonal distribution suggesting that only part of the edge was active (Fig. 13). One of these two examples is a silcrete lamellar flake with a trapezoidal morphology. Another piece with a similar morphology, but no black imprint, presents a polish on its proximal part that suggests a contact with a hard material that could originate from hafting.

Additional evidence on how the Robberg artefacts were hafted is indirectly inferred from the presence of macrofractures (Fig. 14). Four bladelets present typical fractures caused by longitudinal impact during use, indicating these bladelets were inserted axially. The morphology of the macrofractures suggests they likely result from a projectile impact. These bladelets have parallel or convergent edges: one is in quartz, three are in silcrete. None of these bladelets with macrofractures is modified.

The use-wear analysis brings decisive information on the function and economy of the blanks that were produced by the Robberg inhabitants of EBC, with 33 artefacts

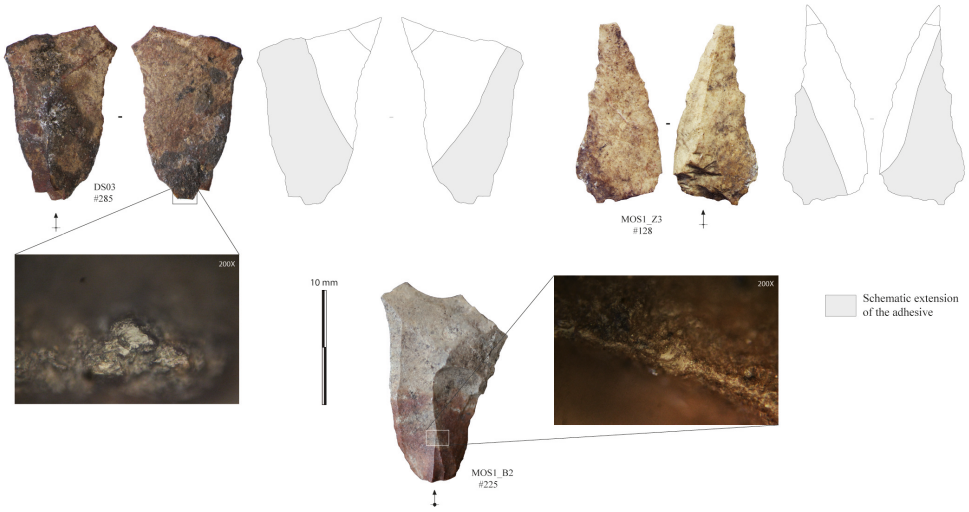

Fig. 13. Bladelets bearing evidences of hafting (all in silcrete). #285 presents a bifacial and symmetric black imprint as well as a polish of hard material contact that suggest the trapezoidal bladelet was hafted obliquely. #128 presents a shallow bifacial black imprint that suggests the asymmetric convergent bladelet was hafted obliquely. #225 presents a polish from a contact with hard material that likely originates from hafting. Notice the similar morphometric characteristics of #225 and #285.

bearing recognizable use-wear traces (Table 5). We can summarize our results into two main categories:

(1) The bladelets (Table 5, Fig. 15). The result of the analysis shows that all different sorts of bladelets were used, regardless of their size, their morphologies and the delineation of their edges (from convex to concave and from irregular to regular). Bladelets testify mostly to processing activities, being primarily used as cutting tools (n = 14). These activities are related to the working of hard materials (n = 4) and soft materials (n = 10) such as hide processing. We notice that one blade shows use-wear traces consistent with a transversal motion on hard material.

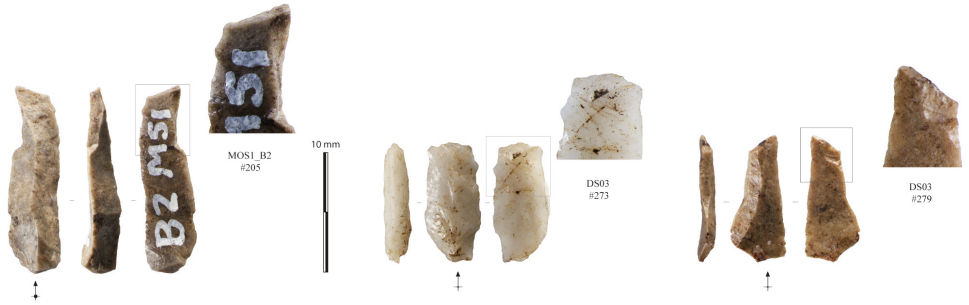

Fig. 14. Bladelets with fractures suggesting a possible projectile impact origin: #205 (silcrete) presents an impact burination; #273 (quartz) presents a bending fracture on its ventral surface; #279 (silcrete) presents a step-terminating fracture that continues parallel to the point's surface and terminates abruptly in a right angle break. Terminology according to Fisher et al. (1984).

TABLE 5

List and results of MOS1 Robberg pieces from Elands Bay Cave analyzed for use-wear traces. Bladelets were selected on the basis of the presence of macroscopic damage such as scars, edge rounding, fractures, potentially linked to tool use (in bracket: number of broken pieces).

					Worked materials and motions										
		Preservation			*longitudinal*		*transversal*			*percussion*					
Typo-techno.	**total**	good	weathered	use-wear traces	soft	hard	hard	wood	undet.	hard	bone	*Hafting*	*projectile impact*	*undet*	**Total**
Unmodified bladelets	94 (46)	46	48	**16**	6	3	-	-	2	-	-	1	2	2	**16**
Modified Bladelets	19 (6)	10	9	**8**	4	1	-	-	-	-	-	1	2	-	**8**
Flakes	6 (0)	3	3	**6**	2	2	1	1	-	-	-	-	-	-	**6**
Blades	2 (2)	1	1	**1**	-	-	1	-	-	-	-	-	-	-	**1**
Pièces esquillées	2 (0)	2	-	**2**	-	-	-	-	-	1	1	-	-	-	**2**
Total	**123 (54)**	**62**	**61**	**33**	**12**	**6**	**2**	**1**	**2**	**1**	**1**	**2**	**4**	**2**	**33**

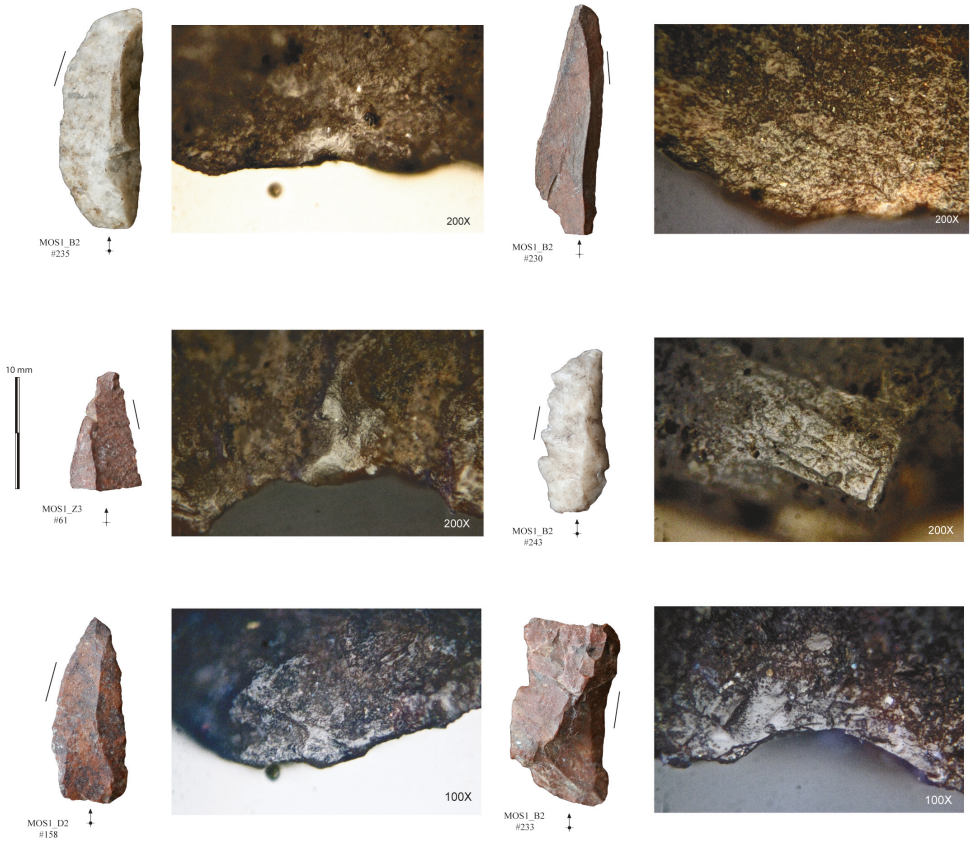

Fig. 15. Bladelets with microscopic use-wear traces. #235 (silcrete) presents a polish related with bone cutting (traces located on both sides of the used edge). #230 (hornfels) presents evidence of animal soft material cutting. #61 (silcrete) presents a polish associated with a slight edge rounding probably related to dry animal hide processing (fracture not morphologically characteristic). #243 (quartz) presents evidence of hard material cutting. #158 is a silcrete bladelet retouched on its right edge with evidence of soft material cutting on the unmodified edge. #233 (silcrete) presents evidence of hard material cutting (traces located on both sides of the used edge).

(2) The flakes (Table 5, Fig. 16). Microscopic observations give clear evidence that small flakes were also part of the functional system of the Robberg groups. All six flakes examined show use-wear traces: one flake was used to scrape wood, one other to scrape hard materials, two testify to a longitudinal motion (e.g. cutting) on hard material and two testify of soft material cutting.

We may finally open a discussion on the bipolar-reduced pieces, or *pièces esquillées*, as the two bipolar-reduced pieces analyzed for use-wear show polishes related to percussive activities on bone (Fig. 16). The nature of the technical task to which this evidence of bone processing corresponds remains uncertain. Although speculating on its origin is very preliminary, the hypothesis of the use of bone as an anvil to fracture the cores seems unlikely. In this case, the contact between bone and tool is too brief and usually

Fig. 16. Flakes and pièces esquillées with microscopic use-wear traces. #436 (silcrete) presents evidence of hard material cutting. #3 (silcrete) presents evidence of soft material cutting. #439 (silcrete) presents evidence of hard material scraping. #84 (silcrete) presents evidence of hard material cutting (fracture not morphologically characteristic). #391 (quartz) presents evidence of wood scraping, to notice the presence of sparse microstriation running perpendicularly to the use edge. #31 (quartz) presents evidence of soft material cutting. #189 and #129 (both in quartz) are two pièces esquillées that present evidence of percussive motions on bone.

causes too much edge damage to allow the preservation of any polish. The observed polishes on the two bipolar-reduced pieces are easily recognizable and could derive from percussive motions (the object forcefully strikes another with the intent of cracking). Amongst a variety of technical methods to work bone, percussive activities played an important role being commonly linked to bone chopping/breaking (Semenov 1964; Skakun et al. 2011; de la Torre & Mora 2010). According to recent experimental results, bone cracking in particular tends to cause patches of polish located over the edges of the working surface (de la Torre et al. 2013).

SYNTHESIS ON THE ROBBERG FROM ELANDS BAY CAVE

The MOS1 technical system

The Robberg technology is based on the production of small products having a maximum length of 25 mm. These products can be generically referred to as bladelets and micro-flakes. We distinguished six different reduction sequences that were used to produce various morphologies. These reduction strategies are independent, meaning they have their own specific rules and geometries. Some cores have more than one surface of removals but a switch from one modality to the other has rarely been observed.

On the basis of our collection, we are inclined to highlight the following main operative steps:

(1) The selection of the raw material and its fragmentation into smaller items. At EBC, the selection was oriented towards quartz and silcrete. Coarse-grained rocks such as local quartzite were barely exploited and only in an opportunistic way. Prior to knapping, EBC tool-makers fractured the rocks by bipolar percussion for quartz blocks and through heat treatment for silcrete. In the latter case, we do not question the intentionality of heat-alteration of the rocks for improving their flaking properties. Rather, we propose that heat treatment may have had a 'side effect': the more or less controlled pyrofracturation as an expected process. The presence of HINC-surfaces on 17 artefacts demonstrates that heat-induced breakage of silcrete was not a criterion for discard and even suggests the intentional use of pyrofracturation as already demonstrated for more recent contexts in Europe, Asia and Australia (Man 1883; Robinson 1938; Binford & O'Connel 1984; Guilbert 2003). Alternatively, flakes detached by free hand percussion on quartz and (pre)heated blocks were selected.

(2) The setting up of the removal surface. The knapper had first to orientate the blocks in order to mentally visualize the future surface of removals. The knapper then had a series of available 'options' to apply in terms of the reduction strategy. But one decisive parameter that seems to transcend all options relates to the 'calibration' of the core. Indeed, we argue that the dimensional range of the bladelets was a decisive criterion at the time of production. Beside morpho-functional arguments (bladelets never exceeded 25 mm long), this hypothesis rests upon a) the existence of different populations of bladelets in terms of dimensions and b) the presence of removals at the base of some of the cores prior to the knapping. This set of observations

suggests the dimensions of the main removals surface, and especially its length, were a crucial parameter for the knapper at the time of setting up the volume of the core.

(3) The combination of free hand and bipolar/anvil percussion. Anvil percussion was regularly used by Robberg inhabitants. The anvil percussion appears to represent an option intended to solve dimensional problems, i.e. to support the diminutive size of the cores during exploitation and to deal with issues of convexities (e.g. many cores, at their stage of discard, present platform angles bracketed between 80 to 90°). This technique was used regardless of the nature of the raw materials, though there is a stronger association with quartz (cf. the number of bipolar-reduced pieces). We argue that anvil percussion did relate to the diminutive size of the cores but also to a core configuration (geometry and dimensions) that was intended to remain 'stable' throughout the reduction. Size mattered for Robberg groups and anvil percussion was ideal to avoid major dimensional transformation throughout the reduction of the core. The absence of platform preparation and the rarity of core rejuvenation (only 12 core tablets in the whole assemblage) could be understood in such a technical context.

(4) The modification of the blanks. EBC inhabitants benefited from a wide set of available morphologies, resulting from the application of different reduction strategies. As expected, we observe a difference between the tools made on bladelets and those made on flakes, dominantly represented by scrapers, notches and denticulates. More surprisingly, we observe that certain morphologies of bladelets (triangular and comma-like) were more frequently modified than others, while they compose a minor part of the production. Retouch on bladelets was light, sometimes very shallow, and oriented toward minor modifications of the blanks.

(5) The microlithic system. We observe that all types of actions were carried out using microlithic blanks, i.e. by microflakes and (micro)bladelets that were dominantly used without any modification. The MOS1 lithic assemblage documents various actions and activities, from projectiles to scraping and cutting actions, though longitudinal motions are best represented in our studied sample. This large range of functions presupposes differences in the way the microlithic products were hafted. The presence of adhesive imprints together with macro- and micro-traces suggests blanks were glued into variable configurations: laterally, axially or obliquely. Bladelets and microflakes were part of a composite technology that seems to have structured the whole production (in terms of dimensions and morphologies of the inserts). Alongside microlithic products, larger blanks (microblades and flakes) appear to have played only a limited functional role.

Techno-economy of the MOS1 Robberg occupations

EBC inhabitants based their raw material provisioning strategies largely on the exploitation of local quartz pebbles. The second preferentially exploited raw material is silcrete. These two raw materials were exploited with similar objectives, but there are differences in the way they were introduced to the site. Quartz is immediately and

commonly available in the surroundings of the site: it was introduced into the shelter in its raw form and entirely exploited *in situ*.

The case is different for silcrete, which mostly originates from distances greater than 30 km. Based on the low number of thermal fragments in our collection, we suggest that silcrete might have been introduced into the site already heat-treated. Together with the low ratio of silcrete cores to silcrete bladelets (ca. 1/40) and with the high diversity of silcrete types, this suggests that the *chaîne opératoire* associated with silcrete was interrupted and fragmented in different places. Our current set of data indicates that EBC inhabitants introduced silcrete as bladelet cores (at different stages of their exploitation) and as (hafted) blanks (predominantly bladelets, but flakes as well). In that perspective, some products would have been transported out of EBC.

Although silcrete only composes 15 % of the lithic assemblage, this raw material appears to represent an important component as suggested by its proportion among the modified pieces (> 30 %). Also, we notice that silcrete bladelets were significantly longer than quartz bladelets. One interpretation would be to consider the influence of the raw material size on the dimensions of the blanks, but this argument does not conform to the assessment of the local geological context where quartz is largely available as blocks of appropriate dimensions. We rather interpret this difference in the context of different raw material economies (*sensu* Perlès 1991), potentially related to differences in mechanical properties.

The main goal of the MOS1 Robberg technological system was the production of small pieces. However, we observe the additional presence of a few larger products in the form of blades and flakes. While blades seem to originate from some initial stages of production, we argue that the larger flakes originate from independent reduction strategies. We observe two patterns for the production of flakes: a local and expedient production based on coarse-grained quartzite, and a non-local silcrete production with products being introduced from at least 30 km. Non-local flakes were used as tools but, additionally, were (later) exploited as cores.

Our functional analysis shows that all sorts of products were used, from bladelets to flakes and from first intention to technical products. These observations support the hypothesis that rocks were exhaustively used in a context of a fairly high economy. We may open a discussion on the bipolar-reduced pieces, as the two *pièces esquillées* analyzed for use-wear show polishes related to percussive activities on bone. Presently, we are tempted to see (some of) the bipolar-reduced pieces as 'janus products', potentially knapped with the intent of being used as a tool and with the intent of being fractured as a core, but only additional data can clarify this question.

The studied sample indicates a trend towards the preferential use of the bladelets with longitudinal actions, suggesting that the fresh cutting edges were the main functional part. But four bladelets indicate their probable use as projectiles. In contrast, flakes and blades were involved in a range of actions that were more diversified, including longitudinal but also transversal actions. But these preliminary ideas need to be tested by a more robust sample.

The MOS1 lithic assemblage documents groups that were collecting rocks from a large area of the West Coast, from the south to the east, as illustrated by silcrete, as well as from the north as showed by some pebbles. The raw material provisioning strategies as documented at EBC represents a flexible system, based on the exploitation

of locally available rocks (quartz being omnipresent in this area) and on the transport of a diversified tool-kit (small cores and hafted(?) small blanks) made of fine grained heat-treated silcrete. The pattern of rock procurement (*in situ* exploitation of local rocks, brief and various exploitations on non-local rocks, high macroscopic diversity of the rocks, isolated discarded finds) suggests that people were not radiating from EBC but were rather transiting from and to other places, as suggested by the identification of "ghost cores". The techno-economic pattern indicates an intense exploitation of the raw materials, i.e. meaning that all sorts of products were usable. But we do not observe any technical or functional specialization in the activities recorded at EBC. More data are now required to state what the mobility system of the Robberg groups was and how these groups were using EBC within their foraging strategy.

A preliminary diachronic view

The lower Robberg occupations at EBC (the D phase) date back to 19 398–18 790 cal. BP and are separated from the MOS1 occupation by a hiatus of about 4000 years. These lithic assemblage however share some similarities. This starts with the raw material provisioning strategies that are based on the predominant exploitation of local quartz and the additional exploitation of silcrete (Table 6), with, however, a silcrete component that is slightly higher in the D phase (ca. 23 %). We note that in both assemblages, evidence of heat-treated silcrete is common.

Regarding the reduction sequences, our 2011 sample of the lower Robberg is small and doesn't allow the development of a robust description and comparison. However the few cores and blanks of our collection document a strict emphasis on the production of small blanks, predominantly bladelets and micro-bladelets. All the types of reduction strategies identified within the MOS 1 assemblage can be recognized in the D phase, though frontal bladelet cores and bipolar-reduced pieces are dominant.

The bladelets from the lower Robberg fit morphologically within the categories we defined for the layer MOS1. A few blades were found but they remain rare and flakes are mostly associated with the local quartzite, as observed in the MOS 1 assemblage. The typological corpus of the D phase is very limited and only represented by three pieces, including two modified bladelets with a shallow retouch and one silcrete flake intensively transformed (Fig. 3). We point to the presence of one macro-tool bearing a facet that suggests the sandstone pebble was used as an upper grinding stone.

Late Pleistocene occupations from EBC have been well studied and published by Orton (2006). The author has subdivided the sequence he studied into 9 periods. The ones of most interest for the present study are the period A assigned to a Robberg-like phase (dated to 13 600 uncal b.p., including the layer MOS1), the period B assigned to a Late Pleistocene microlithic phase (dating from 13 100 to 11 370 uncal. b.p.) and period C assigned to a transitional phase (dating from 11 050 b.p. and 10 550 uncal b.p.).

First, we have to acknowledge the existence of some differences between our results and the ones published by Orton (2006). The period A is said to contain no formal tools in silcrete, no clear bladelet cores as well as relatively few bladelets (10.5 % of all flakes and blades in Orton 2006). There is no direct explanation for the absence of silcrete formal tools and bladelet cores. But the difference in bladelet proportions between our two studies might find different explanations. For example, the fact that the phase A not only includes the MOS 1 assemblage but is based on a more diversified

TABLE 6

List of the 2011 lithic assemblage associated with the earliest Robberg Stratigraphic Units from Elands Bay Cave.

	Quartz	**Local Silcrete**	**Exotic silcrete**	**Coarse Quartzite**	**Fine Quartzite**	**Chert**	**Hornfels**	**TOTAL**
Flakes	14	4	11	19	2	0	0	**50**
Blades (≥ 15 mm)	0	0	3	0	0	0	0	**3**
Micro-Blades (≥ 12 mm)	3	0	2	1	0	0	0	**6**
Bladelets (≤11 mm)	20	3	28	0	0	1	0	**52**
Micro-bladelets (≤5 mm)	9	1	7	0	0	0	0	**17**
Micro-flakes (≤20 mm)	84	1	16	2	0	0	0	**103**
Cores	10	2	5	0	0	1	0	**18**
Core-reduced pieces	17	0	0	0	0	0	0	**17**
Manuport	0	0	0	0	0	0	0	**0**
Fragments >20 mm	6	1	3	0	0	1	1	**12**
TOTAL	**163**	**12**	**75**	**22**	**2**	**3**	**1**	**278**
Fragments ≤20 mm	294	0	25	2	1	0	0	**322**
TOTAL	**457**	**12**	**100**	**24**	**3**	**3**	**1**	**600**

sample can be an explanation of the differing proportions. Additionally, the difference can relate to the criteria of definition we applied to 'fragments'. Indeed the proportion of bladelets appears to be inversely proportional to the proportion of 'chips' (Orton 2006): this certainly has a meaning in the sequence of changes recorded at EBC, but this should not be regarded as a difference between these two studies.

Orton's study documents a progressive diminution of local quartz from the phase A to the phase C in favour of the coarse-grained local quartzite. This occurs in parallel to a decline in bladelet manufacture, which is interpreted by the author as a progressive transition toward the non-microlithic Oakhurst technology (starting at EBC from ca. 10 000 uncal. b.p.).

The site of EBC presents a discontinuous archaeological and sedimentological record. Changes in topography and landscape at the time of the LGM and during the LG likely explain the punctuated nature of the EBC record. After an ELSA phase dating back to ca. 23–22 000 cal BP, there is an initial Robberg pulse at ca. 19 000 and a second pulse of occupation at ca. 14 500 cal BP. It is as yet not easy to draw clear comparisons between the 19 000 and the 14 500 Robberg lithic technologies. We notice technological and typological differences (in terms of presence and absence of certain categories) but their meaning (changes in activities or temporal trend within the Robberg) is still not understood. Then, as demonstrated by Orton (2006) and suggested by Parkington (1988), EBC seems to record a gradual technological change from the Robberg to the early Holocene occupations.

AN OVERVIEW OF THE SOUTH AFRICAN ROBBERG TECHNOLOGY

Most studies acknowledge the difficulty in recognizing spatial and temporal trends within the Robberg lithic industries. Not all Robberg assemblages are identical to one another, but differences are minor and/or potentially related to specific geologies or site activities.

Robberg industries share a general pattern of rock selection oriented toward fine-grained rocks, quartz included. This varies regionally but mirrors the geological availabilities as emphasized by Mitchell (1988b): the author described the south eastern part of South Africa as chert dominated and the Western Cape area as quartz dominated. The present study of EBC, located in the second region, confirms the clear emphasis toward quartz but we acknowledge as well a selection and use of heat-treated silcrete that played an important role within the procurement strategies.

What unifies the Robberg is first its specific technology based on single platform cores oriented toward the production of (micro-)bladelets (Deacon 1978, 1984; Mitchell 1988c; Wadley 1996), with the common use of the bipolar/anvil technique interwoven with free hand percussion. Several bladelet reduction strategies have been recognized in the literature, although they have been differently described and often grouped into large categories, such as single platform cores and irregular forms, hiding potential differences. We can currently emphasize three main 'types':

(1) The first type represents the bipolar-reduced pieces. This category includes different sorts of bipolar cores and varies regionally, but it is nonetheless documented throughout the sub-continent and can be considered as one characteristic of the Robberg technology.

(2) The second type represents the high-backed cores, once interpreted as tools. This reduction strategy has been identified in several Robberg sites such as Nelson Bay Cave (Deacon 1978), Sehonghong (Binneman & Mitchell 1997) and EBC. Though their internal variability requires better description, the high-backed cores category might also represent one characteristic of the Robberg technology.
(3) The third and last category is more heterogeneous as it includes various bladelets reduction strategies often classified as single-platform cores. At EBC, we subdivided this category into 3 distinct types (the 'narrow-sided', the 'frontal' and the 'conic' bladelet cores). Further studies will acknowledge the relevance or otherwise of these distinctions.

As a general statement, authors often describe cores with an initial shaping that has been limited. This is in agreement with our own study that suggests the reduction strategy is closely related to the morphology of the block *l.s.* selected by the knapper. At Sehonghong, Mitchell (1995) notes the frequent presence of crested bladelets, which would indicate the shaping of more specific core geometries. At EBC, crested bladelets have been identified mostly in the form of partial neo-crests (crests not intended to start the production but to correct the removal surface), which seems also to be the case at Sehonghong on the basis of published illustrations. At EBC, such technical products closely relate to 'narrow-sided' bladelet cores.

Core platforms were rarely prepared, as is illustrated by the dominant proportion of bladelets with plain butts such as at Rose Cottage Cave (Wadley 1993) and EBC. This interestingly goes with the rarity of core rejuvenation products, with the possible exception of Sehonghong (Mitchell 1995) although the ratio of core-tablets to cores remains relatively low (1/37). While the punch technique has been hypothesized, the evidence clearly favours the use of a direct and slightly tangential percussion with a soft stone hammer to produce bladelets. In addition, the use of bipolar knapping is documented in all Robberg sites. Interestingly, anvil percussion is documented in different contexts and applied to different raw materials, to different core geometries and at different stages of reduction.

Present studies show that the reduction strategies were not oriented toward blades but toward (micro)bladelets. Their proportions vary within and between sites, partly because of calculations based on different artefacts categories. The frequency of bladelets reaches up to 25 % at Rose Cottage Cave (Wadley 1996), varies from ca. 20 to 40 % of the lithic assemblages at Sehonghong (Mitchell 1995; Binneman & Mitchell 1997), represents ca. 20 % at Faraoskop (Manhire 1993) and ca. 16–19 % at AK2006/001 (Orton 2008). At EBC, bladelets form 55 % of whole blanks ≥ 20 mm. These variations relate firstly to analysts (see Pargeter & Redondo 2016) and have to be understood within a context that includes a substantial number of fragmented specimens as noticed at Rose Cottage Cave (Wadley 1996), AK2006/001 (Orton 2008) and EBC where 60 % of the bladelets are fragmented. The strong emphasis of Robberg technology on (micro)bladelets cannot be explained by any kind of raw material constraints or availabilities. The quasi-absence of macro-blanks (blades and flakes) defines a Robberg system that was fully microlithic.

No clear cut-size categories have been recognized within bladelets assemblages, though there are a few exceptions. Dimensional variations are generally viewed within a

continuous reduction sequence rather than as independent reduction strategies. So far, the significant differences we observed at EBC, suggesting the existence of different dimensional groups, find some parallels for example with the results published for Sehonghong (Pargeter & Redondo 2016). Further analysis will have to test and clarify the significance of these cut-size categories. However published data as well as our own study suggest the dimensions of the bladelets were a key parameter at the time of their production. At Nelson Bay Cave J. Deacon (1978) described the bladelets as no longer than 20 mm in length; at Sehonghong, Binneman and Mitchell (1997) described the bladelets as quite standardized in size, with mean length ranging from 12 to 24 mm and mean width from 4 to 8 mm; at Bloomplaas H.J. Deacon (1995) described the bladelets as less than 20 mm in length; at Byneskranskop 1 Pargeter (2012) described bladelets with length ranging from ca. 8 to 20 mm and mentioned a mean length of 17.5 mm at Rose Cottage Cave. At EBC, we found that the mean length of the bladelets is comprised between 8 and 16 mm and that complete specimens never exceed 25 mm. These metric data suggest some homogeneity between Robberg sites all over South Africa. This character, long noticed by J. Deacon (1978), Mitchell (1988a) and Wadley (1993), contributes to define the Robberg technology.

From the present literature it is clear that dimensions of the bladelets were a major technical and functional parameter. The possibility that cores were dimensionally calibrated, as hypothesized from the analysis of the MOS1 collection of EBC, seems a specific feature with no equivalent elsewhere. But what is worth mentioning in terms of 'calibration' is the possibility that some of the blanks were intentionally broken to fit the expected size. Intentional breaking might be exemplified by a few bladelets from EBC but this hypothesis requires further attention in order to discriminate intentional breaking from manufacture and post-depositional breaking. But at sites such as Sehonghong (Binneman & Mitchell 1997) and Rose Cottage Cave (Binneman 1997), the analysts mention the presence of several bladelets (hafted and used) with a proximal part that was removed by flaking.

In sites such as Sehonghong, it has been proposed that standardized bladelets were produced from highly distinctive forms of bladelet cores (Mitchell 1995). Standardization of Robberg products is reflected in their narrow dimensional ranges as well as by their morphologies. At EBC, we emphasize the production of three main morphologies of bladelets (parallel, triangular and comma-like), though we notice the clear emphasis on parallel bladelets. Data published by Binneman and Mitchell (1997) suggest bladelets with straight laterals were also dominant among the set of Robberg bladelets from Sehonghong. Similar observations have been made at Rose Cottage Cave (Wadley 1996) where regular parallel-sided bladelets form the main part of all bladelet morphologies.

Bladelets represent the main objective of Robberg production but the functional status of the (micro)flakes must not be underestimated. Flakes are regularly mentioned in Robberg lithic assemblages, though their technical and functional status is not always clearly addressed. At EBC, microflakes come largely from bladelet reduction strategies: either as an objective of production (documenting some latitude) or as technical operations. But two case studies differ. The first one relates to flakes that were produced on the coarse grained local quartzite: in that case, flakes result from an expedient reduction sequence and seem to answer immediate needs. The second example is

illustrated by the introduction of large flakes on fine-grained rocks. These large-flakes show no elaboration in their preparation and seem to have been preferentially transported as 'large' tools and/or cores. Our set of observations suggests the flake component is not a typical feature of the Robberg but is relevant while discussing techno-economic patterns.

The study of the MOS1 lithic collection from EBC shows that a wide range of products was used, regardless of their dimensions, morphologies and technical roles. Several authors have hypothesized the use of bladelets as projectiles (Deacon 1983; Parkington 1984). So far, macro-fractures interpreted as impact damages have not been recognized in many sites: one example potentially relates to a use as a component of a projectile weapon at Sehonghong (Binneman & Mitchell 1997), a few have been found at Nelson Bay Cave and Byneskranskop (Pargeter 2012). The new evidence from EBC, though limited, adds some substance to this hypothesis. All present examples document axial fractures suggesting bladelets were mounted in their longitudinal axis. The hypothesis of a concomitant use as barbs is not yet firmly supported by archaeological evidence.

Insights into Robberg hafting technology rest on the presence of black imprints interpreted as adhesive. Such imprints have been found on three products from EBC and on a large collection of artefacts (n = 44) from Sehonghong (Binneman & Mitchell 1997). If we consider the wide set of evidence (distribution of adhesives on the blanks together with the orientation of impact fractures and micro-wear residues), we can hypothesize a sophisticated composite technology where micro-blanks (bladelets and microflakes) were hafted in different ways: axially, laterally and obliquely. Additionally, some bladelets from Sehonghong (n = 1) and Rose Cottage Cave (n = 13) indicate they have been used on their two laterals suggesting they were turned in their haft/shaft (Binneman 1997; Binneman & Mitchell 1997).

Hafted microliths were not restricted to hunting activities. The use wear study performed at Sehonghong (Binneman & Mitchell 1997) and Rose Cottage Cave (Williamson 1996; Binneman 1997) clearly indicate that small blanks, predominantly bladelets, were involved in various motions (e.g. cutting, scraping) and on various worked materials (e.g. hide, vegetal material, bone). Similar conclusions have been reached at EBC, though the preliminary data suggest possible functional differences between the bladelets (predominantly involved in cutting activities on soft materials) and other blanks (involved in more diversified actions such as cutting and scraping, on soft and hard materials).

The Robberg lithic assemblages seem to indicate a need for fresh cutting edges. Binneman and Mitchell (1997) hypothesized that bladelets were short-lived single task tools, an idea that is supported by our analysis on EBC artefacts. But at the same time, several pieces of evidence indicate a fairly high degree of economy of the raw materials. This is, for example, suggested by some cores from Sehonghong that were used as tools, as well as by some bladelets that were used on both laterals and potentially turned in their haft (Binneman & Mitchell 1997). Such economizing of blanks compares well with our study from EBC.

Formal tools represent a minor component of Robberg lithic assemblages. This class of tools represents less than 1 % of the whole assemblage at sites such as Sehonghong (Binneman & Mitchell 1997), Faraoskop (Manhire 1993), AK2006/001G (Orton 2008),

Umhlatuzana (Kaplan 1989), Nelson Bay Cave (Deacon 1978) and Rose Cottage Cave (Wadley 1996). Our study from EBC differs substantially with a proportion of formal tools that reaches ca. 5 % of the whole assemblage ≥ 20 mm. We do not interpret this difference as a variation in site activities but rather see it as a difference in the way formal tools were recorded. Robberg assemblages, though they present a low degree of formal tools, often contain a fairly significant number of 'modified' pieces with edge scarring. These modifications are qualified as light nibbling (Mitchell 1995; Wadley 1996), shallow, expedient or blunting retouch (Wadley 1993, 1996) and are sometimes classified within the miscellaneous pieces (Orton 2008) or the utilized pieces (Binneman & Mitchell 1997). Robberg retouch is never invasive and its origin is sometimes questionable. In our study, it has been difficult to draw an analytical line between the different types of edge modifications. In search of a better analytical protocol, we decided to record all modifications, regardless of type, extension, invasiveness and origin. The retouch in Robberg assemblages, though it requires better description, can be considered as a technical pattern typifying this industry.

Within the formal typological corpus, the Robberg includes a range of modified bladelets, including backed bladelets. They are documented, for example, at Boomplaas, Nelson Bay Cave (Deacon 1984), Sehonghong (Mitchell 1995) and Rose Cottage Cave (Wadley 1996). However these backed bladelets never adequately typify the lithic assemblages. Other modified bladelets depict some variability that needs to be better described, both technologically and functionally. But one striking element that characterizes Robberg assemblages is the absence of 'microliths'/geometric tools, namely of bladelets or flakes that were intentionally shaped into geometric forms such as triangles, trapezes or crescents and segments. The other Robberg tools, such as denticulates, notches and scrapers, are more ubiquitous and they display little consistency within and between assemblages (see Mitchell 1995). In addition, we may remember the presence of macro-tools within Robberg assemblages, as mentioned at Sehonghong (Mitchell 1995), Rose Cottage Cave (Waldey 1996) as well as in the lower Robberg of EBC.

Albeit limited, some typological variety occurs from site to site. One of the rare examples is provided by the site of Sehonghong where truncated tools have been found in the lower Robberg units (Mitchell 1995). These pieces have been manufactured on bladelets and on flakes. So far, such tools have not been described elsewhere and might typify a phase or a regional expression/adaptation within the Robberg.

Some variations occur from site to site regarding the proportion of bladelets and/or of the types of cores discarded at the site. These variations reflect different mechanisms that relate to site functions, regional adaptations and temporal changes. The differences we noticed at EBC between the quartz and the silcrete (in terms of core types, dimensions and proportions of modified pieces) provide one illustration of the technological variability that might occur within and between Robberg sites.

So far, only a few studies have been able to define temporal trends within the Robberg, partly because of the discontinuous nature of the archaeological record and possibly because of the analytical tools. Regarding the earlier phase of the Robberg, Mitchell's study of the Sehonghong lithic sequence led him to hypothesize a chronological change between the LGM and the LG, though considerable technological continuity throughout the sequence is emphasized (Mitchell 1995). These differences between a LGM and

a LG phase are based on the patterns of core reduction and on potential functional changes in the way bladelets were used. Few other authors have discussed the earliest phases of the Robberg. Kaplan (1989), for example, proposes the distinction between an 'early' and a 'late' Robberg at Umhlatuzana on the basis of the frequencies of *outils écaillés* and bladelets that are higher in the lower phase. It is also worth noticing the recent work at Putslaagte 8 where the 25–22 000 BP lithic group is said to have some Robberg-like characteristics although there are differences with the 21–18 000 BP group classified as more typical Robberg (Mackay et al. 2015). Additionally, Pargeter and Redondo (2016) recently recognized that bladelets from Sehonhong changed in morphology after 18 000 cal. BP.

In the EBC sequence, there is a clear trend at the end of the Robberg toward a larger selection of coarse-grained rocks and the production of flakes (Parkington 1990; Orton 2006). A similar trend has been noticed at Sehonghong (Mitchell 1995), when Robberg inhabitants start to exploit dolerite and hornfels more frequently than opalines, as well as at Nelson Bay Cave (Deacon 1978) where quartzite becomes dominant over quartz. This change in raw material selection and blank production suggests a contemporaneous and potentially gradual technological transformation toward the end of MIS2.

While there are some regional variations and uncertainties regarding the chronology, the present set of data may support the existence of three main stages within the Robberg, though their significance and nature remain to be further evaluated. These stages would be composed of an early phase from 23 000 until 18 000 BP (LGM), an LG phase that would last until 13 000 BP, and a terminal phase that will last until the 'transition' to Holocene technologies sets in. The understanding of these phases might bring new information on how groups adapted and what the details of the Robberg technology imply within the panel of microlithic industries.

TO CONCLUDE

The technological identity of the Robberg is based on an exclusive production of bladelets that were bracketed within a narrow dimensional range (max. of 22–25 mm long, max of 8–10 mm breadth). These bladelets were obtained from various reduction strategies associated with both free hand and anvil percussion. Different morphologies of bladelets were produced but those with parallel laterals were the main component. Modifications of the blanks were limited, in terms of frequency and intensity, and often took the form of irregular and shallow retouch. All these blanks appear to be part of a composite technology and hafted in different positions: laterally, obliquely and axially. These characteristics, together with the 'absence' of blades and geometric tools, contribute to defining the Robberg as a non-geometric microlithic technology and add further variability to the known corpus of Late Pleistocene technologies.

The Robberg is somewhat coherent in technology but is also characterized by a complex system of territorial networks and symbolic communication (Mitchell 2002). Robberg occupations have been found in different contexts, from the coast to high altitudes, from caves to open-air sites, depicting a system adapted to all sorts of different environments. More detailed studies (in terms of technology and subsistence) will help clarify the discussion of the existence and significance of spatial and temporal trends within the Robberg.

The Robberg is characterized by several innovations, one of which is the use of heat treatment applied to silcrete. This technological innovation was only recently discovered in the South African MSA and the question of its precise time frame, its spatial and temporal evolution and the associated procedures is still a matter of debate (Schmidt et al. 2013; Schmidt et al. 2015; Wadley & Prinsloo 2014). The evidences from EBC extends the chronology and known contexts of heat treatment on South Africa's West Coast, with evidence from the Robberg but also from the late MSA and ELSA (Porraz et al. 2016 this issue). Furthermore, if heat treatment was mainly applied to improve the suitability of silcrete for knapping, we observe a side-effect: pyrofracturation of the blocks used to pre-segment blocks before knapping. Although no tempering residues on silcrete artefacts have so far been found on Robberg lithics, the recurrent presence of HINC fracture surfaces indicates that heat treatment was performed without a specific set up of the fires (see Schmidt et al. 2015).

The main innovation associated with the Robberg relates to its microlithic nature. This technology was the solution adopted by Robberg groups to cope with new needs, of internal and/or external origin. One way to understand the spark behind this innovation is to regard the benefits and the implications that might be associated with such an innovation, and to question its context of appearance as well as its variability in space and development in time. We might also refer to other microlithic industries that developed independently and that might give new clues of interpreting the Robberg.

One of the main current questions regards the origin of the Robberg. There are uncertainties regarding the nature and form of the technological succession from the ELSA to the Robberg. And it is presently an assumption to consider the ELSA as one homogeneous tradition. The current set of data shows continuity regarding the production of small products and the use of bipolar percussion. But the ELSA and the Robberg differ regarding the nature of their reduction sequences, the control and regularity of the products as well as their sets of formal tools. More techno-typological studies as well as new controlled excavation and new 14C dating are yet required to clarify this succession. As currently seen, the Robberg seems to appear at ca. 23 000 cal. BP from Limpopo to the West Coast, suggesting a 'rapid' diffusion of groups and/or adoption of ideas throughout the sub-continent.

The appearance of the LGM and the rise of Robberg industries represent an improbable coincidence. However, if the LGM offers a context of appearance, it does not give any direct explanation of what the main changes were that populations had to face. What we observe is that the Robberg technology marks a new stage in local microlithic technology, characterized by a composite technology that durably impacted the sizes and morphologies of the inserts.

The miniaturization of tools changes the way populations had to plan and adapt to available geological resources, giving access to a wider range of raw materials. In the meantime, it presumably represents an easily transportable technology as well as a maintainable and reliable technology with inserts that were quickly and easily replaced (see Mitchell 1988b). These observations (and assumptions) characterize a system that was optimizing time, from procurement to manufacture, and that surely impacted the way populations were territorially organized. Based on the study from EBC, the nature of the raw material provisioning strategies supports the hypothesis that the shelter was occupied by small groups for rather short-term occupations.

The Robberg differs from other sub-contemporaneous industries from Eurasia (e.g. Clarkson et al. 2009; Langlais et al. 2012; Tomasso 2014) or from other industries classified as microlithic (e.g. the Howiesons Poort). One main difference relates to the larger blades that still represent a primary component in these industries while they have 'disappeared' in the Robberg system. Moreover, unlike the Robberg, other composite technologies are associated with geometric forms, which are often interpreted as a change related to the adoption of new hunting weapons.

The understanding of the Robberg, that is, the reasons behind its appearance, has to be integrated within a regional perspective, in other word with regard to the ELSA technologies, environment and symbolisms. But this question should also be addressed with regard to other microlithic industries that might help deciphering what manifestations relate to the historical processes and what manifestations relate to the trend (or '*tendance*', after Leroi-Gourhan 1945). In a technical perspective, the disappearance of the blade (its obsolescence) has been interpreted as one stage of development of composite technologies (Boëda 2013). The Robberg is presently a unique manifestation. While it shares for example strong similarities with the European Mesolithic regarding its miniaturization, the lack of geometrics illustrates a different functional path. The Robberg signs an original technical trajectory and challenges the way we approach and understand broader technical processes such as those of microlithization and geometrization.

NOTE

[1] The limit we established between blades and bladelets follows Tixier (1965).

ACKNOWLEDGEMENTS

We thank the French Ministry of Foreign Affairs, the Deutsche Forschung Gemeinschaft, the University of Cape Town, the Iziko Museum and the South African Heritage Resources Agency for their help and support throughout the Elands Bay Cave project. Many thanks as well to the Laboratoire des Sciences du Climat et de l'Environnement (LSCE) and the Laboratoire de mesure du Carbone 14 (LMC14) for the C14 dating. We thank David Witelson for his help with the English editing as well as Isabelle Théry-Parisot for her help with statistics. Many thanks to Janet Deacon, Lyn Wadley, Jayson Orton, Justin Pargeter and a fifth reviewer for their valuable comments and inputs.

REFERENCES

Barrière, C., Daniel, R., Delporte, H., de Fonton, E., Parent, R., Roche, A.J., Rozoy, J.G., Tixier, J. & Vignard, E. 1969. Epipaléolithique-Mésolithique: les microlithes géométriques. *Bulletin de la Société préhistorique française* **66**: 355–66.

Beaumont, P.B. 1981. The Heuningneskrans Shelter. In: E.A. Voigt, ed., *Guide to archaeological sites in the northern and eastern Transvaal*. Prepared for the Southern African Association of Archaeologists excursion, 6–11 June, pp. 132–45.

Boëda, E. 2001. Détermination des unités techno-fonctionnelles de pièces bifaciales provenant de la couche acheuléenne C'3 base du site de Barbas I. In: D. Cliquet & M. Otte, eds., *Les industries à outils bifaciaux du Paléolithique moyen d'Europe occidentale*. Actes de la Table Ronde internationale organisée à Caen (Basse-Normandie, France). ERAUL 98. Liège: Service de préhistoire, Université de Liège, pp. 51–75.

Boëda, E. 2013. *Techno-logique & technologie: une paléo-histoire des objets lithiques tranchants*. @ rchéo-éditions.

Boëda, E., Geneste, J. M. & Meignen, L. 1990. Identification de chaînes opératoires lithiques du Paléolithique ancien et moyen. *Paléo* **2** (1): 43–80.

Binford, L.R. & O'Connel, J.F. 1984. An Alyawara day: the stone quarry. *Journal of Anthropological Research* **40** (3): 406–32.

Binneman, J. 1997. Usewear traces on Robberg bladelets from Rose Cottage Cave. *South African Journal of Science* **93** (10): 479–81.

Binneman, J.N.F. & Mitchell, P.J. 1997. Usewear analysis of Robberg bladelets from Sehonghong Shelter, Lesotho. *Southern African Field Archaeology* **6**: 42–9.
Brown, K.S., Marean, C.W., Herries, A.I., Jacobs, Z., Tribolo, C., Braun, D., Roberts D.L., Meyer M.C. & Bernatchez, J. 2009. Fire as an engineering tool of early modern humans. *Science* **325** (5942): 859–62.
Cartwright, C., Parkington, J.E. & Porraz, G. 2016. The wood charcoal evidence from renewed excavations at Elands Bay Cave. *Southern African Humanities* **29**: 249–58.
Charrié-Duhaut, A., Porraz, G., Igreja, M., Texier, P.-J. & Parkington, J.E. 2016. Holocene hunter-gatherers and adhesives manufacture in the West Coast of South Africa. *Southern African Humanities* **29**: 283–306.
Callahan, E. 1987. *An evaluation of the lithic technology in Middle Sweden during the Mesolithic and Neolithic*. Uppsala: Societas Archaeologica Upsaliensis 8.
Clark, P.U., Dyke, A.S., Shakun, J.D., Carlson, A.E., Clark, J., Wohlfarth, B., Mitrovica, J.X., Hostetler, S.W. & Marshall McCabe, A. 2009. The Last Glacial Maximum. *Science* **325**: 710–14.
Clarkson, C., Petraglia, M., Korisettar, R., Haslam, M., Boivin, N., Crowther, A., Ditchfield P., Fuller D., Miracle P., Harris C., Connell K., James H. & Connell, K. 2009. The oldest and longest enduring microlithic sequence in India: 35 000 years of modern human occupation and change at the Jwalapuram Locality 9 rockshelter. *Antiquity* **83** (320): 326–48.
Conard, N.J., Porraz, G. & Wadley, L. 2012. What is in a name? Characterising the 'post-Howieson's Poort' at Sibudu. *South African Archaeological Bulletin* **67**: 180–99.
Cowling, R.M., Cartwright, C.R., Parkington, J.E. & Allsopp, J.C. 1999. Fossil wood charcoal assemblages from Elands Bay Cave, South Africa: implications for Late Quaternary vegetation and climates in the winter-rainfall fynbos biome. *Journal of Biogeography* **26** (2): 367–78.
De la Peña, P. 2015. A qualitative guide to recognize bipolar knapping for flint and quartz. *Lithic technology* **40** (4): 1–16.
De la Torre, I. & Mora, R. 2010. A technological analysis of non-flaked stone tools in Olduvai Beds I & II. Stressing the relevance of percussion activities in the African Lower Pleistocene. In: V. Mourre & M. Jarry, eds., *Entre le marteau et l'enclume. La percussion directe au percuteur dur et la diversité de ses modalités d'application. Actes de la table ronde de Toulouse (March 2004). Paléo* **numéro spécial**: 13–34.
De la Torre, I., Benito-Calvo, A., Arroyo, A., Zupancich, A. & Proffitt, T. 2013. Experimental protocols for the study of battered stone anvils from Olduvai Gorge (Tanzania). *Journal of Archaeological Science* **40** (1): 313–32.
Deacon, H.J. 1976. *Where hunters gathered: a study of Holocene Stone Age people in the Eastern Cape*. Claremont: South African Archaeological Society.
Deacon, H.J. 1983. The peopling of the fynbos region. Fynbos paleoecology: a preliminary synthesis. *South African Scientific Programmes Report* **75**: 183–209.
Deacon, H.J. 1995. Two late Pleistocene-Holocene archaeological depositories from the southern Cape, South Africa. *South African Archaeological Bulletin* **50**: 121–31.
Deacon, J. 1978. Changing patterns in the late Pleistocene/early Holocene prehistory of southern Africa as seen from the Nelson Bay Cave stone artefact sequence. *Quaternary Research* **10** (1): 84–111.
Deacon, J. 1984. *The Later Stone Age of southernmost Africa*. Cambridge Monographs in African Archaeology 12. International Series 213. Oxford: BAR.
Deacon, J. 1988. The scale and timing of technological and environmental changes over the last 20 000 years in the southern Cape, South Africa. In: J. Bower & D. Lubell, eds., *Prehistoric cultures and environments in the Late Quaternary of Africa*. Cambridge Monographs in African Archaeology 26. International Series 405. Oxford: BAR, pp. 145–62.
Deacon, J. 1990. Changes in the archaeological record in South Africa at 18 000 BP. In: C. Gamble & O. Soffer, eds., *The World at 18 000 BP: the low latitudes*. London: Unwin Hyman, pp. 170–88.
Deacon, H.J. & Deacon, J. 1999. *Human beginnings in South Africa*. Cape Town: David Philip.
Ehlers, J. & Gibbard, P.L. 2007. The extent and chronology of Cenozoic global glaciation. *Quaternary International* **164**: 6–20.
Elston, R.G. & Kuhn, S.L. 2002. *Thinking small: global perspectives on microlithization*. Arlington, VA: American Anthropological Association.
Féblot-Augustins, J. 1997. *La circulation des matières premières au Paléolithique*. ERAUL 75. Liège: Service de préhistoire, Université de Liège.
Fisher, A., Vemming Hansen, P. & Rassmussen, P. 1984. Macro and micro wear traces on lithic projectile points: experimental results and prehistoric examples. *Journal of Danish Archaeology* 3: 19–46.
Gardin, J.C. 2002. The logicist analysis of explanatory theories in archæology. In: R. Franck, ed., *The explanatory power of models: bridging the gap between empirical and theoretical research in the social sciences*. New York: Springer, pp. 267–84.

Geneste, J.M. 1992. Systèmes techniques de production lithique. Variations techno-économiques dans les processus de réalisation des outillages paléolithiques. *Techniques & Culture*. **17–18**: 1–35.
Gonzales Urquijo, J.E. & Ibanez Estevez, J.J. 2004. *Metodologia de analisis funcional de instrumentos tallados en silex*. Bilbao: Universidad de Deusto.
Guilbert, R. 2003. Les systèmes de débitage de trois sites sauveterriens dans le Sud-Est de la France. *Bulletin de la Société préhistorique française* **100** (3): 463–78.
Hayden, B., ed. 1979. *Lithic use-wear analysis*. New York: Academic Press.
Igreja, M. 2009. Use-wear analysis of non-flint stone tools using DIC microscopy and resin casts: a simple and effective technique. In: M. Igreja & I. Clemente-Conte, eds., *Recent functional studies on non flint stone tools: Methodological improvements and archaeological inferences*, 23–25 May 2008, Lisboa, Proceedings of the workshop. Lisboa: Padrão dos Descobrimentos.
Igreja, M., Clemente-Conte, I. 2009. *Recent functional studies on non flint stone tools: methodological improvements and archaeological inferences*. Lisbon: Padrão dos Descobrimentos.
Igreja, M. & Porraz, G. 2013. Functional insights into the innovative Early Howiesons Poort technology at Diepkloof Rock Shelter (Western Cape, South Africa). *Journal of Archaeological Science* **40** (9): 3475–91.
Inizan, M.L., Reduron-Ballinger, M. & Roche, H. 1999. *Terminology and technology of knapped stone*. Meudon: Centre National de la Recherche Scientifique.
Iovita, R., Schönekeß, H., Gaudzinski-Windheuser, S. & Jäger, F. 2014. Projectile impact fractures and launching mechanisms: results of a controlled ballistic experiment using replica Levallois points. *Journal of Archaeological Science* **48** (1): 73–83.
Jerardino, A., Klein, R.G., Navarro, R.A., Orton, J. & Horwitz, L.K. 2013. Settlement and subsistence patterns since the terminal Pleistocene in the Elands Bay and Lamberts Bay areas. In: A. Jerardino, A. Malan & D. Braun, eds., *The archaeology of the West Coast of South Africa*. Cambridge Monographs in African Archaeology 84. International Series 2526. Oxford: BAR, pp. 85–108.
Kaplan, J.M. 1989. 45 000 years of hunter-gatherer history in Natal as seen from Umhlatuzana Rock Shelter. *South African Archaeological Society Goodwin Series* **6**: 7–16.
Keeley, L.H., 1980. *Experimental determination of stone tool uses: a microwear analysis*. Chicago: University of Chicago Press.
Kelly, R.L. 1995. *The foraging spectrum: diversity in hunter–gatherer lifeways*. Washington, DC: Smithsonian Institution Press.
Klein, R.G. 1974. Environment and subsistence of prehistoric man in the southern Cape Province, South Africa. *World Archaeology* **5** (3): 249–84.
Kuhn, S. 1995. *Mousterian lithic technology and raw material economy: a cave study*. Princeton: Princeton University.
Langlais, M., Costamagno, S., Laroulandie, V., Pétillon, J.M., Discamps, E., Mallye, J.B., Cochard, D. & Kuntz, D. 2012. The evolution of Magdalenian societies in South-West France between 18,000 and 14,000 cal BP: Changing environments, changing tool kits. *Quaternary International* **272**: 138–49.
Lepot, M. 1993. *Approche techno-fonctionnelle de l'outillage lithique Moustérien: essai de classification des parties actives en termes d'efficacité technique*. Masters thesis, University of Paris X.
Leroi-Gourhan, A. 1945. *Evolution des techniques: milieu et techniques*. Paris: Albin Michel.
Leroi-Gourhan, A. 1964. *Le geste et la parole. I: Technique et language. II: La mémoire et les rythmes*. Paris: Albin Michel.
Loftus, E., Sealy, J., & Lee-Thorp, J. 2016. New radiocarbon dates and bayesian models for Nelson Bay Cave and Byneskranskop 1: implications for the South African Later Stone Age sequence. *Radiocarbon* **58** (2): 365–81.
Lombard, M., 2005. Evidence of hunting and hafting during the middle stone age at Sibudu cave, Kwazulu-Natal, South Africa: a multianalytical approach. *Journal of Human Evolution* **48** (3): 279–300.
Lombard, M. & Pargeter, J. 2008. Hunting with Howiesons Poort segments: pilot experimental study and the functional interpretation of archaeological tools. *Journal of Archaeological Science* **35** (9): 2523–31.
Lombard, M., Wadley, L., Deacon, J., Wurz, S., Parsons, I., Mohapi, M., Swart, J. & Mitchell, P. 2012. South African and Lesotho Stone Age sequence updated. *South African Archaeological Bulletin* **67**: 123–44.
Mackay, A., Jacobs, Z., & Steele, T.E. 2015. Pleistocene archaeology and chronology of Putslaagte 8 (PL8) rockshelter, Western Cape, South Africa. *Journal of African Archaeology* **13** (1): 71–98.
Man, E.H. 1883. On the aboriginal inhabitants of the Andaman Islands. *Journal of the Anthropological Institute of Great Britain and Ireland* **12**: 69–116.
Manhire, A. 1993. A report on the excavations at Faraoskop Rock Shelter in the Graafwater district of the south-western Cape. *Southern African Field Archaeology* **2**: 3–23
Miller, C.E., Mentzer, S., Berthold, C., Leach, P., Schulz H., Tribolo, C., Parkington, J.E. & Porraz, G. 2016. Site formation processes of the Middle Stone age deposits from Elands Bay Cave, South Africa. *Southern African Humanities* **29**: 69–128.

Mitchell, P. 1988a. Human adaptation in southern Africa during the Last Glacial Maximum. In: J. Bower & D. Lubell, eds., *Prehistoric cultures and environments in the Late Quaternary of Africa*. Cambridge Monographs in African Archaeology 26. International Series 405. Oxford: BAR, pp. 163–96.

Mitchell, P. 1988b. The Late Pleistocene early microlithic assemblages of southern Africa. *World Archaeology* **20** (1): 27–39.

Mitchell, P. 1988c. *The early Pleistocene microlithic assemblages of southern Africa*. International Series 388. Oxford: BAR.

Mitchell, P. 1990. A palaeoecological model for archaeological site distribution in southern Africa during the Upper Pleniglacial and Late Glacial. In: C. Gamble & O. Soffer, eds, *The World at 18 000 BP: the low latitudes*. London: Unwin Hyman, pp. 189–205.

Mitchell, P. 1995. Revisiting the Robberg: new results and a revision of old ideas at Sehonghong Rock Shelter, Lesotho. *South African Archaeological Bulletin* **50**: 28–38.

Mitchell, P. 2002. *The archaeology of southern Africa*. Oxford: Cambridge University Press.

Mix, A. C., Bard, E., & Schneider, R. 2001. Environmental processes of the ice age: land, oceans, glaciers (EPILOG). *Quaternary Science Reviews* **20** (4): 627–657.

Orton, J. 2006. The Later Stone Age lithic sequence at Elands Bay, Western Cape, South Africa: raw materials, artefacts and sporadic change. *Southern African Humanities* **18** (2): 1–28.

Orton, J. 2008. A late Pleistocene microlithic Later Stone Age assemblage from coastal Namaqualand, South Africa. *Before Farming* **2008** (1): 1–9.

Pargeter, J. 2012. Robberg bladelets as weapon inserts: results of a macrofracture and morphometric analysis on two Robberg assemblages from the southern Cape coast, South Africa. Poster presented at the 2012 Society for Africanist Archaeologists Meetings in Toronto, Canada.

Pargeter, J. & Redondo, M. 2016. Contextual approaches to studying unretouched bladelets: a late Pleistocene case study at Sehonghong Rockshelter, Lesotho. *Quaternary International* **404**: 30–43.

Parkington, J.E. 1976. Coastal settlement between the mouths of the Berg and the Olifants rivers, Cape Province. *South African Archaeological Bulletin* **31**: 127–40.

Parkington, J.E. 1981. The effects of environmental change on the scheduling of visits to the Elands Bay Cave, Cape Province, S.A. In: I. Hodder, G. Isaac & N. Hammond, eds., *Patterns of the past*. Cambridge: Cambridge University Press, pp. 341–59.

Parkington, J.E. 1984. Changing views of the Later Stone Age of South Africa. *Advances in World Archaeology* **3**: 89–142.

Parkington, J.E. 1988. The Pleistocene/Holocene transition in the Western Cape, South Africa: observations from Verlorenvlei. In: J. Bower & D. Lubell, eds., *Prehistoric cultures and environments in the Late Quaternary of Africa*. Cambridge Monographs in African Archaeology 26. International Series 405. Oxford: BAR, pp. 197–206.

Parkington, J 1990. A view from the south: southern Africa before, during and after the Last Glacial Maximum. In: C. Gamble & O. Soffer, eds., *The World at 18 000 BP: the low latitudes*. London: Unwin Hyman, pp. 214–28.

Parkington, J.E. 2016. Elands Bay Cave: keeping an eye on the past. *Southern African Humanities* **29**: 17–32.

Parkington J., Baxter A., Cartwright C., Cowling R.M. & Meadows, M. 2000. Palaeovegetation at the last glacial maximum in the Western Cape, South Africa: wood charcoal and pollen evidence from Elands Bay Cave. *South African Journal of Science* **96** (11–12): 543–546.

Parkington, J.E., Poggenpoel, C., Buchanan, W., Robey, T., Manhire, A. & Sealy, J. 1988. Holocene coastal settlement patterns in the Western Cape. In: G. Bailey & J.E. Parkington, eds., *The archaeology of prehistoric coastlines*. Cambridge: Cambridge University Press, pp. 22–41.

Pelegrin, J. 1995. *Technologie lithique: le Châtelperronien de Roc-de-Combe (Lot) et de la Côte (Dordogne)*. Paris: Centre National de la Recherche Scientifique.

Perlès, C. 1991. Économie des matières premières et économie du débitage: deux conceptions opposées? In: Actes des XI[èmes] Rencontres internationales d'archéologie et d'histoire d'Antibes, *25 ans d'études technologiques en Préhistoire: bilan et perspectives*. Antibes: APDCA, pp. 35–45.

Plisson, H. 1985. *Etude fonctionnelle d'outillages lithiques préhistoriques par l'analyse des micro-usures: recherche méthodologique et archéologique*. PhD thesis, University of Paris I.

Porraz, G. 2008. Middle Palaeolithic mobile toolkits in short-term human occupations. Pié Lombard rockshelter (Provence, France) and Broion cave (Venetia, Italy): two case studies. *Eurasian Prehistory* **6** (1–2): 33–55.

Porraz, G., Texier, P.J., Archer, W., Piboule, M., Rigaud, J.P., & Tribolo, C. 2013. Technological successions in the Middle Stone Age sequence of Diepkloof Rock Shelter, Western Cape, South Africa. *Journal of Archaeological Science* **40** (9): 3376–400.

Porraz, G., Igreja, M. & Texier, P.-J. 2015. Développement sur une discontinuité technique dans la séquence Howiesons Poort de l'abri Diepkloof (Afrique du Sud). In: N.J. Conard & A. Delagnes, eds., *Settlement systems of the Middle Palaeolithic and Middle Stone Age*. Tübingen: Kerns Verlag, pp. 77–104.

Porraz, G., Schmid, V., Miller, C.E., Cartwright, C., Igreja, M., Mentzer, S., Mercier, N., Schmidt, P., Tribolo, C., Conard, N.J., Texier, P.-J. & Parkington, J.E. 2016. Update on the 2011 excavation at Elands Bay Cave (South Africa) and the Verlorenvlei Stone Age. *Southern African Humanities* **29**: 33–68.

Robinson, T.R. 1938. A survival of flake-technique in Southern Rhodesia. *Man* **38**: 224.

Semenov, S.A. 1964. *Prehistoric technology: an experimental study of the oldest tools and artefacts from traces of manufacture and wear*. London: Cory, Adams & Mackay.

Schmid, V., Conard, N.J., Parkington, J.E., Texier, P.-J. & Porraz, G. 2016. The 'MSA 1' of Elands Bay Cave (Western Cape Province, South Africa) in the context of the southern African Early MSA technologies. *Southern African Humanities* **29**: 153–201.

Schmidt, P. 2014. What causes failure (overheating) during lithic heat treatment? *Archaeological and Anthropological Sciences* **6** (2): 107–12.

Schmidt, P., Porraz, G., Slodczyk, A., Bellot-Gurlet, L., Archer, W. & Miller, C.E. 2013. Heat treatment in the South African Middle Stone Age: temperature induced transformations of silcrete and their technological implications. *Journal of Archaeological Science* **40**: 3519–31.

Schmidt, P., Porraz, G., Bellot-Gurlet, L., February, E., Ligouis, B., Paris, C., Texier, P.-J., Parkington, J.E., Miller, C.E., Nickel, K.G. & Conard, N.J. 2015. A previously undescribed organic residue sheds light on heat treatment in the Middle Stone Age. *Journal of Human Evolution* **85**: 22–34.

Schmidt, P. & Mackay, A. 2016. Why was silcrete heat-treated in the Middle Stone Age? An early transformative technology in the context of raw material use at Mertenhof Rock Shelter, South Africa. *Plos One* **11**: e0149243.

Skakun, N., Zhiiin, M. & Terekhina, V. 2011. Technology of processing of bone and antler at Ivanovskoje 7 Mesolithic site, central Russia. *Rivista di Scienze Preistoriche* **61**: 39–58.

Soriano, S., Villa, P. & Wadley, L. 2007. Blade technology and tool forms in the Middle Stone Age of South Africa: the Howiesons Poort and post-Howiesons Poort at Rose Cottage Cave. *Journal of Archaeological Science* **34** (5): 681–703.

Schweitzer, F.R. & Wilson, M.L. 1982. Byneskranskop 1, a late Quaternary living site in the southern Cape Province, South Africa. *Annals of the South African Museum* **78**: 101–232.

Tixier, J. 1965. Procédés d'analyse et questions de terminologie concernant l'étude des ensembles industriels du Paléolithique récent et de l'Epipaléolithique dans l'Afrique du Nord-Ouest. In: W.W. Bishop & J.D. Clark, eds, *Background to evolution in Africa*. Chicago: University of Chicago Press, pp. 771–820.

Tixier, J. 1980. *Préhistoire et technologie lithique, 1*. Meudon: CNRS Editions.

Tomasso, A. 2014. *Territoires, systèmes de mobilité et systèmes de production: La fin du Paléolithique supérieur dans l'arc liguro-provençal*. PhD thesis, University of Nice Sophia Antipolis.

Tribolo, C., Mercier, N., Valladas, H., Miller, C.E., Parkington, J.E. & Porraz, G. 2016. Chronology of the Pleistocene deposits at Elands Bay Cave (South Africa) based on charcoals, burnt lithics, and sedimentary quartz and feldspar grains. *Southern African Humanities* **29**: 129–52.

Villa, P. & Lenoir, M. 2009. Hunting and hunting weapons of the Lower and Middle Paleolithic of Europe. In: M. Richards & J.J. Hublin, eds., *The evolution of hominid diet: integrating approaches to the study of Palaeolithic subsistence*. Dordrecht: Springer, pp. 59–84.

Villa, P., Soriano, S., Tsanova, T., Degano, I., Higham, T., d'Errico, F., Backwell, L., Lucejko, J., Colombini, M.P. & Beaumont, P.B. 2012. Border Cave and the beginning of the Later Stone Age in South Africa. *Proceedings of the national Academy of Sciences* **109** (33): 13208–13.

Wadley, L. 1993. The Pleistocene Later Stone Age south of the Limpopo River. *Journal of World Prehistory* **7** (3): 243–96.

Wadley, L. 1996. The Robberg industry of Rose Cottage Cave, eastern Free State: the technology, spatial patterns and environment. *South African Archaeological Bulletin* **51**: 64–74.

Wadley, L. & Prinsloo, L.C. 2014. Experimental heat treatment of silcrete implies analogical reasoning in the Middle Stone Age. *Journal of human evolution* **70**: 49–60.

Williamson, B.S. 1996. Preliminary stone tool residue analysis from Rose Cottage Cave. *Southern African Field Archaeology* **5**: 36–44.

Woodborne, S., Hart, K. & Parkington, J.E. 1995. Seal bones as indicators of the timing and duration of hunter-gatherer coastal visits. *Journal of Archaeological Science* **22**: 727–40.

Southern African Humanities **29**: 249–58 December 2016 KwaZulu-Natal Museum

The wood charcoal evidence from renewed excavations at Elands Bay Cave, South Africa

[1]**Caroline R. Cartwright**, [2,3]**Guillaume Porraz** and [4]**John Parkington**

[1]Department of Scientific Research, British Museum, London, WC1B 3DG, United Kingdom; CCartwright@britishmuseum.org
[2]CNRS, USR 3336, UMIFRE 25, French Institute of South Africa, Johannesburg, South Africa
[3]Evolutionary Studies Institute (ESI), University of the Witwatersrand, Johannesburg, South Africa
[4]Department of Archaeology, University of Cape Town, South Africa

ABSTRACT

This article presents the results of the anatomical identification by scanning electron microscopy of wood charcoal from excavations in 2011 at Elands Bay Cave (EBC), South Africa. The samples are from Robberg Group D layers (18/19 ka cal BP); the Early Later Stone Age (LSA) Group F layers (22–24 ka cal BP), and the late Middle Stone Age (MSA) Group H-I-J layers (35–39ka cal BP). Noticeable differences in the vegetation are present in LSA layers, which have more diverse thicket elements represented in Groups D and F than in Group H-I-J layers—with their heavier reliance on Afromontane and mesic thicket taxa during the late MSA. Published charcoal results from previous excavations at EBC chart a progressive change over time from xeric thicket and asteraceous shrubland vegetation, through proteoid fynbos and general thicket to mesic thicket, riverine woodland and proteoid fynbos, ultimately to Afromontane forest. Climatic or soil moisture factors may have played a significant part and contributed to some or all of the taxa having very different phytogeographical distributions compared to their modern counterparts, but is also necessary to consider to what extent the people using EBC at different times might have collected (and selected) woody resources from a mosaic of vegetational communities, some local, some far away.

KEY WORDS: wood charcoal, scanning electron microscopy, Later Stone Age, Middle Stone Age, Robberg; vegetation, climate, Western Cape.

This article presents the results of the anatomical identification by scanning electron microscopy of wood charcoal from Robberg 'Group D', Early Later Stone Age (LSA) 'Group F' and late Middle Stone Age (MSA) 'Group H-I-J' within the renewed excavations in 2011 at Elands Bay Cave (EBC), South Africa. The purpose of the 2011 fieldwork season at EBC was to contextualize the lower LSA and MSA archaeological deposits excavated by John Parkington in 1972 and 1978 (Porraz et al. 2016 this issue). Present studies (Porraz et al. 2016 this issue; Tribolo et al. 2016 this issue) suggest that, unlike nearby Diepkloof Rock Shelter (DRS), no Still Bay, Howiesons Poort (HP) or post-HP occupation has yet been recorded at EBC.

Detailed analysis of charcoal from the 1970 excavations at EBC revealed new insights into late and terminal Pleistocene vegetational and climate change in the coastal area of the Western Cape (Cartwright & Parkington 1997; Cowling et al. 1999; Parkington et al. 2000; Cartwright et al. 2014). These charcoal assemblages from EBC at the Last Glacial Maximum (LGM) included Afromontane taxa which showed that the Western Cape coastal belt had higher soil moisture availability during the later and terminal Pleistocene, including at the LGM. We hypothesized, therefore, that during these time periods, westerly cyclonic fronts delivered sustained precipitation on the western slopes of the Cape Fold Belt mountains but decreased movement of moist unstable air across the restricted and possibly cooler Agulhas current left the eastern part of the biome more arid than it is today

ISSN 2305-2791 (online); 1681-5564 (print)

(Cowling et al. 1999). Comparisons with charcoal samples from the LSA and MSA chronostratigraphic sequence at DRS are vital to all EBC analyses (Cartwright 2013), and this comparative research is on-going in terms of its wider palaeoenvironmental and archaeobotanical implications.

METHODS

For the earlier EBC charcoal analysis (Cartwright & Parkington 1997; Cartwright et al. 2014) collection of reference specimens essential for the identification of the archaeological charcoal commenced in the area around the site, and then extended to other locations in the south-western, north-western and southern Cape. In the field, 434 woody taxa were photographed, documented and collected. Some were professionally identified *in situ*, whilst others were brought back for identification at the Bolus Herbarium, Department of Botany, University of Cape Town or at Kirstenbosch National Botanical Garden, Cape Town. Collection was made from a range of substrata and topographical locations with a view to assessing possible microenvironmental variability. The collected woody taxa not only characterised the region around EBC (and DRS) today, but also provided a framework of reference for those represented in the vegetational changes through time evidenced by the archaeological charcoal assemblages (Cartwright et al. 2014). Integral to interpretation is the research currently in progress (under the direction of Richard M. Cowling) with regard to the characterisation of extant vegetational communities in their climatic and habitat envelopes covering steep gradients in temperature and rainfall regimes. Already, such characterisation has resulted in a broad set of available environmental correlates that were crucial to the interpretation of the 1970 EBC charcoal assemblages (Cowling et al. 1999), and it is anticipated that similar outcomes will be forthcoming for both the DRS and the 2011 EBC charcoal being reported here.

In the laboratory each securely-identified woody reference collection specimen was halved; one portion was thin sectioned using standard microtome and staining techniques to provide transverse, radial longitudinal and tangential longitudinal (TS, RLS and TLS) sections of the wood, and the other half was converted to charcoal for anatomical comparative reference purposes (Cartwright & Parkington 1997). None of the taxa represented by woody reference collection specimens had already been described anatomically according to International Association of Wood Anatomists (IAWA) protocols (Wheeler et al. 1989). Thus, before any identification of archaeological charcoals could proceed, Cartwright carried out an intensive microscopical examination and compiled a computerised anatomical feature database and checklist for all the reference collection of woody taxa using the descriptions and features from the IAWA List of Features for Hardwood Identification (Wheeler et al. 1989; InsideWood 2004 onwards). The extremely useful on-line wood anatomy database InsideWood (Wheeler 2011) was not available at the commencement of the EBC (and DRS) projects. But even if it had been available, whilst it is an essential tool for the wood anatomist, and despite comprising 6996 modern wood descriptions and 43 005 modern wood thin section images at the time of writing (June 2016), InsideWood's geographical coverage (did not and) does not extend (at present) to the woody taxa of the western Cape of South Africa, it does not cover gymnosperm woods (softwoods), and it does not document charcoal. However, it still remains a key

resource for the wood anatomist and, with certain cautions, to the charcoal specialist as well (Cartwright 2015). Cartwright updated her original computerised anatomical feature database for Western Cape charcoal using the augmented IAWA feature checklist (InsideWood 2004 onwards) prior to the final phases of identification of Western Cape archaeological charcoal assemblages. Some of the descriptors on this data sheet required modification—particularly those reflecting size and dimension—to accommodate the effects of charring, as had been implemented for EBC 1970 charcoal on an earlier version (Cartwright & Parkington 1997).

The anatomical examination of all EBC 2011 archaeological charcoal was carried out using scanning electron microscopy (SEM). Because of the three-dimensional nature of wood anatomy, each piece of charcoal, irrespective of size, was fractured manually to show TS, RLS and TLS for examination (for full details, see Cartwright & Parkington 1997). Each TS, RLS and TLS charcoal sample was then mounted on an aluminium SEM stub for SEM examination. Charcoal fragments that were very small, in poor condition or from contexts lowest in the stratigraphical sequence were mounted using Leit-C Plast carbon cement (which is a proprietary brand of conductive material with low outgassing properties). After mounting, each stub with its charcoal sample was sputter-coated with gold or platinum to make it conductive in the high vacuum conditions of the Hitachi S4800 field emission (FE) SEM using the secondary electron (SE) detector (for technical details see Cartwright 2013). Although the 2011 EBC charcoal fragments are in remarkably good condition (considering their antiquity), they are often extremely small and so the FE-SEM ultra-resolution and increased range of magnification has proved particularly suitable for these charcoal samples. Well-preserved charcoal samples were mounted as described above and examined uncoated in the Hitachi S-3700N variable pressure (VP) SEM (for methodological and technical details see Cartwright 2013).

RESULTS AND DISCUSSION

Excavations in 2011 at EBC were carried out in sedimentary units, rigorously following the slope of the strata. Hearths were excavated separately with charcoals and ash horizons being differentiated (Miller et al. 2016 this issue; Porraz et al. 2016 this issue). All deposits have been sorted using 3 mm and 1 mm mesh screens. The present study is based on the sorting of the 3 mm screen only.

Three main groups can be defined (Porraz et al. 2016 this issue):

1) The Robberg Group D layers (14C dated to 18/19 ka cal BP)
2) The Early LSA Group F layers (14C dated to 22–24 ka cal BP)
3) The late MSA Group H-I-J layers (14C dated to 34–36 ka cal BP).

Table 1 shows the results of the charcoal identifications presented according to these groups. The present-day distributions and characteristics of the taxa present in Table 1 serve as a framework of reference for interpretation of the archaeological charcoal, particularly with regard to palaeoenvironmental considerations.

Mindful of the very different present-day vegetation of Elands Bay—with low xeric (very dry) scrub and asteraceous shrubs—and also the previous published charcoal results from EBC which chart a progressive change over time from xeric thicket and asteraceous shrubland vegetation, through proteoid fynbos and general thicket to mesic

TABLE 1
Charcoal identifications from groups D, F and H-I-J of EBC 2011 excavations.
Numbers = weight in grams.

	Group D dated to 18/19 ka cal BP	**Group F** dated to 22–24 ka cal BP	**Group H-I-J** dated to 3–39 ka cal BP
General thicket taxa			
Searsia lucida (formerly *Rhus lucida*)	10	7	
Searsia tomentosa (formerly *Rhus tomentosa*)	11	9	6
Searsia undulata (formerly *Rhus undulata)*	15	6	4
Mesic thicket taxa			
Cassine peragua	6	10	12
Cassine schinoides (formerly *Hartogiella schinoides*)	5	8	16
Diospyros glabra	6	8	22
Dodonaea viscosa subsp. *angustifolia* (formerly *Dodonaea angustifolia*)	7	7	28
Gymnosporia buxifolia (formerly *Maytenus heterophylla*)	4	8	14
Heeria argentea	6	12	14
Maytenus oleoides	6	11	10
Olea europaea subsp. *africana*	4	8	30
Afromontane forest taxa			
Celtis africana	2	2	15
Halleria lucida	2	2	17
Kiggelaria africana	3	5	22
Myrsine africana			8
Podocarpus elongatus	4	4	26

thicket, riverine woodland and proteoid fynbos, ultimately to Afromontane forest (Cartwright & Parkington 1997), we can consider the charcoal taxa represented in the 2011 EBC record in more detail.

Group D layers show distinct use of general thicket taxa; Group F layers also to some extent but Group H-I-J layers less so. *Searsia lucida* (waxy-leaved bush) can be classified as a general thicket taxon, though may also be found on edges of forests and on rocky hill-slopes. *S. lucida* shows a preference (although not exclusively so) for wetter locations, including Olifants Alluvium Fynbos, Graafwater Sandstone Fynbos in wetter areas in hills, Leipoldtville Sand Fynbos, Graafwater Flats Strandveld, Kobee Succulent Shrubland, CitrusdalVygieveld (Helme 2007), sandstone fynbos valley bottom/depression wetlands, sandstone fynbos depressions/mountain seeps and alluvial floodplain wetlands (Job et al. 2008). Other thicket taxa include *Searsia tomentosa* (wild currant), which can be found in Renosterveld, on rocky mountain slopes and

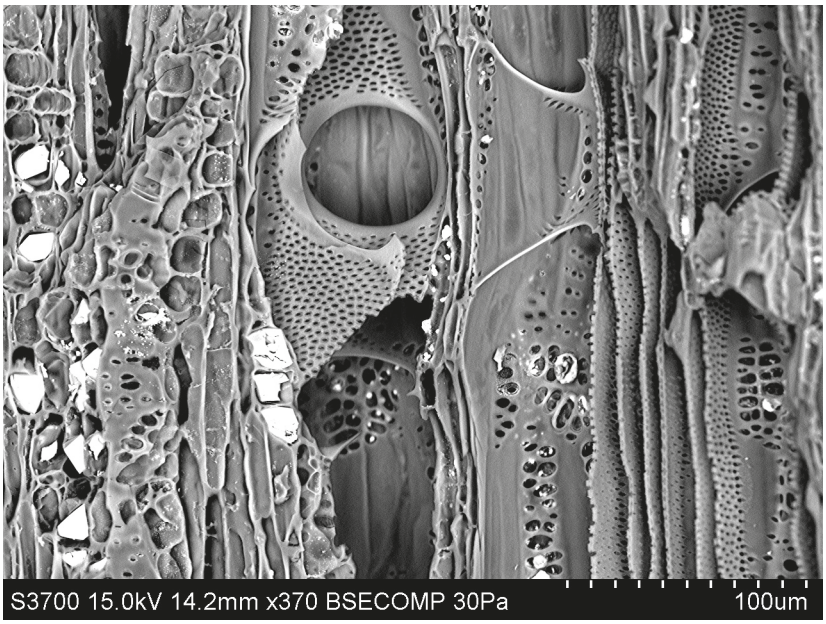

Fig. 1. Variable pressure scanning electron microscope image of *Searsia undulata* (Namaqua kuni-bush) charcoal in radial longitudinal section. Image: Caroline R. Cartwright.

on the edges of low thicket or scrub, and *Searsia undulata* (Namaqua kuni-bush, Fig. 1) *S. undulata* seems to prefer the drier vegetational communities such as Nieuwoudtville-Roggeveld Dolerite Renosterveld (Manning & Goldblatt 1997), Doringrivier Quartzite Karoo, Kobee Succulent Shrubland and Citrusdal Vygieveld (Helme 2007). It occurs alongside *Cassine peragua* (forest spoonwood), *Dodonaea viscosa* var. *angustifolia* (sand-olive), *Heeria argentea* (rockwood/kliphout), *Olea europaea* subsp. *africana* (wild olive), *Maytenus oleoides* (mountain maytenus/rock candlewood), *Diospyros glabra* (blueberry bush) and *S. lucida* in thicket vegetation on rocky slopes and in forest margins and it is of significance that the association of these taxa is clear in Groups D and F layers, and to some extent in Group H-I-J layers (Table 1).

Group D layers exploit the mesic thicket category, Group F layers even more so and Group H-I-J layers show a marked reliance on these taxa. *Cassine* species can be found at the present day in mesic thicket as well as in Afrotemperate forest and its margins and on riverine fringes; Groups D and F layers, and particularly those in Group H-I-J show consistent selection of *C. peragua* (see Cartwright 2013 for a detailed taxonomic discussion) and *C. schinoides* (spoonwood) is present in an altitude range of 100 to 1800 m in Afrotemperate forest, on rocky mountain slopes, in wooded kloofs (ravines) and in thicket. *D. glabra* sometimes forms part of general thicket vegetation and sometimes within mesic thicket at forest-margins and on rocky hill-slopes. It has been recorded in pockets of Afromontane vegetation in mountain kloofs as well as in Olifants Alluvium Fynbos, Graafwater Sandstone Fynbos and Vanrhynsdorp Shale Renosterveld, and on alluvial floodplain wetlands (Low et al. 2004; Helme 2007; Job et al. 2008). *D. viscosa* var. *angustifolia*, *O. europaea* subsp. *africana* and *H. argentea* can also be found in association within Graafwater Sandstone Fynbos in kloofs (Low et

al. 2004). *O. europaea* subsp. *africana*, in addition to occurring in thicket and woodland (where it may attain a height of 12 m), can also be found in riverine valley bottom wetland sandstone fynbos vegetation. *Gymnosporia buxifolia* (spike-thorn) occurs in a variety of thicket, fynbos and strandveld vegetation, including Hopefield Sand Fynbos, Leipoldtville Sand Fynbos, Namaqualand Sand Fynbos, Swartland Shale Renosterveld, Saldanha Flats Strandveld, West Coast Strandveld, Langebaan Fynbos/Thicket Mosaic, Graafwater Flats Strandveld and Namaqualand Strandveld (Helme 2007). *H. argentea* is recorded as being common in thicket patches of Graafwater Sandstone Fynbos, but on the west coast, only one example of *H. argentea* forest has survived in the Lambert's Bay area on a sandstone inselberg "a remnant from long ago, perhaps when sea levels were further out and the climate was much wetter than it is now … the nearest patch is now at least 25 km inland, in more mesic habitats" (Helme 2007: 67 and Plate 32). *M. oleoides* occurs in Graafwater Sandstone Fynbos (Helme 2007) on rocky slopes and at forest margins.

Maps (some interactive) of these different vegetation zones at the present day (mentioned above) can be found on the Biodiversity GIS (BGIS)South African National Biodiversity Institute (SANBI) websites at http://bgis.sanbi.org/gcbc/vegetationTypes.asp and http://bgis.sanbi.org/vegmap/map2009_2012.asp.

We have already noted that the charcoal evidence from the 1970 excavations at EBC indicated a predominance of Afromontane taxa which suggested that the Western Cape coastal belt had higher soil moisture availability during the later and terminal Pleistocene, including at the LGM (Cartwright & Parkington 1997; Cowling et al. 1999; Parkington et al. 2000; Cartwright et al. 2014). Charcoal from Group H-I-J layers of the 2011 excavations at EBC show a more marked dependence on such taxa than in Groups D and F layers. *Celtis africana* (white stinkwood), Figure 2, and *Podocarpus elongatus* (Breede River yellowwood), Figure 3, are found today in Southern and Eastern Cape Afrotemperate woodlands in sheltered mountain gorges alongside taxa such as *Cassine* (Cowling et al. 1997). *C. africana* is usually associated with higher rainfall or moister places (Cowling et al. 1999) and can be found in rocky outcrops (in small and scrubby form) as well as full-grown in Afrotemperate forests. The phenotypic plasticity of *P. elongatus* has already been noted (Cowling & Homes 1992; Cowling et al. 1999; Cartwright et al. 2014) but it is worth reiterating this adaptive capacity for plants and trees to survive in changed environments and in a variety of vegetational communities, as it is directly relevant to their presence at EBC and the processes whereby they arrived at the site over time. *P. elongatus*, for example, whilst often to be found in pockets of Afromontane/Afrotemperate forests in kloofs, along rivers and adjacent to wetlands, can also occur in the wetter areas of different types of fynbos including Graafwater Sandstone Fynbos (in hills) and Olifants Alluvium Fynbos (Cowling & Homes 1992; Low et al. 2004; Helme 2007). The fact that *Podocarpus* is useful source of resin might account for its sustained presence in the archaeological record at EBC (and other sites in the Western Cape, such as DRS).

Halleria lucida (tree fuchsia) has a mostly eastern distribution at the present day in coastal and karroid scrub, at forest and river margins and on rocky slopes. Helme (2007) does not record *H. lucida* for the Sandveld of the Western Cape, but does note the presence of the shrubby *H. ovata* along stream banks in the Citrusdal region and in fynbos locations in the Olifants River Mountains (Helme & Raimondo 2007;

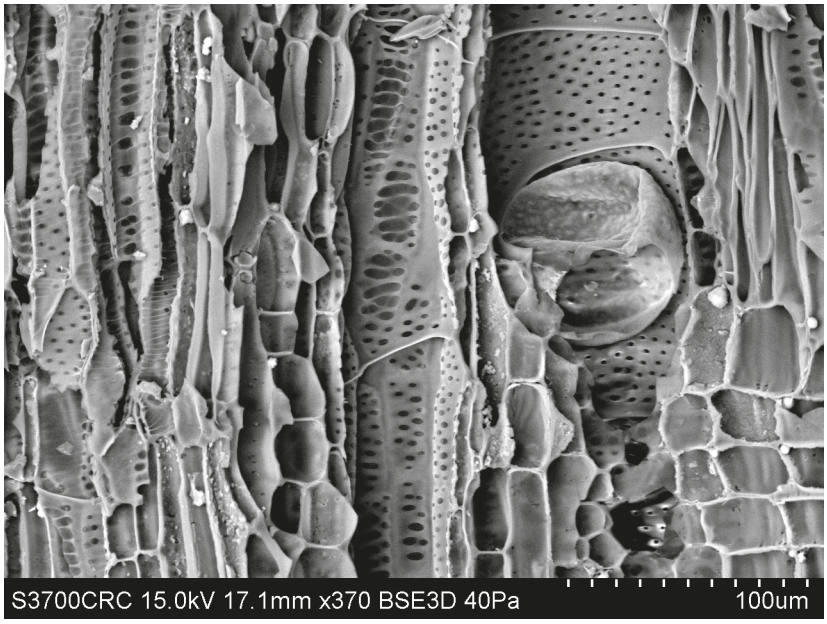

Fig. 2. Variable pressure scanning electron microscope image of *Celtis africana* (white stinkwood) charcoal in radial longitudinal section. Image: Caroline R. Cartwright.

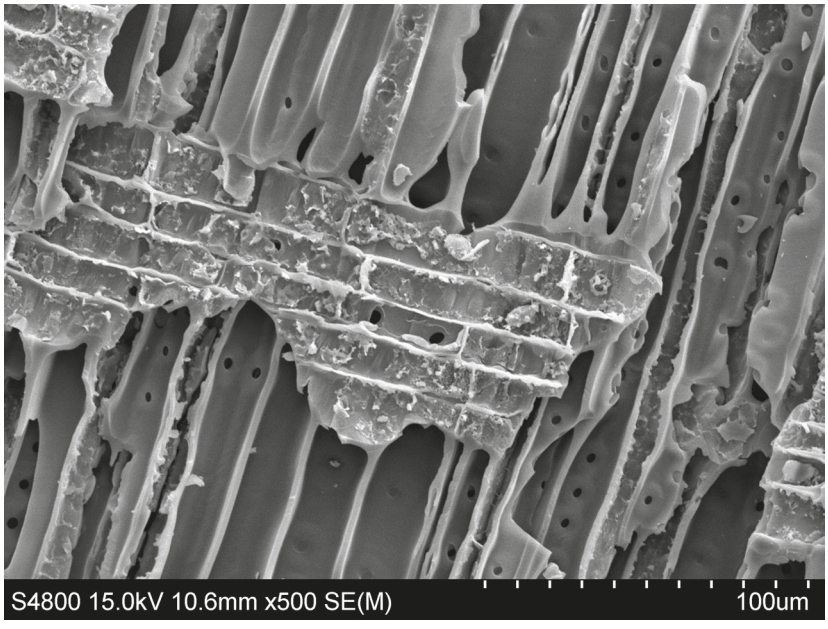

Fig. 3. Field emission scanning electron microscope image of *Podocarpus elongatus* (Breede River yellowwood) charcoal in radial longitudinal section. Image: Caroline R. Cartwright.

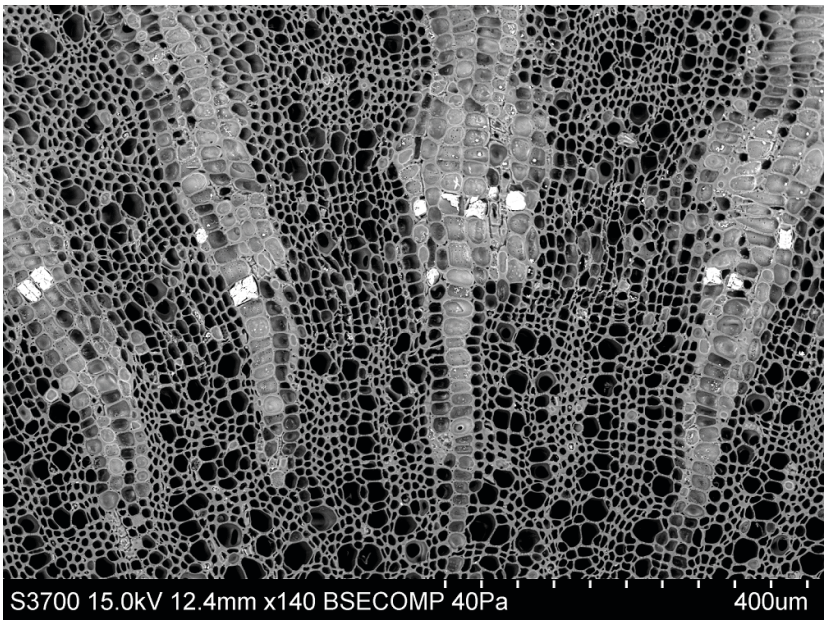

Fig. 4. Variable pressure scanning electron microscope image of *Myrsine africana* (Cape myrtle) charcoal in transverse section. Image: Caroline R. Cartwright.

Raimondo et al. 2009). *Kiggelaria africana* (wild peach) is widely distributed in (mostly southern, eastern and north-eastern) coastal and inland Afrotemperate forests, along streams and on rocky hillsides. *Myrsine africana* (Cape myrtle), Figure 4, also has a wide distribution and can be found in forests, rocky hill-tops and fynbos.

The charcoal from the 2011 excavations at EBC contributes further evidence of the nature of vegetation change prompted by climatic variability during the LGM in the Western Cape. Comparing such evidence from the charcoal on West Coast sites to the broader picture of LGM change more widely in South Africa is far more complex, not least because the vegetation across South Africa is extremely diverse, and far more archaeological sites yielding well-stratified sequences containing identifiable charcoal need to be excavated and analysed. More meaningful than comparisons of individual taxa across South Africa in general will be comparisons on a region-by-region basis where the changes of vegetational communities as attested from the evidence of well-dated sequences of archaeological charcoal can be interpreted against the framework of present-day vegetation for that biogeographical region. Furthermore, patterns of vegetation and vegetational changes over time have been influenced and shaped by climatic controls that are fundamentally different on the east coast of South Africa compared to that of the west coast. Consequently, we have held back at this stage from making unsubstantiated comparisons over wide areas. It is crucial to understand west coast variability fully before attempting inter-regional reconstructions, particularly as the non-woody plant material (seeds and fruits) from EBC is not yet processed and available for study. Adding this dimension of evidence could significantly alter our reconstruction of vegetational communities over time, as well as providing enhanced information about resource selection and availability.

CONCLUSIONS

The 2011 EBC charcoal evidence (Table 1) shows some noticeable differences in the vegetation present in LSA layers, which have more diverse thicket elements represented in Groups D and F than in Group H-I-J layers—with their heavier reliance on Afromontane and mesic thicket taxa during the late MSA. The published charcoal results from previous excavations at EBC chart a progressive change over time from xeric thicket and asteraceous shrubland vegetation, through proteoid fynbos and general thicket to mesic thicket, riverine woodland and proteoid fynbos, ultimately to Afromontane forest. As has been seen for these results (e.g. Cowling et al. 1999), whilst climatic or soil moisture factors may have played a significant part and contributed to some or all of the taxa having very different phytogeographical distributions compared to their modern counterparts, it is also necessary to consider to what extent the people using EBC at different times might have collected (and selected) woody and other botanical resources from a mosaic of vegetational communities, some local, some far away (see Charrié-Duhaut et al. 2016 this issue).

REFERENCES

Cartwright, C.R. 2013. Identifying the woody resources of Diepkloof Rock Shelter (South Africa) using scanning electron microscopy of the MSA wood charcoal assemblages. *Journal of Archaeological Science* **40**: 3463–74.

Cartwright, C.R. 2015. Invited review. The principles, procedures and pitfalls in identifying archaeological and historical wood samples. *Annals of Botany* **116**: 1–13.

Cartwright, C.R. & Parkington, J.E. 1997. The wood charcoal assemblages from Elands Bay Cave, southwestern Cape: principles, procedures and preliminary interpretation. *South African Archaeological Bulletin* **52**: 59–72.

Cartwright, C.R., Parkington, J.E. & Cowling, R.M. 2014. Chapter 5. Understanding Late and Terminal Pleistocene vegetation change in the Western Cape, South Africa: the wood charcoal evidence from Elands Bay Cave. In: C.J. Stevens, S. Nixon, M.A. Murray & D.Q. Fuller, eds., *Archaeology of African plant use*. Walnut Creek, California: Left Coast Press, pp. 59–72.

Charrié-Duhaut, A., Porraz, G., Igreja M., Texier P.-J, & Parkington J.E. 2016. Holocene hunter-gatherers and adhesives manufacture in the West Coast of South Africa. *Southern African Humanities* **29**: 283–306.

Cowling, R.M., Cartwright, C.R., Parkington, J.E. & Allsopp, J.C. 1999. Fossil wood charcoal assemblages from Elands Bay Cave, South Africa: implications for Late Quaternary vegetation and climates in the winter-rainfall fynbos biome. *Journal of Biogeography* **26**: 367–78.

Helme, N. 2007. *Botanical report: fine scale vegetation mapping in the Sandveld.* Cape Town: CapeNature.

Helme, N.A. & Raimondo, D. 2007. *Halleria ovata* Benth. National Assessment: Red List of South African Plants version 2013.1. (Accessed September 2013)

InsideWood. 2004 onwards. http://insidewood.lib.ncsu.edu/search (accessed December 2012).

Job, N., Snaddon, C.D., Nel, J., Smith-Adao, L. & Day, L. 2008. *C.A.P.E. fine-scale planning project: aquatic ecosystems of the Saldanha-Sandveld planning domain.* Cape Town: CapeNature.

Low, A.B., Mustart, P. & Van der Merwe, H. 2004. Greater Cederberg Biodiversity Corridor: provision of biodiversity profiles for management. Rondebosch: COASTEC.

Manning, J. & Goldblatt, P. 1997. *Nieuwoudtville, Bokkeveld Plateau and Hantam*. South African Wild Flower Guide 9. Cape Town: Botanical Society of South Africa.

Miller, C.E., Mentzer, S., Berthold C., Leach P., Tribolo C., Parkington J. & Porraz, G. 2016. Site-formation processes of the Middle and Later Stone Age deposits from Elands Bay Cave, South Africa. *Southern African Humanities* **29**: 69–128.

Parkington, J., Cartwright, C.R., Cowling, R.M., Baxter & A., Meadows, M. 2000. Palaeovegetation at the last glacial maximum in the western Cape, South Africa: wood charcoal and pollen evidence from Elands Bay Cave. *South African Journal of Science* **96**: 543–6.

Porraz, G., Schmid, V.C., Miller, C.E., Tribolo, C., Cartwright, C.R., Charrié-Duhaut, A., Igreja, M., Mentzer, S., Mercier, N., Schmidt, P., Conard, N.J., Texier, P.-J. & Parkington J.E.2016. Update on the 2011 excavation at Elands Bay Cave (South Africa) and the Verlorenvlei Stone Age. *Southern African Humanities* **29**: 33–68.

Raimondo, D., Von Staden, L., Foden, W., Victor, J.E., Helme, N.A., Turner, R.C., Kamundi, D.A. & Manyama, P.A. 2009. *Red list of South African plants*. Strelitzia 25. Pretoria: South African National Biodiversity Institute.

Tribolo, C., Mercier, N., Valladas, H., Miller, C.E., Parkington, J.E. & Porraz, G. 2016. Chronology of the Pleistocene deposits at Elands Bay Cave (South Africa) based on charcoals, burnt lithics, and sedimentary quartz and feldspar grains. *Southern African Humanities* **29**: 129–52.

Wheeler, E.A. 2011. InsideWood – a web resource for hardwood anatomy. *IAWA Journal* **32**: 199–211.

Wheeler, E.A., Baas, P. & Gasson, P.E. 1989. IAWA list of microscopic features for hardwood identification. *IAWA Bulletin* **10**: 219–332.

Southern African Humanities **29**: 259–82 December 2016 KwaZulu-Natal Museum

Large mammal and tortoise bones from Elands Bay Cave (South Africa): implications for Later Stone Age environment and ecology

[1]**Richard G. Klein** and [2]**Kathryn Cruz-Uribe**

[1]Program in Human Biology, Building 20, Inner Quad, Stanford University, Stanford, CA 94305, United States of America; rklein1@me.com

[2]Office of the Chancellor, Indiana University East, 2325 Chester Blvd, Richmond, IN 47374, United States of America; kathcruz@iue.edu

ABSTRACT

Elands Bay Cave has provided abundant large mammal and angulate tortoise bones from three Later Stone Age occupational pulses, bracketed by radiocarbon between 13 600 and 7800 b.p., 4300 and 3100 b.p., and 1800 and 300 b.p. (the radiocarbon ages here and below are uncalibrated). The mammal bones come from thirty-four species as large or larger than the Cape dune molerat. Fur seals, steenbok/grysbok, and molerat dominate heavily. Other species occur mainly as traces, especially in deposits postdating 9600 b.p. Fur seal bones appear first in layers dated to about 11 000 b.p., where together with intertidal shells, they record the post-glacial rise in sea level that brought the coastline to approximately its current position about 1400 years later. The terrestrial mammals record a change from moister, grassier surroundings before about 9600 b.p. to drier, scrubbier ones afterwards. Deposits dated between 12 000 and 10 000 b.p. document the youngest known occurrence of the large, extinct Cape zebra. Median tortoise size suggests that local human collectors were most numerous about 10 000 b.p., coincident with the time when the density of occupational debris implies especially intensive human use of the cave. Average fur seal age suggests people were present mainly in the August–October interval when dead or exhausted 9–11 month old seals would have been especially abundant on the nearby shore.

KEY WORDS: Elands Bay Cave, Later Stone Age ecology, Cape zebra, seasonality of occupation.

We note at the outset that publications on Elands Bay Cave (EBC) have long relied on uncalibrated radiocarbon dates, and we continue that practice here, where we have used b.p. (as opposed to BP) to emphasize lack of calibration. Parkington (2016 this issue) employs the same uncalibrated dates and presents a table with calibrated equivalents. The calibrated ages are mainly somewhat older, especially those calculated from uncalibrated dates beyond 8000 b.p. The principal advantage of calibrated ages is that they can be compared directly to the calendar ages produced by other dating methods. The principal disadvantage is that they depend on calibration assumptions that are subject to change.

John Parkington's excavations at Elands Bay Cave in the 1970s showed that bones were not preserved in the Middle Stone Age (MSA) layers, and that they were abundant only in Later Stone Age (LSA) deposits that postdate 13 600 b.p. Excavations subsequent to Parkington's, conducted in 2011 (Porraz et al. 2016 this issue), focused on the deposits older than 13 600 b.p. and did not add to the available bone samples. Parkington's excavations identified more than 300 discrete field units within the fossiliferous deposits, but most contained too few items for meaningful numeric analysis. The individual units were thus grouped into 19 successive clusters or 'packages', each containing field units that were similar in content and age (Parkington 2016 this issue). Radiocarbon determinations fix the sequence in time (Parkington

ISSN 2305-2791 (online); 1681-5564 (print)

2006: chapter 4, 2016 this issue) and they reveal three main occupational/depositional pulses: (1) packages 19–10, between 13 600 and 7800 b.p.; (2) packages 9–6, between 4300 and 3100 b.p.; and (3) packages 6–1, between 1800 and 300 b.p. Occupational/depositional gaps separate the pulses.

Bones were rare and perhaps mostly intrusive in packages older than 19 and we therefore focus on the contents of packages 19 to 1. Our purpose is to summarize the implications of the large mammal and tortoise bones for the environment and ecology of the cave occupants. We define a 'large mammal' as one in which adults weigh at least 0.75 kg. This definition specifically excludes small rodents, insectivores, and other 'microfaunal' species that were probably introduced to EBC mainly by barn owls and that D.M. Avery (1983) and Matthews (1999) analyzed. In local terms, our definition of large mammal includes all species as large or larger than the Cape dune molerat (*Bathyergus suillus*). In our discussion below, we emphasize conspicuous changes in large mammal species frequencies through time. To estimate frequencies, we employ both the Number of Identifiable Specimens (NISP) assigned to each species and the Minimum Number of Individuals (MNI) that the specimens must represent. Klein and Cruz-Uribe (1984) outline the assumptions behind the MNI calculations. Table 1 lists the species for the fauna as a whole and the NISPs and MNIs for each species by package. The text provides Linnaean names only for species that are not listed in the table. The table differs in detail from a similar one we presented once before (Klein & Cruz-Uribe 1987), which was based on a significantly smaller sample and on a different higher-order grouping of field provenience units. The basic patterning, however, remains the same.

IDENTIFICATION ISSUES

The EBC bones are well preserved but often fragmented, and the mammals definitely or possibly include several closely related species whose incomplete bones are difficult to separate. The problem pertains particularly to hares, zebras, rhinoceroses, pigs, and bovids. Hare bones, for example, could come from Cape hare (*Lepus capensis*), scrub hare (*Lepus saxatilis*), or red rock hare (*Pronolagus crassicaudatus*), and variation in bone size suggests that at least two of these species are present. However, we could not make species identifications strictly on morphology, and we have therefore assigned the hare bones simply to family.

We separated relatively complete zebra bones and teeth between quagga and the significantly larger extinct Cape zebra, but we were forced to assign some fragmentary specimens only to a composite category that could include both species. Similarly, we were able to assign some rhinoceros and pig bones to black rhinoceros and bushpig respectively, but we could not eliminate the possibility that other specimens represent white rhinoceros (*Ceratotherium simum*) and warthog (*Phacochoerus aethiopicus*). Thus, in addition to black rhinoceros and bushpig, Table 1 lists categories that include all rhinoceros and suid bones, including ones we identified as black rhinoceros and bushpig and others we could not identify to species.

The bovids present the biggest problem, because in general, we could identify species only from teeth and horncores. We assigned most postcranial bones simply to size categories, which we labeled small, small-medium, large-medium, and large. These categories correspond closely to ones used by other analysts of African Quaternary

faunas (Thackeray 1979; Bunn et al. 1980; Brain 1981; Voigt 1983; Brink 1987; Marean 1992; Plug 1993; Thompson 2010; Faith 2013a; Reynard et al. 2016). With respect to the bovid species in Table 1, small bovids include steenbok, Cape grysbok, and klipspringer; small-medium bovids include springbok, common duiker, and sheep; large-medium bovids include blue antelope and Cape hartebeest; and large bovids include eland and bovines. The listings for individual species in Table 1 are based strictly on dentitions and horncores, while the listings for size categories are based on all elements, including dentitions and horncores.

There is the additional problem that we could not separate grysbok and steenbok, except on nearly complete mandibles or horncores, and we could not securely allocate bovine teeth among cattle (*Bos taurus*), Cape buffalo (*Syncerus caffer*), and extinct large, long-horned buffalo (*Syncerus antiquus*). The result is that Table 1 has listings for grysbok and steenbok separately (based on mandibles and horncores) and for steenbok/grysbok (based on all cranial elements). It also includes a bovine (cattle/buffalo) category without further separation. Judging by size and stratigraphic provenience, most bovine teeth probably come from Cape buffalo, but an especially large deciduous premolar from package 18 could come from the long-horned buffalo. Arguably, a fragmentary bovine mandible with second and third molars from package 1 represents cattle, since package 1 probably postdates the time when cattle were introduced locally and buffalo were not recorded nearby historically (Skead 2011). However, we could not assign it to cattle versus buffalo on morphology alone.

In a previous publication (Klein 1981), one of us presented a mortality profile for EBC grysbok/steenbok, based on dental crown heights. The profile was problematic, partly because it included specimens from both species, and partly because rapid breeding in such small antelopes obscures the difference between the two theoretical types of mortality—catastrophic and attritional—on which paleobiologists usually base interpretation (Klein & Cruz-Uribe 1984). With these two problems in mind, we have not revisited grysbok/steenbok mortality here. The teeth of other species are too rare for mortality profile construction.

THE BONE COLLECTOR

We focus on the implications of large mammal and tortoise bones for changing prehistoric human landscape use near EBC, but in advance, we must establish who or what accumulated the bones. Otherwise, we might confuse faunal changes that reflect changing human ecology with changes due to changes in the bone-collector. Besides Stone Age people, the main alternative collectors to consider are hyenas or other carnivores, porcupines, and large raptors (Brain 1981). Jackal bones are relatively common in packages 13–10, and the presence of pups and possible jackal burrows suggests that jackals may temporarily have occupied the cave. They could then be responsible for some of the small mammal bones that are common in the same packages. However, in general, carnivores and porcupines are precluded throughout the EBC sequence by the rarity of bones with carnivore or porcupine tooth marks. In contrast, cut-marked bones implying a significant human contribution are abundant. Hyenas are further ruled out by the absence of coprolites, which are always numerous where hyena-chewed bones are common, and also by the rarity of bones from other terrestrial carnivores (Table 1, Fig. 1). Carnivore bones, especially from large species

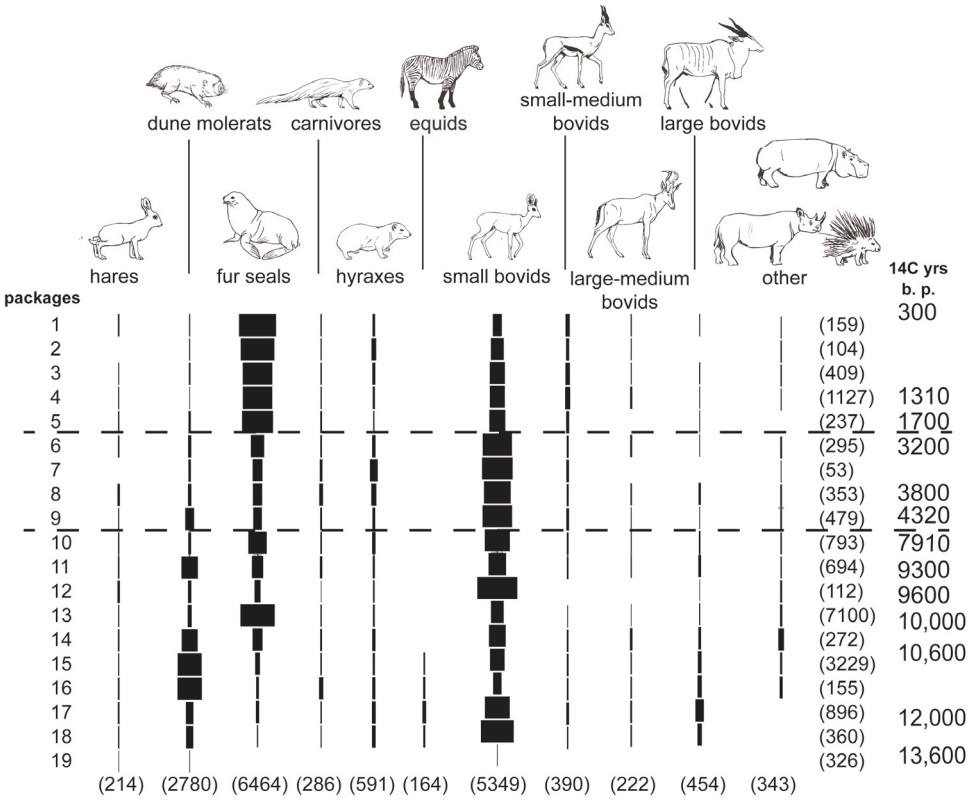

Fig. 1. Taxonomic frequency variation through the Elands Bay Cave sequence. The bars are proportional to the NISPs of each taxon in each package. Total NISPs per taxon and package are presented in parentheses in the margins. Dashed lines mark the main occupational/depositional gaps.

like lion (*Panthera leo*), spotted hyena (*Crocuta crocuta*), and brown hyena (*Hyaena brunnea*), are far more frequent in hyena-accumulated assemblages than in archaeological ones (Cruz-Uribe 1991), probably because hyenas interact with large carnivores more frequently than people do. Finally, of course, with regard to EBC, the extraordinary abundance of artefacts and other cultural debris implies that people (and not carnivores or porcupines) accumulated the overwhelming majority of bones.

An important role for raptors is more difficult to exclude. Black eagles (*Aquila verreauxii*) roost on a cliff close to EBC today, and Brain (1981) points out that when eagles roost nearby, bones they drop could enter a cave catchment. Black eagles prey preferentially on hyraxes (Gargett 1990; Boshoff et al. 1991; Armstrong & Avery 2014), which are relatively common in the EBC fauna, and they also take small antelope, which are substantially more abundant (Table 1, Fig. 1). However, eagle feeding produces a distinctive pattern of hyrax skeletal part representation in which skulls and mandibles dominate heavily, followed distantly by rearlimb bones and even more distantly by forelimb bones (Cruz-Uribe & Klein 1998). Figure 2 shows that the EBC hyrax pattern differs sharply from the one for eagles, and it thus appears unlikely that black eagles contributed significantly to the EBC fauna.

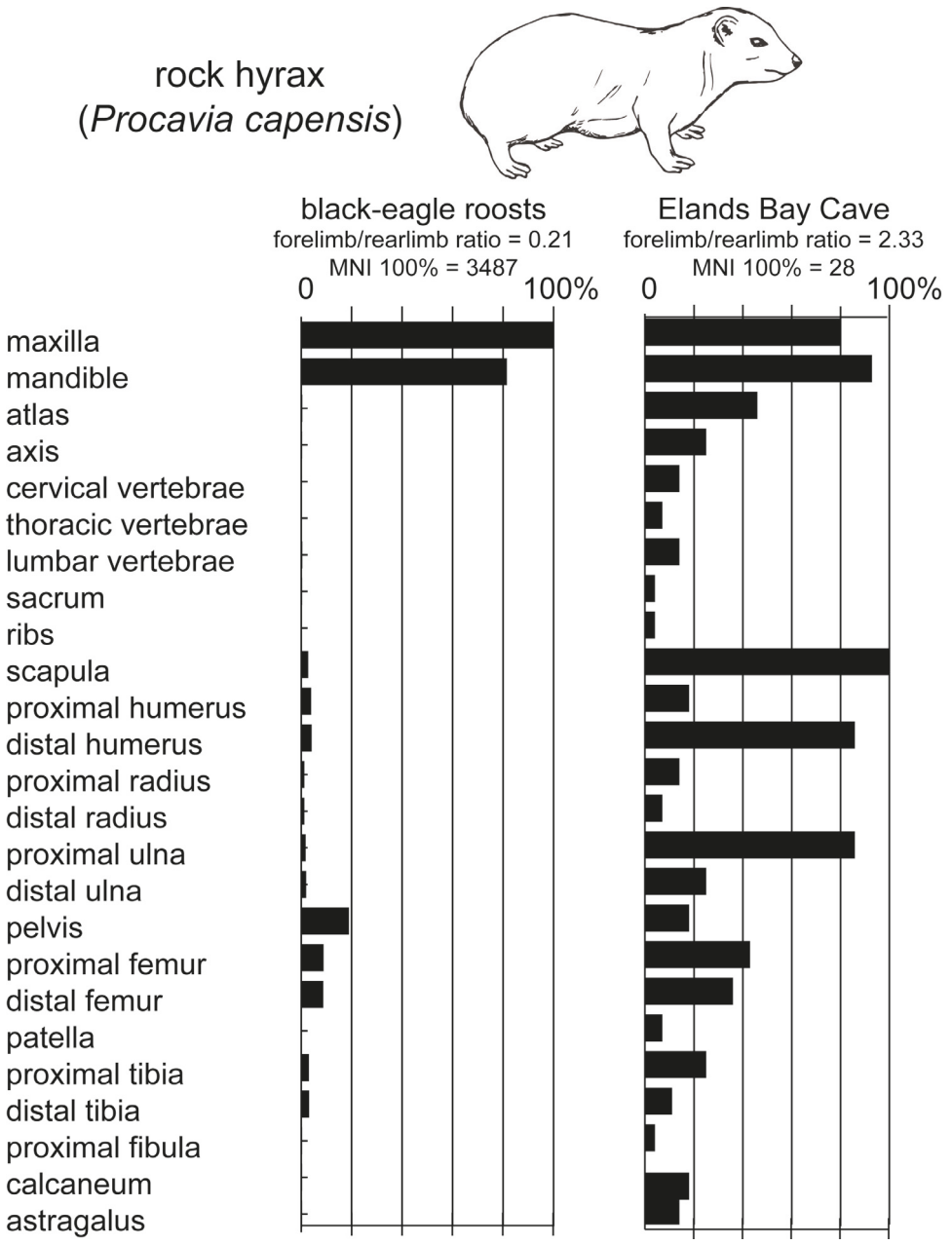

Fig. 2. Hyrax skeletal part representation in modern black-eagle roosts and in the LSA deposits of Elands Bay Cave. In each sample, the abundance of a skeletal part is indicated by the Minimum Number of Individuals (MNI) it must represent as a proportion of the largest MNI. Boshoff et al. (1991) and Klein and Cruz-Uribe (1996) describe the black-eagle roosts.

We cannot, however, rule out a role for Cape eagle owls (*Bubo capensis*), particularly in accumulating the dune molerat bones that abound in packages 20 to 14 (Table 1, Fig. 1). Cape eagle owls feed on molerats, and they sometimes roost in caves (Brain 1981; Avery 1990). We have suggested that Cape eagle owls rather than people accumulated most of the dune molerat bones in the MSA layers at Die Kelders Cave 1, where molerat bones dominate heavily (Grine et al. 1991; Avery et al. 1997) and where probable raptor gastric acid attack conspicuously etched or reduced the size of some specimens (Klein & Cruz-Uribe 2000). We saw no such obvious examples among the EBC molerat bones, but a microscopic study might reveal subtle etching on some (Andrews 1990).

SPECIES FREQUENCIES AND ENVIRONMENTAL CHANGE

Figure 1 illustrates frequency change in mammals through the EBC sequence, based on the NISPs from Table 1. We do not argue that the NISPs in the table or the figure closely mirror the past abundance of different species nearby or that they reflect the frequency with which people obtained various species. In fact, we think that large species like rhinoceros, hippopotamus, and the larger bovids were usually more common nearby and that people also obtained them more often than the table or figures suggest. This is because historic observations indicate that hunter-foragers often fail to return many bones of large animals to camp sites like EBC (Yellen 1977; O'Connell et al. 1990; Bartram 1993; Bunn 1993). However, even if our NISP estimates need not mirror the numbers of each species that people saw or obtained at any one time, they can inform on changes in local Stone Age ecology through time. Some of the NISP changes may result from technological or social change, but the most conspicuous ones coincide closely with local, regional or global environmental change, and it is environmental change that most economically explains them.

Table 1 lists 34 larger mammal species, but Figure 1 shows that just three species or species groups dominate the EBC fauna. These are the dune molerat, the Cape fur seal, and small bovids, mainly grysbok/steenbok, and it is their frequency fluctuations that largely shape Figure 1. Grysbok/steenbok bones tend to be common in all packages, but molerat and seal bones vary sharply in frequency among packages. The most conspicuous breaks in the sequence occur between packages 14 and 13 and packages 6 and 5. Package 13 records a sudden jump in the abundance of seal bones, which was accompanied by a sharp increase in shells and in bones of fish and shore birds (Parkington 2006: chapter 4). The overall increase in coastal food debris surely reflects the late glacial rise in sea level, which brought the coast to nearly its present position when package 13 formed about 9600 b.p. The drop in molerat bones in package 13 may reflect the drowning of favorable molerat habitat on the sandy coastal plain, more intensive human occupation resulting in less intensive eagle-owl use, or some combination of these factors.

Figure 1 shows that seal numbers decline in package 12 and do not return to package 13 levels until the accumulation of package 5, roughly 1700 b.p. The reason for reduced seal numbers in packages 12 to 6 could be a combination of fluctuating sea levels and of climatic conditions that altered the intensity or seasonality of seal exploitation from the cave. Fluctuating sea level is perhaps a more likely explanation for lower seal numbers in packages 12 to 10, and climate, specifically relatively dry conditions, for lower numbers in packages 9 to 6. Whichever factor was more important, seal age

distributions described below suggest that seasonality of occupation may have shifted slightly between packages 10 and below and packages 9 and above.

Table 1 shows frequency variation in the ungulates, which after dune molerats were the main terrestrial species the EBC people exploited and which could therefore be expected to reveal changes in prehistoric human ecology. Historically, the most common ungulates near EBC were steenbok and common duiker (Skead 2011). Both are browsers that prosper in the kind of shrubby vegetation that abounds near Elands Bay. Historically, the only obligate grazer recorded nearby was the hartebeest, and it was relatively rare. Table 1 shows that something akin to the historic situation probably obtained throughout the EBC sequence. Thus, grysbok/steenbok dominate heavily in nearly all packages. Common duiker is the next most abundant bovid in most units, and hartebeest occurs sporadically from the bottom to the top.

However, Table 1 also reveals some stratigraphic variation. Most notably, various large ungulates tend to be more common in packages 19 to 10 than in packages 9 to 1, and the larger species include two that were historically extraregional. These are the bushpig (in package 15) and the southern reedbuck (in packages 19 and 11). Both species require more mesic conditions than those near Elands Bay historically, and their fossil occurrence implies greater precipitation during at least part of the interval between 13 600 and 7900 b.p. when packages 19 to 10 formed. Conceivably, the abundance of hedgehog in this interval (Table 1) also implies more moisture, since hedgehogs live only in much wetter environments today. More indirectly, greater rainfall between 13 600 and 7900 b.p. is implied by the relatively large size of the dune molerats and hyraxes in packages 19 to 10 versus those in packages 5 to 1 and especially 9 to 6 (Klein 1991; Klein & Cruz-Uribe 1996). Faunal remains from other sites on or near the South African west and south coasts also suggest greater rainfall, or perhaps more effective rainfall under cooler temperatures, between about 14 000 and 8000 b.p. (Avery 1983; Klein 1983; Faith 2013b).

The reedbuck may also indicate grassier vegetation, which is more firmly suggested by the occurrence of zebra bones, particularly in packages 19 to 15. Finally, vegetational change at roughly 9600 b.p. is implied by the tendency for steenbok to become more numerous relative to grysbok beginning with packages 14 or 13 (Table 1). As already indicated, both steenbok and grysbok are primarily browsers, but historically, grysbok were more abundant in the relatively dense shrubland in the strip paralleling the South African south coast known informally as the southern Cape, while steenbok were more common in the sparser coastal strandveld or beach scrub in the strip along the west coast, known informally as the western Cape, that includes Elands Bay. Together with other changes in the large mammals, the shift towards steenbok dominance probably echoes a shift implied by charcoals (Cartwright & Parkington 1997; Cowling et al. 1999; Parkington & Fisher 2006, Cartwright et al. 2016 this issue) and microfauna (Avery 1983) from more mesic shrubland before 9600 b.p. near EBC to more xeric coastal strandveld after 9600 and especially after 4300 b.p. (February 1992). Less complete pollen evidence from EBC, not yet published, broadly supports the charcoal results.

In sum, changes in mammal species frequencies document both the late glacial rise in sea level and climatic/vegetational change across the Last Glacial/Present Interglacial (Holocene) boundary near Elands Bay. The vegetational change is also recorded in

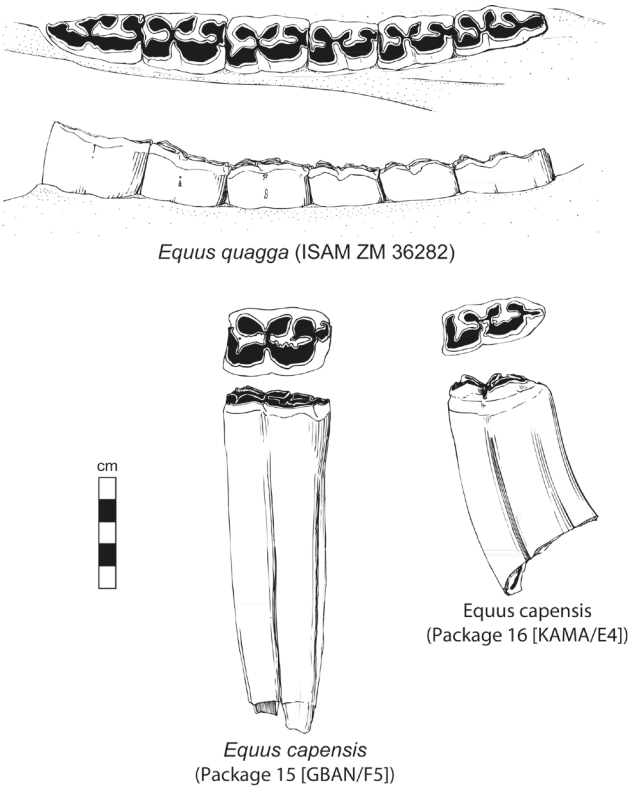

Fig. 3. Left mandibular cheek teeth of *Equus capensis* from Elands Bay Cave compared to the left mandibular dentition of a recent plains zebra (Drawings by Katharine Scott). Square brackets enclose the EBC field units and excavation squares from which the teeth came.

the charcoals, but the mammals suggest it was subtler than simultaneous vegetational change in the southern Cape. In contrast to the situation near EBC, terminal last glacial faunas in the southern Cape were heavily dominated by large grazing species (Klein 1983). The numbers and diversity of grazers declined sharply in the early Holocene, suggesting that a shrubland-bush-forest mosaic like the historic one largely replaced a last glacial mosaic in which grasses were much more important. The interregional contrast suggests that precipitation change from the Last Glaciation to the Holocene was much greater in the southern Cape.

EXTINCTIONS AND INTRODUCTIONS

The EBC fauna includes one or possibly two historically extinct species and one or possibly two introduced domestic species. The extinct species are the Cape zebra (Fig. 3), represented in packages 19 to 15, and possibly the long-horned buffalo, which may be represented by a large bovine deciduous premolar in package 18. Both the Cape zebra remains and the putative long-horned buffalo tooth date between 12 500 and 10 000 b.p. This interval brackets the latest known occurrences of the same species elsewhere in southern Africa (Klein 1983), and it coincides with the Last Glacial/

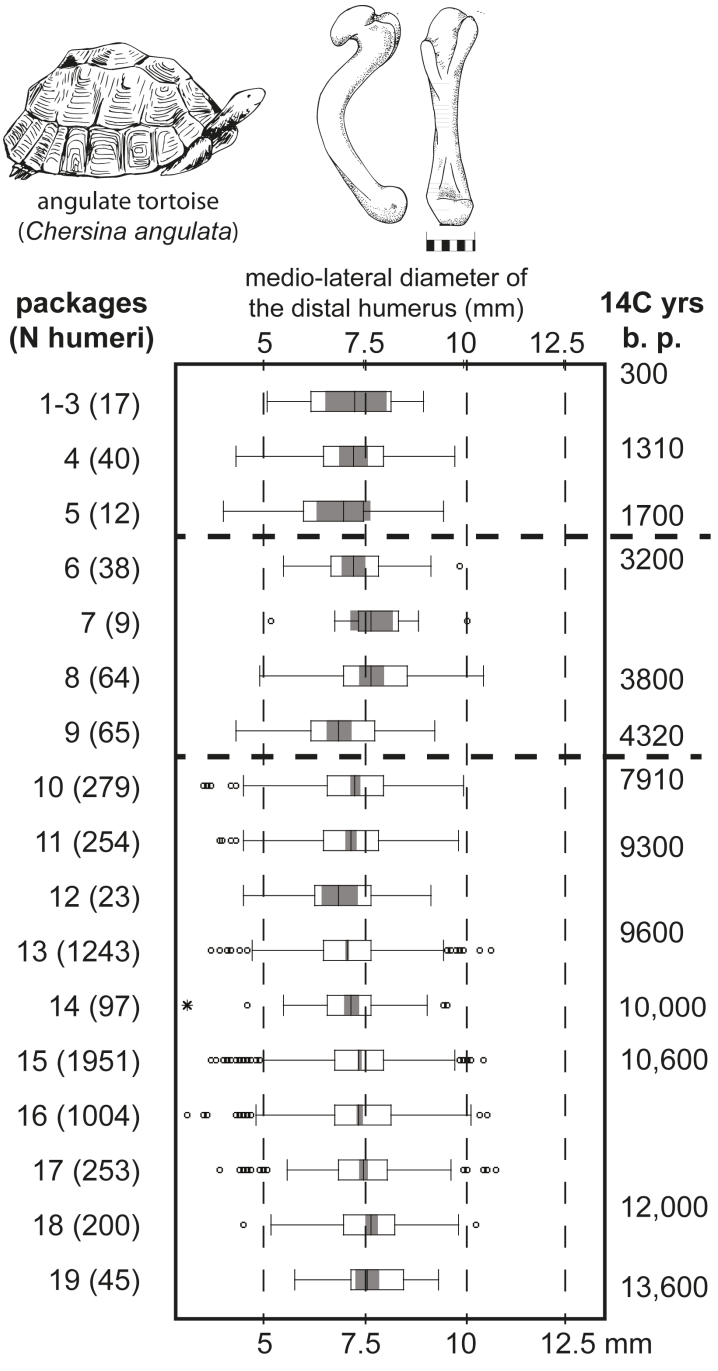

Fig. 4. Boxplots summarizing the mediolateral diameters of angulate tortoise distal humeri in Elands Bay Cave packages from youngest (top) to oldest (bottom). The number in parentheses to the left of each boxplot is the number of humeri in the corresponding package. Horizontal dashed lines mark depositional/occupational gaps.

Holocene transition. It is therefore tempting to ascribe the extinctions to environmental change. However, both species survived comparable change during the transition from the Penultimate Glaciation to the Last Interglacial roughly 128 000 b.p. The difference during 12 500–10 000 b.p. may have been the presence of much more sophisticated LSA (vs. MSA) hunter-gatherers, who applied the final blow to species already suffering from less favorable environmental conditions.

The EBC fauna also contains one of the latest archaeological records of the blue antelope, in package 8, dated to roughly 3800 b.p. Like the long-horned buffalo and especially the Cape zebra, the blue antelope appears to have prospered more under glacial than interglacial conditions, and it is relatively rare in Holocene sites (Klein 1987). It survived, however, to the historic period just east of the Hottentots Holland Mountains, in a small triangle defined by Swellendam, Caledon, and Bredasdorp (Skinner & Chimimba 2005). The last individual was observed around AD 1800.

With regard to introduced species, undoubted sheep remains occur in packages 4, 3, and 1, all younger than 1600 b.p., and there is a possible cattle dentition in package 1, which probably formed between 500 and 300 b.p. Both EBC occurrences postdate the earliest regional records of sheep and cattle. Older sheep are known at Kasteelberg, Die Kelders, Boomplaas, Blombos Cave, and possibly other western and southern Cape sites (Sealy & Yates 1994; Henshilwood 1996). The oldest well-documented sheep are dated to roughly 2000 b.p. at Blombos Cave, where the date may closely approximate the actual time of introduction. Older cattle are known at Kasteelberg, where they were present at least 1300 b.p. (Smith 1992), but the time of cattle introduction remains uncertain. Neither sheep nor ?cattle are abundant at EBC, and Table 1 shows that fur seals and grysbok/steenbok far outnumber both sheep and ?cattle even in the youngest packages. In addition, seal and other bones in these packages show little or none of the dog-chewing that altered large numbers of like-aged bones at Kasteelberg and the Dune Field Midden (Cruz-Uribe & Klein 1994). Assuming that herders kept dogs more commonly than hunter-foragers, the implication may be that EBC remained primarily a hunting-gathering station even after herders and herding-foraging were regionally well established.

AVERAGE TORTOISE SIZE AND HUMAN POPULATION DENSITY

At most archaeological sites in the western Cape and the adjacent southwestern Cape, west of Mossel Bay, tortoise bones abound, and EBC obeys the rule. Carapace fragments show that the angulate or bowsprit tortoise, *Chersina angulata*, dominates heavily at EBC, as it does at other sites on or near the west and southwest coasts. The tiny common padloper or parrot-beaked tortoise, *Homopus areolatus*, also usually occurs but in much smaller numbers. The abundance of tortoises at western and southwestern Cape sites stands in contrast to their rarity in deep sequences at Klasies River Cave 1 (Klein 1976), Nelson Bay Cave (Inskeep 1987), and Boomplaas Cave (Deacon 1979) on the south-central Cape coast and its hinterland further east. The difference implies a long-standing environmental contrast that persisted even during 'glacial' periods. Together with the subtler shifts in terrestrial mammal species frequencies at EBC, the persistent abundance of tortoises suggests that climatic/vegetational change occurred within narrower confines than it did in the south-central Cape.

In most EBC packages, angulate tortoise bones are sufficiently abundant to estimate average tortoise size, and it is on this that we focus. The single most common measurable bone is the distal humerus, and for size estimates we rely especially on its mediolateral diameter. Figure 4 summarizes our results in a boxplot format produced by the Macintosh program Data Desk (Velleman 2014). In each plot, the vertical line near the centre is the median, the open rectangle encloses the middle half of the data (between the 25th and 75th percentiles), the hachured rectangle is the 95 % confidence interval for the median, and the vertical lines at the ends mark the range of more or less continuous data. Circles or star bursts indicate extreme values (points that are far removed from the main body of data). The number of specimens in each package is given in parentheses. Samples for which the 95 % confidence intervals for the median do not overlap differ significantly in the conventional statistical sense. The samples from packages 1 to 3 were individually too small for meaningful display, so they are lumped in the figure.

The figure shows that median tortoise size varies significantly among packages in a wave-like pattern. The largest tortoises are in packages 19 and 18, dated to roughly 13 500–12 000 b.p., and in packages 8 and 7, dated to roughly 3800–3300 b.p. The smallest tend to be in packages 14 to 11, centred on 10 000–9300 b.p., and in packages 5 to 1, postdating 1700 b.p.

Unlike mammals, tortoises grow continuously until their physiology collapses, and the most likely explanation for tortoise size fluctuation is thus a change in the intensity of human collection. Prehistoric collectors, probably mostly women and children, would have needed no special technology nor faced special risk. They would probably have taken the largest tortoises first, since these would be most visible and the ones with the most food value. An increase in the number of collectors would then drive down average tortoise size, which means that smaller tortoise size is likely to imply a larger human population.

In support of an association between smaller tortoises and larger human populations, we note that the small tortoises in EBC packages 14–11 occur with artefactual and faunal debris implying especially intense occupation. This in turn probably reflects the most favorable conditions for hunting and gathering at any point in the EBC sequence. The small tortoises of packages 5–1 probably accumulated under much less favorable (drier) circumstances, but they are associated with the regional introduction of pastoralism. Pastoralism could have prospered only if it permitted larger human populations, and the Kasteelberg sites show that pastoralists (or more precisely pastoralist-foragers) collected large numbers of tortoises (Klein & Cruz-Uribe 1989).

The large tortoises of packages 19 and 18 antedate the terminal Pleistocene occupation buildup that peaked in package 13, while those of packages 8 and 7 are associated with faunal and floral evidence for relatively dry conditions that probably depressed hunter-gatherer populations just as earlier more mesic conditions had promoted them. Even drier conditions could explain the preceding occupational gap between packages 10 and 9 for which we lack faunal evidence.

A similar relationship between tortoise size and environmental or economic change marks the long MSA and LSA sequences at Die Kelders Cave 1 and Byneskranskop Cave 1 on the southwestern Cape coast (Klein & Cruz-Uribe 1983). Variation in limpet size through the EBC sequence parallels the tortoise pattern in Figure 4 (Parkington

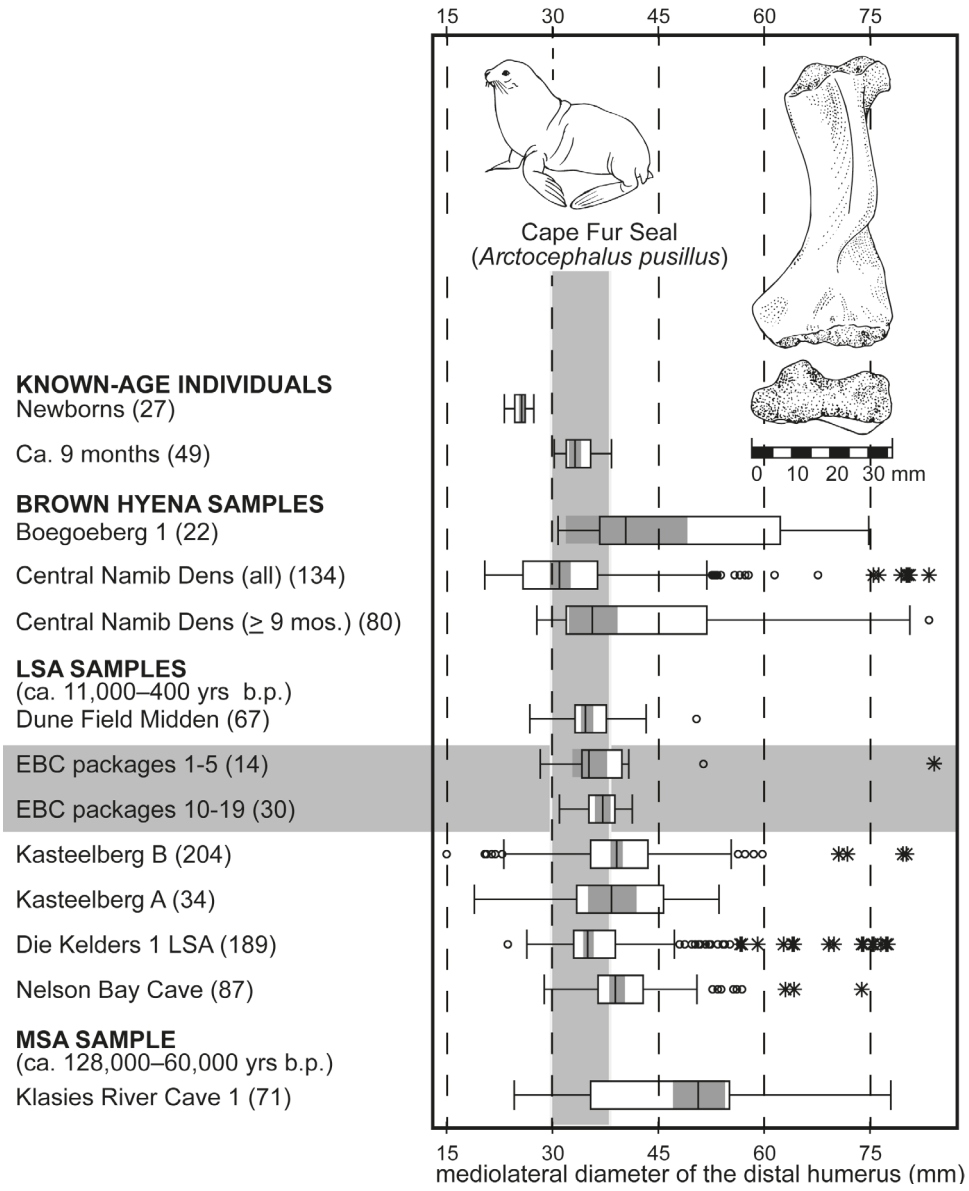

Fig. 5. Boxplots summarizing the mediolateral diameters of fur seal distal humeri in modern newborns and 9-month olds and in fossil samples from the Dunefield Midden (Parkington et al. 1992; Parkington 2006: chapter 3), Elands Bay Cave, Kasteelberg A and B (Smith 1987, 1992; Klein & Cruz-Uribe 1989; Cruz-Uribe & Klein 1994), Die Kelders Cave 1 (Schweitzer 1979; Avery et al. 1997; Klein & Cruz-Uribe 2000), Nelson Bay Cave (Deacon 1984; Inskeep 1987), Boegoeberg 1 (Klein et al. 1999), Klasies River Mouth Cave 1 (Singer & Wymer 1982; Deacon 1995), and the Central Namib Desert brown hyena dens (Skinner & Van Aarde 1991; Skinner et al. 1995).

2008) and the most economic explanation is that both patterns primarily reflect human collection intensity and population density. A driver linked directly to environmental change is especially unlikely, since tortoises and limpets occupy radically different ecosystems. Taken with artifactual and other faunal evidence, the sum suggests that the densest human populations occurred near Elands Bay in the transition from the Last Glaciation to the Holocene about 10 000 b.p., and again in the very late Holocene, after 1700 b.p.

SEASON OF HUMAN OCCUPATION

The EBC fauna not only reflects human subsistence and demography over a period of more than 13 000 years, but also illuminates an aspect of local settlement systems, namely, the seasonal scheduling of visits to the cave. In addressing this topic, we build on the pioneering work of Parkington (1972), who recognized that Cape fur seal bones have special potential for showing the time(s) of year when people occupied EBC and other coastal sites.

The Cape fur seal inhabits the coastal waters around southwestern Africa from roughly Algoa Bay (Port Elizabeth) on the southeast to southern Angola on the northwest (David 1989; Skinner & Chimimba 2005). Until 1941, when fur seals were locally afforded protection from human predation, they bred almost exclusively on offshore rocks. The vast majority of births occurred within a few weeks in late November and early December, and adults forced the young from the rocks about nine months later. In recent times, large numbers of 9–11-month-old seals then washed up ashore, exhausted or dead. It is the tightly seasonal fur seal birth season and the consequent seasonal peak in on-shore availability that allow estimates of when prehistoric people were present at sites like EBC. If archaeological seal ages cluster tightly around 9–11 months, site occupation probably centred tightly on the August–October period of 9–11-month-old seal superabundance. If ages cluster more loosely around 9–11 months, site visits included not only the August–October interval, but probably other times as well. And if ages fail to cluster near the 9–11-month average, then visits probably fell largely outside the August–October interval.

Fossil seal bones may be 'aged' by comparison to bones from known-age animals, and we have established the broad relationship between seal age and bone size from known-age skeletons at the Iziko South African Museum and the South African Department of Sea Fisheries. The known-age collections comprise mainly newborns and individuals about 9–11 months old. Various skeletal elements are suitable for age determination, but we rely primarily on the distal humerus, because it is relatively durable and is thus common in fossil samples. The most consistently available dimension is the mediolateral diameter or 'breadth' of the distal end. The dimensions of other bones, including the mediolateral diameter of the distal femur and the 'short length' of the mandible (defined by Woodborne et al. 1995) provide the same basic results, but the patterning is less compelling, because it is based on fewer specimens.

Figure 5 uses the same boxplot format we described in the last section to summarize fur seal distal humerus breadths at EBC and in five other LSA assemblages, all postdating 11 000 b.p., in an MSA assemblage that accumulated at Klasies River Cave 1 between roughly 128 000 and 60 000 b.p., and in two brown hyena accumulated

assemblages described more fully below. The caption to Figure 5 lists sources for all the sites. To aid interpretation, the figure includes boxplots for samples of modern newborn and 9-month old seals, and it extends the range for 9-month olds through the other boxplots.

The figure shows that in most samples, median fur-seal-distal-humerus breadth lies within or just outside the range for known 9-month-olds, and we conclude that bone accumulation at the relevant sites encompassed at least part of the August–October interval when 9–11-month-old seals are readily available. The most obvious exception to the rule is the MSA sample from Klasies River Cave 1, where median distal humerus breadth is substantially and significantly above the 9-month median. We suggest from this that bone accumulation at Klasies River 1 occurred mainly outside the peak period of 9–11-month-old availability, or more generally, that the Klasies River MSA people followed a qualitatively distinct seasonal round.

Our conclusion for EBC is unambiguous. For each of the two temporally discrete humerus samples for which we could calculate boxplots, the median lies squarely within the range for known 9-month-olds, and the clustering around the median is remarkably tight. Larger samples might show that the median in the younger sample, centred on about 1000 b.p., is significantly smaller than the median in the older sample, dating mainly to around 10 000 b.p., but both samples imply seasonal visits centred tightly on the August–October interval.

It is particularly instructive to compare the EBC boxplots to those for the two brown hyena samples near the centre of Figure 5. The sample labeled 'Central Namib' was accumulated between AD 1990 and 1996 in dens adjacent to a fur seal breeding colony about 20 km south of Luderitz, Namibia (Skinner & van Aarde 1991; Skinner et al. 1995). The other was accumulated in a fossil den at Boegoeberg 1, near Alexander Bay, Northern Cape, South Africa. Hyenas occupied the fossil den during a relatively cool, moist interval antedating 37 000 b.p. In keeping with hyena access to a breeding colony, the 143 humeri in the Central Namib sample include 54 from newborn individuals. The abundance of newborn specimens explains why Central Namib median distal humerus breadth is so small, and the rarity or absence of newborn specimens at EBC and other archaeological sites implies that none were located near breeding colonies. When the newborn specimens are removed from the Central Namib sample for heuristic purposes, the median humerus breadth becomes more like that in the EBC samples, but the degree of breadth dispersion becomes much greater. This is because the Central Namib brown hyenas remain at the coast throughout the year, including times when 9–11-month old seals are rare. The comparable or greater degree of dispersion in the fossil Boegoeberg 1 hyena sample also illustrates non-seasonal bone accumulation. However, in this instance, like the MSA and LSA people represented in the figure, the hyenas clearly did not have access to a breeding colony.

In sum, we conclude that the prehistoric occupants of EBC timed their coastal visits to include the August–October peak in young seal availability. The EBC seabird sample might allow a more precise estimate of when people were present (Avery 1990), but if people occupied EBC outside the peak of young seal abundance, they collected remarkably few seals. More likely, at times when 9–11-month old seals were rare, the people moved to other locales along the coast or to the interior, as Parkington (1972) suggested.

Fig. 6. Small and large bovid skeletal part representation at Elands Bay Cave. In each sample, the abundance of a skeletal part is indicated by the Minimum Number of Individuals (MNI) it must represent as a percentage of the largest MNI.

BOVID SKELETAL PART REPRESENTATION

In most African archaeological sites, including EBC, bovids are the most common terrestrial mammals, and it is important to ask how they were obtained. Binford (1984) suggested that hunting is implied when high-utility skeletal parts dominate a bovid assemblage, while scavenging is indicated when lower utility parts are more common. He defined the utility of a part as its food (= meat, marrow and grease) value. He reasoned that only early access to a carcass via hunting would yield an abundance of high-utility parts. Late access, after carnivore ravaging, would produce mainly low-utility parts.

In general, the highest utility bovid parts are proximal limb bones like the humerus, radius, femur, and tibia. Distal limb bones (podials, metapodials, and phalanges) and cranial bones tend to have much lower utility. Binford analyzed the frequencies of bovid parts in the MSA layers of Klasies River Cave 1 and noted that smaller bovids were well-represented by a range of skeletal parts, while larger bovids were well represented only by distal limb and cranial bones. He concluded therefore that the Klasies River MSA people hunted small bovids and mainly scavenged large ones.

Figure 6 graphs small and large bovid skeletal part representation at EBC. As an aid to interpretation, horizontal gray bars highlight distal limb elements. The figure shows that EBC recalls Klasies River in that small bovids are well-represented by a relatively wide range of skeletal parts, including proximal limb bones, while large bovids are well-represented only by cranial bones and distal limb bones. This might mean that the EBC people, like their Klasies River predecessors, mainly hunted small bovids and scavenged large ones.

However, the same contrast in skeletal part representation between smaller and larger bovids characterizes Stone Age camp sites throughout the world (Klein 1989), including sites like Kasteelberg B, where the smaller and larger bovids are mainly domestic species. The ubiquity of the pattern precludes scavenging versus hunting as a general explanation, and it suggests that other factors, dependent mainly on animal or carcass size, are highly relevant. These factors could include (1) cost-benefit considerations, whereby people often found that it was more efficient to process high-utility parts of large bovids in the field than to carry them to base camps; and (2) the absolute utility of particularly desirable large (vs. small) bovid parts, which led people to reduce many of them to unidentifiable fragments.

If these two factors explain the contrast in Figure 6, skeletal part representation does not reveal how the EBC people obtained large bovids, and there is no alternative, less ambiguous line of evidence. However, in regard to weaponry and numbers, the EBC people probably broadly resembled recently observed Hadza hunter-gatherers in northern Tanzania, and we suggest that Hadza behavior provides at least a rough guide to ancient EBC practice. The Hadza obtain 75–80 % of large mammal carcasses by active hunting and 20–25 % by scavenging (O'Connell et al. 1988, 1992). We note also that, like other historically observed hunter-gatherers in tropical or temperate latitudes, the Hadza cannot survive on hunting and scavenging alone, and they maintain a reliable nutrient flow only by routine exploitation of berries, roots, fruit, honey, tortoises, and other gathered resources. Undoubtedly the EBC people also relied heavily on gathered foods, although except for shellfish and tortoises, these have left no visible trace at EBC.

SUMMARY

Analysis of the large mammal and tortoise bones from Elands Bay Cave supports the following main conclusions:

1. Later Stone Age people rather than carnivores, porcupines, or raptors accumulated the large majority of animal bones at EBC.
2. Mammal species frequency fluctuations through the EBC sequence mainly reflect regional environmental change, including (a) a rise in sea level that brought the coastline to near its present position 10 000–9600 b.p., and (b) a shift from more mesic, grassier conditions before 9600 b.p. to drier, more shrubby conditions afterwards.
3. Variation in average tortoise size through the sequence suggests that human populations were densest roughly 10 000 b.p., when local conditions for hunting-gathering were most favorable, and again after 1700 b.p., when hunting-gathering was supplemented by pastoralism.
4. Seal bones in seal-rich units dating to about 10 000 and 1000 b.p. respectively indicate that people occupied EBC largely in the August-October interval when 9–11-month old seals could be harvested on nearby beaches.

ACKNOWLEDGEMENTS

We thank John Parkington for the opportunity to study the Elands Bay Cave fauna, the Iziko South African Museum for research facilities, and Graham Avery, John Parkington, Teresa Steele, and Aurore Val for helpful comments on a draft.

REFERENCES

Andrews, P. 1990. *Owls, caves, and fossils*. Chicago: University of Chicago Press.

Armstrong, A. & Avery, G. 2014. Taphonomy of Verreaux's Eagle (*Aquila verreauxii*) prey accumulations from the Cape Floral Region, South Africa: implications for archaeological interpretations. *Journal of Archaeological Science* **52** (0): 163–83.

Avery, D.M. 1983. Palaeoenvironmental implications of the small Quaternary mammals of the Fynbos region. In: H.J. Deacon, Q.B. Hendey, & J.J.N. Lambrechts, eds, *Fynbos paleoecology: a preliminary synthesis*. Pretoria: Council for Scientific and Industrial Research, pp. 139–55.

Avery, G. 1990. *Avian fauna, palaeoenvironments and palaeoecology in the Late Quaternary of the western and southern Cape, South Africa*. PhD thesis, University of Cape Town.

Avery, G., Cruz-Uribe, K., Goldberg, P., Grine, F.E., Klein, R.G., Lenardi, M.J., Marean, C.W., Rink, W.J., Schwarcz, H.P., Thackeray, A.I. & Wilson, M.L. 1997. The 1992–1993 excavations at the Die Kelders Middle and Later Stone Age cave site, South Africa. *Journal of Field Archaeology* **24** (3): 263–91.

Bartram, L.E. 1993. Perspectives on skeletal part profiles and utility curves from eastern Kalahari ethnoarchaeology. In: J. Hudson, ed., *From bones to behavior: ethnoarchaeological and experimental contributions to the interpretation of faunal remains*. Carbondale, IL: Center for Archaeological Investigations, Southern Illinois University at Carbondale, pp. 115–37.

Binford, L.R. 1984. *Faunal remains from Klasies River Mouth*. Orlando, FL.: Academic Press.

Boshoff, A.F., Palmer, N.G., Avery, G., Davies, R.A.G. & Jarvis, M.J.F. 1991. Biogeographical and topographical variation in the prey of black eagles in the Cape Province, South Africa. *Ostrich* **62**: 59–72.

Brain, C.K. 1981. *The hunters or the hunted? An introduction to African cave taphonomy*. Chicago: University of Chicago Press.

Brink, J.S. 1987. The archaeozoology of Florisbad, Orange Free State. *Memoirs van die Nasionale Museum (Bloemfontein)* **24**: 1–151.

Bunn, H.T. 1993. Bone assemblages at base camps: a further consideration of carcass transport and bone destruction by the Hadza. In: J. Hudson, ed., *From bones to behavior: ethnoarchaeological and experimental contributions to the interpretation of faunal remains*. Carbondale, IL: Center for Archaeological Investigations, Southern Illinois University at Carbondale, pp. 156–68.

Bunn, H.T., Harris, J.W.K., Isaac, G.L., Kaufulu, Z., Kroll, E., Schick, K., Toth, N. & Behrensmeyer, A.K. 1980. FxJj 50: an early Pleistocene site in northern Kenya. *World Archaeology* **12**: 109–36.

Cartwright, C. & Parkington, J.E. 1997. The wood charcoal assemblages from Elands Bay Cave, southwestern Cape: principles, procedures and preliminary interpretation. *South African Archaeological Bulletin* **52**: 59–72.

Cartwright, C.R., Porraz, G. & Parkington, J.E. 2016. The wood charcoal evidence from renewed excavations at Elands Bay Cave (South Africa). *Southern African Humanities* **29**: 249–58.

Cowling, R.M., Cartwright, C.R., Parkington, J.E. & Allsopp, J.C. 1999. Fossil wood charcoal assemblages from Elands Bay Cave, South Africa: implications for Late Quaternary vegetation and climates in the winter-rainfall fynbos biome. *Journal of Biogeography* **26** (2): 367–78.

Cruz-Uribe, K. 1991. Distinguishing hyena from hominid bone accumulations. *Journal of Field Archaeology* **18**: 467–86.

Cruz-Uribe, K. & Klein, R.G. 1994. Chew marks and cut marks on animal bones from the Kasteelberg B and Dune Field Midden Later Stone Age sites, western Cape Province, South Africa. *Journal of Archaeological Science* **21**: 35–49.

Cruz-Uribe, K. & Klein, R.G. 1998. Hyrax and hare bones from modern South African eagle roosts and the detection of eagle involvement in fossil bone assemblages. *Journal of Archaeological Science* **25** (2): 135–47.

David, J.H.M. 1989. Seals. In: A.I.L. Payne & R.J.H. Crawford, eds, *Oceans of life of Southern Africa*. Cape Town: Vlaeberg Publishers, pp. 288–302.

Deacon, H.J. 1979. Excavations at Boomplaas Cave – a sequence through the Upper Pleistocene and Holocene in South Africa. *World Archaeology* **10** (3): 241–57.

Deacon, H.J. 1995. Two late Pleistocene-Holocene archaeological depositories from the southern Cape, South Africa. *South African Archaeological Bulletin* **50**: 121–31.

Deacon, J. 1984. Later Stone Age people and their descendants in southern Africa. In: R.G. Klein, ed., *Southern African prehistory and paleoenvironments*. Rotterdam: A.A. Balkema, pp. 221–328.

Faith, J.T. 2013a. Taphonomic and paleoecological change in the large mammal sequence from Boomplaas Cave, western Cape, South Africa. *Journal of Human Evolution* **65** (6): 715–30.

Faith, J.T. 2013b. Ungulate diversity and precipitation history since the Last Glacial Maximum in the Western Cape, South Africa. *Quaternary Science Reviews* **68**: 191–9.

February, E. 1992. Archaeological charcoals as indicators of vegetation change and human fuel choice in the late Holocene at Elands Bay, Western Cape Province, South Africa. *Journal of Archaeological Science* **19** (3): 347–54.

Gargett, V. 1990. *The black eagle*. Randburg (South Africa): Acorn Books.

Grine, F.E., Klein, R.G. & Volman, T.P. 1991. Dating, archaeology, and human fossils from the Middle Stone Age levels of Die Kelders, South Africa. *Journal of Human Evolution* **21**: 363–95.

Henshilwood, C.S. 1996. A revised chronology for the arrival of pastoralism in southernmost Africa: new evidence of sheep at ca. 2000 b.p. from Blombos Cave, South Africa. *Antiquity* **70** (270): 945–9.

Inskeep, R.R. 1987. *Nelson Bay Cave, Cape Province, South Africa: the Holocene levels*. International Series 357. Oxford: B.A.R.

Klein, R.G. 1976. The mammalian fauna of the Klasies River Mouth sites, southern Cape Province, South Africa. *South African Archaeological Bulletin* **31**: 75–96.

Klein, R.G. 1981. Stone Age predation on small African bovids. *South African Archaeological Bulletin* **36**: 55–65.

Klein, R.G. 1983. Palaeoenvironmental implications of Quaternary large mammals in the Fynbos Biome. In: H.J. Deacon, Q.B. Hendey, & J.J.N. Lambrechts, eds, *Fynbos paleoecology: a preliminary synthesis*. Pretoria: Council for Scientific and Industrial Research, pp. 116–138.

Klein, R.G. 1987. The extinct blue antelope. *Sagittarius* **2** (3): 20–3.

Klein, R.G. 1989. Why does skeletal part representation differ between smaller and larger bovids at Klasies River Mouth and other archeological sites? *Journal of Archaeological Science* **16**: 243–56.

Klein, R.G. 1991. Size variation in the Cape dune molerat (*Bathyergus suillus*) and Late Quaternary climatic change in the southwestern Cape Province, South Africa. *Quaternary Research* **36**: 243–56.

Klein, R.G. & Cruz-Uribe, K. 1983. Stone age population numbers and average tortoise size at Byneskranskop Cave 1 and Die Kelders Cave 1, southern Cape Province, South Africa. *South African Archaeological Bulletin* **38**: 26–30.

Klein, R.G. & Cruz-Uribe, K. 1984. *The analysis of animal bones from archaeological sites*. Chicago: University of Chicago Press.

Klein, R.G. & Cruz-Uribe, K. 1987. Large mammal and tortoise bones from Elands Bay Cave and nearby sites, western Cape Province, South Africa. *Papers in the Prehistory of the Western Cape, South Africa*. International Series 332. Oxford: B.A.R., pp. 132–63.

Klein, R.G. & Cruz-Uribe, K. 1989. Faunal evidence for prehistoric herder-forager activities at Kasteelberg, Vredenburg Peninsula, western Cape Province, South Africa. *South African Archaeological Bulletin* **44**: 82–97.

Klein, R.G. & Cruz-Uribe, K. 1996. Size variation in the rock hyrax (*Procavia capensis*) and late Quaternary climatic change in South Africa. *Quaternary Research* **46**: 193–207.

Klein, R.G. & Cruz-Uribe, K. 2000. Middle and Later Stone Age large mammal and tortoise remains from Die Kelders Cave 1, Western Cape Province, South Africa. *Journal of Human Evolution* **38**(1): 168–195.

Klein, R.G., Cruz-Uribe, K., Halkett, D., Hart, T. & Parkington, J.E. 1999. Paleoenvironmental and human behavioral implications of the Boegoeberg 1 late Pleistocene hyena den, Northern Cape Province, South Africa. *Quaternary Research* **52** (3): 393–403.

Marean, C.W. 1992. Implications of late Quaternary mammalian fauna from Lukenya Hill (south-central Kenya) for paleoenvironmental change and faunal extinctions. *Quaternary Research* **37**: 239–55.

Matthews, T. 1999. Taphonomy and the micromammals from Elands Bay Cave. *South African Archaeological Bulletin* **54**: 133–40.

O'Connell, J.F., Hawkes, K. & Blurton Jones, N. 1988. Hadza scavenging: implications for Plio-Pleistocene subsistence. *Current Anthropology* **29**: 356–63.

O'Connell, J.F., Hawkes, K. & Blurton Jones, N. 1990. Reanalysis of large mammal body part transport among the Hadza. *Journal of Archaeological Science* **17**: 301–16.

O'Connell, J.F., Hawkes, K. & Blurton Jones, N. 1992. Patterns in the distribution, site structure and assemblage composition of Hadza kill-butchering sites. *Journal of Archaeological Science* **19**: 319–45.

Parkington, J.E. 1972. Seasonal mobility in the Late Stone Age. *African Studies* **31** (4): 223–44.

Parkington, J.E. 2006. *Shorelines, strandlopers and shell middens*. Cape Town: Creda Communications.

Parkington, J.E. 2008. Limpet sizes in stone age archaeological contexts at the Cape, South Africa: changing environment or human impact? In: A. Antczak & R. Cipriani, eds., *Early human impact on megamolluscs*. Oxford: Archaeopress, pp. ?–?.

Parkington, J.E. 2016. Elands Bay Cave: keeping an eye on the past. *Southern African Humanities* **29**: 17–32.

Parkington, J.E. & Fisher, J.W. 2006. Small mammal bones on Later Stone Age sites from the Cape (South Africa): consumption and ritual events. *Archeological Papers of the American Anthropological Association* **16**: 71–9.

Parkington, J.E., Nilssen, P., Vermuelen, C. & Henshilwood, C. 1992. Making sense of space at Dunefield Midden campsite, western Cape, South Africa. *Southern African Field Archaeology* **1**: 63–70.

Plug, I. 1993. The macrofaunal and molluscan remains from Tloutle, a Later Stone Age site in Lesotho. *Southern African Field Archaeology* **2**: 44–8.

Porraz, G., Schmid, V., Miller, C.E., Cartwright, C., Igreja, M., Mentzer, S., Mercier, N., Schmidt, P., Tribolo, C., Valladas, H., Conard, N.J., Texier, P.-J. & Parkington, J.E. 2016. Update on the 2011 excavation at Elands Bay Cave (South Africa) and the Verlorenvlei Stone Age. *Southern African Humanities* **29**: 33–68.

Reynard, J.P., Discamps, E., Wurz, S., van Niekerk, K.L., Badenhorst, S. & Henshilwood, C.S. 2016. Occupational intensity and environmental changes during the Howiesons Poort at Klipdrift Shelter, southern Cape, South Africa. *Palaeogeography, Palaeoclimatology, Palaeoecology* **449**: 349–64.

Schweitzer, F.R. 1979. Excavations at Die Kelders, Cape Province, South Africa: the Holocene deposits. *Annals of the South African Museum* **78** (10): 101–233.

Sealy, J.C. & Yates, R. 1994. The chronology of the introduction of pastoralism to the Cape, South Africa. *Antiquity* **68**: 58–67.

Singer, R. & Wymer, J.J. 1982. *The Middle Stone Age at Klasies River Mouth in South Africa*. Chicago: University of Chicago Press.

Skead, C.J. 2011. *Historical incidence of the large mammals in the broader Western and Northern Cape*. 2nd edition. Port Elizabeth: Centre for African Conservation Ecology, Nelson Mandela Metropolitan University.

Skinner, J.D. & Chimimba, C.T. 2005. *The mammals of the southern African subregion*. 3rd edition. Cambridge: Cambridge University Press.

Skinner, J.D. & Van Aarde, R.J. 1991. Bone collecting by brown hyenas *Hyaena brunnea* in the Central Namib Desert, Namibia. *Journal of Archaeological Science* **18**: 513–23.
Skinner, J.D., Van Aarde, R.J. & Goss, R.A. 1995. Space and resource use by brown hyenas *Hyaena brunnea* in the Namib Desert. *Journal of Zoology, London* **237**: 123–31.
Smith, A.B. 1987. Seasonal exploitation of resources on the Vredenburg Peninsula after 2000 BP. In: J.E. Parkington & M. Hall, eds, *Papers in the prehistory of the western Cape, South Africa*. International Series 332. Oxford: B.A.R., pp. 393–402.
Smith, A.B. 1992. Origins and spread of pastoralism in Africa. *Annual Review of Anthropology* **21**: 125–41.
Thackeray, J.F. 1979. An analysis of faunal remains from archaeological sites in southern South West Africa (Namibia). *South African Archaeological Bulletin* **34**: 18–33.
Thompson, J.C. 2010. Taphonomic analysis of the Middle Stone Age faunal assemblage from Pinnacle Point Cave 13B, Western Cape, South Africa. *Journal of Human Evolution* **59** (3–4): 321–39.
Velleman, P.F. 2014. *DataDesk 7 User's Manual*. Ithaca, NY: DataDescription, Inc.
Voigt, E.A. 1983. *Mapungubwe: an archaeozoological interpretation of an Iron Age community*. Transvaal Museum Monograph 1. Pretoria: Transvaal Museum.
Woodborne, S., Hart, K. & Parkington, J.E. 1995. Seal bones as indicators of the timing and duration of hunter-gatherer coastal visits. *Journal of Archaeological Science* **22**: 727–40.
Yellen, J.E. 1977. Cultural patterning in faunal remains: evidence from the !Kung Bushmen. In: D. Ingersoll, J.E. Yellen & W. MacDonald, eds, *Experimental archaeology*. New York: Columbia University Press, pp. 271–331.

TABLE 1

The Number of Specimens (NISP) and the Minimum Number of Individuals (MNI) from which they must come in depositional packages 22 to 1 at Elands Bay Cave. The NISP totals for each taxon include bones that could not be assigned to a package. They are therefore larger than the totals in Figure 1, which are based only on bones assigned to packages.

	1		2		3		4		5		6		7		8		9		10		11	
	NISP	MNI	**NISP**	MNI	**NISP**	MNI	**NISP**	MNI	**NISP**	MNI	**NISP**	MNI	**NISP**	MNI	**NISP**	MNI	**NISP**	MNI	**NISP**	MNI	**NISP**	MNI
hedgehog (*Erinaceus frontalis*)	**-**	-	**-**	-	**-**	-	**1**	1	**1**	1	**-**	-	**-**	-	**-**	-	**1**	1	**11**	3	**10**	3
hare(s) (Leporidae gen. et sp. indet.)	**3**	1	**-**	-	**3**	1	**9**	2	**3**	1	**5**	1	**-**	-	**13**	1	**4**	1	**11**	2	**11**	1
Cape dune molerat (*Bathyergus suillus*)	**2**	1	**1**	1	**8**	1	**3**	2	**8**	1	**15**	3	**2**	1	**19**	2	**78**	5	**35**	5	**216**	13
porcupine (*Hystrix africaeaustralis*)	**-**	-	**-**	-	**-**	-	**3**	1	**-**	-	**1**	1	**-**	-	**4**	1	**1**	1	**-**	-	**-**	-
baboon (*Papio ursinus*)	**-**	-	**-**	-	**1**	1	**9**	1	**2**	1	**1**	1	**-**	-	**3**	1	**-**	-	**1**	1	**1**	1
Cape fur seal (*Arctocephalus pusillus*)	**106**	4	**63**	2	**217**	5	**596**	11	**132**	4	**69**	3	**9**	1	**56**	3	**71**	3	**259**	6	**137**	3
black-backed jackal (*Canis mesomelas*)	**1**	1	**-**	-	**1**	1	**8**	1	**-**	-	**4**	1	**2**	1	**9**	1	**2**	1	**3**	1	**10**	1
Cape fox (*Vulpes chama*)	**-**	-	**-**	-	**-**	-	**-**	-	**-**	-	**-**	-	**-**	-	**-**	-	**-**	-	**-**	-	**-**	-
striped polecat (*Ictonyx striatus*)	**-**	-	**-**	-	**1**	1	**-**	-	**-**	-	**-**	-	**-**	-	**-**	-	**1**	1	**-**	-	**6**	2
honey badger (*Mellivora capensis*)	**-**	-	**-**	-	**-**	-	**-**	-	**-**	-	**1**	1	**-**	-	**-**	-	**1**	1	**-**	-	**-**	-
Egyptian mongoose (*Herpestes ichneumon*)	**-**	-	**-**	-	**-**	-	**-**	-	**1**	1	**-**	-	**-**	-	**-**	-	**-**	-	**-**	-	**1**	1
Cape gray mongoose *(Galerella pulverulenta)*	**1**	1	**1**	1	**1**	1	**5**	1	**3**	1	**-**	-	**-**	-	**2**	1	**4**	2	**8**	1	**2**	1
African wildcat (*Felis libyca*)	**-**	-	**-**	-	**1**	1	**-**	-	**1**	1	**1**	1	**-**	-	**1**	1	**1**	1	**-**	-	**2**	1
caracal *(Caracal caracal)*	**-**	-	**-**	-	**1**	1	**1**	1	**-**	-	**-**	-	**-**	-	**8**	2	**-**	-	**1**	1	**1**	1
leopard (*Panthera pardus*)	**-**	-	**-**	-	**1**	1	**-**	-	**-**	-	**-**	-	**-**	-	**-**	-	**2**	1	**2**	1	**-**	-
aardvark (*Orycteropus afer*)	**-**	-	**-**	-	**1**	1	**1**	1	**-**	-	**-**	-	**-**	-	**1**	1	**-**	-	**2**	1	**1**	1
rock hyrax (*Procavia capensis*)	**6**	2	**8**	2	**18**	2	**36**	4	**3**	1	**15**	4	**7**	2	**29**	2	**19**	2	**42**	3	**20**	2
African savanna elephant (*Loxodonta africana*)	**-**	-	**-**	-	**1**	1	**-**	-	**-**	-	**-**	-	**-**	-	**-**	-	**-**	-	**1**	1	**-**	-
quagga (*Equus quagga*)	**-**	-	**-**	-	**-**	-	**-**	-	**-**	-	**-**	-	**-**	-	**-**	-	**-**	-	**1**	1	**-**	-
Cape zebra (*Equus capensis*)	**-**	-	**-**	-	**-**	-	**-**	-	**-**	-	**-**	-	**-**	-	**2**	1	**-**	-	**1**	1	**1**	1
quagga or Cape zebra (*Equus* sp indet.)	**-**	**-**	**-**	**-**	**-**	**-**	**-**	**-**	**-**	**-**	**-**	**-**	**-**	**-**	**-**	**-**	**-**	**-**	**-**	**-**	**-**	**-**

TABLE 1 (*continued*)

The Number of Specimens (NISP) and the Minimum Number of Individuals (MNI) from which they must come in depositional packages 22 to 1 at Elands Bay Cave. The NISP totals for each taxon include bones that could not be assigned to a package. They are therefore larger than the totals in Figure 1, which are based only on bones assigned to packages.

	1		2		3		4		5		6		7		8		9		10		11	
	NISP	MNI	**NISP**	MNI	**NISP**	MNI	**NISP**	MNI	**NISP**	MNI	**NISP**	MNI	**NISP**	MNI	**NISP**	MNI	**NISP**	MNI	**NISP**	MNI	**NISP**	MNI
black rhinoceros (*Diceros bicornis*)	**-**	-	**-**	-	**-**	-	**-**	-	**-**	-	**-**	-	**-**	-	**-**	-	**-**	-	**-**	-	**1**	1
black rhinoceros and indet. rhinocerotid	**-**	-	**-**	-	**-**	-	**-**	-	**-**	-	**-**	-	**-**	-	**-**	-	**-**	-	**1**	1	**1**	1
hippopotamus (*Hippopotamus amphibius*)	**-**	-	**-**	-	**-**	-	**1**	1	**-**	-	**-**	-	**-**	-	**1**	1	**1**	1	**-**	-	**-**	-
bushpig (*Potamochoerus larvatus*)	**-**	-	**-**	-	**-**	-	**-**	-	**-**	-	**-**	-	**-**	-	**-**	-	**-**	-	**-**	-	**-**	-
bushpig and indet. suid	**-**	-	**-**	-	**-**	-	**-**	-	**-**	-	**-**	-	**-**	-	**-**	-	**-**	-	**-**	-	**1**	1
eland (*Taurotragus oryx*)	**-**	-	**-**	-	**-**	-	**1**	1	**-**	-	**-**	-	**-**	-	**2**	1	**-**	-	**2**	1	**3**	1
blue antelope (*Hippotragus leucophaeus*)	**-**	-	**-**	-	**-**	-	**-**	-	**-**	-	**-**	-	**-**	-	**1**	1	**-**	-	**1**	1	**-**	-
southern reedbuck (*Redunca arundinum*)	**-**	-	**-**	-	**-**	-	**-**	-	**-**	-	**-**	-	**-**	-	**-**	-	**-**	-	**-**	-	**1**	1
red hartebeest (*Alcelaphus buselaphus*)	**1**	1	**-**	-	**-**	-	**5**	2	**-**	-	**-**	-	**-**	-	**2**	1	**-**	-	**-**	-	**1**	1
springbok (*Antidorcas marsupialis*)	**-**	-	**-**	-	**-**	-	**-**	-	**-**	-	**-**	-	**-**	-	**-**	-	**-**	-	**-**	-	**1**	1
common duiker (*Sylvicapra grimmia*)	**1**	1	**-**	-	**1**	1	**14**	3	**3**	1	**1**	1	**-**	-	**1**	1	**5**	1	**6**	1	**3**	2
klipspringer (*Oreotragus oreotragus*)	**-**	-	**-**	-	**-**	-	**-**	-	**-**	-	**-**	-	**-**	-	**-**	-	**-**	-	**1**	1	**-**	-
steenbok (*Raphicerus campestris*)	**1**	1	**-**	-	**-**	-	**11**	3	**4**	1	**3**	2	**-**	-	**2**	2	**-**	-	**4**	2	**4**	3
Cape grysbok (*Raphicerus melanotis*)	**-**	-	**1**	1	**1**	1	**1**	1	**-**	-	**1**	1	**-**	-	**1**	1	**3**	2	**7**	3	**5**	2
steenbok/grysbok (*Raphicerus* spp.)	**5**	1	**5**	1	**27**	4	**59**	11	**14**	2	**25**	5	**3**	1	**24**	5	**19**	3	**86**	10	**31**	6
sheep (*Ovis aries*)	**1**	1	**-**	-	**2**	1	**9**	2	**-**	-	**-**	-	**-**	-	**-**	-	**-**	-	**-**	-	**-**	-
buffalo(s)/cattle (Bovini gen. et sp. indet.)	**1**	1	**-**	-	**-**	-	**-**	-	**-**	-	**-**	-	**-**	-	**1**	1	**-**	-	**-**	-	**-**	-
small bovid - all	**26**	2	**25**	1	**116**	6	**316**	11	**71**	3	**165**	6	**31**	2	**180**	7	**270**	8	**378**	10	**228**	22
small-medium bovid - all	**11**	1	**5**	1	**31**	2	**96**	4	**11**	1	**8**	1	**2**	1	**10**	1	**19**	2	**19**	1	**14**	2
large-medium bovid - all	**2**	1	**1**	1	**4**	1	**37**	2	**-**	-	**9**	1	**-**	-	**7**	1	**3**	1	**6**	1	**9**	1
large bovid - all	**1**	1	**-**	-	**3**	1	**5**	1	**1**	-	**1**	1	**-**	-	**10**	1	**1**	1	**13**	1	**23**	1

TABLE 1 (*continued*)

The Number of Specimens (NISP) and the Minimum Number of Individuals (MNI) from which they must come in depositional packages 22 to 1 at Elands Bay Cave. The NISP totals for each taxon include bones that could not be assigned to a package. They are therefore larger than the totals in Figure 1, which are based only on bones assigned to packages.

	12		13		14		15		16		17		18		19		20		21		22		ALL	
	NISP	MNI	**NISP**	MNI	**NISP**	MNI	**NISP**	MNI	**NISP**	MNI	**NISP**	MNI	**NISP**	MNI	**NISP**	MNI	**NISP**	MNI	**NISP**	MNI	**NISP**	MNI	**NISP**	MNI
hedgehog (*Erinaceus frontalis*)	**1**	1	**68**	8	**5**	2	**25**	5	**7**	2	**1**	1	**4**	1	**-**	-	**-**	-	**-**	-	**-**	-	**152**	20
hare(s) (Leporidae gen. et sp. indet.)	**4**	1	**75**	4	**5**	2	**34**	3	**19**	2	**5**	1	**6**	1	**1**	1	**-**	-	**-**	-	**-**	-	**237**	10
Cape dune molerat (*Bathyergus suillus*)	**6**	1	**486**	34	**82**	7	**1474**	71	**118**	9	**46**	3	**86**	6	**24**	4	**3**	1	**-**	-	**-**	-	**2973**	157
porcupine (*Hystrix africaeaustralis*)	**1**	1	**6**	1	**-**	-	**26**	2	**-**	-	**4**	1	**2**	1	**-**	-	**1**	1	**-**	-	**-**	-	**51**	2
baboon (*Papio ursinus*)	**-**	-	**3**	1	**-**	-	**12**	2	**7**	1	**-**	-	**-**	-	**-**	-	**-**	-	**-**	-	**-**	-	**40**	3
Cape fur seal (*Arctocephalus pusillus*)	**11**	1	**4380**	69	**47**	4	**245**	6	**43**	3	**4**	1	**10**	1	**3**	1	**-**	-	**-**	-	**-**	-	**6666**	103
black-backed jackal (*Canis mesomelas*)	**-**	-	**29**	2	**1**	1	**4**	1	**-**	-	**-**	-	**-**	-	**-**	-	**1**	1	**-**	-	**-**	-	**82**	3
Cape fox (*Vulpes chama*)	**-**	-	**1**	1	**-**	-	**-**	-	**-**	-	**-**	-	**-**	-	**-**	-	**-**	-	**-**	-	**-**	-	**1**	1
striped polecat (*Ictonyx striatus*)	**-**	-	**11**	2	**2**	1	**15**	2	**6**	2	**-**	-	**-**	-	**-**	-	**-**	-	**-**	-	**-**	-	**43**	6
honey badger (*Mellivora capensis*)	**-**	-	**-**	-	**-**	-	**1**	1	**1**	1	**-**	-	**2**	1	**-**	-	**-**	-	**-**	-	**-**	-	**7**	1
Egyptian mongoose (*Herpestes ichneumon*)	**-**	-	**2**	1	**-**	-	**-**	-	**-**	-	**-**	-	**-**	-	**-**	-	**-**	-	**-**	-	**-**	-	**4**	1
Cape gray mongoose *(Galerella pulverulenta)*	**-**	-	**24**	3	**1**	1	**12**	3	**2**	1	**-**	-	**-**	-	**-**	-	**-**	-	**-**	-	**-**	-	**73**	7
African wildcat (*Felis libyca*)	**-**	-	**2**	1	**-**	-	**3**	1	**2**	1	**3**	1	**-**	-	**-**	-	**-**	-	**-**	-	**-**	-	**22**	2
caracal *(Caracal caracal)*	**-**	-	**11**	1	**1**	1	**12**	1	**2**	1	**-**	-	**1**	1	**-**	-	**-**	-	**1**	1	**-**	-	**43**	2
leopard (*Panthera pardus*)	**-**	-	**15**	1	**1**	1	**5**	1	**-**	-	**-**	-	**1**	-	**-**	-	**-**	-	**-**	-	**-**	-	**27**	1
aardvark (*Orycteropus afer*)	**0**	-	**8**	1	**2**	1	**10**	1	**1**	1	**4**	1	**3**	1	**-**	-	**-**	-	**-**	-	**-**	-	**35**	2
rock hyrax (*Procavia capensis*)	**2**	1	**179**	12	**13**	1	**97**	7	**50**	3	**20**	5	**12**	2	**8**	1	**1**	1	**-**	-	**-**	-	**650**	30
African savanna elephant (*Loxodonta africana*)	**-**	-	**1**	1	**-**	-	**2**	1	**1**	1	**1**	-	**-**	-	**-**	-	**-**	-	**-**	-	**-**	-	**7**	1
quagga (*Equus quagga*)	**-**	-	**-**	-	**-**	-	**2**	1	**3**	1	**1**	1	**5**	1	**1**	1	**1**	1	**-**	-	**-**	-	**15**	1
1111Cape zebra (*Equus capensis*)	**-**	-	**4**	1	**-**	-	**36**	2	**29**	1	**5**	1	**6**	1	**2**	1	**1**	1	**-**	-	**-**	-	**91**	3
quagga or Cape zebra *(Equus* sp. indet.)	**-**	-	**-**	-	**-**	-	**34**	2	**22**	1	**4**	1	**-**	-	**-**	-	**-**	-	**-**	-	**-**	-	**62**	3

TABLE 1 (*continued*)

The Number of Specimens (NISP) and the Minimum Number of Individuals (MNI) from which they must come in depositional packages 22 to 1 at Elands Bay Cave. The NISP totals for each taxon include bones that could not be assigned to a package. They are therefore larger than the totals in Figure 1, which are based only on bones assigned to packages.

	12		13		14		15		16		17		18		19		20		21		22		ALL	
	NISP	MNI	**NISP**	MNI	**NISP**	MNI	**NISP**	MNI	**NISP**	MNI	**NISP**	MNI	**NISP**	MNI	**NISP**	MNI	**NISP**	MNI	**NISP**	MNI	**NISP**	MNI	**NISP**	MNI
black rhinoceros (*Diceros bicornis*)	**-**	-	**-**	-	**-**	-	**-**	-	**1**	1	**5**	1	**-**	-	**-**	-	**-**	-	**-**	-	**-**	-	**7**	1
black rhinoceros and indet. rhinocerotid	**-**	-	**2**	1	**-**	-	**10**	1	**6**	1	**6**	1	**2**	1	**4**	1	**-**	-	**-**	-	**-**	-	**32**	2
hippopotamus (*Hippopotamus amphibius*)	**-**	-	**2**	1	**-**	-	**18**	2	**3**	2	**-**	-	**-**	-	**-**	-	**-**	-	**-**	-	**-**	-	**27**	2
bushpig (*Potamochoerus larvatus*)	**-**	-	**-**	-	**-**	-	**1**	1	**-**	-	**-**	-	**-**	-	**-**	-	**-**	-	**-**	-	**-**	-	**1**	1
bushpig and indet. suid	**-**	-	**-**	-	**-**	-	**3**	1	**1**	-	**-**	-	**1**	1	**-**	-	**-**	-	**-**	-	**-**	-	**6**	1
eland (*Taurotragus oryx*)	**-**	-	**13**	4	**3**	1	**43**	8	**35**	4	**7**	2	**5**	2	**1**	1	**-**	-	**-**	-	**-**	-	**121**	11
blue antelope (*Hippotragus leucophaeus*)	**-**	-	**-**	-	**-**	-	**2**	1	**2**	1	**-**	-	**-**	-	**-**	-	**-**	-	**-**	-	**-**	-	**6**	1
southern reedbuck (*Redunca arundinum*)	**-**	-	**-**	-	**-**	-	**-**	-	**-**	-	**-**	-	**-**	-	**1**	1	**-**	-	**-**	-	**-**	-	**3**	1
red hartebeest (*Alcelaphus buselaphus*)	**-**	-	**3**	1	**-**	-	**12**	2	**2**	1	**-**	-	**3**	1	**-**	-	**-**	-	**-**	-	**-**	-	**29**	4
springbok (*Antidorcas marsupialis*)	**-**	-	**-**	-	**-**	-	**-**	-	**-**	-	**-**	-	**-**	-	**-**	-	**-**	-	**-**	-	**-**	-	**1**	1
common duiker (*Sylvicapra grimmia*)	**1**	1	**15**	3	**3**	1	**36**	3	**8**	2	**2**	1	**-**	-	**-**	-	**-**	-	**-**	-	**-**	-	**112**	11
klipspringer (*Oreotragus oreotragus*)	**1**	1	**-**	-	**-**	-	**3**	1	**-**	-	**-**	-	**2**	1	**-**	-	**-**	-	**-**	-	**-**	-	**6**	1
steenbok (*Raphicerus campestris*)	**7**	3	**25**	8	**1**	1	**5**	4	**3**	1	**-**	-	**-**	-	**-**	-	**-**	-	**-**	-	**-**	-	**70**	18
Cape grysbok (*Raphicerus melanotis*)	**-**	-	**15**	5	**2**	1	**21**	6	**8**	3	**-**	-	**-**	-	**-**	-	**-**	-	**-**	-	**-**	-	**67**	20
steenbok/grysbok (*Raphicerus* spp.)	**22**	5	**255**	27	**10**	3	**248**	23	**89**	10	**28**	3	**7**	1	**-**	-	**2**	1	**-**	-	**-**	-	**1071**	83
sheep (*Ovis aries*)	**-**	-	**-**	-	**-**	-	**-**	-	**-**	-	**-**	-	**-**	-	**-**	-	**-**	-	**-**	-	**-**	-	**13**	3
buffalo(s)/cattle (Bovini gen. et sp. indet.)	**-**	-	**8**	3	**1**	1	**7**	1	**9**	2	**1**	1	**1**	1	**1**	1	**-**	-	**-**	-	**-**	-	**33**	5
small bovid - all	**86**	5	**1673**	32	**86**	3	**868**	23	**408**	11	**222**	6	**146**	6	**31**	2	**6**	1	**7**	2	**3**	1	**5719**	85
small-medium bovid - all	**1**	1	**36**	3	**6**	1	**72**	3	**35**	2	**5**	1	**6**	1	**-**	-	**2**	1	**-**	-	**-**	-	**421**	13
large-medium bovid - all	**-**	-	**22**	2	**11**	1	**52**	3	**23**	1	**7**	1	**23**	2	**3**	1	**-**	-	**1**	1	**2**	1	**234**	4
large bovid - all	**-**	-	**64**	4	**9**	1	**157**	9	**107**	4	**22**	2	**21**	2	**7**	1	**1**	1	**1**	1	**-**	-	**483**	15

Southern African Humanities **29**: 283–306 December 2016 KwaZulu-Natal Museum

Holocene hunter-gatherers and adhesive manufacture in the West Coast of South Africa

[1]**Armelle Charrié-Duhaut**, [2,3]**Guillaume Porraz**, [4]**Marina Igreja**, [5]**Pierre-Jean Texier** and [6]**John E. Parkington**

[1]CNRS, UMR 7140, Université de Strasbourg, Laboratoire de Spectrométrie de Masse des Interactions et des Systèmes (LSMIS), Strasbourg, France; acharrie@unistra.fr
[2]CNRS, USR 3336, Institut Français d'Afrique du Sud, Johannesburg, South Africa; guillaume.porraz@mae.u–paris10.fr
[3]Evolutionary Studies Institute, University of the Witwatersrand, Johannesburg, South Africa
[4]ENVARCH, CIBIO-INBIO, University of Porto, Portugal; maraujo_mar@yahoo.com
[5]CNRS, PACEA, Université de Bordeaux; pierre.texier@u–bordeaux.fr
[6]Department of Archaeology, University of Cape Town, South Africa; john.parkington@uct.ac.za

ABSTRACT

Elands Bay Cave provides the opportunity to characterize Holocene technologies and hunter-gatherers adaptations in the West Coast of South Africa. In this paper, we discuss the question of adhesives uses and manufactures by applying a biomolecular and technological analysis to three unpublished organic artefacts recovered from the 1970s excavation. The first piece is a large handle made of adhesive and with a tear-drop shape (the 'handle'), the second piece is a kind of pencil grip wrapping a microlithic quartz segment (the 'grip'), and the last piece takes the form of a macro-residue likely sealing the perforation of an ostrich eggshell flask (the 'sealant'). The results of our study document the selection and transformation of *Podocarpus* resin, mixed with quartz sand to produce adhesive. One case study (the sealant) suggests that fat was added to the recipe in order to modify the adhesive's properties. The paper provides a unique insight into Holocene organic technologies and fuels ideas on how hunter-gatherers adapted and took benefit from local natural resources. We suggest that *Podocarpus*, in South Africa, has been specifically chosen for adhesive manufacture since, at least, the MIS4.

KEY WORDS: South Africa, Elands Bay Cave, Later Stone Age, Holocene, macro-residues, hafting, adhesive, Ostrich eggshell, backed tool, microliths, Podocarpus, Diterpenoids

The use of natural substances may represent a common practice among past hunter-gatherer societies, but archaeological evidences remain very limited. Natural substances encompass all sorts of plant and animal materials and there is sometimes confusion regarding the appropriate terminology. The first distinction to operate concerns the raw substances coming out of plant materials (exudates, gums, resins, saps) on the one hand, and the substances that have been 'manufactured' (tar, pitch, adhesive) on the other. Basically, all these raw materials are exudates, liquids seeping from a plant. They include resins (mixture of terpenoids or phenolic structures), gums and mucilages (polysaccharides structures) and latex (Langenheim 2003). It is completely different from sap, an aqueous solution which carries nutrients through the phloem or xylem tissue of plants. As described below, following the family, genus or species of the plant, the corresponding resin has a diagnostic distribution of compounds called biomarkers allowing identification (Mills & White 1977, 1994). Some have special names: myrrhs from *Commiphora* species, Olibanum from *Boswellia* species, dammar for the resin of Dipterocarpaceae family or mastic from the trees mainly of the genus *Pistacia* of the Anacardiaceae family. Regarding the "manufactured" materials derived from plants, tars obtained by pyrolysis of wood are well known for their specific properties such as their viscous and sticky textures or their hydrophobicity. Birch bark tar and pitch

ISSN 2305-2791 (online); 1681-5564 (print)

(softwood tar from conifers) have been widely used in prehistoric times (Hayek et al. 1990; Pollard & Heron 1996).

In the present paper, we deal more specifically with the manufacture and use of adhesives. This is a material composed of one or several more organic natural substances, mixed or not with other components (mineral, fibrous, etc.), which has been shaped or intentionally applied to a surface in order to give it new properties. Adhesives could have been used for different purposes, for example to seal or waterproof containers, but its main known use in prehistory relates to hafting technology (Helwig et al. 2014; Regert & Rolando 2002; Regert 2004).

Adhesives can be regarded as the first synthetic material produced in human history, i.e. the first natural substance chemically transformed to be used. The manufacture of an adhesive is a combination of different technological steps and know-hows, from the acquisition of the natural substances to their transformation and application. Such a manufacture implies complex cognitive capacities and requires a favorable context in terms of socio-economic structures and technical knowledge (Haidle 2010; Wadley 2010; Sykes in press).

The manufacture of an adhesive is a function naturally of the available resources but recipes reflect the types of property (or adherence) that were sought by the manufacturer. How the adhesive suits the need and how it resists through time are two of the main attributes that constraint the *chaîne opératoire* of an adhesive.

The oldest evidences of adhesives manufacture date back to the late Middle Pleistocene at the site of Campitello (Italy). There, two flakes have been found with a lump of birch bark tar at their base (Mazza et al. 2006). Following later examples date back from the Last interglacial. Another proof comes from the site of Königsaue (Germany) where two pieces of birch pitch have been found (Koller et al. 2001; Grünberg 2002). The excavation of the site of Inden-Altdorf (Germany) has recovered 39 tools bearing residues and gives evidence for the use of an adhesive substance (Pawlik & Thissen 2011).

The other Middle Palaeolithic examples where adhesive has been found document the use of bitumen. This is the case at the site of Umm-el-Tlel (Syria) where several Levallois flakes and points showing basal bitumen imprints have been found (Boëda, Bonilauri, Connan, Jarvie, Mercier, Tobey, Valladas & Sakhel 2008; Boëda, Bonilauri, Connan, Jarvie, Mercier, Tobey, Valladas, Sakhel & Muhesen 2008), together with a lump of oil-stained sands (Connan 1999). Evidence of bitumen use has also been observed in the Mousterian lithic assemblage from the nearby site of Hummal (Syria, Hauck et al. 2013). Another example is known from the late Mousterian site of Gura Cheii-Râsnov (Romania) where one flake has been found with a lateral imprint (Cârciumaru et al. 2012).

The range of direct evidence seems to increase with the Upper Palaeolithic and, later on, with the Mesolithic. There are traces from three burins of the late Aurignacian of Les Vachons (Dinnis et al. 2009) where pitch resin has been recognized. A recent study on geometrics from the late Upper Palaeolithic site of Ohalo II in the Near East (Yaroshevich et al. 2013) indicates that both calcareous and organic substances were used as adhesives. And adhesives have also been macroscopically identified at Lascaux Cave (Leroi-Gourhan & Allain 1979) and in Mesolithic sites from Germany (Yates et al. 2015). There are a few other examples where shaft, adhesives and lithic tools have

been found together. It is the case at the Magdalenian site of Pincevent (France) where two bladelets have been found attached with adhesive on an osseous point (Leroi-Gourhan 1983), and at the Mesolithic site of Tlokowo (Poland) where geometrics were found inserted and glued into the grooves of a bone point (Sulgostowska 1993). A final example is provided by the site of Loshult (Sweden) where lithic pieces have been found glued with birch tar onto a wooden arrow (Petersson 1951).

All these examples provide strong evidence that adhesive was part of the technological repertoire of hunter-gatherers since at least the MIS7. The set of evidences become even clearer if we open our argumentation to indirect hafting traces (e.g. Rots 2003; Rots et al. 2006; Conard et al. 2012), which suggest that adhesive might have been involved or required. One of these indirect evidences would be provided by the tang of the North African Aterian points (Tixier 1959; Iovita 2011).

In Africa, few studies have dealt with the question of adhesives technology. Adhesives imprints or residues presently known are documented in the Nubian site of Sodmein Cave in Egypte (Rots et al. 2011), in the Still Bay (SB) and Howiesons Poort (HP) of Sibudu Cave (Lombard 2006, 2008, Wadley & Mohapi 2008) and in the HP of Diepkloof Rock Shelter (Igreja & Porraz 2013) in South Africa, and have also been reported from the Early Later Stone Age (LSA) site of Nasampolai in Kenya (Ambrose 1998). These evidences become more numerous through time, especially in South Africa, where adhesives have been reported in the Early LSA of Border Cave (Villa et al. 2012), in the Late Pleistocene Robberg of Elands Bay Cave (Porraz et al. 2016 this issue) and Sehonghong (Binneman & Mitchell 1997), as well as in the Holocene of Melkhoutboom (Deacon 1976) and Boomplaas (Deacon & Deacon 1980; Deacon 1984). So far, only few chemical analyses have been applied to such material. They concern adhesives from the HP of Diepkloof (Charrié-Duhaut et al. 2013) and Sibudu (Soriano et al. 2015) and from the Early LSA of Border Cave (Villa et al. 2012). All these studies indicate hunter-gatherers made use of a conifer resin, likely resin of *Podocarpus* (Yellowwood) as identified for the sites of Diepkloof and Border Cave.

This overview from the literature reports increasing evidence of the manufacture and use of adhesives from the Middle to the end of the late Pleistocene. This reflects that these organic materials could be preserved through time, but has also to be understood in the light of new (microlithic) technologies that have been adopted by hunter-gatherer groups. Our set of data suggests that at least from the MIS 2, the manufacture of adhesives was a familiar technological capacity among hunter-gatherers groups.

But the increasing set of archaeological evidences does not go together with a diversification in uses: in fact, all current evidence from the Pleistocene documents the use of adhesives in relation to hafting technologies. The diversification in uses seems only to develop from the Holocene. The Neolithic provides examples of ceramics being fixed with glue (Mitkidou et al. 2008); the Holocene LSA provides examples of ostrich eggshell (OES) containers being sealed with adhesive (Deacon & Deacon 1999; Henderson 2002). Other examples are derived from the historic period: bitumen has for example been used as a mortar in construction, to waterproof and seal containers, to caulk boats, and to create domestic and ornamental objects (Connan 1999).

In this paper, we aim to fuel the discussion on how adhesives were manufactured by hunter-gatherers and how this manufacture varied with uses. We focus on the Holocene

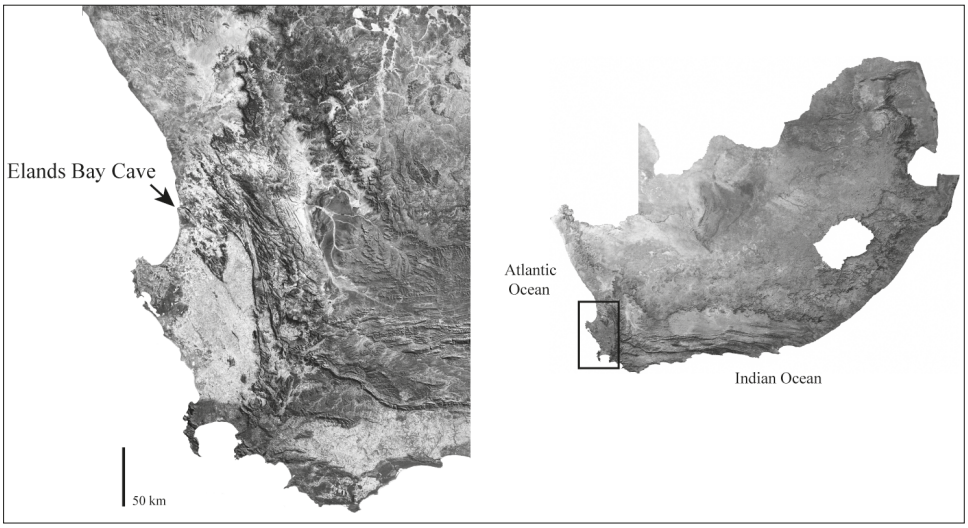

Fig. 1. Location of Elands Bay Cave (South Africa).

sequence of Elands Bay Cave (EBC) where various organic artefacts have been found. Three different organic LSA artefacts have been selected for the study: 1) a large handle made of adhesive and with a tear-drop shape, 2) an adhesive pencil grip wrapping a quartz segment, and 3) a strip of adhesive circling the opening of an OES flask.

Most adhesives such as resin, tar or waxes are amorphous. These are substances without form, without crystalline structure or cellular organization and as such their identification requires chemical analysis. In this study, we provide results from both Fourier transform infrared spectroscopy (FTIR) and mass spectrometry analyses, together with a comprehensive description of the main technological steps and inferences involved in the adhesive's manufacture. We comment further on the technological implications of our study and argue that, in South Africa, *Podocarpus* was specifically chosen to produce adhesive since, at least, the MIS4.

SITE AND MATERIAL

EBC is located on the West Coast of South Africa, about 200 km north of Cape Town (Fig. 1). The site was excavated by John E. Parkington in the 1970s and exposes long and well-stratified deposits dominantly accumulated during the LSA. The upper part of the deposits represents a shell midden that started forming during the early Holocene (Parkington 2016 this issue). A relatively long suite of radiocarbon age determinations indicates the shell midden represents 3 main pulses of human occupation ranging from 11 000 to 8 000 b.p., 4 350 to 3 300 b.p., and 2 250 to 300 b.p. (Parkington 2016 this issue).

These upper deposits are characterized by substantial assemblages of archaeological materials including a range of terrestrial and marine fauna, lithic artefacts, ochre, worked wood, worked bones, charcoals and seeds. Some pieces were individualized, separated and labelled during excavation as they were showing evidences of organic macro-residues. Three of them have been selected for this study.

Fig. 2. Illustrations of the tear-drop shaped handle (credit photo: P.-J. Texier; drawing: Jaqui Peterson).

The tear-drop shaped handle (Fig. 2)

This first piece studied by us is one of two hefty pieces described at the time of recovery as 'mastic' (see below for a description of the second piece). Both come from the lowermost unit (JOFR) in the fill of a sleeping hollow excavated about 3750 years ago into existing terminal Pleistocene deposits by mid Holocene cave occupants. This 'excavation' uncovered and disturbed an earlier human burial that might have been the original context of the pieces presently under study. It is possible but not demonstrable that these two artefacts are contemporary. The human remains are 8000 years old.

This organic artefact has a tear-drop shape and a hole on its truncated, narrower extremity. It has a size of a palm and presents attributes of a handle. It weighs 43.3 g and is 63 mm long, but is slightly damaged on one extremity. The base of the handle is 46 mm width and 26 mm thick, its top is 31 mm width and 22 mm thick.

The handle presents a homogeneous external surface of a brownish yellow color (Munsell soil color chart: 10YR6/8). The surface exposes multiple small cracks that make a pattern similar to desiccation features. Some of these cracks are filled up by secondary minerals. This external surface is locally smoothed at its base and presents vegetal imprints. Quartz grains are also visible.

The handle is composed of three distinct 'layers': an external layer of about 2 mm thick, a middle layer of 4 to 8 mm thick and an internal layer of 2 to 3 mm thick. The internal layer resembles the external layer but is slightly lighter in color. The middle layer has a dark color and is shiny, as if it was 'vitrified'.

The hole is slightly off-centered and presents a diamond to circular shape. It is 43 mm deep and has a diameter of ca. 5 mm that seems to be constant throughout. The wall of the hole, as visible on its extremity, is not smoothed but present patterns on the form of 'positive veins', suggesting it has been formed in contact with an organic material such as a stick or a bone point.

Two main functional hypotheses can be proposed. One is to consider that the handle represents a reserve of resin that would have been collected around a stick and transported into the site for a future use. Such examples are reported from

Melkhoutboom cave (Deacon 1976) on the form of a 'stick with mastic', as well as from Boomplaas cave (Deacon 1984) in the form of three lumps of adhesive, including one piece with wood attached on it. But the piece from EBC differs substantially from these examples. While the pieces from Melkhoutboom and Boomplaas caves have an irregular and asymmetric shape, the handle from EBC presents a symmetric shape and a set of technical stigmata suggesting it is a finished and desired form.

The organic tool inserted into the handle is not present anymore. But its imprint is the one of a regular artefact indicating it has been worked. The collection of EBC presents several organic tools, either in wood or bone. All of them are pointed. One identified wood tool presents an oval section and a diameter of 6 mm, suggesting that the variability of organic tools manufactured at EBC is compatible with the hypothesis that the piece was designed for handling such an artefact. The polished surfaces at the base of the piece suggest it was handled several times and also support this interpretation.

Though part of the extremity of the handle is missing, the absence of polishing at the side of the hole indicates the tool was well fixed into the handle and/or that no rotating motions were involved. The set of observations suggests the hole has not been drilled into the handle, but results either from the molding of the resin directly around the organic tool, or from the inserting of the tool into the resin while it was still plastic enough.

These observations, together with the presence of vegetal imprints, indicate that the resin was not liquid while it was worked, but malleable. The existence of three different layers could be indicative of different steps in the covering of the organic tool. But the contact between these layers and their structure rather suggest they could represent different degrees of alteration or consolidation. The cracks that are observable on the external surface of the tear-drop didn't form on technical joints of manufacture, suggesting it was molded from one large piece of malleable adhesive. We observed no finger imprints, but several vegetal imprints are visible, indicating these plant parts were involved while the handle was being shaped. We consider four main hypotheses: 1) the vegetal substances/structures were used to maintain the soft resin, 2) the vegetal substance was used to help/control the drying of the resin, 3) the vegetal substance was part of the composition of the resin, or 4) the handle was held in a leaf package.

The macroscopic observation indicates the resin was mixed with millimetric quartz grains. One fragment of charcoal is present on the surface of the handle. Its isolation and position suggest this charcoal could be an indirect trace of manufacture, for example that could have occurred while the adhesive was (re-)heated.

The pencil-grip (Fig. 3)

The pencil-grip adhesive, as well as a small collection of quite distinctive silcrete, ochre stained flakes, came from the excavated unit of the human burial immediately below JOFR. The piece is likely to have been placed in the burial at about 8000 years ago.

This piece is a small backed quartz segment held in place in an organic holder. The whole piece weights 2.3 g. The piece is complete, though the imprint still visible on the ventral face of the quartz tool might suggest the adhesive was a little bit more invasive.

The backed artefact is made of a quartz flake. This tool is 21 mm long, with a

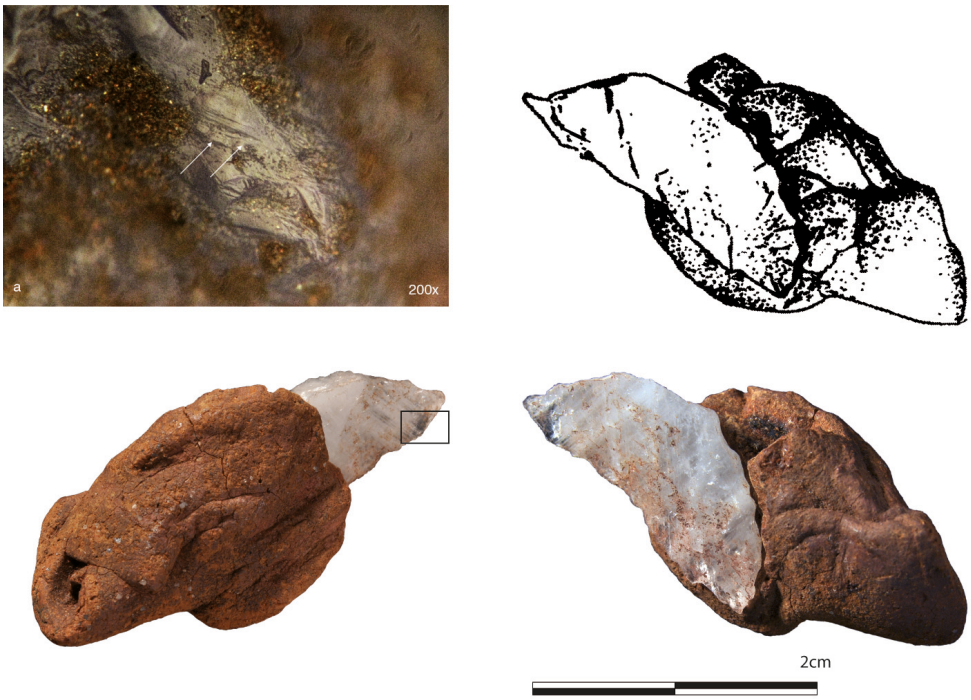

Fig. 3. Illustrations of the pencil grip wrapping a microlithic backed tool (credit photo: P.-J. Texier; drawing: Jaqui Peterson) with detail of the use-wear polish and striation.

maximum breadth of 9 mm and a maximum thickness of 4 mm. It corresponds to a segment with a semi- lunate shape, the back having been partly shaped by bipolar percussion. The segment has a rectilinear profile and a sharp edge with an irregular delineation. The edge presents micro-scars localized toward the apex. The use-wear analysis shows the presence of a polish together with striations (Fig. 3) that indicate the tool was used as a knife in a longitudinal motion.

The adhesive forms a small piece of about 24 mm long, 10 mm width and 15 mm thick. It is of brown color (Munsell soil color chart: 10YR4/3) and is homogeneous at a macroscopic scale. On its thickest part, the adhesive presents a blackish and shiny color. Multiple small cracks are visible as well as many quartz grains and a few shallow vegetal imprints. Prominent surfaces are smoothed.

There is no indication or marks that the adhesive was used to fix the tool into a wood or bone handle. The adhesive is complete and its shape suggests it was wrapped directly around the backed piece. Moreover, some surfaces of the handle are polished, suggesting a direct handling. Regarding the size of the piece and the types of functional traces, it is hypothesized that the lithic tool was involved in fine cutting or scribing activities.

The segment only fits in one way and so we have assumed that the tool was 'open' on one side (where the thumb presses) and that the segment could be easily changed. We see this as a kind of pencil grip that, in our case study, could only work if the object was held in the right hand with the right thumb doing the pressing.

The original morphology of the adhesive is the one of a foil that has been wrapped. It presents an irregular conic morphology with its maximum thickness being located on the contact with the tool. The morphology suggests that the foil, before being wrapped, had a pseudo-rectangular morphology and was about 25 mm width, 40 mm long and 2 to 4 mm thick. The quartz backed tool was positioned on the side of the adhesive foil and pinched by gripping until the two extremities recovered each other's marginally. The segment had been pressed into the mastic (and indeed there is an impression of one side of the segment in the mastic) and then held in place by the pressure of the thumb against it. A pleat was made at one extremity to adapt the global geometry of the handle and strengthen its adherence. It is a unique configuration of stone backed tool and holding device.

Our observations indicate the adhesive was moulded around the backed tool while it was plastic enough. Regarding the size of the piece and its nature, we expect that the adhesive has been moulded by hand, though no finger imprints are visible. One possibility is that those technical marks would have been erased with use. Alternatively, the craftsman may have made use of vegetation to manipulate the resin, explaining the presence of shallow vegetal imprints on the indurated adhesive (cf. the handle).

The macroscopic observation shows the adhesive has a rich load in quartz grains. No other additives, mineral or organic, are macroscopically visible.

The OES sealant (Fig. 4)

The third artifact is much younger than the other two and comes from a stratigraphic unit (DOLL) with an uncalibrated radiocarbon date of 950 years b.p.

The piece is an angular fragment of an ostrich eggshell water flask, with a maximum width of 36 mm and a maximum length of 25 mm. The light color of the surface of the eggshell suggests the OES has not been affected by post-depositional burning. Both perforation and macro-residue predate the breakage of the eggshell.

The presence of a perforation shaped by percussion indicates the OES was used as a flask or a container, presumably holding fresh water. The edge of the perforation is well polished, suggesting repeated contacts with another medium. The diameter of the perforation is estimated to be 10 to 12 mm. Although the fragment is small, its natural curvature suggests the hole was opened on the apex of the eggshell. No engravings or scratches are observed on the surface of the eggshell. So far, no engraved OES has been found in the related archaeological layers, which is consistent with the regional record. Generally in the Western Cape coastal region, terminal Holocene ostrich eggshell water flasks are not marked, although in the earlier Holocene such marking ('decoration') is more commonly found.

The macro-residue circling the perforation is of very dark grayish brown color (Munsell soil color chart: 10YR3/2), with a portion being even darker. The adhesive extends strictly on the external surface of the OES and almost reached the edge of the perforation. The macro-residue forms a strip with a regular width of about 10 mm. The maximum thickness of the macro-residue is on the middle of the strip and is about 2 mm. Some cracks are observable, as well as quartz grains and small fragments of shell (less than 2 mm).

Other examples of OES flasks with adhesive circling the perforation are known from the sites of Connies Limpet Bar (Parkington 2006) and Thoma's Farm (Henderson

Fig. 4. Photograph of the OES sealing-strip (credit photo: P.-J. Texier).

2002). Some of them have even been found with a vegetal cork that was used to seal the flask. From that perspective, the role of the adhesive is to ensure the impermeability of the cork. In our studied case, this hypothesis is directly supported by the functional traces observed on the hole, which is well polished on its whole thickness, suggesting a cork was sunk inside the hole and removed several times.

The adhesive is well smoothed which indicates it was applied and manipulated directly by hand while the adhesive was still malleable. The adhesive looks very resinous and includes small quartz grains, shell fragments as well as one isolated small charcoal.

ANALYTICAL METHODS

Having described the three organic artefacts under study, we propose to refer to them afterwards simply as: the 'handle', the 'grip' and the 'sealant'. We move from description of form to shorthand that refers essentially to the functional use of the pieces.

Protocols applied to archaeological pieces were adapted in order to minimize the quantity to be analyzed. For the handle, two samples were analyzed with the aim to highlight variations in manufacture or alteration. One of these two samples come from the outside layer and weight 5 mg, the other comes from the medium layer and weights 4.6 mg. Both samples originate from the top of the handle, already partly broken. For the grip, one sample of 4 mg was analyzed and for the sealant, one sample of less than 1 mg was analyzed. For these two specimens, samples were taken from broken parts.

Recent resins

The set of archaeological samples was complemented by a recent local resin originating from *Heeria argentea* (common name: Kliphout, Rockwood) that exudes spontaneously from the tree and by a dichloromethane/methanol (60:40 v/v) extract of recent bark from *Podocarpus elongatus* (common name: Yellowwood), both collected in South Africa. These two taxa are known sources of exploitable resin (Langenheim 2003): they still exist in the site area and were identified in the charcoal from both 'Joe Frazer' (JOFR) and 'Dolly' (DOLL) layers (Cartwright et al. 2014). They belong to two different plant families, easily distinguished based in their molecular composition in terpenic components (Mills & White 1977; Langenheim 2003). *P. elongatus* (Podocarpaceae family) is a part of Gymnosperm group (naked seed-producing plants) characterized by diterpene molecular markers (skeletal comprising 20 carbon atoms and up to three

cycles). It is clear that the composition of the bark extract and the resin may differ, but the biomarker families of *P. elongatus* must be identical and present in each. *Heeria argentea* (Anacardiaceae family) belongs to dicotyledons Angiosperms (flowering plants), characterized by triterpene molecular markers (skeletal with four or five cycles comprising 30 carbon atoms).

Reagents
All solvents were HPLC grade (Sigma Aldrich, purity: 99.9 %) and were used without further purification. Pyridine and *N,O*-bis(trimethyl)silyltrifluoroacetamide (BSTFA) containing 1 % trimethylchlorosilane (TMCS) were purchased from Sigma Aldrich. To avoid any contamination, only dichloromethane cleaned glassware was used. Silica gel, cotton and Fontainebleau sand were extracted in soxhlet with dichloromethane.

Extraction, purification, silylation
The resins and the macroresidues finely ground in an agate mortar were fully solubilized ultrasonically for 5 min with dichloromethane. After concentration under nitrogen flow the organic extract was purified by gravity flow column chromatography (silica gel support, eluents: dichloromethane/ethyl acetate 50:50 v/v and dichloromethane/methanol 60:40 v/v). The combined elution fractions were again concentrated to dryness. Resulting extract was then engaged in the silylation reaction. 40 µl pyridine and 200 µl BSTFA with 1 % TMCS were added. The reaction medium was heated for 2 hours at 70°C and then evaporated to dryness before being injected in GC-MS.

ATR - FTIR analysis
Samples were directly deposited on the measuring cell. Absorbance was collected in the range of 4000–400 cm^{-1} with 4 cm^{-1} resolution at a temperature of 18°C. ATR cell of the Bruker Alpha spectrometer consists of a diamond platinum crystal.

Mass spectrometric analysis
GC-MS analyses were carried out using a Focus GC gas chromatograph interfaced with an ISQ mass detector ThermoScientific (splitless mode injector, HP–5 MS column, 30 m x 0.25 mm i.d., 0.25 µm film thickness, temperature program: 40°C (1 min), 40–100°C (10°C/min), 100–320°C (4°C/min), isothermal 320°C (30 min). GC-MS interface was set at 320°C. Helium was used as carrier gas (1.5 $mL.min^{-1}$). Mass spectra were produced at 70eV, source 180°C, in full detection mode over 40–800 amu. Peak assignment was based on interpretation of mass spectra and comparison with spectra available in literature and NIST library 2.0.

The matrix assisted laser desorption-ionization mass spectrometry (MALDI-MS) analyses were conducted on a Bruker Autoflex II MALDI - Time of Flight (TOF) - mass spectrometer (Bruker Daltonics, Bremen, Germany). The device was featured with a pulsed nitrogen laser emitting at 337 nm and operated at an extraction voltage of 20 kV. The samples were dissolved in a mixture acetonitrile/methanol 1:1 (v/v) with 0.1 % trifluoroacetic acid (TFA) and deposited on a stainless steel target as dry droplets with a saturated solution of sinapic acid (SA) in the same mixture. Gated suppression was applied in order to prevent any saturation of the detector

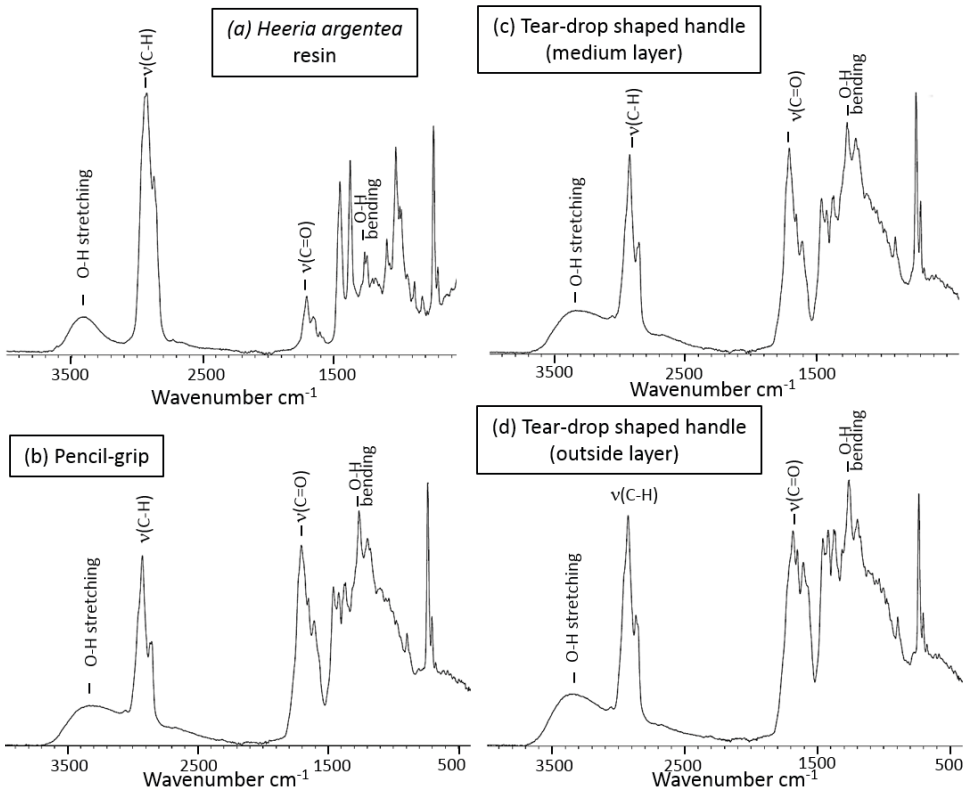

Fig. 5. FTIR spectra of (a) resin Heeria argentea, (b) the macro-residue from the grip, (c) the medium layer and (d) the outside layer from the handle.

by matrix ions. A total of 1000 laser shots were averaged for each spectrum and acquisitions were realized in reflector mode with positive ionization, with a laser power optimized and kept constant for the different samples. Bruker Pepmix II was used for calibration and spectra were processed with the Bruker FlexAnalysis software (version 3.4).

RESULTS

Preliminary analysis by ATR-FTIR

For a long time, FTIR has been used extensively in an archaeological context for the study of adhesives (e.g. Masschelein-Kleiner et al. 1968). Especially in ATR mode, this technique has the advantage of being non-destructive and the sample in powder form can be recovered. It is particularly suited to the analysis of pure organic materials with a low level of alteration. The presence of an inorganic base can indeed hide the organic signal and only the major components will be detected. Based on intermolecular bonds and on the presence of specific functional groups, it provides access to a diagnostic fingerprint of various natural substances such as resins or waxes and is useful for initial interpretations.

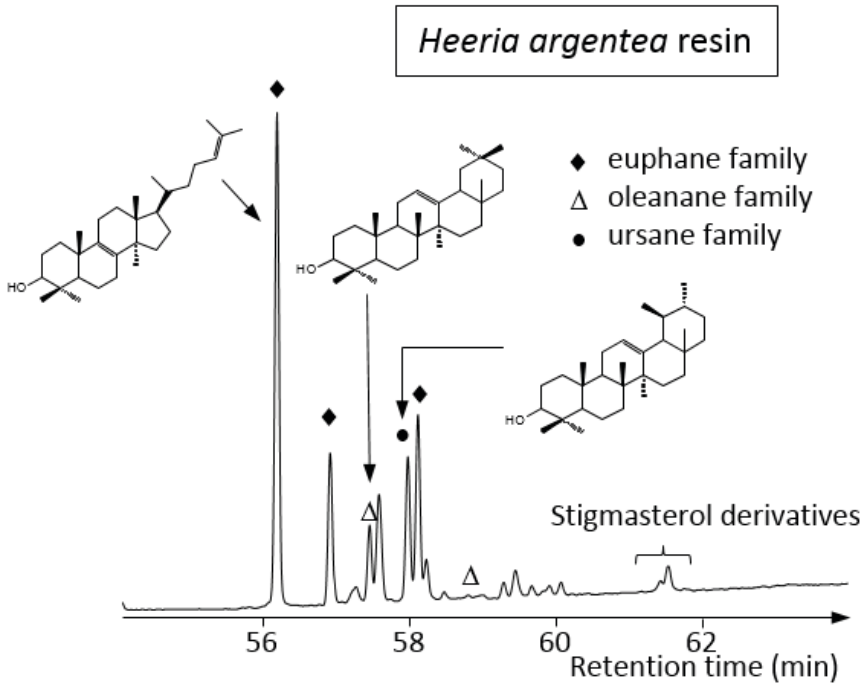

Fig. 6. GC-MS total ion current traces of the silylated extract from Heeria argentea.

According to literature data and reference spectra available in the laboratory, the spectra of dichloromethane extract from *Heeria argentea* resin and samples from the handle and the grip show a typical absorbance profile of a vegetal resin (Derrick et al. 1999; Colombini et al. 2009) (Fig. 5). The carboxylic acids present in resins leads to strong C–H and C=O stretching vibration (ν(C–H) at 2927 and 2868cm^{-1}, ν(C=O) at 1706cm^{-1}). Other bands can be clearly assigned: O–H stretching at 3420 cm^{-1}, aromatic ring stretching at 1607 cm^{-1}, CH_2 and CH_3 bending at 1459 and 1367 cm^{-1}, O–H bending at 1264 cm^{-1}, C–O stretching and bending in the range 1281–1198 cm^{-1}.

Unsurprisingly, the bands corresponding to oxygenated functionalities are more important in archaeological samples against fresh resins, reflecting a higher degree of alteration. They will also appear more clearly from the film surface than in the core of the handle.

Molecular analysis by GC-MS

The biomolecular approach used in this study is based on the identification of diagnostic molecular markers also called biomarkers derived from naturally-occurring substances by the means of mass spectrometric techniques (Charrié-Duhaut et al. 2009). The resulting diagnostic molecular fingerprints permit us both to define the biological origin of pure natural products or in admixture (plant, animal, families, and species) and to evaluate states of alteration (natural ageing or anthropic transformations). In the particular case of resins, specific series of terpenic skeletons are characteristics of plants families, or even of genera and species (Mills & White 1977; Langenheim

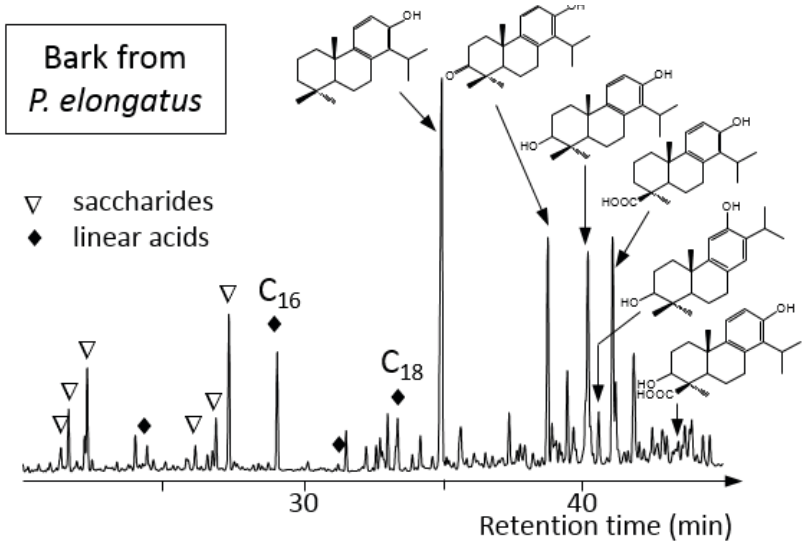

Fig. 7. GC-MS total ion current traces of the silylated extract of bark from Podocarpus elongatus.

2003). This will be illustrated below by comparing the molecular fingerprints of the two recent plant samples of known taxonomy and used as reference. This also explains why it is so essential to identify precisely the carbon skeleton of the components present in archaeological samples. Indeed, even if changes of functional groups occur, cyclic carbon structure is preserved. The latter can be used as a molecular marker to connect a degraded substance in archaeological context to its recent equivalent and to get an idea of the transformation processes that took place (Lampert et al. 2002; Burger et al. 2011; Charrié & Leprovost 2012; Charrié-Duhaut et al. 2013.).

Heeria argentea *and* Podocarpus elongatus

Heeria argentea is a South African endemic, specifically in the Western Cape area. Few studies of this taxon are reported in the literature and no molecular markers are described to the best of our knowledge, unlike *Pistacia* genus which is another member of Anacardiaceae family but not native to South Africa. The GC-MS total ion current traces of the silylated total extract consist mainly of triterpenoid structures (Fig. 6). The presence of such tetra- and pentacyclic components with retention time greater than 50 minutes provides evidence for an Angiosperm contribution and is expected for a plant from the Anacardiaceae family. The major compounds are based on euphane skeleton with a hydroxyl group at position 3 and double bonds in the ring B and in the side-chain (Appendix A) such as lanosterol. The pentacyclic triterpenoids belong to both oleanane and ursane families (β-amyrin and α-amyrin respectively). Stigmasterol derivatives ubiquitous in higher plants were also detected.

As expected, the GC-MS total ion current trace of the silylated total extract of bark from *Podocarpus elongatus* is more complex (Fig. 7). Linear structures (acids, alcohols) and components derived from sitosterol/stigmasterol generally observed in higher land plants such as stigmasta-3,5-dien-7-one, are present. Saccharides whose origin is certainly the cellulose of the bark are also detected. Concerning terpene

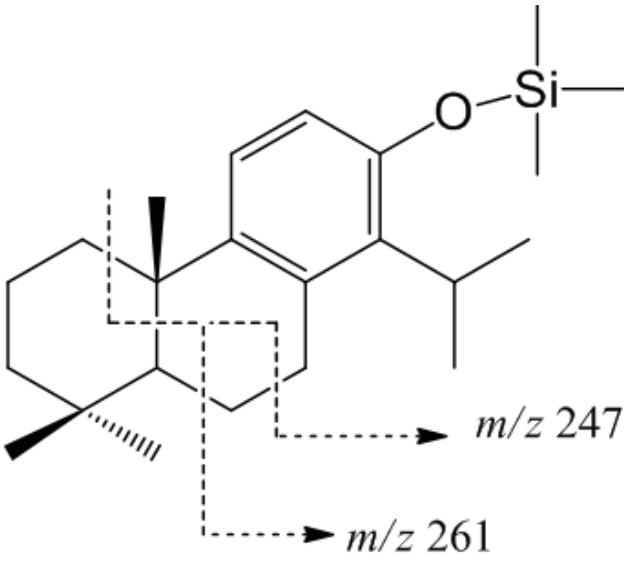

Fig. 8. Diagnostic mass fragmentations of trimethylsilylated derivatives from totarol.

skeletons, only phenolic diterpenic structures are present (retention times between 30 and 45 minutes). These latter compounds are used to precisely define the biological origin of natural substances. As mentioned above, diterpenic biomarkers indicate a Gymnosperm contribution, mainly conifer precursors. The specific molecular fingerprints of abietane skeletons are used to distinguish the different families in the group of conifers, especially of southern hemisphere conifers resins: Araucariaceae, Cupressaceae, Pinaceae, Podocarpaceae, Taxodiaceae (Mangoni & Caputo 1967; Bendall & Cambie 1995; Otto & Wilde 2001; Langenheim 2003; Cox et al. 2007). The basic principles are for instance: 'phenolic' abietanes divided into three groups according to the position of substituents on the aromatic ring (totarol, sempervirol, ferruginol) are absent in Pinaceae, predominance of ferruginol derivatives associated with totarol and sempervirol derivatives characterize Cupressaceae family, totarol and ferruginol are biomarkers for Podocarpaceae. We should also mention that the distinction of compounds belonging to all three families of 'phenolic' abietanes is not easy because of the similarity of mass spectra and therefore special care must be taken for precise structural identification (Enzell & Wahlberg 1970). As an example, according to Cox et al. (2007), the distinction between the three diagnostic unsubstituted phenols (totarol, ferruginol, sempervirol) is based on the intensity of the fragment *m*/*z* 247 compared to the fragment *m*/*z* 261 (Fig. 8), which is much more important for the totarol and this is indeed the case in this sample. The major components of the extract of present bark are totarol, 3-ketototarol (prominent M-7 ion in the fragmentation pattern *ie m*/*z* 315), 3-hydroxytotarol (prominent M-15-90 ion in the fragmentation pattern *ie m*/*z* 341), 4-carboxynortotarol (prominent M-15-118 ion in the fragmentation pattern *ie m*/*z* 327), 3-hydroxy-4-carboxynortotarol and 3-hydroxyferruginol. This molecular fingerprint is that expected for *Podocarpus elongatus*.

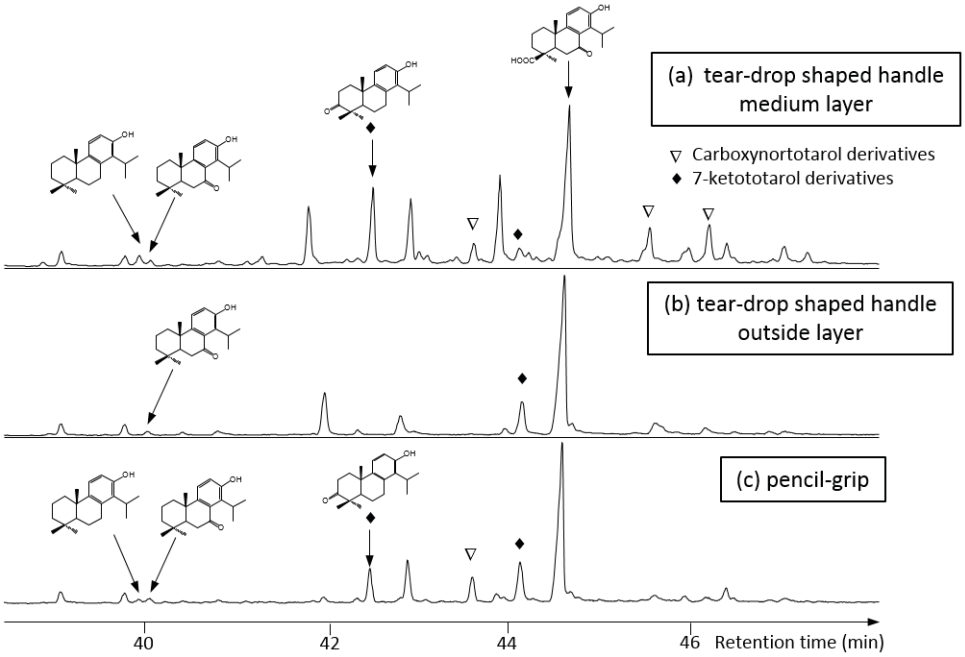

Fig. 9: GC-MS total ion current traces of the silylated extract of the macroresidue corresponding to (a) the medium layer and (b) the outside layer from the handle, (c) the grip.

The handle

The GC-MS total ion current traces of both outside and medium layers display a relatively small number of compounds with similar retention time. The compounds are divided into two main groups. The first with retention time between 50 and 60 min corresponds to the compounds of the family of sitosterol and stigmasterol. As before, they are indicators of higher land plant material. The second consists of diterpene structures related to totarol (Fig. 9a–b). The distributions are, however, quite different from that observed in bark extract described above. Regarding first the middle layer, totarol is still detected but is not at all major as in the bark. Only another compound is common to both: 3-ketototarol. Other structures based on totarol skeletons include more oxygen functionalities. Although little information on these oxidized components is available in the literature, structural proposals can be made on the basis of mass spectra. Derivatives with a carboxyl group at the 19-position and/or a ketone at the 7-position appear mostly (Fig. 9a–b). The major compound is the 4-carboxy, 7-ketototarol. From a chemical point of view, the benzylic position of phenolic structures (the 7-position) is extremely sensitive to oxidation. So it is no surprising to find such degradation byproducts, easily formed both by anthropogenic transformations or natural ageing. Although having a different physical appearance, molecular fingerprint corresponding to the outer layer has little difference with respect to the middle layer. Only small differences in intensity are visible. The material constituting the handle is therefore *Podocarpus* resin. No other component seems to be present as no other biomarkers appear on the GC-MS traces.

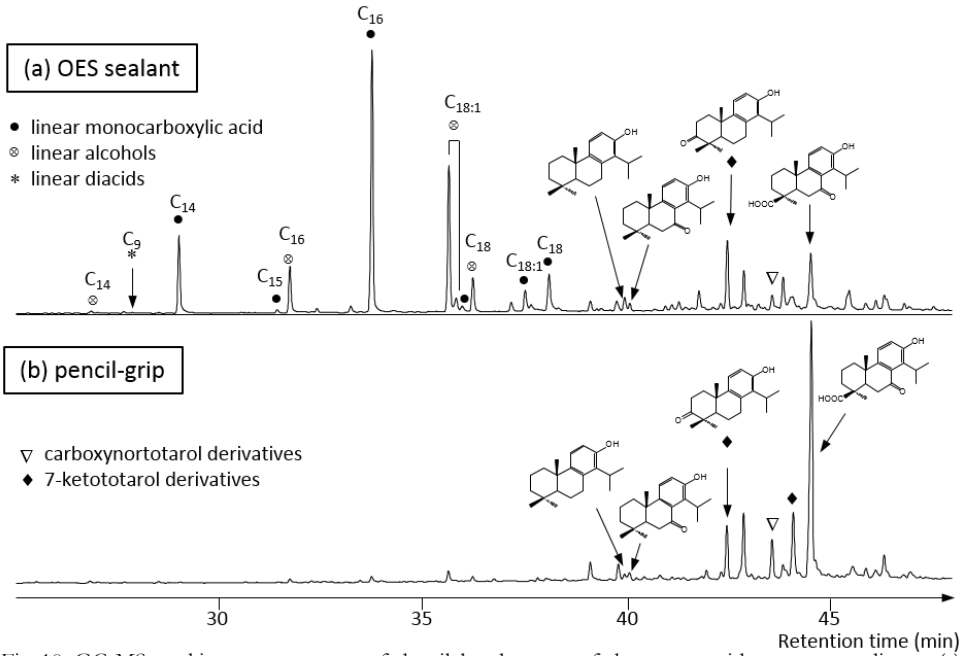

Fig. 10. GC-MS total ion current traces of the silylated extract of the macroresidue corresponding to (a) the sealant, (b) the grip.

The grip

The GC-MS total ion current trace corresponding to the leaf handle is very similar to the preceding ones and is clearly related to *Podocarpus* resin (Fig. 9c). As mentioned above, no other biomarkers were detected, indicating the use of pure plant material. There is no indication of heating.

The sealant

Despite the small quantities available, the applied protocol allowed the precise molecular composition of this coating to be established. A diterpenic distribution related to the family of totarol similar to that presented above is clearly observed indicating once again the contribution of a *Podocarpus* resin. This sample differs from the previous as linear structures are clearly present (Fig. 10a). Their fingerprint is dominated by linear monocarboxylic acids (even predominance, ranging from C_{14} to C_{18}, presence of the mono-unsaturated C_{18} acid) and linear alcohols (even predominance, ranging from C_{14} to C_{18}). Only one linear diacid (α,ω–dicarboxylic acid) is detected in low abundance: this is the term C9 also called azelaic acid. Such structures are usually fat characteristics. Based on the GC/MS data, it is very difficult to accurately determine its biological origin. This is especially true when the level of degradation is high. Indeed alteration processes lead to the loss of molecular markers allowing for example to differentiate a plant oil from an animal fat (Bastien 2011).The hypothesis of an animal fat is however encouraged by the fact that very few unsaturated fatty acids and diacids (their degradation products) are present (almost absent). Contribution of external contamination cannot be excluded. This fingerprint is strongly different from the one observed in a hafting adhesive at Diepkloof

Rock Shelter (Charrié-Duhaut et al. 2013), where linear diacids predominate linear monocarboxylic acids. It also doesn't correspond to the distribution of linear structures shown by Villa et al. (2012) suggesting the presence of bio-polyester derived from suberin. Further analysis would need to be undertaken to achieve for the biological origin of fat (measurement of carbon isotopic ratio ^{13}C vs ^{12}C of the fatty acids for instance).

Resin or tar?

The various studies on archaeological plant residues always raises the question of the use of an optionally heated resin or of making a tar? This is especially true when corresponding charcoals are found on the site. This involves different technologies, know-how and therefore cognitive functions. At the macromolecular as well as molecular level, it is difficult to distinguish. However some indications are in favor of one of the two assumptions. Plant tars are obtained by heating wood under reduced oxygen atmosphere. Some have been widely used since ancient times as the well-known pitch deriving from *Pinaceae* or the birch bark tar. The intense heating required to produce tar is accompanied by an aromatization of compounds through thermal dehydrogenation or decarboxylation (Robinson et al. 1987; Bailly 2015). This modification of the molecular composition demonstrated for pitch or birch bark tar should be present if *Podocarpus* wood was intensively heated to produce tar. Such aromatic structures were not detected in the samples from EBC. Another clue for molecular characterization of tar is the identification of molecules resulting from thermal degradation of the cellulose and lignin such as phenolic dimers (Bailly 2015), which is not the case in this study. According to Villa et al. (2012), suberin-containing pitch is also characterized by the presence of linear monocarboxylic acids and α,ω–dicarboxylics acids. Low abundance of these compounds has been detected in the OES sealant, which also contains fat, and are absent in the two other samples. MALDI-MS analyzes were undertaken to provide additional data on this specific issue. The mass spectra acquired for tars (analyzes performed on reference and archaeological birch bark tar and ancient pitch) show a regular distribution typical of a polymer. This is probably a lignocellulosic polymer finding its origin in the use of wood as raw material. This distribution is not found in the resins or in the tear-drop shaped handle from EBC. In the mass spectrum corresponding to this sample only diterpenes, more or less oxidized, appear (Fig. 11). For the three samples from EBC, it is reasonable to conclude in favor of resin rather than tar, resin that could have been slightly heated to gain malleability. Indeed, moderate heating probably induces little change in the molecular composition of the resin and will be very difficult to demonstrate.

SYNTHESIS AND MAIN IMPLICATIONS

Even if the pieces studied differ in terms of form, function and chronology, the *chaînes opératoires* present certain similarities. First of all, our results indicate a common use of *Podocarpus* to create adhesive. As charcoals from *P. elongatus* were found on the site (Cartwright et al. 2014), we hypothesize that this species likely provided the resin used. However, other species of *Podocarpus* exist in South Africa (*P. falcatus, P. latifolius)* and distinction between species on the basis of biomarkers needs further clarification. Furthermore, terpenoid resins are quite resistant to natural decay, which is not the case of other natural substances like proteinaceous binders or plant gums. This may result

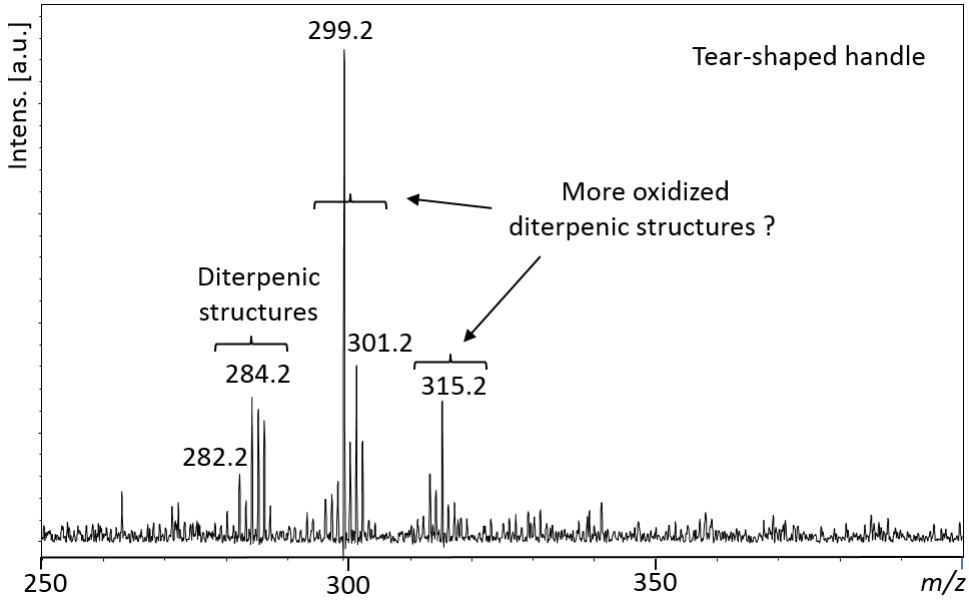

Fig. 11. Mass spectra MALDI–TOF corresponding to the medium layer from the handle. Matrix: SA 10 mg/mL in ACN/H20 1:1 (v/v), 0.1 % TFA; Reflector mode, positive ionization.

in a preferential preservation of the resins and we must keep in mind that the *chaînes opératoires* could be more complex.

The resin was mixed with a load of quartz grains in varying amounts. One fragment of shell found in the sealant would suggest the mineral load might have been acquired directly on the Atlantic beach at the foot of the shelter. Though we ignore the exact protocol, the transformation of the resin requires it to be heated for softening, until the right consistency and transformation are achieved. Our observations converge to recognize that the adhesive was malleable and not liquid when applied. Rare fragments of charcoals observed in two of the three artefacts might suggest the adhesive was heated during its application, possibly in direct contact with embers and purportedly to control softening. The application and shaping of the adhesive were likely made by hand. The presence of vegetal imprints on the two handles suggests their use was part of the process of modelling.

Macroscopically, no ochre or bone fragment has been observed. But the fingerprint of the sealant indicates the presence of (animal?) fat. While we cannot avoid the possibility that this results from pollution, we have to acknowledge the peculiarities required by the process of sealing in terms of properties. Unlike the other two pieces where adhesive exist as a solidified form, the seal needed to be "sticky". The addition of fat, during manufacture or during use, could have been part of the recipe to create and keep the properties of that adhesive.

There are other artefacts from EBC that reflect the use of adhesive. This is the case for a few adzes, which are tools that have supposedly been used in woodworking activities. The presence of macro-scars on the working edges suggests adzes were involved in a hard motion requiring the use of a haft. The manufacture and use of wood

and bone handles and hafts are inferred from many archaeological contexts but direct observations are few. Part of the explanation for this might lie in our results here, as the Holocene record of EBC indicates that hafting technology was commonly made up only of adhesive, at least for tools that were involved in (light) domestic activities such as cutting.

Our record adds substantial data to the discussion on composite technologies, microlithic and interchangeable tools. When there is use of a haft, the adhesive is here to ensure the good maintenance of the haft and the tool. In that case, the shape of the tool has to adapt to the handle, which contributes to normalize the production. In our examples, the grip adhesive and the microlithic backed piece form one single piece. In other words, the shape has not been influenced by the need of interchangeability: this was an ad hoc wrapping of adhesive finger protection around a specific quartz segment.

While there are many debates about microlithic backed tool manipulation and use, this piece provides a good example that microlithic and geometrics tools do not need automatically implicate their use in projectiles. The microlithic backed tool from EBC described here was used as a knife, in longitudinal action, just being wrapped into an adhesive in order to protect the hand and facilitate its prehension. As emphasized in many other contexts, microliths are not monolithic tools used in only a limited way (Elston & Kuhn 2002; Wadley & Mohapi 2008) and could have been involved in a whole range of activities including hunting and domestic tasks.

CONCLUSION

South Africa is characterized by a rich ecological diversity and includes different ecozones that define a wide range of constraints and opportunities, fueling the question of how hunter-gatherers adapted and diversified their practices. Archaeologically, one scientific advantage lies in the quality of the organic preservation, with Late Pleistocene plant remains being well documented and studied.

The study of archaeological plant remains, predominantly found in the form of charcoals, seeds and more occasionally as leaves, allows different kinds of investigation and interpretation (Sievers & Muasya 2011; Wadley 2012; Lennox & Bamford 2015; Sievers 2015). While these plant remains are good indicators of past environments, they also document a suite of behaviors that can be interpreted with reference to their known properties (as poisons, repellants, medicines, hallucinogens, etc.). Although these interpretations are no demonstration, the set of archaeological observations grows and converges to indicate that some plants were preferentially selected, suggesting some properties were understood and researched by hunter-gatherers groups. Our study on Holocene adhesive brings a new kind of evidence on how hunter-gatherers used and took benefits from their environments.

There are uncertainties regarding the recipes, the exact nature of the *chaînes opératoires* as well as the importance of each step during the adhesive's manufacture. This process of clarification requires a large set of experiments in order to evaluate the nature of the pyrotechnic management and in order to discriminate what reflects choices and preferences and what relates to constraints. This process of understanding also requires a larger set of archaeological observations, starting with macroscopic descriptions. Adhesives are recorded in different sites of South Africa, with many examples found in LSA contexts. Presently, the use of adhesive has been recorded for three types of

functional tasks: 1) to glue tools into their haft, 2) to create handles, 3) to seal OES containers (as strips to seal flasks, as cork or as spout). But within these broad categories, variability in recipes is expected.

The impact of mastering adhesive manufacture could have had major effects on other technologies and could represent one of the key innovations from the Late Pleistocene. Among the different properties that could characterize an adhesive, malleability appears to be a key property that could have durably influenced the technology of past hunter-gatherer groups.

One biomolecular analysis of adhesive presently done in South Africa relates to the Late HP of Diepkloof and dates back to ca 55 000 years ago, although evidence of adhesive use at the site goes back much earlier in time (Igreja & Porraz 2013). These analyses have recognized *Podocarpus resin* as the organic substance that was used to produce adhesive (Charrié-Duhaut et al. 2013). Similarly, 2000 km east of Diepkloof, the analysis of an adhesive coming from the Early LSA layers of Border Cave, dated to 43 000 BP, also demonstrates a composition based on *Podocarpus* (Villa et al. 2012). Our analysis from EBC expands this suite of observations and recognizes *Podocarpus* as the natural substance used to create adhesive during the Holocene of the West Coast of South Africa. These independent results converge to recognize that the resin of *Podocarpus* was preferentially collected by South African hunter-gatherers to produce adhesive since, at least, the MIS 4. We argue that the exploitation of *Podocarpus* may represent a lasting tradition and adaptation that is similar to the one recorded in Western Europe where birch is well known for having been used preferentially by prehistoric groups (Regert 2004). The use of *Podocarpus* resin would represent a knowledge that transcended changes in technological traditions.

ACKNOWLEDGEMENTS

We are indebted to L. Bom (Faculté de Chimie, Strasbourg, France) for the loan of equipment. We thank the Department of Archaeology at the University of Cape Town for help and assistance, the Iziko museum for providing access to the EBC collections as well as the South African Heritage Resources Agency (SAHRA). All chemical studies were performed in the Laboratory of Mass Spectrometry of Interactions and Systems (Strasbourg, France). We would like to thank Lyn Wadley, Martine Regert as well as a third anonymous reviewer for their constructive remarks.

REFERENCES

Bailly, L. 2015. *Caractérisation moléculaire et isotopique de goudrons et résines archéologiques dérivés de conifères en contexte maritime*. PhD thesis, University of Strasbourg.

Bastien, C. 2011. *Etude chimique des substances contenues dans une collection exceptionnelle de poteries provenant de Deir-el-Médineh (Egypte): une population et ses produits*. PhD thesis, University of Strasbourg.

Bendall, J.G. & Cambie, R.C. 1995. Invited review: Totarol: a non-conventional diterpenoid. *Australian Journal of Chemistry* **48**: 883–917.

Boëda, É., Bonilauri, S., Connan, J., Jarvie, D., Mercier, N., Tobey, M., Valladas, H. & Sakhel, H.A. 2008b. New evidence for significant use of bitumen in Middle Palaeolithic technical systems at Umm el Tlel (Syria) around 70,000 BP. *Paléorient* **34**: 67–83.

Boëda, É., Bonilauri, S., Connan, J., Jarvie, D., Mercier, N., Tobey, M., Valladas, H., Sakhel, H.A. & Muhesen, S. 2008a. Middle Palaeolithic bitumen use at Umm el Tlel around 70,000 BP. *Antiquity* **82**: 853–61.

Binneman, J.N.F., & Mitchell, P.J. 1997. Use wear analysis of Robberg bladelets from Sehonghong Shelter, Lesotho. *Southern African Field Archaeology* **6**: 42–9.

Burger, P., Charrié-Duhaut, A., Connan, J. & Albrecht, P. 2011. Taxonomic characterisation of fresh Dipterocarpaceae resins by gas chromatography-mass spectrometry (GC-MS): providing clues for identification of unknown archaeological resins. *Archaeological and Anthropological Sciences* **3**: 185–200.

Cartwright, C.R., Parkington, J.E. & Cowling, R.M. 2014. Understanding Late and Terminal Pleistocene vegetation change in the Western Cape, South Africa: the wood charcoal evidence from Elands Bay Cave. In: C.J. Stevens, S. Nixon, M.A. Murray & D.Q. Fuller, eds., *Archaeology of African plant use*. Walnut Creek, California: Left Coast Press, pp. 59–72.

Charrié, A. & Leprovost, C. 2012. Biomarqueurs et GC/MS: des principes clés pour la caractérisation, la conservation et la restauration des objets du patrimoine. Application à un adhésif végétal néolithique. *Spectra Analyse* **825**: 32–39.

Charrié-Duhaut, A., Burger, P., Maurer, J., Connan, J. & Albrecht, P. 2009. Molecular and isotopic archaeology: top grade tools to investigate organic archaeological materials. *C. R. Chimie* **12:** 1140–53.

Charrié-Duhaut, A., Porraz, G., Cartwright, C., Igreja, M., Connan, J., Poggenpoel, C. & Texier P.-J. 2013. First molecular identification of a hafting adhesive in the Late Howiesons Poort at Diepkloof Rock Shelter (Western Cape, South Africa). *Journal of Archaeological Science* **40** (9): 3506–18.

Colombini, M.P., Giachi, G., Iozzo, M. & Ribechini, E. 2009. An Etruscan ointment from Chiusi (Tuscany, Italy): its chemical characterization. *Journal of Archaeological Science* **36**: 1488–95.

Cox, R.E., Yamamoto, S. & Simoneit, B. 2007. Oxygenated di- and tricyclic diterpenoids of southern hemisphere conifers. *Biochemical Systematics and Ecology* **35** (6): 342–62.

Cârciumaru, M., Ion, R.M., Niţu, E.C. & Ştefănescu, R. 2012. New evidence of adhesive as hafting material on Middle and Upper Palaeolithic artefacts from Gura Cheii-Râşnov Cave (Romania). *Journal of Archaeological Science* **39**: 1942–50.

Conard, N.J., Porraz, G., & Wadley, L. 2012. What is in a name? Characterizing the 'post-Howieson's Poort' at Sibudu. *South African Archaeological Bulletin* **67**: 180–99.

Connan, J. 1999. Use and trade of bitumen in antiquity and prehistory: molecular archaeology reveals secrets of past civilizations. *Philosophical Transactions of the Royal Society B: Biological Sciences* **354**: 33–50.

Deacon, H.J. 1976. *Where hunters gathered: a study of Holocene Stone Age people in the Eastern Cape* (No. 1). South African Archaeological Society.

Deacon, J. 1984. *The Later Stone Age of southernmost Africa*. Oxford: British Archaeological Reports 213.

Deacon, H.J., & Deacon, J. 1980. The hafting, function and distribution of small convex scrapers with an example from Boomplaas Cave. *South African Archaeological Bulletin* **35**: 31–7.

Deacon, H.J., & Deacon, J. 1999. *Human beginnings in South Africa: uncovering the secrets of the Stone Age*. Cape Town: David Philip Publishers.

Derrick, M.R., Stulik, D. & Landry, J.M. 1999. *Infrared spectroscopy in conservation science: scientific tools for conservation*. The Getty Conservation Institute. Los Angeles.

Dinnis, R, Pawlik, A & Gaillard, C. 2009. Bladelet cores as weapon tips? Hafting residue identification and micro-wear analysis of three carinated burins from the late Aurignacian of Les Vachons, France. *Journal of Archaeological Science* **36**: 1922–34.

Elston, R.G. & Kuhn, S.L. 2002. *Thinking small: global perspectives on microlithization*. Arlington, VA: American Anthropological Association.

Enzell, C.R. & Wahlberg, I. 1970. Mass spectrometric studies of diterpenes. *Acta Chemica Scandinavica* **24**: 2498–510.

Grünberg, J.M. 2002. Middle Palaeolithic birch-bark pitch. *Antiquity* **76**: 15–16.

Haidle, M.N. 2010. Working-memory capacity and the evolution of modern cognitive potential. *Current Anthropology* **51**: 149–66.

Hayek, E.W.H., Krenmayr, P., Lohninger, H., Jordis, U., Moche, W. & Sauter, F. 1990. Identification of archaeological and recent wood tar pitches using gas chromatography/mass spectrometry and pattern recognition. *Analytical Chemistry* **62**: 2038–43.

Hauck, T.C., Connan, J., Charrié-Duhaut, A., Le Tensorer, J.M. & al Sakhel, H. 2013. Molecular evidence of bitumen in the Mousterian lithic assemblage of Hummal (Central Syria). *Journal of Archaeological Science* **40**: 3252–62.

Helwig, K., Monahan, V., Poulin, J. & Andrews, T.D. 2014. Ancient projectile weapons from ice patches in northwestern Canada: identification of resin and compound resin-ochre hafting adhesives. *Journal of Archaeological Science* **41**: 655–65.

Henderson, Z. 2002. A dated cache of ostrich-eggshell flasks from Thomas' Farm, Northern Cape Province, South Africa. *South African Archaeological Bulletin* **57**: 38–40.

Igreja, M., & Porraz, G. 2013. Functional insights into the innovative Early Howiesons Poort technology at Diepkloof Rock Shelter (Western Cape, South Africa). *Journal of Archaeological Science* **40**: 3475–91.

Iovita, R. 2011. Shape Variation in Aterian tanged tools and the origins of projectile technology: a morphometric perspective on stone tool function. *Plos One* **6** (12): e29029.

Koller, J., Baumer, U. & Mania, D. 2001. Pitch in the Palaeolithic: investigations of the Middle Palaeolithic 'resin remains' from Königsaue. In: G.A. Wagner & D. Mania, eds, *Frühe Menschen in Mitteleuropa-Chronologie, Kultur & Umwelt*: pp. 99–112.

Lampert, C.D., Glover, I.C., Heron, C., Stern, B., Shoocongdej, R. & Thompson, G.B. 2002. Characterization and radiocarbon dating of archaeological resins from Southeast Asia. In: K.A. Jakes, ed., *Archaeological chemistry: materials, methods, and meaning.* ACS Symposium Series. Washington D.C.: American Chemical Society, pp. 84–109.

Langenheim, J.H. 2003. *Plant resins; chemistry, evolution, ecology and ethnobotany*. Portland, Cambridge: Timber Press.

Lennox, S.J., & Bamford, M. 2015. Use of wood anatomy to identify poisonous plants: charcoal of *Spirostachys africana*. *South African Journal of Science* **111***:* 1–9.

Leroi-Gourhan, A. 1983. Une tête de sagaie à armature de lamelles de silex à Pincevent (Seine-et-Marne). *Bulletin de la Société préhistorique française* **80**: 154–6.

Leroi-Gourhan, A. & Allain, J. 1979. *Lascaux inconnu*. XII Supplément à Gallia Préhistoire. Paris: Editions du CNRS.

Lombard, M. 2006. First impressions of the functions and hafting technology of Still Bay pointed artefacts from Sibudu Cave. *Southern African Humanities* **18** (1): 27–41.

Lombard, M. 2008. Finding resolution for the Howiesons Poort through the microscope: micro-residue analysis of segments from Sibudu Cave, South Africa. *Journal of Archaeological Science* **35**: 26–41.

Mangoni, L. & Caputo, R.1967. Sempervirol, a novel type of diterpene phenol. *Tetrahedron Letters* **8**: 673–5.

Masschelein-Kleiner, L., Heylen, J. & Tricot-Marckx, F. 1968. Contribution à l'analyse des liants, adhésifs et vernis anciens. *Studies in Conservation* **13**: 105–21.

Mazza, P.P.A., Martini, F., Sala, B., Magi, M., Colombini, M.P., Giachi, G., Landucci, F., Lemorini, C., Modugno, F. & Ribechini, E. 2006. A new Palaeolithic discovery: tar-hafted stone tools in a European mid-Pleistocene bone-bearing bed. *Journal of Archaeological Science* **33***:* 1310–18.

Mills, J.S. & White, R. 1977. Natural resins of art and archaeology: their sources, chemistry and identification. *Studies in Conservation* **22**: 12–31.

Mills, J.S. & White, R. 1994. *The organic chemistry of museum objects*. 2nd edition. Oxford: Butterworth-Heinemann.

Mitkidou, S., Dimitrakoudi, E., Urem-Kotsou, D., Papadopoulou, D., Kotsakis, K., Stratis, J.A. & Stephanidou-Stephanatou, I. 2008. Organic residue analysis of Neolithic pottery from North Greece. *Microchimica Acta* **160**: 493–8.

Otto, A. & Wilde, V. 2001. Sesqui-, di- and triterpenoids as chemosystematic markers in extant conifers – a review. *Botanical Review* **67**: 141–238.

Parkington, J.E. 2006. *Shorelines, strandlopers and shell middens*. Krakadouw Trust. Cape Town.

Parkington, J.E. 2016. Elands Bay Cave: keeping an eye on the past. *Southern African Humanities* **29**: 17–32.

Pawlik, A. F. & Thissen, J. P. 2011. Hafted armatures and multi-component tool design at the Micoquian site of Inden-Altdorf, Germany. *Journal of Archaeological Science* **38**: 1699–1708.

Petersson, M. 1951. Mikrolithen als Pfeilspitzen. Ein Fund aus dem Lille Loshult Moor Ksp. Loshult, Skane. *Meddelanden fran Lunds Universitets Historiska Museum* **4**: 123–37.

Pollard, A.M. & Heron, C. 1996. *Archaeological chemistry*. Cambridge: The Royal Society of Chemistry.

Porraz, G., Igreja, M., Schmidt, P. & Parkington, J. 2016. A shape to the microlithic Robberg from Elands Bay Cave (South Africa). *Southern African Humanities* **29**: 203–47.

Regert, M. & Rolando, C. 2002. Identification of archaeological adhesives using direct inlet electron ionization mass spectrometry. *Analytical Chemistry* **74**: 965–75.

Regert, M. 2004. Investigating the history of prehistoric glues by gas chromatography-mass spectrometry. *Journal of Separation Science* **27**: 244–54.

Robinson, N., Evershed, R.P., Higgs, W.J., Jerman, K. & Eglinton, G. 1987. Proof of pine wood origin for pitch from Tudor (Mary Rose) and Etruscan shipwrecks: application of analytical organic chemistry in archaeology. *Analyst* **112**: 637–44.

Rots, V. 2003. Towards an understanding of hafting: the macro-and microscopic evidence. *Antiquity* **77** (298): 805–15.

Rots, V., Pirnay, L., Pirson, P. & Baudoux, O. 2006. Blind tests shed light on possibilities and limitations for identifying stone tool prehension and hafting. *Journal of Archaeological Science* **33**: 935–52.

Rots, V., Van Peer, P. & Vermeersch, P.M. 2011. Aspects of tool production, use, and hafting in Palaeolithic assemblages from Northeast Africa. *Journal of Human Evolution* **60** (5): 637–64.

Sievers, C. 2015. Nuts for dinner? *Cladium mariscus* in the Middle Stone Age at Sibudu, South Africa. *Transactions of the Royal Society of South Africa* **70** (3): 213–18.

Sievers, C. & Muasya, A. M. 2011. Identification of the sedge *Cladium mariscus* subsp. *jamaicense* and its possible use in the Middle Stone Age at Sibudu, KwaZulu-Natal. *Southern African Humanities* **23**: 77–86.

Soriano, S, Villa, P., Delagnes, A, Degano, I., Pollarolo L., Lucejko, J.J., Henshilwood, C. & Wadley, L. 2015. The Still Bay and Howiesons Poort at Sibudu and Blombos: understanding Middle Stone Age technologies. *PLoS ONE* **10** (7): e0131127.

Sulgostowska, Z. 1993. Mesolithic bone point with flint inserts from Tlokowo, Olsztyn Voivodeship: a technological assessment. *Archeologia Polski* **38**: 78.

Sykes, R.W. In press. To see a world in a hafted tool: birch pitch composite technology, cognition and memory in Neanderthals. In: F. Coward, R. Hosfield, M. Pope & F. Wenban-Smith, eds., *Settlement, society and cognition in human evolution: landscapes in the mind*. Cambridge: Cambridge University Press.

Tixier, J. 1959. Les pièces pédonculées de l'Atérien. *Libyca* **VI–VII**: 127–57.

Villa, P., Soriano, S., Tsanova, T., Degano, I., Higham, T., d'Errico, F., Backwell, L., Lucejko, J., Colombini, M.P., Beaumont, P.B. 2012. Border Cave and the beginning of the Later Stone Age in South Africa. *Proceedings of the National Academy of Sciences* **109** (33): 13208–13.

Wadley, L. 2010. Compound-adhesive manufacture as a behavioral proxy for complex cognition in the Middle Stone Age. *Current Anthropology* **51**: 111–19.

Wadley, L. 2012. Two 'moments in time' during Middle Stone Age occupations of Sibudu, South Africa. *Southern African Humanities* **24**: 79–97.

Wadley, L. & Mohapi, M. 2008. A segment is not a monolith: evidence from the Howiesons Poort of Sibudu, South Africa. *Journal of Archaeological Science* **35**: 2594–605.

Yaroshevich, A., Nadel, D. & Tsatskin, A. 2013. Composite projectiles and hafting technologies at Ohalo II (23 ka, Israel): analyses of impact fractures, morphometric characteristics and adhesive remains on microlithic tools. *Journal of Archaeological Science* **40**: 4009–23.

Yates, AB., Smith, A.M., Bertuch, F., Gehlen, B., Gramsch, B., Heinen, M., Joannes-Boyau, R., Scheffers, A., Parr, J. & Pawlik, A. 2015. Radiocarbon-dating adhesive and wooden residues from stone tools by Accelerator Mass Spectrometry (AMS): challenges and insights encountered in a case study. *Journal of Archaeological Science* **61**: 45–58.

APPENDIX A

Structures of natural products mentioned in the text.

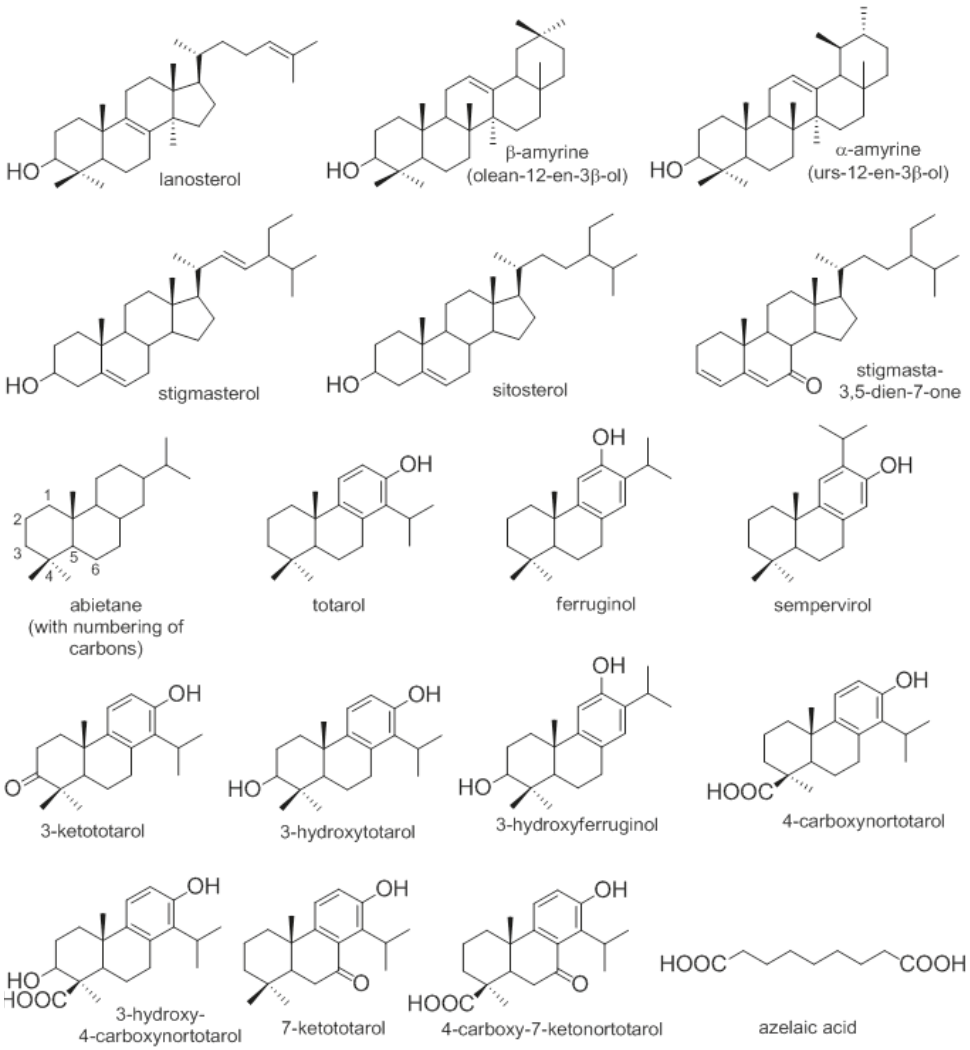

INSTRUCTIONS TO AUTHORS

General

Southern African Humanities is published annually and is a vehicle for research of an archaeological, anthropological and historical nature that is relevant to southern Africa. All contributions are published in English (British Standard). It is understood that manuscripts submitted to *Southern African Humanities* have not been offered to any other journal for prior or simultaneous publication. While there is no limit on the length of manuscripts, length should be appropriate for the topic. Papers are considered by at least two independent referees before acceptance. Authors are welcome to suggest suitable referees.

Preparation of manuscript

The manuscript should be in 12 pt font and 1.5 spaced. Number manuscript pages consecutively beginning with the title page. Give full details of the title of the manuscript, name(s) of author(s), postal address and email address if available, each on a separate line.

An abstract of not more than 200 words should summarise the essence of the paper. Avoid references in the abstract. Select a set of up to 12 key words or phrases (index terms).

Consider the journal's printed page size (127 × 192 mm) when preparing illustrations and tables. Illustrations (including graphs) and their captions or legends should form a separate unit. Explain abbreviations in the legends, or (if too numerous) collect them elsewhere in a list. Do not use very fine lines or dots in illustrations that require significant reduction. Similarly, use lettering of sufficient size to permit reduction.

Tables should include headings and explanations, and should be numbered consecutively. References in the text to illustrations and tables: Fig. 1; Figs 1–3; Table 1. Use lower case (fig., figs, table, pl., pls) when referring to items reproduced in another publication.

References

Two systems of referencing are acceptable, the Harvard author-date system and the endnote system. For the Harvard system, arrange citations in the text by date from earliest to latest. References within the text are as follows: (Davies 1974; Ngubane 1977; Deacon & Deacon 1999; Jolles 2001); Cooke (1963); Wright and Hamilton (1989); (Kuper 1980, 1982; Maggs 1984a, b); Jacobson et al. (1991). Cite page numbers as follows: (Dlamini 2001: 127).

List all publications cited in the text in full in the list of references. Arrange authors in alphabetical order, with multiple papers by the same author arranged chronologically. Cite all authors. Do not capitalize words unnecessarily. Give names of journals in full.

List website citations alphabetically according to author (if available) or website title, date of 'publication' (if available) and website address. Include date of access. In text, cite using author, date and, if relevant, website page address. Use the website title in place of author if the author is not obvious.

Treat each reference as a separate paragraph. Do not insert hard returns, tabs, spaces, etc. into the reference.

Examples

Anderson, A.A. 1888. *Twenty-five years in a wagon in the gold regions of Africa*. 2nd edition. London: Chapman & Hall.

Bleek, W.H.I. & Lloyd, L. 2005. *Lloyd and Bleek Collection*. Site accessed May 2006. http://www.lloydbleekcollection.uct.ac.za/uct/originals/ef/89a38bac.jpg.

Burrett, R.S. 1998. *Investigating Pfupi: a Later Stone Age industrial tradition in northeastern Zimbabwe*. MSc dissertation, University of the Witwatersrand.

Van de Merwe, N.J. 1975. Cannabis smoking in 13–14th century Ethiopia. In: V. Rubin, ed., *Cannabis and culture*. The Hague: Mouton, pp. 77–80.

Dlamini, N. 2001. The Battle of Ncome project; state memorialism, discomforting spaces. *Southern African Humanities* **13**: 125–38.

Endnotes are indicated by consecutive superior figures. Initial references must be in full, as follows:

J.C.H. Cable, K. Scott & P.L. Carter, 'Excavations at Good Hope Shelter, Underberg District, Natal', *Annals of the Natal Museum* **24** (1), 1980, pp. 1–34.
T.M.O'C. Maggs, *Iron Age communities of the southern Highveld*. Pietermaritzburg: Council of the Natal Museum, 1976.

Subsequent references to the works are abbreviated, but must provide an unambiguous indication of the source of the information:

Cable et al., 'Good Hope Shelter'; Maggs, *Iron Age communities*, p. 30.

Quotation marks

Use double quotation marks for quoted text, single quotation marks to highlight words. Quotations longer than 35 words should be set apart from the text in an indented block without quotation marks.

Initial Submission

Submit an electronic version of the manuscript to the editor by email or on a CD/DVD. Preferably submit all components of the paper (text, tables, figures) as a single .pdf file to facilitate the refereeing process. Graphics may be of reduced quality sufficient for evaluation by the reviewers. Initial submission of only a hard copy is possible but may slow down the review process. In the latter case, please send the printed version in triplicate and illustrations in duplicate (authors should keep the originals until the paper is accepted). Print hard copies on one side of the paper (A4 or a similar format).

Final submission

Supply the final text as a Word document. Illustrations can be submitted as original artwork or in standard electronic graphic formats (e.g. .tif, .jpg, .eps and .pdf). **The required resolutions for illustrations are as follows.**

Photographs: 400 dpi at print size. Maximum print size is 27 × 192 mm, which at the required resolution contains 2000 × 3024 pixels.

Line art (e.g. maps, graphs, site plans, artefact drawings): 1200 dpi at print size. Maximum print size is 127 × 192 mm, which at the required resolution contains 6000 × 9071 pixels.

Please do NOT USE your graphic programme to invent pixels.

Editorial process

All final submissions are checked to ensure that the author has dealt appropriately with the recommendations of the referees. The paper is then subjected to copy-editing and returned to the author for further input if necessary. Papers are then made up in the journal style and .pdf proofs sent to the author for checking. Once the author's corrections are implemented, each paper is checked again by the copy-editor. Finally, each paper is proof-read by a member of the editorial committee before it is posted online. The editorial committee reserves the right to suggest, recommend and/or require changes at any stage during the process. The file posted online is the same file used to generate the printed article.

Address all correspondence to

The Editor, Southern African Humanities
KwaZulu-Natal Museum,
P. Bag 9070,
Pietermaritzburg,
3200 South Africa;
e-mail: editor@nmsa.org.za;
www.sahumanities.org